# CURRENT INTELLIGENCE BULLETIN 70

# Health Effects of Occupational Exposure to Silver Nanomaterials

**Centers for Disease Control and Prevention**
National Institute for Occupational Safety and Health

**On the cover:**

Silver nanomaterials and products or processes using silver nanomaterials.

Clockwise from top left and ending with center:

Composite image of cells 24 hours post-exposure to silver nanoparticles coated with polyvinylpyrrolidone. Nanoparticles, endoplasmic reticulum, nuclei, and mitochondria shown in white, red, blue, and green, respectively. Photo by Robert M. Zucker, U.S. EPA.

Silver metal (Ag), crystal structure. Photo by ©Molekuul/Getty Images.

Printed circuit boards and components, which frequently use silver. Photo by ©Isti2/Getty Images.

Silver nanoparticles within macrophages in lung tissue. Photo by NIOSH.

Silver nanoparticles imaged by scanning electron microscope. Photo by NIOSH.

Sock fabric, which is among textiles that frequently contain silver as an antimicrobial agent. Photo by ©Gojak/Getty Images.

A tradesperson uses an airless sprayer to apply paint containing silver biocide. Photo by Bruce Lippy, CPWR.

# Current Intelligence Bulletin 70

# Health Effects of Occupational Exposure to Silver Nanomaterials

DEPARTMENT OF HEALTH AND HUMAN SERVICES
Centers for Disease Control and Prevention
National Institute for Occupational Safety and Health

## Disclaimer

Mention of any company or product does not constitute endorsement by the National Institute for Occupational Safety and Health (NIOSH), Centers for Disease Control and Prevention (CDC). In addition, citations of websites external to CDC/NIOSH do not constitute CDC/NIOSH endorsement of the sponsoring organizations or their programs or products. Furthermore, CDC/NIOSH is not responsible for the content of these websites. All web addresses referenced in this document were accessible as of the publication date.

## Get More Information

Find NIOSH products and get answers to workplace safety and health questions:

1-800-CDC-INFO (1-800-232-4636) | TTY: 1-888-232-6348
CDC/NIOSH INFO: cdc.gov/info | cdc.gov/niosh
Monthly *NIOSH eNews*: cdc.gov/niosh/eNews

## Suggested Citation

NIOSH [2021]. Current Intelligence Bulletin 70: health effects of occupational exposure to silver nanomaterials. By Kuempel E, Roberts JR, Roth G, Dunn KL, Zumwalde R, Drew N, Hubbs A, Trout D, and Holdsworth G. Cincinnati, OH: U.S. Department of Health and Human Services, Centers for Disease Control and Prevention, National Institute for Occupational Safety and Health, DHHS (NIOSH) Publication No. 2021-112, https://doi.org/10.26616/NIOSHPUB2021112.

DHHS (NIOSH) Publication No. 2021–112

DOI: https://doi.org/10.26616/NIOSHPUB2021112

May 2021

# Foreword

When the U.S. Congress passed the Occupational Safety and Health Act of 1970 (Public Law 91–596), it established the National Institute for Occupational Safety and Health (NIOSH). Through the Act, Congress charged NIOSH with recommending occupational safety and health standards and describing exposure limits that are safe for various periods of employment. These recommendations include but are not limited to the exposures at which no workers will suffer diminished health, functional capacity, or life expectancy because of their work experience.

The growing use in commerce of nanomaterials (materials with one or more dimension smaller than about 100 nm) has resulted in increased awareness and understanding of the associated potential hazards. Since the early 2000s, NIOSH has been assessing and addressing the potential occupational safety and health effects of high-volume nanomaterials, including silver nanomaterials. Elemental silver has been in commerce for centuries. In 1988 NIOSH adopted a recommended exposure limit (REL) for total silver of 10 micrograms per cubic meter ($\mu g/m^3$) as an 8-hour time-weighted average (TWA) concentration to protect workers from developing argyria (bluish-gray pigmentation to the skin and mucous membranes) and argyrosis (bluish-gray pigmentation to the eyes). The previous authoritative assessments of occupational exposure to silver did not account for particle size.

Recent studies in animals have demonstrated that biologic activity and potential adverse health effects are related to particle size. Adverse health effects of nanoscale silver particles, such as early stage lung inflammation and liver hyperplasia, have been observed in rats following inhalation exposure. NIOSH considers these responses of pulmonary inflammation and liver hyperplasia to be relevant to workers and estimated the risks to workers based on these animal data. This led NIOSH to determine that it is reasonable and prudent to establish a REL for nanoscale silver. The NIOSH REL for silver nanomaterials (≤100 nm primary particle size) is 0.9 $\mu g/m^3$ as an airborne respirable 8-hour TWA concentration. In addition, NIOSH continues to recommend a REL of 10 $\mu g/m^3$ as an 8-hour TWA concentration for total silver (metal dust, fume, and soluble compounds) as Ag. NIOSH further recommends the use of workplace exposure assessments, engineering controls, safe work procedures, training and education, and established medical surveillance approaches to protect workers.

NIOSH recommends that employers disseminate this information to workers and customers and requests that professional and trade associations and labor organizations inform their members about the potential hazards of occupational exposure to silver nanomaterials.

NIOSH appreciates the time and effort of the expert peer, stakeholder, and public reviewers whose comments and input strengthened this document.

John Howard, M.D.
Director, National Institute for Occupational Safety and Health
Centers for Disease Control and Prevention

# Abstract

Nanoscale silver particles are some of the most widely used nanomaterials in commerce, with numerous uses in consumer and medical products. Workers who produce or use silver nanomaterials are potentially exposed to those materials in the workplace. Previous authoritative assessments of occupational exposure to silver did not account for particle size. The National Institute for Occupational Safety and Health (NIOSH) assessed potential health risk from exposure to silver nanomaterials by evaluating more than 100 studies of silver nanomaterials in animals or cells. In studies that involved human cells, silver nanomaterials were associated with toxicity (cell death and DNA damage) that varied according to the size of the particles. In animals exposed to silver nanomaterials by inhalation or other routes of exposure, silver tissue concentrations were elevated in all organs tested. Exposure to silver nanomaterials in animals was associated with decreased lung function, inflamed lung tissue, and histopathological (microscopic tissue) changes in the liver and kidney. In the relatively few studies that compared the effects of exposure to nanoscale or microscale silver, nanoscale particles had greater uptake and toxicity than did microscale particles. To date, researchers have not reported health effects in workers exposed to silver nanomaterials.

To assess the risk of health effects from exposure to silver nanoparticles quantitatively, NIOSH evaluated the data from two published subchronic (intermediate duration) inhalation studies in rats. These studies revealed lung and liver effects that included early-stage lung inflammation and liver bile duct hyperplasia. NIOSH researchers used the data from these studies to estimate the dose of silver nanoparticles that caused these effects in rats. They then calculated the corresponding dose that would be expected to cause a similar response in humans, accounting for uncertainties in those estimates. From this evaluation, NIOSH derived a recommended exposure limit (REL) for silver nanomaterials ($\leq$100 nm primary particle size) of 0.9 micrograms per cubic meter ($\mu g/m^3$) as an airborne respirable 8-hour time-weighted average (TWA) concentration. In addition, NIOSH continues to recommend a REL of 10 $\mu g/m^3$ as an 8-hour TWA for total silver (metal dust, fume, and soluble compounds, as Ag). NIOSH further recommends the use of workplace exposure assessments, engineering controls, safe work procedures, training and education, and established medical surveillance approaches to protect workers.

# Executive Summary

## Introduction

Nanotechnology is an enabling technology involving structures generally defined as having one, two, or three external dimensions in the range of approximately 1 to 100 nanometers (nm) [ISO 2008]. Nanoscale substances may have physical (including morphological) and chemical properties that differ from those of the same substances as larger particles or in bulk [Wijnhoven et al. 2009]; such useful properties may be exploited by manufacturers. One prominent example of these substances is silver nanomaterials, which are used in the manufacture of electronics and textiles and have been used as pigments, catalysts, and antimicrobials [Wijnhoven et al. 2009; Nowack et al. 2011]. The United States produced an estimated 20 tons of silver nanomaterials in 2010 [Hendren et al. 2011], and an estimated 450–542 tons were produced worldwide in 2014 [Future Markets, Inc. 2013]. A more recent study by Giese et al. [2018] indicated high uncertainty in estimates of total nanomaterial production. Estimates for silver nanomaterial production globally ranged from 5.5 to 100,000 tons annually [Giese et al. 2018].

The current Occupational Safety and Health Administration (OSHA) permissible exposure limit (PEL), the Mine Safety and Health Administration (MSHA) PEL, and the National Institute for Occupational Safety and Health (NIOSH) recommended exposure limit (REL) are each 10 micrograms per cubic meter ($\mu g/m^3$) as an 8-hour time-weighted average (TWA) concentration (total mass sample) of silver (metal dust, fume, and soluble compounds, as Ag) [NIOSH 1988, 2007; OSHA 1988, 2012a; 30 CFR 57.5001]. The PEL and REL for total silver are based on preventing workers from developing argyria, which is bluish-gray pigmentation to the skin and mucous membranes, and argyrosis, which is bluish-gray pigmentation to the eyes (see Terminology/Glossary and Section 1.4, Human Health Basis, for the NIOSH REL).

When the current REL of 10 $\mu g/m^3$ for total silver was developed, it did not include a specific evaluation of silver nanomaterials. More recent studies in animals and cells have shown that the fate and biologic activity of silver are affected by physical-chemical characteristics such as particle size [Park et al. 2011c; Kim et al. 2012; Gliga et al. 2014; Braakhuis et al. 2014], shape [Stoehr et al. 2011], solubility, and surface properties [Johnston et al. 2010; Foldbjerg et al. 2011; Beer et al. 2012]. Studies in animals have shown exposure-related adverse lung and liver effects in rats following subchronic inhalation exposure to silver nanoparticles (AgNPs) of 15–20 nm in diameter [Sung et al. 2009, Song et al. 2013].

## Occupational Exposure and Human Evidence

Workers can be exposed to silver throughout its life cycle, including ore extraction, smelting and refining, product fabrication, use, disposal, and recycling. Workplace exposures to silver have been reported to occur during brazing and soldering operations ($\leq$ 6.0 $\mu g/m^3$ TWA) [NIOSH 1973, 1981,1998]; during manufacturing of silver nitrate and silver oxide

(39–378 μg/m$^3$ TWA) [Rosenman et al. 1979, 1987]; during smelting and refining of silver (1–100 μg/m$^3$ TWA) [DiVincenzo et al. 1985]; and during reclamation of silver from photographic film (5–240 μg/m$^3$ TWA) [Pifer et al. 1989; Williams and Gardner 1995; NIOSH 2000]. These early studies provide little information on airborne-particle characteristics, and it is likely that the fumes generated while melting silver or during brazing and soldering contained AgNPs and/or agglomerates of AgNPs. More recent studies have shown exposures to AgNPs in the workplace [Park et al. 2009; Lee et al. 2011b; Lee et al. 2012a,b; Miller et al. 2010; Lewis et al. 2012; Lee et al. 2013b]. Measurements of airborne concentration of silver nanoparticles in workers' personal breathing zones were reported to range from 0.02 to 2.43 μg/m$^3$ TWA during their production [Lee et al. 2011b; Lee et al. 2012a,b]. Airborne concentrations ranged from 13 to 94 μg/m$^3$ TWA at a precious metal processing facility where melting and electrorefining of silver occurred [Miller et al. 2010].

Published reports of adverse health effects on workers occupationally exposed to silver, though limited, indicate that long-term exposure to silver can cause localized (in dermal and mucous membranes) and generalized (systemic) argyria [ATSDR 1990; Drake and Hazelwood 2005; Wijnhoven et al. 2009; Johnston et al. 2010; Lansdown 2012]. Ocular argyrosis has been observed in workers exposed to either soluble or insoluble silver, but no deficits in visual performance could be attributed to the silver deposits [Rosenman et al. 1979; Pifer et al. 1989]. Other studies have revealed cases of abnormal kidney function or acute respiratory distress [Parikh et al. 2014; Rosenman et al. 1987] in silver workers compared with unexposed workers, but such exposure often occurred concurrently with exposure to cadmium and solvents. Relatively few studies have been published on worker exposures to silver nanomaterials [Lee et al. 2011b, 2012a,b; Park et al. 2009; Miller et al. 2011]. These studies did not show adverse health effects and did not characterize the nanomaterial exposures in detail. In a case study, acute silver poisoning was reported in a young worker after an exposure to silver vapors from melting silver ingots continuously for 4 hours in a small closed room without ventilation [Forycki et al. 1983].

## Cellular Studies

In vitro studies provide information on the cellular toxicological mechanisms associated with AgNPs and the effect of physicochemical properties. These findings may be relevant to potential in vivo mechanisms (at least qualitatively, as equivalent doses may not be estimable). Key findings from in vitro studies of effects from exposure to either AgNPs or ionic silver include increased levels of reactive oxygen species (ROS) [Hussain et al. 2005a; Carlson et al. 2008; Foldbjerg et al. 2009; Kim et al. 2009c], induction of oxidative stress management genes [Kim et al. 2009c; Miura and Shinohara 2009], and increased percentages of apoptotic cells [Hsin et al. 2008; Foldbjerg et al. 2009; Miura and Sinohara 2009]. Results of some cellular assay studies indicate that ionic silver can be more potent than AgNPs in causing apoptosis [Foldbjerg et al. 2009] and reducing cell viability [Carlson et al. 2008; Greulich et al. 2009; Kim et al. 2009c; Miura and Shinohara 2009], whereas results of other studies provide evidence of a relationship between increasing generation of intracellular ROS and decreasing particle size.

Reactive oxygen species generation was statistically significantly elevated after exposure of rat alveolar macrophages to 15-nm-diameter AgNPs, but not after exposure to 30- or 55-nm-diameter AgNPs at the 10–50 μg/mL doses [Carlson et al. 2008]. DNA damage and high levels of apoptosis and necrosis were associated with exposure to either AgNPs or ionic

silver [Foldbjerg et al. 2009, 2011]. Statistically significant increases in bulky DNA adducts were observed at doses from 2.5 μg/mL of AgNPs; however, pretreatment with the antioxidant N-acetyl-L-cysteine (NAC) (10 mM; 1 hour prior to Ag exposure) inhibited the formation of bulky adducts [Foldbjerg et al. 2009, 2011]. AgNP surface chemistry and activity affect the kinetics of ion release, and AgNP dissolution processes generate additional ROS as a byproduct [Liu et al. 2010b]. These in vitro studies suggest nanoscale silver particles may be more toxic than microscale silver particles in both the lungs and extrapulmonary organs; however, results were more variable in rodent studies that compared the toxicity of nanoscale and microscale silver particles. Although several studies showed greater toxic effects following exposure to smaller particles [Park et al. 2010b, Philbrook et al. 2011, Silva et al. 2016; Sieffert et al., 2015], some studies found that the larger particles were more toxic [Silva et al. 2015; Botelho et al. 2016]. The differences of effect in the in vivo studies could be due to variations in route of exposure, form of silver, dose, and the target tissue. The in vitro findings also indicate that dissolution of AgNPs accounts for some degree of the observed toxicity, although the effects cannot be fully apportioned to the measured dissolved fraction of silver.

## Animal Studies

The most comprehensive information on the potential toxicity of AgNPs comes from experimental animal studies. In vivo studies of rats exposed to AgNPs by subchronic inhalation provide evidence of (1) the uptake of silver ions and nanoparticles in the blood and subsequent distribution to all major organs and tissues, including liver, kidneys, testes, ovaries, olfactory bulb, and brain [Sung et al. 2008, 2009; Song et al. 2014]; (2) perturbation of lung function and induction of inflammatory responses [Sung et al. 2008, 2009; Song et al. 2013]; and (3) histopathologic changes in the kidney and notably in the liver, where bile duct hyperplasia and necrosis were identified [Sung et al. 2009]. These effects were reported after inhalation exposure to AgNPs (primary particle diameter, 15–20 nm) at airborne concentrations of 49 or 133 μg/m$^3$ (6 hr/d, 5 d/wk) for 12–13 weeks. Following exposure to AgNPs by various routes (inhalation, oral, intravenous), statistically significant increases in the amount of silver have been observed in major organs and tissues, including the lungs, liver, spleen, kidneys, olfactory bulb, brain, and blood in both male and female rats [Ji et al. 2007b; Kim et al. 2008; Sung et al. 2009; Kim et al. 2010a; Lankveld et al. 2010; Lee et al. 2013d]; these increases appear to be sex-specific, with the most commonly reported difference being a significantly greater accumulation of silver in the kidneys of female rats [Sung et al. 2009; Kim et al. 2010a, 2011; Song et al. 2013; Dong et al. 2013]. Inhalation and oral exposure to silver nanomaterials are likely to be the most relevant routes in the workplace, from airborne or dermal (hand to mouth) exposure. Findings from intravenous studies provide additional information about transformation of silver nanomaterial and potential modes of action at sites of toxicity. Most of the effects observed in animal studies following exposure to silver nanomaterials by any route have been reported to be in the lungs, liver, and kidneys, although some findings in the brain and reproductive organs (Sections 5.2.1, 5.22., 5.3) suggest that further study in these tissues may be warranted.

In a 13-week (90-day) inhalation study by Sung et al. [2008, 2009], lung function deficits (decreased tidal volume, minute volume, and peak inspiration flow), inflammation responses, and alveolar accumulation of macrophages were observed [Sung et al. 2008]. In a subsequent 12-week inhalation (and 12-week recovery) study from the same laboratory [Song et al. 2013], the alveolar inflammation had resolved in the female rats and had

resolved in all but one of the male rats at the high dose 12 weeks after cessation of exposure. Acute and shorter subacute exposure studies have ranged in degree of pulmonary inflammation and lung injury but have a commonality in the trend of responses; the majority of studies show degrees of resolution of responses over time following exposure [Kwon et al. 2012; Roberts et al. 2013; Seiffert et al. 2016; Silva et al. 2016; Stebounova et al. 2011].

Although the biological interactions with inhaled AgNPs are not fully understood, the possible mechanisms include dissolution and release of soluble silver species, and particle transformation through sulfidation (binding with sulfur) or opsonization (binding with protein), which can stabilize the silver [Liu et al. 2011; Loeschner et al. 2011; Bachler et al. 2013]. AgNPs are considered to have a greater potential for dissolution and release of ions than microscale particles, because of the increased surface area per unit mass of nanoparticles [Wijnhoven et al. 2009]. Only a few studies in animals have compared the effects of exposure to different sizes of silver particles (micro- and nano-diameter); these studies showed that exposure to nanoscale silver particles in rodents resulted in a greater retained mass dose [Braakhuis et al. 2014], increased alveolar macrophage uptake [Anderson et al. 2015], a higher degree of acute pulmonary inflammation [Anderson et al. 2015; Braakhuis et al. 2014], and greater cytotoxicity (both severity and duration) [Anderson et al. 2015], in addition to increased nasal cavity deposition, transport to the olfactory bulb, and microglial cell activation [Patchin et al. 2016].

## Published Occupational Exposure Limits (OELs) for Silver Nanoparticles

Aschberger et al. [2011], Christensen et al. [2010], and Stone et al. [2009] derived OELs for AgNPs of ~0.1–0.67 μg/m$^3$ as 8-hour TWAs, based on the rat subchronic inhalation data reported in Sung et al. [2008, 2009]. Christensen et al. [2010] described the European Chemicals Agency (ECHA) [2012] guidelines that were followed, starting with the rat no observed adverse effect level (NOAEL) for lung or liver effects, or the lowest observed adverse effect level (LOAEL) for lung function deficits. The rat NOAEL and LOAEL were adjusted by differences in rat and human exposure conditions and by uncertainty factors (UFs). The OEL estimates depended on the animal NOAEL or LOAEL (49 or 133 μg/m$^3$) and the UFs (75–250) used in the assessments. In another assessment, Swidwinska-Gajewska and Czerczak [2015] derived a maximum admissible concentration for silver nano-objects of 10 μg/m$^3$ as an 8-hour TWA inhalable fraction.

Weldon et al. [2016] estimated an 8-hour TWA OEL of 0.19 μg/m$^3$ for AgNPs, based on the silver tissue dose and liver–bile duct hyperplasia response in female rats [Sung et al. 2009]. Liver bile duct hyperplasia was considered to be the critical (i.e., most sensitive) effect, which was specific and quantifiable. The human-equivalent concentration (HEC) was estimated by applying dosimetric adjustment factors (DAFs) [U.S. EPA 1994] to the rat benchmark dose or concentration (BMD or BMC) estimates. The 8-hour TWA OEL was derived from an estimated animal effect level of 25.5 μg/m$^3$ and by applying a total DAF of 4.5 and total UF of 30. Further details are reported in Appendix G.

## NIOSH Quantitative Risk Assessment

In the absence of information on health effects from human exposure to AgNPs, NIOSH considered the subchronic inhalation data on rats [Sung et al. 2008, 2009; Song et al. 2013]

to be the best available for evaluating the potential occupational health hazards of AgNPs. This is consistent with the use of an exposure route relevant to humans (inhalation) and the use of positive effect in either humans or animals for health hazard classification [29 CFR 1910.1200, A.0.3.3; OSHA Health Hazard Criteria, available at https://www.osha.gov/dsg/hazcom/hazcom-appendix-a.html]. In testing for toxicity of airborne agents, inhalation exposures in animals are often the most appropriate measurements [Harkema et al. 2013]. The airborne exposure concentrations in these rat studies ranged from 49 to 515 μg/m$^3$, a range which spans the 100 μg/m$^3$ 8-hr TWA OEL (ACGIH TLV® and MAK) for inhalable, insoluble silver (Table 1-3). No statistically significant dose-related changes in rat body weight or organ weight were reported, and no toxicity that interfered with the study interpretation [Bucher et al. 1996; Oberdörster 1997] was described [Sung et al. 2009; Song et al. 2013]. The pulmonary clearance rates of silver were similar to the normal rates for alveolar macrophage–mediated clearance (i.e., no evidence of overloading) (Section 6.2.1). Thus, the adverse lung and liver effects associated with exposure to AgNPs in these rat studies were considered to be relevant to humans. The lung and liver effects associated with exposure to AgNPs in the rat subchronic inhalation studies are consistent with the definition of Specific Target Organ Toxicity following Repeated Exposure (STOT-RE) [29 CFR 1910.1200, A.9].

Lung inflammation and lung function deficits were observed in both male and female Sprague-Dawley rats following inhalation of AgNPs for 13 and 12 weeks, respectively, as reported by Sung et al. [2008, 2009] and Song et al. [2013]. The inflammation (chronic, alveolar) was reported to be of minimal severity on the basis of histopathologic evaluation [Sung et al. 2009; Song et al. 2013], and the inflammation had resolved by 12 weeks post-exposure in 8 of the 9 rats in the high-exposure group (381 μg/m$^3$) [Song et al. 2013]. Pulmonary fibrosis was not reported as having been observed in either study at the AgNP inhaled doses in these studies [Sung et al. 2009; Song et al. 2013]. These findings indicate that the rat pulmonary inflammation response to AgNPs following subchronic inhalation is an early-stage effect of minimal severity. However, long-term studies on potential pulmonary effects following chronic exposure to AgNPs are not available.

NIOSH considers the response of pulmonary inflammation to be relevant to workers. Persistent inflammation in animals or humans can damage tissue. Persistent (chronic) or poorly controlled inflammation is a very common cause of disease in humans, including in the lungs [Kumar et al. 2015]. Pulmonary inflammation and other adverse lung effects have been associated with some occupational exposures to airborne respirable particles [NIOSH 1995, 2011]. In hazard assessment, information on related materials is an additional consideration [29 CFR 1910.1200, A.0.3.2]. In particular, the classic inflammatory mediator *endotoxin* is implicated in occupational lung disease from inhalation of organic dusts, particularly cotton dust [Castellan et al. 1987; Wang et al. 2005]. In addition, inflammation is implicated in occupational lung diseases from inhaled inorganic particles, the pneumoconioses [Bisson et al. 1987; Rom 1991].

Adverse effects in the liver were also associated with exposure to AgNPs in rats. The finding of liver bile duct hyperplasia in rats [Sung et al. 2009, Kim et al. 2010a] from exposure to AgNPs is consistent with the pathway in which silver is eliminated from the blood via biliary excretion and eventually from the body in the feces [DiVincenzo et al. 1985; Wölbling et al. 1988]. The clinical significance of bile duct hyperplasia as an isolated lesion is not well known, but some evidence suggests that when accompanied by hepatobiliary injury, it is translationally relevant to humans. Some evidence suggests that cholangiocellular carcinoma can develop from bile duct hyperplasia [Kurashina et al. 2006]. Hyperplasia is one

of several factors believed to be involved in the development of cholangiocarcinoma, the biliary tract cancer of the liver [Rizvie and Gores 2014; Rizvi et al. 2014]. In rats exposed to AgNPs, the bile duct hyperplasia was accompanied by additional evidence of liver abnormalities, which includes liver necrosis at the higher exposures [Sung et al. 2009; Kim et al. 2010a]. On the basis of these findings, NIOSH considers the response of bile duct hyperplasia in a subchronic inhalation study in rats [Sung et al. 2009] to be a potential adverse effect of relevance to workers.

The risk assessment methods applied to the rat subchronic inhalation data included benchmark dose (BMD) modeling to estimate the doses associated with early-stage adverse lung and liver responses. Human-equivalent exposure concentrations were estimated as described below.

## Physiologically Based Pharmacokinetic (PBPK) Modeling

NIOSH used the results from a peer-reviewed, published physiologically based pharmacokinetic (PBPK) model for AgNPs [Bachler et al. 2013] to estimate the 45-year working lifetime exposure concentrations associated with argyria at the lowest reported silver skin-tissue dose in humans (Section A.5.3). These estimates were 47, 78, and 253 μg/m$^3$, respectively, for ionic, 15-nm-, and 100-nm-diameter silver (Table A-7). These estimates are approximately 5 to 25 times greater than the current NIOSH REL of 10 μg/m$^3$ (8-hour TWA, total mass sample) of soluble or insoluble silver [NIOSH 2007], which suggests a relatively low risk of argyria at the REL for total silver, assuming equal response at equivalent mass tissue dose of silver. No data were available on exposure to AgNPs and development of argyria in animals or humans; thus, the PBPK model provides estimates based on historical data of occupational exposures to silver of unknown particle size(s) and type(s).

The PBPK model of Bachler et al. [2013] was also used to estimate the 45-year working lifetime AgNP exposure concentrations that would result in tissue doses equivalent to those associated with the NOAEL or benchmark dose estimates for pulmonary inflammation or liver bile duct hyperplasia in the rat subchronic inhalation studies [Sung et al. 2009; Song et al. 2013]. The estimated HECs to the rat NOAELs for lung and liver effects were 0.19 to 3.8 μg/m$^3$ for total silver and 6.2 to 195 μg/m$^3$ for soluble/active tissue doses, depending on particle size (15-nm- or 100-nm-diameter AgNPs) (Table A-9). NIOSH considers the PBPK model (Appendix A) to be a useful tool for exploratory analysis of HEC estimates, including at different durations of exposure and particle sizes and types of AgNPs. However, because of the greater complexity of the model and its assumptions, additional data are needed for further evaluation and validation (e.g., as discussed in U.S. EPA [2006]).

## Dosimetric Adjustment Factor (DAF) Method

NIOSH used dosimetric adjustments to estimate the HECs to the rat doses associated with early-stage lung and liver effects in the subchronic inhalation studies [Sung et al. 2009; Song et al. 2013]. DAF methods have been used for many years in the risk assessment of inhaled particles [U.S. EPA 1994], including for AgNPs [Weldon et al. 2016]. NIOSH preferred the DAF method to the PBPK model (Appendix A) due to the nature of the data available, as well as the complexity and data needs of these models and methods (Section 6.2, Figure 6-1). NIOSH considered the DAF method to be a reasonable match to the available data for silver nanomaterials.

The rat exposure-response data were first modeled with the U.S. EPA [2012b] benchmark dose software, to estimate a benchmark concentration associated with a 10% increase in either liver bile duct hyperplasia or pulmonary inflammation, as the 95% lower confidence limit estimate ($BMCL_{10}$). DAFs were then applied to the rat $BMCL_{10}$ estimates to derive the HEC estimates. The total DAF included individual factors based on the following data from animals and humans: ventilation rates (volume of air inhaled per day), respiratory tract deposition fractions of inhaled particles, and respiratory tract surface area or body weight. A DAF was not used to adjust for interspecies differences in clearance of AgNPs because of uncertainty about the dissolution and clearance rate differences between animals and humans; instead, a UF was applied. The lowest HEC was 23.1 μg/m$^3$, based on the pulmonary inflammation data from male and female rats in both subchronic inhalation studies [Sung et al. 2009; Song et al. 2013] (Section 6.2.3).

## NIOSH Recommended Exposure Limit (REL) Derivation

NIOSH applied well-established risk assessment methods [ICRP 1994; U.S. EPA 1994, 2002, 2012b, 2015] to derive a REL for silver nanomaterials based on rat data of lung and liver effects following subchronic (13-week) inhalation exposure to AgNPs [Sung et al. 2009; Song et al. 2013]. Adverse effects in these rat studies evaluated for potential adverse health risk in workers included liver bile duct hyperplasia and pulmonary inflammation. Dosimetric adjustments were used to estimate equivalent concentrations in humans, and UFs were applied to the lowest HEC estimate to derive a REL for silver nanomaterials. In applying these methods, NIOSH uses scientific data when available; and when data are not available, UFs are used. A sensitivity analysis examined the influence of the various risk assessment methods and assumptions (Section 6.4.6). This analysis showed that, over the range of assumptions and uncertainties considered in the risk assessment methods for AgNPs, the OEL estimates derived by NIOSH and others are all relatively low airborne mass concentrations (0.1 to 2 μg/m$^3$) compared to the current NIOSH REL of 10 μg/m$^3$ for total silver (metal dust, fume, and soluble compounds, as Ag) and to the other OELs for silver (up to 100 μg/m$^3$) (Table 1-3).

The lowest HEC estimate of 23 μg/m$^3$ was used as the point of departure (PoD) to derive a REL for silver nanomaterials. A total UF of 25 (to account for uncertainty in animal-to-human toxicodynamics, human interindividual variability, and subchronic-to-chronic exposure) (Table 6-6) was applied to the PoD estimate (i.e., 23 μg/m$^3$ / 25 = 0.9 μg/m$^3$) (Table 6-7). Thus, the NIOSH REL for silver nanomaterials (≤100 nm primary particle size) is 0.9 μg/m$^3$ as an airborne respirable 8-hour TWA concentration.

The NIOSH REL for silver nanomaterials is based on prevention of early-stage adverse health effects in the lungs and liver of workers. The animal studies that provided the quantitative data for developing the REL involved airborne exposure to AgNPs with primary particle diameter of ~15–20 nm [Sung et al. 2009; Song et al. 2013]. In the few in vivo and in vitro studies that compare the effects of exposure to nanoscale or microscale silver particles, the findings generally show greater uptake and toxicity of nanoscale compared with microscale silver particles (Sections 4, 5, and 6.1.3). On the basis of evaluation of the available evidence, NIOSH has determined that it is reasonable and prudent to define the REL of 0.9 μg/m$^3$ (8-hour TWA) as being applicable to all silver nanomaterials, i.e., ≤100 nm primary particle size. The upper particle size of 100 nm for nanoscale particles [ISO 2008] is not a health-based definition but is based on particle size definitions and sampling conventions (see Terminology/Glossary definitions of "Nanomaterials," "Silver nanoparticles

(AgNPs)," and "Primary particle, aggregate, and agglomerate"). Employers and risk managers may choose to exercise additional precaution if workers have potential exposure to silver particles of similar size range to nanoscale silver. Findings from the literature indicate that workplace exposures can, in some situations, be controlled at or below the REL (Section 2; Table 2-1).

## Recommendations

Silver is produced and used in the workplace in varying particle size fractions, including fine (which is defined as all particle sizes collected by respirable particle sampling) and ultrafine or nanoscale (defined as the fraction of respirable particles with a primary particle size of ≤100 nm) (Section 7.1). NIOSH recommends that effective risk management practices be implemented for all processes that produce or use silver nanomaterials so that worker exposures do not exceed the NIOSH REL for either silver nanomaterials or total silver. The NIOSH REL for total silver (metal dust, fume, and soluble compounds, as Ag) is 10 μg/m$^3$ (8-hour TWA), measured as a total airborne mass concentration [NIOSH 1988, 2003, 2007]. The NIOSH REL for silver nanomaterials (primary particle size of ≤100 nm) is 0.9 μg/m$^3$ (8-hour TWA), measured as a respirable airborne mass concentration.Until the results from animal research studies can fully explain the mechanisms (e.g., shape, size, chemistry, functionalization) that potentially increase or decrease toxicity, all types of AgNPs should be considered a respiratory hazard and occupational exposures should be controlled at the REL of 0.9 μg/m$^3$.

Exposure measurement and sample analysis are needed to determine if an airborne respirable particle sample includes silver nanomaterials (Chapter 7). If the samples indicate that airborne concentrations of silver exceed the NIOSH RELs for total silver or silver nanomaterials, then control technologies (Section 7.2) should be implemented and personal protective equipment (Section 7.6) used until control technologies are fully implemented and demonstrated effective.

NIOSH further recommends that employers who formulate, use, or otherwise handle silver nanomaterials or products containing silver nanomaterials develop a risk management program (see Chapter 7), with worker input, including these components:

- Identification of processes and job tasks where there is potential for exposure to silver nanomaterials. Comprehensive assessment of exposures (including exposures to other potential hazards and the potential for home contamination) should be performed as part of job hazard analysis, and a hazard communication program should be developed following the OSHA Hazard Communication Standard (HCS) [29 CFR 1910.1200(h)] or MSHA Hazard Communication Standard [30 CFR 47].
- Development of criteria and guidelines for selecting, installing, and evaluating engineering controls (such as LEV, dust collection systems), with the objective of controlling worker airborne exposure to total silver (metal dust, fume, and soluble compounds, as Ag) below the NIOSH REL of 10 μg/m$^3$ (8-hour TWA) and to silver nanomaterials (primary particle size ≤100 nm) below the NIOSH REL of 0.9 μg/m$^3$ (8-hour TWA).
- Routine systematic evaluation of worker exposure to silver nanomaterials at least annually, and/or whenever there is a change in a process or task associated with potential exposure to silver nanomaterials. Changes could include frequency, volume, duration, equipment, and procedures/processes.

- An education and training program for recognizing potential exposures and using good work practices to prevent exposure to silver, including the safe handling of silver nanomaterials.
- Development of procedures for selecting and using personal protective equipment (PPE) such as clothing, gloves, and respirators.
- Development of a respiratory protection program following the OSHA respiratory protection standard (29 CFR 1910.134) or MSHA respiratory standards (30 CFR 56/57/5005, or 30 CFR 72.710) if respiratory protection is used.
- Development of spill control plans and routine cleaning procedures for work areas with a HEPA-filtered vacuum or wet-wipes. Do not use dry sweeping or air hoses. Avoid using or handling silver nanomaterials in powder form, where possible, and ensure silver nanomaterials are stored in tightly sealed containers and labeled in accordance with the HCS.
- Provision of facilities for hand washing to reduce the potential for dermal and oral exposures, and encouragement of workers to use these facilities before eating or leaving the worksite.
- Use of established medical surveillance approaches for workers potentially exposed to silver, including silver nanomaterials.

## Future Research Needs

Uncertainties in evaluating the health risks of silver nanomaterials may be reduced as new information becomes available from currently ongoing research studies, such as the National Institute of Environmental Health Sciences nanoGo consortium research [Schug et al. 2013] and the National Toxicology Program (NTP). As new studies become available, NIOSH may assess the results and determine whether additional recommendations are needed to protect workers' health.

This page intentionally left blank.

# Contents


Foreword . . . . . iii
Abstract . . . . . iv
Executive Summary . . . . . v
Introduction . . . . . v
Occupational Exposure and Human Evidence . . . . . v
Cellular Studies . . . . . vi
Animal Studies . . . . . vii
Published Occupational Exposure Limits (OELs) for Silver Nanoparticles . . . . . viii
NIOSH Quantitative Risk Assessment . . . . . viii
Physiologically Based Pharmacokinetic (PBPK) Modeling . . . . . x
Dosimetric Adjustment Factor (DAF) Method . . . . . x
NIOSH Recommended Exposure Limit (REL) Derivation . . . . . xi
Recommendations . . . . . xii
Future Research Needs . . . . . xiii
Abbreviations and Definitions . . . . . xxi
Terminology/Glossary . . . . . xxvii
Terms Related to Silver and Silver Nanomaterials . . . . . xxvii
Terms Used in Risk Assessment . . . . . xxviii
Acknowledgments . . . . . xxxiii
Invited Expert Reviewers . . . . . xxxiv
1 Introduction . . . . . 1
1.1 Background . . . . . 1
1.2 Bases for Current Occupational Exposure Limits . . . . . 3
1.3 Scientific Literature Review . . . . . 4
1.4 Human Health Basis for the Current NIOSH REL . . . . . 6
2 Occupational Exposures to Silver . . . . . 9
3 Human Evidence of Internal Dose and Potential Adverse Health Effects . . . . . 19
3.1 Background . . . . . 19
3.2 Human Studies of Lung Deposition of Airborne Silver Nanoparticles . . . . . 19
3.3 Biomonitoring Studies in Humans . . . . . 20
3.4 Health Effects in Workers with Exposure to Silver . . . . . 21
3.5 Health Effects in Humans with Nonoccupational Exposure to Silver . . . . . 25

4 Cellular and Mechanistic Studies Overview . . . . . 27
4.1 Overview of Cell-based Silver Nanoparticle (AgNP) Studies . . . . . 27
4.2 AgNP Exposure Increases Cytotoxicity and Oxidative Stress . . . . . 27
4.3 AgNP Exposure Induces Genotoxicity . . . . . 28
4.4 Other Cellular Effects of AgNP Exposure . . . . . 28
4.5 Effects of AgNP Size, Functionalization, and Ion Release . . . . . 29
5 Animal Studies Overview . . . . . 31
5.1 Toxicokinetic Findings . . . . . 31
5.1.1 Pulmonary Exposure—Inhalation . . . . . 31
5.1.2 Nonpulmonary Routes of Exposure . . . . . 32
5.1.3 Sex Differences . . . . . 33
5.1.4 Physicochemical Properties Affecting Kinetics . . . . . 33
5.2 Toxicological Effects . . . . . 35
5.2.1 Pulmonary Exposure . . . . . 35
5.2.2 Dermal, Oral, and Parenteral Exposure . . . . . 35
5.2.3 Sex Differences . . . . . 36
5.2.4 Potential Mechanisms of Toxicity . . . . . 37
5.2.5 Physicochemical Properties . . . . . 37
5.3 General Conclusions . . . . . 38
6 Hazard and Risk Evaluation of Silver Nanomaterials and Recommended Exposure Limit . . . . . 39
6.1 Hazard Identification . . . . . 39
6.1.1 Lung Effects . . . . . 39
6.1.2 Liver Effects . . . . . 40
6.1.3 Biological Mode of Action and Physical-Chemical Properties . . . . . 42
6.2 Quantitative Risk Assessment of Silver Nanoparticles . . . . . 44
6.2.1 Animal Studies . . . . . 44
6.2.2 Basis for Conducting a Quantitative Risk Assessment . . . . . 46
6.2.3 Point of Departure from Animal Data ($PoD_{animal}$) . . . . . 46
6.2.4 Human-Equivalent Concentration Estimates . . . . . 47
6.3 Derivation of NIOSH Recommended Exposure Limit (REL) for Silver Nanomaterials . . . . . 52
6.4 Risk Characterization . . . . . 53
6.4.1 Relevance of Animal Responses to Humans . . . . . 53
6.4.2 Biologically Active Dose Metric . . . . . 54
6.4.3 Human-Equivalent Tissue Dose . . . . . 54
6.4.4 Working Lifetime Equivalent Concentration . . . . . 56
6.4.5 Areas of Uncertainty . . . . . 56
6.4.6 Sensitivity Analysis . . . . . 57
6.5 Summary . . . . . 58
7 Recommendations . . . . . 69
7.1 Exposure Assessment for Silver Nanomaterials . . . . . 70

7.2 Engineering Controls . . . . . 73
7.3 Worker Education and Training . . . . . 79
7.4 Cleanup and Disposal . . . . . 79
7.5 Dermal Protection . . . . . 80
7.6 Respiratory Protection . . . . . 81
7.7 Occupational Health Surveillance . . . . . 81
7.7.1 Hazard Surveillance . . . . . 82
7.7.2 Medical Screening and Surveillance . . . . . 82

8 Research Needs . . . . . 85

9 References . . . . . 87

APPENDIX A: Physiologically Based Pharmacokinetic (PBPK) Modeling . . . . . 115
A.1 Background and Objectives . . . . . 116
A.1.1 Particle Mechanisms . . . . . 116
A.1.2 Model Evaluation Criteria . . . . . 116
A.1.3 PBPK Model Structure and Development . . . . . 118
A.2 Evaluation of Rat Subchronic Data and PBPK Model Predictions . . . . . 120
A.2.1 Lungs . . . . . 120
A.2.2 Liver . . . . . 121
A.3 Effect Level Estimates in Rats and Humans . . . . . 122
A.4 PBPK Model Estimates . . . . . 124
A.4.1 Overview of PBPK Modeling Runs . . . . . 124
A.4.2 Comparison of Model-Predicted and Measured Lung and Liver Tissue Burdens in Rats . . . . . 124
A.4.3 Human-Equivalent Working Lifetime Exposure Concentrations . . . . . 130
A.4.4 Worker Body Burden Estimates of Silver From Diet and Occupational Exposures . . . . . 130
A.4.5 Estimated Working Lifetime Exposure Concentrations Associated with Argyria . . . . . 132
A.4.6 Estimated Silver Tissue Burdens in Workers with Inhalation Exposure to 10 μg/m$^3$ of AgNP . . . . . 134
A.4.7 Estimated 45-year Working Lifetime Airborne Exposure Concentrations Equivalent to Rat Effect Levels . . . . . 136
A.5 Evaluation of PBPK Modeling Results . . . . . 136
A.5.1 Utility of PBPK Modeling Estimates . . . . . 136
A.5.2 Comparison of Human Data to Rat-Based Estimates . . . . . 138
A.5.3 Argyria Risk . . . . . 138
A.5.4 Lung Inflammation Risk . . . . . 139
A.5.5 Bile Dust Hyperplasia Risk . . . . . 140
A.5.6 Silver Nanoparticle Form . . . . . 141

APPENDIX B: Statistical Analyses Supplement . . . . . 143
B.1 Benchmark Dose Modeling of Rat Subchronic Inhalation Studies . . . . . 144

B.2 No Observed Adverse Effect Level (NOAEL) Estimation of Rat Liver Bile Duct Hyperplasia . . . 153
B.2.1 Background . . . 153
B.2.2 Data . . . 153
B.2.3 Analysis . . . 154
B.2.4 Conclusion . . . 155
B.3 Pooled Data Analysis of Rat Subchronic Pulmonary Inflammation . . . 155
B.3.1 Background . . . 155
B.3.2 Analyses . . . 156
B.3.3 Conclusions . . . 166
B.4 Exploration of Pooling Rat Subchronic Liver Effects Data . . . 168
B.4.1 Background . . . 168
B.4.2 Analysis . . . 168
B.4.3 Conclusion . . . 174
B.5 Evaluation of Biomarker Findings in Silver Jewelry Workers . . . 174
B.5.1 Summary of findings . . . 174
B.5.2 Statistical evaluation of findings . . . 175
B.6 Conclusions . . . 176
B.7 References . . . 177

APPENDIX C: Literature Search Strategy . . . 179

APPENDIX D: In Vitro/Mechanistic Studies . . . 185
D.1 Oxidative Stress/Induction of Apoptosis . . . 186
D.2 DNA Damage/Genotoxicity . . . 195
D.3 Changes in Gene Expression/Regulation . . . 201
D.4 Modeling the Perturbation of the Blood–Brain Barrier . . . 203
D.5 Impact of Silver Nanoparticles on Keratinocytes . . . 204
D.6 Effect of Silver Nanoparticles on Platelet Activation . . . 204
D.7 Antitumor and Antimicrobial Activity of Silver Nanoparticles . . . 204
D.8 Dermal Absorption (in Vitro) . . . 225

APPENDIX E: Toxicological and Toxicokinetic Effects of Silver Nanoparticles in Experimental Animal Studies . . . 227
E.1 Inhalation Exposure . . . 228
E.1.1 Toxicokinetics . . . 228
E.1.2 Toxicological Effects . . . 228
E.2 Oral Exposure . . . 238
E.2.1 Toxicokinetics . . . 238
E.2.2 Toxicological Effects . . . 241
E.3 Exposure via Other Routes . . . 255
E.3.1 Dermal . . . 255
E.3.2 Intratracheal Instillation, Oropharyngeal Aspiration, or Intranasal Instillation . . . 257
E.3.3 Subcutaneous, Intravenous, or Intraperitoneal Injection . . . 264

APPENDIX F: Rat Respiratory Parameters Pertaining to Interspecies Equivalent Dose Estimation . . . . . 317
F.1 Estimating Lung Tissue Concentration of Silver Relative to Steady-State Tissue Concentration in Rats . . . . . 318
F.2 Rat Ventilation Rates . . . . . 318
F.3 Rat Measured and Dosimetry Model–Predicted Lung Burdens . . . . . 319
F.4 Interspecies Dose Normalization Factors . . . . . 320
APPENDIX G: Other Quantitative Risk Assessments for Silver Nanoparticles . . . . . 325
G.1 Christensen et al. [2010] . . . . . 326
G.2 Weldon et al. [2016] . . . . . 326
G.3 Ji and Yu [2012] . . . . . 328
G.4 Acute Inhalation Exposure to Silver . . . . . 328

This page intentionally left blank.

# Abbreviations and Definitions

| | |
|---|---|
| AB | Alamar Blue |
| ACGIH | American Conference of Governmental Industrial Hygienists |
| Ag | silver |
| Ag+ | ionic silver |
| AgCl | silver chloride |
| $Ag_2CO_3$ | silver carbonate |
| Ag/Cu | silver copper |
| $AgNO_3$ | silver nitrate |
| $Ag_2O$ | silver oxide |
| $Ag_3PO_4$ | silver phosphate |
| $Ag_2S$ | silver sulfide |
| $Ag_2SO_4$ | silver sulfate |
| AgNP | silver nanoparticle |
| AgNW | silver nanowire |
| AIC | Akaike information criterion |
| $Al_20_3$ | aluminum oxide |
| ALT | alanine aminotransferase |
| AMG | auto-metallography |
| AP | alkaline phosphatase |
| ATSDR | Agency for Toxic Substances and Disease Registry |
| BAL | bronchoalveolar lavage |
| BMC | benchmark concentration |
| BMCL | 95% lower confidence limit estimate of BMC |
| $BMCL_{10}$ | 95% lower confidence limit estimate of the BMC which is associated with a 10% increase over background in the proportion of animals with an adverse response |
| BMD | benchmark dose |
| BMDL | 95% lower confidence limit estimate of BMD |
| $BMDL_{10}$ | 95% lower confidence limit estimate of the BMD which is associated with a 10% increase over background in the proportion of animals with an adverse response |
| BMR | benchmark response |

| | |
|---|---|
| BW | body weight |
| °C | degrees Celsius |
| $C_6H_5Ag_3O_7$ | silver citrate |
| CIB | Current Intelligence Bulletin |
| CKAP4 | cytoskeleton-associated protein 4 |
| cm | centimeter |
| $cm^2$ | centimeter squared |
| CMAD | count median aerodynamic diameter |
| CMC | carboxymethyl cellulose |
| CPC | condensation particle counter |
| DAF | dosimetric adjustment factor |
| DCF | dichlorofluorescein |
| DNA | deoxyribonucleic acid |
| EC50 | median effective concentration |
| ECHA | European Chemicals Agency |
| EDS | energy dispersive X-ray spectroscopy |
| ESP | electrostatic precipitator |
| EU | European Union |
| °F | degrees Fahrenheit |
| FAAS | flame atomic absorption spectrometry |
| FITC | fluorescein isothiocyanate |
| FMPS | fast mobility particle sizer |
| FSH | follicle stimulation hormone |
| g | gram |
| GD | gestation day |
| GJIC | gap-junction intercellular communication |
| GM | geometric mean |
| GP | glutathione peroxidase |
| GSD | geometric standard deviation |
| GSH | glutathione |
| HEC | human equivalent concentration |
| HED | human equivalent dose |
| HEPA | high-efficiency particulate air |
| hMSC | human mesenchymal stem cell |
| hr | hour |
| HT | hydroxytryptamine |

| | |
|---|---|
| $IC_{50}$ | median inhibitory concentration |
| ICP-MS | inductively coupled plasma-mass spectroscopy |
| Ig | immunoglobulin |
| INEL | indicative no-effect level |
| ISO | International Organization for Standardization |
| JNK | c-Jun NH2-terminal kinase |
| kg | kilogram |
| L | liter |
| L/min | liters per minute |
| $LC_{50}$ | concentration resulting in a mortality of 50% |
| LCL | lower confidence limit |
| $LD_{50}$ | median lethal dose |
| LDH | lactate dehydrogenase |
| LEV | local exhaust ventilation |
| LFA | long amosite fibers |
| LH | luteinizing hormone |
| lpm | liters per minute |
| LOAEL | lowest observed adverse effect level |
| MALDI-TOFMS | matrix-assisted laser desorption/ionization–time-of-flight mass spectrometry |
| MEF | mouse embryonic fibroblasts |
| MES | mouse embryonic stem |
| mg/L | milligram per liter |
| $mg/m^3$ | milligram per cubic meter |
| min | minute |
| mL | milliliter |
| MMAD | mass median aerodynamic diameter |
| MNPCE | micronucleated polychromatic erythrocytes |
| MoA | mode of action |
| MPPD | multiple-path particle dosimetry |
| MTD | maximum tolerated dose *or* minimally toxic dose |
| mRNA | messenger ribonucleic acid |
| MSHA | Mine Safety and Health Administration |
| MWM | Morris water maze |
| NA | not applicable |
| $NaBH_4$ | sodium borohydride |
| NAC | N-acetyl cysteine |

| | |
|---|---|
| NAG | N-acetyl-B-D glucosaminidase |
| ND | nondetectable |
| ng/cm$^2$ | nanograms per square centimeter |
| ng/g | nanograms per gram |
| NIEHS | National Institute of Environmental Health Sciences |
| NIOSH | National Institute for Occupational Safety and Health |
| NIST | National Institute of Standards and Technology |
| nm | nanometer |
| nm$^2$/cm$^3$ | square nanometer per cubic centimeter |
| NOAEL | no observed adverse effect level |
| NTRC | Nanotechnology Research Center |
| OEB | occupational exposure band |
| OECD | Organisation for Economic Cooperation and Development |
| OEL | occupational exposure limit |
| OSHA | Occupational Safety and Health Administration |
| PBPK | physiologically based pharmacokinetic [model] |
| PBS | phosphate buffered saline |
| PCR | polymerase chain reaction |
| PI | propidium iodide |
| PKC | protein kinase C |
| PoD | point of departure, used in quantitative risk assessment |
| PPE | personal protective equipment |
| PSM | process safety management |
| PtD | Prevention through Design |
| PVP | polyvinylpyrrolidone |
| PVR | poliovirus receptor |
| QRA | quantitative risk assessment |
| RBC | red blood cell |
| RCC | relative cell count |
| REL | recommended exposure limit |
| RNA | ribonucleic acid |
| ROS | reactive oxygen species |
| RT-PCR | reverse transcription polymerase chain reaction |
| SD | standard deviation |
| SEGs | similarly exposed groups |
| SEM | scanning electron microscope |

| | |
|---|---|
| SFA | short fibers of amosite |
| SLC7A13 | solute carrier family 7, member 13 |
| SOD | superoxide dismutase |
| SOP | standard operating procedures |
| SPECT | single-photon emission computerized tomography |
| SPMS | scanning mobility particle sizer |
| STEM | scanning transmission electron microscopy |
| TEM | transmission electron microscopy |
| TGF-β | transforming growth factor–beta |
| THF | tetrahydrofuran |
| $TiO_2$ | titanium dioxide |
| TLV® | threshold limit value |
| TWA | time-weighted average |
| UF | uncertainty factor |
| µg | microgram |
| µg/dL | microgram per deciliter |
| µg/g | microgram per gram |
| µg/kg | microgram per kilogram |
| µg/L | microgram per liter |
| $\mu g/m^3$ | microgram per cubic meter |
| µg/mL | microgram per milliliter |
| µL | microliter |
| µm | micrometer |
| U/L | units per liter |
| UCL | upper confidence limit |
| U.S. EPA | U.S. Environmental Protection Agency |
| WBC | white blood cell |
| WHO | World Health Organization |
| wk | week |
| wt | weight |
| yr | year |
| % | percent |

This page intentionally left blank.

# Terminology/Glossary

A number of terms used in the field of nanotechnology have specialized meanings, and definitions of certain terms have important biologic, legal, regulatory, and policy implications. Experimental animal and in vitro studies cited in this report frequently describe exposures to 'silver,' 'nanosilver,' 'nanoscale silver,' 'silver nanoparticles (AgNPs),' or 'silver nanowires (AgNWs)' without always providing complete information on particle dimension, species, and other physical-chemical properties. The absence of such information, especially from some in vitro studies, limits the ability to compare the toxicological outcomes reported in the in vitro studies with the exposure concentrations and doses that brought about AgNP-related effects observed in the in vivo studies.

Terms used in the risk assessment of silver nanomaterials are also defined in this section.

## Terms Related to Silver and Silver Nanomaterials

**Nanomaterials:** The International Organization for Standardization (ISO) has developed nomenclature and terminology for nanomaterials [ISO 2008]. According to ISO 27687:2008, a *nano-object* is a material with one, two, or three external dimensions in the size range of approximately 1–100 nanometers (nm). Subcategories of a nano-object are (1) *nanoplate,* a nano-object with one external dimension at the nanoscale (1–100 nm); (2) *nanofiber,* a nano-object with two external dimensions at the nanoscale (a nanotube is defined as a *hollow nanofiber*, and a nanorod is defined as a *solid nanofiber*); and (3) *nanoparticle,* a nano-object with all three external dimensions at the nanoscale. Nano-objects are commonly incorporated in a larger matrix or substrate called a *nanomaterial.* The term 'silver nanomaterial' used by NIOSH in this *Current Intelligence Bulletin* includes various forms of engineered AgNPs and AgNWs, including silver nanoparticles that are functionalized, coated, or embedded into polymetric matrices.

**Silver nanoparticles (AgNPs):** This document focuses primarily on exposure to engineered AgNPs. Methods of AgNP synthesis include the Lee-Meisel or Creighton method (involving silver salts and reducing agents); high-temperature reduction in porous solid matrices; vapor-phase condensation of a metal onto a solid support; laser ablation of a metal target into a suspending liquid; photo-reduction of silver ions; chemical vaporization; dry powder dispersion; and electrolysis of a silver salt solution. Most reports of the in vitro and in vivo studies described in this document do not note the source of exposure to AgNPs. In addition, workers employed in industries using silver have potential exposures to AgNPs, such as those generated as a fume during the melting and electrorefining of silver or during brazing/soldering operations.

**Primary particle, aggregate, and agglomerate:** A primary particle is the smallest identifiable subdivision of a particulate system [BSI 2005]. In many circumstances, primary AgNPs can aggregate or agglomerate into secondary particles with dimensions greater than 100 nm. These two terms have specific meanings [ISO 2006]: an *aggregate* is a heterogeneous group

of nanoparticles held together by relatively strong forces (for example, covalent bonds) and thus not easily broken apart. An *agglomerate* is a group of nanoparticles held together by relatively weak forces, including van der Walls forces, electrostatic forces, and surface tension. Aggregates and agglomerates of silver particles can occur in work environments where engineered AgNPs are synthesized and handled (such as during removal from the reactor or handling of "free" powder forms of AgNPs) and where fumes are generated during the melting of silver and silver alloys and during silver brazing or soldering. The extent to which AgNPs occurred as an aggregate or agglomerate in the cited studies with workers and in the in vitro and in vivo studies was often not described by the authors. Whether the constituent primary particles remained agglomerated or aggregated during the entire study period is also unknown.

**Colloid:** The term 'colloid' used in the cited studies refers to an assemblage of AgNPs suspended within a given medium that are smaller than microscale (less than $10^{-6}$ m). For example, Wijnhoven et al. [2009] refers to colloidal silver as comprising silver particles primarily in the range of 250–400 nm, thereby distinguishing nanoscale silver from colloidal silver.

**Fume:** Hinds [1999] defines a fume as "a solid-particle aerosol produced by the condensation of vapors or gaseous combustion products. These submicrometer particles are often clusters or chains of primary particles. The latter are usually less than 0.05 μm (50 nm)." The secondary agglomerates can be substantially larger (on the scale of 1 μm) and usually fall within the respirable size fraction of a sample.

**Argyria:** Argyria is frequently described as a gray-blue discoloration of the skin, mucous membranes, and/or internal organs as a result of exposure to silver. Argyria may occur in an area of repeated or abrasive dermal contact with silver or silver compounds, or it may occur more extensively over widespread areas of skin after long-term oral or inhalation exposure. Localized argyria can occur in the eyes (argyrosis), where gray-blue patches of pigmentation are formed without evidence of tissue reaction. Generalized argyria is recognized by widespread pigmentation of the skin due to the deposition of silver complexes and by a silver-induced increase in melanin [Hathaway and Proctor 2004].

## Terms Used in Risk Assessment

These definitions are based on or adapted from those in the NIOSH [2020] *Current Intelligence Bulletin 69: Practices in Occupational Risk Assessment*, unless otherwise cited.

**Acute exposure:** A one-time or short-term exposure with a duration of less than or equal to 24 hours [U.S. EPA 1994].

**Adverse effect:** Change in the morphology, physiology, growth, development, reproduction, or life span of an organism, system, or population that results in an impairment of functional capacity, an impairment of the capacity to compensate for additional stress, or an increase in susceptibility to other influences.

**Aerosol:** All-inclusive term. A suspension of liquid or solid particles in air [U.S. EPA 1994].

**Benchmark dose (BMD):** A dose that produces a predetermined change in the response rate of an adverse effect relative to the background response rate of this effect. The dose may be as administered or as measured in biological tissues or fluids.

**Benchmark concentration (BMC):** An exposure concentration of a substance (e.g., in air) that produces a predetermined change in the response rate of an adverse effect relative to the background response rate of this effect.

**Benchmark response (BMR):** A predetermined change in the response rate of an adverse effect relative to the background response rate of this effect. A BMR is typically in the low dose region of the data (e.g., 10% increase over background response).

**Critical effect:** The first adverse effect, or its known precursor, that occurs as the dose rate increases; designation is based on evaluation of overall data base [U.S. EPA 1994].

**Chronic exposure:** Multiple exposures occurring over an extended period of time or a significant fraction of the animal's or the individual's lifetime [U.S. EPA 1994].

**Dose:** Total amount of an agent administered to, taken up by, or absorbed by an organism, system, or (sub) population.

**Dose-response:** The relationship between the amount of an agent administered to, taken up by, or absorbed by an organism, system, or population and the change developed in that organism, system, or population in reaction to the agent.

**Dosimetric adjustment factor (DAF):** A multiplicative factor used to adjust observed animal or epidemiological data to estimate a human equivalent concentration (HEC) for an exposure scenario of interest. For inhaled particles, DAFs include factors to account for interspecies differences in ventilation rate, particle deposition fraction, and surface area of the respiratory tract region(s) of interest [adapted from U.S. EPA 1994].

**Exposure:** Contact between an agent and a target. Contact takes place at an exposure surface over an exposure period.

**Exposure assessment:** The process of estimating or measuring the distribution of the magnitude, frequency, and duration of exposure to an agent, along with the number and characteristics of the population exposed. Ideally, it describes the sources, pathways, routes, and uncertainties in the assessment.

**Exposure duration:** The length of time over which continuous or intermittent contacts occur between an agent and a target.

**Exposure route:** The way in which an agent enters a target after contact (e.g., by ingestion, inhalation, or dermal absorption).

**Hazard:** The inherent property of an agent (or situation) having the potential to cause an adverse effect when an organism, system, or population is exposed to that agent.

**Hazard assessment:** The process of identifying the type and nature of adverse effects that an agent has an inherent capacity to cause in an organism, system, or population. Hazard assessment is the first of the four main steps of a risk assessment.

**Human-equivalent concentration:** The airborne concentration of a substance at the animal point of departure (PoD), which has been estimated by application of dosimetric adjustment factors (DAFs) for the respiratory tract region(s) of interest [adapted from U.S. EPA 1994].

**Lowest observed adverse effect level (LOAEL):** The lowest dose or concentration at which there are statistically significant increases in the frequency or severity of biologically significant adverse effects between the exposed population and its appropriate control group [adapted from U.S. EPA 1994].

**Mechanism of action:** A more detailed understanding and description of events, often at the molecular level, than is meant by mode of action.

**Mode of action (MoA):** A sequence of key events and processes, starting with interaction of an agent with a cell, proceeding through operational and anatomical changes, and resulting in disease such as cancer.

**No observed adverse effect level (NOAEL):** The highest dose or concentration at which there are no statistically significant increases in the frequency or severity of biologically significant adverse effects between the exposed population and its appropriate control group; some effects may be produced at this dose level, but they are not considered adverse or precursors of adverse effects observed [adapted from U.S. EPA 1994].

**Occupational exposure limit (OEL):** The allowable concentration or intensity of a hazardous agent in the worker's work environment over a period of time. Generally expressed as an 8-hour time-weighted average or as a short-term exposure limit of 15 or 30 minutes.

**Point of departure (PoD):** A point on the dose-response curve from experimental or observational data, which is a dose associated with a level of no or low effect, and which is estimated without significant extrapolation beyond the data. A PoD is often a NOAEL, LOAEL, or BMD estimate from an animal study.

**Risk assessment:** The determination of the relationship between the predicted exposure and adverse effects in four major steps: hazard identification, dose–response assessment, exposure assessment, and risk characterization.

**Risk characterization:** The qualitative and, wherever possible, quantitative determination, including attendant uncertainties, of the probability of occurrence of known and potential adverse effects of an agent in workers under defined exposure conditions.

**Physiologically based pharmacokinetic (PBPK) modeling:** A mathematical modeling technique to predict the absorption, distribution, metabolism, and/or elimination of exogenous substances in animals or humans.

**Subchronic exposure:** Multiple or continuous exposures occurring for approximately 10% of an experimental species' lifetime, usually over 3 months [U.S. EPA 1994].

**Target:** Any biological entity that receives an exposure or a dose (e.g., an organ, an individual, or a population).

**Validity:** The quality of being logically or factually sound; the extent to which the measure describes that which is being measured.

**Uncertainty factor (UF):** One of several factors, generally 3- to 10-fold, used in deriving the recommended exposure limit (REL) from experimental data. UFs are intended to account for (1) the variation in sensitivity among the members of the human population, (2) the uncertainty in extrapolating laboratory animal data to humans, (3) the uncertainty in

extrapolating from data obtained in a study that is of less-than-lifetime exposure, (4) the uncertainty in using LOAEL data rather than NOAEL data, and (5) the inability of any single study to adequately address all possible adverse outcomes in humans [U.S. EPA 1994].

**Uptake:** The process by which an agent crosses an absorption barrier.

This page intentionally left blank.

# Acknowledgments

This *Current Intelligence Bulletin* (CIB) was developed by the scientists and staff of the National Institute for Occupational Safety and Health (NIOSH), Division of Science Integration (formerly Education and Information Division, EID), Nanotechnology Research Center (NTRC), with individual contributions by external collaborators. Paul Schulte is the Director of DSI and Co-Manager of the NTRC; Charles Geraci is the Associate Director for Emerging Technologies and Co-Manager of the NTRC; and Laura Hodson is the Coordinator of the NTRC.

This document was authored by Eileen Kuempel, Jenny R. Roberts, Gary Roth, Kevin L. Dunn, Ralph Zumwalde, Nathan Drew, Ann Hubbs, Doug Trout, and George Holdsworth. Eileen Kuempel, Gary Roth, and Nathan Drew are from NIOSH DSI/NTRC; Ralph Zumwalde (retired) is formerly from NIOSH/DSI/NTRC; Jenny R. Roberts and Ann Hubbs are from the NIOSH Health Effects Laboratory Division (HELD); and Kevin L. Dunn and Douglas Trout are from the NIOSH Division of Field Studies and Engineering (DFSE). The late George Holdsworth of the Oak Ridge Institute for Science and Education (ORISE) provided an initial hazard review of the toxicology studies under contract to NIOSH.

The data analyses were performed by Eileen Kuempel and Nathan Drew, DSI/NTRC, and by Gerald Bachler, formerly with Institute for Chemical and Bioengineering, Zurich, Switzerland, who provided the PBPK modeling estimates of airborne exposure concentrations of silver nanoparticles and internal tissue doses. Sherri Fendinger, DSI/Science Applications Branch (SAB), performed the scientific literature searches for this revised document. Paul Schulte, Kathleen MacMahon (DSI), Paul Middendorf, Tara Hartley, Gerald Joy, Ann Berry, Roger Rosa, and John Piacentino, NIOSH Office of the Director, and John A. Decker, formerly in the NIOSH Office of the Director, provided scientific and policy reviews of the external review draft documents. Emily Norton, Anne Blank, Katie Shahan, and Nura Sadeghpour, NIOSH Office of the Director, provided health communications review.

The following NIOSH researchers provided scientific and technical input during the internal review of this document:

Kathleen MacMahon, Christine Whittaker, Randall Smith, and James Couch (all in DSI), and David Dankovic, formerly in DSI

Aleksandr Stefaniak, NIOSH Respiratory Health Division

Bean Chen, formerly in HELD

Lee Portnoff, NIOSH National Personal Protective Technology Laboratory (NPPTL), and Pengfei Gao, formerly in NPPTL

Kevin H. Dunn and Matthew Dahm, DFSE

Steven M. Schrader, formerly in the NIOSH Division of Applied Research and Technology

Editorial services for this document were provided by Seleen Collins, Ellen Galloway, and John Lechliter, DSI. Graphic design services were provided by Vanessa Williams and Elizabeth Clements, DSI.

## Invited Expert Reviewers

**Scientific peer reviewers of the 2018 draft document:** Dhimiter Bello, Harvard School of Public Health, Harvard Center for Nanotechnology and Nanotoxicology; James E. Lockey, Emeritus, University of Cincinnati, College of Medicine, Department of Environmental Health; Vicki Stone, Institute of Biological Chemistry, Biophysics and Bioengineering, School of Engineering and Physical Sciences, Heriot-Watt University, Edinburgh, UK; and Lisa M. Sweeney, UES, Inc., assigned to U.S. Air Force School of Aerospace Medicine

**Expert reviewers of specific sections of the updated 2018 draft document:** Lisa M. Sweeney, Andrew Maier, formerly with the University of Cincinnati and currently with Cardno Chemrisk; and David Malarkey, National Institutes of Health/National Institute of Environmental Health Sciences

**Scientific peer reviewers of the 2016 draft document:** Karin Aschberger, European Commission, Joint Research Centre, Institute for Health and Consumer Protection; Terry Gordon, New York University, School of Medicine; Thomas Peters, University of Iowa; and Q. Jay Zhao, U.S. Environmental Protection Agency

**Invited expert reviewer of the 2016 draft document:** Günter Oberdörster, Emeritus, University of Rochester Medical College

# 1 Introduction

This *Current Intelligence Bulletin* (CIB) presents an assessment of the potential health risks to workers occupationally exposed to silver, with emphasis on workers' exposure to silver nanomaterials. First, the CIB presents (1) workplace exposure data for silver; (2) information on the absorption, systemic distribution, metabolism, and excretion of silver; (3) an assessment of toxicological data from experimental animal studies; and (4) an analysis of in vitro and mechanistic studies. The CIB then presents, on the basis of those data, (5) an assessment of the health risk to workers exposed to silver and silver nanomaterials and (6) a recommended exposure limit (REL) for silver and silver nanomaterials. Finally, the CIB provides recommendations for (7) assessing exposure to silver nanomaterials, (8) managing associated risks, and (9) conducting future research related to silver nanomaterials.

## 1.1 Background

Silver (Ag) is a rare, naturally occurring element. It is often found as a mineral ore deposit—in association with copper, lead-zinc, and gold—from which it is extracted [USGS 2014]. In 2018, the United States produced approximately 900 metric tons of silver [USGS 2019]. Chemically, silver is the most reactive of the noble metals, but it does not oxidize readily; rather, it tarnishes by combining at ordinary temperatures with sulfur ($H_2S$). Silver is slightly harder than gold and is very ductile and malleable. Silver can form many different inorganic and organic complexes, and its most stable oxidation states are elemental ($Ag^0$) and monovalent silver ion ($Ag^+$), although other cationic states ($Ag^{+2}$, $Ag^{+3}$) exist as well [USGS 2014]. The most abundant silver compounds are silver sulfide ($Ag_2S$), silver nitrate ($AgNO_3$), and silver chloride (AgCl).

Elemental silver has been commercially available for decades and used in applications as diverse as coins and medals, electrical components and electronics, jewelry and silverware, dental alloy, explosives, and biocides [Wijnhoven et al. 2009; Nowack et al. 2011; USGS 2014]. For centuries the antimicrobial potential of silver (medicinal silver colloids) for healing wounds and preserving materials [Nowack et al. 2011] has been recognized, and within the last century silver has been used in antimicrobial tonics, in bandages for wound care, and in the processing of radiographic and photographic materials [Quadros and Marr 2010; Hendren et al. 2011].

Within the past decade, the demand has increased for production of silver nanomaterials to create different nanostructures such as spheres and wires [Wijnhoven et al. 2009]. These nanostructures of silver are typically commercialized as powders, flakes, and grains and are sold in suspensions (such as in water, alcohol, or surfactant), colloidal preparations, and dry powders [Future Markets, Inc. 2013]. These various silver compounds have differing physical-chemical properties, such as solubility and surface charge, which all may affect their fate and biologic activity. Silver nanomaterials are increasingly being used in consumer and medical products, mainly to take advantage of their high antimicrobial activity. The consumer products and applications include coatings, paints, conductive inks, soaps and laundry detergents, refrigerator and laundry machine components, cooking utensils, medical instruments (dressings, catheters, pacemakers), drug delivery devices, water purifiers, textiles, antibacterial sprays, personal care products (toothpaste, shampoo, cosmetics), air filters, and humidifiers [Quadros and Marr 2010]. Additionally, different nano-forms of silver can be used in the field of electronics (e.g., transparent conducting films, transparent electrodes for flexible devices, flexible thin-film tandem solar cells) [Reidy et al.

2013]. These applications exploit their conductivity and electrical properties rather than antimicrobial properties. The Woodrow Wilson International Center for Scholars "Project on Emerging Nanotechnologies" (http://www.nanotechproject.org/) lists over 100 consumer products containing silver nanomaterials, although the nanomaterial content of many of these products could not be verified [Vance et al. 2015]. It was estimated that 20 tons of silver nanomaterials were produced in the United States in 2010 [Hendren et al. 2011], and an estimated worldwide production of 450 to 542 tons/yr was projected for 2014 [Future Markets, Inc. 2013]. A more recent study by Giese et al. [2018] indicated high uncertainty in estimates of total nanomaterial production. Estimates for silver nanomaterial production globally ranged from 5.5 to 100,000 tons annually [Giese et al. 2018]. As new products utilizing silver nanomaterials are produced and applications expanded, the potential for worker and consumer exposure to airborne silver nanomaterials (such as AgNPs) is also expected to expand throughout the materials' life cycle (that is, during synthesis, use, disposal, and recycling).

Numerous methods have been used to synthesize silver nanomaterials, which can be arbitrarily divided into traditional and nontraditional categories [Evanoff and Chumanov 2005; Chen and Schluesener 2008; Quadros and Marr 2010]. Traditional methods include solution-phase synthesis techniques that are based on various modifications of the Lee-Meisel or Creighton method, in which different silver salts and reducing agents are used. The most common traditional method for the synthesis of AgNPs is the reduction of $AgNO_3$ with $NaBH_4$. The nontraditional methods include silver particle synthesis through high-temperature reduction in porous solid matrices; vapor-phase condensation of a metal onto a solid support; laser ablation of a metal target into a suspending liquid; photoreduction of silver ions; chemical vaporization; dry powder dispersion; and electrolysis of a silver salt solution.

Although each method has certain advantages and disadvantages, the selection of a method typically depends on the nature of the nanomaterial application. After synthesis, AgNPs can be coated with a metallic, semi-metallic oxide, or metallic oxide layer or coated/embedded into organic polymeric matrices such as poly-(dimethylsiloxane), poly-(4-vinylpyridine), polystyrene, polymethacrylate, and Teflon. These coatings are used to tailor the surface chemical properties of the AgNPs to particular applications and to protect them from chemically aggressive environments.

The metallic forms of silver nanomaterials can form stable suspensions in which the AgNPs slowly dissolve into silver ions [U.S. EPA 2012a]. Silver nanomaterials may also include other insoluble particulate forms, such as silver carbonate ($Ag_2CO_3$), silver citrate ($C_6H_5Ag_3O_7$), silver phosphate ($AgPO_4$), silver oxide ($Ag_2O$), silver sulfate ($Ag_2SO_4$), and silver sulfide ($Ag_2S$). However, specific salts of silver, including nitrate ($AgNO_3$), are soluble in water [WHO 2002]. The highly insoluble forms of silver typically have a low dissolution rate for releasing silver ions, whereas the completely soluble forms of silver (such as $AgNO_3$) have a high ion dissolution release potential in water. Factors that can affect the dissolution of AgNPs in water include size [Ma et al. 2012], surface coatings [Zook et al. 2011; Li et al. 2012a; Tejamaya et al. 2012], pH [Elzey and Grassain 2010], and the solution concentration of sulfur or sodium chloride [Kent and Vikesland 2012]. Also, as the particle size of silver decreases, the potential for releasing silver ions via dissolution increases because of rising surface availability per mass of silver [Wijnhoven et al. 2009]. The local environment (including physiological conditions) can affect particle dissolution and condensation rates. Simulated digestions have shown variable potential for dissolution and reforming of AgNPs following ingestion and for variation in stable particle size, depending on conditions within physiological ranges [Walczak et al. 2012; Axson et al. 2015, Bove et al. 2017].

Although the overall amount of animal toxicological information is small and the studies have been comparatively short, the knowledge base includes these findings: (1) by various routes of exposure,

AgNPs in the body can be absorbed and become transported to target tissues; (2) lung inflammation and lung function decrements have been observed at certain exposure concentrations of AgNPs following subchronic inhalation in rats, suggesting the potential for chronic adverse health effects; and (3) the liver and (to a lesser extent) the kidney represent the primary target organs for systemic accumulation of silver and adverse effects associated with exposure to AgNPs. The studies also indicate that the higher surface volume ratio of AgNPs, compared with larger respirable-size silver particles, is a cause of concern because it makes AgNPs potentially more reactive than larger silver particles and makes it more difficult to predict how they will interact with biological systems (Table 1-1).

**Table 1-1. Differences between ionic, nanoparticulate, and bulk silver.**

| Ions | Nanoparticles | Bulk (microscale) particles |
|---|---|---|
| • Dissolved throughout entire fluid volume<br>• May condense into solid ($Ag^0$) particles<br>• Infiltrate cells easily<br>• Form complexes with compounds, based on reactive group chemistry | • Greater surface area per unit mass<br>• Higher potential rate of dissolution or growth<br>• Cellular uptake via active processes<br>• High affinity for larger biomolecules<br>• Greater oxidative capacity | • Smaller surface area per unit mass<br>• Lower potential rate of dissolution or growth<br>• Lower uptake by most cells<br>• Limited binding of biomolecules<br>• Lower oxidative capacity |

Adapted from Reidy et al. [2013].

## 1.2 Bases for Current Occupational Exposure Limits

The accumulation of silver over time (body burden) has been shown to result in a condition known as argyria. This condition, a pathologic consequence of prolonged silver exposure, has been described as a blue-grey discoloration of the skin and mucous membranes (argyria) or as a localized condition of the eyes (argyrosis) [Harker and Hunter 1935; Hill and Pillsbury 1939]. Exposure to the soluble forms of silver has frequently been associated with the development of argyria [ATSDR 1990; Drake and Hazelwood 2005; Wijnhoven et al. 2009; Johnston et al. 2010; Lansdown 2012]. Generalized occupational argyria in exposed workers can occur as a result of the absorption of silver through the lungs, the digestive tract, or wounds in the skin.

Prevention of argyria is the basis for the current occupational exposure limits (OELs) in the United States and other countries. The Occupational Safety and Health Administration (OSHA) permissible exposure limit (PEL), Mine Safety and Health Administration (MSHA) PEL, and National Institute for Occupational Safety and Health (NIOSH) recommended exposure limit (REL) are all 10 μg/m$^3$ (total dust) for silver (metal dust, fume, and soluble compounds, as Ag) as an 8-hour time-weighted average (TWA) concentration [OSHA 1988, 2012a; NIOSH 1988, 2007; 30 CFR 57.5001]. The term *fume* is not included in the *NIOSH Pocket Guide* [NIOSH 2007] definition of the NIOSH REL and OSHA PEL for silver (total dust). However, fume is included in the other references for the NIOSH REL and OSHA PEL for silver, i.e., "metal dust, fume, and soluble compounds, as Ag" [NIOSH 1988; OSHA 1988, 2012a]. The American Conference

of Governmental Industrial Hygienists (ACGIH) threshold limit values (TLVs®) [ACGIH 2001; TLV® updated in 1992] and the German MAK Commission MAK (Maximum Workplace Concentration) values are also 10 μg/m$^3$ for soluble silver but are higher, at 100 μg/m$^3$, for insoluble silver compounds (Table 1-3). The evidence basis and derivation of the NIOSH REL are discussed in Section 1.4.

A growing body of toxicological evidence indicates that exposure to some forms and particle sizes of silver may pose a greater health risk to workers than other forms and sizes. Experimental animal studies with rats (for up to 3 months) exposed to AgNP concentrations of approximately 100 μg/m$^3$ (10 times the current OSHA PEL and NIOSH REL) showed mild adverse lung effects, including pulmonary inflammation and lung function deficits that persisted after the end of exposure. Bile duct hyperplasia has also been observed in rats after the inhalation of relatively low-mass concentrations of silver and AgNPs (Appendix E, Table E-5).

It is not known how universal these adverse effects are, that is, whether they occur in animals exposed to all forms and particle sizes of silver. However, inflammation is important in the pathogenesis of particle-induced lung disease in both humans and animals. In particular, the classic inflammatory mediator *endotoxin* is implicated in occupational lung disease from inhalation of organic dusts, particularly cotton dust [Castellan et al. 1987; Wang et al. 2005]. In addition, inflammation is implicated in occupational lung diseases from inhaled inorganic particles, the pneumoconioses [Bisson et al. 1987; Rom 1991]. In terms of bile duct hyperplasia, hyperplasia is believed to be one of several factors involved in the development of cholangiocarcinoma, the biliary tract cancer of the liver [Rizvie and Gores 2014; Rizvi et al. 2014]. Most important, it is not known whether similar adverse health effects occur in humans following exposure to AgNPs. The extent to which workers are exposed to silver in the workplace, including exposure to silver nanomaterials, is also unclear because of limited published exposure data.

## 1.3 Scientific Literature Review

NIOSH conducted a comprehensive review of the literature to identify the scientific information available on occupational exposure to silver nanomaterials and potential adverse health effects associated with exposure. The scientific data and information include published journal articles on exposure measurement in the workplace, medical monitoring in workers, and toxicology studies in animals and cell systems. Three main literature searches were conducted from 2012 to 2020 (Table 1-2). The initial search was conducted by the Oak Ridge Institute for Science and Education (ORISE). Subsequent literature searches were conducted by NIOSH, using the online databases and specific search terms and dates described in Appendix C.

The initial literature search was performed by ORISE in 2012, using several online databases and with no date restrictions (Appendix C). The search focused on experimental (in vivo) and cellular (in vitro) studies with silver nanomaterials. Search terms included silver nanoparticles and other relevant key words (e.g., toxicology, physical and chemical properties, dosimetry). NIOSH conducted literature searches in 2013 and 2014 to identify additional studies with information on exposure and response to silver or silver nanomaterials. These searches were conducted to update the initial search conducted by ORISE and to expand those searches to include studies on occupational exposures. Search terms were selected to ensure that all in vivo and in vitro toxicology studies with silver or silver nanomaterials were identified, as well as all studies describing workplace exposures to silver or silver nanomaterials (Appendix C). The findings from this combined literature search were reported in the December 18, 2015, external review draft of the CIB, which underwent review in 2016.

The second main literature search was conducted by NIOSH in 2016 in response to external review comments in 2016 on the 2015 draft CIB. The purpose was to update the scientific literature review to include studies newly published, between January 1, 2011 (to provide overlap with previous searches),

**Table 1-2. Literature searches on silver nanomaterials.**

| Purpose | Dates Conducted | Scope |
|---|---|---|
| Initial search, retrieval and evaluation by ORISE; update and expansion by NIOSH | 2012–2014 | Experimental animal (in vivo) and cellular (in vitro) studies with silver nanoparticles; toxicology, characterization, dosimetry; workplace exposures |
| Update and expand previous searches; add focused searches | 2016–2017 | Silver nanomaterial exposures in humans, animals, and in vitro; rat biliary hyperplasia in response to silver nanoparticle exposures |
| Search for any new subchronic or chronic toxicity studies of rodents or occupational studies | 2019–2020 | Subchronic or chronic inhalation studies of silver nanomaterials in rodents; workplace exposure studies |

Abbreviations. ORISE: Oak Ridge Institute for Science and Education; NIOSH: National Institute for Occupational Safety and Health.

and September 30, 2016 (the end date of the second main search). It also sought to expand the literature in the following areas: exposure to silver nanomaterials in humans, animals (including lung, oral, or dermal routes of exposure), and zebrafish, as well as in vitro (cellular) and cell-free study areas. NIOSH conducted two additional searches in October 2016 focused on the kinetics of silver nanoparticles in biological systems and on reproductive outcome studies that had been published since January 2011. A focused literature search on the biological significance of the rat biliary hyperplasia response to silver nanoparticles was performed by NIOSH in January 2017. The findings from the 2016–2017 literature searches were reported in the August 24, 2018, revised external review draft of the CIB.

In April 2019, NIOSH conducted the third main literature search. This was a specific search to determine if any additional subchronic or chronic studies in rodents or any studies in humans had been published that might pertain to the risk assessment and derivation of the REL. No additional relevant studies were found. A focused literature search was conducted by NIOSH in December 2019 and January 2020 for studies on the consequences of persistent lung inflammation and its role in hazard classification based on animal studies. Further information on the databases, search terms, and results are reported in Appendix C.

NIOSH evaluated the relevance of these literature search results initially by examining the titles and abstracts of the publications. The publications selected for full review included all studies of occupational exposure to silver or silver nanomaterials, all in vivo studies on silver nanoscale or microscale particles, and any in vitro studies that provided information on the role of physicochemical properties on the toxicity of microscale or nanoscale silver. NIOSH obtained all relevant publications available in English-language text. These publications were individually reviewed and considered for inclusion on the basis of relevance to occupational exposures or to toxicology in humans, animals, or cell systems. All of the occupational exposure studies and in vivo and in vitro studies on silver nanoscale or microscale particles that met the search and selection criteria were included in this document.

The total number of publications on silver nanomaterials evaluated in this review includes seven studies of exposure in workers, 111 studies in animals, and 75 studies in cell systems. Of these, the primary studies that NIOSH selected for the quantitative risk assessment and derivation of the REL

for silver nanomaterials are the two published subchronic inhalation studies of rats exposed to silver nanoparticles (Section 6). All other publications of studies involving animals or cells were used in evaluations of the biodistribution and clearance of silver, the toxicological effects associated with exposure, the possible biological modes of action, and the physicochemical properties of silver nanomaterials that may affect the toxicity observed in the experimental studies.

## 1.4 Human Health Basis for the Current NIOSH REL

The NIOSH REL of 10 μg/m$^3$ (total dust) for silver (metal dust, fume, and soluble compounds, as Ag) [NIOSH 1988, 2003, 2007] was set to prevent argyria and was based on findings in workers exposed to airborne silver. The existing NIOSH REL is the same as the OSHA PEL and uses the same evidence basis [OSHA 1988, 2012a]. The derivation of the REL and PEL [OSHA 1988] is based on an earlier ACGIH TLV, as described below.

These OELs in the United States are based on early case reports of argyria in humans ingesting silver [Hill and Pillsbury 1939]. A total mass body burden of approximately 3.8 g (1 to 5 g) of silver was associated with argyria [OSHA 1988]. The occupational airborne exposure concentration that would result in an equivalent body burden of silver was calculated. ACGIH estimated a total deposition of approximately 1.5 g if a worker were exposed at the TLV of 100 μg/m$^3$ for 25 years, based on a worker air intake of 10 m$^3$/day and 25% retention of inhaled silver [ACGIH 2001].

That is,

$$1.5\ g = 0.1\ mg/m^3 \times 10\ m^3\ /8\ hr \times 8\ hr/d \times 5\ d/wk \times 50\ wk/yr \times 25\ yr \times 0.25\ [RF] \times (1g/1{,}000\ mg)$$

Although it is not stated explicitly in the documentation of the PEL and REL, the "body retention fraction" (RF) is a constant factor that represents the assumed total fraction of the inhaled dose of silver that is retained in the body (e.g., 0.25). This includes the fraction deposited in any region of the respiratory tract and retained in the lungs or other tissues (i.e., following absorption into the blood or lymph, transported to other organs, and retained in other organs). The remaining 0.75 of the inhaled dose is assumed not to be deposited in the respiratory tract or to be cleared from the body after deposition. The use of the factor in the total dose estimate means that a constant proportion of the Ag is retained, regardless of the inhaled dose. No uncertainty factors (UFs) appear to have been used in deriving this TLV.

Over a full working lifetime of 45 years, the body burden of silver would be estimated to be higher (i.e., ~2.8 g, assuming 45 years worked at 8 hours/day, 40 hours/week, 50 weeks/year, as well as the same volume of air inhaled per day [10 m$^3$] and total RF). If a higher RF of 0.50 is assumed (as discussed below), then the 45-year body burden would be estimated to be ~5.6 g, which exceeds the average (3.8 g) and minimum (1 g) body burdens associated with argyria in humans [OSHA 1988; ACGIH 2001].

The OSHA PEL [OSHA 1988] and NIOSH REL [NIOSH 1988] are based on an earlier ACGIH TLV® of 10 μg/m$^3$ for silver, which was derived from the same human data [Hill and Pillsbury 1939] but assumed that an estimated fraction of 0.5 of inhaled silver was retained in the body (i.e., deposited and not cleared). The PEL of 10 μg/m$^3$ was based on the following estimates [OSHA 1988]. The retained body burden of silver associated with argyria in humans was estimated to be 1 to 5 g (from Hill and Pillsbury [1939]). Based on the assumption of the lower value of 1 g silver body burden, an 8-hour TWA concentration of 50 μg/m$^3$ was estimated for a 20-year exposure duration [NIOSH 1988; OSHA 1988]. The PEL of 10 μg/m$^3$ provides a "safety factor" or "safety margin" of five [OSHA 1988] (assuming a 20-year exposure duration).

These calculations of the airborne exposure concentration (X mg/m$^3$) associated with the target

human body burden (as reported above) can be calculated as follows:

X mg/m$^3$ = Body burden (mg)/[Exposure duration (d) × Air intake per workday (m$^3$/d) × Body retention fraction, or RF]

An example calculation based on the equation above and using the information provided [NIOSH 1988; OSHA 1988] suggests a slightly lower 8-hour TWA concentration associated with a lower body burden estimate for argyria:

0.042 mg/m$^3$ = 1,000 mg/(5,000 d × 9.6 m$^3$/d × 0.5)

where 1 g (or 1,000 mg) is the minimum estimated body burden associated with argyria [NIOSH 1988; OSHA 1988]; 5,000 is the number of exposure days in 20 years (5 d/wk*50 wk/yr*20 yr); 9.6 m$^3$/d is the volume of air inhaled per workday (light activity, reference worker value); and 0.5 is the RF (unitless). Based on this example calculation, the original "safety factor" of five is closer to four (0.042 mg/m$^3$ effect level for argyria in humans vs. 0.01 mg/m$^3$ PEL).

Using the same target human body burden (1 g) of silver, retention fraction, and air intake but assuming 45 years of exposure (5 days/week, 50 weeks/year) would result in an estimated airborne concentration of 18 µg/m$^3$ (8-hour TWA). Thus, assuming a 45-year working lifetime exposure, instead of a 20-year exposure duration, would result in a lower safety factor of <2 from the human argyria effect level and the current NIOSH REL and OSHA PEL of 10 µg/m$^3$ (8-hour TWA).

Airborne sampling for silver according to the NIOSH REL and other OELs (Table 1-3) is based on the total airborne mass concentration, as Ag (NIOSH Methods 7300, 7301, and 7306) [NIOSH 2017a]. These sampling criteria include collection of all particle sizes that can be inhaled in the human respiratory tract (approximately 1 nm to 100 µm in diameter). Inhaled particles depositing anywhere in the respiratory tract could potentially contribute to the body burden of silver either at the site of deposition (if retained) or at distal sites (if absorbed).

**Table 1-3. Current OELs for silver in the United States and other countries.**

| Authority | Particle Size | Form | OEL (µg/m$^3$) | Reference |
|---|---|---|---|---|
| NIOSH REL | Metal dust, fume, and soluble compounds, as Ag; total mass fraction | Soluble or insoluble | 10 | NIOSH [1988, 2003, 2007] |
| OSHA PEL* | Metal dust, fume, and soluble compounds, as Ag; total mass fraction | Soluble or insoluble | 10 | OSHA [1988, 2012a] |
| MSHA PEL | Metal and soluble compounds; total mass fraction | Metal and soluble compounds | 10 | 30 CFR 57.5001, which cites ACGIH [1974] |
| ACGIH TLV* | Metal dust and fume; inhalable fraction | Soluble<br>Insoluble | 10<br>100 | ACGIH [2001; TLV* updated in 1992] |
| MAK† | Inhalable fraction | Silver salts (as Ag)<br>Silver (Ag) | 10<br>100 | DFG [2013] |

*Current regulatory limit in the United States.
†Maximum Workplace Concentration (Germany).

This page intentionally left blank.

# 2 Occupational Exposures to Silver

Worker exposure to silver can occur throughout the life cycle of the metal (ore extraction, melting/refining, product fabrication, use, disposal, recycling) [Maynard and Kuempel 2005]. Inhalation and dermal contact with silver are considered to be the main exposure routes [ATSDR 1990; Wijnhoven et al. 2009]. Published information on worker exposure to silver includes study findings of airborne silver during brazing and soldering operations [NIOSH 1973, 1981, 1998]; fabrication of silver jewelry [NIOSH 1992; Armitage et al. 1996]; recovery of silver from photographic fixer solutions [Williams and Gardner 1995; NIOSH 2000]; production of silver oxide and silver nitrate [Rosenman et al. 1979, 1987; Moss et al. 1979]; refinement of silver [Williams and Gardner 1995]; reclamation of silver [Pifer et al. 1989; Armitage et al. 1996]; handling of insoluble silver compounds [DiVincenzo et al. 1985; Wölbling et al. 1988]; and MSHA personal health samples datasets [MSHA 2020]. The reports of these studies lack information on the physical-chemical characteristics (such as particle size or species) of the aerosol to which workers were exposed, although it's likely that aerosols/fumes generated during brazing/soldering [NIOSH 1973, 1981, 1998], the melting of silver alloys [NIOSH 1992], the refinement of silver [Williams and Gardner 1995], and the recovery of silver from photographic fixer solutions [Williams and Gardner 1995; NIOSH 2000] contained nanometer-size silver particles and/or agglomerates of silver particles. In several workplace studies, airborne exposure to AgNPs was measured during the synthesis of engineered AgNPs [Park et al. 2009; Lee et al. 2011b; Lee et al. 2012a,b] and during the electrorefining of silver [Miller et al. 2010]. Workplace findings of the potential for dermal absorption of silver during handling of colloidal suspension (gel form) and liquid AgNPs also have been reported [Ling et al. 2012]. Table 2-1 summarizes reported workplace exposures to silver.

NIOSH has reported on several workplace studies in which workers were found to be exposed to silver and other airborne contaminants during brazing/soldering and milling operations at an air conditioning equipment company [NIOSH 1973], a metal fabrication facility [NIOSH 1981], and a manufacturer of construction equipment [NIOSH 1998]. Workers were found to be exposed to airborne silver concentrations that ranged from nondetectable to 6 μg/m$^3$ during brazing and soldering operations while they assembled air conditioning equipment [NIOSH 1973], in which the use of exposure controls was minimal. At the other two manufacturing facilities, workers performing brazing and soldering were exposed to airborne silver concentrations that were below the OSHA PEL and NIOSH REL of 10 μg/m$^3$ [NIOSH 1981] or ranged from nondetectable to 0.015 μg/m$^3$ [NIOSH 1998]. In both facilities, controls were used to minimize worker exposure.

NIOSH also reported on a survey at a manufacturer of silver jewelry [NIOSH 1992], in which workers were potentially exposed to silver, copper, lead, and cadmium fume as well as to carbon monoxide and nitrogen dioxide. Exposure to silver was detected during the metal casting operation, in which 100 ounces of an Ag/Cu alloy was melted with an air-acetylene and oxy–natural gas torch. The operation took approximately 84 minutes, and the airborne silver concentration to which the worker was exposed during this time was 54 μg/m$^3$. Local exhaust ventilation (LEV) was used during the casting operation.

The highest airborne silver concentrations found in NIOSH workplace studies were at a precious metal recycling facility [NIOSH 2000] during the recovery of silver from photographic fixer solutions. Silver was recovered by the "metallic replacement method," in which steel wool and fiberglass were used within a recovery cartridge to extract the

dissolved silver ions from the fixer solution. The cartridges were then placed into silicon carbide or clay graphite crucibles and heated at a temperature of 2200°F to 2300°F to separate silver from the impurities. A personal sample collected on a worker during the silver recovery process revealed an airborne TWA silver concentration of 140 μg/m$^3$. Area airborne samples collected over the full work shift at this facility revealed silver concentrations that ranged from 9 to 190 μg/m$^3$.

MSHA reports miner exposures to silver dust and silver fume through the personal health sample dataset in the Mine Data Retrieval System. As of January 2020, the public database contained approximately 220 samples with exposures exceeding 0.9 μg/m$^3$, with a range up to 1,275 μg/m$^3$ [MSHA 2020].

Airborne exposure to engineered AgNPs has been documented during their synthesis in a liquid-phase production process [Park et al. 2009]. The airborne release of AgNPs was evaluated at the reactor (wet chemical method), dryer, and grinding processes with use of a scanning mobility particle sizer (SMPS), to determine the size and particle number concentration, and with an electrostatic precipitator (ESP) to collect samples for particle characterization by transmission electron microscopy (TEM). Exposure measurements of AgNPs taken at the opening of the reactor showed the release of particles with diameters of 50 to 60 nm, which agglomerated into 100-nm particles shortly after their release. Particle measurements taken before the reactor door was opened ($6.1 \times 10^4$ particles/cm$^3$) increased to $9.2 \times 10^4$ particles/cm$^3$ when it was opened. After a 24-hour aging process, the silver colloidal suspension was transferred from the reactor, filtered, and deposited in a dryer to remove volatile organic materials and water. Airborne particle concentrations determined after the drying of the silver suspension indicated a doubling in the number of AgNPs that were 60 to 100 nm in diameter, compared with background particle number measurements. Prior to packaging, the dried AgNPs were ground to reduce agglomeration; measurements taken at the opening of the grinder detected the release of airborne AgNPs 30 to 40 nm in diameter.

Lee et al. [2011b, 2012a] reported on the airborne release of engineered AgNPs during the synthesis of AgNPs <100 nm at two different facilities. Facility A used a large-scale pilot reactor operated at negative pressure in which various silver-containing precursors (wire, powder, liquid) were fed through an inductively coupled argon plasma (ICP) torch, where they were vaporized in argon plasma. Silver atoms were condensed to predominantly 20- to 30-nm particles in a temperature gradient and then amassed in a collector. Facility B synthesized silver nanoparticles (1 kg/day) by mixing sodium citrate with silver nitrate and pumping the solution into a reactor that was housed in a ventilated fume hood.

Worker and area exposure measurements detected airborne silver concentrations up to 0.1 μg/m in Facility A and 0.4 μg/m$^3$ in Facility B [Lee et al. 2011b]. Two of five workers who were involved in AgNP manufacturing at Facility A also participated in a health surveillance study [Lee et al. 2012a]. The two had been employed at the facility for 7 years. One worker was reported to have been exposed to an airborne silver concentration of ~0.3 μg/m$^3$ and the other worker to a concentration of ~1.35 μg/m$^3$. Levels of silver in the blood of the two workers were 0.0135 and 0.034 micrograms per deciliter (μg/dL), and those in the urine were 0.043 μg/dL and nondetectable, which the authors noted as below the normal ranges presented in other studies. All clinical chemistry and hematologic parameters were found to fall within the normal range, and the workers reported no adverse health effects.

A follow-up study was conducted to evaluate workplace exposures over 3 days [Lee et al. 2012b]. Personal and area samples were collected for silver determination and for particle characterization by means of scanning transmission electron microscopy (STEM) and energy-dispersive X-ray spectroscopy (EDS). Real-time airborne particle size and count concentrations were also determined, with an SMPS and a condensation particle counter (CPC). The highest airborne concentrations for silver were detected in the injection room, where silver powder along with acetylene and oxygen gas were introduced into the reactor to manufacture

AgNPs. The personal samples of workers who spent a total of 10 to 20 minutes per day in the injection room had TWA silver concentrations that ranged from 0.04 to 2.43 μg/m$^3$ during those time periods. The use of exposure controls was not reported, but workers were required to wear half-facepiece respirators.

TWA silver concentrations determined from area samples collected in the injection room ranged from 5 to 288.7 μg/m$^3$, whereas area samples collected for silver at other locations in the facility had concentrations ≤1.3 μg/m$^3$ (sampling durations ranged from 159 to 350 minutes). Analysis of area and personal airborne samples by STEM showed the preponderance of AgNPs as agglomerates. Real-time aerosol monitoring with the SMPS revealed particle number concentrations that ranged from 224,622 to 2,328,608 particles/cm$^3$, and measurements by CPC revealed concentrations of 533 to 7,770 particles/cm$^3$.

Lee et al. [2013b] also reported on total airborne particulate, silver, carbon, and volatile organic compounds at a printed electronics facility. Personal and area samples were taken in the proximity of the three roll-to-roll or roll-to-plate presses at the facility during operation and cleaning. Analysis was conducted by ICP-MS and STEM. Particulate number and size were assessed by SMPS-CPC and a dust monitor. TWA silver concentrations were 2 to 3 μg/m$^3$ during cleaning and 3 to 24 μg/m$^3$ during operation. Particle concentrations and sizes were measured but were not quantitatively attributable to the silver fraction. Use of PPE at the facility was minimal and incorrect (workers did not use it or used it for insufficient periods of time, without proper storage); ventilation systems and fume hoods were often not functioning or were set up incorrectly (such as by using unconventional fittings and repair materials); and waste disposal was handled in ways that would not protect workers from spills or evolved gases.

Airborne exposure to AgNPs was also reported to occur during the melting and electrorefining of silver feedstock [Miller et al. 2010]. A survey of worker exposures at a precious metals refinery yielded results from personal and area samples collected for metal determination as well as airborne particle number concentrations via a Fast Mobility Particle Sizer (FMPS). A handheld ESP was also used to collect airborne aerosols for TEM characterization. Concentrations in personal airborne samples for total silver (from use of NIOSH Method 7303) ranged from 13 to 94 μg/m$^3$, whereas those in area samples ranged from 4 to 39 μg/m$^3$. Concentrations in all area samples analyzed for soluble silver compounds (with use of ISO Method 15202) were <2 μg/m$^3$.

TEM and EDS analysis of ESP samples indicated the presence of silver, lead, selenium, antimony, and zinc, with all metals in the nanometer size range. AgNPs were the primary aerosol, with a mean diameter of ~10 nm, in samples collected near the furnace; samples collected at other worksites contained agglomerated AgNPs with diameters of ~100 nm. Airborne particle number measurements made with an FMPS in work areas on the electrorefining floor and around the furnaces during mold pours were >$10^6$/cm$^3$, representing up to a 1,000-fold increase in particle number concentration over baseline background particle concentrations.

Lewis et al. reported on an exposure to various metals (including silver) associated with loading and unloading catalysts for petroleum refining [Lewis 2012]. Depending on the particular process, loading and unloading can take multiple shifts (up to 96 hours). Area and personal samples were analyzed by ICP-atomic emission spectroscopy. In all cases, TWA silver concentration was <6 μg/cm$^3$. Workers used PPE such as goggles, full-body coveralls, impervious gloves and boots, and either a half-mask air-purifying respirator or a supplied-air respirator for certain operations.

**Table 2-1. Summary of occupational exposures to silver.**

| Source of Exposure | Exposure Details and Airborne Silver Concentrations | Comments | Reference |
|---|---|---|---|
| Brazing, silver soldering, and milling at an air conditioning equipment facility | Personal samples (7): ND–6.0 μg/m$^3$ TWA<br>Area samples (4): ND–6.0 μg/m$^3$ TWA | No clinical signs of argyria<br>No LEV used | NIOSH [1973] |
| Brazing, milling, and sanding at a metal fabrication facility | Personal samples (20): 0.001–0.01 μg/m$^3$ TWA | No clinical signs of argyria<br>LEV used | NIOSH [1981] |
| Brazing at a manufacturer of construction equipment | Personal samples (99): ND–15 μg/m$^3$ TWA | No clinical signs of argyria<br>LEV used | NIOSH [1998] |
| Casting of a silver alloy at a silver jewelry manufacturing facility | Personal sample (1): 54 μg/m$^3$ (84 min) | No medical assessment performed<br>LEV used | NIOSH [1992] |
| Silver recovery from photographic fixer solutions | Personal sample (1): 140 μg/m$^3$ TWA<br>Area samples (5): 9–190 μg/m$^3$ TWA | No medical assessment performed<br>Local exhaust in furnace room not operating correctly | NIOSH [2000] |
| Manufacturing of silver nitrate and silver oxide | Personal samples (6): 39–378 μg/m$^3$ TWA | No mention of exposure controls<br>Medical assessment of 30 workers found<br>— 6 workers with generalized argyria<br>— 20 workers with argyrosis<br>— 10 workers with decreased vision | Rosenman et al. [1979] |

(Continued)

**Table 2-1 (Continued). Summary of occupational exposures to silver.**

| Source of Exposure | Exposure Details and Airborne Silver Concentrations | Comments | Reference |
|---|---|---|---|
| Silver processing facility (silver salts and metallic silver) | Area samples: 1–310 μg/m³ TWA (soluble silver compounds), 3–540 μg/m³ TWA (insoluble silver compounds) | No mention of exposure controls<br>Medical assessment of 50 workers found<br>— 9 workers with argyrosis (soluble silver exposure)<br>— No symptoms of argyrosis in workers exposed to insoluble silver | Wölbling et al. [1988] |
| Reclamation of silver from photographic film, paper, and liquid wastes (insoluble silver halides) | Personal and area samples (>100) over a 30-yr period: 5–240 μg/m³ TWA | No mention of exposure controls<br>Medical assessment of 27 workers found<br>— No cases of argyria<br>— 7 workers with some form of ocular argyrosis | Pifer et al. [1989] |
| Smelting and refining of silver and the preparation of silver salts for photosensitized products | Personal and area samples (62) over a 2-month period: 1–100 μg/m³ TWA | No mention of exposure controls<br>Biologic samples for silver in blood, urine, and feces measured for 37 workers<br>— Mean blood silver concentration was 0.011 μg/mL, with over 80% having detectable levels<br>— Two workers had detectable levels of silver in urine, at 0.007 and 0.011 μg/g<br>— Mean fecal concentration of silver was 15 μg/g in samples and 1.5 μg/g in control, with detection in all samples | DiVincenzo et al. [1985] |

(Continued)

**Table 2-1 (Continued). Summary of occupational exposures to silver.**

| Source of Exposure | Exposure Details and Airborne Silver Concentrations | Comments | Reference |
|---|---|---|---|
| Manufacturing precious metal powder (silver nitrate, silver oxide, silver chloride, silver cadmium oxide) | Personal samples (OSHA inspection):<br>40–350 μg/m$^3$ TWA | No mention of exposure controls; some workers reported to wear respirators<br>Biologic samples for blood and urine silver showed raised levels in 92% of studied workers relative to the control group<br>Acute irritation found for eyes and kidney | Rosenman et al. [1987] |
| Six worksites: Silver reclamation, bullion production, jewelry manufacture, bullion/coin/tableware production, and chemical production (two factories) | No assessment of airborne silver concentrations reported | No mention of exposure controls<br>Blood silver levels measured for workers at all six worksites<br>— Reclamation workers: 1.3–20 μg/L<br>— Workers from the other 5 worksites: 0.1–16 μg/L<br>— Jewelry workers had lowest levels: 0.2–2.8 μg/L | Armitage et al. [1996] |
| Two worksites: silver reclamation from X-rays and photographic film, and silver refinery | Samples taken during silver reclamation (3):<br>Area, 85 μg/m$^3$ (3 hr) at incinerator; Personal, 1030 and 1360 μg/m$^3$ (<15 min) at pulverizing area<br>Samples taken during silver refining:<br>Area, 110–170 μg/m$^3$ (229 min) at silver refining casting area;<br>Personal, 100 μg/m$^3$ (224 min) and 59–96 μg/m$^3$ (28 min) at silver refining casting area | Improvements in exposure control instituted<br>Medical assessment of a worker at each site for argyrosis and argyria:<br>— Worker involved in silver reclamation (silver halides and oxide): no argyrosis<br>— Worker involved in silver refining (soluble compounds; silver nitrate): argyrosis | Williams and Gardner [1995] |

(Continued)

**Table 2-1 (Continued). Summary of occupational exposures to silver.**

| Source of Exposure | Exposure Details and Airborne Silver Concentrations | Comments | Reference |
|---|---|---|---|
| Production of nanoscale silver (liquid-phase production process; silver nitrate with nitric acid) | No quantitative silver exposure measurements; only particle count concentrations | Improvements in exposure control instituted | Park et al. [2009] |
| Production of nanoscale silver at two facilities: Facility C used inductively coupled plasma torch with electric atomizer; Facility D used sodium citrate and silver nitrate | Personal breathing zone samples (2) at Facility C: 0.12–1.02 μg/m$^3$ (TWA)<br>Area samples (8) at<br>Facility C: 0.02–0.34 μg/m$^3$ (TWA)<br>Personal breathing zone samples (2) at Facility D: 0.38–0.43 μg/m$^3$ (TWA)<br>Area samples (8) at<br>Facility D: 0.03–1.18 μg/m$^3$ (TWA) | Facility C: The reactor and collector processes were performed under vacuum to control release of airborne silver<br>Facility D: The wet process reacting silver nitrates with citrate prevented release of airborne silver particles | Lee et al. [2011b] |
| Production of nanoscale silver at Facility C, as described in Lee et al. [2011b] | Personal samples (2):<br>— Worker 1, 0.35 μg/m$^3$ (TWA)<br>— Worker 2, 1.35 μg/m$^3$ (TWA) | Biologic samples for silver<br>— Worker 1: blood (0.034 μg/dl); urine (0.043 μg/dl)<br>— Worker 2: blood (0.030 μg/dl); urine (ND)<br>Some engineering controls used as well as PPE | Lee et al. [2012a] |

(Continued)

**Table 2-1 (Continued). Summary of occupational exposures to silver.**

| Source of Exposure | Exposure Details and Airborne Silver Concentrations | Comments | Reference |
|---|---|---|---|
| Production of nanoscale silver at Facility C, as described in Lee et al. [2011b] | Samples were collected over 3 days.<br>Personal samples (6):<br>Worker 1, 1.55–4.99 μg/m$^3$ (2.43 μg/m$^3$ TWA)<br>Worker 2, 0.09–1.35 μg/m$^3$ (0.04 μg/m$^3$ TWA)<br>Area samples (28):<br>0.02–426.43 μg/m$^3$ (0.01–288.73 μg/m$^3$ TWA) | Highest silver concentrations found in the injection room, in which silver powder and acetylene/oxygen gas were injected into the reactor<br>Particle number concentration ranged from 911,170 to 1,631,230 cm$^3$ during reactor operation<br>Particle size: 15–710 nm during reactor operation<br>Natural ventilation used; workers wore half-mask respirators | Lee at al. [2012b] |
| Precious metal processing facility; melting and electro-refining of silver | Total silver:<br>Personal, full-shift samples (6):<br>13–94 μg/m$^3$<br>Area samples (14):<br>4–39 μg/m$^3$ | Highest personal exposures to silver found on electrorefining floor<br>Particle number concentrations >10$^6$, with highest at furnaces/pouring<br>~10-nm-diameter particles<br>Ventilation controls during pouring of molten metal | Miller et al. [2010] |
| Petroleum refinery; Loading and unloading solid catalysts | Total silver:<br>Personal, 54- to 543-min samples (13):<br><3 μg/m$^3$<br>Area, 54- to 1505-min samples (54):<br><6 μg/m$^3$ | Catalysts can take 8–72 h to load and 8–96 h to unload<br>PPE includes respirator, goggles, full-body coveralls, gloves, and boots<br>Other metallic co-contaminants and dust detected and assayed | Lewis et al. [2012] |

(Continued)

**Table 2-1 (Continued). Summary of occupational exposures to silver.**

| Source of Exposure | Exposure Details and Airborne Silver Concentrations | Comments | Reference |
|---|---|---|---|
| Electronic printing facilities; roll-to-roll and roll-to-plate printing operation and cleaning | Total silver:<br>Operating press, 93- to 158-min samples: 4–24 μg/m$^3$<br>Cleaning, 128- to 157-min samples: 2–3 μg/m$^3$ | "Conductive nano-ink, mostly silver nanoparticles or carbon nanotubes" used<br>LEV and fume hoods<br>Minimal PPE usage, improper PPE filter storage, fume hoods and LEV systems defeated; authors recommended resolutions to these issues<br>Risks related to organic solvent exposure noted | Lee et al. [2013] |

LEV = local exhaust ventilation; ND = nondetectable; PPE = personal protective equipment; TWA = time-weighted average.

This page intentionally left blank.

# 3 Human Evidence of Internal Dose and Potential Adverse Health Effects

## 3.1 Background

The majority of reports on workplace exposure and health assessments of workers exposed to silver lack sufficient detail to adequately determine the physical-chemical characteristics (such as particle size and silver species) of the aerosol to which workers were exposed. However, it's reasonable to infer that some workers had exposure to nanometer-sized particles, on the basis of known characteristics of particles that are typically present: (1) in fumes generated during brazing and soldering or the melting of silver alloys or silver recycled materials, (2) during the recovery of silver from photographic fixer solutions, and (3) during the handling of colloidal silver. Because of silver's many potential uses, workers can be exposed to a range of particle sizes and forms of silver that could enter the body by different routes [Drake and Hazelwood 2005]. Ingestion can be an important route of entry for silver compounds and colloidal silver [Silver 2003], whereas inhalation of dusts or fumes containing silver occurs primarily in occupational settings [ATSDR 1990]. Skin contact can also occur in occupational settings from the handling of silver and silver-containing materials [ATSDR 1990].

Several factors are known to influence the ability of a metal to produce toxic effects on the body; these include the solubility of the metal at the biologic site (affected by particle size and pH of the surrounding media), the nature of any surface coating or binding material, the surface activity of the metal, the ability of the metal to bind to biologic sites, and the degree to which metal complexes are formed and sequestered or metabolized and excreted. Published studies appear to indicate that some forms of silver may be more toxic than others. The majority of health data from workers exposed to silver indicate that long-term inhalation or ingestion of silver compounds (especially soluble forms of silver) can cause irreversible pigmentation of the skin and mucous membranes (argyria) and/or the eyes (argyrosis), in which the affected area becomes bluish-gray or ash gray [ATSDR 1990; Drake and Hazelwood 2005; Wijnhoven et al. 2009; Johnston et al. 2010; Lansdown 2012]. Generalized argyria has often been reported to occur following the ingestion or application of silver-containing medicines, but it has also been observed to varying degrees in workers exposed to silver compounds during the production, use, and handling of silver nitrate and silver oxide [Moss et al. 1979; Rosenman et al. 1979; Williams 1999] and silver salts (nitrate and chloride) [Wölbling et al. 1988]; during the reclamation of silver from photographic film [Buckley 1963; Pifer et al. 1989; Williams and Gardner 1995]; and during the handling of silver in photosensitized products [DiVincenzo et al. 1985]. Localized argyria has also been reported to be due to the following: application of burn creams containing silver [Wan et al. 1991]; silver soldering [Scrogges et al. 1992]; contact with silver jewelry [Catsakis and Sulica 1978; Murdaca et al. 2014]; use of silver acupuncture needles [Tanita et al. 1985; Sato et al. 1999], catheters [Saint et al. 2000], or dental amalgams [Catsakis and Sulica 1978; Piña et al. 2012]; and accidental puncture wounds [Rongioletti et al. 1992].

## 3.2 Human Studies of Lung Deposition of Airborne Silver Nanoparticles

Limited data are available on the deposition of inhaled AgNPs in humans and absorption from the

lungs (i.e., transport across epithelial cell membranes and entry into the lymph or blood circulatory system) [Muir and Cena 1987; Cheng et al. 1996]. Muir and Cena [1987] exposed three male volunteers to air containing AgNPs with a mean count diameter of 9 nm (geometric standard deviation [GSD] = 2.0) and at a concentration of $2 \times 10^5$ particles/cm$^3$. Airborne particles were size-separated by a parallel-plate diffusing battery and counted with a nucleus particle counter. The particle size distribution of the aerosol was obtained before and after each inhalation experiment, and the mean differed only slightly from 9 nm. The sampling of inhaled and exhaled air was undertaken at a fixed flow rate of 2 L/min. Particle deposition in the respiratory tract was determined by relating the concentrations of particles inhaled to the concentrations of particles exhaled by the subjects. The subjects breathed at a normal resting lung volume. Particle deposition was found to increase from 20% to 90% as the breathing cycle (duration of breath, including both inspiration and expiration) increased from 2 to 10 seconds, but it was not affected by tidal volume (volume of air inhaled and exhaled at each breath; 0.5–3 L tested).

In another lung deposition study with AgNPs, 10 male human subjects were exposed to four different particle sizes (4, 8, 20, and 150 nm in diameter) of silver wool (99.9% pure) via an evaporation–condensation method at two constant flow rates of 167 and 333 cm$^3$ per second [Cheng et al. 1996]. Airborne concentrations of AgNPs were measured with a condensation particle counter (CPC). Each subject was repeatedly measured for aerosol deposition during 32 combinations of experimental conditions. Lung deposition efficiencies for 4-nm particles ranged from about 25% to 65% with nose-in/mouth-out breathing and 25% to 62% with mouth-in/nose-out breathing. For 8-nm particles, respective deposition efficiencies were 14% to 49% and 14% to 45%. The respective ranges for 20-nm particles were 2% to 35% and 3% to 28%. For 150-nm particles, deposition efficiencies were 0% to 15% for both breathing methods.

Although the values of deposition efficiencies varied among the 10 subjects, particle deposition in the lung appeared to result from diffusion, with AgNP deposition observed to increase as the particle diameter and flow rate decreased. The interindividual variability of particle deposition efficiencies was correlated with the intersubject variations in nasal dimensions (as measured by total surface area), smaller cross-sectional area, and complexity of the airway shape.

## 3.3 Biomonitoring Studies in Humans

Although no data are available on the body burdens in workers resulting from inhaled silver nanoparticles, some biomonitoring data are available on workers exposed to airborne silver (particle size not specified). Such information provides the best available data on internal doses, for comparison to the animal study data.

Following a study of 37 male silver-production workers (most with 5 or more years of experience in production areas), DiVincenzo et al. [1985] reported workplace airborne exposure measurements of 1 to 100 µg/m$^3$. These researchers compared the estimated total silver dose in workers to the estimated dose associated with argyria (that is, approximately 2.3 g by intravenous injection [Hill and Pillsbury 1939, cited in DiVincenzo et al. 1985], or 23–115 mg, on 1% to 5% silver retention in the body from measurements in mammals exposed to radionuclides of silver [Scott and Hamilton 1948, 1950; Fruchner et al. 1968, cited in DiVincenzo et al. 1985]). DiVincenzo et al. [1985] estimated an annual dose of 14 µg/kg in workers, by assuming the lower cited value of 1% retention of silver after uptake in the body by diet (oral) or workplace (inhalation) exposure [DiVincenzo et al. 1985]. They then estimated a worker airborne exposure concentration of 30 µg/m$^3$ from fecal excretion data, which is within the measured air concentration range. The estimated annual dose of retained silver in a 70-kg worker was approximately 1 mg. Given the 23- to 115-mg retained dose estimated to be associated with argyria, DiVincenzo et al. [1985] estimated that at least 22 years of workplace

exposure would be required for development of argyria. Although different assumptions were used in deriving these estimates, the results are similar to the estimates used as the basis for the NIOSH REL (Section 6.1).

A study of 50 workers in the silver processing industry (44 males, 6 females) investigated associations between the airborne exposure concentration and duration and the clinical symptoms or silver concentrations in skin samples [Wölbling et al. 1988]. About half of the workers (52%) handled only metallic silver and 46% were exposed to silver salts (silver nitrate or silver chloride); one worker was exposed to both forms of silver. No cases of generalized argyria were observed, although 8 of the 23 silver salt workers had localized argyria (especially in mucous membranes of the eyes, mouth, and nose). No cases of localized argyria were observed among the metallic silver workers. Airborne concentrations ranged from 1 to 310 μg/m³ in the "salts" group and from 3 to 540 μg/m³ in the "metal" group. Worker exposure durations were 3 to 20 years. The lowest concentration associated with localized argyria (ocular) was 2 to 4 μg/m³, although no relationship was observed between the exposure concentration or duration and the signs of argyrosis. The silver concentrations in skin (0.01–0.11 μg/g) were within the range of previously reported values and were not associated with argyria. In another study, argyria was observed in a worker (silver polisher) with 3.7 μg/g silver in skin [Treibig and Valentin 1982, cited in Wölbling et al. 1988].

## 3.4 Health Effects in Workers with Exposure to Silver

Rosenman et al. [1979] reported findings of respiratory symptoms and argyria in workers ($n$ = 30) involved with the manufacturing of silver nitrate and silver oxide. Sixteen of the 30 had worked for 5 or more years. All the workers were white males, and the average age was 34.6 years. Chest radiographic findings and results of clinical examination of respiratory function were predominantly normal. Two workers were found to have small, irregular opacities on chest X-rays; one of the workers was reported to have had previous exposure to asbestos. None of the workers had evidence of restrictive pulmonary disease, and obstructive changes in pulmonary function were attributed to smoking.

Ten of the 30 workers complained of abdominal pain, which appeared to be associated ($p < 0.25$) with silver found in the blood. There was a history of X-ray-documented ulcers in six of these workers and a history of upper gastrointestinal bleeding in two others. Decreased vision at night was also reported by 10 workers and was associated with the length of employment; however, no changes in visual performance could be attributed to silver deposits. The cross-sectional study did identify six workers with generalized argyria and 20 with argyrosis. At the time of the study, no exposure measurements were taken; however, personal airborne measurements made 4 months before the study revealed 8-hour TWA silver concentrations ranging from 39 to 378 μg/m³ (total mass).

A follow-up study of these 30 workers [Moss et al. 1979] also revealed evidence of argyrosis and burns of the skin from contact with silver nitrate in 27 and a history of ocular burns in 11. An in-depth ophthalmic examination was conducted to determine if workers suffered from any visual deficits from their exposure. A direct relationship was shown between the amount of discoloration of the cornea and the length of time worked. As reported in the previous study [Rosenman et al. 1979], no functional deficits were found, although some workers complained of decreased night vision.

Wölbling et al. [1988] reported on a cross-sectional study of 50 workers (44 males and 6 females employed ≥1 year) at a silver processing plant to determine if symptoms of exposure differed between those exposed predominantly to insoluble silver ($n$ = 26) and those exposed exclusively to soluble silver compounds of silver nitrate and silver chloride ($n$ = 23). Ten subjects, not occupationally exposed to silver, were used as a control group. Length of exposure ranged from 3 to 20 years. Exposure concentrations ranged from 1 to 310 μg/m³ for workers exposed to

soluble silver compounds and from 3 to 540 μg/m³ for those exposed to insoluble silver compounds. Among workers in the soluble exposure group, discoloration (argyrosis) was observed in the eyes of 5, the mouths of 2, the nose of 1, and the nape of the neck of 1. No symptoms of argyria or argyrosis were seen in workers in the insoluble exposure group.

Skin biopsies analyzed for silver revealed a concentration of 0.03 to 13.5 ppm for the soluble group (median of 0.115 ppm), 0.03 to 0.77 ppm for the insoluble group (median of 0.085 ppm), and 0.01 to 0.11 ppm for the control group (median of 0.02 ppm). Silver concentrations found in the skin biopsy specimens and air did not correlate with either ocular deposits or duration of exposure. The authors concluded that the occurrence of argyria and argyrosis depends on individual susceptibility.

Pifer et al. [1989] reported on a clinical assessment of 27 silver reclamation workers exposed primarily to insoluble silver halides. An equal number of workers not occupationally exposed were selected as a control group. Airborne silver concentrations ranged from 5 to 240 μg/m³ (total mass). Silver was found in the blood of 21 silver reclamation workers, with a mean concentration of 0.01 μg/mL. Only one worker had a detectable level of urinary silver; silver was not detected in the blood or the urine of the control group. Silver was measured in all fecal samples collected, with a mean concentration of 16.8 μg/g for exposed workers ($n$ = 18) and 1.5 μg/g for unexposed workers ($n$ = 22).

Clinical examinations and skin biopsies revealed no cases of generalized argyria. Twenty of the 27 reclamation workers exhibited some degree of internal nasal septal pigmentation, and 7 of 24 workers were found to have ocular silver deposits, in the conjunctiva and/or cornea. Optometric and contrast sensitivity test results revealed no deficits in visual performance. No abnormalities were revealed during tests of renal and pulmonary function or on chest radiographs. The researchers concluded there was no evidence that chronic exposure to insoluble silver halides had detrimental health effects on exposed workers at the concentrations measured.

DiVincenzo et al. [1985] reported on workers exposed to different species of silver during the smelting and refining of silver and preparation of silver salts for use in photosensitized products. The absorption and excretion of silver were monitored by measuring blood, urine, fecal, and hair concentrations in 37 male workers occupationally exposed primarily to insoluble silver compounds; a group of 35 unexposed workers served as a control population. Personal and area airborne samples were collected for silver.

The 8-hour TWA exposure to silver over a 2-month monitoring period (62 samples) ranged from about 1 to 100 μg/m³ (total mass). Measured concentrations of silver in the blood, urine, and feces were 0.011 μg/mL, <0.005 μg/mL, and 15 μg/mL, respectively. The concentration of silver in the hair was higher for the silver workers than for controls (130 ± 160 vs. 0.57 ± 0.56 μg/g). Using fecal excretion as an index of exposure for calculating body burden of silver and assuming that 1% to 5% of the silver was retained in the body, the authors concluded that a minimum of 24 years of continuous workplace exposure would be necessary for workers to retain enough silver to develop argyria.

Williams and Gardner [1995] reported on the medical evaluation of two workers who were employed by a company involved in the reclamation of silver from old X-rays and photographic film. The reclamation and refining process required incineration of the film, pulverization of the ash, and extraction of the silver, followed by an electrolytic process involving nitric acid to obtain the desired purity prior to casting of the silver. The two workers had been employed for less than 7 years and were reported to be asymptomatic, with no evidence of argyria. A personal exposure measurement for one of the workers (Case 1) during the incineration of films was 85 μg/m³ (180 minutes), and airborne concentrations of 1030 and 1360 μg/m³ (<115 minutes) were measured in the pulverizing area. A blood silver determination for this worker at the time of environmental exposure assessments was 49 μg/L. The second worker (Case 2) was involved in mainly silver refinement and was reported to have

airborne concentrations of 110 to 170 μg/m³ (229 minutes) and 100 μg/m³ (224 minutes) during the casting of silver. Short-term personal samples indicated exposure concentrations of 59 to 96 μg/m³ (28 minutes), and background airborne concentrations in the electrolytic area of the refinery were 30 to 70 μg/m³. The background concentrations of silver were attributed to the presence of silver compounds from the electrolytic tanks rather than from the casting process.

Follow-up visits to the plant revealed no change in the clinical outcome of the first worker (Case 1) exposed to silver halides and silver oxide. This was consistent with the report of Pifer et al. [1989] that exposure to insoluble silver compounds appeared to be relatively benign in causing argyria. Follow-up clinical assessment of the second worker (Case 2) revealed the onset of argyria, attributed to exposure to soluble silver compounds (silver nitrate) and metallic silver. Subsequent follow-up of this worker over a 5-year period [Williams 1999] indicated an average blood silver concentration of 11.2 μg/L (range, 6–19 μg/L). During this period, no progression of argyria was noted.

In a cross-sectional study of workers manufacturing silver (silver nitrate, silver oxide, silver chloride, silver cadmium oxide) and other metal powders, Rosenman et al. [1987] observed upper respiratory irritation, such as sneezing, stuffy or runny nose, and chest tightness, in 15 of 27 workers (56%). The average age of the 27 workers was 41, and they had worked at the plant for an average of 8.1 years. Kidney function was also evaluated. The urinary enzyme N-acetyl-B-D glucosaminidase (NAG) was found to be statistically significantly elevated in four of the exposed workers and was correlated with blood silver concentrations and age. The exposed population mean NAG concentration was also statistically significantly higher ($p < 0.01$) than that found in the control population. In addition, the estimated creatine clearance rate was significantly lower ($p < 0.05$) in exposed workers compared to controls. Because of concurrent exposure to known nephrotoxins, such as cadmium and solvents, the authors could not determine if exposure to silver was responsible. Also, 96% of the workers had elevated urine silver concentrations (0.5–52.0 μg/L), and 92% had elevated blood silver concentrations (0.05–6.2 μg/100 mL). No correlation was found between raised blood and urine silver concentrations and the work area. However, this lack of an association may have been due to the workers' use of respiratory protection. An OSHA health inspection conducted at the plant revealed 8-hour TWA silver concentrations ranging from 40 to 350 μg/m³ (total mass).

Although it is unclear whether there is a relationship between airborne exposure to silver and blood silver concentrations, Armitage et al. [1996] suggested that blood silver concentrations determined on a group level could be used to evaluate the overall effectiveness of workplace control measures. A total of 98 blood samples from occupationally exposed workers and 15 control blood samples from agricultural workers were analyzed for silver. Samples were collected from workers at factories involved in silver reclamation, jewelry manufacture, bullion production, silver chemical manufacture, and tableware production. A normal range of blood silver concentrations was found for the agricultural workers, with a mean of <0.1 μg/L. Reclamation workers were found to have some of the highest silver concentrations in the blood, ranging from 1.3 to 20 μg/L (average, 6.8 μg/L), whereas workers involved in refining silver to produce bullion, coins, and chemicals had blood silver concentrations that ranged from 0.1 to 16 μg/L (average, 2.5 μg/L).

Workers employed in industries as silver refiners and those involved in the production of silver nitrate had the highest blood silver concentrations, whereas workers in jewelry production had the lowest, ranging from 0.2 to 2.8 μg/L. No evidence of argyria was found in any of these workers. Murdaca et al. [2014] found evidence of argyria in a case study of a jewelry worker, but the exposure was not quantified. Aktepe et al. [2015] reported statistically significantly increased DNA damage and oxidative stress among silver jewelry workers. DNA damage was quantified by alkaline comet assay of endogenous mononuclear leukocytes; total

antioxidant, total oxidant status, and remaining free thiol groups were also quantified. Exposure was not assessed. The effects of silver exposure in jewelers may also be confounded by the presence of cadmium [Parikh et al. 2014]. A statistical evaluation of the results reported by Aktepe et al. [2015] is provided in Section B.4.

Likewise, Cho et al. [2008] reported normal hematology and clinical chemistry values for a subject whose serum silver level reached 15.44 μg/dL (normal range, 1.1–2.5 μg/dL) and urinary silver level reached 243.2 μg/L (normal range, 0.4–1.4 μg/L) after exposure to aerosolized silver at a mobile telephone subunit facility. The aerosol, which was reported to contain alcohol and acetone in addition to silver, was used for plating metal parts. Exposure controls were not used during the plating of silver, and the worker did not wear respiratory protection. No information was provided on silver species or particle size. The worker developed generalized argyria of the face, and a biopsy of the epidermal basal layer of the skin revealed the presence of silver granules.

Two studies evaluated health effects in workers exposed to AgNPs [Lee et al. 2011b; Lee et al. 2012a]. Exposure information from those studies is described in Section 2. Lee et al. [2011b, 2012a] reported that workers were exposed to airborne engineered AgNPs during particle synthesis (via an inductively coupled argon plasma process in one facility and the mixing of sodium citrate/silver nitrate in a second facility). Although traces of silver were detected in the blood and urine, all clinical chemistry and hematologic parameters were within the normal ranges, and no adverse health effects were reported for these workers. Other recent study reports of health effects in workers exposed to silver did not note particle sizes or exposure concentrations (Section 3.3).

In a case report, acute silver poisoning occurred in a young worker (age 27 years) who experienced a single "massive" exposure to silver vapors during the melting of silver ingots of "high purity" for 4 hours in a closed room without ventilation [Forycki et al. 1983]. The next day (approximately 14 hours later), the man developed headache and moderate dyspnea (shortness of breath). His symptoms worsened, and he was admitted to the hospital. His condition continued to deteriorate, with signs including "considerable" peripheral cyanosis; quick, shallow breathing; and elevated heart rate and blood pressure. Chest X-ray showed a pattern of "shock lung." The patient was put on artificial ventilation for a total of 18 days. After 4 weeks of treatment, the patient was moved to a rehabilitation facility and completely recovered. This case report suggests that very high (although unmeasured) exposure to silver vapor, which would be anticipated to include AgNP fume, caused severe acute respiratory health effects in the worker.

In summary, these studies of health effects in workers included those with exposures to silver particles of various types (soluble, insoluble) and from various processes (manufacturing, processing, and reclamation). Some of the findings included lung, liver, and kidney adverse effects, although none of these were statistically significantly associated with the measured airborne exposure concentrations or the blood or urine concentrations of silver. None of these study reports included the particle size. Argyria and argyrosis were the only effects clearly associated with measured silver exposure, and they were not associated with functional effects. The sample sizes in these studies were relatively small (a few workers in case studies to a few dozen workers), which may have limited the power to detect statistically significant effects related to exposure. The duration of exposure was generally short, relative to a full working lifetime. Some of the study reports noted confounding exposures to other toxic substances, including other metals (notably, cadmium) [Parikh et al. 2014; Rosenman et al. 1987; NIOSH 1992]. In addition, these studies were primarily of male workers, which would not allow for detection of possible gender-related effects, as observed in the animal studies (Section 5.2.3).

## 3.5 Health Effects in Humans with Nonoccupational Exposure to Silver

Trop et al. [2006] reported on a burn victim who had an argyria-like condition and elevated activities of liver-specific plasma enzymes when an Acticoat™ dressing (containing ionic AgNPs) was applied to his wound. No mention was made of silver being sequestered in the liver, although this was possible because levels of the metal were elevated in plasma and urine. As reported by the authors, local treatment with Acticoat™ dressings for 7 days caused the plasma activities of alanine aminotransferase (ALT) and aspartate aminotransferase (AST) to rise incrementally to 233 and 78 units per liter (U/L), respectively (upper limits of normal: 33 U/L for ALT and 37 U/L for AST). The concentration of silver in blood plasma was 107 micrograms per kilogram (µg/kg); this value subsequently dropped toward normal levels (13.3 µg/kg after 97 days) when Acticoat™ dressings were changed on day 8 to dressings containing betadine ointment. C-reactive protein level was also elevated, in parallel with plasma silver levels, reaching a maximum concentration of 128 milligrams per liter (mg/L) after 4 days. The level of this liver-synthesized marker for acute inflammation was back to normal (5 mg/L) after 8 silver treatment–free days.

In a prospective study of 30 patients with graft-requiring burns, Vlachou et al. [2007] found increased concentrations of silver in serum (median, 56.8 micrograms per liter [µg/L]; range, 4.8–230 µg/L) when Acticoat™ dressings were applied to the wounds. The authors found no changes in hematologic or clinical chemistry parameters indicative of toxicity associated with the silver absorption, and at the 6-month follow-up, the median serum level had declined to 0.8 µg/L. However, the absence of any toxicological effects of silver deposition from Acticoat™ dressings reported by Vlachou et al. [2007] contrasts with the findings of Trop et al. [2006].

It is unclear whether the liver perturbations were caused by silver deposition or were a response to the burns themselves. Thus, a review by Jeschke [2009] drew attention to the profound structural and metabolic changes in the liver of burn victims. Hepatic responses to thermal injury such as the formation of edema, release of proinflammatory cytokines, and activity of AST, ALT, and alkaline phosphatase (AP) have been shown to increase by up to 200% in the rat burn model [Jeschke et al. 2009].

The findings from burn victims treated with Acticoat™ do not provide adequate data to determine a threshold level of plasma silver that might be associated with the elevation of AST and ALT. The fluctuation in these markers of liver function deficits in the worker described by Trop et al. [2006] might be a consequence of thermal injury rather than wound treatment with silver [Jeschke 2009; Jeschke et al. 2009].

This page intentionally left blank.

# 4 Cellular and Mechanistic Studies Overview

## 4.1 Overview of Cell-based Silver Nanoparticle (AgNP) Studies

The effects of AgNP exposure have been studied extensively in mammalian cell models, especially murine- or human-derived lung or liver models [Hussain et al. 2005a; Shannahan et al. 2015; Gliga et al. 2014; Nymark et al. 2013; Kawata et al. 2009; Kim et al. 2009c]. AgNP exposure is reported to result in increased oxidative stress levels [Hussain et al. 2005a; Carlson et al. 2008; Foldbjerg et al. 2009; Kim et al. 2009c], the upregulation of pro-inflammatory cytokines [Carlson et al. 2008; Gaiser et al. 2013; Sarkar et al. 2015], and genotoxicity [Kermanizadeh et al. 2013; Piao et al. 2011; Gliga et al. 2014; Nymark et al. 2013] in several cell models. Other mechanisms of AgNP toxicity indicated in the literature include inhibited selenoprotein synthesis [Srivastava et al. 2012], induction of the unfolded protein response [Huo et al. 2015], cell cycle arrest [Beer et al. 2012; Chairuangkitti et al. 2013; Foldbjerg et al. 2012; Lee et al. 2011a], and disruption of the cytoskeleton [Guo et al. 2016; Ma et al. 2011]. Pretreatment with antioxidants mitigates many of the endpoints discussed above [Avalos et al. 2015; Chairuangkitti et al. 2013; Hsin et al. 2008; Kawata et al. 2009; Kim et al. 2009c].

Studies have indicated that although many toxic effects of AgNPs may be mediated through Ag ion release and that cells are often more sensitive to Ag ions than AgNPs [Beer et al. 2012; Foldbjerg et al. 2012], certain effects differ between AgNP- and ion-exposed samples [Liu et al. 2010b; Arai et al. 2015; Garcia-Reyero et al. 2014; Guo et al. 2016]. There are also indications that particle shape may affect inhalation toxicity [Schinwald et al. 2012; Schinwald and Donaldson 2012; Kenyon et al. 2012] and that smaller AgNPs have greater cytotoxic and genotoxic effects than larger AgNPs [Park et al. 2011c; Kim et al. 2012; Gliga et al. 2014; Sahu et al. 2014a; 2014b; 2016a; 2016b]. There remain few comparisons between different types of AgNP functionalization in the literature, a deficiency which prevents assessing many specific functionalizations or drawing a conclusion on their effects.

## 4.2 AgNP Exposure Increases Cytotoxicity and Oxidative Stress

A wide range of cellular assays have also been used to examine the oxidative stress and apoptotic effects of AgNPs in vitro. Key findings following exposure to either AgNPs or ionic silver include increased levels of reactive oxygen species (ROS) [Hussain et al. 2005a; Carlson et al. 2008; Foldbjerg et al. 2009; Kim et al. 2009c], induction of oxidative-stress-management genes [Kim et al. 2009c; Miura and Shinohara 2009], increased percentage of apoptotic cells [Hsin et al. 2008; Foldbjerg et al. 2009; Miura and Sinohara 2009], and attenuation of cytotoxic effects of silver by N-acetylcysteine (a glutathione precursor, ligand for ionic silver, and ROS scavenger) [Avalos et al. 2015; Chairuangkitti et al. 2013; Hsin et al. 2008; Kawata et al. 2009; Kim et al. 2009c].

A number of studies indicate that ionic silver can be more potent than AgNPs in some cellular assays for causing apoptosis [Foldbjerg et al. 2009] and reducing cell viability [Carlson et al. 2008; Greulich et al. 2009; Kim et al. 2009c; Miura and Shinohara 2009]. However, other studies provide evidence of a correlation between the increase in intracellular ROS and decreasing particle size [Carlson et al. 2008], and high levels of apoptosis and necrosis for both AgNPs and ionic silver [Foldbjerg et al. 2009, 2011].

Additionally, AgNP exposure has been linked to upregulation of pro-inflammatory mediators. Rat alveolar macrophages increased expression of tumor necrosis factor (TNF)-α, macrophage inflammatory protein (MIP)-2, and interleukin (IL)-1β after exposure to AgNP supernatant [Carlson et al. 2008], indicating these effects are likely a result of Ag ion release from AgNPs. In human monocyte–derived macrophages responding to *Mycobacterium tuberculosis* infection, it was demonstrated that although AgNPs increased expression of IL-1β and IL-8, AgNPs also decreased expression of IL-10 as well as nuclear factor (NF)-κB, potentially demonstrating compromisation of immune responses [Sarkar et al. 2015]. Upregulation of IL-1β, IL-8, IL-10, TNF-α, monocyte chemoattractant protein (MCP)-1, and IL-1RI transcripts has been demonstrated in human hepatoblastoma cells, and a greater response was observed after exposure to 10-nm AgNPs than to 30- to 50-nm AgNPs [Gaiser et al. 2013].

## 4.3 AgNP Exposure Induces Genotoxicity

AgNP exposure has also been linked to genotoxicity. DNA fragmentation as assayed by single-cell gel electrophoresis, or comet assay, has been detected in human liver [Paino et al. 2015; Kermanizadeh et al. 2013; Piao et al. 2011], lung [AshaRani et al. 2009; Gliga et al. 2014; Nymark et al. 2013], and mesenchymal stem cells [Hackenberg et al. 2011]. Markers of DNA damage response activation have also been observed following AgNP exposure, specifically H2AX phosphorylation in human liver cells [Kim et al. 2009c], lung cells [Gliga et al. 2014], and mouse embryonic stem cells and fibroblasts [Ahmed et al. 2008], as well as upregulation of DNA damage response and repair proteins [Ahmed et al. 2008]. AgNPs were also observed to induce micronucleus formation in Chinese hamster ovary cells [Kim et al. 2013a], human lymphoblastoid cells [Li et al. 2012b], and human liver and colorectal cancer cells [Sahu et al. 2014a; 2014b; 2016a; 2016b].

AgNP-induced oxidative stress and the resulting high level of ROS are potential reasons for the observed DNA perturbations causing DNA breaks and oxidative adducts. Both oxidative stress and genotoxicity were observed in the presence of Ag ions as well as AgNPs, and in each case these were mitigated by antioxidant pretreatment with N-acetylcysteine [Kim et al. 2009c; Foldbjerg et al. 2011]. It was also indicated that particle size had a statistically significant effect on genotoxicity. In colorectal cancer cells, 20-nm and 50-nm AgNPs induced micronuclei, but only 20-nm AgNPs induced micronuclei in liver cells [Sahu et al. 2014a; 2014b; 2016a; 2016b]. A similar size-dependent toxicity was observed in lung cells, where 10-nm AgNPs induced DNA fragmentation but larger particles did not [Gliga et al. 2014].

Interpretation of these in vitro findings in comparison with those from in vivo studies (Sections 5.2.1, E.1.2, E.2.1) is challenging. Study protocols and controls are highly variable across studies. Additionally, genotoxicity studies of transformed or cancer-derived cell lines may have limited relevance to predicting effects in vivo in animals and humans. The doses in in vitro studies can be much higher than those in vivo, and thus the in vitro results may not be predictive of the outcomes at much lower doses in vivo.

## 4.4 Other Cellular Effects of AgNP Exposure

Besides the cytotoxic, genotoxic, and ROS-generation-related effects, AgNP exposure has been linked to other endpoints. AgNP and Ag ions (from $Ag_2SO_4$) have been shown to interfere with selenoprotein synthesis in keratinocytes (HaCat) and pneumocytes (A549), specifically by preventing incorporation of selenium ions [Srivastava et al. 2012]. In bronchial epithelial (16HBE) cells, but not hepatoblastoma (HepG2) and human umbilical vein endothelial (HUVEC) cells, AgNP (20-nm) and Ag ions (from AgNO3) have been shown to trigger the unfolded protein response and upregulation of pro-apoptotic markers specific to that

pathway, relative to the mitochondrial pathway [Huo et al. 2015]. Several studies have indicated that AgNP exposure causes cell cycle arrest in fibroblasts (L929) [Wei et al. 2010] and pneumocytes (A549) [Beer et al. 2012; Chairuangkitti et al. 2013; Foldbjerg et al. 2012; Lee et al. 2011a]. Further, it has been noted that this effect was not caused by Ag microparticles [Wei et al. 2010] and is linked to the dissolved ion concentration [Beer et al. 2012; Foldbjerg et al. 2012] but is independent of ROS-dependent pathways [Chairuangkitti et al. 2013].

Alteration of cell cycle–related gene expression in fibroblasts [Ma et al. 2011] and hepatoblastoma (HepG2) cells [Kawata et al. 2009] was also documented. Cytoskeletal fiber-length reduction was observed following AgNP exposure in umbilical vein endothelial cells [Guo et al. 2016], and this effect was reflected at the gene expression level in fibroblasts [Ma et al. 2011]. Increased sensitivity of cystic fibrotic bronchial epithelial cells to AgNP-induced cytotoxicity has been reported [Jeanett et al. 2016]. Finally, AgNP exposure may increase the responsiveness of breast cancer cells to radiation exposure [Swanner et al. 2015].

## 4.5 Effects of AgNP Size, Functionalization, and Ion Release

The comparative in vitro cytotoxicity of elemental AgNPs and ionic silver has been examined in studies with mammalian cells, including human mesenchymal stem cells [Greulich et al. 2009; 2011], human monocytic cells [Foldbjerg et al. 2009], human HEPG2 hepatoma cells [Kawata et al. 2009; Kim et al. 2009c], human HeLa S3 cells [Miura and Shinohara 2009], human lung cells [Gliga et al. 2014], human umbilical vein endothelial cells [Guo et al. 2016], Neuro-2A and HepG2 cells [Kennedy et al. 2014], mouse macrophages [Arai et al. 2015], rat alveolar macrophages [Hussain et al. 2005b; Carlson et al. 2008], and mouse spermatogonia stem cells [Braydich-Stolle et al. 2010]. The results from these studies indicate that (1) the cellular uptake and toxicity can be modulated when AgNPs are functionalized with monosaccharides [Kennedy et al. 2014], (2) the mammalian cytotoxic response to elemental AgNPs appears to be influenced by the particles' physical and chemical characteristics, and (3) the response is similar to that observed with ionic silver, especially for AgNPs with small diameters (less than ~30 nm) [Park et al. 2011c; Kim et al. 2012; Gliga et al. 2014; Sahu et al. 2014a; 2014b; 2016a; 2016b].

Comparatively few reports of in vivo studies of AgNPs in experimental animals are available, whereas information on in vitro (cellular) studies with AgNPs is extensive. The in vitro studies indicate that AgNP uptake and localization in the cell appear to be dependent on the cell type. The surface properties and size of AgNPs also appear to be important factors. In summary, adverse physiologic and biochemical responses have been observed with AgNPs in isolated cells, including (1) formation of ROS, (2) cellular disruption, (3) impairment of cellular respiration, (4) DNA perturbation, and (5) stimulation of apoptosis. Unfortunately, insufficient information is available to compare the effective concentrations for the toxicological effects of AgNPs in the in vitro studies with the exposure concentrations and doses that brought about the agent-related responses in the in vivo studies. One of the reasons for this is the lack of sufficient characterization of the AgNPs used in experiments under the exposure conditions utilized, which makes it difficult to correlate any observed effect to the AgNP properties and the available dose (which may be affected by media components). The studies do indicate, however, that the larger surface area per unit mass of AgNPs, compared with larger respirable-size silver particles, is a cause of concern because it makes AgNPs potentially more reactive than larger silver particles and makes it more difficult to predict how they will interact with biologic systems [Reidy et al. 2013].

Exposure to AgNPs has also been found to generate more ROS than silver ions, suggesting that the ROS production is due to specific characteristics of AgNPs and not only to ion release [Liu et al. 2010b].

Although the dissolution of AgNPs accounts for at least a degree of toxicity observed with AgNP exposure, the effects cannot always be fully apportioned to the measured dissolved fraction of silver. Although certain AgNPs may have low solubility in certain media and conditions, their contact with biologic receptors may cause the release of ions that could be sustained over a long period. In addition to different dissolution rates in different biological media, soluble silver may undergo transformation to secondary particles (including zerovalent AgNPs) within biological fluids where the redox potential is available and this, in turn, could potentially affect toxicity in vitro and in vivo [Liu et al. 2012].

Differences in the intracellular behavior of AgNPs and dissolved ions have also been observed, including activation of differing response pathways [Garcia-Reyero et al. 2014] and differences in protein-binding tendencies (with AgNPs binding to proteins of high molecular weight and Ag ions binding to metallothioneins) [Arai et al. 2015]. Necrotic (rather than apoptotic) cell death may be more common after exposure to silver ions than after exposure to AgNPs [Guo et al. 2016].

Information is limited on the role of particle shape on the capacity to induce toxicity, but Stoehr et al. [2011] found AgNWs (length, 1.5–25 μm; diameter, 100–160 nm) to be more toxic to alveolar epithelial A549 cells than AgNPs (30 nm) and silver microparticles (<45 μm) at concentrations that overlapped in both mass and surface area. No effects were observed with AgNPs and silver microparticles on A549 cells, whereas AgNWs induced strong cytotoxicity, loss in cell viability, and early calcium influx that appeared to be independent of the length of the AgNWs.

In vitro studies provide information on the influence of physicochemical properties on the toxicity of AgNPs. However, it is not clear to what extent the mechanism of action for AgNP toxicity is related to specific physical-chemical properties, including particle size and shape, surface area, and release rate of silver ions, and it may involve a combination of these properties. Exposure of cells to silver particles and/or silver ions may elicit toxicity by different modes of action. Although the specific mechanisms may not be fully understood, most in vitro studies have shown that nanoscale particles are more toxic than microscale particles. A more detailed description of the in vitro studies of silver is provided in Appendix D.

# 5 Animal Studies Overview

## 5.1 Toxicokinetic Findings

Available data suggest that AgNPs or silver ions eluted from AgNPs can be absorbed via the inhalation, oral, parenteral, or dermal routes in humans and experimental animals. Differences in rate and degree of absorption varied according to route of exposure, particle size, degree of aggregation, dissolution rate, and/or nature of any surface coating or binding material, properties which may also be important in terms of toxicity. Although the rate of absorption varies by route of exposure, cumulative evidence on the systemic distribution of silver (irrespective of route of exposure to AgNPs) has shown the liver, spleen, and kidneys to be the primary organs in which silver accumulates [Takenaka et al. 2001; Kim et al. 2008; Sung et al. 2009; Song et al. 2013; Loeschner et al. 2011; Korani et al. 2011, 2013; Lankveld et al. 2010; Park et al. 2011a; Dziendzikowska et al. 2012; Lee et al. 2013a,d; Smulders et al. 2014; Huo et al. 2015; Bergin et al. 2016; Boudreau et al. 2016; Chen et al. 2016; Hendrickson et al. 2016; Recordati et al. 2016; Qin et al. 2016; Tiwari et al. 2017; Dasgupta et al. 2019]. Silver has also been shown to distribute to the brain and ovaries/testes following pulmonary and nonpulmonary routes of exposure (Figure 5.1) [Ji et al. 2007b; Kim et al. 2008; Kim et al. 2009b;Tang et al. 2008, 2009; Takenaka et al. 2001; Sung et al. 2008; Lankveld et al. 2010; Kim et al. 2010b; Park et al. 2010b; Park et al. 2011a; Dziendzikowska et al. 2012; van der Zande et al. 2012; Xue et al. 2012; Genter et al. 2012; Lee et al. 2013a,d; Braakhuis et al. 2014; Wen et al. 2015; Fennell et al. 2016; Patchin et al. 2016; Wang et al. 2016; Wesierska et al. 2018].

It is important to note that most studies that examine organ burden use the standard technique of either ICP-MS or -AES. This spectrometry-based technique does not distinguish between the particle or ionic form of the material without phase extraction, and silver has the propensity to precipitate from solution in the presence of chloride in various tissues during the digestion process, which may lead to an underestimation of tissue burden in some studies [Liu 2012; Loza et al. 2014, 2018; Poitras et al. 2015; Su and Sun 2015].

### 5.1.1 Pulmonary Exposure—Inhalation

Silver concentrations in lung tissue were observed following a subchronic (12-week) inhalation study in male and female rats [Song et al. 2013] in a dose-dependent manner. The silver concentrations following 12 weeks of exposure gradually cleared from the lung tissue during a 12-week post-exposure (recovery) period, but the lung silver concentration remained statistically significantly elevated ($p < 0.01$) relative to controls at the highest exposure concentration of 381 μg/m³. The lung clearance half-times ($T_{1/2}$) ranged from 28.5 to 112.9 days across dose groups and sexes (with no clear differences by either factor, in Tables X and XI of Song et al. [2013]). Silver concentrations also increased in a dose-dependent manner in all nonpulmonary tissues examined in male and female rats (except for brain in females) [Song et al. 2013]. During the 12-week recovery period, silver gradually cleared from most nonpulmonary tissues but remained statistically significantly elevated (relative to controls) in the liver and spleen at the high dose in male and female rats, as well as in the eyes in male rats at the medium and high doses. The distribution of silver to the eyes in rats following inhalation exposure [Song et al. 2013] appears to be consistent with argyrosis observed in humans exposed to silver (Chapter 3).

The absorption and distribution of AgNPs via the inhalation route were studied in female F344 rats

following a single 6-hour exposure to AgNPs at 133 μg/m$^3$; four animals per time point were killed and examined at 0, 1, 4, or 7 days post-exposure [Takenaka et al. 2001]. Immediately after exposure, silver was detected at elevated concentrations in the lungs, nasal cavity, liver, and blood, but the concentrations declined over time. A total of 1.7 μg of silver was measured in the lungs immediately after exposure had ended, although only 4% of the initial pulmonary burden remained after 7 days. Nanoparticles were detected in the blood on the first day (8.9 ng Ag per g tissue wet weight). The level of silver in blood decreased to approximately 4% of the initial dose, as silver was distributed systemically to organs including liver, kidney, heart, and tracheobronchial lymph nodes.

Distribution to internal organs following inhalation exposure has also been demonstrated in studies aimed at assessing toxicity, including a subchronic exposure study by Sung et al. [2009], a 28-day inhalation study by Ji et al. [2007b], a 4-day inhalation study by Braakhuis et al. [2014], a 1-day exposure by Kwon et al. [2012], and an inhalation study by Patchin et al. [2016]. Depending on duration of exposure, dose, and possibly particle characteristics, silver was measured in varying degrees in liver, kidney, spleen, olfactory bulb, brain, heart, and whole blood. A more detailed description of these and other inhalation studies, as well as studies utilizing alternative pulmonary exposure methods (intranasal instillation, oropharyngeal aspiration, intratracheal instillation), is provided in Appendix E.

### 5.1.2 Nonpulmonary Routes of Exposure

Recent studies have demonstrated that the liver is also a major site of redistribution when silver nanoparticles are administered via gavage, intranasal instillation, or intravenous injection [Lankveld et al. 2010; De Jong et al. 2013; Davenport et al. 2015; Hendrickson et al. 2016; Recordati et al. 2016; Wang et al. 2016] (Section E.1). For example, when citrate- or polyvinylpyrrolidone (PVP)-coated silver nanoparticles were intravascularly injected in mice, the spleen and liver had the highest silver concentrations at 1 day after exposure [Recordati et al. 2016]. In rats, intravenous exposure to 20-nm AgNPs showed redistribution preferentially to the liver, followed by kidneys and spleen, whereas larger nanoparticles in the vasculature were preferentially redistributed to the spleen, followed by liver and lung [Lankveld et al. 2010]. In a 13-week gavage study of AgNPs, silver accumulated in all major organs, including the liver. Organs of female rats accumulated more silver than the organs of male rats, and more silver accumulated in organs of rats receiving 10-nm AgNPs than those receiving 75- or 110-nm AgNPs [Boudreau et al. 2016]. Similarly, the liver is a major site of silver accumulation in AgNP inhalation studies [Takenaka et al. 2001; Song et al. 2013].

Within the liver of rats repeatedly injected intravenously with silver nanoparticles, silver has been reported to accumulate in Kupffer cells, in endothelial cells, and at sites of inflammation [De Jong et al. 2013]. In rats in a 13-week AgNP gavage study, silver granules were identified in liver portal triads by TEM [Boudreau et al. 2016]. In addition, in multiple tissues, AgNPs often accumulate within cells, whereas soluble silver tends to accumulate extracellularly, suggesting important differences in their biodistribution [Boudreau et al. 2016]. In the mouse injection study, silver accumulated in Kupffer cells, in portal and sinusoidal endothelial cells, and to a lesser extent in hepatocytes 1 day after a single injection [Recordati et al. 2016]. The accumulation of silver in Kupffer cells and liver endothelial cells is consistent with the scavenging functions of these cells in the mammalian liver [Krenkel and Tacke, 2017; Sorensen et al, 2012; Sorenson et al., 2015]. Kupffer cells are phagocytic cells, whereas liver endothelial cells tend to remove material by endocytosis, and both of these features are shared among mammalian species, suggesting that the finding of AgNP uptake by these cells in rats may be important in humans as well [Krenkel and Tacke, 2017; Sorenson et al., 2015].

Although rodent studies have generally not shown argyria or argyrosis in rodents exposed to silver by

any route, Walker [1971] described the distribution of silver in the tissues of "argyric" rats. Male Sprague-Dawley rats (age 8 weeks) were exposed to 6, 12, or 24 mM $AgNO_3$ in drinking water for 10 weeks, followed by 4 weeks of plain drinking water. Blocks of kidney, skin, eye, liver, and muscle were taken for electron microscopy. Rats given the lowest dose of 6 mM $AgNO_3$ "rapidly developed brown stained muzzles and teeth" [Walker 1971]. This change in tooth and muzzle skin color may be the rodent equivalent of argyria in humans. Boudreau et al. [2016] also reported the distribution of silver to the eyes in male and female Sprague-Dawley/CD-23 rats (exposed orally to 9, 13, or 36 mg/kg of 10, 75, or 110 nm AgNP, or 100, 200, or 400 mg/kg silver acetate daily for 13 weeks) (Section E.2.1). Toxicity studies of nanoscale or microscale silver in rodents have generally not examined the skin or eyes for color changes, because these are not commonly considered target tissues.

### 5.1.3 Sex Differences

Sex differences in biodistribution have also been observed in rodents. Following oral exposure in Sprague-Dawley rats, Lee et al. [2013a] found that silver accumulated in the gonads of both sexes; however, the levels in the testes persisted longer than in the ovaries. Persistence of silver in the testes over time, as well as in the brain, was also observed in rats following oral exposure [Van der Zande et al. 2012]. One commonality across studies examining sex differences in silver absorption and distribution, irrespective of route of exposure or species, was an increase in silver levels in the kidneys of females (Sung et al. 2008; Sung et al. 2009; Song et al. 2013; Dong et al. 2013; Xue et al. 2012; Kim et al. 2008; Park et al. 2010a; Lee et al. 2013a; Kim et al. 2009a; Kim et al. 2010a; Boudreau et al. 2016]. The accumulation of silver in the kidneys appears to be sex-specific, on the basis of results from 28-day, 90-day, and 12-week inhalation studies [Sung et al. 2009; Kim et al. 2011; Song et al. 2013; Dong et al. 2013] and 90-day oral studies [Kim et al. 2010a].

Both inhalation and oral exposure studies indicate that female rats have two to four times more silver accumulation than males in all kidney regions. In particular, the glomerulus in the kidney cortex of Fischer 344 female rats was found to contain a higher accumulation than in males [Kim et al. 2009a]. The AgNPs were also preferentially accumulated in the basement membranes of the renal tubules in the cortex, in the medium and terminal parts of the inner and outer medulla of female rats; they also were detected in the cytoplasm and nuclei of the interstitial cells in the inner medulla of the kidneys [Kim et al. 2009a]. These sex differences have been suggested to be associated with metabolism and hormonal regulation, because the kidneys are a target organ for several hormones, such as thyroid hormones and testosterone [Kim et al. 2009a]. Increased levels of silver in the spleen and gastrointestinal tract of female Sprague-Dawley rats compared to male rats were reported following oral exposure [Boudreau et al. 2016].

### 5.1.4 Physicochemical Properties Affecting Kinetics

In terms of the physical and chemical properties of AgNPs, studies indicate that solubility and size are critical factors in absorption and distribution of AgNPs. In general, soluble or "ionic" silver was absorbed faster and in greater quantity than AgNPs following pulmonary exposure [Arai et al. 2015; Wen et al. 2015] and oral exposure [Loeschner et al. 2012; Park et al. 2013; Bergi et al. 2016; Qin et al. 2016; Boudreau et al. 2016]. Smaller AgNPs were absorbed and distributed to a greater degree than larger silver particles following oral exposure [Boudreau et al. 2016], intravenous exposure [Lankveld et al. 2010; Dziendzikowska et al. 2012; Tang et al. 2008; Recordati et al. 2016], and pulmonary exposure [Braakhius et al. 2014; Patchin et al. 2016]. The effect of particle size on the biodistribution of AgNPs remains largely unstudied for dermal exposure.

Few studies have directly compared the effects of surface coating of AgNPs on kinetics following pulmonary and oral exposure. In a study by

Bergin et al. [2016], no differences were observed in biodistribution following oral exposure to PVP- or citrate-coated AgNPs. In a study of the pulmonary clearance of PVP- and citrate-coated AgNPs, Anderson et al. [2015] found a greater rate of clearance for the 20-nm PVP-coated material versus the 20-nm citrate-coated material. Systemic distribution was not examined by Anderson et al. [2015]. Following intravenous exposure of citrate- or PVP-coated nanoparticles, these nanoparticles showed a similar distribution pattern [Pang et al. 2016; Recordati et al. 2016]; however, polyethylene glycol (PEG)-coated materials (which are relatively neutral in charge and have a high affinity for binding protein) were more biopersistent, followed by branched polyethyleneimine (BPEI)-coated materials, compared to citrate- or PVP- coated materials [Pang et al., 2016]. Regardless of coating, silver distributed primarily to the liver and spleen. Ashraf et al. [2015] demonstrated that both uncoated AgNPs and dextran-coated AgNPs also target the liver and spleen following intravenous exposure; however, recognition and uptake of dextran-coated AgNPs were slower. Further research is needed to more fully elucidate the effects of coating and particle shape on the absorption, distribution, metabolism, and excretion of AgNPs by various routes of exposure, including following long-term exposure.

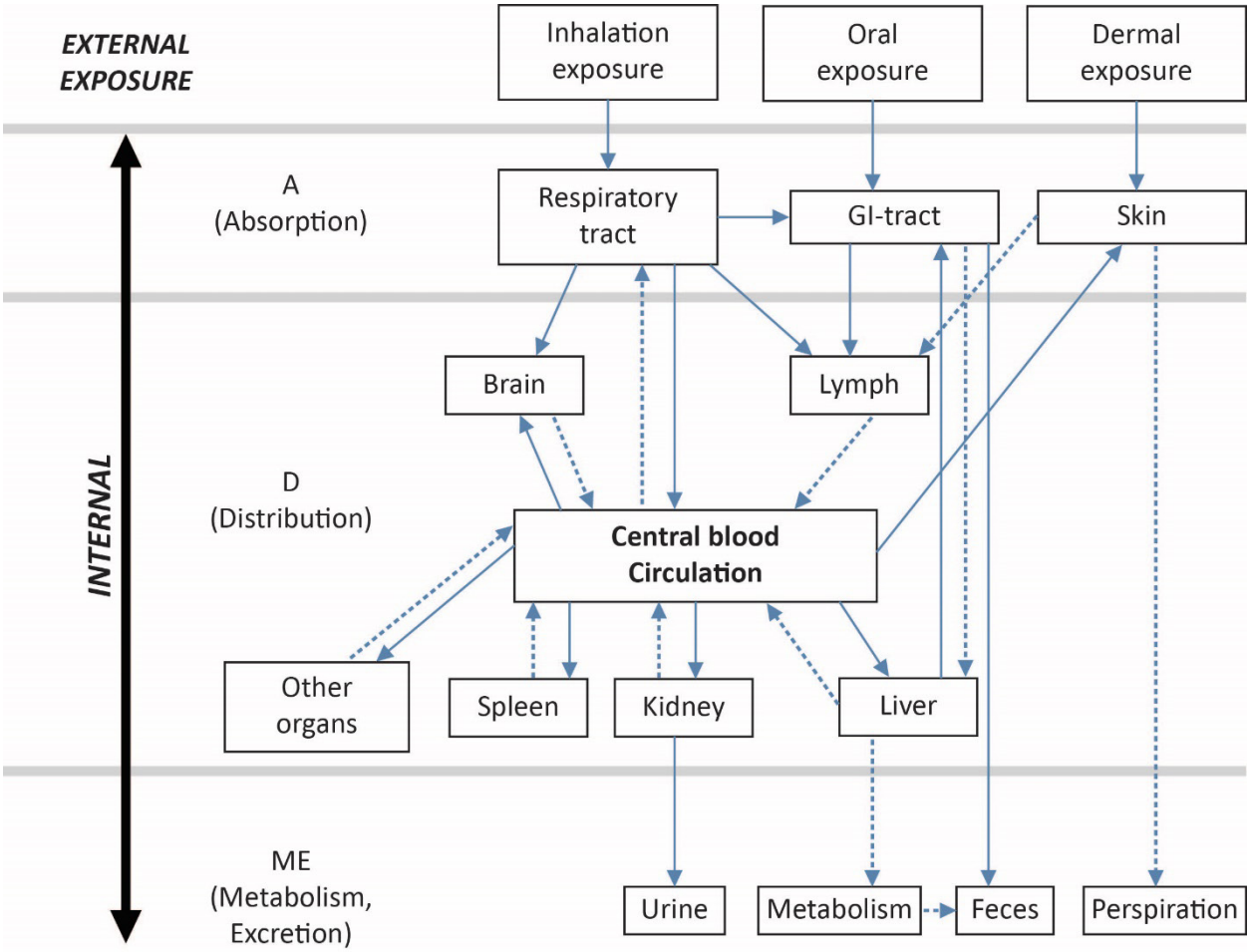


**Figure 5.1.** Systemic distribution of silver. The solid lines represent confirmed routes for silver (including AgNPs); the dashed lines represent possible routes and other organ sites (such as the heart and reproductive organs). Adapted from Hagens et al. [2007] and Oberdörster et al. [2005].

## 5.2 Toxicological Effects

### 5.2.1 Pulmonary Exposure

Inhalation studies in mammalian models provide the most physiologically relevant data for evaluating toxicity following respiratory exposure. The most comprehensive dataset on the potential toxicity of silver comes from studies of animals exposed by subchronic inhalation to silver nanoparticles [Sung et al. 2008, 2009; Kim et al. 2011; Song et al. 2013; Dong et al. 2013]. In these studies, male and female rats were exposed to silver nanoparticles with diameters ranging from 2 to 65 nm (median of 16 nm) at three different doses for 12 to 13 weeks. There was a dose-dependent accumulation of silver in the lung, liver, kidneys, blood, and brain [Song et al. 2013; Sung et al. 2009], as well as in the spleen, eyes, testes, and ovaries, with a greater degree of silver accumulation in the kidneys of female rats [Song et al. 2013]. Lung function changes and histopathological lesions in the lung occurred at the highest dose (381 μg/m$^3$) [Song et al. 2013; Sung et al. 2008; 2009], with lung function deficits persisting up to 12 weeks post-exposure in male rats, whereas female rats showed gradual recovery in lung responses over the 12-week post-exposure period [Song et al. 2013]. Systemically, bile duct hyperplasia and hepatocellular necrosis were observed in both male and female rats following exposure [Sung et al. 2008, 2009]. Genotoxicity studies were performed in the same animals from the subchronic inhalation studies. Kim et al. [2011] found no changes in micronucleus induction in bone marrow; however, Dong et al. [2013] did find variations in gene expression profiles when comparing the kidneys of male and female rats.

Following acute and subacute inhalation, lung inflammation ranged from nonexistent to minimal/moderate, with varying degrees of resolution over time [Stebounova et al. 2011; Kwon et al. 2012; Roberts et al. 2013; Braakhuis et al. 2014; Sieffert et al. 2016; Silva et al. 2016]. Lung function deficits, where present, were transient [Sieffert et al. 2016]. Goblet cell hypertrophy and hyperplasia were noted in one study [Hyun et al. 2008]. Systemic toxicity was also observed following acute or subacute inhalation exposure, including effects in liver [Ji et al. 2007b] and in brain [Lee et al. 2010; Patchin et al. 2016].

Pulmonary inflammation and lung function, with varying degrees of resolution over time, were also observed following acute or repeated aspiration, intranasal instillation, or intratracheal instillation [Park et al. 2011b; Roberts et al. 2012; Kaewamatawong et al. 2014; Smulders et al. 2014; Seiffert et al. 2015; Silva et al. 2015; Botehlo et al. 2016]. Mucosal erosion in the nasal cavity was also noted [Genter et al. 2012]. As with inhalation studies, exposure by aspiration or instillation resulted in systemic effects in the liver [Gosens et al. 2015; Huo et al. 2015], spleen [Genter et al. 2012; Davenport et al. 2015], kidney [Huo et al. 2015], and brain [Liu et al. 2012; Davenport et al. 2015]. No chronic studies on carcinogenicity, reproductive toxicity, or developmental toxicity following pulmonary exposure have been reported.

A recent study report may be the first to note that inhaled silver nanoparticles in mice accumulated in placental and fetal tissues and were associated with an adverse pregnancy outcome [Campagnolo et al. 2017]. An increased number of resorbed fetuses were observed in female mice that had been exposed to 18- to 20-nm silver nanoparticles by nose-only inhalation at an airborne concentration of 640 μg/m$^3$, for 4 hours each day during the first 15 days of gestation. The silver nanoparticles were freshly produced by a spark generator in an inert argon atmosphere. Estrogen plasma levels were reduced in the mothers, and inflammatory mediators were elevated in the lungs and placenta [Campagnolo et al. 2017].

### 5.2.2 Dermal, Oral, and Parenteral Exposure

Dermal exposure represents another potential route of occupational exposure. Data specifically related to AgNP exposure are limited. Several studies show minimal to no effect following acute exposure

[Kim et al. 2013b; Maneewattanapinyo et al. 2011]. In the acute and subacute studies where effects were observed, topical irritation at the contact site and focal inflammation/edema were observed [Korani et al. 2011, Samberg et al. 2010], and in one subacute study epidermal hyperplasia and graying of the skin were noted [Samberg et al. 2010]. Only one set of studies examined subchronic exposure, which resulted in skin effects similar to acute exposure and also caused histopathological changes in the liver and spleen [Korani et al. 2011] and in kidney and bone [Korani et al. 2013].

Effects observed in the liver, either as histopathological changes in tissue or changes in blood chemistry indicative of liver injury/disease, have also been extensively reported in relation to oral and parenteral routes of exposure [Kim et al. 2009b; Kim et al. 2010b; Tiwari et al. 2011; Lee et al. 2013b; Kim et al. 2008; Park et al. 2010a; Kim et al. 2010a; Yun et al. 2015; Elle et al. 2013; Katsnelson et al. 2013; Recordati et al. 2016; Qin et al. 2016; Wang et al. 2013; Dasgupta et al. 2019]. Kidney is also a likely target organ following exposure via oral and parenteral routes, with evidence of tissue and blood chemistry changes [Kim et al. 2010b; Park et al. 2010a; Yun et al. 2015; Qin et al. 2016]. Both oral and parenteral exposure also result in changes to blood hemocytology, including red blood cells, white blood cells, platelets, and hemoglobin [Tiwari et al. 2011; Katsnelson et al. 2013; Park et al. 2013; Qin et al. 2016], which may suggest other potential target organs such as the spleen.

Results from studies focusing on neurological effects in response to oral or parenteral exposure to AgNPs in terms of behavioral responses, memory responses, and biochemical changes in the brain have been variable; when effects have been noted, these have included changes in neurotransmitter levels and changes in gene expression [Rahman et al. 2009; Hadrup et al. 2012c; Dabrowska-Bouta et al. 2016; Wesierska et al. 2018]. Studies of intranasal instillation of AgNPs in rodents have shown oxidative stress in the brain, but effects on learning and memory were mixed [Genter et al. 2012; Liu et al. 2012; Wen et al. 2015]. These studies suggest that the brain may be a target organ for AgNPs and that the ionic form of silver may translocate to the brain to a greater degree than the particle form. However, more research is needed on the potential for neurotoxicity following AgNP exposure.

Reproductive toxicity was evaluated following oral, intravenous, and intraperitoneal exposure to AgNPs. In studies that observed toxicity, the most commonly observed effects in adult and prepubertal males included morphological abnormalities in the seminiferous tubules, reduction in spermatogenesis, and damage to and decreased viability of sperm [Gromadzka-Ostrowska et al. 2012; Sleiman et al. 2013; Miresmaeili et al. 2013; Mathiaas et al. 2014; Thakur et al. 2014; Lafuente et al. 2016]. Because effects in pregnant dams and in embryos/fetuses are highly variable, it is difficult to draw general conclusions related to pregnancy and embryo development [Philbrook et al. 2011; Austin et al. 2012; Mahabady et al. 2012; Wang et al. 2013; Yu et al. 2014; Kovvuru et al. 2015].

Effects in the gastrointestinal tract specific to oral exposure included a shift in microbiota populations in the gut after subchronic exposure [Williams et al. 2015], inflammation in the microvillus and damage to microvilli [Sharare et al. 2013], and increased goblet cells and secretions in mucins [Jeong et al. 2010]. The inflammatory effects are similar to those observed in respiratory mucosa [Hyun et al. 2008; Genter et al. 2012].

### 5.2.3 Sex Differences

As discussed above, differences were noted between male and female rats in absorption and biodistribution, irrespective of the route of exposure, with the most prominent difference reported to be increased levels of Ag in the kidney of females. In vivo studies have also correlated this difference with toxicity in the kidney of females. Dong et al. [2013] demonstrated that gene expression was differentially regulated in males and females following inhalation of AgNPs. Studies have shown increased kidney calcifications following oral exposure, which correlated with increased serum calcium [Yun et al.

2015], and have also shown increased allantoin in urine, indicative of oxidative stress [Hadrup et al. 2012a]. In addition to effects in kidneys, studies indicate oral exposure may also result in sex-related effects in the liver, although the findings vary in this regard. A number of studies have indicated increased serum liver enzymes in females [Kim et al. 2008; Park et al. 2010a; Yun et al. 2015]; however, Qin et al. [2016] demonstrated a greater increase in serum liver enzymes in males versus females. Blood cell profiles also differed between sexes following oral exposure, with increased white blood cells in females [Qin et al. 2016; Yun et al. 2015] and increased platelets in males [Yun et al. 2015]. Williams et al. [2015] found differences between sexes in effects on the gut microbiota as well.

### 5.2.4 Potential Mechanisms of Toxicity

Studies of AgNP-induced toxicity, irrespective of route of exposure, indicate oxidative stress as one of the primary mechanisms of toxicity in target organs. Following pulmonary exposure to AgNPs, evidence of oxidative stress in the lung has been indicated in lavage fluid as increased malonaldehyde (MDA) [Liu et al. 2013a; Seiffert et al. 2015, 2016] and as alterations or increases in glutathione (GSH), super oxide dismutase (SOD), and nitric oxide (NO) [Liu et al. 2013a]. Changes in GSH and SOD have also been measured in lung tissue [Kaewamatawong et al. 2014; Gosens et al. 2015] and the nasal cavity [Genter et al. 2012]. In addition, thiol-containing proteins, specifically metallothioneins, which are important in protecting against metal toxicity and oxidative stress, are increased in lung tissue [Kaewamatawong et al. 2014; Smulders et al. 2015a]. Increased GSH in spleen and Hmox1 expression in brain have also been measured after pulmonary exposure [Davenport et al. 2015]. Huo et al. [2015] found increased endoplasmic reticular stress in liver, kidney, and lung and increased apoptosis in lung and liver following pulmonary exposure; however, direct correlations of these parameters to oxidative stress were not delineated. Oxidative stress in target organs has also been evaluated following oral and parenteral routes of exposure. Oral exposure has resulted in increased MDA and NO in serum [Elle et al. 2013; Shrivastava et al. 2016] and superoxide anion in heart and liver [Elle et al. 2013], increased metallothionein in liver and kidney [Shrivastava et al. 2016], and increased markers of oxidative stress and DNA damage in urine [Hadrup et al. 2012b; Shrivastava et al. 2016]. Following parenteral exposure, increased levels of ROS have been measured in blood, lung, liver, and kidney, along with apoptosis in lung, liver, and kidney [Tiwari et al. 2011; Kim et al. 2010b], and an increase in apoptosis and oxidative stress–related gene expression was detected in the brain [Rohman et al. 2009].

### 5.2.5 Physicochemical Properties

As described earlier, a number of physical and chemical properties of nanomaterials have been considered to be important factors in toxicity, including shape, size, degree of agglomeration, surface area, chemical composition, surface charge, surface chemistry (coatings, capping agents, functional modifications), and dissolution rate. In turn, these factors, in combination with a specific route of exposure (different cell types, pH, surrounding physiologic fluids, etc.) influence the toxicokinetics of the materials (cellular uptake and tissue absorption, distribution, metabolism, and excretion of the material). The in vivo AgNP studies reviewed in detail in Appendix E for any given route of exposure are diverse in terms of species used, AgNP primary particle size and form, particle dose, use of reference materials/controls, and degree of characterization of particles as it relates to physical and chemical properties of the material.

One of the more consistent findings across studies appears to indicate that more soluble forms and small particle sizes of silver may be more toxic than larger particles [Johnston et al. 2010; Park et al. 2011a; Hadrup et al. 2012a,b; Gromadska-Ostrowska et al. 2012; Kim et al. 2012; Park et al. 2013; Gliga et al. 2014, Katsnelson et al. 2013; Arai et al. 2015; Qin et al. 2016; Silva et al. 2016]. These

studies indicate that AgNPs, because of their small particle size and large surface area per unit mass, facilitate the more rapid dissolution of ions than the equivalent bulk material, potentially leading to increased toxicity. This, coupled with the particles' capacity to adsorb biomolecules and interact with biologic receptors, may mean that AgNPs can reach subcellular locations, leading to potentially higher localized concentrations of ions once those particles start to dissolve or subsequently transform to other valence states or other Ag complexes in different biological fluids in situ. A small number of studies suggest larger particles may induce toxicity to a greater degree, depending on primary particle size and coating [Anderson et al. 2015b; Silva et al. 2015; Botelho et al. 2016]; however, the majority of the data suggest that the smaller particles are associated with increased biodistribution and toxicity. Whether this is related to the material itself (coating, solubility, agglomeration) or the specific toxicological parameter being investigated is unclear. Studies also show that although toxicity may be increased with increasing solubility, solubility does not account entirely for toxicity, and particles contribute to toxicity as well [Hadrup et al. 2012c; Holland et al. 2015; Qin et al. 2016]. Findings from studies that have compared surface coatings of the materials (primarily citrate or PVP) vary widely, and data available on AgNPs are insufficient to draw conclusions regarding coating and shape.

## 5.3 General Conclusions

As mentioned above, studies varied in the species, strain, dose, size, and form/coating of AgNPs (PVP, citrate, spark generated, CMC, colloidal), degree of characterization of the materials, and incorporation of controls or reference particles for different particle properties, making cross-study comparisons challenging. Despite these differences and with some exceptions, several broad conclusions can be drawn from the in vivo animal studies reviewed in this document.

Particle size and degree of solubility likely affect distribution of silver and, in turn, toxicity, with greater distribution or a higher rate of distribution and increasing toxicity with decreasing size and increasing solubility, irrespective of the route of exposure.

Sex differences in distribution and toxicity have been demonstrated, with the most common difference a greater accumulation of silver in the kidneys of females, irrespective of route of exposure (oral, intravenous, or pulmonary).

Dose-dependent effects are demonstrated in the primary organ systems related to the route of exposure (skin, lung, gastrointestinal tract); however, organ systems exposed to silver following absorption and distribution of AgNPs may be more sensitive to the toxic effects of silver. Liver is likely a target organ following AgNP exposure. In most studies, toxicological effects were demonstrated in liver, irrespective of the route of exposure or sex. Kidney and spleen are also likely target organs, depending on the route of exposure. Neurological and reproductive studies demonstrate long-term persistence of silver in the brain and testes; however, toxicological outcomes vary, and more studies are needed across various routes of exposure in this area to correlate distribution with toxicity.

When toxicity is observed following exposure to AgNPs, oxidative stress–induced tissue injury is indicated as one of the primary mechanisms.

A more detailed description of the experimental animal studies of silver can be found in Appendix E.

# 6 Hazard and Risk Evaluation of Silver Nanomaterials and Recommended Exposure Limit

## 6.1 Hazard Identification

### 6.1.1 Lung Effects

In the absence of data on human exposure to AgNPs, the findings from subchronic inhalation studies in rats [Sung et al. 2008, 2009; Song et al. 2013] were determined to be the best available data to evaluate the potential occupational health hazard of AgNPs. Although chronic exposure data are preferred, data from subchronic inhalation studies in animals are considered acceptable for deriving reference concentrations [U.S. EPA 1994], which involves risk assessment methods similar to those used in deriving OELs.

The lung effects associated with exposure to AgNPs in the rat subchronic inhalation studies are consistent with the definition of "specific target organ toxicity arising from repeated exposure to a substance or mixture" (STOT - RE) [OSHA Health Hazard Criteria, 29 CFR 1910.1200, A.9]. Lung inflammation and lung function deficits occurred in both male and female Sprague-Dawley rats following inhalation of AgNPs for 13 and 12 weeks, respectively, as reported by Sung et al. [2008, 2009] and Song et al. [2013]. The inflammation (chronic, alveolar) was reported to be of minimal severity in histopathologic evaluation [Sung et al. 2009; Song et al. 2013]. The lung inflammation had resolved by 12-week post-exposure in all but one rat exposed to the high dose of AgNPs (381 mg/m$^3$) [Song et al. 2013].

NIOSH considers the pulmonary inflammation observed in these rat studies to be relevant to humans. It is an early-stage adverse effect associated with inhalation exposure to AgNPs. In selecting an endpoint in risk assessment, it is important to understand the progression of disease and to select a measurable adverse effect as early in the process or with the least severity of effect as possible [NIOSH 2020].

Persistent (chronic) inflammation is a common cause of disease in humans, including in the lungs [Kumar et al. 2015]. Although the available AgNP inhalation studies in rats have been limited to subchronic duration of exposure or dose, chronic pulmonary inflammation with epithelial injury and dysfunctional resolution is associated with pulmonary fibrosis attributable to nonoccupational as well as occupational causes [Cotton et al, 2017; Meyer, 2017; Oberdörster et al, 1994]. In addition, pulmonary inflammation is implicated in occupational diseases associated with inhalation of organic and inorganic particles [Bisson et al. 1987; Castellan et al. 1987; Rom et al. 1991; Wang et al. 2005].

The pulmonary inflammation responses to silver nanoparticles observed in rats after subchronic inhalation are consistent with pulmonary responses to other respirable particles, including nanoparticles, following subchronic inhalation exposure in animals [NIOSH 2011, 2013]. However, the pulmonary inflammation was not persistent in most of the rats exposed to AgNPs after exposure was discontinued in a recovery study, resolving by 12 weeks post-exposure in all but one rat [Song et al. 2013]. In addition, pulmonary fibrosis was not documented in rats following subchronic inhalation of AgNPs [Sung et al. 2009; Song et al. 2013]. These findings indicate that the rat pulmonary inflammation response to AgNPs following subchronic inhalation is an early-stage effect of minimal severity.

Exposures at which this response is not observed therefore may be unlikely to be associated with adverse effects with chronic exposure. The selection of the rat pulmonary inflammation response in the risk assessment is consistent with "a measurable adverse effect as early in the process or with the least severity of effect as possible" that is relevant to occupational exposures in humans [NIOSH 2020].

Lung function deficits were also noted in both of the subchronic inhalation studies in rats [Sung et al. 2008; Song et al. 2013], including decreases in tidal volume, minute volume, peak inspiration flow, and peak expiration flow. The 49-$\mu g/m^3$ exposure concentration was a LOAEL for lung function deficits in female rats in the study by Sung et al. [2008], but in the study by Song et al. [2013], 381 $\mu g/m^3$ was the NOAEL (that is, no lung function deficits were observed at that concentration) in female rats. These results show large variability in the female lung function responses in the two studies. For male rats, 133 $\mu g/m^3$ was the NOAEL for lung function deficits in Sung et al. [2008], and it was 49 $\mu g/m^3$ in Song et al. [2013]. The difference in the number of rats in each exposure group ($n$ = 10 males and $n$ = 10 females in Sung et al. [2008]; $n$ = 5 males and $n$ = 4 females in Song et al. [2013]) may have contributed to the variability in responses observed in the two studies. The lung function deficits were dose-related, although it is unclear whether the level of reduced lung function reported from these rat studies would be considered clinically significant in humans (as discussed in Christensen et al. [2010]). In addition to lung function deficits, pulmonary inflammation was observed in these rats, as discussed below.

The NOAEL for pulmonary inflammation was 133 $\mu g/m^3$ in male and female rats in a study by Sung et al. [2009]. Song et al. [2013] reported that 117 $\mu g/m^3$ was the LOAEL in male rats and a NOAEL in female rats. In male rats, lung inflammation was observed at 117 $\mu g/m^3$, which had resolved by 12 weeks post-exposure (but was persistent in the 381-$\mu g/m^3$ group). In female rats, lung inflammation was not observed at 117 $\mu g/m^3$, and the inflammation observed in the 381-$\mu g/m^3$ exposure group had resolved by 12 weeks post-exposure. The rat lung inflammation data from the end of the subchronic inhalation (13 weeks [Sung et al. 2009] and 12 weeks [Song et al. [2013]) were used for the quantitative risk assessment (Table 6-1) (Section 6.3). NIOSH considers persistent pulmonary inflammation to be a relevant potential adverse health effect in workers because it has been associated with occupational exposures to some hazardous airborne particles [NIOSH 2011, 2013].

### 6.1.2 Liver Effects

NIOSH considers the liver effects observed in the subchronic (13-week) inhalation study in rats [Sung et al. 2009] to be relevant to estimating risk in workers. The liver effects associated with exposure to AgNPs in this rat study are consistent with the definition of "specific target organ toxicity arising from repeated exposure to a substance or mixture" (STOT - RE) [OSHA Health Hazard Criteria, 29 CFR 1910.1200, A.9]. Sung et al. [2009] observed bile duct hyperplasia of minimum or greater severity in male and female rats exposed to silver nanoparticles at 515 $\mu g/m^3$. The NOAEL for liver effects was 133 $\mu g/m^3$ (Section B.1). Silver was shown to accumulate in the liver in a dose-dependent manner [Song et al. 2013] (Section 5.1). In 3 of 10 female rats in the high-dose (515 $\mu g/m^3$) group, the bile duct hyperplasia was accompanied by a pattern of individual hepatocellular necrosis, which was not seen in control rats. One of these female rats had bile duct hyperplasia of moderate severity with concurrent moderate centrilobular fibrosis, necrosis, and pigmentation [Sung et al. 2009]. One of the affected rats also had moderate multifocal hepatocellular necrosis [Sung et al, 2009]. The presence of foci of minimal necrosis in two control rats, albeit with a different pattern, complicates the interpretation. No data were available to assess persistence of the liver effects in the rats following subchronic inhalation.

The finding of bile duct hyperplasia in rats [Sung et al. 2009, Kim et al. 2010a] from exposure to AgNPs is consistent with the elimination pathway through

the liver. Silver in the blood is removed via biliary excretion and eliminated from the body primarily in the feces, as noted in studies of workers [DiVincenzo et al. 1985; Wölbling et al. 1988].

Bile duct hyperplasia is often associated with aging in rats (which is not the case in the subchronic studies) [Eustis et al. 1990]. When bile duct hyperplasia is accompanied by inflammatory cells and/or oval cell proliferation, it can be caused by exposure to a toxic substance [NTP 2014]. The clinical significance of bile duct hyperplasia as an isolated lesion is not well known, but some evidence suggests that when accompanied by hepatobiliary injury, it is translationally relevant to humans. Some evidence suggests that cholangiocellular carcinoma can develop from bile duct hyperplasia [Kurashina et al. 2006]. Minimal biliary hyperplasia as an isolated finding in rats is sometimes considered non-adverse, particularly in the Sprague-Dawley rat, where the hyperplasia may be reversible after a recovery period [Hailey et al. 2014]. However, the authors of the review reaching that conclusion also noted that "serum or tissue markers of hepatocellular injury may serve as a sentinel for potential untoward biliary epithelial proliferations" [Hailey et al. 2014]. On the basis of these findings, NIOSH considers the response of bile duct hyperplasia in a subchronic inhalation study in rats [Sung et al. 2009] to be a potential adverse effect.

In addition, oral studies that examined liver effects in rats provide relevant supporting information. A subchronic (13-week) oral exposure study did not show hepatocellular necrosis in any of the 20 control rats, but focal, multifocal, or lobular hepatocellular necrosis was seen in rats in each of the exposed groups (2/10, 2/10, and 2/10 affected females in the low-, medium-, and high-exposure groups; 4/10, 5/10, and 4/10 affected males in the low-, medium-, and high-exposure groups) [Kim et al. 2010a]. In addition, clinical chemistry in the oral toxicity study supporting liver damage included elevation of serum cholesterol in male rats in the medium- and high-exposure groups and in female rats in the high-exposure group; increased alkaline phosphatase (AP) in female rats at the highest exposure; and increased total bilirubin in male rats in the medium-exposure group [Kim et al. 2010a]. Biliary hyperplasia, usually of minimal severity, was also higher after oral silver nanoparticle exposure. The concomitant presence of hepatocellular necrosis, biliary hyperplasia, and clinical pathology abnormalities in the oral toxicity studies indicates that the liver effects in male rats in the medium- and high-exposure groups and in female rats in the high-exposure group were adverse in this study [Kim et al. 2010a].

In a 28-day oral toxicity study of 42-nm-diameter silver nanoparticles in mice, AP and AST were increased in the serum of male and female mice at the highest exposure (1 mg/kg), and alanine transaminase was also increased in the female mice in this exposure group [Park et al. 2010]. Similarly, serum AP was increased in male and female Sprague-Dawley rats exposed to 1030.5 mg/kg AgNPs orally for 13 weeks [Yun et al. 2015].

Because of serum and/or histopathologic evidence of liver damage in rats or mice exposed to silver nanoparticles by the oral or intravascular routes, NIOSH considers the concomitant bile duct hyperplasia and single-cell hepatocellular necrosis observed in the group of female rats exposed by inhalation (515 μg/m$^3$ for 13 weeks) [Sung et al. 2009] to be a potential adverse effect. The bile duct hyperplasia of minimum or greater severity in male and female rats exposed by inhalation to 515 μg/m$^3$ is interpreted as part of an apparent continuum of silver nanoparticle–induced hepatobiliary damage and is therefore also considered potentially adverse [Sung et al. 2009]. In addition, the studies of silver nanoparticle biodistribution and acute hepatotoxicity from nonpulmonary routes of exposure (Section 5.1) provide additional relevant information to the interpretation of bile duct changes seen in subchronic toxicity studies. On the basis of the findings described in this section, NIOSH considers the rat bile duct hyperplasia response to AgNPs to be a potential adverse health effect in workers.

### 6.1.3 Biological Mode of Action and Physical-Chemical Properties

Few studies have directly compared the effects of nanoscale and microscale silver particles. Of those that do, the in vivo studies showed greater uptake and toxicity of nanoscale silver particles than microscale silver particles [Roberts et al. 2013; Braakhuis et al. 2014; Anderson et al. 2015; Patchin et al. 2016]. In addition, the in vitro studies generally showed greater effects following exposure to smaller particles [Park et al. 2010b, Philbrook et al. 2011, Silva et al. 2016; Sieffert et al., 2015], although some in vitro studies found that the larger particles were more toxic [Silva et al. 2015; Botelho et al. 2016].

According to the available toxicology information from studies in animals (reviewed in Section 5 and Appendix E), the biochemical and biophysical processes that may influence the dose-response relationships and the potential adverse health risk of occupational exposure to silver nanoparticles include the following:

- The dissolution rate of silver particles in the lungs and other tissues is associated with particle size and is faster for nanoscale than microscale particles.
- The binding of silver particles or ions to proteins and thiol groups in the body modifies the bioactivity of silver and increases silver uptake in liver and excretion.
- The toxicity of silver is related both to the release of ions (which occurs at a higher rate for nanoscale silver) and to the retention of silver particles in tissues.

Current knowledge on these biochemical and biophysical processes is based primarily on acute or short-term studies of silver. The role of these processes on the toxicity of silver nanoparticles following repeated exposures is not well known. Both poorly soluble and soluble particles can potentially cause adverse effects when inhaled into the lungs. The silver ions are typically associated with acute effects, which may resolve if the exposure does not continue [Roberts et al. 2013], although repeated exposures could result in higher doses of both ions and particles (which may also release ions over time, depending on site of disposition in the body and reaction with cellular proteins and other compounds). Ions released from soluble particles (such as $AgNO_3$) can react with cells and damage cell membranes, resulting in cell death [Cronholm et al. 2013; Zhang et al. 2014]. Smaller particles with greater surface area per unit mass would have a greater potential for ion release [Johnston et al. 2010].

Poorly soluble particles that are deposited in the pulmonary region of the lungs at doses that are not effectively cleared can trigger inflammatory responses, and particles that interact with epithelial cells lining the alveoli and translocate to the lung interstitial tissue can elicit fibrotic responses [NIOSH 2011, 2013]. Pulmonary fibrosis has not been found in the animal subchronic inhalation studies of inhaled AgNPs [Sung et al. 2008, 2009; Song et al. 2013] or in studies of workers in silver production or processing [DiVincenzo et al. 1985]. Inhalation is often the route associated with the highest potential for exposure in the workplace [Park et al. 2009; Miller 2010; Lee et al. 2011b; Lee et al. 2012a]; however, the applications and uses of silver nanomaterials could also influence the potential routes of exposure, including dermal and hand-to-mouth (oral) exposures. In addition to inhalation, workers may be exposed to silver particles or ions through dermal exposure or ingestion (for instance, as a result of mucociliary clearance of silver particles from the respiratory tract).

A study in rats showed that nanoscale (15-nm diameter) silver was more toxic than microscale (410-nm diameter) silver following subacute inhalation exposure (4 days, 6 hours/day) to similar airborne particle concentrations (179 or 167 $mg/m^3$, respectively); that is, pulmonary inflammation was observed in rats exposed to the nanoscale silver but not in those exposed to microscale silver [Braakhuis et al. 2014]. The two particle sizes were generated by different methods: the smaller NPs were made with a Palas spark generator, and the larger particles were

purchased as PVP-coated NPs and generated by nebulization. The inflammation in the rats exposed to the 15-nm-diameter AgNPs resolved by 7 days post-exposure. The 15-nm particles were shown to have a higher alveolar (pulmonary) deposition fraction than the 410-nm particles, resulting in a 3.5 times higher deposited mass dose (and 66,000 higher particle number dose). The 15-nm particles were observed in the rat lungs to have been reduced in size to <5 nm within 24 hours, suggesting relatively rapid dissolution in vivo of the nanoscale silver.

Acute inhalation studies in rodents suggest that soluble forms of silver are more biologically active and inflammogenic than poorly soluble silver particles [Braakhius et al. 2014; Roberts et al. 2013]. Decreased particle size has been associated with an increased rate of dissolution [Braakhius et al. 2014], suggesting that the greater toxicity of nanoscale to microscale silver is due in part to the increased generation of ionic silver. Some in vitro studies found that soluble silver was more bioactive than AgNPs (including reduction in mitochondrial function and decreased cell viability) [Foldbjerg et al. 2011; van der Zande et al. 2012]. However, at least one in vitro study showed that AgNP was more damaging to cells than was silver in solution [Piao et al. 2011]. The mechanism of AgNP activity may be different from that of soluble silver.

The size and composition of silver to which workers may be exposed can vary, depending on the product being manufactured, production method, and job/task within the facility. Workers can be exposed to a mixture of silver particle sizes (nanoscale or larger respirable or inhalable sizes) [Lee et al. 2011b]. In addition, workers can potentially be exposed to silver compounds (such as silver nitrate and silver acetate), which can exhibit different biologic availability and activity depending on the associated moieties. Potential worker exposure can occur during the use of silver in various applications and depends on the form of the silver or silver compound (such as dry powder or colloidal silver) [Drake et al. 2005]. In the case of colloidal silver compounds (such as used for disinfectant sprays), the ionic silver component can vary with the age of the product [Liu and Hurt 2010].

Studies in workers have shown that soluble forms of silver have been more frequently associated with the development of argyria than poorly soluble forms [as reviewed in ATSDR 1990; Drake and Hazelwood 2005; Wijnhoven et al. 2009] (Chapters 2 and 3). If the inflammation response is related to the release rate of ions during dissolution of the AgNPs, then the soluble/active portion of the dose estimates from the PBPK model [Bachler et al. 2013] may be more closely associated with the inflammation responses in the lungs, including with repeated exposures (up to a 45-year working lifetime).

A primary goal of occupational health risk assessment is to evaluate exposure-related adverse effects in experimental animals that are relevant to humans and to estimate exposure levels that would not likely result in adverse health effects in workers, even if exposed for up to a 45-year working lifetime. Understanding the physicochemical properties that influence their uptake and bioactivity is important to assessing the health risk of exposure to airborne particles. The inhalable and respirable mass fractions that deposit in the respiratory tract can be estimated with low uncertainty, based on aerosol measurement data and deposition models (e.g., MPPD [ARA 2011]). In contrast, the fate of AgNPs after deposition in the respiratory tract is an area of higher uncertainty, which pertains to the potential adverse effects of exposure to silver dust or fumes (including nanoparticles), especially with chronic exposure.

Animal studies have measured silver in various organs in the body, including lungs, liver, kidneys, and brain. The adverse effects observed in rats following subchronic inhalation exposures to AgNPs include chronic alveolar (pulmonary) inflammation and reduced lung function as well as biliary hyperplasia and necrosis associated with exposure to AgNPs [Sung et al. 2008, 2009; Song et al. 2013], suggesting that effects occur at both the site of entry and systemically. The role of silver nanoparticles vs.

ions in causing these effects cannot be determined from these studies. That is, effects could be due to the primary AgNPs used in exposure, ions formed by the dissolution of those AgNPs in vivo, and/or secondary AgNPs formed by condensation of those ions in vivo.

## 6.2 Quantitative Risk Assessment of Silver Nanoparticles

### 6.2.1 Animal Studies

The published rat subchronic inhalation data [Sung et al. 2008, 2009; Song et al. 2013] were used in this NIOSH risk assessment. These rat studies have also been evaluated in other risk assessments for silver nanoparticles [Stone et al. 2009; Christensen et al. 2010; Aschberger et al. 2011; Swidwinska-Gajewska and Czerczak 2015; Weldon et al. 2016]. Lung and liver effects in male and female rats were observed to be associated with exposure concentration or tissue dose of silver nanoparticles (Section 6.1). These subchronic studies were conducted according to current OECD and GLP guidelines [OECD 1995; Sung et al. 2009], and a standard subchronic inhalation exposure protocol was followed. Male and female rats were exposed by whole body inhalation to one of three exposure concentrations in each study, ranging from 49 to 515 μg/m$^3$ of airborne silver nanoparticles (18–20 nm in diameter, generated by a ceramic heater) [Ji et al. 2007a] or to air only (controls). The silver tissue doses were measured in the lungs, liver, and other organs. Exposure durations were 6 hr/d for 13 weeks in Sung et al. [2008, 2009] and 6 hr/d for 12 weeks in Song et al. [2013], followed by 12 weeks of recovery.

The airborne exposure concentration span in these rat studies (49 to 515 μg/m$^3$) covers the concentration of 100 μg/m$^3$, which is the ACGIH TLV® and MAK OEL for inhalable silver (Table 1-3). These exposure concentrations are considerably below those associated with the highest recommended exposure concentration of 100,000 μg/m$^3$ (100 mg/m$^3$) in an experimental animal study, according to standard toxicology methods for inhaled particles [Lewis et al. 1989]. An exposure concentration of 100 mg/m$^3$ could also be considered the MTD (i.e., maximum tolerated dose [Oberdörster 1995, 1997] or minimally toxic dose [Bucher et al. 1996]), because the MTD is recommended as the highest exposure concentration to be used in an experimental study [Bucher et al. 1996; Oberdörster 1997]. No evidence of toxicity that interferes with the study interpretation should be observed at the MTD [Bucher et al. 1996]. It is also recognized that the MTD would be lower for more toxic particles [Oberdörster 1997].

Particle clearance kinetics are relevant to evaluate with regard to the estimation of dose and response in rodents and humans. In rodents, overloading of lung clearance of particles occurs when particle exposures exceed the capacity of normal clearance mechanisms. This phenomenon has been observed with lung exposures to poorly soluble low toxicity (PSLT) particles of various sizes and shapes in rats and mice [Bolton et al. 1983; Morrow 1988; Ferin et al. 1992; Elder et al. 2005; Pauluhn 2011]. The particle volume dose was shown to be most closely associated with overloading of PSLT particles of various microscale diameters and different densities; the responses to overloading doses include decreased pulmonary clearance and increased particle retention rates [Morrow 1988; Oberdörster et al. 1992a].

In rats or mice exposed to nanoscale as well as microscale PSLT particles, the particle surface area dose was more closely associated with the overloading of lung clearance and increased neutrophilic inflammation [Tran et al. 1999; Oberdörster et al. 1992b; Elder et al. 2005]. In overloaded rats, as the retained particle dose increases, the sequence of responses includes persistence of pulmonary inflammation, development of fibrosis, mutagenesis, and eventually tumorigenesis [Oberdörster 1995; Driscoll et al. 1996, 1997; IARC 2010].

In humans, lung clearance kinetics differ from those in rats [Stöber et al. 1967; Snipes 1989; Kuempel et al. 2001; Gregorratto et al. 2010; ICRP 2015].

Humans have slower long-term particle clearance and increased lung retention that occur at lower doses than those associated with overloading in rats (~1–3 mg/g lung tissue [assuming 1-g average lung weight]) [Stöber et al. 1967; Snipes 1989; Muhle et al. 1991; Oberdörster 1995]. For example, in workers with dusty jobs, such as coal miners, retained particle mass lung burdens can reach >10 mg/g lung [Kuempel et al. 2001]. Pulmonary clearance rates in humans are approximately 10 times slower than in rats (first-order retention half-times of ~60 days in rats vs. ~693 days or greater in humans) [Snipes 1989; Pauluhn 2014; Bailey et al. 1985; ICRP 2015]. Several reviews describe in more detail the overloading in rats and implications to humans [ILSI 2000; Pauluhn 2014; Morfeld et al. 2015; Borm et al. 2015]. In the subchronic inhalation studies of AgNPs in rats [Song et al. 2009; Sung et al. 2013], overloading of lung particle clearance does not appear to be a factor in the observed responses.

Following subchronic inhalation exposure to AgNPs, the clearance rates of silver from the rat lungs [Song et al. 2013] were generally within the normal range of 60 to 90 days for pulmonary clearance of poorly soluble low-toxicity particles [Pauluhn 2014]; these findings suggest that overloading of particle clearance had not occurred. However, for AgNPs, it is expected that the clearance rates may be faster than those for poorly soluble particles, given that dissolution as well as macrophage-mediated clearance would be expected to occur. The rat pulmonary clearance half-times ranged from 28 to 43 days at the lowest (49 $\mu g/m^3$) and highest (381 $\mu g/m^3$) exposure concentrations of AgNPs. Longer clearance half times of 85 and 113 days were reported at the medium (117 $\mu g/m^3$) exposure concentration in male and female rats, respectively (Tables F-1 and F-2); however, these findings are not consistent with dose-dependent overloading of clearance and may instead reflect variability in experimental measurement. The pulmonary inflammation that was observed in rats at the end of the 12-week inhalation exposure to AgNPs (medium- and high-dose groups) had resolved by the end of the 12-week recovery period in all but one rat (male, high dose group) [Song et al. 2013]; this finding is another indication that the inhalation MTD had not been exceeded [Oberdörster 1995]. In addition, no statistically significant dose-related changes were observed in body weights or organ weights in Sung et al. [2009], or in body weights in Song et al. [2013] (organ weights not reported in the latter study), at the 1% level of significance. In addition, no toxicity that interfered with the study interpretation was reported in either study [Sung et al. 2009; Song et al. 2013]. No mortality occurred during or after exposure in Song et al. [2013]; however, one rat died during an ophthalmological examination in Sung et al. [2009]. Overall, these results suggest that pulmonary clearance was not overloaded and that the exposures did not exceed the MTD in these rat subchronic inhalation studies.

Subchronic studies in rodents are regularly used in quantitative risk assessment (QRA) and OEL derivation when adequate data from humans or chronic studies in animals are not available, as is the case for AgNMs. Chronic studies, if available, would be preferred for predicting adverse health effects from long-term exposures, such as over a working lifetime [U.S. EPA 1994]. NIOSH considers the subchronic inhalation studies and the supporting toxicological literature from in vivo and in vitro studies to be useful in the evaluation of the potential occupational health risks of inhaling silver nanoparticles. The subchronic inhalation studies used in the risk assessment [Sung et al. 2009; Song et al. 2013] were reported to be performed according to OECD and GLP protocols and guidelines [OECD 1995; Sung et al. 2009].

Other publications have also evaluated the health hazards and derived exposure limits for silver nanomaterials [Stone et al. 2009; Christensen et al. 2010; Aschberger et al. 2011; Swidwinska-Gajewska and Czerczak 2015; Weldon et al. 2016], based on the findings of the rat subchronic inhalation studies of silver nanoparticles [Sung et al. 2009; Song et al. 2013]. In the NIOSH updated literature searches, no additional subchronic (or chronic) inhalation studies of nanoscale or microscale silver were

found to have been published since those reported in the previous external review draft [NIOSH 2016a] (Section 1.3).

### 6.2.2 Basis for Conducting a Quantitative Risk Assessment

Although information is limited for assessing the potential adverse health effects of occupational exposure to AgNPs, the following evidence provides the rationale for conducting a QRA and developing a REL. First, the effects in the lungs and liver of rats are associated with the airborne exposure to silver nanoparticles and to the retained target-tissue dose of silver. These effects, which include early-stage pulmonary inflammation and bile duct hyperplasia (accompanied by liver necrosis at higher concentrations) are considered to be adverse and potentially clinically significant in humans. That is, if workers were exposed to equivalent airborne concentrations of silver over a period of time, it is assumed that they could also develop these effects. Second, silver is a high-volume nanomaterial with an increasing number of workers potentially exposed. Under the current REL for silver (total dust) of 10 μg/m$^3$ (8-hour TWA concentration), workers would be at higher estimated risk of developing these early-stage adverse lung and liver effects. For these reasons, and as discussed further in Sections 6.1.1 and 6.1.2, NIOSH concluded that there is a reasonable scientific basis for (1) assessing the risk of adverse health effects in workers from the rat subchronic inhalation data and (2) developing a REL for AgNPs.

Other assessments that utilized these rat data were evaluated for comparison to the NIOSH risk assessment and REL derivation for AgNPs. The studies by Christensen et al. [2010] and Weldon et al. [2011] were examined in more detail regarding the methods used to derive an OEL from the rat subchronic inhalation data. The assessments by Stone et al. [2009], Christensen et al. [2010], and Aschberger et al. [2011] are similar in the data and methods used, as are the OEL estimates derived. Among those studies, NIOSH selected the Christensen et al. [2010] study for further evaluation because it focuses on AgNPs only and provides more specific information. The Swidwinska-Gajewska and Czerczak [2015] assessment did not derive an OEL for the respirable fraction of AgNPs and so was not examined further in this context. The Weldon et al. [2016] assessment was selected for further evaluation because it utilizes another methodology for deriving an OEL for respirable AgNPs, which includes dosimetric adjustment methods similar to those used in the NIOSH risk assessment for AgNPs. Figure 6-2 shows the steps in the NIOSH risk assessment and REL derivation for AgNPs.

### 6.2.3 Point of Departure from Animal Data ($PoD_{animal}$)

A point of departure in the animal studies ($PoD_{animal}$) was an estimate of the exposure or dose associated with a level of no or low effect, typically an adverse health effect to be prevented in humans. The $PoD_{animal}$ in this risk assessment was estimated from the rat data on airborne exposure concentration, and the rat lung or liver response data were modeled with benchmark dose software (BMDS) [U.S. EPA 2012b]. The $PoD_{animal}$ in these analyses was the $BMCL_{10}$, which is the benchmark concentration, 95% lower confidence limit estimate, of the exposure concentration associated with an added 10% response compared to the control (unexposed) rats. The dose associated with a small increase in response (e.g., 10% added to background) has long-standing use as a benchmark response [Crump 1984]. The exposure-response data and BMDS modeling results for liver or lung effects are shown in Figures 6-2 and 6-3, respectively.

The $BMCL_{10}$ estimates for liver bile duct hyperplasia were 50.5 and 92.5 μg/m$^3$ in female and male rats, respectively (Table B-5). These estimates are lower than the NOAEL of 133 μg/m$^3$ for the liver bile duct hyperplasia response in male and female rats in Sung et al. [2009] but higher than the estimate by Weldon et al. [2016] of 25.5 μg/m$^3$ in female rats (based on a linear model of the relationship

between the liver tissue dose and the airborne silver concentration). The $BMCL_{10}$ estimates for all liver abnormalities were lower than those for liver bile duct hyperplasia in both this analysis (Table B-12) and that of Weldon et al. [2016]; however, bile duct hyperplasia was selected as the liver endpoint for use in risk assessment in both analyses, because it is a specific, quantifiable endpoint in rats that is considered relevant to humans. The lower $BMCL_{10}$ estimate in female rats (50.5 μg/m$^3$) was selected as the $PoD_{animal}$ for bile duct hyperplasia; the model fit to these data are shown in Figure 6-3.

The $BMCL_{10}$ estimate for pulmonary inflammation (minimum or higher severity) was 62.8 μg/m$^3$, based on the pooled male and female rat data from both subchronic inhalation studies [Sung et al. 2009; Song et al. 2013] (Figure 6-4; Table B-11). This endpoint was not used in the risk assessments of Christensen et al. [2010] or Weldon et al. [2016] (Appendix G). NIOSH found that the pooled data were sufficiently homogenous to be adequately fit with the same exposure-response model. That is, the airborne exposure concentration was sufficient to explain the variability in the rat pulmonary inflammation response to inhaled AgNPs without having to account for differences in study or sex (Appendix B).

## 6.2.4 Human-Equivalent Concentration Estimates

Three methods have been used by NIOSH and others to estimate human-equivalent concentrations (HECs) from the rat subchronic inhalation effect levels: the uncertainty factor method; the dosimetric adjustment factor (DAF) method; and PBPK modeling. HECs have been estimated with each of these methods. Details of these analyses can be found in this section and in Appendixes A, B, and G.

NIOSH evaluated all of these methods and determined that the DAF method was a reasonable match to the available data for silver nanoparticles. This determination was based on consideration of the nature of the data available and the complexity of the models and methods (Figure 6-1). In the DAF method, data are used to estimate the HEC from the $PoD_{animal}$ by accounting for differences in the deposited mass dose of inhaled silver in the respiratory tract of humans or rats. In applying this method, NIOSH uses scientific data when available to derive the individual DAFs; and when data are not available, uncertainty factors (UFs) are used. NIOSH also considers the PBPK model (Appendix A) to be a useful tool for exploratory analysis of HEC estimates, including at different durations of exposure and particle sizes and types of AgNPs. However, because of the greater complexity of the model and its assumptions, additional data are needed for further evaluation and validation (e.g., as discussed in U.S. EPA [2006]).

### *6.2.4.1 Dosimetric Adjustment Factor (DAF) Method*

NIOSH used a DAF method to account for the factors that influence the internal dose of inhaled particles across species and to extrapolate the dose estimates from animals to humans [ICRP 1994]. A benchmark dose is a statistics-based dose estimate that is preferred as the effect level when sufficient dose-response data are available; otherwise, a NOAEL is typically used [U.S. EPA 2012b]. The basis for the DAF method has been described by U.S. EPA [1994] and Jarabek et al. [2005]. NIOSH and others have used a DAF method in deriving OEL estimates for carbon nanotubes [NIOSH 2013a]. A recent application of these methods on silver nanoparticles has been reported by Weldon et al. [2016] (discussed further in Appendix G.2).

For inhaled particles, the key factors that influence the estimated particle dose in animals and humans include the following:

(a) Ventilation rates

(b) Deposition fraction of inhaled particles

(c) Exposure, clearance, and retention kinetics

(d) Interspecies dose normalization

Deposition fraction by respiratory tract region is based on the airborne particle size, the breathing pattern (e.g., nasal and/or oral), and the lung airway geometry. The respiratory tract region of interest is where the adverse effects are observed in the animal and/or human studies and represented in the dose-response data being analyzed.

Ventilation rate is the inhaled air volume per unit of time and depends on the basal metabolic rate in each species as well as breathing rate associated with activity level. The air intake per 8-hour workday (light exercise) [ICRP 1994] or the rat exposure (6-hour) day is used in this analysis.

Exposure duration and clearance kinetics determine the total deposited particle dose and the retained dose over time. Clearance or retention of inhaled particles depends on the biological clearance mechanisms in the respiratory tract region (e.g., alveolar macrophage-mediated clearance of particles in the pulmonary region; mucociliary clearance from the tracheobronchial region; expectoration or swallowing of particles in the nasopharyngeal region). Clearance can also be influenced by dissolution, as evidence suggests for silver nanoparticles [Song et al. 2013; Braakhuis et al. 2014]. Dissolution depends on chemical composition, particle size, and the biological medium. To the extent that the dissolution and transfer rates of soluble particles into blood depend primarily on the physicochemical properties of the material, the biokinetics of soluble particles may be similar across species [Dahl et al. 1991].

Normalization of the delivered dose adjusts for the differences across species that determine the effective dose (e.g., particle mass dose per unit of tissue surface area). The dose normalization, and thus the effective dose metric, depends on the biological mode of action.

Estimates for each of these factors are included in the total DAF to the extent that data are available. The data values used for these individual DAFs in the NIOSH risk assessment are described in Section 6.2.4.2.

The human-equivalent concentration PoD (HEC_PoD) is estimated by adjusting the animal PoD by the DAF as follows:

[Equation 6-1]

$$HEC\_PoD = PoD_{animal} / DAF$$

where $PoD_{animal}$ is the animal effect level selected for the PoD and DAF is the dosimetric adjustment factor, estimated as shown below:

[Equation 6-2]

$$DAF = (VE_H/VE_A) \times (DF_H/DF_A) \times (RT_H/RT_A) \times (NF_A/NF_H)$$

where VE is the ventilation rate (e.g., as total volume of air inhaled per exposure day, $m^3/d$) in humans (H) or animals (A); DF is the deposition fraction in the target respiratory tract region; RT is retention half-time of particles in the lungs; and NF is the interspecies dose normalization factor (e.g., by mass, surface area, or volume of target tissue).

The version of the DAF shown in Equation 6-2 is from NIOSH [2013, in Section A.6.3.1 of that document], and it is similar to other versions reported by U.S. EPA [1994], Jarabek et al. [2005], and Pauluhn [2010]. The DAF version in Equation 6-2 was also used by Weldon et al. [2016] for silver nanoparticles (discussed in Section G.2).

An advantage of using a DAF method to estimate the HEC_PoD is that it is a clear, evidence-based method that can be systematically applied and evaluated for the influence of alternative estimates. A disadvantage of this method is that it is not a comprehensive, biologically based model and assumes linear (proportional) relationships in the animal and human parameters that influence the inhaled dose. Factors that are not accounted for in the DAF method are typically addressed with UFs (Section 6.2.4.3). An example of the DAF and UF methods used by Weldon et al. [2013] and Christensen et al. [2010] to derive an OEL for silver nanoparticles is provided in Sections G.1 and G.2.

### 6.2.4.2 Selection of DAF values

The individual parameter values used to estimate the total DAF (Equation 6-2) are shown in Tables 6-3 and 6-4. Table 6-3 shows the factors applied to the exposure concentration associated with liver bile duct hyperplasia in female rats, and Table 6-4 shows the factors applied to the exposure concentration associated with pulmonary inflammation in male and female rats.

**DAF 1 — Ventilation rates:** Measured ventilation rates in humans, based on reference worker values [ICRP 1994], were used in these analyses. The parameter values and calculations to estimate the rat DAF 1 in the NIOSH analyses are provided in Section F.2. In Table 6-3, the rat ventilation rate is based on the female rat estimated average body weight (Section F.2) because the dose-response model of the data for liver bile duct hyperplasia in female rats [Sung et al. 2009] resulted in a lower (more sensitive) BMC estimate than that in male rats (Table B-5). In Table 6-4, the rat ventilation rate is based on the male rat estimated average body weight (Section F.2) because the pulmonary inflammation data on male rats [Song et al. 2013] were sufficient for dose-response modeling, whereas those on female rats were not (Table B-2). The pooled dose-response data for pulmonary inflammation in male and female rats [Sung et al. 2009; Song et al. 2013] were later found to be adequately modeled and provide a statistically better estimate of the BMD (Section B.1; Table B-11). The ventilation rates were 0.053 and 0.084 $m^3$/d for female and male rats, respectively, in the NIOSH analyses. These values are similar to the value of 0.1015 $m^3$/d used by Weldon et al. [2016] for female rats. Other measured or estimated values of the rat ventilation rate are discussed in Section F.2, and these values vary widely.

In the assessments of both NIOSH and Weldon et al. [2016], differences in the human and rat exposure durations were taken into account by adjusting for the total volume of air inhaled in 1 day by workers or by rats, as described above. Christensen et al. [2010] adjusted the rat NOAEL for human ventilation rate for light work vs. resting (10 vs. 6.7 $m^3$/d) (Section G.1).

**DAF 2 — Deposition fraction of inhaled particles:** Particle deposition fractions in the NIOSH analysis of the liver bile duct hyperplasia endpoint were based on the total respiratory tract dose of AgNPs in humans and rats because the total deposited dose of silver was considered to be a relevant dose metric for the systemic endpoint of liver bile duct hyperplasia. Weldon et al. [2016] used only the pulmonary deposition fraction (further discussion on the respiratory tract regions evaluated is under DAF 4). The DAF 2 value in rats from this NIOSH analysis also differs from that used by Weldon et al. [2016] (Equation G-8), because the MPPD v. 3.04 model for Sprague-Dawley rats [ARA 2015; Miller et al. 2014] was used in this analysis (corresponding to the Sprague-Dawley rats used in the Sung et al. [2009] and Song et al. [2013] studies), rather than the MPPD v. 2.11 Long-Evans rat model used by Weldon et al. [2016]. The Long-Evans was the only rat model available in the earlier version of MPPD (v. 2.11). The total respiratory tract deposition fraction of 0.95 for 18-nm silver nanoparticles in the Sprague-Dawley rat model (Table 6-3) is greater than a total respiratory tract deposition fraction of 0.62 based on the Long-Evans rat model (MPPD v. 3.04, default values for 300-g rat), apparently because of the greater deposition efficiency of the nanoparticles in the nasal–pharyngeal (head) region in the Sprague-Dawley rat (i.e., ~0.8 vs. 0.2 for Sprague-Dawley vs. Long-Evans rats, estimated in MPPD v. 3.04 for 18-nm CMD particles). As a result, the estimated deposition fraction of particles in the pulmonary region is substantially lower in Sprague-Dawley rats (0.0635) (Table 6-4) than in Long-Evans rats (0.28 from MPPD v. 3.04; or 0.29 reported by Weldon et al. [2016]). Christensen et al. [2010] did not adjust for differences in particle deposition in the respiratory tract in rats and humans. The oral dose that the rats may have received from grooming and ingesting silver nanoparticles that deposited on the fur during the whole-body inhalation exposure is unknown, although whole-body inhalation is the most common method for

chronic exposure studies [NIOSH 2020]. Inhalation provides a natural route of exposure and is preferable for the introduction of toxicants into the lungs [Driscoll et al. 2000].

**DAF 3 — Exposure, clearance, and retention kinetics:** In the NIOSH assessment, DAF 3 values were not used because of the lack of specific information on AgNPs and the uncertainty about the clearance rates of silver across species (Table 6-7). Faster pulmonary clearance rates of AgNPs, possibly due to dissolution, compared to those for poorly soluble particles are suggested in the rat subchronic inhalation studies [Sung et al. 2009; Song et al. 2013]. Much lower retained-mass lung burdens of silver were reported in the rat studies than would be expected from MPPD modeling of poorly soluble particles (Section F.3; Tables F-3 and F-4). Thus, NIOSH addressed the uncertainty in the long-term clearance and retention kinetics of AgNPs through the selection of UFs (Section 6.2.4.3). This approach is consistent with previous practice in DAF methods [U.S. EPA 1994; Jarabek et al. 2005], where a subchronic-to-chromic UF is applied in estimating the HEC when the $PoD_{animal}$ is based on subchronic rather than chronic data. Accounting for a possibly lower effect level at chronic exposure than estimated from subchronic data is supported by evidence that a steady-state tissue concentration of silver was not reached by the end of the 12-week exposure. That evidence suggests that higher retained tissue doses of silver would be expected at chronic exposures to the same airborne exposure concentration (assuming first-order clearance kinetics without overloading in rats) (Section F.1).

In contrast, Weldon et al. [2016] adjusted for assumed differences in interspecies clearance rates of AgNPs based on first-order clearance rates of poorly soluble particles [Snipes 1989] that were used by Pauluhn [2010] for carbon nanotubes, i.e., a human/rat ratio of 10 (Table 6-7). NIOSH notes that other information suggests that particle dissolution kinetics across species may be similar if the rates of dissolution and transfer of silver into blood depend on the physicochemical properties of the material rather than species-specific physiological factors [Dahl et al. 1991]. Thus, to the extent that the retention kinetics depend on dissolution of the silver nanoparticles, the retention rates may be similar across species. However, the dissolution rates can also depend on particle size [Braakhuis et al. 2014]. In the analysis by Christensen et al. [2010], clearance was not taken into account, and a simple adjustment for daily exposure time in rats vs. humans (6 vs. 8 hours) was used in that analysis. The limited information available on which to select an evidence-based DAF 3 is a large source of uncertainty in these assessments.

**DAF 4 — Interspecies dose normalization:** The factor used to normalize dose across species pertains to the target tissue associated with the benchmark response and the biological model of action. For the rat liver bile duct hyperplasia response, NIOSH used the total respiratory tract surface area (Table 6-3) to normalize the deposited dose of silver nanoparticles across species. This is because AgNPs depositing anywhere in the respiratory tract would have the potential to reach the liver (e.g., through AgNP translocation and/or dissolution into the systemic circulation, and/or oral exposure through swallowing). For the critical effect of pulmonary inflammation, NIOSH used the pulmonary target tissue surface area to normalize the rat dose to humans (Table 6-4), because the pulmonary inflammation response is associated with the particle dose in that region of the respiratory tract.

The human-to-rat ratios of either the total respiratory tract surface areas or the pulmonary region surface areas are similar within a given source (e.g., ~260 for either total or alveolar surface area ratios from Miller et al. [2010] or ~160 from U.S. EPA [1994]) (Section F.4; Table F-5). The alveolar surface area values for humans or rats reported by Stone et al. [1992] are greater than those reported in the other sources, although the ratios of values are similar to those reported by Miller et al. [2011] (Table F-5). The differences in the reported values may relate to the degree of inflation of the lungs during the measurements. [Note that the interspecies dose normalization ratio (DAF 4) is expressed

as A/H as calculated in this document (Equations 6-1, 6-2, and G-8). Thus, the equivalent ratio to ~260 H/A (Table F-5) is 0.0038 A/H (Table G-1).]

In the analysis of Weldon et al. [2016], the pulmonary surface area was used to normalize dose across species, although the critical effect used was the rat liver bile duct hyperplasia. They acknowledge that "[t]he deposition and subsequent dissolution of AgNP can occur throughout the respiratory tract" but considered the dose of silver in the pulmonary region to be the largest fraction, given the much faster clearance of particles in the upper airways. [As noted above, NIOSH considered that the AgNP depositing anywhere in the respiratory tract had the potential to reach the liver. In addition, the deposition fraction of inhaled particles in the total respiratory tract is higher than that in the pulmonary region, i.e., >60–90% vs. ~6–39% (Tables 6-3 and 6-4).] However, in practice, there is little effect of using either the pulmonary (alveolar) surface area or the total respiratory tract surface area for dose normalization; this is because the alveolar surface area makes up most of the total respiratory tract surface area, and the ratios across species are similar on the basis of either alveolar or total surface area (within a given study, based on the same methods) (Table F-5; Table G-1).

Alternative normalization metrics such as the total alveolar macrophage cell volume in humans or rats related to a pulmonary overload mechanism (e.g., as used by Pauluhn [2010]) could result in a different ratio (e.g., differing by a factor of ~4.5 compared to pulmonary surface area [NIOSH 2013a]); however, the overload mechanism for poorly soluble particles has not been reported for silver nanoparticles. As shown in Song et al. [2013], the lung burdens gradually cleared after the end of exposure (consistent with normal first-order clearance), while the lung burdens in rats exposed at the high dose (381 μg/m$^3$) remained statistically significantly elevated (relative to controls) at 12 weeks post-exposure.

**Total DAF:** The HEC is estimated by dividing the $PoD_{animal}$ by the total DAF (Equation 6-1) (Table 6-7). The data-based HEC estimate is further divided by UFs to account for uncertainties in the data used to estimate the HEC (Section 6.3) (Table 6-7). A health-based default is proposed for the DAF to be no less than 1 (i.e., assuming HEC is not greater than the $PoD_{animal}$). This default is used for the liver bile duct hyperplasia response (shown in Table 6.3).

#### *6.2.4.3 Uncertainty Factor Method and Selection*

UFs are used in the derivation of OELs from animal bioassay data to account for the uncertainty and variability in the scientific data available to extrapolate the animal dose to the human population (e.g., workers). When sufficient information is available, the HECs are first estimated by DAF adjustment of the $PoD_{animal}$ (Section 6.2.4.1 and 6.2.4.2). Where information is lacking, UFs are applied to the HEC to adjust for the main sources of uncertainty, as discussed in this section. UFs are used to estimate a safe exposure level for most of the exposed population, including sensitive subgroups [Dankovic et al. 2015].

The values of UFs typically used in occupational health risk assessment are shown in Table 6-5. These UFs include the following factors: (1) animal to human ($UF_A$) to account for possible interspecies differences in the toxicokinetics (influencing the internal dose) or toxicodynamics (influencing the biological response) in extrapolating the $PoD_{animal}$ to the average human; (2) human interindividual ($UF_H$) to account for interindividual variability in the human population, including sensitive subgroups; (3) LOAEL to NOAEL ($UF_L$) to adjust for the use, if applicable, of a higher effect level than the NOAEL or $BMDL_{10}$; (4) subchronic to chronic ($UF_s$) to account for the possibility that the subchronic critical effect that is the basis for the $PoD_{animal}$ could develop at a lower dose, or the incidence or severity of the effect could increase, with a chronic exposure duration; and (5) $UF_D$ to account for insufficient data and adjust for the possibility of identifying a lower PoD or a more sensitive effect if additional studies were available [Dankovic et al. 2015].

Although additional subchronic or chronic inhalation studies are preferred, the two well-designed subchronic inhalation studies [Sung et al. 2009; Song et al. 2013] more than meet the minimum data base criteria for estimating an inhalation reference concentration [U.S. EPA 1994; U.S. EPA 2002]. An oral subchronic study in rats is also available [Kim et al. 2010a], which provides supporting information regarding the liver effects associated with exposure to AgNPs [Sung et al. 2009] (Section 6.1.2). A number of studies in animals and cell systems provide information about possible biological and physicochemical mechanisms pertaining to the toxicity of silver nanomaterials (Sections 4 and 5). Based on these available data, NIOSH did not consider a $UF_D$ to be needed, which is consistent with other published risk assessments of AgNPs [Christensen et al. 2010; Weldon et al. 2016]. The findings of exposure-related lung and liver effects that include relatively early-stage, low-severity effects in the rat studies of AgNPs also suggest that a $UF_D$ was not needed in this assessment.

Table 6-6 summarizes the scientific evidence related to each of the UFs used in this assessment, as well as the values NIOSH considered to be appropriate to apply to the HEC. These UFs included the following values: $UF_A$ (1 for the TK portion of $UF_A$ since the DAF method was used to estimate the HEC; 2.5 for uncertainty in the TD portion); $UF_H$ ($\sqrt{10}$, or 3.16, for uncertainty in worker interindividual variability); $UF_L$ (1 since a LOAEL was not used); and $UF_S$ ($\sqrt{10}$, or 3.16, for uncertainty about the possible higher incidence or severity of effects with chronic exposure). The total UF was 25. Regarding the subchronic to chronic adjustment, NIOSH considered the available evidence to be insufficient to account for possible interspecies differences in the long-term retention kinetics of silver nanoparticles in estimating the HEC (Section 6.2.4.1); thus, it used $UF_S$ to adjust for uncertainty in the rat subchronic PoD. The value of $UF_S$ was based on the findings from studies that examined the subchronic and chronic exposure-response data [Naumann and Weideman 1995; Kalberlah et al. 2002]. The need to adjust for uncertainty in the subchronic to chronic PoD based on the rat subchronic inhalation studies is evidenced in the finding that the rat lung tissue doses of silver had not yet reached steady-state (as estimated in Section F.1), suggesting that higher lung burdens (and hence higher response) could be observed with longer exposure.

In other risk assessments of AgNPs, Christensen et al. [2010] used a $UF_S$ of 2, whereas Weldon et al. [2016] included a factor of 10 in their DAF for the estimated higher relative pulmonary retention half-time in humans (Sections G.1 and G.2). The total UF used in the NIOSH risk assessment was lower than that used in the assessments by Weldon et al. [2016] and Christensen et al. [2010] (Table 6-7). An overall consideration in the selection of the UFs in the NIOSH assessment was the early-stage, low severity of the adverse effects in rats used in the assessment (liver bile duct hyperplasia and pulmonary inflammation, which resolved in most rats after the end of exposure).

## 6.3 Derivation of NIOSH Recommended Exposure Limit (REL) for Silver Nanomaterials

A REL is estimated by dividing the lowest HEC by a total UF (Equation 6-1) (Table 6-7). The HEC is a human-equivalent estimate of the rat effect level, based on the pooled exposure-response data on pulmonary inflammation in male and female rats at the end of subchronic (12- or 13-week) inhalation exposure to silver nanoparticles [Sung et al. 2009; Song et al. 2013]. The rat effect level estimate ($BMCL_{10}$) is the benchmark exposure concentration, 95$^{th}$ percentile lower confidence limit estimate, of silver nanoparticles associated with an added 10% of rats developing pulmonary inflammation of minimal or higher severity, based on histopathological examination. The HEC estimate to the rat $BMCL_{10}$ of 23 $\mu g/m^3$ was derived from available data for dosimetric adjustment (Section 6.3).

The UFs used in occupational risk assessment (Table 6-5) were evaluated for application to the HEC estimates from the rat subchronic inhalation data. A total UF of 25 is suggested for the HEC (Table 6-6). That is, HEC_PoD / total UF = REL, or 23.1 μg/m$^3$ / 25 = 0.92 μg/m$^3$, or 0.9 μg/m$^3$ after rounding. Thus, the NIOSH recommended exposure limit (REL) for silver nanomaterials (≤100 nm primary particle size) is 0.9 μg/m$^3$, as an airborne respirable 8-hour TWA concentration.

The NIOSH REL for silver nanomaterials is set to protect workers from developing pulmonary inflammation due to airborne exposure to silver nanoparticles (15–20 nm in diameter) and is established from rat subchronic inhalation data. In addition, the REL should protect workers from developing liver bile duct hyperplasia, because the lower HEC estimate was used to derive the REL (Table 6-7). Similarly, the NIOSH REL for silver nanomaterials should protect workers from developing argyria, because much higher exposure concentrations (47–253 μg/m$^3$) over a 45-year working lifetime were estimated from the PBPK model of Bachler et al. [2013] to be equivalent by mass to the human skin tissue doses associated with argyria (Table A-10). The REL for silver nanomaterials based on rat data of subchronic inhalation exposure to 15- to 20-nm-diameter silver nanomaterials should also protect workers exposed to larger silver nanomaterials (up to 100-nm diameter), because the toxicological evidence suggests that the smaller nanoparticles are more toxic (Chapters 4 and 5).

NIOSH recommends that effective risk management control practices be implemented so that worker exposures to silver nanomaterials do not exceed the NIOSH REL of 0.9 μg/m$^3$ (8-hour TWA), measured as a respirable airborne mass concentration. Until the results from animal research studies can fully explain the mechanisms (e.g., shape, size, chemistry, functionalization) that potentially increase or decrease toxicity, all types of AgNPs should be considered a respiratory hazard and occupational exposures should be controlled at the REL of 0.9 μg/m$^3$. As new data become available, NIOSH may reevaluate these recommendations to determine whether additional recommendations are needed to protect workers' health.

## 6.4 Risk Characterization

This risk characterization section includes an evaluation of the overall evidence and a discussion of uncertainties in the available information. The main areas of uncertainty include limited available animal data (for one type of silver nanoparticles) and extrapolation of the rat subchronic early effect levels to workers with long-term exposures. These and related areas of uncertainty are discussed further below.

### 6.4.1 Relevance of Animal Responses to Humans

The utility of the rat as an animal model has been well established for particle inhalation studies. Many of the toxicity studies follow the OECD guidelines, which recommend the rat as the preferred species for inhalation toxicity studies [OECD 2009, 2018a, 2018b]. Qualitatively, the lung and liver effects appear to be relevant to humans (Section 6.2). The pulmonary inflammation and liver bile duct hyperplasia responses were early stage and included minimal or more severe lesions [Sung et al. 2008, 2009; Song et al. 2013]. As noted in Sections 1.2 and 6.1.2, hyperplasia is believed to be one of several factors involved in the development of cholangiocarcinoma, the biliary tract cancer of the liver [Rizvie and Gores 2014; Rizvi et al. 2014]. Minimal biliary hyperplasia as an isolated finding in rats is sometimes considered non-adverse and can occur in aged rats [Hailey et al. 2014; Eustis et al. 1990]. However, the rats in the subchronic study were not aged, and biliary hyperplasia was sometimes accompanied by evidence of hepatocellular injury, including necrosis [Sung et al. 2009]. The concomitant presence of both hepatocellular injury and biliary hyperplasia in rats is more frequently a concern than biliary hyperplasia alone [Hailey et al. 2014]. Thus, as noted in Section 6.1.2, biliary hyperplasia is considered to be potentially adverse. The lowest effect level estimates (as airborne

concentration or tissue dose) associated with those responses were used to estimate human equivalent tissue doses and airborne concentration (as 8-hour TWA for up to a 45-year working lifetime).

Areas of uncertainty include the extrapolation of these subchronic effects in rats to workers who may be exposed for up to a 45-year working lifetime. One study investigated the biopersistence of the lung effects in rats and the retention of silver in tissues [Song et al. 2013]. The lung inflammatory effects had generally resolved 12 weeks after the end of the 12-week inhalation exposure to 14-nm-diameter silver nanoparticles. Clearance of silver from the lung and other tissues was observed, and the lung tissue doses of silver were no longer statistically significantly elevated at the 49- and 117-µg/m$^3$ exposure concentrations. These findings suggest silver was cleared by normal clearance processes and that overloading of lung clearance had not occurred at the animal doses used in the risk assessment (i.e., NOAEL or $BMDL_{10}$). Pulmonary fibrosis was not reported as having been observed in rats exposed to silver nanoparticles [Sung et al. 2008, 2009; Song et al. 2013]. This finding is consistent with a biological mode of action of the silver ion release and/or the nanoparticles (prior to clearance) being related to the early lung effects, and with the observed recovery from those effects noted in the rats. However, the hematoxylin and eosin staining and examination by light microscopy in these studies do not exclude the possibility that subtle fibrosis, if it occurred, may not have been visible. It is also relevant to consider that workers could potentially be exposed daily during a working lifetime and thus could have a sustained pulmonary inflammation response to silver nanoparticles. Such sustained pulmonary inflammation is associated with the development of pulmonary interstitial fibrosis from non-occupational as well as occupational causes [Cotton et al. 2017; Meyer 2017; Oberdörster et al. 1994].

A limitation in the available data is the absence of information on the persistence of the adverse effects observed in the liver, including liver bile duct hyperplasia and necrosis [Sung et al. 2009]. Another area of uncertainty is the potential for adverse effects in other organs, especially with chronic exposures.

### 6.4.2 Biologically Active Dose Metric

The biologically active tissue dose causing the adverse lung and liver effects is not well understood. The most predictive dose metric could include the total particle mass (including silver that is biologically sequestered through binding with proteins and sulfhydryl groups) and/or the soluble/active silver particles (which are capable of releasing reactive ions). Only the PBPK model [Bachler et al. 2013] provides estimates of tissue doses (although Weldon et al. [2010] used a linear regression model to associate the airborne exposures and tissue concentrations). To date, no data are available to assess which of these dose metrics (total and/or soluble/active) is most closely associated with potential long-term effects in animals or humans. However, smaller particle size and ion release are associated with acute pulmonary effects [Roberts et al. 2013; Braakhuis et al. 2014]. Assumptions about the biologically active dose metric have a large influence on the estimates of the HECs in the PBPK modeling (Table A-9).

### 6.4.3 Human-Equivalent Tissue Dose

Human data on silver tissue doses in the general population or in workers provide reference points from which to evaluate the findings from the rat studies (Sections A.5.2, A.5.4, and A.5.5). The rat tissue concentrations of silver in the liver at the estimated effect levels [BMD ($BMDL_{10}$)] for bile duct hyperplasia were 0.023 (0.012) µg/g for males and 0.010 (0.06) µg/g for females (Table B-7). These estimates are similar to or lower than the average human background concentrations of silver in liver tissue of 0.017 µg/g, e.g., from dietary sources [ICRP 1960], or to the upper range of silver concentration measured in liver tissue in unexposed workers of 0.032 µg/g [Brune 1980]. The finding that the rat effect levels (liver tissue doses of silver) associated with liver bile duct hyperplasia are similar to the "background" level of silver in liver tissue in

the general human population [ICRP 1960] raises questions about the relevance of the finding to humans, because adverse liver effects have not been reported to be associated with silver exposure in workers or in the general population. A possible explanation is that the silver nanoparticles in the rat inhalation studies might have been more toxic (e.g., due to smaller particle size or other factors) than the silver to which the general population is exposed in the diet (orally) or the airborne silver to which workers were exposed. The worker studies revealed argyria and argyrosis associated with exposure to airborne silver particles (of various types and sizes) but did not reveal adverse liver effects in those workers (Section 3.3).

Another possible explanation is that the earlier stage bile duct hyperplasia (based on histopathology examination) reported to occur in the rat studies would not have been detected in the studies of workers since examinations to identify such lesions were not performed. The human studies were relatively small in terms of the number of workers examined and did not cover a full 45-year working lifetime, both factors which may have reduced the likelihood of detecting adverse liver effects, if any, associated with exposure to silver in workers. In addition, the silver to which workers were exposed was not reported to be nanoscale silver and may also have been different forms of silver.

Analytical measurement error could have been another factor. If the silver tissue doses were underestimated because of analytical challenges (e.g., as reported in NIEHS studies, Society of Toxicology 2015 annual meeting), the actual silver tissue mass dose associated with the adverse effects might have been higher than measured (and thus, the human background tissue levels could be below the true rat effect level). However, no information is available to assess this question, and only the one rat subchronic inhalation study report [Sung et al. 2009] has noted liver effects. The persistence of those effects is unknown.

The lung tissue concentrations of silver (nanoparticles and/or ions) in the rat studies were similar to or higher than those reported to occur in lung tissues of unexposed workers (0.06 μg/g) or smelter workers (0.28 μg/g) [Brune 1980] (Table A-5). The rat lung tissue concentration of silver at the BMD ($BMDL_{10}$) was 0.145 (0.033) μg/g (males, Song et al. [2013]) (Tables A-1 and B-8). The measured lung tissue concentrations of silver varied widely between the two rat subchronic studies, which at the NOAEL (no statistically significant inflammation) ranged from 0.081 μg/g for males in Song et al. [2013] to 5.45 μg/g for males in Sung et al. [2009].

No adverse pulmonary health effects have been reported to be associated with long-term occupational exposure to silver (Section 3.3); however, as noted above, the human studies were relatively small and exposures were less than a full working lifetime. Acute adverse lung effects were reported to occur in workers exposed to airborne concentrations of silver that were likely very high (although unmeasured), including silver nanoparticles emitted from heating silver [Forycki et al. 1983]. Qualitatively, the rat lung responses are considered relevant to workers (Section 6.1.1). Although the clinical significance of these early-stage effects is uncertain, the rat pulmonary inflammation response is consistent with "a measurable adverse effect as early in the process or with the least severity of effect as possible" [NIOSH 2020].

The current evidence on the role of particle dissolution and ion release on the acute lung effects [Roberts et al. 2013; Braakhuis et al. 2014] suggests that the soluble/active particle dose may be the most biologically relevant dose metric for the pulmonary effects. Given that workers could be exposed daily over a working lifetime, the REL estimates based on the soluble/active dose metric (Table A-10) may be the most relevant estimates for prevention of lung inflammation. Much lower concentrations (0.19–0.83 μg/m$^3$) are estimated for the total silver dose metric. The biological mode of action and relevant dose metric for liver bile duct hyperplasia are also uncertain.

### 6.4.4 Working Lifetime Equivalent Concentration

The estimation of working lifetime equivalent concentration depends on the deposition fraction of silver nanoparticles in the respiratory tract and on the clearance or retention of silver after deposition. The deposited dose of silver nanoparticles in humans or rats can be estimated with low uncertainty because of the availability of respiratory tract deposition models, which have been validated in a number of studies for microscale particles (and less extensively for nanoscale particles). The deposition efficiency in the respiratory tract depends on the airborne particle size distribution (aerodynamic diameter for microscale particles and thermodynamic for nanoscale). However, the fate of inhaled silver nanoparticles after deposition is not well known. Some information on the biokinetics of silver uptake, retention, and clearance is available from an earlier study of workers [DiVincenzo et al. 1985]. The airborne particle size of silver in that study was not reported, although the smelting and refining processes described could have included exposure to nanoscale silver aerosols.

### 6.4.5 Areas of Uncertainty

Uncertainties in hazard and risk assessments based on the rat subchronic inhalation studies [Sung et al. 2011; Song et al. 2013] include the following:

- Clinical significance to humans of the early-stage lung and liver effects in the rat subchronic inhalation study.
- Quantification of the tissue doses associated with the adverse effects in rats, and extrapolation of those doses to humans for up to a working lifetime.
- Role of the soluble/active vs. total silver tissue burden on the dose-response relationships for lung or liver effects.
- Lack of chronic studies in rats and on the potential for other adverse effects (e.g., neurotoxicity).

Information is lacking on whether the early-stage adverse lung and liver effects in the rat studies result in functional impairment. Inconsistent results were reported from the two studies within the same rat sex [Sung et al. 2008, 2009; Song et al. 2013]. For example, lung function deficits were measured in female rats at 49 μg/m$^3$ (LOAEL) [Sung et al. 2008] but not at 381 μg/m$^3$ (NOAEL) [Song et al. 2013]. The variability in these and other lung responses results in uncertainty about the functional significance of the lung effects in rats or as extrapolated to humans. No information is available on whether bile duct hyperplasia would lead to a clinically adverse effect.

Information on the chemical composition and physical state of AgNPs is limited in the rat studies and in the human studies as well. Thus, there is uncertainty about the extent to which the total silver or the soluble silver portion contributed to the adverse lung and liver effects associated with inhalation exposure to silver nanoparticles in the rat studies. In addition, to the extent that differences in the physicochemical characteristics of the silver particles influence the kinetics and toxicity of silver, the findings from the two subchronic inhalation studies used to derive the REL [Sung et al. 2009; Song et al. 2013] may differ from the findings of studies using other forms of silver. Despite the reported differences in the methods used to generate the silver nanoparticles and in the particle composition or coating, the general conclusions from the literature are that the small size and greater solubility of silver nanoparticles result in increased toxicity (Section 5.6).

The potential for adverse effects in organs other than the lungs and liver is unknown, especially with chronic exposure. For example, the potential for neurotoxic effects from inhalation of silver nanoparticles [Hubbs et al. 2011] is suggested from the exposure-related, statistically significant increase in silver in the brain tissue in one of the rat subchronic inhalation studies [Sung et al. 2009]. However, the lack of an exposure-related increase in the brain tissue dose in the other rat subchronic inhalation study [Song et al. 2013] raises uncertainty about the

extent of translocation of silver to the brain following inhalation exposure to nanoparticles and/or about the reliability of quantifying silver in tissue. In the latter study, the silver concentration in the brain tissue of unexposed (control) rats was fourfold higher (0.004 μg/g in females; not measured in males) than that in control rats in the Sung et al. [2009] study (0.001 μg/g in female or male rats). Those measurements were at the end of the inhalation exposure in both studies (week 12 or 13).

### 6.4.6 Sensitivity Analysis

Because of the limited available data for risk assessment of silver nanoparticles, a comprehensive sensitivity analysis was not feasible. However, the risk assessment included consideration of several alternative estimates. These include (1) an array of estimates of the dose of silver associated with the adverse lung and liver effects observed in the rat studies (Section 6.2.3) and (2) alternative assumptions that were examined in the estimation of the human-equivalent dose (Section 6.2.4). In addition, several response endpoints were evaluated from the rat study for possible PoDs in estimating the human-equivalent concentrations (Section 6.1). A range of PoD estimates was evaluated, including NOAEL and LOAEL, as well as $BMCL_{10}$ or $BMDL_{10}$ estimates (based, respectively, on either airborne exposure concentrations or internal tissue doses of silver) (Table A-1).

Alternative data and assumptions were evaluated in the application of the DAF and UF methods (Section 6.2.4). In the PBPK modeling method, alternative assumptions on particle size and solubility were considered in the PBPK model–based estimates of Ag tissue dose and equivalent airborne exposure concentrations (Tables A-7 through A-10); different durations of exposure (i.e., 15, 30, or 45 years) were evaluated (Table A-8); and comparisons were made of the PBPK model estimates to the limited available data on silver tissue doses in humans (Section A.5.2; Tables A-4 and A-5).

These findings showed that estimates of the animal effect levels and the HEC estimates varied by a factor of up to three orders of magnitude, depending on the animal effect level estimate (NOAEL, LOAEL, or $BMCL_{10}$) (Tables A-1 and 6-8), the particle size and type (15- to 100-nm-diameter particle or ionic Ag) (Tables A-7 and A-9), and the assumed biologically relevant dose metric (soluble/active or total silver) (Table A-9).

Also evaluated was the influence of the different risk assessment methodologies on the OELs derived by NIOSH in this document (Section 6.3) and by others [Christensen et al. 2010; Weldon et al. 2016]. The data used to derive these OELs (Table 6-7) were from the same subchronic inhalation studies [Sung et al. 2008, 2009; Song et al. 2013]. However, these risk assessments selected different rat responses as the critical effect (i.e., lung function deficits, lung inflammation, or liver bile duct hyperplasia); different PoD estimate types (NOAEL, LOAEL, or $BMCL_{10}$); and different dose metrics (airborne exposure or tissue dose of silver). In addition, these risk assessments used different DAFs and UFs, which vary by up to an order of magnitude (Section 6.2.4). The HEC and OEL estimates also vary by about an order of magnitude (Table 6-7). However, each of these OEL estimates for silver nanomaterials, by NIOSH and others, is a lower airborne mass concentration (0.1 to 2 $\mu g/m^3$) than the current NIOSH REL of 10 $\mu g/m^3$ for total silver (metal dust, fume, and soluble compounds, as Ag) and the other OELs for silver (up to 100 $\mu g/m^3$) (Table 1-3).

The sources of uncertainty that could not be evaluated quantitatively were characterized with regard to the available scientific evidence and needs for future research (Sections 6.4.5 and 8). These areas of uncertainty include (1) the clinical significance to humans of the adverse effects observed in the rat studies (discussed in Section 6.4.1), (2) the role of particle dissolution and clearance of AgNPs on the doses associated with the adverse effects observed in rats (described in Section 6.4.2), and (3) the potential for chronic adverse effects not observed in the subchronic studies (discussed in Sections 6.4.3 and 6.4.4). Nevertheless, despite these uncertainties, the overall review of the information shows

a coherent pattern indicative of a potential hazard and risk to workers from exposure to silver nanomaterials. As new information becomes available, the uncertainties may be reduced in the risk estimates of occupational exposure to silver nanomaterials.

## 6.5 Summary

The two subchronic inhalation studies in rats exposed to AgNPs [Sung et al. 2009; Song et al. 2013] were used by NIOSH and others to evaluate the potential occupational health risk of exposure to AgNPs and to develop OELs for silver nanomaterials (Section 6.3). The airborne exposure concentrations in these rat studies ranged from 49 to 515 μg/m$^3$, which spans the 100 μg/m$^3$ OEL (ACGIH TLV® and MAK) for inhalable silver (Table 1-3). These rat study exposure concentrations are considered to be below the MTD dose because no statistically significant dose-related changes were reported in body or organ weights, and no toxicity that interfered with the study interpretation was observed [Sung et al. 2009; Song et al. 2013]. The pulmonary clearance rates of silver were similar to normal rates for alveolar macrophage–mediated clearance of poorly soluble particles (i.e., no evidence of overloading) (Section 6.2.1).

The observed lung and liver effects in rats associated with subchronic inhalation of silver nanoparticles are considered to be relevant to humans (Section 6.4.1), although the clinical significance of these early-stage effects is uncertain (Section 6.4.5). The rat pulmonary inflammation response at the LOAEL resolved by 12 weeks post-exposure [Song et al. 2013] and pulmonary fibrosis was not reported as having been observed, suggesting that the pulmonary effects of AgNP exposure in the rat studies were early-stage and were not persistent (Section 6.4.1). Liver effects included hyperplasia at lower doses and necrosis at higher doses in the one subchronic inhalation study that showed liver effects [Sung et al. 2009]; however, no information on the persistence of these rat liver effects was available.

As described in the sensitivity analysis (Section 6.4.6), the HEC estimates from the rat effect levels vary according to the rodent data selected and the dosimetric methods applied (Tables 6-3, 6-4, and A-9). The smallest HEC estimates are from PBPK model estimates of the total silver tissue dose after a 45-year working lifetime exposure (Table A-10). Studies in rodents suggest that the soluble/active form may be the most biologically relevant dose metric for the observed acute inflammation responses [Roberts et al. 2013; Braakhuis et al. 2014] (Section 6.1.3). However, the role of the different forms of silver on long-term effects is not well understood and may involve both ionic and particulate forms of silver, as suggested from shorter-term studies both in vitro and in vivo (Sections 4.5 and 5.2.5).

In the external review draft (January 7, 2016) of this CIB, NIOSH considered the evidence to be insufficient to derive an OEL that is specific to particle size. Since that draft, a new risk assessment on silver nanoparticles was published [Weldon et al. 2016], and comments received from peer and public reviewers prompted NIOSH to reevaluate the available data and risk assessment methods. Although no new evidence was available in animals or humans that could be used in quantitative risk assessment, the current document provides a more comprehensive risk assessment with additional evaluations and comparisons of the available data and methods. An updated literature search provides further evidence of increased toxicity of nanoscale silver relative to microscale silver from in vivo and in vitro studies, as well as additional information on the biological modes of action and dose metrics. Uncertainties are discussed with regard to the estimated worker-equivalent concentrations that are based on the rodent subchronic effect levels. The OEL estimates depend on the data and methods used and the uncertainty factors applied (Section 6.4.6).

The OELs for silver nanoparticles derived in the risk assessment by NIOSH (Section 6.3) and others [Christensen et al. 2010; Weldon et al. 2013] vary by approximately an order of magnitude (Table

6-7); however, these OEL estimates are all substantially lower than the NIOSH REL of 10 μg/m³ for total airborne silver (Section 6.4.6) (Table 1-3).

The overall findings from the quantitative risk assessment indicate that a REL of 0.9 μg/m³ would protect workers from developing adverse lung and liver effects, as observed in rodents exposed to silver nanoparticles. These findings are consistent with general guidance on the application of an OEL for the "bulk material" to a nanoscale form of the material when data are insufficient to develop a nanomaterial-specific OEL [ISO 2014, 2016], i.e., the NIOSH REL of 10 μg/m³ for silver would be reduced by a factor of ~10 in applying those nanomaterial control-banding strategies. Workplace airborne exposures to silver nanomaterials were reported to be at concentrations as low as 0.02 μg/m³ (as silver metal) [Lee et al. 2011b] (Section 2); these findings provide evidence that silver can be measured at and controlled to airborne concentrations below the NIOSH REL of 0.9 μg/m³.

On the basis of the hazard review and quantitative risk assessment of AgNPs provided in this CIB and on prudent occupational health practice, NIOSH recommends that worker airborne exposures be controlled to below the REL of 0.9 μg/m³ for silver nanomaterials, as an 8-hour TWA concentration.

**Table 6-1. Rat subchronic inhalation study data for silver nanoparticles: response proportion for pulmonary inflammation (chronic, alveolar, minimal).***

| Rat Study and Sex | Response Proportion at Indicated Concentration† | | | |
|---|---|---|---|---|
| | 0 μg/m³ | 49 μg/m³ | 133 μg/m³ | 515 μg/m³ |
| Sung et al. [2009], Male | 2/10 | 3/10 | 2/10 | 8/9 |
| Sung et al. [2009], Female | 3/10<br>0 μg/m³ | 2/10<br>49 μg/m³ | 0/10<br>117 μg/m³ | 8/10<br>381 μg/m³ |
| Song et al. [2013], Male | 0/5 | 0/5 | 3/5 | 5/5 |
| Song et al. [2013], Female | 0/4 | 0/4 | 0/4 | 4/4 |

*Histopathology results from Tables 9 and 10 of Sung et al. [2009] and from Table XII in Song et al. [2013]; data at end of 13-week exposure in Sung et al. [2009] or at end of 12-week exposure in Song et al. [2013].
†Pooled response proportion (responders/total rats) by exposure concentration: 5/29 at 0 μg/m³; 5/29 at 49 μg/m³; 3/9 at 117 μg/m³; 2/20 at 133 μg/m³; 9/9 at 381 μg/m³; 16/19 at 515 μg/m³. $BMDL_{10}$ estimate is 62.8 μg/m³ (Table B-11).

**Table 6-2. Rat subchronic inhalation study data for silver nanoparticles: response proportion for liver bile duct hyperplasia (minimum or moderate).***

| Rat Study and Sex | Response Proportion at Indicated Exposure Concentration† | | | |
|---|---|---|---|---|
| | 0 μg/m³ | 49 μg/m³ | 133 μg/m³ | 515 μg/m³ |
| Sung et al. [2009], Male | 0/10 | 0/10 | 1/10 | 4/9 |
| Sung et al. [2009], Female | 3/10 | 2/10 | 4/10 | 9/10 |

*Histopathology results from Tables 9 and 10 of Sung et al. [2009]; data at end of 13-week exposure. These data could not be pooled because of heterogeneity in the male and female exposure-response data (Appendix B).
†$BMDL_{10}$ estimates are 92.5 and 50.5 μg/m³ for male and female rats, respectively (Table B-5).

**Table 6-3. Dosimetric adjustment factors (DAFs) proposed by NIOSH, applicable to liver bile duct hyperplasia response in female Sprague-Dawley rats after subchronic inhalation of silver nanoparticles [Sung et al. 2009].**

| Adjustment Factor: Human (H) or Animal (A)* | Human DAF | Rat DAF | Basis |
|---|---|---|---|
| 1. Ventilation per exposure day ($m^3$/d) (VE) (H/A)† | 9.6 | 0.053 | Human: male reference worker, 70 kg BW [ICRP 1994]<br>Rat: 196 g average female BW [Sung et al. 2009]; 0.15 L/min [U.S. EPA 1994] |
| 2. Deposition fraction, by respiratory tract region (DF) (H/A) | 0.6634 | 0.949 | Total respiratory tract, both species‡ |
| 3. Lung retention rate, long-term (RT) (H/A) | NA | NA | Clearance adjustment for subchronic to chronic differences in rat and humans addressed in uncertainty factors [Jarabek et al. 2005] given uncertain dissolution kinetics. |
| 4. Normalization of dose (A/H), surface area ($m^2$) | 63.8979 | 0.24647 | Total respiratory tract [Miller et al. 2011; U.S. EPA 1994] |
| **Total DAF** | 0.488§ | | Less than 1 |
| Default DAF | 1 | | Assume HEC is not greater than $PoD_{animal}$ |

Abbreviations: BW: body weight; HEC: human-equivalent concentration; NA: not applicable or not applied; $PoD_{animal}$: point of departure in animals (Section 6.2.3).

*Indicates order of factors in ratio in Equation 6-2.

†Air intake per exposure day ($m^3$/8-hour d) in humans is the reference worker average value [ICRP 1994]; in rats, this value calculation was based on average body weight, as shown in Section F.2.

‡MPPD v. 3.04 [ARA 2015] input parameters:

- Particle characteristics: 0.018 µm diameter (CMD); 1.5 GSD; density 10.5 g/$cm^2$ [Sung et al. 2009].
- Human: Yeh/Schum symmetric model in MPPD 3.04; oronasal normal augmenter; no inhalability adjustment; 1143 mL tidal vol; 17.5 breaths/min (equals 20 L/min [ICRP 1994]).
- Rat: Sprague-Dawley, symmetric model MPPD v. 3.04; BW 196 g; and associated MPPD parameters: 1.37 mL tidal vol; 131 breaths/min; inhalability adjustment.

§From Equation 6-2: 0.488 = (9.6 $m^3$/d / 0.053 $m^3$/d) × (0.6634/0.949) × (0.24647 $m^2$ / 63.8979 $m^2$)

**Table 6-4. Dosimetric adjustment factors (DAFs) proposed by NIOSH, applicable to pulmonary inflammation response in male and female Sprague-Dawley rats after subchronic inhalation of silver nanoparticles [Sung et al. 2009; Song et al. 2013].**

| Adjustment Factor: Human (H) or Animal (A)* | Human DAF | Rat DAF | Basis |
|---|---|---|---|
| 1. Ventilation per exposure day ($m^3$/d)† (VE) (H/A) | 9.6 | 0.084 | Human: male reference worker, 70 kg BW [ICRP 1994]<br>Rat: 345 g average BW male [Sung et al. 2009]; 0.23 L/min [U.S. EPA 1994] |
| 2. Deposition fraction, by respiratory tract region (DF) (H/A) | 0.386 | 0.0635 | Alveolar (pulmonary) region, both species‡ |
| 3. Lung retention rate, long-term (RT) (H/A) | NA | NA | Clearance adjustment for subchronic to chronic differences in rat and humans addressed in uncertainty factors [Jarabek et al. 2005], given uncertain dissolution kinetics |
| 4. Normalization of dose (A/H), surface area ($m^2$) | 102 | 0.4 | Alveolar surface area [Stone et al. 1992; NIOSH 2011, 2013] |
| **Total DAF** | 2.72§ | | |

NA: not applicable or not applied; BW: body weight.

*Indicates order of factors in ratio in Equation 6-2.

†Air intake per exposure day ($m^3$/8-hour d) in humans is the reference worker average value [ICRP 1994]; in rats, this value was calculated on the basis of average body weight, as shown in Section F-2.

‡MPPD v. 3.04 [ARA 2015] input parameters:

- *Particle characteristics*: 0.018 μm diameter (CMD); 1.5 GSD; density 10.5 g/$cm^2$ [Sung et al. 2009].
- *Human*: Yeh/Schum symmetric model in MPPD 3.04; oronasal normal augmenter; no inhalability adjustment; 1143 mL tidal vol; 17.5 breaths/min (equals 20 L/min [ICRP 1994]).
- *Rat*: Sprague-Dawley, symmetric model MPPD v. 3.04; BW 345 g and associated MPPD parameters: 2.42 mL tidal volume; 111 breaths/min; inhalability adjustment.

§From Equation 6-2: 2.72 = (9.6 $m^3$/d /0.084 $m^3$/d) × (0.386/0.0635) × (0.4 $m^2$/102 $m^2$)

**Table 6-5. Uncertainty factors in occupational risk assessment.***

| Factor | Source of Uncertainty or Variability | Default Values in Workers |
|---|---|---|
| $UF_A$ | Animal to human: Toxicokinetics (TK)<br>Toxicodynamics (TD) | Allometric scaling (TK)<br>2.5–3 (TD) |
| $UF_H$ | Human interindividual variability in TK and TD: workers | 3–5 |
| $UF_L$ | LOAEL to NOAEL adjustment | 1–10 |
| $UF_S$ | Subchronic to chronic exposure and effects | 2–100 |
| $UF_D$ | Database insufficiency | Not specified |

*Adapted from Table II of Dankovic et al. [2015], who cite ECHA (current version [2012]). A modifying factor (MF) is sometimes also used to adjust for uncertainties not addressed by the uncertainty factor (UF) [Dankovic et al. 2015].

**Table 6-6. Uncertainty factors (UFs) applied in estimating the human-equivalent concentration to the rat effect levels following subchronic inhalation exposure to silver nanoparticles.[*†]**

| Factor[‡] | Proposed Value | Rationale |
|---|---|---|
| Animal to human ($UF_A$) | 1 (TK)<br>2.5 (TD) | TK: Animal to human dose adjusted by the total respiratory tract deposition fractions and body weights (liver bile duct hyperplasia) or pulmonary deposition fractions and alveolar epithelial cell surface area (pulmonary inflammation); insufficient data regarding possible clearance rate differences, which are addressed in UFs<br>TD: No chemical-specific information on animal to human sensitivity; default TD estimate of 2.5 from WHO/IPCS [2005] |
| Human interindividual variability ($UF_H$) | √10<br>(3.16) | No chemical-specific information on which to base this factor, which includes both TK and TD considerations; worker population factors typically 3-5 [Dankovic et al. 2015]; because human studies of silver exposure (particle size unknown) have not suggested a sensitive subpopulation (Section 3), a minimum default value of ~3 appears to be reasonable |
| LOAEL used as PoD ($UF_L$) | 1 | Not applicable because rat $BMCL_{10}$ estimates were used as the PoDs |
| Subchronic to chronic ($UF_S$) | √10<br>(3.16) | Rat tissue concentrations of silver appear not to have reached steady-state in these subchronic studies (based on clearance half-time estimates) [Song et al. 2013], suggesting higher dose accumulation with chronic exposure, possibly causing increased incidence or severity of response; default estimate of ~3 used [Naumann and Weideman 1995; Kalberlah et al. 2002] |
| **Total UF** | 25 | |

$BMCL_{10}$: benchmark dose estimate, 95% lower confidence limit estimate; DAF: dosimetric adjustment factor; HEC: human-equivalent concentration; LOAEL: lowest observed adverse effect level; PoD: point of departure; TD: toxicodynamic; TK: toxicokinetic; UF: uncertainty factor.

*The rat PoDs were $BMCL_{10}$ estimates of bile duct hyperplasia or lung inflammation of minimal severity observed by histopathology examination in Sung et al. [2009] and Song et al. [2013] (Section 6.2.3).

†UFs were applied after application of DAFs to the rat PODs. The DAF and UF methods used by NIOSH are described in Section 6.2.4.

‡An additional factor for database insufficiency or severity of effects ($UF_D$ in Table 6-5) was considered not applicable to these analyses.

**Table 6-7. Summary of the scientific values used in the derivation of the NIOSH recommended exposure limit (REL) for silver nanomaterials, with comparison to values used in other studies.**

| Rat Effect Endpoint and Sex [Study Reference] | Rat PoD, µg/m³ | Total DAF | HEC, µg/m³ | Total UF | OEL Estimate (8-hour TWA), µg/m³ |
|---|---|---|---|---|---|
| **NIOSH (Sections 6.2.3 and 6.2.4; Tables 6-3 and 6-4)** | | | | | |
| Liver bile duct hyperplasia, $BMCL_{10}$, female [Sung et al. 2009] | 50.5 | 1* | 50.5 | 25 | 2.0 |
| Pulmonary inflammation, $BMCL_{10}$, pooled data for male and female [Sung et al. 2009; Song et al. 2013] | 62.8 | 2.72 | 23.1 | 25 | 0.92† |
| **Weldon et al. [2016] (Section G-2; Equation G-8)** | | | | | |
| Liver bile duct hyperplasia, $BMCL_{10}$, female [Sung et al. 2009] | 25.5 | 4.51 | 5.66 | 30 | 0.19 |
| **Christensen et al. [2010] (Section G-1)** | | | | | |
| Lung function decrement, LOAEL, female [Sung et al. 2008] | 49 | 2‡ | 25 | 75§<br>250§ | 0.33<br>0.1 |
| Lung and liver effects, NOAEL, male and female [Sung et al. 2009] | 133 | 2‡ | 67 | 100 | 0.67 |

*Default value (Table 6-3).

†The NIOSH REL for silver nanomaterials is based on this lower estimate.

‡Note that this is the inverse of the factor used in Christensen et al. [2010], who multiplied the rat effect level (NOAEL or LOAEL) by the DAF to obtain the HEC (vs. dividing as shown in these analyses); the DAF of 2 is from Equation G-1 [i.e., 1/(6 hr/8 hr × 6.7 $m^3$/10 $m^3$)]; note that the term adjustment factor, not DAF, was used by Christensen et al. [2010].

§Two different exposure scenarios in Christensen et al. [2010].

DAF: dosimetric adjustment factor; HEC: human-equivalent concentration; OEL: occupational exposure limit (including NIOSH REL); PoD: point of departure; TWA: time-weighted average (exposure concentration); UF: uncertainty factor.

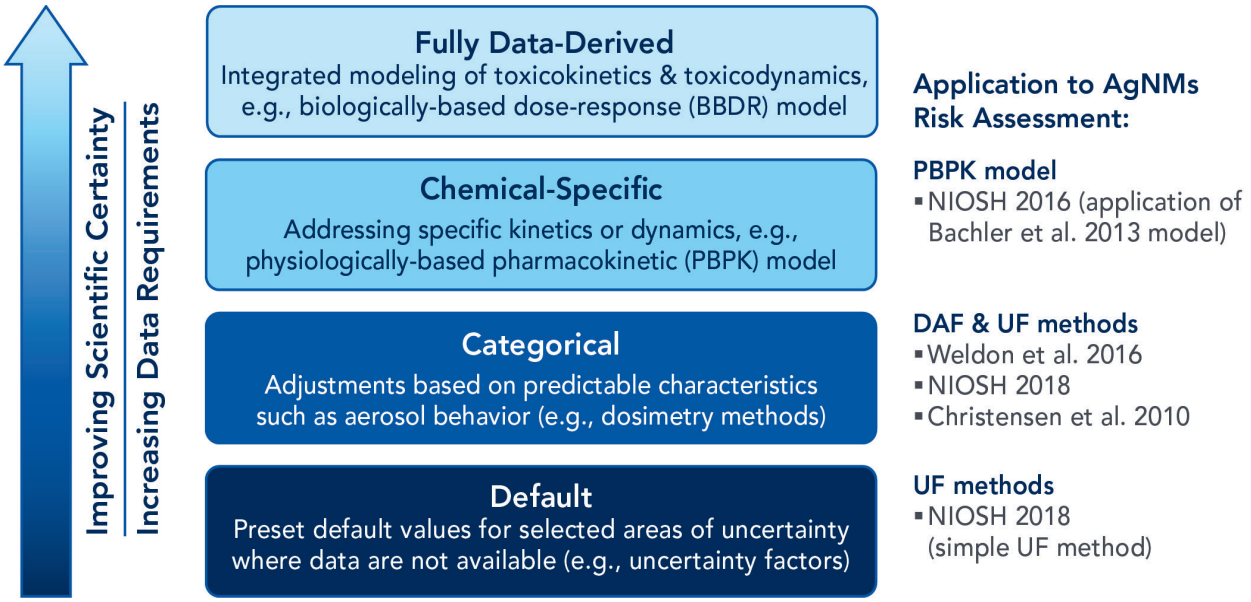


**Figure 6-1.** Hierarchy of risk assessment methods, with consideration of the available scientific data and the model complexity and data needs, as applied to silver nanomaterials (AgNMs). (Figure adapted from Dankovic et al. [2015] and Kuempel et al. [2015].)

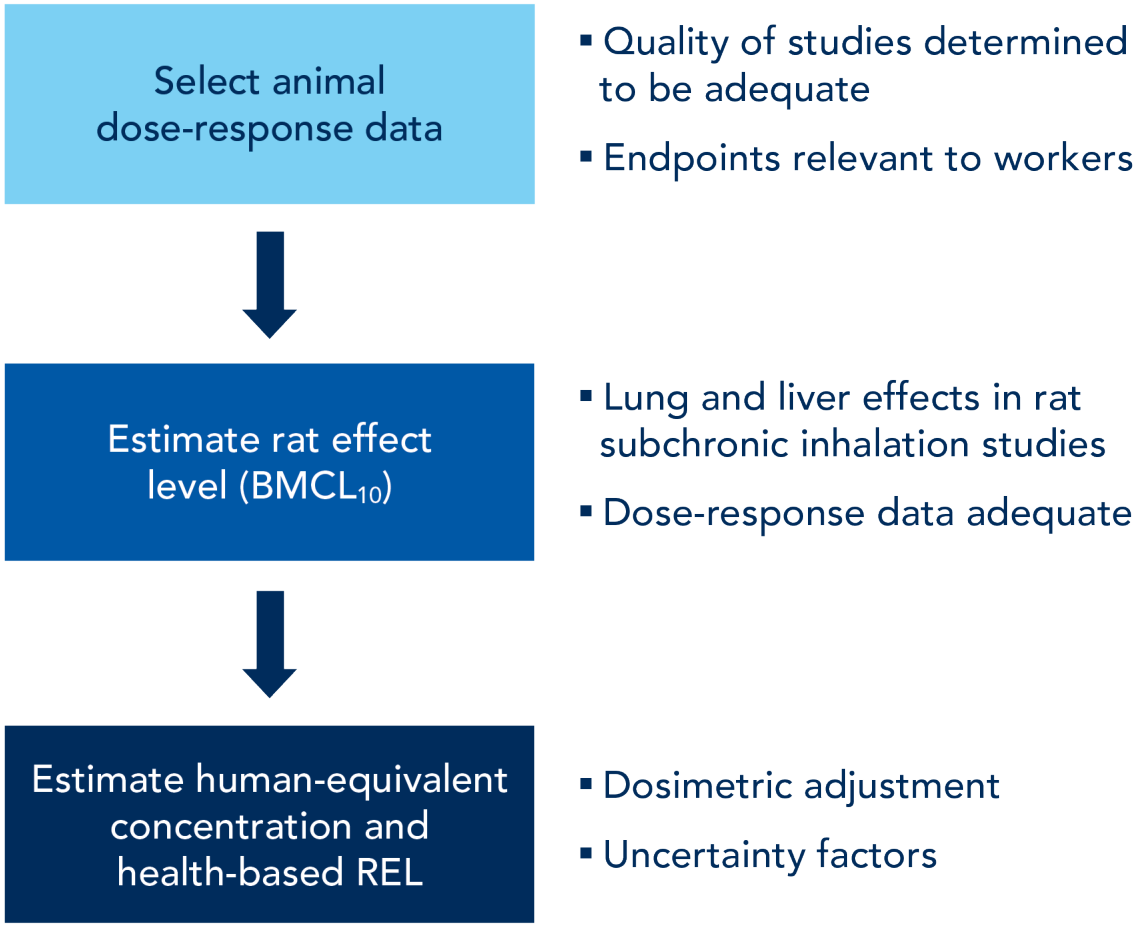


**Figure 6-2.** Summary of main steps in quantitative risk assessment and derivation of a recommended exposure limit (REL) for silver nanomaterials. The dose-response data used are from two rat subchronic inhalation studies [Sung et al. 2008, 2009; and Song et al. 2013]. Estimated $BMCL_{10}$: benchmark concentration, 95% lower confidence limit, is associated with 10% added risk of early-stage lung or liver effects (minimal or higher severity at histopathological examination) in rats. Risk assessment methods and data used are described in Sections 6.2.

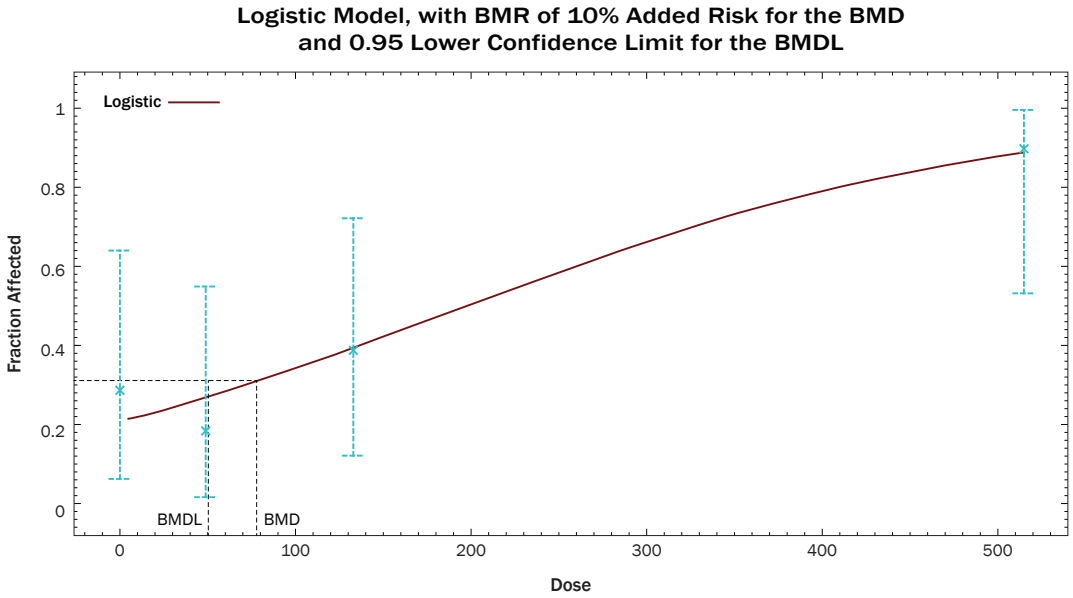


**Figure 6-3.** Exposure-response model (logistic) fit to the airborne concentration of silver nanoparticles (μg/m$^{3)}$ and bile duct hyperplasia proportion in female rats [Sung et al. 2009]. (Data and model results in Tables B-1 and B-5; same as Figure B-2.)

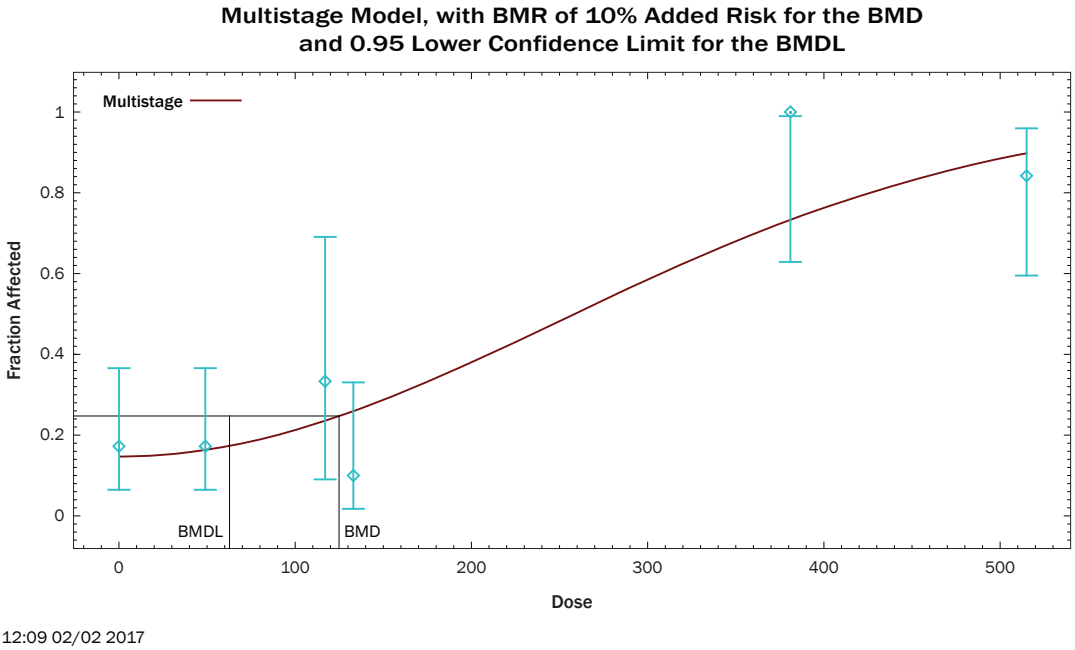


**Figure 6-4.** Exposure-response model (multistage polynomial degree 3) fit to the pooled data on airborne concentration of silver nanoparticles (μg/m$^3$) and chronic alveolar inflammation in male and female rats [Sung et al. 2009; Song et al. 2013]. (Data and model results in Table B-11; same as Figure B-9.)

This page intentionally left blank.

# 7 Recommendations

NIOSH recommends that risk management control practices be implemented so that worker exposures to silver nanomaterials (primary particle size ≤100 nm; metal dust, fume, and soluble compounds, as Ag) do not exceed the NIOSH REL of 0.9 μg/m$^3$ (8-hour TWA), measured as a respirable airborne mass concentration. A nanoparticle is defined as having a primary particle size of ≤100 nm [ISO 2008]. These terms are discussed in more detail in the Terminology/Glossary definitions of the terms *nanomaterials*, *silver nanoparticles (AgNPs)*, and *primary particle, aggregate, and agglomerate*. Exposure measurement and analysis methods are needed to determine whether an airborne respirable particle sample includes silver nanomaterials (Section 7.1).

The NIOSH REL for silver nanomaterials is based on prevention of early-stage adverse health effects in the lungs and liver in workers. The animal studies that provided the quantitative data for developing the REL involved airborne exposure to AgNPs with primary particle diameter of ~15–20 nm [Sung et al. 2009; Song et al. 2013]. In the relatively few in vivo and in vitro studies that compare the effects of exposure to nanoscale or microscale silver particles, the findings generally show greater uptake and toxicity of nanoscale versus microscale silver particles (Sections 4, 5, and 6.1.3). By evaluating the available evidence, NIOSH has determined that it is reasonable and prudent to define the REL of 0.9 μg/m$^3$ (8-hour TWA) as being applicable to all silver nanomaterials, i.e., ≤100 nm primary particle size. The upper particle size of 100 nm for nanoscale particles [ISO 2008] is not a health-based definition but is based on particle size definitions and sampling conventions (see Terminology/Glossary). Employers and risk managers may choose to exercise additional precaution if workers have potential exposure to silver particles of size ranges similar to nanoscale silver.

Findings from the literature indicate that workplace exposures can in some situations be controlled at or below the REL (Section 2). For example, workplace airborne exposure concentrations of silver nanomaterials were reported to be as low as 0.02 μg/m$^3$ (as silver metal) [Lee et al. 2011b] (Table 2-1). These findings provide evidence that silver can be measured at and controlled to airborne concentrations below the NIOSH REL of 0.9 μg/m$^3$.

The NIOSH REL of 10 μg/m$^3$ for total silver (metal dust, fume, and soluble compounds, as Ag) [NIOSH 1988, 2003, 2007] continues to apply. Worker exposures to silver should not exceed the NIOSH REL for silver nanomaterials or the NIOSH REL for total silver.

Development of a risk management program should include management and employee involvement. An effective risk management program will include these elements:

1. A written program that follows the OSHA Hazard Communication Standard [20 CFR 1910.1200]. This should include (a) identification of processes and job tasks where there is potential for exposure to silver nanomaterials and (b) training of workers on how to recognize and prevent potential exposures.
2. Routine systematic and comprehensive evaluation of worker exposures by all routes to silver nanomaterials, periodically and/or whenever there is a change in a process or task associated with potential exposure to silver nanomaterials. Changes could include frequency, volume, duration, equipment, and procedures/processes.
3. Development of criteria and guidelines for selecting, installing, and evaluating engineering controls (such as LEV, dust collection systems), with the objective of controlling worker airborne

exposure to silver nanomaterials (metal dust, fume, and soluble compounds, as Ag) below the NIOSH REL of 0.9 μg/m³ (respirable mass, 8-hour TWA) and exposure to total airborne silver (metal dust, fume, and soluble compounds, as Ag) below the NIOSH REL of 10 μg/m³ (total mass, 8-hour TWA).

4. Development of procedures for selecting and using personal protective equipment (PPE; clothing, foot coverings, gloves, respirators) and development of a respiratory protection program that follows the OSHA respiratory protection standard (29 CFR 1910.134) if respiratory protection is used.
5. Development of spill control plans and routine cleaning procedures for work areas, using a HEPA-filtered vacuum or wet-wipes. Do not use dry sweeping or air hoses. Avoid using or handling silver nanomaterials in powder form, where possible, and ensure silver nanomaterials are stored in tightly sealed containers and appropriately labeled.
6. Provision of facilities for hand washing to reduce the potential for dermal and oral exposures, and encouragement of workers to use these facilities before eating or leaving the worksite.
7. Use of established medical surveillance approaches for workers potentially exposed to silver, including silver nanomaterials.

## 7.1 Exposure Assessment for Silver Nanomaterials

NIOSH continues to recommend the REL of 10 μg/m³ (8-hour TWA) for total silver (metal dust, fume, and soluble compounds, as Ag) [NIOSH 1988, 2003, 2007]. Sampling and analysis methods for total silver are described in the *NIOSH Manual of Analytical Methods* (NIOSH Methods 7300, 7301, and 7306) [NIOSH 2017a]. In addition, NIOSH is recommending an airborne respirable mass concentration of 0.9 μg/m³ as an 8-hour TWA concentration to evaluate and monitor worker exposure to silver nanomaterials (primary particle size ≤100 nm). The REL for silver nanomaterials applies to the airborne mass fraction of particles with a primary particle size of 100 nm or less in any single dimension, including agglomerates composed of these primary particles (Figure 7-1).

Although there are currently no personal sampling devices available to specifically measure the mass concentration of these ultrafine particles, there are

Particle size categories are inherent in the exposure sampling and measurement methods [NIOSH 2017]:

- **Total silver (Ag)** includes airborne silver particles
- **Respirable Ag** is a fraction of the total Ag sample, and includes all silver nanoparticles (AgNP)
- **Silver nanoparticles (AgNP)** are a fraction of both the respirable and the total Ag samples

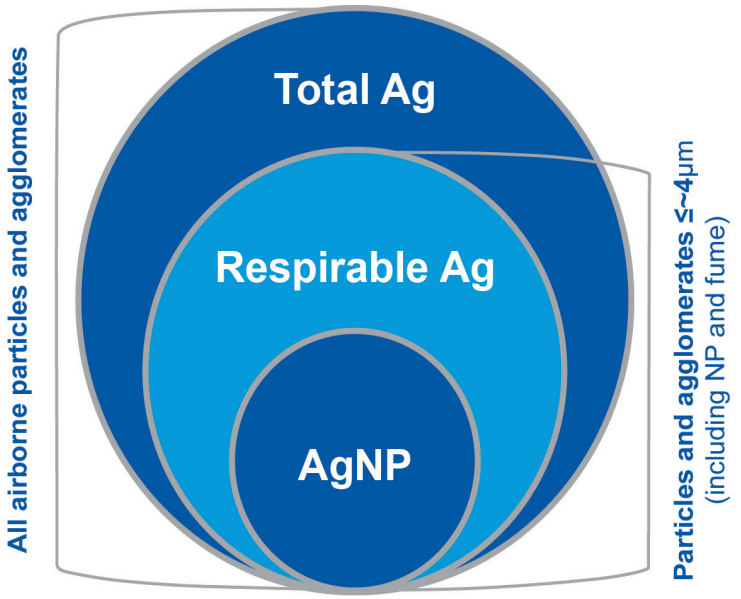


**Figure 7-1.** Airborne silver particle size categories.

several valid aerosol methods for collecting these ultrafine particles as part of a larger sample. Note that a combination of methods may be necessary to properly characterize exposure (Figure 7-2). Multiple combinations of size-selective samplers and analytical methods can capture the data necessary to conduct an exposure assessment of airborne silver nanomaterials. NIOSH provides the following procedures as one example for conducting an exposure assessment of silver nanomaterials.

1. Use a size-selective sampler (such as a standard respirable cyclone) to collect airborne ultrafine particles and fume. Two separate samples, both obtained with a standard respirable cyclone, should be collected simultaneously on mixed cellulose ester (MCE) filters, because NIOSH Method 7300 is a destructive analysis (the entire sample is consumed in analysis) and further analysis may be required.
2. Analyze the respirable sample by NIOSH Method 7300 [NIOSH 2003] to determine the mass of silver present, accounting for wall loss as described by the *NIOSH Manual of Analytical Methods*. Results below 0.9 μg/m$^3$ will affirm that exposures are below the REL for silver nanomaterials, and thus the duplicate sample may be discarded. [NIOSH Method 7300 has a limit of detection (LOD) of approximately 42 ng Ag per MCE filter. Note that LODs are specific to the instrumentation and protocols used by a given laboratory.]
3. If the result is above 0.9 μg/m$^3$, then further characterize the duplicate sample with an electron microscope equipped with X-ray energy dispersive spectroscopy (EDS) to be more specific to ultrafine particles. This analysis can identify particles and agglomerates of primary particles of 100 nm or less, allowing determination of the mass fraction to which the silver nanomaterial REL of 0.9 μg/m$^3$ is applicable.
4. Once the exposure is well characterized and controlled below the REL, use samples collected with the chosen size-selective sampler and analyzed with NIOSH Method 7300 to monitor exposure, without the need for microscopy samples. If a monitoring sample result is above 0.9 μg/m$^3$ for AgNP, exposure monitoring should be repeated with microscopy samples until exposures are controlled below the REL.

An important first step in applying any risk management program is to develop a job hazard analysis of the processes and job activities that place workers at risk of exposure (such as the handling of large volumes of silver nanomaterials, silver brazing/soldering operations, and other high-temperature processes involving silver), as described in https://www.osha.gov/Publications/osha3071.pdf. When applicable, the job hazard analysis should include an initial assessment of a bulk sample of the material and/or documentation from the manufacturer to determine the presence of silver nanomaterials. The job hazard analysis can be used to determine the number of workers potentially exposed and to qualitatively determine which workers and processes are likely to have the greatest potential for exposure.

Several exposure assessment strategies can be used to determine workplace exposures [NIOSH 1977; Corn and Esmen 1979; Leidel and Busch 1994; Rappaport et al. 1995; Lyles et al. 1997; Bullock and Ignacio 2006; Ramachandran et al. 2011; McNally et al. 2014]. These strategies can be tailored to a specific workplace, depending on available resources, the number of workers, and the complexity of the work environment (such as process type and rate of operation, exposure control methods, and physical state and properties of material). One approach for determining worker exposures to airborne silver concentrations would be to initially target similarly exposed groups (SEGs) of workers [Corn and Esmen 1979; Leidel and Busch 1994]. This initial sampling effort may be more time efficient and require fewer resources for identifying workers with exposures to silver above the REL. However, this measurement strategy may produce incomplete and upwardly biased exposure estimates if the exposures are highly variable [Kromhout 2009]. Therefore, repeated measurements on randomly selected workers may be required to account for between- and within-worker variations in exposure concentrations [Rappaport

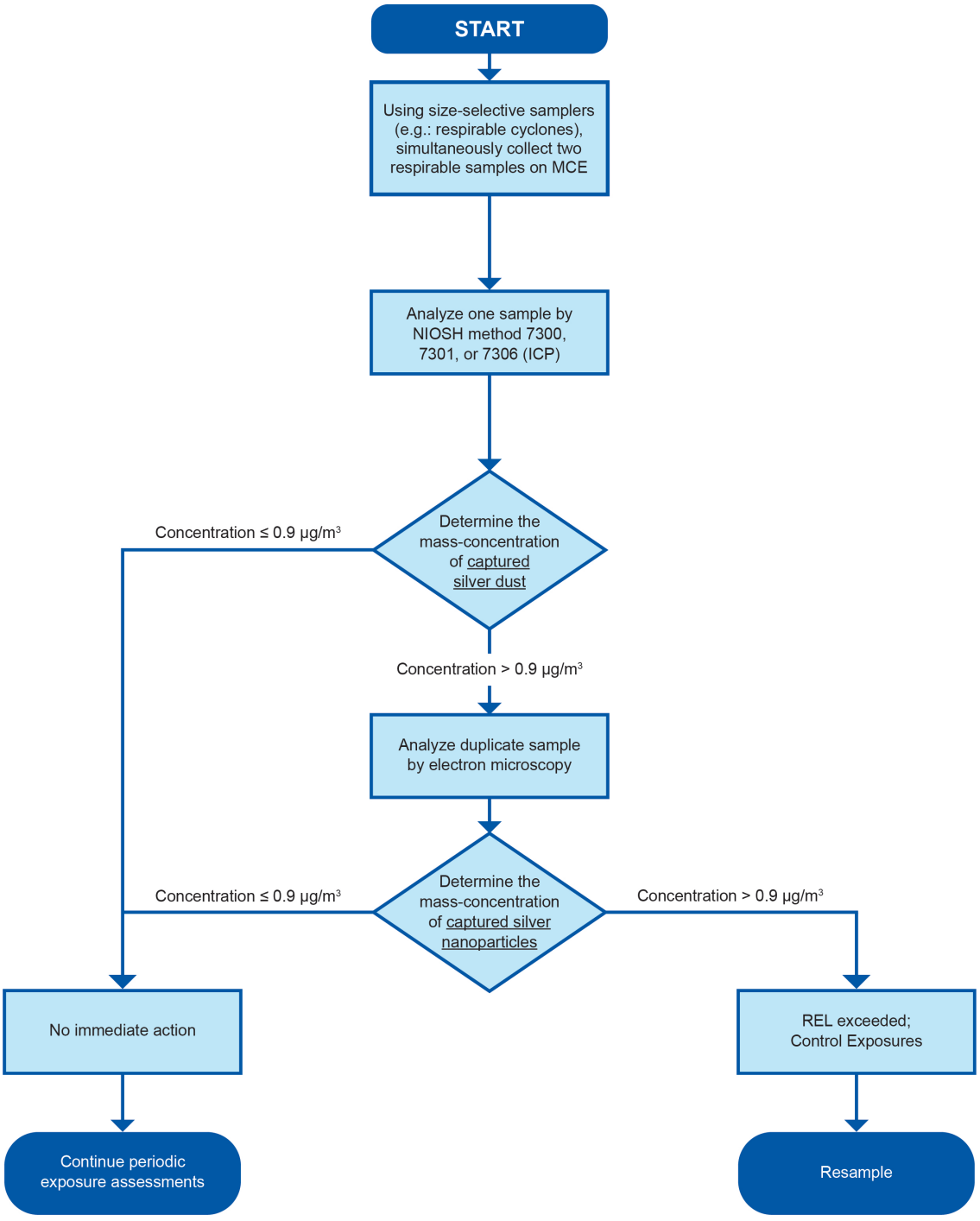


**Figure 7-2.** Exposure assessment protocol for silver nanoparticles in an aerosol of unknown particle size distribution containing Ag and other particulates. For exposure assessment of total silver, see NIOSH Methods 7300, 7301, and 7306 [NIOSH 2017a]. MCE: mixed cellulose ester; ICP: inductively coupled argon plasma method; REL: recommended exposure limit.

et al. 1995; Lyles et al. 1997]. If workplace exposure measurement data for silver are available, as well as information on exposure variability, it may be possible to use a Bayesian model that combines expert knowledge with existing exposure measurement data to estimate workers' exposures [McNally et al. 2014].

Because there is no "best" exposure measurement strategy that can be applied to all workplaces, multiday random sampling of workers (all workers, if the exposed workforce is small) may be needed to accurately assess the airborne concentrations of silver to which workers are exposed. Additionally, the concentration mapping and job task–related measurement tools described by Ramachandran et al. [2011] would further complement the randomly-selected-worker method. In cases where resources and/or health and safety expertise are limited, consultation with an expert may be required.

Although the REL is not applicable to surface sampling, the potential adverse health effects of dermal exposure to silver reported in animal studies (Section E.3.1) suggest that dermal exposure should be minimized. Additionally, minimizing surface concentrations of silver reduces the likelihood of transferring silver nanomaterials out of the process areas. NIOSH recommends periodic surface-wipe sampling in process areas as well as office and common areas, using NIOSH Method 9100 and analysis by NIOSH Method 7300 or 7301 to validate containment of contaminates and the effectiveness of housekeeping procedures.

Brookhaven National Laboratory has published internal surface-wipe sampling criteria for metals [2014]. These criteria include acceptable surface levels for two categories: equipment release and housekeeping. The equipment release level, or the acceptable surface level of silver for transfer of equipment to non-operational areas or the public, is 1 µg/100 $cm^2$. To meet the housekeeping criteria, surface levels should be below 15 µg/100 $cm^2$ during operational periods [Brookhaven National Laboratory 2014]. Surface contamination of silver should be maintained below 15 µg/100 $cm^2$ for process areas and below 1 µg/100 $cm^2$ for non-process areas.

## 7.2 Engineering Controls

One of the best ways to prevent adverse health effects from exposure to a hazardous material is to eliminate exposure and minimize risks early in the design or redesign of manufacturing and downstream-user processes (see NIOSH Prevention through Design [PtD], at www.cdc.gov/niosh/topics/PtD/). The concept of PtD is to design out or minimize hazards, preferably early in the design process. This can be accomplished through the establishment of a process safety management (PSM) program that is consistent with the requirements of the OSHA Process Safety Management Standard [29 CFR 1910.119 (c) – (o)]. PSM entails the development and implementation of programs or systems to ensure that the practices and equipment used in potentially hazardous processes are adequate and appropriately maintained.

An integral part of the PSM program is a process hazard analysis prior to the initiation of work, to identify where sources of exposure to silver and other hazardous materials may occur so that process equipment can be designed or redesigned to minimize the risk of exposure. As part of the assessment, the health and safety professional should evaluate the potential magnitude and extent of emissions to determine the risk of exposure to workers. This initial assessment is an important first step toward identifying possible exposure control strategies.

Controlling exposures to occupational hazards is the fundamental method of protecting workers. Traditionally, a hierarchy of controls has been used as a means of determining how to implement feasible and effective control measures [NIOSH 2013b]. Following the hierarchy normally leads to implementation of inherently safer systems, where the risk of illness or injury has been substantially reduced. Elimination and substitution are generally most effective if implemented when a process is in

the design or development stage. If done early, implementation is simple, and in the long run it can result in substantial savings (such as in the cost of protective equipment and the initial and operation costs for the ventilation system) [NIOSH 2013b]. For an existing process, elimination or substitution of the material may require major changes in equipment and/or procedures in order to reduce the potential hazard.

When elimination or substitution is not feasible, the use of engineering controls can be an effective control strategy for minimizing exposure to hazards associated with processes and job tasks. Well-designed engineering controls can be highly effective in protecting workers and will typically be independent of worker interactions. The use of engineering controls to reduce worker exposure to all forms and particle sizes of silver is an effective means of minimizing health concerns and works best when it is part of an overall risk management program that includes worker exposure evaluation, education/training, administrative controls, and use of PPE.

Different types of exposure control systems can be used, depending on the configuration of the process and the degree of exposure control required [ACGIH 2013; NIOSH 2013b]. For example, source enclosure (that is, isolating the generation source from the worker) and well-designed local exhaust ventilation (LEV), equipped with high-efficiency particulate air (HEPA) filters, can be effective for capturing airborne silver particles at the source of exposure [NIOSH 2013b]. The selection of an appropriate exposure control system should take into account the extent to which the airborne concentration of silver nanomaterials is to be reduced (such as below the NIOSH REL of 0.9 μg/m$^3$), the quantity and physical form of the material (such as dispersible silver powder, a liquid slurry, or a matrix), the task duration, the frequency with which workers may come into contact with silver or silver-containing material, and the characteristics of the task itself (such as how much energy is imparted to the material during sonication or powered sanding/cutting).

For instance, working with materials containing silver nanomaterials (such as encapsulated in a fabric or solid material) may require a different type of exposure control system than would be needed for working with large quantities of silver nanomaterials in a highly dispersed free (powder) form. Specific processes (such as high-temperature melting of silver) and job tasks (such as silver brazing/soldering) have the potential to generate an aerosol or fume containing silver and therefore should incorporate exposure controls at the exposure source. Likewise, the manufacturing/synthesis of engineered silver nanomaterials and the handling of dry powders should be performed in enclosed systems and, when warranted, HEPA-ventilated systems. HEPA filtration has been shown to be effective in capturing nanoparticles and should be considered in situations where emissions may be regular, where processes are repeated, and where higher quantities are used in a way that may lead to emissions. Research quantities of silver nanomaterials in laboratories can be safely handled if appropriate exposure-containment systems are used, such as a constant-velocity (variable air-volume) laboratory fume hood or air-curtain hood [Tsai et al. 2010] or a glove box to minimize worker exposure [NIOSH 2012]. These exposure control systems should be properly designed, tested, and routinely maintained and evaluated to ensure maximum efficiency [ACGIH 2010].

NIOSH found that in two facilities conducting brazing and soldering operations, airborne concentrations of silver (including silver nanoparticles) were less than 0.015 μg/m$^3$, measured as personal breathing zone TWA concentrations. Engineering controls included "canopy-type" ventilation hoods equipped with LEV; this was discharged directly through the roof of the building at high velocity, both downwind and approximately 50 or more feet from air intakes [NIOSH 1998].

Lee et al. [2011b; 2012a,b] examined silver nanoparticle production processes in two facilities. The first facility used an inductively coupled plasma torch to vaporize various silver feedstocks, which were then condensed into nanoparticles, effectively a type of

vapor-condensation synthesis process. The first study recorded silver concentrations in area samples between 0.02 and 0.34 μg/m³, with personal samples of 0.12 and 1.20 μg/m³ [Lee et al. 2011b], though a subsequent visit to the site showed increased ranges of 0.01 to 288.73 μg/m³ for area samples and 0.02 to 2.43 μg/m³ for personal samples [Lee 2012b]. The only engineering control discussed was natural ventilation, which in combination with the closed system maintained airborne silver concentrations at approximately 1 μg/m³. The greatest exposures occurred during the process of workers introducing feedstock; exposure was controlled with half-mask respirators and by limiting worker time on this task [Lee 2012b]. Exposures from vapor-condensation and other airborne synthesis processes can frequently be reduced by optimization of reactor design and processes and by using hoods or enclosures and LEV [Virji and Stefanaik 2014].

The second facility studied by Lee et al. [2011b] used two processes for silver nanoparticle production: a wet-chemistry reaction of sodium citrate and silver nitrate, and attrition milling. Both processes occurred in the same space, and silver concentrations ranged from 0.03 to 1.18 μg/m³ in area samples and from 0.38 to 0.43 μg/m³ in personal samples. It was indicated that the workplace was "equipped with a fume hood and well ventilated" [Lee et al. 2011b]. Although exposures from liquid and solid processes have been less studied, it has been indicated that emissions from wet-chemistry processes are lower than from vapor phase processes, but that milling represents a possible source of emission; fume hoods and LEV have been applied effectively to these methods as well [Virji and Stefanaik 2014].

In one study of such wet-chemistry processes, Park et al. [2009] examined a facility that used nitric acid and silver nitrate to produce a colloidal suspension, which was then filtered, dried, and milled. A vent hood was installed above the reactor, and ventilation facilities were in place near the grinding location. It was observed that opening the grinder door increased airborne particle concentrations and irregularities in concentration; moreover, it was shown that activating the ventilation system directly reduced this irregularity. The authors also noted that particles on the floor were readily disturbed by workers and therefore represented an additional potential exposure. The authors suggest that it would be better if the grinding room were airtight (while maintaining ventilation facilities) to prevent exposures to other zones [Park et al. 2009].

Table 7-1 provides examples of the types of engineering and other exposure control measures that could be used at various processes and job tasks to help control worker exposures to silver nanomaterials. In some cases, a combination of approaches may be necessary to accomplish exposure control goals (such as installing a continuous liner system inside a ventilated booth).

**Table 7-1. Engineering controls to reduce silver exposures below the NIOSH RELs.***

| Process and/ or Task Activity | Potential Sources of Exposure | Exposure Controls |
|---|---|---|
| **Pilot and Research & Development Operations** | Generally *small quantities* of AgNPs/ AgNWs (such as μg and mg) during<br>• Synthesis of AgNPs/AgNWs, including chemical vapor deposition, solution phase synthesis, and dry powder dispersion<br>• Harvesting of AgNPs after synthesis<br>• Removal of silver nanomaterials from a substrate<br>• Powder transfer (AgNPs/AgNWs)<br>• Reactor cleaning | • Constant-velocity fume hood or nanomaterial enclosure with HEPA-filtration exhaust when warranted<br>• HEPA-filtration exhaust enclosure (such as glove box isolator)<br>• Biologic safety cabinet<br>• Note: LEV or some type of enclosure control (glove box) may be required at the reactor and during the harvesting of material. |
| **Research Laboratory Operations** | Generally *small quantities* of AgNPs/ AgNWs (such as μg and mg) during<br>• Handling (such as mixing, weighing, blending, transferring) of AgNPs/AgNWs in free powder form or sonication of AgNP or AgNW liquid suspension | • Constant-velocity fume hood or nanomaterial-handling enclosure with HEPA-filtration exhaust when warranted<br>• HEPA-filtration exhaust enclosure (such as glove box isolator)<br>• Biologic safety cabinet |
| **Manufacturing and Synthesis of AgNPs and AgNWs** | Generally *large quantities* of AgNPs/ AgNWs (≥ kg amounts) during<br>• Synthesis of AgNPs (chemical vapor deposition, solution phase synthesis, and dry powder dispersion)<br>• Harvesting of AgNPs after synthesis<br>• Removal of silver nanomaterials from a substrate<br>• Powder transfer of silver nanomaterials<br>• Drum and bag filling<br>• Reactor cleaning<br>• Coating of AgNPs/AgNWs | • Dedicated ventilated room (such as a down-flow room) for reactor with HEPA-filtration exhaust, potentially in conjunction with localized controls listed below<br>• LEV at source of potential exposure when isolation or total enclosure of the process is not possible<br>• Ventilated bagging/weighing stations and/or unidirectional down-flow ventilation booth<br>• Non-ventilation options, including a continuous liner off-loading system for bagging operations<br>• Ventilated bag dumping stations for product transfer |

(Continued)

**Table 7-1. Engineering controls to reduce silver exposures below the NIOSH RELs.***

| Process and/ or Task Activity | Potential Sources of Exposure | Exposure Controls |
|---|---|---|
| **Use of AgNPs and AgNWs to produce enabled materials** | 1. Generally *small quantities* of AgNP/AgNW powder or liquid suspensions during<br>• Mixing, weighing, and transferring of AgNPs/AgNWs<br>• Incorporation of AgNPs/AgNWs into matrices and coatings<br>• Spraying of AgNPs/AgNWs on surfaces | 1. Options<br>• Transfer of AgNPs/AgNWs in sealed, unbreakable, labeled containers<br>• Constant velocity fume hood or nanomaterial handling enclosure (with filtered exhaust when warranted)<br>• HEPA-filtration exhaust enclosure (such as glove box isolator)<br>• Biologic safety cabinet |
| | 2. Generally *large quantities* of AgNPs or AgNWs in powder or liquid suspensions during<br>• Blending or pouring into other matrices<br>• Impregnating of textile materials and spray coating of surfaces | 2. Options<br>• Isolation techniques such as a dedicated ventilated room or process enclosure with HEPA-filtration exhaust<br>• Process-based controls such as ventilated bagging/weighing station and unidirectional down-flow booth<br>• Non-ventilation options such as continuous liner off-loading systems for bagging operations<br>• Ventilated bag dumping stations for product transfer |

(Continued)

**Table 7-1. Engineering controls to reduce silver exposures below the NIOSH RELs.***

| Process and/ or Task Activity | Potential Sources of Exposure | Exposure Controls |
|---|---|---|
| | 3. *Small pieces* of AgNP- and AgNW-enabled textiles, fabrics, materials, and composites during handling:<br>• Grinding, sanding, cutting, drilling, or other mechanical energy applied to materials containing AgNPs or AgNWs | 3. Options<br>**For small pieces of AgNP/AgNW-enabled textiles, fabrics, materials, and composites**<br>• Constant-velocity fume hood or nanomaterial handling enclosure with filtered exhaust when warranted<br>• HEPA-filtration exhaust enclosure (such as glove box isolator)<br>• Biologic safety cabinet<br>• Localized dust-suppression techniques, including ventilation-based (power tool–type) or mist/water-based, where appropriate<br>**For large pieces of AgNP/AgNW-enabled materials/composites, where use of isolation techniques (such as large ventilated enclosures) are not feasible**<br>• Ventilated process enclosure or unidirectional down-flow booth with HEPA-filtered exhaust<br>• LEV at exposure source with HEPA-filtered exhaust<br>• Localized dust-suppression techniques, including ventilation-based (power tool–type) or mist/water-based, where appropriate |
| **Processes requiring application of high temperatures to Ag metals and alloys** | Fumes generated during brazing, soldering, welding, and melting of Ag and Ag alloys | • LEV-based welding fume control approaches should be used, including ventilated enclosing hoods, fixed slot/plenum ventilated worktables, or moveable capture hoods (such as a welding fume extraction unit)<br>• Process-based controls, such as ventilated production welding booths, may be required for large-scale applications where fumes may be generated |

*Note: Factors that influence the selection of appropriate engineering controls and other exposure control strategies include the physical form (such as dry dispersible powder, fume, liquid slurry, or a matrix/composite), task duration, frequency, quantity of the Ag (including AgNPs and AgNWs) handled, and task characteristics (how much energy is imparted to the material). **The airborne concentration of silver at the potential source of emission should be measured to confirm the effectiveness of the exposure control measures.** See NIOSH documents *Current Strategies for Engineering Controls in Nanomaterial Production and Downstream Handling Process* [NIOSH 2013b] and *General Safe Practices for Working with Engineered Nanomaterials in Research Laboratories* [NIOSH 2012] for guidance on the selection of appropriate exposure control strategies.

## 7.3 Worker Education and Training

Establishing a safety and health program that includes educating and training workers on the potential hazards of silver, including exposure to silver nanomaterials, is critical to preventing adverse health effects from exposure. Research has shown that immediate and long-term objectives can be attained with training when: (1) workers are educated about the potential hazards of their job, (2) knowledge and work practices become improved, (3) workers are provided the necessary skills to perform their jobs safely, and (4) management shows commitment and support for workplace safety [NIOSH 2010]. Requirements for the education and training of workers, as specified in the OSHA Hazard Communication Standard (29 CFR 1910.1200) [OSHA 2012b] and as described by Kulinowski and Lippy [2011] for workers exposed to nanomaterials, provide a minimum set of guidelines that can be used for establishing an education and training program. Workers who should receive training include those who work directly with silver nanomaterials, those who are likely to come into contact with or work in close proximity to silver nanomaterials, and managers or supervisors who are responsible for assignment and oversight of those workers' tasks.

The establishment and oversight of the program should be described in one or more standard operating procedures to (1) ensure management's commitment to control exposures; (2) identify and communicate potential hazards to workers; (3) evaluate workplace exposures to silver; (4) identify and implement engineering controls and effective work practices; (5) establish documentation; and (6) periodically review the adequacy of exposure controls and other preventive practices. Management should systematically review and update these procedures and convey to workers the actions taken to resolve and/or improve workplace conditions.

A program for educating workers should also include both instruction and "hands on" training that address the following:

- The potential health risks associated with exposure to silver
- Potential routes of exposure to silver
- Recognizing effects of exposure
- The safe handling of silver nanomaterials and materials containing silver nanomaterials to minimize the likelihood of inhalation exposure and skin contact, including the proper use of engineering controls, PPE (such as respirators, foot coverings, and gloves), and good work practices
- Procedures and tools for avoiding handling silver nanomaterials in powder form where possible; ensuring silver nanomaterials are stored in tightly sealed containers; cleaning work areas with a HEPA-filtered vacuum or wet-wipes; avoiding use of dry sweeping or air hoses; and using hand washing facilities before eating, smoking, or leaving the worksite
- Instructions for reporting health symptoms
- The availability and benefits of medical surveillance and screening programs.

## 7.4 Cleanup and Disposal

Procedures should be developed to protect workers from exposure to silver, with special emphasis on the safe cleanup and removal of silver nanomaterials from contaminated surfaces. Inhalation and dermal exposures will likely present the greatest risks. The potential for inhalation exposure during cleanup will be influenced by the likelihood of silver nanomaterials becoming airborne, with bulk silver nanomaterials (powder form) presenting a greater inhalation potential than silver nanomaterials in solution (liquid form), and liquids in turn presenting a greater potential risk than silver nanomaterials in encapsulated materials.

It would be prudent to base strategies for dealing with spills and contaminated surfaces on the use of current good practices, together with available information on exposure risks. Standard approaches

for cleaning powder spills can be used for cleaning surfaces contaminated with silver. These include using HEPA-filtered vacuum cleaners, wiping up silver (in powder form) with damp cloths, and wetting the powder before wiping. Liquid spills containing silver nanomaterials can typically be cleaned up with absorbent materials or liquid traps. If vacuum cleaning is employed, extreme caution should be taken that HEPA filters are installed properly and that bags and filters are changed according to the manufacturer's recommendations. Dry sweeping or air hoses should not be used to clean work areas. Task-specific PPE (i.e., designated for spill control) may be needed, depending on the amount of the spill and its location. A plan should be in place describing the steps that should be taken to address the issue and the type of PPE that should be used.

Waste (including all cleaning materials) and other contaminated materials (such as gloves) should be collected in a separate waste stream and be disposed of in compliance with all applicable regulations (federal, state, and local).

## 7.5 Dermal Protection

Although there are no regulations or guidelines for the selection of clothing or other apparel protective against exposure specific to silver, OSHA requires employers to ensure that employees wear appropriate PPE for their work tasks [OSHA 29 CFR 1910.132 (d)(1)].

If exposure to AgNPs can occur from the dermal route, PPE (such as protective clothing, including gloves) is recommended when all technical measures to eliminate or control exposure to Ag, including silver nanomaterials, have not been successful, or there is a potential for dermal exposure to damaged or abraded skin.

Several performance criteria should be considered when selecting the appropriate PPE [Gao et al. 2014; NIOSH 2016; Johnson et al. 2000; Johnson 2016]:

- Penetration potential
- Durability (resistance to wear, tear, abrasions, punctures, and chemical degradation)
- Dexterity/flexibility
- Decontamination ability (for multi-use PPE)
- Comfort
- Compatibility with other equipment and interface regions (such as the glove/coat interface)
- Heat stress
- Communication limitations

The challenge when selecting appropriate protective clothing is to strike a balance between comfort and protection. Garments that provide the highest level of protection are also the least comfortable to wear for long periods, whereas garments that are probably the least protective are the most breathable and comfortable to wear. The limited experimental evidence suggests that airtight fabrics made of nonwoven textiles are more efficient in protecting workers against nanoparticles than fabrics made of woven cotton or polyester [Golanski et al. 2009; Golanski et al. 2010]. The efficiency of commercial gloves in preventing dermal exposure to nanoparticles varies, depending on the glove material, its thickness, and the manner in which it is used (such as long exposure times and other chemical exposures) [NanoSafe 2008; Golanski et al. 2009, 2010]. The proper selection of gloves should take into account their resistance to chemical attack by the nanomaterial and, if it is suspended in liquids, by the liquid itself [USDOE 2008]. If protective gloves (such as powder-free nitrile, neoprene, and latex gloves) are used, consider all activities such as working with sharp instruments, which may require additional cut-proof gloves as well as chemical protective gloves [http://nioshsciencepolicy.cdc.gov/PDF/97-135.pdf]. Special attention should also be given to the proper removal and disposal of contaminated gloves to prevent skin contamination. Gloves should be visually inspected for tears before and during use and routinely replaced. Irrespective of glove use, it is also important to eliminate hand-to-mouth activity to prevent a dermal exposure from becoming an oral exposure.

If the job hazard analysis notes a substantial possibility of hazardous materials outside the work area or of possible risk of home contamination, additional measures may be required to mitigate these risks. Such measures are described in the *Report to Congress on Workers' Home Contamination Study Conducted Under the Worker's Family Protection Act* (29 U.S.C. 671a) and may include changing garments in designated areas or washing the skin or garments [NIOSH 1995].

## 7.6 Respiratory Protection

The decision to use respiratory protection should be based upon hazard assessment and risk management practices to keep worker inhalation exposure below prescribed occupational exposure limits. When engineering controls and work practices cannot reduce worker airborne exposures below the NIOSH REL of 10 μg/m$^3$ (8-hour TWA) for total airborne silver (metal dust, fume, and soluble compounds, as Ag) [NIOSH 1988, 2003, 2007] or the NIOSH REL of 0.9 μg/m$^3$ (respirable mass, 8-hour TWA) for silver nanomaterials (primary particle size ≤100 nm), workers should be provided respiratory protection. The use of respirators may also be advisable for certain tasks that place workers at risk of potentially high peak concentrations of silver, such as cleanup of silver nanomaterial spills or debris (free form); maintenance of equipment used to process silver nanomaterials; large processes involving the electrorefining of silver; and cleaning and/or disposal of filtration systems used to capture airborne silver nanomaterials.

When selecting the appropriate respirator, the respirator program manager should consider the presence of other potentially hazardous aerosols, such as chemicals [Rengasamy and Eimer 2011]. On the basis of this information, the respirator program manager may decide to choose a respirator with a higher assigned protection factor or one with a higher level of filtration performance (such as changing from an N95 to a P100). Studies on the filtration performance of N95 filtering facepiece respirators have found that the mean penetration levels for 40-nm particles range from 1.4% to 5.2%, indicating that N95 and higher-performing respirator filters would be effective at capturing airborne AgNPs [Bałazy et al. 2006; Rengasamy et al. 2007, 2008]. Recent studies show that nanoparticles <20 nm are also effectively captured by NIOSH-approved filtering facepiece respirators [Rengasamy et al. 2008, 2009]. Other classes of respirators also can provide a higher level of protection (Table 7-2). The publication *NIOSH Respirator Selection Logic 2004* provides guidance for selecting an appropriate respirator [NIOSH 2005].

The OSHA respiratory protection standard (29 CFR 1910.134) requires establishment of a respiratory program for both voluntary and required respirator use. Elements of the standard include (1) a medical evaluation of each worker's ability to perform the work while wearing a respirator; (2) regular training of personnel; (3) periodic workplace exposure monitoring; (4) respirator fit-testing; and (5) respirator maintenance, inspection, cleaning, and storage. The program should be evaluated regularly, and respirators should be selected by the person who is in charge of the program and knowledgeable about the workplace and the limitations associated with each type of respirator.

## 7.7 Occupational Health Surveillance

Occupational health surveillance involves the ongoing systematic collection, analysis, and dissemination of exposure and health data on groups of workers for the purpose of preventing illness and injury. Occupational health surveillance is an essential component of an effective occupational safety and health program [Harber et al. 2003; Baker and Matte 2005; NIOSH 2006; Wagner and Fine 2008; Trout and Schulte 2010], and NIOSH continues to recommend occupational health surveillance as an important part of an effective risk management program. Occupational health surveillance includes the elements of hazard and medical surveillance.

**Table 7-2. Respiratory protection for exposure to silver.**

| Workplace Airborne Concentrations of Silver or Conditions of Use * Options | Minimum Respiratory Protection |
|---|---|
| 0.9–9.0 μg/m$^3$ (up to 10 × REL) | Any filtering facepiece respirator or air-purifying, elastomeric half-facepiece respirator equipped with appropriate type of particulate filter; † any negative-pressure (demand), supplied-air respirator equipped with a half-mask |
| ≤22.5 μg/m$^3$ (up to 25 × REL) | Any powered, air-purifying respirator equipped with a hood or helmet and a HEPA filter; any continuous-flow supplied-air respirator equipped with a hood or helmet |
| ≤45.0 μg/m$^3$ (up to 50 × REL) | Any air-purifying full-facepiece respirator equipped with N-100, R-100, or P-100 filter; any powered air-purifying respirator equipped with a tight-fitting half-facepiece and a HEPA filter; any negative-pressure (demand) supplied-air respirator equipped with a full facepiece; any continuous-flow supplied-air respirator with a tight-fitting half-facepiece; any negative-pressure (demand) self-contained respirator equipped with a full facepiece |
| ≤900 μg/m$^3$ (up to 1,000 × REL) | Any pressure-demand supplied-air respirator equipped with a full facepiece |

* The protection offered by a given respirator is contingent upon (1) the respirator user's adhering to complete program requirements (such as those required by OSHA in 29 CFR 1910.134), (2) the use of NIOSH-certified respirators in their approved configuration, and (3) individual fit testing to rule out those respirators for which a good fit cannot be achieved.

† The appropriate type of particulate filter means any 95- or 100-series (N, R, or P) filter. Note: N-95 or N-100 series filters should not be used in environments where there is potential for exposure to oil mists.

Note: Complete information on the selection of respirators can be found at (1) OSHA 3352-02 2009, *Assigned Protection Factors for the Revised Respiratory Protection Standard*, at https://www.osha.gov/Publications/3352-APF-respirators.html, and (2) NIOSH, at https://www.cdc.gov/niosh/docs/2005-100/default.html.

### 7.7.1 Hazard Surveillance

Hazard surveillance includes hazard and exposure assessment (see Sections 7 and 7.1). Development of the job hazard analysis (discussed in Section 7.1) includes identification of hazards in the workplace and review of the best available information concerning toxicity of materials; such information may come from databases, texts, the literature, and regulations or recommendations (such as from NIOSH or OSHA). Human studies, such as epidemiologic investigations and case series or reports, and animal studies may also provide valuable information. Currently, there are limited toxicological data and a lack of epidemiologic data pertaining to silver nanomaterials with which to make a complete hazard assessment. Exposure assessment involves evaluating relevant exposure route(s) (inhalation, ingestion, dermal, and/or injection), amount, duration, and frequency, as well as whether exposure controls are in place and how protective they are. Hazard surveillance for AgNPs provides information that is used in evaluating and implementing workplace controls.

### 7.7.2 Medical Screening and Surveillance

Medical surveillance targets actual health events or a change in a biologic function of an exposed

person or persons. Medical surveillance involves ongoing evaluation of the health status of a group of workers through the collection and aggregate analysis of health data, for the purpose of preventing disease and evaluating the effectiveness of intervention programs (primary prevention). NIOSH recommends medical surveillance of workers when they are exposed to hazardous materials and therefore are at risk of adverse health effects from such exposures. Medical screening is a form of medical surveillance used to detect early signs of work-related illness in individual workers. It involves administering tests to apparently healthy persons to detect those with early stages of disease or risk of disease.

Medical screening and surveillance provide a second line of defense, behind the implementation of engineering, administrative, and work practice controls (including personal protective equipment). Integration of hazard and medical surveillance is key to an effective occupational health surveillance program [Trout and Schulte 2010; Schulte and Trout 2011; Schulte et al. 2016].

NIOSH has previously concluded that workers occupationally exposed to airborne concentrations of silver above the NIOSH REL for total silver (10 μg/m$^3$, 8-hour TWA) may potentially be at risk of developing argyria [NIOSH 1988, 2007]. On the basis of the evidence summarized in this document, NIOSH concludes that workers occupationally exposed to airborne concentrations of silver above the NIOSH REL for silver nanomaterials (0.9 μg/m$^3$, 8-hour TWA) may potentially be at risk of developing early-stage adverse lung and liver effects.

Currently there is insufficient scientific and medical evidence to recommend the specific medical screening of workers potentially exposed to silver nanomaterials. Medical screening programs pertaining to workers' total silver exposure may be in place at some workplaces. Workers exposed to silver nanomaterials who are included in such programs (based on total silver exposure) should continue in those programs per the usual practice of those workplaces.

As research into the potential hazards of silver nanomaterials continues, periodic reassessment of available data is critical to determine whether specific medical screening may be warranted. In the interim, the following recommendations related to occupational health surveillance are provided for workplaces where workers may be exposed to silver nanomaterials in the course of their work [NIOSH 2009]:

- Take prudent measures to control exposures to silver nanomaterials;
- Conduct hazard surveillance as the basis for implementing controls; and
- Use established medical surveillance approaches [NIOSH 2009].

This page intentionally left blank.

# 8 Research Needs

Additional data and information are needed to ascertain the occupational safety and health concerns of working with all forms of silver. Data are particularly needed on sources of exposure to silver nanomaterials (such as AgNPs and AgNWs) and on factors that influence workers' exposure; exposure control measures (such as engineering controls) and work practices that are effective in reducing worker exposures to below the NIOSH REL; and appropriate measurement methods and exposure metrics for characterizing workplace exposures. In vitro and in vivo studies with silver of different physical-chemical properties are needed to better understand the role of particle size, shape, surface charge, chemical composition, dissolution rate, and surface treatment in causing toxicity. Chronic inhalation studies in animals may provide information about the long-term potential for adverse health effects in workers.

The following types of research and findings are needed to determine appropriate risk management practices for protecting workers occupationally exposed to silver, including silver nanomaterials:

1. Identification of industries or occupations in which exposures to silver may occur, including trends in the production and use of silver nanomaterials
2. Description of work tasks and scenarios with a potential for exposure to silver nanomaterials by inhalation, dermal, oral, and other routes
3. Information on measurement methods and exposure metrics to quantify worker exposure to silver nanomaterials, including information on the utility and limitations of those methods for quantifying exposures
4. Development of methods for assessment of silver nanomaterials that expand capabilities and improve risk management, such as with real-time monitoring or spatial and temporal mapping
5. Workplace exposure measurement data from the industries, jobs, and tasks where silver nanomaterials are manufactured and used
6. Studies on the design and effectiveness of control measures (such as engineering controls, work practices, PPE) being used in the workplace to minimize worker exposure to silver, including silver nanomaterials
7. Case reports or other health information demonstrating potential health effects in workers exposed to silver nanomaterials
8. Epidemiologic studies of workers, including quantitative exposure estimates by silver type and particle size
9. In vitro and in vivo studies to better understand the physicochemical properties of AgNPs and how those properties affect AgNP toxicology, including particle size and size dispersion (monodispersity, polydispersity), shape, zeta potential, surface coating, agglomeration, age of sample, ion-producing potential, and dissolution rate; in vitro and in vivo studies to determine the effect of surface modifications, including coatings, on toxicity
10. Long-term studies to elucidate the biological mechanisms of the toxicity of silver nanomaterials, including interactions with cellular and subcellular structures, cellular bioprocessing, and underlying molecular events following particle speciation or dissolution
11. Long-term animal inhalation exposure studies with AgNPs and AgNWs of different compositions and dimensions to assess biodistribution/accumulation and chronic effects, including

the use of an accepted AgNP reference material (e.g., National Institute of Standards and Technology [NIST 2015]) as a control

12. Studies to determine genotoxicity and potential effects in other target organs, including the central nervous system and reproductive system, following longer exposure durations
13. Further validation of the PBPK models of silver nanomaterials (e.g., Bachler et al. [2013], used in the NIOSH risk assessment) to estimate silver tissue doses in rodents and humans by particle size and solubility, including utilization of experimental data on the interactions between silver nanoparticles and biological compounds and possible changes in particle properties that could influence the toxicokinetics
14. Studies of potential biomarkers of adverse lung or liver effects associated with exposure to silver nanoparticles
15. Investigation of the human health effects of chronic AgNP exposure, including cumulative risks by inhalation, oral, and/or dermal routes of exposure
16. Determination of any age, sex, or other group differences in AgNP sensitivity to better inform risk assessment.

# 9 References


ACGIH [1974]. TLVs® Threshold Limit Values for chemical substances in workroom air adopted by the American Conference of Government Industrial Hygienists for 1973. J Occup Med *16*(1):39–58.

ACGIH [2001]. Silver and compounds. In: Documentation of threshold limit values and biological exposure indices. 7th ed. Vol. 1. Cincinnati, OH: American Conference of Governmental Industrial Hygienists.

ACGIH [2010]. Industrial ventilation: a manual of recommended practice for operation and maintenance. Cincinnati, OH: American Conference of Governmental Industrial Hygienists.

ACGIH [2013]. Industrial ventilation: a manual of recommended practice for design. Cincinnati, OH: American Conference of Governmental Industrial Hygienists.

Ahamed M, Karns M, Goodson M, Rowe J, Hussain SM, Schlager JJ, Hong Y [2008]. DNA damage response to different surface chemistry of silver nanoparticles in mammalian cells. Toxicol Appl Pharmacol *233*(3):404–410.

Aktepe N, Kocyigit A, Yukselten Y, Taskin A, Keskin C, Celik H [2015]. Increased DNA damage and oxidative stress among silver jewelry workers. Biol Trace Elem Res *164*(2):185–191, https://doi.org/10.1007/s12011-014-0224-0.

Amato C, Hussain S, Hess K, Schlager J [2006]. Interaction of nanomaterials with mouse keratinocytes. The Toxicologist *90*(1-S):168.

Anderson DS, Patchin ES, Silva RM, Uyeminami DL, Sharmah A, Guo T, Das GK, Brown JM, Shannahan J, Gordon T, Chen LC, Pinkerton KE, van Winkle LS [2015a]. Influence of particle size on persistence and clearance of aerosolized silver nanoparticles in the rat lung. Toxicol Sci *144*(2):366–381.

Anderson DS, Silva RM, Lee D, Edwards PC, Sharmah A, Guo T, Pinkerton KE, van Winkle LS [2015b]. Persistence of silver nanoparticles in the rat lung: influence of dose, size and chemical composition. Nanotoxicology *9*(5):591–602.

ARA [2011]. Multiple-path particle deposition (MPPD 2.1): a model for human and rat airway particle dosimetry. Raleigh, NC: Applied Research Associates, Inc.

ARA [2015]. Multiple-path particle dosimetry model (MPPD v. 3.4). Raleigh, NC: Applied Research Associates, Inc.

Arai Y, Miyayama T, Hirano S [2015]. Difference in the toxicity mechanism between ion and nanoparticle forms of silver in the mouse lung and in macrophages. Toxicology *328*:84–92, https://www.sciencedirect.com/science/article/pii/S0300483X14002534?via%3Dihub.

Armitage SA, White MA, Wilson HK [1996]. The determination of silver in whole blood and its application to biological monitoring of occupationally exposed groups. Ann Occup Hyg *40*(3):331–338.

Arora S, Jain J, Rajwade JM, Paknikar KM [2008]. Cellular responses induced by silver nanoparticles: in vitro studies. Toxicol Lett *179*(2):93–100.

Arora S, Jain J, Rajwade JM, Paknikar KM [2009]. Interactions of silver nanoparticles with primary mouse fibroblasts and liver cells. Toxicol Appl Pharmacol *236*(3):310–318.

AshaRani PV, Mun GLK, Hande MP, Valiyaveettil S [2009]. Cytotoxicity and genotoxicity of silver nanoparticles in human cells. ACS Nano *3*(2):279–290.

Aschberger K, Micheletti C, Sokull-Kluttgen B, Christensen FM [2011]. Analysis of currently available data for characterising the risk of engineered

nanomaterials to the environment and human health–lessons learned from four case studies. Environ Int *37*:1143–1156.

Ashraf A, Sharif R, Ahmad M, Masood M, Shahid A, Anjum DH, Rafique MS, Ghani S [2015]. In vivo evaluation of the biodistribution of intravenously administered naked and functionalised silver nanoparticles in rabbit. IET Nanobiotechnol *9*(6):368–374.

ATSDR [1990]. Toxicological profile for silver. TP-90-24. Atlanta, GA: Agency for Toxic Substances and Disease Registry.

Austin CA, Umbreit TH, Brown KM, Barber DS, Dair BJ, Francke-Carroll S, Feswick A, Saint-Louis MA, Hikawa H, Siebein KN, Goering PL [2012]. Distribution of silver nanoparticles in pregnant mice and developing embryos. Nanotoxicology *6*(8):912–922.

Avalos A, Haza AI, Mateo D, Morales P [2015]. Effects of silver and gold nanoparticles of different sizes in human pulmonary fibroblasts. Toxicol Mech Methods *25*(4):287–295, https://doi.org/10.3109/15376516.2015.1025347.

Avalos Funez A, Isabel Haza A, Mateo D, Morales P [2013]. In vitro evaluation of silver nanoparticles on human tumoral and normal cells. Toxicol Mech Methods *23*(3):153–160, https://doi.org/10.3109/15376516.2012.762081.

Axson JL, Stark DI, Bondy AL, Capracotta SS, Maynard AD. Philbert, MA, Bergin IL, Ault AP [2015]. Rapid kinetics of size and pH-dependent dissolution and aggregation of silver nanoparticles in simulated gastric fluid. J Phys Chem C *119*(35):20632–20641, https://pubs.acs.org/doi/10.1021/acs.jpcc.5b03634.

Bachler G, von Goetz N, Hungerbühler K [2013]. A physiologically based pharmacokinetic model for ionic silver and silver nanoparticles. Intl J Nanomed *8*:3365–3382.

Bachler G, Losert S, Umehara Y, von Goetz N, Rodriguez-Lorenzo L, Petri-Fink A, Rothen-Rutishauser B, Hungerbuehler K [2015a]. Translocation of gold nanoparticles across the lung epithelial tissue barrier: combining in vitro and in silico methods to substitute in vivo experiments. Part Fibre Toxicol *12*:18.

Bachler G, von Goetz N, Hungerbühler K [2015b]. Using physiologically based pharmacokinetic (PBPK) modeling for dietary risk assessment of titanium dioxide ($TiO_2$) nanoparticles. Nanotoxicology *9*(3):373–380.

Bailey MR, Fry FA, James AC [1985]. Long-term retention of particles in the human respiratory tract. J Aerosol Sci *16*:295–305.

Baker EL, Matte TP [2005]. Occupational health surveillance. In: Rosenstock L, Cullen E, Brodkin R, eds. Textbook of clinical occupational and environmental medicine. Philadelphia, PA: Elsevier Saunders, https://www.osha.gov/medical-surveillance.

Bałazy A, Toivola M, Reponen T, Podgorski A, Zimmer A, Grinshpun SA [2006]. Manikin-based performance evaluation of N95 filtering facepiece respirators challenged with nanoparticles. Ann Occup Hyg *50*(3):259–269.

Beer C, Foldbjerg R, Hayashi Y, Sutherland DS, Autrup H [2012]. Toxicity of silver nanoparticles: nanoparticle or silver ion? Toxicol Lett *208*:286–292.

Bell RA, Kramer JR [1999]. Structural chemistry and geochemistry of silver-sulfur compounds: critical review. Environ Toxicol Chem *18*(1):9–22.

Bergin IL, Wilding LA, Morishita M, Walacavage K, Ault AP, Axson JL, Stark DI, Hashway SA, Capracotta SS, Leroueil PR, Matnard AD, Philbert MA [2016]. Effects of particle size and coating on toxicological parameters, fecal elimination kinetics, and tissue distribution of acutely ingested silver nanoparticles in a mouse model. Nanotoxicology *10*(3):352–360.

Bisson G, Lamoureux G, Begin R [1987]. Quantitative gallium 67 lung scan to assess the inflammatory activity in the pneumoconioses. Semin Nucl Med *17*(1):72–80.

Bolton RE, Vincent HJ, Jones AD, Addison J, Beckett ST [1983]. An overload hypothesis for pulmonary clearance of UICC amosite fibers inhaled by rats. Br J Ind Med *40*:264–272.

Borm P, Cassee FR, Oberdörster G [2015]. Lung particle overload: old school—new insights? Part Fibre Toxicol *12*:10.

Botelho DJ, Leo BF, Massa CB, Sarkar S, Tetley TD, Chung KF, Chen S, Ryan MP, Porter AE, Zhang J, Schwander SK, Gow AJ [2016]. Low-dose AgNPs reduce lung mechanical function and innate immune defense in the absence of cellular toxicity. Nanotoxicology *10*(1):118–127.

Boudreau MD, Imam MS, Paredes AM, Bryant MS, Cunningham CK, Felton RP, Jones MY, Davis KJ, Olson GR [2016]. Differential effects of silver nanoparticles and silver ions on tissue accumulation, distribution, and toxicity in the Sprague Dawley rat following daily oral gavage administration for 13 weeks. Toxicol Sci *150*:131–160.

Bove P, Malvindi MA, Kote SS, Bertorelli R, Summa M, Sabella S [2017]. Dissolution test for risk assessment of nanoparticles: a pilot study. Nanoscale *9*(19):6315–6326, https://pubs.rsc.org/en/content/articlehtml/2017/nr/c6nr08131b.

Braakhuis H, Gosens I, Krystek P, Boere J, Cassee F, Fokkens P, Post J, van Loveren H, Park M [2014]. Particle size dependent deposition and pulmonary inflammation after short-term inhalation of silver nanoparticles. Particle Fibre Toxicol *11*:49.

Braakhuis HM, Giannakou C, Peijnenburg WJ, Vermeulen J, van Loveren H, Park MV [2016]. Simple *in vitro* models can predict pulmonary toxicity of silver nanoparticles. Nanotoxicology *10*(6):770–779, https://doi.org/10.3109/17435390.2015.1127443.

Braydich-Stolle LK, Lucas B, Schrand A, Murdock RC, Lee T, Schlager JJ, Hussain SM, Hofmann MC [2010]. Silver nanoparticles disrupt GDNF/Fyn kinase signaling in spermatogonial stem cells. Toxicol Sci *116*(2):577–589.

Brookhaven National Laboratory [2014]. IH75190 surface wipe sampling procedure. Upton, NY: Brookhaven National Laboratory, https://www.bnl.gov/esh/shsd/sop/pdf/IH_SOPS/IH75190.pdf.

Brouwer D, van Duuren-Stuurman B, Berges M, Jankowska E, Bard D, Mark D [2009]. From workplace air measurement results toward estimates of exposure? Development of a strategy to assess exposure to manufactured nano-objects. J Nanopart Res *11*(8):1867–1881.

Brune D, Nordberg G, Wester PO [1980]. Distribution of 23 elements in the kidney, liver and lungs of workers from a smeltery and refinery in North Sweden exposed to a number of elements and of a control group. Sci Total Environ *16*(1):13–35.

BSI [2005]. Publicly available specification: Vocabulary—nanoparticles. London, UK: British Standards Institute. Document no. PAS 71:2005, pp. 32.

Bucher JR, Portier CJ, Goodman JI, Faustman EM, Lucier GW [1996]. Workshop overview—National Toxicology Program studies: Principles of dose selection and applications to mechanistic based risk assessment. Fundam Appl Toxicol *31*:1–8.

Buckley WR [1963]. Localized argyria. Arch Derm *88*:531–539.

Bullock W, Ignacio JS, eds. [2006]. A strategy for assessing and managing occupational exposures. 3rd ed. Fairfax, VA: AIHA Press.

Campagnolo L, Massimiani M, Vecchione L, Piccirilli D, Toschi N, Magrini A, Bonanno E, Scimeca M, Castagnozzi L, Buonanno G, Stabile L, Cubadda F, Aureli F, Fokkens PH, Kreyling WG, Cassee FR, Pietroiusti A [2017]. Silver nanoparticles inhaled during pregnancy reach and affect the placenta and the foetus. Nanotoxicology *11*(5):687–698.

Carlson C, Hussain SM, Schrand AM, Braydich-Stolle LK, Hess KL, Jones RL, Schlager JJ [2008]. Unique cellular interaction of silver nanoparticles: size-dependent generation of reactive oxygen species. J Phys Chem B *112*(43):13608–13619.

Castellan RM, Olenchock SA, Kinsley KB, Hankinson JL [1987]. Inhaled endotoxin and decreased

spirometric values. An exposure-response relation for cotton dust. N Engl J Med *317*(10):605–610.

Catsakis LH, Sulica VI [1978]. Allergy to silver amalgams. Oral Surg *46*:371–375.

Chairuangkitti P, Lawanprasert S, Roytrakul S, Aueviriyavit S, Phummiratch D, Kulthong K, Chanvorachote P, Maniratanachote R [2013]. Silver nanoparticles induce toxicity in a549 cells via ROS-dependent and ROS-independent pathways. Toxicol In Vitro *27*(1):330–338, https://dx.doi.org/10.1016/j.tiv.2012.08.021.

Chang AL, Khosravi V, Egbert B [2006]. A case of argyria after colloidal silver ingestion. J Cutan Pathol *33*(12):809–811.

Chen R, Zhao L, Bai R, Liu Y, Han L, Xu Z, Chen F, Autrup H, Long D, Chen C [2016]. Silver nanoparticles induced oxidative and endoplasmic reticulum stresses in mouse tissues: implications for the development of acute toxicity after intravenous administration. Toxicol Res *01 March* (2):602–608.

Chen X, Schluesener HJ [2008]. Nanosilver: a nanoproduct in medical application. Toxicol Lett *176*(1):1–12.

Cheng KH, Cheng YS, Yeh HC, Guilmette RA, Simpson SQ, Yang YH, Swift DL [1996]. In vivo measurements of nasal airway dimensions and ultrafine aerosol deposition in the human nasal and oral airways. J Aerosol Sci *27*(5):785–801.

Cho EA, Lee WS, Kim KM, Kim S-Y [2008]. Occupational generalized argyria after exposure to aerosolized silver. J Dermatol *35*:759–760, https://doi.org/10.1111/j.1346-8138.2008.00562.x.

Cho W-S, Duffin R, Donaldson K [2012]. Zeta potential and solubility to toxic ions as mechanisms of lung inflammation caused by metal/metal oxide nanoparticles. Toxicol Sci *126*(2):469–477.

Chrastina A, Schnitzer JE [2010]. Iodine-125 radiolabeling of silver nanoparticles for in vivo SPECT imaging. Int J Nanomed *5*:653–659.

Christensen FM, Johnston HJ, Stone V, Aitken RJ, Hankin S, Peters S, Aschberger K [2010]. Nano-silver—feasibility and challenges for human health risk assessment based on open literature. Nanotoxicology *4*(3):284–295.

Chuang H-C, Hsiao T-C, Wu C-K, Chang H-H, Lee C-H, Chang C-C, Cheng T-J [2013]. Allergenicity and toxicology of inhaled silver nanoparticles in allergen-provocation mice models. Int J Nanomed *8*:4495–4506.

Coccini T, Manzo L, Bellotti V, De Simone U [2014]. Assessment of cellular responses after short- and long-term exposure to silver nanoparticles in human neuroblastoma (sh-sy5y) and astrocytoma (d384) cells. Sci World J *2014*:ID 259765, https://doi.org/10.1155/2014/259765.

Connolly M, Fernandez-Cruz ML, Quesada-Garcia A, Alte L, Segner H, Navas JM [2015]. Comparative cytotoxicity study of silver nanoparticles (AgNPs) in a variety of rainbow trout cell lines (rtl-w1, rth-149, rtg-2) and primary hepatocytes. Int J Environ Res Public Health, *12*(5):5386–5405, https://www.mdpi.com/1660-4601/12/5/5386.

Corn M, Esmen N [1979]. Workplace exposure zones for classification of employee exposure to physical and chemical agents. Am Industr Hyg Assoc *40*:47–57.

Cotton CV, Spencer LG, New RP, Cooper RG [2017]. The utility of comprehensive autoantibody testing to differentiate connective tissue disease associated and idiopathic interstitial lung disease subgroup cases. Rheumatology *56*:1264–1271.

Cronholm P, Karlsson HL, Hedberg J, Lowe TA, Winnberg L, Elihn K, Wallinder IO, Möller L [2013]. Intracellullar uptake and toxicity of Ag and CuO nanoparticles: a comparison between nanoparticles and their corresponding metal ions. Small *9*(7):970–982.

Crump KS [1984]. A new method for determining allowable daily intakes. Fund Appl Toxicol *4*(5):854–871.

Dabrowska-Bouta B, Zieba M, Orzelska-Gorka J, Skalska J, Sulkowski G, Frontczak-Baniewicz

M, Talarek S, Listos J, Struzynska L [2016]. Influence of a low dose of silver nanoparticles on cerebral myelin and behavior of adult rats. Toxicology *363*:29–36.

Dankovic DA, Naumann BD, Maier A, Dourson ML, Levy LS [2015]. The scientific basis of uncertainty factors used in setting occupational exposure limits. J Occup Environ Hyg *12*(Suppl 1):S55–S68.

Dasgupta N, Ranjan S, Ramalingam C, Gandhi M [2019]. Silver nanoparticles engineered by thermal co-reduction approach induces liver damage in Wistar rats: acute and sub-chronic toxicity analysis. 3 Biotech *9*:125.

Davenport LL, Hsieh H, Eppert BL, Carreira VS, Krishan M, Ingle T, Howard PC, Williams MT, Vorhees CV, Genter MB [2015]. Systemic and behavioral effects of intranasal administration of silver nanoparticles. Neurotoxicol Teratol *51*:68–76.

De Jong WH, Van Der Ven LT, Sleijffers A, Park MV, Jansen EH, Van Loveren H, Vandebriel RJ [2013]. Systemic and immunotoxicity of silver nanoparticles in an intravenous 28 days repeated dose toxicity study in rats. Biomaterials *34*:8333–8343.

Deng F, Olesen P, Foldbjerg R, Dang DA, Guo X, Autrup H [2010]. Silver nanoparticles upregulate connexin43 expression and increase gap junctional intercellular communication in human lung adenocarcinoma cell line A549. Nanotoxicology *4*:186–195.

DFG [2013]. Deutsche Forschungsgemeinschaft. List of MAK and BAT values 2013. Weinheim, Germany: Wiley-VCH Veriag GmbH & Co. KGaA. ISBN: 978-3-527-33616-6.

DiVincenzo GD, Giordano CJ, Schriever LS [1985]. Biologic monitoring of workers exposed to silver. Int Arch Occup Environ Health *56*:207–215.

Dong MS, Choi JY, Sung JH, Kim JS, Song KS, Ryu HR, Lee JH, Bang IS, An K, Park HM, Song NW, Yu IJ [2013]. Gene expression profiling of kidneys from Sprague-Dawley rats following 12-week inhalation exposure to silver nanoparticles. Toxicol Mech Methods *23*(6):437–448.

Drake PL, Hazelwood KJ [2005]. Exposure-related health effects of silver and silver compounds: a review. Ann Occup Hyg *49*(*7*):575–585.

Driscoll KE, Carter JM, Howard BW, Hassenbein DG, Pepelko W, Baggs RB, Oberdörster G [1996]. Pulmonary inflammatory, chemokine, and mutagenic responses in rats after subchronic inhalation of carbon black. Toxicol Appl Pharmacol *136*:372–380.

Driscoll KE, Deyo LC, Carter JM, Howard BW, Hassenbein DG, Bertram TA [1997]. Effects of particle exposure and particle-elicited inflammatory cells on mutation in rat alveolar epithelial cells. Carcinogenesis *18*(2):423–430.

Driscoll KE, Costa DL, Hatch G, Henderson R, Oberdörster G, Salem H, Schlesinger RB [2000]. Intratracheal instillation as an exposure technique for the evaluation of respiratory tract toxicity: uses and limitations. Toxicol Sci *55*(1):24–35.

Duan N, Mage T [1997]. Combination of direct and indirect approaches for exposure assessment. J Expo Anal Environ Epidemiol *7*(4):439–470.

Dziendzikowska K, Gromadzka-Ostrowska J, Lankoff A, Oczkowski M, Krawczynska A, Chwastowska J, Sadowska-Bratek M, Chajduk E, Wojewodzka M, Dusinska M, Kruszewski M [2012]. Time-dependent biodistribution and excretion of silver nanoparticles in male Wistar rats. J Appl Toxicol *32*:920–928.

ECHA [2012]. Guidance on information requirements and chemical safety assessment. Chapter R.8: Characterisation of dose [concentration]-response for human health. Version: 2.1. European Chemicals Agency (ECHA). ECHA-2010-G-19-EN, https://www.echa.europa.eu/documents/10162/13632/information_requirements_r8_en.pdf.

Elder A, Gelein R, Finkelstein JN, Driscoll KE, Harkema J, Oberdorster G [2005]. Effects of subchronically inhaled carbon black in three species. I. Retention kinetics, lung inflammation, and histopathology. Toxicol Sci *88*(2):614–629.

Elle RE, Gaillet S, Vide J, Romain C, Lauret C, Rugani N, Cristol JP, Rouanet JM [2013]. Dietary exposure to silver nanoparticles in Sprague-Dawley

rats: effects on oxidative stress and inflammation. Food Chem Toxicol *60*:297–301.

Elzey S, Grassian VH [2010]. Agglomeration, isolation, and dissolution of commercially manufactured silver nanoparticles in aqueous environments. J Nanoparticle Res *12*:1945–1958.

Eustis SL, Boorman GA, Harada T, Popp JA [1990]. Liver. In: Boorman GA, Eustis SL, Elwell MR, Montgomery CA Jr, MacKenzie WF, eds. Pathology of the Fischer rat: reference and atlas. New York: Academic Press.

Exposure limits for airborne contaminants. 30 CFR 57.5001.

Evanoff DD, Chumanov G [2005]. Synthesis and optical properties of silver nanoparticles and arrays. Chem Phys Chem *6*:1221–1231.

Fennell TR, Mortensen NP, Black SR, Snyder RW, Levine KE, Poitras E, Harrington JM, Wingard CJ, Holland NA, Pathmasiri W, Sumner SC [2017]. Disposition of intravenously or orally administered silver nanoparticles in pregnant rats and the effect on the biochemical profile in urine. J Appl Toxicol *37*(5):530–544.

Ferin J, Oberdörster G, Penney DP [1992]. Pulmonary retention of ultrafine and fine particles in rats. Am J Respir Cell Mol Biol *6*:535–542.

Foldbjerg R, Dang DA, Autrup H [2011]. Cytotoxicity and genotoxicity of silver nanoparticles in the human lung cancer cell line, A549. Arch Toxicol *85*(7):743–750.

Foldbjerg R, Irving ES, Hayaski Y, Sutherland DS, Thorsen K, Autrup H, Beer C [2012]. Global gene expression profiling of human lung epithelial cells after exposure to nanosilver. Toxicol Sci *130*(1):145–157.

Foldbjerg R, Olesen P, Hougaard M, Dang DA, Hoffmann HJ, Autrup H [2009]. PVP-coated silver nanoparticles and silver ions induce reactive oxygen species, apoptosis and necrosis in THP-1 monocytes. Toxicol Lett *190*(2):156–162.

Forycki Z, Zegarski W, Bardzik J, Swica P [1983]. Acute silver poisoning through inhalation. Bull Inst Marit Trop Med Gdynia *34*(3-4):199-203.

Furchner JE, Richmond CR, Drake GA [1968]. Comparative metabolism of radionuclides in mammals-IV. Retention of silver 110m in the mouse, rat, monkey and dog. Health Physics *15*:505–514.

Future Markets, Inc. [2013]. The global nanotechnology and nanomaterials industry. Technology Report No. 68, https://www.futuremarketsinc.com/.

Gaiser BK, Hirn S, Kermanizadeh A, Kanase N, Fytianos K, Wenk A, Haberl N, Brunelli A, Kreyling WG, Stone V [2013]. Effects of silver nanoparticles on the liver and hepatocytes in vitro. Toxicol Sci *131*(2):537–547, https://doi.org/10.1093/toxsci/kfs306.

Gao P, Behar JL, Shaffer R [2014]. Considerations for selection of PPE to protect against nanoparticle dermal exposure. In Daniel Anna, ed. Chemical Protective Clothing. 2nd printing of 2nd ed. Fairfax, VA: AIHA Press, pp. 511–555.

Gao P, Jaques PA, Hsiao T, Shepherd A, Eimer BC, Yang M, Miller A, Gupta B, Shaffer R [2011]. Evaluation of nano- and submicron particle penetration through ten nonwoven fabrics using a wind-driven approach. J Occup Environ Hyg *8*(1):13–22.

Garcia T, Lafuente D, Blanco J, Sanchez DJ, Sirvent JJ, Domingo JL, Gomez M [2016]. Oral subchronic exposure to silver nanoparticles in rats. Food Chem Toxicol *92*:177–187.

Garcia-Reyero N, Kennedy AJ, Escalon BL, Habib T, Laird JG, Rawat A, Wiseman S, Hecker M, Denslow N, Steevens JA, Perkins EJ [2014]. Differential effects and potential adverse outcomes of ionic silver and silver nanoparticles in vivo and in vitro. Environ Sci Technol *48*(8):4546–4555, https://doi.org/10.1021/es4042258.

Genter MB, Newman NC, Shertzer HG, Ali SF, Bolon B [2012]. Distribution and systemic effects of intranasally administered 25 nm silver nanoparticles in adult mice. Toxicol Pathol *40*(7):1004–1013.

Giese B, Klaessig F, Park B, Kaegi R, Steinfeldt M, Wigger H, von Gleich AV, Gottschalk F [2018]. Risks, release and concentrations of engineered nanomaterial in the environment. Sci Rep *8*(1):1565: 1–18, https://doi.org/10.1038/s41598-018-19275-4.

Gliga AR, Skoglund S, Wallinder IO, Fadeel B, Karisson HL [2014]. Size-dependent cytotoxicity of silver nanoparticles in human lung cells: the role of cellular uptake, agglomeration and Ag release. Particle Fibre Toxicol *11*:11, doi:10.1186/1743-8977-11-11.

Golanski L, Guiot A, Rouillon F, Pocachard J, Tardif F [2009]. Experimental evaluation of personal protection devices against graphite nanoaerosols: fibrous filter media, masks, protective clothing, and gloves. Hum Exp Toxicol *28*(6–7):353–359.

Golanski L, Guiot A, Tardif F [2010]. Experimental evaluation of individual protection devices against different types of nanoaerosols: graphite, $TiO_2$ and Pt. J Nanopart Res *12*(1):83–89.

Gopinath P, Gogoi SK, Sanpui P, Paul A, Chattopadhyay A, Ghosk SS [2010]. Signaling gene cascade in silver nanoparticle induced apoptosis. Colloids and Surface B: Biointerfaces *77*:240–245.

Gosens I, Kermanizadeh A, Jacobsen NR, Lenz A-G, Bokkers B, de Jong, WH, Krystek P, Tran L, Stone V, Wallin H, Stoeger T, Cassee FR [2015]. Comparative hazard identification by a single dose lung exposure of zinc oxide and silver nanomaterials in mice. PLOS ONE, doi:10.1371/journal.pone.0126934.

Gregoratto D, Bailey MR, Marsh JW [2010]. Modelling particle retention in the alveolar-interstitial region of the human lungs. J Radiol Prot *30*(3):491–512.

Greulich C, Diendorf J, Simon T, Eggeler G, Epple M, Koller M [2011]. Uptake and intracellular distribution of silver nanoparticles in human mesenchymal stem cells. Acta Biomaterialia *7*:347–354.

Greulich C, Kittler S, Epple M, Muhr G, Koller M [2009]. Studies on the biocompatibility and the interaction of silver nanoparticles with human mesenchymal stem cells (hMSCs). Arch Surg *394*:495–502.

Gromadzka-Ostrowska J, Dziendzikowska K, Lankoff A, Dobrzynska M, Instanes C, Brunborg G, Gajowik A, Radzikowska J, Wojewodzka M, Kruszewski M [2012]. Silver nanoparticles effects on epididymal sperm in rats. Toxicol Lett *214*:251–258.

Guo H, Zhang J, Boudreau M, Meng J, Yin JJ, Liu J, Xu H [2016]. Intravenous administration of silver nanoparticles causes organ toxicity through intracellular ROS-related loss of inter-endothelial junction. Part Fibre Toxicol *13*:21, doi: 10.1186/s12989-016-0133-9.

Haberl N, Hirn S, Wenk A, Diendorf J, Epple M, Johnston BD, Krombach F, Kreyling WG, Schleh C [2013]. Cytotoxicity and proinflammatory effects of PVP-coated silver nanoparticles after intratracheal instillation in rats. Beilstein J Nanotechnol *4*:933–940.

Hackenberg S, Scherzed A, Kessler M, Hummel S, Technau A, Froelich K, Ginzkey C, Koehler C, Hagen R, Kleinsasser N [2011]. Silver nanoparticles: evaluation of DNA damage, toxicity and functional impairment in human mesenchymal stem cells. Toxicol Lett *201*(1):27–33.

Hadrup N, Lam HR, Loeschner K, Mortensen A, Larsen EH, Frandsen H [2012b]. Nanoparticulate silver increases uric acid and allantoin excretion in rats, as identified by metabolomics. J Appl Toxicol *32*:929–933.

Hadrup N, Loeschner K, Bergstrom A, Wilcks A, Gao X, Vogel U, Frandsen HL, Larsen EH, Lam HR, Mortensen A [2012a]. Subacute oral toxicity investigation of nanoparticulate and ionic silver in rats. Arch Toxicol *86*:543–551.

Hadrup N, Loeschner K, Mortensen A, Sharma AK, Qvortrup K, Larsen EH, Lam HR [2012c]. The similar neurotoxic effects of nanoparticulate and ionic silver *in vivo* and *in vitro*. Neurotoxicology *33*:416–423.

Hagens WI, Oomen AG, de Jong WH, Cassee FR, Sips A [2007]. What do we (need to) know about the kinetic properties of nanoparticles in the body? Reg Tox Pharm *49*:217–229.

Hailey JR, Nold JB, Brown RH, Cullen JM, Holder JC, Jordan HL, Ennulat D, Miller RT [2014]. Biliary proliferative lesions in the Sprague-Dawley rat: adverse/non-adverse. Toxicol Pathol *42*:844–854.

Hamilton RF, Buckingham S, Holian A [2014]. The effect of size on Ag nanosphere toxicity in macrophage cell models and lung epithelial cell lines is dependent on particle dissolution. Int J Mol Sci *15*(4):6815–6830, https://doi.org/10.3390/ijms15046815.

Han JW, Gurunathan S, Jeong JK, Choi YJ, Kwon DN, Park JK, Kim JH [2014]. Oxidative stress mediated cytotoxicity of biologically synthesized silver nanoparticles in human lung epithelial adenocarcinoma cell line. Nanoscale Res Lett *9*(1):459, doi: 10.1186/1556-276X-9-459.

Hansen RE, Roth D, Winther JR [2009]. Quantifying the global cellular thiol-disulfide status. Proc Natl Acad Sci USA *106*(2):422–427.

Harber P, Conlon C, McCunney RJ [2003]. Occupational medical surveillance. In: McCunney RJ, ed. A practical approach to occupational and environmental medicine. Philadelphia, PA: Lippincott, Williams, & Wilkins.

Harkema JR, Nikula KJ, Haschek WM [2013]. Respiratory system. In: Haschek W, Rousseaux C, Wallig M, eds. Haschek and Rousseaux's handbook of toxicologic pathology. Vol. III. Systems toxicologic pathology. 3rd ed. Cambridge, MA: Academic Press, pp. 1935–2003.

Harker JM, Hunter D [1935]. Occupational argyria. Br J Dermatol Syphilis *November*:441–455.

Hathaway GJ, Proctor NH [2004]. Chemical hazards of the workplace. 5th ed. Hoboken, NJ: John Wiley & Sons, 632–634.

Hazard communication (HazCom). 30 CFR 47.

Hazard communication. 29 CFR 1910.1200.

He Y, Du Z, Ma S, Liu Y, Li D, Huang H, Jiang S, Cheng S, Wu W, Zhang K, Zheng X [2016]. Effects of green-synthesized silver nanoparticles on lung cancer cells in vitro and grown as xenograft tumors in vivo. Int J Nanomed *11*:1879–1887, https://doi.org/10.2147/IJN.S103695.

Hendren CQ, Mesnard X, Droge J, Wiesner MR [2011]. Estimating production data for five engineered nanomaterials as a basis for exposure assessment. Environ Sci Technol *45*:2562–2569.

Hendrickson OD, Klochkov SG, Novikova OV, Bravova IM, Shevtsova EF, Safenkova IV, Zherdev AV, Bachurin SO, Dzantiev BB [2016]. Toxicity of nanosilver in intragastric studies: biodistribution and metabolic effects. Toxicol Lett *Jan 22*(241): 184–192.

Herzog F, Clift MJ, Piccapietra F, Behra R, Schmid O, Petri-Fink A, Rothen-Rutishauser B [2013]. Exposure of silver-nanoparticles and silver-ions to lung cells in vitro at the air-liquid interface. Part Fibre Toxicol, *10*:11, https://dx.doi.org/10.1186/1743-8977-10-11.

Herzog F, Loza K, Balog S, Clift MJ, Epple M, Gehr P, Petri-Fink A, Rothen-Rutishauser B [2014]. Mimicking exposures to acute and lifetime concentrations of inhaled silver nanoparticles by two different in vitro approaches. Beilstein J Nanotechnol, *5*:1357–1370, https://doi.org/10.3762/bjnano.5.149.

Hill WR, Pillsbury DM [1939]. Argyria: the pharmacology of silver. Baltimore, MD: The Williams and Wilkins Company.

Hinds WC [1999]. Aerosol technology: properties, behavior, and measurement of airborne particles, 2nd ed. New York: John Wiley & Sons, p. 5.

Holland NACM, Becak DP, Shannahan JH, Brown JM, Carratt SA, Van Winkle LS, Pinkerton KE, Wang CM, Munusamy P, Baer DR, Sumner SJ, Fennell TR, Lust RM, Wingard CJ [2015]. Cardiac ischemia reperfusion injury following instillation of 20 nm citrate-capped nanosilver. J Nanomed Nanotechnol, https://doi.org/10.4172/2157-7439.s6-006.

Hsin YH, Chen CF, Huang S, Shih TS, Lai PS, Chueh PJ [2008]. The apoptotic effect of nanosilver is mediated by a ROS- and JNK-dependent

mechanism involving the mitochondrial pathway in NIH3T3 cells. Toxicol Lett *179*(3):130–139.

Hubbs AF, Mercer RR, Benkovic SA, Harkema J, Sriram K, Schwegler-Berry D, Goravanahally MP, Nurkiewicz TR, Castranova V, Sargent LM [2011]. Nanotoxicology—a pathologist's perspective. Toxicologic Pathol *39*:301–324.

Huo L, Chen R, Zhao L, Shi X, Bai R, Long D, Chen F, Zhao Y, Chang YZ, Chen C [2015]. Silver nanoparticles activate endoplasmic reticulum stress signaling pathway in cell and mouse models: the role in toxicity evaluation. Biomaterials *61*:307–315, https://doi.org/10.1016/j.biomaterials.2015.05.029.

Hussain S, Hess K, Gearhart JM, Geiss KT, Schlager JJ [2005b]. Toxicity assessment of silver nanoparticles (Ag 15, 100 nm) in alveolar macrophages. Toxicol Sci *84*(1-S):350.

Hussain SM, Hess KL, Gearhart JM, Geiss KT, Schlager JJ [2005a]. In vitro toxicity of nanoparticles in BRL 3A rat liver cells. Toxicol In Vitro *19*(7):975–983.

Hyun J-S, Lee BS, Ryu HY, Sung JH, Chung KH, Yu IJ [2008]. Effects of repeated silver nanoparticles exposure on the histological structure and mucins of nasal respiratory mucosa in rats. Toxicol Lett *182*:24–28.

IARC [2010]. IARC monographs on the evaluation of carcinogenic risks to humans. In: carbon black, titanium dioxide, and talc. International Agency for Research on Cancer, World Health Organization. Vol. 93. Geneva: WHO Press.

ICRP [1960]. Report of Committee II on permissible dose for internal radiation, 1959. Annals of the ICRP. Tarrytown, NY: International Commission on Radiological Protection, ICRP Publication No. 2, pp. 1–40.

ICRP [1994]. Human respiratory tract model for radiological protection. In: Smith H, ed. Annals of the ICRP. Tarrytown, NY: International Commission on Radiological Protection, ICRP Publication No. 66.

ICRP [2015]. Occupational intakes of radionuclides: Part 1. Tarrytown, NY: International Commission on Radiological Protection, ICRP Publication No. 130. Ann ICRP *44*:2.

ILSI (International Life Sciences Institute) [2000]. The relevance of the rat lung response to particle overload for human risk assessment: a workshop consensus report. Inhal Toxicol *12*:1–17.

ISO [2006]. Workplace atmospheres; ultrafine, nanoparticle and nano-structured aerosols, exposure characterization and assessment. Geneva: International Standards Organization. Document No. ISO/TC 146/SC2/WGI N324.

ISO [2008]. Nanotechnologies: terminology and definitions for nano-object, nanoparticle, nanofibre and nanoplate. ISO/TS 27687:2008. Vienna, Austria: International Organization for Standardization.

Ito S [2011]. Pharmacokinetics 101. Paediatr Child Health *16*(9):535–536.

Jang S, Park JW, Cha HR, Jung SY, Lee JE, Jung SS, Kim JO, Kim SY, Lee CS, Park HS [2012]. Silver nanoparticles modify VEGF signaling pathway and mucus hypersecretion in allergic airway inflammation. Internat J Nanomed *7*:1329–1343.

Jeannet N, Fierz M, Schneider S, Kunzi L, Baumlin N, Salathe M, Burtscher H, Geiser M [2016]. Acute toxicity of silver and carbon nanoaerosols to normal and cystic fibrosis human bronchial epithelial cells. Nanotoxicology *10*(3):279–291, https://doi.org/10.3109/17435390.2015.1049233.

Jeong GN, Jo UB, Ryu HY, Kim YS, Song KS, Yu IJ [2010]. Histochemical study of intestinal mucins after administration of silver nanoparticles in Sprague-Dawley rats. Arch Toxicol *84*:63–69.

Jeschke MG [2009]. The hepatic response to thermal injury: is the liver important for postburn outcomes? Mol Med *15*:337–351.

Jeschke MG, Gauglitz GG, Song J, Kulp GA, Finnerty CC, Cos RA, Barral JM, Herndon DN, Boehning D [2009]. Calcium and ER stress mediate

hepatic apoptosis after burn injury. J Cell Mol Med *13*:1857–1865.

Johnson AT [2016]. Respirator masks protect health but impact performance: a review. J Biol Eng *10*:4, doi:10.1186/s13036-016-0025-4. PMID: 26865858; PMCID: PMC4748517.

Johnson AT, Scott WH, Lausted CG, Coyne KM, Sahota MS, Johnson MM, Grace Yeni-Komshian, Caretti DM [2000]. Communication using a telephone while wearing a respirator. Am Ind Hygiene Assoc J *61*(2): 264–267, https://doi.org/10.1080/15298660008984535.

Ji JH, Jung JH, Yu IJ, Kim SS [2007a]. Long-term stability characteristics of metal nanoparticle generator using small ceramic heater for inhalation toxicity studies. Inhal Toxicol *19*(9):745–751.

Ji JH, Jung JH Kim SS, Yoon J-U, Park JD Choi BS, Chung YH, Kwon IH, Jeong J, Han BS, Shin JH, Sung JH, Song KS, Yu IJ [2007b]. Twenty-eight-day inhalation toxicity study of silver nanoparticles in Sprague-Dawley rats. Inhalation Toxicol *19*:857–871.

Ji JH, Yu IJ [2012]. Estimation of human equivalent exposure from rat inhalation toxicity study of silver nanoparticles using multi-path particle dosimetry model. Toxicology Research, The Royal Society of Chemistry, https://doi.org/10.1039/c2tx20029e.

Johnston HJ, Hutchison G, Christensen FM, Peters S, Hankin S, Stone V [2010]. A review of the in vivo and in vitro toxicity of silver and gold particulates: particle attributes and biological mechanisms responsible for the observed toxicity. Crit Rev Tox *40*(4):328–346.

Juling S, Bachler G, von Gotz N, Lichtenstein D, Bohmert L, Niedzwiecka A, Selve S, Braeuning A, Lampen A [2016]. In vivo distribution of nanosilver in the rat: the role of ions and de novo-formed secondary particles. Food Chemical Toxicol *97*: 327–335.

Jun E-AH, Lim K-M, Kim K, Bae ON, Noh JY, Chung KH, Chung JH [2011]. Silver nanoparticles enhance thrombus formation through increased platelet aggregation and procoagulant activity. Nanotoxicology *5*(2):157–167.

Kaewamatawong T, Banlunara W, Maneewattanapinyo P, Thammachareon C, Ekgasit S [2014]. Acute and subacute pulmonary toxicity caused by a single intratracheal instillation of colloidal silver nanoparticles in mice: pathobiological changes and metallothionein responses. J Environ Pathol Toxicol Oncol *33*(1):59–68.

Kalberlah F, Fost U, Schneider K [2002]. Time extrapolation and interspecies extrapolation for locally acting substances in case of limited toxicological data. Ann Occup Hyg *46*(2):175–185.

Kalishwaralal K, Banumathi E, Pandian SBRK, Deepak V, Muniyandi J, Eom SH, Gurunathan S [2009]. Silver nanoparticles inhibit VEGF induced cell proliferation and migration in bovine retinal endothelial cells. Colloids Surf B Biointerfaces *73*(1):51–57.

Katnelson BA, Privalova LI, Gurvich VB, Makeyev OH, Shur VY, Beikin YB, Sutunkova MP, Kireyeva EP, Minigalieva IA, Loginova NV, Vasilyeva MS, Korotkov AV, Shuman EA, Vlasova LA, Shishkina EV, Tyurnina AE, Kozin RV, Valamina IE, Pichugova SV, Tulakina LG [2013]. Comparative in vivo assessment of some adverse bioeffects of equidimensional gold and silver nanoparticles and the attenuation of nanosilver's effects with a complex of innocuous bioprotectors. Internat J Mol Sci *14*:2449–2483.

Kawata K, Osawa M, Okabe S [2009]. In vitro toxicity of silver nanoparticles at noncytotoxic doses to HepG2 human hepatoma cells. Environ Sci Technol *43*:6046–6051.

Kennedy DC, Orts-Gil G, Lai C-H, Miller L, Haase A, Luch A, Seeberger PH [2014]. Carbohydrate functionalization of silver nanoparticles modulates cytotoxicity and cellular uptake. J Nanobiotechnology *20*:59.

Kenyon A, Antonini JM, Mercer RR, Schwegler-Berry D, Schaeublin NM, Hussain SM, Oldenburg SJ, Roberts JR [2012]. Pulmonary toxicity associated

with different aspect ratio silver nanowires after intratracheal instillation in rats. Society of Toxicology Annual Meeting, San Francisco, CA, March 11–15, 2012. Toxicol Sci: The Toxicologist *126*(1):A652, p. 141.

Kermanizadeh A, Gaiser BK, Hutchison GR, Stone V [2012]. An in vitro liver model: assessing oxidative stress and genotoxicity following exposure of hepatocytes to a panel of engineered nanomaterials. Part Fibre Toxicol *9*:28, https://dx.doi.org/10.1186/1743-8977-9-28.

Kermanizadeh A, Pojana G, Gaiser BK, Birkedal R, Bilanicova D, Wallin H, Jensen KA, Sellergren B, Hutchison GR, Marcomini A, Stone V [2013]. In vitro assessment of engineered nanomaterials using a hepatocyte cell line: cytotoxicity, pro-inflammatory cytokines and functional markers. Nanotoxicology *7*(3):301–313, https://dx.doi.org/10.3109/17435390.2011.653416.

Kim E, Chu YC, Han JY, Lee DH, Kim YJ, Kim H-C, Lee SG, Lee SJ, Jeong SW, Kim JM [2010b]. Proteomic analysis of silver nanoparticle toxicity in rat. Toxicol Environ Health Sci *2*:251–262.

Kim E, Maeng J-H, Lee DH, Kim JM [2009b]. Correlation of biomarkers and histological responses in manufactured silver nanoparticle toxicity. Toxicol Environ Health Sci *1*:8–16.

Kim E, Lee JH, Kim JK, Lee GH, Ahn K, Park JD, Yu IJ [2016]. Case study on risk evaluation of printed electronics using nanosilver ink. Nano Converg *3*(1):2.

Kim HR, Park YJ, Shin DY, Oh SM, Chung KH [2013a]. Appropriate in vitro methods for genotoxicity testing of silver nanoparticles. Environ Health Toxicol *28*:e2013003, https://dx.doi.org/10.5620/eht.2013.28.e2013003.

Kim J, Kuk E, Yu K, Kim J, Park S, Lee H, Kim S, Park Y, Park YH, Hwang C, Kim Y, Lee Y, Jeong D, Cho M [2007]. Antimicrobial effects of silver nanoparticles. Nanomedicine *3*:95–101, as cited in Hackenberg et al. [2011].

Kim JS, Song KS, Sung JH, Ryu HR, Choi BG, Cho HS, Lee JK, Yu IJ [2013b]. Genotoxicity, acute oral and dermal toxicity, eye and dermal irritation and corrosion and skin sensitization evaluation of silver nanoparticles. Nanotoxicology *7*(5):953–960.

Kim JS, Sung JH, Ji JH, Song KS, Lee JH, Kang CS, Yu IJ [2011]. In vivo genotoxicity of silver nanoparticles after 90-day silver nanoparticle inhalation exposure. Saf Health Work *2*(1):34–38.

Kim K-J, Sung WS, Suh BK, Moon SK, Choi J-S [2009d]. Antifungal activity and mode of action of silver nano-particles on *Candida albicans*. Biometals *22*(2):235–242.

Kim S, Choi JE, Choi J, Chung KH, Park K, Yi J, Ryu DY [2009c]. Oxidative stress-dependent toxicity of silver nanoparticles in human hepatoma cells. Toxicol In Vitro *23*(6):1076–1084.

Kim TH, Kim M, Park HS, Shin US, Gong MS, Kim HW [2012]. Size-dependent cellular toxicity of silver nanoparticles. J Biomed Mater Res Part A *100A:*1033–1043.

Kim W-Y, Kim J, Park JD, Ryu HY, Yu IJ [2009a]. Histological study of gender differences in accumulation of silver nanoparticles in kidneys of Fischer 344 rats. J Toxicol Environ Health Part A *72*:1279–1284.

Kim YS, Kim JS, Cho HS, Rha DS, Park JD, Choi BS, Lim R, Chang HK, Chung YH, Kwon IH, Jeong J, Han BS, Yu IJ [2008]. Twenty-eight day oral toxicity, genotoxicity, and gender-related tissue distribution of silver nanoparticles in Sprague-Dawley rats. Inhal Toxicol *20*:575–583.

Kim YS, Song MY, Park JD, Song KS, Ryu HR, Chung YH, Chang HK, Lee JH, Oh KH, Kelman BJ, Hwang IK, Yu IJ [2010a]. Subchronic oral toxicity of silver nanoparticles. Particle Fibre Toxicol *7*:20.

Kitter S, Greulich C, Diendorf J, Koller M, Epple M [2010]. Toxicity of silver nanoparticles increases during storage because of slow dissolution under release of silver ions. Chem Mater *22*:4548–4554.

Klaassen CD [1979]. Biliary excretion of silver in the rat, rabbit, and dog. Tox Applied Pharm *5:*49–55.

Korani M, Rezayat SM, Gilani K, Arbabi Bidgoli S, Adeli S [2011]. Acute and subchronic dermal toxicity of nanosilver in guinea pig. Int J Nanomed *6*:855–862.

Korani M, Rezayat SM, Arbadi Bidgoli S [2103]. Sub-chronic dermal toxicity of silver nano particles in guinea pigs: special emphasis to heart, bone, and kidney toxicities. Iranian J Pharmaceut Res *12*(3):511–519.

Kovvuru P, Mancilla PE, Shirode AB, Murray TM, Begley TJ, Reliene R [2015]. Oral ingestion of silver nanoparticles induces genomic instability and DNA damage in multiple tissues. Nanotoxicology *9*(2):162–171.

Krenkel O, Tacke F [2017]. Liver macrophages in tissue homeostasis and disease. Nature Rev Immunol *17*:306–321.

Kreyling WG, Hirn S, Möller W, Schleh C, Wenk A, Celik G, Lipka J, Schäffler M, Haberl N, Johnston BD, Sperling R, Schmid G, Simon U, Parak WJ, Semmler-Behnke M [2014]. Air-blood barrier translocation of tracheally instilled gold nanoparticles inversely depends on particle size. ACS Nano *28*;8(1):222–233.

Kromhout H [2009]. Design of measurement strategies for workplace exposures. Occup Environ Med *59*(5):349–354.

Kuempel ED, O'Flaherty EJ, Stayner LT, Smith RJ, Green FHY, Vallyathan V [2001]. A biomathematical model of particle clearance and retention in the lungs of coal miners. I. Model development. Regul Toxicol Pharmacol *34*(1):69–87.

Kuempel ED, Tran CL [2002]. Comparison of human lung dosimetry models: implications for risk assessment. Ann Occup Hyg *46*(Suppl 1):337–341.

Kuempel ED, Sweeney LM, Morris JB, Jarabek AM [2015]. Advances in inhalation dosimetry models and methods for occupational risk assessment and exposure limit derivation. J Occup Environ Hyg *12*(Suppl 1):S18–S40.

Kuhlbusch TA, Asbach C, Fissan H, Gohler D, Stintz M [2011]. Nanoparticle exposure at nanotechnology workplaces: a review. Part Fibre Toxicol *8*:22.

Kulinowski K, Lippy B [2011]. Training workers on risks of nanotechnology. Washington, DC: National Clearinghouse for Worker Safety and Health Training, National Institute of Environmental Health Sciences (NIEHS) Worker Education and Training Program (WETP), https://tools.niehs.nih.gov//wetp/index.cfm?id=537.

Kumar V, Abbas AK, Aster JC [2015]. Robbins and Cotran. Pathologic basis of disease. 9th ed. Philadelphia, PA: Elsevier/Saunders.

Kurashina M, Kozuka S, Nakasima N, Hirabayasi N, Masafumi I [2006]. Relationship of intrahepatic bile duct hyperplasia to cholangiocellular carcinoma. Cancer *61*(12):2469–2474.

Kwan KH, Yeung KW, Liu X, Wong KK, Shum HC, Lam YW, Cheng SH, Cheung KM, To MK [2014]. Silver nanoparticles alter proteoglycan expression in the promotion of tendon repair. Nanomedicine *10*(7):1375–1383, https://doi.org/10.1016/j.nano.2013.11.015.

Kwon J-T, Minai-Tehrani A, Hwang S-K, Kim J-E, Shin J-Y, Yu K-N, Chang S-H, Kim D-S, Kwon Y-T, Choi I-J, Cheong Y-H, Kim JS, Cho M-H [2012]. Acute pulmonary toxicity and body distribution of inhaled metallic silver nanoparticles. Toxicol Res *28*(1):25–31.

Lafuente D, Garcia T, Blanco J, Sanchez DJ, Sirvent JJ, Domingo JL [2016]. Effects of oral exposure to silver nanoparticles on the sperm of rats. Reprod Toxicol *60*:133–139.

Landsiedel R, Fabian E, Ma-Hock L, et al. [2012]. Toxico-/biokinetics of nanomaterials. Arch Toxicol *86*(7):1021–1060.

Lankveld DP, Oomen AG, Krystek P, Neigh A, Troost-de Jong A, Noorlander CW, Eijkeren JC,

Geertsma RE, De Jong WH [2010]. The kinetics of the tissue distribution of silver nanoparticles of different sizes. Biomaterials *31*:8350–8361.

Lansdown ABG [2012]. Silver and gold. In: Bingham and Cohrssen, eds. Patty's toxicology. 6th ed. Vol. 1. New York: John Wiley & Sons.

Larese FF, D'Agostin F, Crosera M, Adami G, Renzi N, Bovenzi M, Maina G [2009]. Human skin penetration of silver nanoparticles through intact and damaged skin. Toxicology *255*:33–37.

Lee H-Y, Choi Y-J, Jung E-J, Yin H-Q, Kwon J-T, Kim J-E, Im H-T, Cho M-H, Kim, J-H, Kim H-Y, Lee B-H [2010]. Genomics-based screening of differentially expressed genes in the brains of mice exposed to silver nanoparticles via inhalation. J Nanopart Res *12*:1567–1578.

Lee JH, Ahn K, Kim SM, Jeon KS, Lee JS, Yu IJ [2012b]. Continuous 3-day exposure assessment of workplace manufacturing silver nanoparticles. J Nanopart Res *14*:1134, https://doi.org/10.1007/s11051-012-1134-8.

Lee JH, Kim YS, Song KS, Ryu HR, Sung JH, Park JD, Park HM, Song NW, Shin BS, Marshak D, Ahn K, Lee JE, Yu IJ [2013a]. Biopersistence of silver nanoparticles in tissues from Sprague-Dawley rats. Particle Fibre Toxicol *10*:36.

Lee JH, Kwon M, Ji JH, Kang CS, Ahn KH, Han JH, Yu IJ [2011b]. Exposure assessment of workplaces manufacturing nanosized $TiO_2$ and silver. Inhalation Toxicol *23*:226–236, https://www.tandfonline.com/doi/full/10.3109/08958378.2011.562567.

Lee JH, Mun J, Park JD, Yu IJ [2012a]. A health surveillance case study of workers who manufacture silver nanomaterials. Nanotoxicology *6*:667–669, https://doi.org/10.3109/17435390.2011.600840.

Lee JH, Sohn EK, Ahn JS, Ahn K, Kim KS, Lee JH, Lee TM, Yu IJ [2013b]. Exposure assessment of workers in printed electronics workplace. Inhal Toxicol *25*:8.

Lee TY, Liu MS, Huang LJ, Lue SI, Lin LC, Kwan AL, Yang RC [2013c]. Bioenergetic failure correlates with autophagy and apoptosis in rat liver following silver nanoparticle intraperitoneal administration. Particle Fibre Toxicol *10*:40.

Lee Y, Kim P, Yoon J, Lee B, Choi K, Kil K-H, Park K [2013d]. Serum kinetics, distribution and excretion of silver in rabbits following 28 days after a single intravenous injection of silver nanoparticles. Nanotoxicology *7*(6):1120–1130.

Lee YS, Kim DW, Lee YH, Oh JH, Yoon S, Choi MS, Lee SK, Kim JW, Lee K, Song CW [2011a]. Silver nanoparticles induce apoptosis and G2/M arrest via PKCzeta-dependent signaling in A549 lung cells. Arch Toxicol, doi:10.1007/s00204-011-0714-1.

Leidel NA, Busch KA [1994]. Statistical design and data analysis requirements. In: Harris RL, Cralley LJ, Cralley LV, eds. Patty's industrial hygiene and toxicology, 3rd ed. Vol. 3, Part A. New York: John Wiley and Sons, pp. 453–582.

Levard C, Hotze EM, Lowry GV, Brown GE [2012]. Environmental transformations of silver nanoparticles: impact on stability and toxicity. Environ Sci Technol *46*(13):6900–6914.

Levard C, Reinsch BC, Michel FM, Oumahi C, Lowry GV, Brown GE [2011]. Sulfidation processes of PVP-coated silver nanoparticles in aqueous solution: impact on dissolution rate. Environ Sci Technol *45*(12):5260–5266.

Lewis RC, Gaffney SH, Le MH, Unice KM, Paustenbach DJ [2012]. Airborne concentrations of metals and total dust during solid catalyst loading and unloading operations at a petroleum refinery. Int J Hyg Envir Health *215*:514–521.

Lewis TR, Morrow PE, McClellan RO, Raabe OG, Kennedy GL, Schwetz BA, Goehl TJ, Roycroft JH, Chhabra RS [1989]. Establishing aerosol exposure concentrations for inhalation toxicity studies. Toxicol Appl Pharmacol 99:377–383.

Li M, Panagi Z, Avgoustakis K, Reineke J [2012a]. Physiologically based pharmacokinetic modeling

of PLGA nanoparticles with varied mPEG content. Int J Nanomed *7*:1345–1356.

Li PW, Kuo TH, Chang JH, Yeh JM, Chan WH [2010]. Induction of cytotoxicity and apoptosis in mouse blastocysts by silver nanoparticles. Toxicol Lett *197*(2):82–87.

Li S-D, Huang L [2008]. Pharmacokinetics and biodistribution of nanoparticles. Mol Pharm *5*(4):496–504.

Li Y, Chen DH, Yan J, Chen Y, Mittelstaedt RA, Zhang Y, Biris AS, Heflich RH, Chen T [2012b]. Genotoxicity of silver nanoparticles evaluated using the Ames test and *in vitro* micronucleus assay. Mutation Res *745*:4–10.

Ling MP, Lin WC, Liu CC, Huang YS, Chueh MJ, Shih TS [2012]. Risk management strategy to increase the safety of workers in the nanomaterials industry. J Haz Mat *Aug 30*(229–230):83–93, https://doi.org/10.1016/j.jhazmat.2012.05.073.

Liu H, Yang D, Yang H, Zhang H, Zhang W, Fang Y, Lin Z, Tian L, Lin B, Yan J, Xi Z [2013a]. Comparative study of respiratory tract immune toxicity induced by three sterilization nanoparticles: silver, zinc oxide and titanium dioxide. J Haz Mat *Mar 15*(248–249):478–486.

Liu J, Hurt RH [2010]. Ion release kinetics and particle persistence in aqueous nano-silver colloids. Environ Sci Technol *44*(6):2169–2175.

Liu J, Sonshine DA, Shervani S, Hurt RH [2010b]. Controlled release of biologically active silver from nanosilver surfaces. ACS Nano *4*:6903–6913.

Liu J, Wang Z, Liu FD, Kane AB, Hurt RH [2012]. Chemical transformation in biological environments. ACS Nano *6*(11):9887–9899.

Liu P, Huang Z, Gu N [2013b]. Exposure to silver nanoparticles does not affect cognitive outcome or hippocampal neurogenesis in adult mice. Ecotoxicol Environ Safety *87*:124–130.

Liu W, Wu Y, Wang C, Li HC, Wang T, Liao CY, Cui L, Zhou QF, Yan B, Jiang GB [2010a]. Impact of silver nanoparticles on human cells: effect of particle size. Nanotoxicology *4*(3):319–330.

Liu Y, Guan W, Ren G, Yang Z [2012]. The possible mechanism of silver nanoparticle impact on hippocampal synaptic plasticity and spatial recognition in rats. Toxicol Lett *209*:227–231.

Loeschner K, Hadrup N, Qvortrup K, Larsen A, Gao X, Vogel U, Mortensen A, Lam HR, Larsen EH [2011]. Distribution of silver in rats following 28 days of repeated oral exposure to silver nanoparticles or silver acetate. Particle Fibre Toxicol *8*:18.

Lok C-N, Ho C-M, Chen R, He Q-Y, Yu W-Y, Sun H, Tam PK-H, Chiu J-F, Che C-M [2006]. Proteomic analysis of the mode of antibacterial action of silver nanoparticles. J Proteome Res *5*:916–924.

Loza K, Diendorf J, Sengstock C, Ruiz-Gonzalez L, Gonzalez-Calbet JM, Vallet-Regi M, Koller M, Epple M [2014]. The dissolution and biological effects of silver nanoparticles in biological media. J Mat Chem B *2*:1634–1643.

Loza K, Epple M [2018]. Silver nanoparticles in complex media: as easy procedure to discriminate between metallic silver nanoparticles, reprecipitated silver chloride, and dissolved silver species. RSC Adv *8*:24386–24391.

Lyles RH, Kupper LL, Rappaport SM [1997]. A lognormal distribution-based exposure assessment method for unbalanced data. Ann Occup Hyg *41*(1):63–76.

Ma J, Lü X, Huang Y [2011]. Genomic analysis of cytotoxicity response to nanosilver in human dermal fibroblasts. J Biomed Nanotechnol *7*:263–275.

Mahabady MK [2012]. The evaluation of teratogenicity of nanosilver on skeletal system and placenta of rat fetuses in prenatal period. Afr J Pharmacy Pharmacol *6*(6):419–424.

Maneewattanapinyo P, Banlunara W, Thammacharoen C, Ekgasit S, Kaewamatawong T [2011]. An evaluation of acute toxicity of colloidal silver nanoparticles. J Vet Med Sci *73*(11):1417–1423. E-pub June 29.

Mathias FT, Romano RM, Kizys ML, Kasamatsu T, Giannocco G, Chiamolera MI, Dias-da-Silva MR, Romano MA [2014]. Daily exposure to silver nanoparticles during prepubertal development decreases adult sperm and reproductive parameters. Informa Healthcare, 17 February, https://doi.org/10.3109/17435390.2014.889237.

Maynard AD, Kuempel ED [2005]. Airborne nanostructured particles and occupational health. J Nanopart Res *7*:587–614.

McNally K, Warren N, Fransman W, Entink RK, Schinkel J, van Tongeren M, Cherrie JW, Kromhout H, Schneider T, Tielemans E [2014]. Advanced REACH tool: a Bayesian model for occupational exposure assessment. Ann Occup Hyg *55*(5):551–565.

Mei N, Zhang Y, Chen Y, Guo X, Ding W, Ali SF, Biris AS, Rice P, Moore MM, Chen T [2012]. Silver nanoparticle-induced mutations and oxidative stress in mouse lymphoma cells. Environ Mol Mutagen *53*:409–419.

Meyer KC [2017]. Pulmonary fibrosis, part I: epidemiology, pathogenesis, and diagnosis. Expert Rev Respir Med *11*(5):343–359.

Miller A, Drake PL, Hintz P, Habjan M [2010]. Characterizing exposures to airborne metals and nanoparticle emissions in a refinery. Ann Occup Hyg *54*(5):504–513.

Miller FJ, Kimbell JS, Preston RJ, Overton JH, Gross EA, Conolly RB [2011]. The fractions of respiratory tract cells at risk in formaldehyde carcinogenesis. Inhal Toxicol *23*:689–706.

Minchenko DO, Yavorovsky OP, Zinchenko TO, Komisarenko SV, Minchenko OH [2012]. Expression of circadian genes in different rat tissues is sensitive marker of in vivo silver nanoparticles. Mat Sci Engin, https://doi.org/10.1088/1757-899X/40/1/012016.

Miresmaeili SM, Halvaei I, Fesahar F, Fallah A, Nikonahad N, Taherinejad M [2013]. Evaluating the role of silver nanoparticles on acrosomal reaction and spermatogenic cells in rat. Iran J Reprod Med *11*(5):423–430.

Miura N, Shinohara Y [2009]. Cytotoxic effect and apoptosis induction by silver nanoparticles in HeLa cells. Biochem Biophys Res Commun *390*(3):733–737.

Morfeld P, Bruch J, Levy L, Ngiewih Y, Chaudhuri I, Muranko HJ, Myerson R, McCunney RJ [2015]. Translational toxicology in setting occupational exposure limits for dusts and hazard classification—a critical evaluation of a recent approach to translate dust overload findings from rats to humans. Part Fibre Toxicol *12*:3.

Morrow PE [1988]. Possible mechanisms to explain dust overloading of the lungs. Fundam Appl Toxicol *10*:369–384.

Moss AP, Sugar A, Hargett NA, Atkin A, Wolkstein M, Rosenman KD [1979]. The ocular manifestations and functional effects of occupational argyrosis. Arch Ophthalmol *97*:906–908.

MSHA [2020]. Mine Data Retrieval System. Department of Labor, Mine Safety and Health Administration, https://www.msha.gov/mine-data-retrieval-system#msha-datasets (accessed 24 Jan 2020).

Muhle H, Bellmann B, Creutzenberg O, Dasenbrock C, Ernst H, Kilpper R, MacKenzie JC, Morrow P, Mohr U, Takenaka S, Mermelstein R [1991]. Pulmonary response to toner upon chronic inhalation exposure in rats. Fund Appl Toxicol *17*:280–299.

Muir DC, Cena K [1987]. Deposition of ultrafine aerosols in the human respiratory tract. Aerosol Sci Technol *6*:183–190.

Murdaca F, Feci L, Acciai S, Biagioli M, Fimiani M [2014]. Occupational argyria. G Ital Dermatol Venereol *149*(5):629–630.

Nallathamby PD, Xu X-HN [2010]. Study of cytotoxic and therapeutic effects of stable and purified silver nanoparticles on tumor cells. Nanoscale *2*(6):942–952.

NanoSafe [2008]. Are conventional protective devices such as fibrous filter media, respirator cartridges, protective clothing and gloves also efficient for nanoaerosols? DR-325/326-200801-1. Brussels: European Commission (EC), https://www.nanosafe.org/cea-tech/pns/nanosafe/en/Documents/DR1_s.pdf.

Naumann BD, Sargent EV, Starkman BS, Fraser WJ, Becker GT, Kirk GD [1996]. Performance-based exposure control limits for pharmaceutical active ingredients. Am Ind Hyg Assoc J *57*:33–42.

Naumann BD, Weideman PA [1995]. Scientific basis for uncertainty factors used to establish occupational exposure limits for pharmaceutical active ingredients. Hum Ecol Risk Assess *1*:590–613.

NIOSH [1973]. Health Hazard Evaluation (HHE) report: Dunham-Bush, Incorporated, West Hartford, Connecticut. By Vandervort R, Polakoff PL, Flesch JP, Lowry LK. Cincinnati, OH: U.S. Department of Health and Human Services, Public Health Service, Centers for Disease Control, National Institute for Occupational Safety and Health (NIOSH). NIOSH HHE Report No. 72-84-31, NTIS No. PB 229627.

NIOSH [1977]. Occupational exposure sampling strategy manual. Cincinnati, OH: U.S. Department of Health and Human Services, Public Health Service, Centers for Disease Control, National institute for Occupational Safety and Health, DHHS (NIOSH) Publication No. 77-173.

NIOSH [1981]. Health Hazard Evaluation (HHE) report: General Electric Company, Lynn, Massachusetts. By McManus KP, Baker EL. Cincinnati, OH: U.S. Department of Health and Human Services, Public Health Service, Centers for Disease Control, National Institute for Occupational Safety and Health (NIOSH), NIOSH HHE Report No. 80-084-927.

NIOSH [1988]. Silver (metal dust and fume). CDC-NIOSH 1988 OSHA PEL Project Documentation: List by Chemical Name: Silver, https://www.cdc.gov/niosh/pel88/7440-22.html.

NIOSH [1992]. Hazard Evaluation and Technical Assistance (HETA) report: Langers Black Hills Silver Jewelry, Inc., Spearfish, South Dakota. By Kiefer M. Cincinnati, OH: U.S. Department of Health and Human Services, Centers for Disease Control and Prevention, National Institute for Occupational Safety and Health (NIOSH), NIOSH HETA Report No. 92-097-2238.

NIOSH [1995]. Report to Congress on Workers' Home Contamination Study Conducted Under the Worker's Family Protection Act (29 U.S.C. 671a). Cincinnati, OH: U.S. Department of Health and Human Services, Centers for Disease Control and Prevention, National Institute for Occupational Safety and Health (NIOSH), DHHS (NIOSH) Publication No. 95-123.

NIOSH [1998]. Hazard Evaluation and Technical Assistance (HETA) report: Caterpillar Inc., York, Pennsylvania. By Tepper A, Blade LM. Cincinnati, OH: U.S. Department of Health and Human Services, Centers for Disease Control and Prevention, National Institute for Occupational Safety and Health (NIOSH), NIOSH HETA Report No. 95-0001-2679.

NIOSH [2000]. Hazard Evaluation and Technical Assistance (HETA) report: OmniSource Corporation, Precious Metal Recycling Facility, Ft. Wayne, Indiana. By Gwin KK, Nemhauser JB. Cincinnati, OH: U.S. Department of Health and Human Services, Centers for Disease Control and Prevention, National Institute for Occupational Safety and Health (NIOSH), NIOSH HETA Report No. 2000-0041-2796.

NIOSH [2003]. Method 7300 and 7301 Elements by ICP (supplement issued March 15, 2003). In: NIOSH manual of analytical methods (NMAM®). Cincinnati, OH: U.S. Department of Health and Human Services, Centers for Disease Control and Prevention, National Institute for Occupational Safety and Health, DHHS (NIOSH) Publication No. 94-113, https://www.cdc.gov/niosh/docs/2003-154/pdfs/7300.pdf.

NIOSH [2005]. NIOSH respirator selection logic. Cincinnati, OH: U.S. Department of Health and Human Services, Centers for Disease Control and Prevention, National Institute for Occupational Safety and Health, DHHS (NIOSH) Publication No. 2005-100.

NIOSH [2006]. Criteria for a recommended standard: occupational exposure to refractory ceramic fibers. Cincinnati, OH: U.S. Department of Health

and Human Services, Centers for Disease Control and Prevention, National Institute for Occupational Safety and Health, DHHS (NIOSH) Publication No. 2006-125.

NIOSH [2007]. NIOSH pocket guide to chemical hazards. Cincinnati, OH: U.S. Department of Health and Human Services, Centers for Disease Control and Prevention, National Institute for Occupational Safety and Health, DHHS (NIOSH) Publication No. 2005-149, https://www.cdc.gov/niosh/npg/npgd0557.html.

NIOSH [2009]. Interim guidance for medical screening and hazard surveillance for workers potentially exposed to engineered nanoparticles. Cincinnati, OH: U.S. Department of Health and Human Services, Centers for Disease Control and Prevention, National Institute for Occupational Safety and Health, DHHS (NIOSH) Publication No. 2009-116.

NIOSH [2010]. A systematic review of the effectiveness of training and education for the protection of workers. By Robson L, Stephenson C, Schulte P, Amick B, Chan S, Bielecky A, Wang A, Heidotting T, Irvin E, Eggerth D, Peters R, Clarke J, Cullen K, Boldt L, Rotunda C, Grubb P. Toronto: Institute for Work & Health; Cincinnati, OH: U.S. Department of Health and Human Services, Centers for Disease Control and Prevention, National Institute for Occupational Safety and Health, DHHS (NIOSH) Publication No. 2010-127.

NIOSH [2011]. Current Intelligence Bulletin 63: occupational exposure to titanium dioxide. Cincinnati, OH: U.S. Department of Health and Human Services, Centers for Disease Control and Prevention, National Institute for Occupational Safety and Health, DHHS (NIOSH) Publication No. 2011-160.

NIOSH [2012]. General safe practices for working with engineered nanomaterials in research laboratories. Cincinnati, OH: U.S. Department of Health and Human Services, Centers for Disease Control and Prevention, National Institute for Occupational Safety and Health, DHHS (NIOSH) Publication No. 2012-147.

NIOSH [2013a]. Current Intelligence Bulletin 65: occupational exposure to carbon nanotubes and nanofibers. By Zumwalde R, Kuempel E, Birch E, Trout D, Castranova V. Cincinnati, Ohio: U.S. Department of Health and Human Services, Centers for Disease Control and Prevention, National Institute for Occupational Safety and Health. DHHS (NIOSH) Publication No. 2013-14.

NIOSH [2013b]. Current strategies for engineering controls in nanomaterial production and downstream handling processes. Cincinnati, OH: U.S. Department of Health and Human Services, Centers for Disease Control and Prevention, National Institute for Occupational Safety and Health, DHHS (NIOSH) Publication No. 2014-102.

NIOSH [2015]. Promoting health and preventing disease and injury through workplace tobacco policies. Cincinnati, OH: U.S. Department of Health and Human Services, Centers for Disease Control and Prevention, National Institute for Occupational Safety and Health, DHHS (NIOSH) Publication No. 2015-113.

NIOSH [2016]. NIOSH criteria for a recommended standard: occupational exposure to heat and hot environments. By Jacklitsch B, Williams WJ, Musolin K, Coca A, Kim J-H, Turner N. Cincinnati, OH: U.S. Department of Health and Human Services, Centers for Disease Control and Prevention, National Institute for Occupational Safety and Health, DHHS (NIOSH) Publication 2016-106.

NIOSH [2017a]. NIOSH Manual of Analytical Methods. 5th ed. Ashley K, O'Connor PF, eds. Cincinnati, OH: U.S. Department of Health and Human Services, Centers for Disease Control and Prevention, National Institute for Occupational Safety and Health, DHHS (NIOSH) Publication No. 2014-151.

NIOSH [2017b]. Reproductive health and the workplace, https://www.cdc.gov/niosh/topics/repro/default.html (accessed May 17, 2019).

NIOSH [2020]. Current Intelligence Bulletin: NIOSH practices in occupational risk assessment. Cincinnati, OH: U.S. Department of Health and Human Services,

Centers for Disease Control and Prevention, National Institute for Occupational Safety and Health. DHHS (NIOSH) Publication No. 2020-106.

NIST [2015]. National Institute of Standards and Technology (NIST): silver nanoparticle test material, https://www-s.nist.gov/srmors/view_report.cfm?srm=8017.

Nowack B, Kurg HF, Height M [2011]. 120 Years of nanosilver history: implications of policy makers. Environ Sci Technol *45*:1177–1183.

NTP [2014]. National Toxicology Program: NTP nonneoplastic lesion atlas. Liver, bile duct-hyperplasia, by Maronpot RR, https://ntp.niehs.nih.gov/nnl/hepatobiliary/liver/bdhyperp/index.htm.

Nymark P, Catalan J, Suhonen S, Jarventaus H, Birkedal R, Clausen PA, Jensen KA, Vippola M, Savolainen K, Norppa H [2013]. Genotoxicity of polyvinylpyrrolidone-coated silver nanoparticles in BEAS 2b cells. Toxicology *313*(1):38–48, https://doi.org/10.1016/j.tox.2012.09.014.

Oberdörster G, Ferin J, Morrow PE [1992a]. Volumetric loading of alveolar macrophages (AM): a possible basis for diminished AM-mediated particle clearance. Exp Lung Res *18*:87–104.

Oberdörster G, Ferin J, Gelein F, Soderholm SC, Finkelstein J [1992b]. Role of the alveolar macrophage in lung injury: studies with ultrafine particles. Environ Health Perspect *97*:193–199.

Oberdörster G, Ferin J, Lehnert BE [1994]. Correlation between particle size, in vivo particle persistence, and lung injury. Environ Health Perspect *102*(Suppl 5):173–179.

Oberdörster G [1995]. Lung particle overload: implications for occupational exposures to particles. Regul Toxicol Pharmacol *21*(1):123–135.

Oberdörster G [1997]. Pulmonary carcinogenicity of inhaled particles and the maximum tolerated dose. Environ Health Perspect *105*(Suppl 5):1347–1355.

Oberdörster G, Oberdörster E, Oberdörster J [2005]. Nanotoxicology: an emerging discipline evolving from studies of ultrafine particles. Environ Health Perspect *113*(7):823–839; erratum *118*(9):A380.

OECD [2004]. OECD guideline for the testing of chemicals. Skin absorption: in vitro method. Paris: Organisation for Economic Co-operation and Development, https://ntp.niehs.nih.gov/iccvam/suppdocs/feddocs/oecd/oecdtg428-508.pdf.

OECD [2006]. Report on the regulatory uses and applications in OECD member countries of (quantitative) structure-activity relationships [(Q)SAR] models in the assessment of new and existing chemicals. Paris: Organisation for Economic Co-operation and Development, Environment Health and Safety Publications, Series on Testing and Assessment, No. 58, ENV/JM/MONO(2006)25.

OECD [2007]. Guidance document on the validation of (quantitative) structure-activity relationships [(Q)SAR] models. Paris: Organisation for Economic Co-operation and Development, Environment Health and Safety Publications, Series on Testing and Assessment, No. 69, ENV/JM/MONO(2007)2.

OECD [2009]. Test no. 403: Acute inhalation toxicity. OECD guidelines for the testing of chemicals, section 4. Paris: Organisation for Economic Co-operation and Development (OECD) Publishing, https://doi.org/10.1787/9789264070608-en.

OECD [2018a]. Test no. 412: Subacute inhalation toxicity: 28-day study. OECD guidelines for the testing of chemicals, section 4. Paris: Organisation for Economic Co-operation and Development (OECD) Publishing, https://doi.org/10.1787/9789264070783-en.

OECD [2018b]. Test no. 413: Subchronic inhalation toxicity: 90-day study. OECD guidelines for the testing of chemicals, section 4. Paris: Organisation for Economic Co-operation and Development (OECD) Publishing, https://doi.org/10.1787/9789264070806-en.

OSHA [1988]. Silver (metal dust and fume). Federal Register *53*(109):21215. Proposed rules: air contaminants. Federal Register *53*:20960-21393.

OSHA [2012a]. Silver, metal and soluble compounds (as Ag): chemical sampling information. Washington, DC: U.S. Department of Labor, https://www.osha.gov/dts/chemicalsampling/data/CH_267300.html.

OSHA [2012b]. Safety data sheets. Hazard Communication Standard (HCS). Washington, DC: U.S. Department of Labor, https://www.osha.gov/Publications/OSHA3514.html.

OSHA [2013]. United States Code of Federal Regulations, 29CFR Part 1910.1000, Air Contaminants, final rule. Vol. 54. Washington, DC: Occupational Safety and Health Administration, p. 2702.

Paino IM, Zucolotto V [2015]. Poly(vinyl alcohol)-coated silver nanoparticles: activation of neutrophils and nanotoxicology effects in human hepatocarcinoma and mononuclear cells. Environ Toxicol Pharmacol *39*(2):614–621, https://doi.org/10.1016/j.etap.2014.12.012.

Pang C, Brunelli A, Zhu C, Hristozov D, Liu Y, Semenzin E, Wang W, Tao W, Liang J, Marcomini A, Chen C, Zhao B [2016]. Demonstrating approaches to chemically modify the surface of Ag nanoparticles in order to influence their cytotoxicity and biodistribution after single dose acute intravenous administration. Nanotoxicology *10*(2):129–139.

Parikh JM, Dhareshwar S, Sharma A, Karanth R, Ramkumar VS, Ramaiah I [2014]. Acute respiratory distress in a silversmith. Indian J Occup Environ Med *18*(1):27–28.

Park EJ, Bae E, Yi J, Kim Y, Choi K, Lee SH, Yoon J, Lee BC, Park K [2010a]. Repeated-dose toxicity and inflammatory responses in mice by oral administration of silver nanoparticles. Environ Toxicol Pharmacol *30*:162–168.

Park E-J, Choi K, Park K [2011b]. Induction of inflammatory responses and gene expression by intratracheal instillation of silver nanoparticles in mice. Arch Pharm Res *34*(2):299–307.

Park EJ, Yi J, Kim Y, Choi K, Park K [2010b]. Silver nanoparticles induce cytotoxicity by a Trojan-horse type mechanism. Toxicol In Vitro *24*(3):872–878.

Park J, Kwak BK, Bae E, Lee J, Kim Y, Choi K Yi J [2009]. Characterization of exposure to silver nanoparticles in a manufacturing facility. J Nanopart Res *11*:1705–1712.

Park K [2013]. Toxicokinetic differences and toxicities of silver nanoparticles and silver ions in rats after single oral administration. J Toxicol Environ Health, Part A *76*(22):1246–1260.

Park K, Park E-J, Chun IK, Choi K, Lee SH, Yoon J, Lee BC [2011a]. Bioavailability and toxicokinetics of citrate-coated silver nanoparticles in rats. Arch Pharm Res *34*:153–158.

Park M, Neigh AM, Vermeulen JP, de la Fonteyne L, Verharen HW, Briede JJ, van Loveren H, de Jong WH [2011c]. The effect of particle size on the cytotoxicity, inflammation, developmental toxicity and genotoxicity of silver. Biomaterials *32*:9810-9817.

Patchin ES, Anderson DS, Silve RM, Uyeminami DL, Scott GM, Guo T, Van Winkle LS, Pinkerton KE [2016]. Size-dependent deposition, translocation, and microglial activation of inhaled silver nanoparticles in the rodent nose and brain. Environ Health Perspect, https://doi.org/10.1289/EHP234.

Pauluhn J [2010]. Multi-walled carbon nanotubes (Baytubes): approach for derivation of occupational exposure limit. Regul Toxicol Pharmacol *57*(1):78–89.

Pauluhn J [2011]. Poorly soluble particulates: searching for a unifying denominator of nanoparticles and fine particles for DNEL estimation. Toxicology *279*(1-3):176–188.

Pauluhn J [2014]. Derivation of occupational exposure levels (OELs) of low-toxicity isometric biopersistent particles: how can the kinetic lung overload paradigm be used for improved inhalation toxicity study design and OEL-derivation? Part Fibre Toxicol *20*;11:72.

Philbrook NA, Winn LM, Nabiul Afrooz ARM, Saleh NB, Walker VK [2011]. The effect of $TiO_2$ and Ag nanoparticles on reproduction and development of *Drosophila melanogaster* and CD-1 mice. Toxicol Appl Pharm *257*:429–436.

Piao MJ, Kang KA, Lee IK, Kim HS, Kim S, Choi JY, Choi J, Hyun JW [2011]. Silver nanoparticles induce oxidative cell damage in human liver cells through inhibition of reduced glutathione and induction of mitochondria-involved apoptosis. Toxicol Lett *201*(1):92–100.

Pifer JW, Friedlander BR, Kintz RT, Stockdale DK [1989]. Absence of toxic effects in silver reclamation workers. Scand J Work Environ Health *15*:210–221.

Piña RA, Martinez MM, Rizo VHT, Lopes MA, Almeida OP. Cutaneous amalgam tattoo in a dental professional: an unreported occupational argyria. Br J Dermatol *167*:1184–1185.

Poitras EP, Levine MA, Harrington JM, Essader AS, Fennell TR, Snyder RW, Black SL, Sumner SS, Levine KE [2015]. Development of an analytical method for assessment of silver nanoparticle content in biological matrices by inductively coupled plasma mass spectrometry. Biol Trace Elem Res *163*:184–192.

Qin G, Tang S, Li S, Lu H, Wang Y, Zhao P, Lin B, Zhang J, Peng L [2016]. Toxicological evaluation of silver nanoparticles and silver nitrate in rats following 28 days of repeated oral exposure. Environ Toxicol, https://doi.org/10.1002/tox.22263.

Quadros ME, Marr LC [2010]. Environmental and human health risks of aerosolized silver nanoparticles. J Air Waste Mgmt *60*:770–781.

Rahman MF, Wang J, Patterson TA, Saini UT, Robinson BL, Newport GD, Murdock RC, Schlager JJ, Hussain SM, Ali SF [2009]. Expression of genes related to oxidative stress in the mouse brain after exposure to silver-25 nanoparticles. Toxicol Lett *187*:15–21.

Ramachandran G, Ostraat M, Evans DE, Methner MM, O'Shaughnessy P, D'Arcy J, Geraci CL, Stevenson E, Maynard A, Rickabaugh K [2011]. A strategy for assessing workplace exposures to nanomaterials. J Occup Environ Hyg *8*:673–685.

Rappaport SM, Lyles RH, Kupper LL [1995]. An exposure-assessment strategy accounting for within—and between—worker sources of variability. Ann Occup Hyg *39*(4):469–495.

Recordati C, De Maglie M, Bianchessi S, Argentiere S, Cella C, Mattiello S, Cubadda F, Aureli F, D'Amato M, Raggi A, Lenardi C, Milani P, Scanziani E [2016]. Tissue distribution and acute toxicity of silver after single intravenous administration in mice: nano-specific and size-dependent effects. Part Fibre Toxicol *13*:12.

Reidy B, Haase A, Luch A, Dawson KA, Lynch I [2013]. Mechanisms of silver nanoparticle release, transformation and toxicity: a critical review of current knowledge and recommendations for future studies and applications. Materials *6*:2295–2350.

Rengasamy S, Eimer BC [2011]. Total inward leakage of nanoparticles through filtering facepiece respirators. Ann Occup Hyg *55*(3):253–263.

Rengasamy S, Eimer BC, Shaffer RE [2009]. Comparison of nanoparticle filtration performance of NIOSH-approved and CE-marked particulate filtering facepiece respirators. Ann Occup Hyg *53*(2):117–128.

Rengasamy S, King WP, Eimer B, Shaffer RE [2008]. Filtration performance of NIOSH-approved N95 and P100 filtering-facepiece respirators against 4-30 nanometer size nanoparticles. J Occup Environ Hyg *5*(9):556–564.

Rengasamy S, Verbofsky R, King WP, Shaffer RE [2007]. Nanoparticle penetration through NIOSH-approved N95 filtering-facepiece respirators. J Int Soc Respir Protect *24*:49–59.

Rizvi S, Gores GJ [2014]. Molecular pathogenesis of cholangiocarcinoma: hepatobiliary tumors. Digestive Disorders *32*:564–569.

Rizvi S, Borad MJ, Patel T, Gores GJ [2014]. Cholangiocarcinoma: molecular pathways and therapeutic opportunities. Seminars Liver Dis *34*(4):456–464.

Roberts JR, Kenyon A, Young SH, Schwegler-Berry D, Hackley VA, MacCuspie RI, Stefaniak AB, Kashon ML, Chen BT, Antonini JM [2012]. Pulmonary toxicity following repeated intratracheal instillation of dispersed silver nanoparticles in rats. The Toxicologist *126*(Suppl 1):141.

Roberts JR, McKinney W, Kan H, Krajnak K, Frazer DG, Thomas TA, Waugh S, Kenyon A, MacCuspie RI, Hackley VA, Castranova V [2013]. Pulmonary and cardiovascular responses of rats to inhalation of silver nanoparticles. J Toxicol Environ Health, Part A *76*:651–668.

Rom WN [1991]. Relationship of inflammatory cell cytokines to disease severity in individuals with occupational inorganic dust exposure. Am J Ind Med *19*(1):15–27.

Rongioletti F, Buffa RE [1992]. Blue nevi-like dotted occupational argyria. J Am Acad Dermatol *27*:1015–1016.

Rosenman KD, Moss A, Kon S [1979]. Argyria: clinical implication of exposure to silver nitrate and silver oxide. J Occup Med *21*:430–435.

Rosenman KD, Seixas N, Jacobs I [1987]. Potential nephrotoxic effects of exposure to silver. Br J Ind Med *44*:267–272.

Rouse JG, Yang J, Ryman-Rasmussen JP, Barron AR, Monteiro-Riviere NA [2007]. Effects of mechanical flexion on the penetration of fullerene amino acid-derivatized peptide nanoparticles through skin. Nano Lett *7*(1):155–160.

Ryman-Rasmussen JP, Riviere JE, Monteiro-Riviere NA [2006]. Penetration of intact skin by quantum dots with diverse physicochemical properties. Toxicol Sci *91*(1):159–165.

Sahu SC, Njoroge J, Bryce SM, Yourick JJ, Sprando RL [2014a]. Comparative genotoxicity of nanosilver in human liver hepg2 and colon caco2 cells evaluated by a flow cytometric in vitro micronucleus assay. J Appl Toxicol *34*(11):1226–1234, https://doi.org/10.1002/jat.3065.

Sahu SC, Njoroge J, Bryce SM, Zheng J, Ihrie J [2016a]. Flow cytometric evaluation of the contribution of ionic silver to genotoxic potential of nanosilver in human liver hepg2 and colon caco2 cells. J Appl Toxicol *36*(4):521–531, https://doi.org/10.1002/jat.3276.

Sahu SC, Roy S, Zheng J, Ihrie J [2016b]. Contribution of ionic silver to genotoxic potential of nanosilver in human liver hepg2 and colon caco2 cells evaluated by the cytokinesis-block micronucleus assay. J Appl Toxicol *36*(4):532–542, https://doi.org/10.1002/jat.3279.

Sahu SC, Roy S, Zheng J, Yourick JJ, Sprando RL [2014b]. Comparative genotoxicity of nanosilver in human liver hepg2 and colon caco2 cells evaluated by fluorescent microscopy of cytochalasin b-blocked micronucleus formation. J Appl Toxicol *34*(11):1200–1208, https://doi.org/10.1002/jat.3028.

Sahu SC, Zheng J, Graham L, Chen L, Ihrie J, Yourick JJ, Sprando RL [2014c]. Comparative cytotoxicity of nanosilver in human liver hepg2 and colon caco2 cells in culture. J Appl Toxicol *34*(11):1155–1166, https://doi.org/10.1002/jat.2994.

Saint S, Veenstra DL, Sullivan SD [2000]. The potential clinical and economic benefits of silver alloy urinary catheters in preventing urinary tract infection. Arch Intern Med *160:*2670–2675.

Samberg M, Oldenburg SJ, Monteiro-Riviere NA [2010]. Evaluation of silver nanoparticle toxicity in skin in vivo and keratinocytes in vitro. Environ Health Perspect *118*:407–413.

Samberg ME, Loboa EG, Oldenburg SJ, Monteiro-Riviere NA [2012]. Silver nanoparticles do not influence stem cell differentiation but cause minimal toxicity. Nanomedicine *7*(8):1197–1209.

Sarkar S, Leo BF, Carranza C, Chen S, Rivas-Santiago C, Porter AE, Ryan MP, Gow A, Chung KF, Tetley TD, Zhang JJ, Georgopoulos PG, Ohman-Strickland PA, Schwander S [2015]. Modulation of human macrophage responses to mycobacterium tuberculosis by silver nanoparticles of different size and surface modification. PLoS One, *10*(11):e0143077, https://doi.org/10.1371/journal.pone.0143077.

Sato S, Sueki H, Nishijima A [1999]. Two unusual cases of argyria: the application of an improved tissue processing method for X-ray microanalysis of

selenium and sulphur in silver-laden granules. Br J Dermatol *140*:158–163.

Sayes CM, Fortner J, Guo W, Lyon D, Boyd AM, Ausman KD, Tao YJ, Sitharaman B, Wilson LJ, Hughes JB, West JL, Colvin VL [2004]. The differential cytotoxicity of water soluble fullerenes. Nano Lett *4*(10):1881–1887.

Schaeblin NM, Estep CA, Roberts JR, Hussain SM [2011]. Silver nanowires induced inflammation in an in vitro human alveolar lung model. Society of Toxicology Annual Meeting, Washington, DC, March 6–10, 2011. Toxicol Sci: The Toxicologist *120*(Suppl 2):A2181, p. 468.

Schinwald A, Chernova T, Donaldson K [2012]. Use of silver nanowires to determine thresholds for fibre length-dependent pulmonary inflammation and inhibition of macrophage migration in vitro. Particle Fibre Toxicol *9*:47.

Schinwald A, Donaldson K [2012]. Use of back-scatter electron signals to visualize cell/nanowire interactions in vitro and in vivo; frustrated phagocytosis of long fibres in macrophages and compartmentalization in mesothelial cells in vivo. Particle Fibre Toxicol *9*(34):1–13, https://doi.org/10.1186/1743-8977-9-34.

Schug TT, Nadadur SS, Johnson AF [2013]. Nano GO Consortium: a team science approach to assess engineered nanomaterials: reliable assays and methods. Environ Health Perspect *121*:A176–A177, https://doi.org/10.1289/ehp.1306866.

Schulte PA, Iavicoli I, Rantanen JH, Dahmann D, Iavicoli S, Pipke R, Guseva Canu I, Boccuni F, Ricci M, Polci ML, Sabbioni E, Pietroiusti A, Mantovani E [2016]. Assessing the protection of the nanomaterial workforce. Nanotoxicology *10*(7):1013–1019.

Schulte PA, Trout DB [2011]. Nanomaterials and worker health: medical surveillance, exposure registries, and epidemiologic research. J Occup Environ Med *53*(6 Suppl):S3–7.

Scott KG, Hamilton JG [1948]. The metabolism of silver. J Clin Invest *27*:555–556.

Scott KG, Hamilton JG [1950]. The metabolism of silver in the rat with radiosilver used as an indicator. Univ Calif (Berk) Publ Pharmacol *2*:241–262.

Scrogges MW, Lewis JS, Proia AD [1992]. Corneal argyrosis associated with silver soldering. Cornea *11*(3):264–269.

Seiffert J, Buckley A, Leo B, Martin NG, Zhu J, Dai R, Hussain F, Guo C, Warren J, Hodgson A, Gong J, Ryan MP, Zhang J, Porter A, Tetley TD, Gow A, Smith R, Chung KF [2016]. Pulmonary effects of spark-generated silver nanoparticles in Brown Norway and Sprague-Dawley rats. Resp Res *17*:85.

Seiffert J, Hussain F, Wiegman C, Li F, Bey L, Baker W, Porter A, Ryan MP, Chang Y, Gow A, Zhang J, Zhu J, Tetley TD, Chung KF [2015]. Pulmonary toxicity of instilled silver nanoparticles: influence of size, coating, and rat strain. PLOS ONE *10*(3):e0119726, https://doi.org/10.1371/journal.pone.0119726.

Shahare B, Yashpal M, Singh G [2013]. Toxic effects of repeated oral exposure of silver nanoparticles on small intestine mucosa of mice. Toxicol Mech Methods *23*(3):161–167.

Shannahan JH, Podila R, Aldossari AA, Emerson H, Powell BA, Ke PC, Rao AM, Brown JM [2015]. Formation of a protein corona on silver nanoparticles mediates cellular toxicity via scavenger receptors. Toxicol Sci *143*(1):136–146, https://doi.org/10.1093/toxsci/kfu217.

Sharma HS, Hussain S, Schlager J, Ali SF, Sharma A [2010]. Influence of nanoparticles on blood–brain barrier permeability and brain edema formation in rats. Acta Neurochir Suppl *106*:359–364.

Shrivastava R, Kushwaha P, Bhutia YC, Flora SJS [2016]. Oxidative stress following exposure to silver and gold nanoparticles in mice. Toxicol Ind Health *32*(8):1391–1404.

Silva RM, Anderson DS, Franzi LM, Peake JL, Edwards PC, van Winkle LS, Pinkerton KE [2015]. Pulmonary effects of silver nanoparticle size, coating, and dose over time upon intratracheal instillation. Toxicol Sci *144*(1):151–162.

Silva RM, Anderson DS, Peake J, Edwards PC, Patchin ES, Guo T, Gordon T, Chen LC, Sun X, van Winkle LS, Pinkerton KE [2016]. Aerosolized silver nanoparticles in the rat lung and pulmonary response over time. Toxicologic Pathol *44*(5):673–686.

Silva RM, Xu J, Saiki C, Donaldson DS, Franzi LM, Vulpe CD, Gilbert B, van Winkle LS, Pinkerton KE [2014]. Short versus long nanowires: a comparison of in vivo pulmonary effects post instillation. Particle Fibre Toxicol *11*:52, https://doi.org/10.1186/s12989-014-0052-6.

Silver S [2003]. Bacterial silver resistance: molecular biology and uses and misuses of silver compounds. FEMS Microbiol Rev *27*:341–353.

Sleiman HK, Romano RM, de Oliveira CA, Romano MA [2013]. Effects of prepubertal exposure to silver nanoparticles on reproductive parameters in adult male Wistar rats. J Toxicol Environ Health Part A *76:*1023–1032.

Smijs TGM, Bouwstra JA [2010]. Focus on skin as a possible post of entry for solid nanoparticles and the toxicological impact. J Biomed Nanotechnol *6*(5):469–484.

Smock KJ, Schmidt RL, Hadlock G, Stoddard G, Grainger DW, Munger MA [2014]. Assessment of orally dosed commercial silver nanoparticles on human ex vivo platelet aggregation. Nanotoxicology *8*(3):328–333.

Smulders S, Larue C, Sarret G, Castillo-Michel H, Vanoirbeek J, Hoet PHM [2015a]. Lung distribution, quantification, co-localization and speciation of silver nanoparticles after lung exposure in mice. Toxicol Lett *238*:1–6.

Smulders S, Luyts K, Brabants G, Golanski L, Martens J, Vanoirbeek J, Hoet PH [2015b]. Toxicity of nanoparticles embedded in paints compared to pristine nanoparticles, in vitro study. Toxicol Lett *232*(2):333–339, https://doi.org/10.1016/j.toxlet.2014.11.030.

Smulders S, Luyts K, Brabants G, Van Landuyt K, Kirschhock C, Smolders E, Golanski L, Vanoirbeek J, Hoet PHM [2014]. Toxicity of nanoparticles embedded in paints compared with pristine nanoparticles in mice. Toxicol Sci *141*(1):132–140.

Snipes MB [1989]. Long-term retention and clearance of particles inhaled by mammalian species. Crit Rev Toxicol *20*(3):175–211.

Song KS, Sung JH, Ji JH, Lee JH, Lee JS, Ryu HR, Lee JK, Chung YH, Park HM, Shin BS, Chang HK, Kelman B, Yu lJ [2013]. Recovery from silver-nanoparticle-exposure-induced inflammation and lung function changes in Sprague Dawley rats. Nanotoxicology *7*(2):169–180.

Sørensen KK, McCourt P, Berg T, Crossley C, Couteur DL, Wake K, Smedsrød B [2012]. The scavenger endothelial cell: a new player in homeostasis and immunity. Am J Physiol Regul Integr Comp Physiol *303*:R1217–R1230.

Sørensen KK, Simon-Santamaria J, McCuskey RS, Smedsrød B [2015]. Liver sinusoidal endothelial cells. Comprehens Physiol *5*:1751–1774.

Soto K, Garza KM, Murr LE [2007]. Cytotoxic effects of aggregated nanomaterials. Acta Biomaterialia *3*:351–358.

Sriram MI, Kanth SBM, Kalishwaralal K, Gurunathan S [2010]. Antitumor activity of silver nanoparticles in Dalton's lymphoma ascites tumor model. Int J Nanomed *5*:753–762.

Srivastava M, Singh S, Self WT [2012]. Exposure to silver nanoparticles inhibits selenoprotein synthesis and the activity of thioredoxin reductase. Environ Health Perspect *120*(1):56–61, https://ehp.niehs.nih.gov/doi/10.1289/ehp.1103928.

Stebounova LV, Adamcakova-Dodd A, Kim JS, Park H, O'Shaughnessy PT, Grassian VH, Thorne PS [2011]. Nanosilver induces minimal lung toxicity or inflammation in a subacute murine inhalation model. Particle Fibre Toxicol *8*:5.

Stöber W, Einbrodt HJ, Klosterkötter W [1967]. Quantitative studies of dust retention in animal and human lungs after chronic inhalation. In: Davis CN,

ed. Inhaled particles and vapours II. Oxford, UK: Pergamon, pp. 409–418.

Stoehr LC, Gonzalez E, Stampfl A, Casals E, Duschl A, Puntes V, Oostingh GJ [2011]. Shape matters: effects of silver nanospheres and wires on human alveolar epithelial cells. Particle Fibre Toxicol *8*:36, https://particleandfibretoxicology.biomedcentral.com/articles/10.1186/1743-8977-8-36.

Stone KC, Mercer RR, Freeman BA, Chang LY, Crapo JD [1992]. Distribution of lung cell numbers and volumes between alveolar and nonalveolar tissue. Am Rev Respir Dis *146*(2):454–456.

Stone V, Hankin SM, Aitken RJ, Aschberger K, Baun A, Christensen FM, et al. [2009]. ENRHES — engineered nanoparticles—review of health and environmental safety. EU 7th Research Framework Programme. Final report.

Su CK, Hung CW, Sun YC [2014a]. In vivo measurement of extravasation of silver nanoparticles into liver extracellular space by push-pull-based continuous monitoring system. Toxicol Lett *227*(2):84–90.

Su CK, Liu HT, Hsia SC, Sun YC [2014b]. Quantitatively profiling the dissolution and redistribution of silver nanoparticles in living rats using a knotted reactor-based differentiation scheme. Anal Chem *86*(16):8267–8274.

Su C-L, Chen T-T, Chang C-C, Chuang K-J, Wu C-K, Liu W-T, Ho KF, Lee K-Y, Ho S-C, Tseng H-E, Chuang H-C, Cheng T-J [2013]. Comparative proteomics of inhaled silver nanoparticles in healthy and allergen provoked mice. Internat J Nanomed *8*:2783–2799.

Su K, Sun Y-C [2015]. Considerations of inductively coupled plasma mass spectrometry techniques for characterizing the dissolution of metal-based nanomaterials in biological tissues. J Anal Atomic Spectrometry *30*:1689–1705.

Sun X, Wang Z, Zhai S, Cheng Y, Liu J, Liu B [2013]. In vitro cytotoxicity of silver nanoparticles in primary rat hepatic stellate cells. Mol Med Rep *8*(5):1365–1372, https://doi.org/10.3892/mmr.2013.1683.

Sung JH, Ji HJ, Yoon JU, Kim DS, Song MY, Jeong J, Han BS, Han JH, Chung YH, Kim J, Kim TS, Chang HK, Lee EJ, Lee JH, Yu IJ [2008]. Lung function changes in Sprague-Dawley rats after prolonged inhalation exposure to silver nanoparticles. Inhalation Toxicol *20*:567–574.

Sung JH, Ji JH, Park JD, Yoon JU, Kim DS, Jeon KS, Song MY, Jeong J, Han BS, Han JH, Chung YH, Chang HK, Lee JH, Cho MH, Kelman BJ, Yu IJ [2009]. Subchronic inhalation toxicity of silver nanoparticles. Toxicol Sci *108*:452–461.

Sung JH, Ji JH, Song KS, Lee JH, Choi KH, Lee SH, Yu IJ [2011]. Acute inhalation toxicity of silver nanoparticles. Toxicol Ind Health *27*:149–154.

Swanner J, Mims J, Carroll DL, Akman SA, Furdui CM, Torti SV, Singh RN [2015]. Differential cytotoxic and radiosensitizing effects of silver nanoparticles on triple-negative breast cancer and non-triple-negative breast cells. Int J Nanomed *10*:3937–3953, https://doi.org/10.2147/IJN.S80349.

Swidwinska-Gajewska AM, Czerczak S [2015]. Nanosilver: occupational exposure limits. In Polish. Med Pr *66*:429–442.

Takenaka S, Karg E, Roth C, Schulz H, Ziesenis A, Heinzmann U, Schramel P, Heyder J [2001]. Pulmonary and systemic distribution of inhaled ultrafine silver particles in rats. Environ Health Perspect *109*(Suppl 4):547–551.

Tang J, Xiong L, Wang S, Wang J, Liu L, Li J, Wan Z, Xi T [2008]. Influence of silver nanoparticles on neurons and blood–brain barrier via subcutaneous injection in rats. Appl Surface Sci *255*:502–504.

Tang J, Xiong L, Wang S, Wang J, Liu L, Li, J, Yuan F, Xi T [2009]. Distribution, translocation and accumulation of silver nanoparticles in rats. J Nanosci Nanotechnol *9*:4924–4932.

Tang J, Xiong L, Zhou G, Wang S, Wang J, Liu L, Li J, Yuan F, Lu S, Wan Z, Chou L, Xi T [2010]. Silver nanoparticles crossing through and distribution in the blood–brain barrier in vitro. J Nanosci Nanotechnol *10*:6313–6317.

Tanita Y, Kato T, Hanada K, Tagami H [1985]. Blue macules of localized argyria caused by implanted acupuncture needles. Arch Dermatol *121*:1550–1552.

Tejamaya M, Romer I, Merrifield RC, Lead JR [2012]. Stability of citrate, PVP, and PEG coated silver nanoparticles in ecotoxicology media. Environ Sci Technol, https://pubs.acs.org/doi/10.1021/es2038596.

Teodoro JS, Simoes AM, Duarte FV, Rolo AP, Murdoch RC, Hussain SM, Palmeira CM [2011]. Assessment of the toxicity of silver nanoparticles in vitro: a mitochondrial perspective. Toxicol In Vitro *25*(3):664–670, https://doi.org/10.1016/j.tiv.2011.01.004.

Thakur M, Gupta H, Singh D, Mohanty I, Maheswari U, Vanage G, Joshi DS [2014]. Histopathological and ultrastructural effects of nanoparticles on rat testis following 90 days (chronic study) of repeated oral administration. J Nanobiotech *12*:42.

Tiwari DK, Jin T, Behari J [2011]. Dose-dependent in-vivo toxicity assessment of silver nanoparticle in Wistar rats. Toxicol Mech Methods *21*(1):13–24.

Tran CL, Cullen RT, Buchanan D, Jones AD, Miller BG, Searl A, Davis JMG, Donaldson K [1999]. Investigation and prediction of pulmonary responses to dust. Part II. In: Investigations into the pulmonary effects of low toxicity dusts. Parts I and II. Suffolk, UK: Health and Safety Executive, Contract Research Report 216/1999.

Trickler WJ, Lantz SM, Murdock RC, Schrand AM, Robinson BL, Newport GD, Schlager JJ, Oldenburg SJ, Paule MG, Slikker W Jr, Hussain SM, Ali SF [2010]. Silver nanoparticle induced blood–brain barrier inflammation and increased permeability in primary rat brain microvessel endothelial cells. Toxicol Sci *118*:160–170.

Triebig G, Valentin H [1982]. Occupational disease argyrosis: current aspects. In German. Verhandlungen der Deutschen Gesellschaft für Arbeitsmedizin *22*:239–243.

Trop M, Novak M, Rodl S, Hellbom B, Kroell W, Goessler W [2006]. Silver-coated dressing Acticoat caused raised liver enzymes and argyria-like symptoms in burn patient. J Trauma *60*:648–652.

Trout DB, Schulte PA [2010]. Medical surveillance, exposure registries, and epidemiologic research for workers exposed to nanomaterials. Toxicology *269*(2–3):128–135.

Tsai S, Huang RF, Ellenbecker MJ [2010]. Airborne nanoparticle exposures while using constant-flow, constant-velocity, and air-curtain isolated fume hoods. Ann Occup Hyg *54*(1):78–87.

U.S. DOE [2008]. Approach to nanomaterial ES & H. Washington, DC: U.S. Department of Energy, Nanoscale Science Research Centers, https://www.energy.gov/science/office-science.

U.S. EPA [1994]. Methods for derivation of inhalation reference concentrations and application of inhalation dosimetry. Washington, DC: U.S. Environmental Protection Agency, Office of Research and Development, EPA/600/8-90/066F, https://www.epa.gov/risk/methods-derivation-inhalation-reference-concentrations-and-application-inhalation-dosimetry.

U.S. EPA [2002]. A review of the reference dose and reference concentration processes. Washington, DC: Risk Assessment Forum, U.S. Environmental Protection Agency, EPA/630/P-02/002F.

U.S. EPA [2004]. Risk assessment guidance for superfund, Vol. I: Human health evaluation manual. Washington, DC: Office of Emergency and Remedial Response Toxics Integration Branch, U.S. Environmental Protection Agency, EPA/540/R/99/005, https://www.epa.gov/risk/risk-assessment-guidance-superfund-volume-i-human-health-evaluation-manual-supplemental.

U.S. EPA [2006]. Approaches for the application of physiologically based pharmacokinetic (PBPK) models and supporting data in risk assessment. Washington, DC: U.S. Environmental Protection Agency, Office of Research and Development, EPA/600/R-05/043F.

U.S. EPA [2012a]. Nanosilver: summary of human health data for registration review. Washington,

DC: Office of Chemical Safety and Pollution Prevention. PC Code: 072599, Case No. 5042.

U.S. EPA [2012b]. Benchmark dose technical guidance. Washington, DC: U.S. Environmental Protection Agency. EPA/100/R-12/001.

U.S. EPA [2014]. Benchmark Dose Software (BMDS) version 2.5. Washington, DC: Environmental Protection Agency, National Center for Environmental Assessment, https://www.epa.gov/bmds.

U.S. EPA [2015]. Benchmark Dose Software (BMDS) version 2.6.0.1 (build 88, 6/25/2015). Washington, DC: Environmental Protection Agency, National Center for Environmental Assessment, https://www.epa.gov/bmds.

USGS [2014]. Mineral commodity summaries, January 2013. Washington, DC: U.S. Geological Survey, https://www.usgs.gov/centers/nmic/silver-statistics-and-information.

USGS [2019]. Mineral commodity summaries, February 2019. Washington, DC: U.S. Geological Survey, https://www.usgs.gov/centers/nmic/silver-statistics-and-information.

Van der Zande M, Vandebriel RJ, Van Doren E, Kramer E, Rivera ZH, Serrano-Rojero CS, Gremmer ER, Mast J, Peters RJB, Hollman PCH, Hendriksen PJM, Marvin HJP, Peijnenburh ACM, Bouwmeester H [2012]. Distribution, elimination, and toxicity of silver nanoparticles and silver ions in rats after 28-day oral exposure. ACS Nano *6*(8):7427–7442.

Vance ME, Kuiken T, Vejerano EP, McGinnis SP, Hochella MF, Rejeski D, Hull MS [2015]. Nanotechnology in the real world: redeveloping the nanomaterial consumer products inventory. Beilstein J Nanotechnol *6*(1):1769–1780.

Virji MA, Stefaniak AB [2014]. A review of engineered nanomaterial manufacturing processes and associated exposures. In: Comprehensive materials processing. Vol. 8. Bassim N, ed. London: Elsevier Ltd., pp. 103–125.

Vlachou E, Chipp E, Shale E, Wilson YT, Papini R, Moiemen NS [2007]. The safety of nanocrystalline silver dressings on burns: a study of systemic silver absorption. Burns *33*:979–985.

Wadhera A, Fung M [2005]. Systemic argyria associated with ingestion of colloidal silver. Dermatol Online J *11*(1):12.

Wagner GR, Fine LJ [2008]. Surveillance and health screening in occupational health. In: Wallace RB, ed. Maxcy-Rosenau-Last Public health and preventive medicine. 15th ed. New York: McGraw-Hill Medical Publishing, pp. 759–793.

Wahlberg JE [1965]. Percutaneous toxicity of metal compounds. Arch Environ Health *11*:201–204. Wan AT, Conyers RAJ, Coombs CJ, Masterton JP [1991]. Determination of silver in blood, urine and tissue of volunteers and burn patients. Clin Chem *37*:1683–1687.

Walczak AP, Fokkink R, Peters R, Tromp P, Rivera ZEH, Rietjens IMCM, Hendriksen PJM, Bouwmeester H [2012]. Behaviour of silver nanoparticles and silver ions in an in vitro human gastrointestinal digestion model. Nanotoxicology *7*(7):1198–1210, https://doi.org/10.3109/17435390.2012.726382.

Wang XR, Zhang HX, Sun BX, et al. [2005]. A 20-year follow-up study on chronic respiratory effects of exposure to cotton dust. Eur Respir J *26*(5):881-886.

Wang Z, Qu G, Su L, Wang L, Yang Z, Jiang J, Liu S, Jiang G [2013]. Evaluation of the biological fate and the transport through biological barriers of nanosilver in mice. Curr Pharm Des *19*(37):6691–6697.

Wei L, Tang J, Zhang Z, Chen Y, Zhou G, Xi T [2010]. Investigation of the cytotoxicity mechanism of silver nanoparticles in vitro. Biomed Mater *5*(4):044103.

Wen R, Yang X, Hu L, Sun C, Zhou Q, Jiang G [2016]. Brain-targeted distribution and high retention of silver by chronic intranasal instillation of silver nanoparticles and ions in Sprague-Dawley rats. J Appl Toxicol *36*:445–453.

Wesierska M, Dziendzikowska K, Gromadzka-Ostrowska J, Dudek J, Polkowska-Motrenko H, Audinot JN, Gutleb AC, Lankoff A, Kruszewski M [2018]. Silver ions are responsible for memory impairment induced by oral administration of silver nanoparticles. Toxicol Lett *290*:133–144.

Wheeler MW, Bailer AJ [2007]. Properties of model-averaged BMDLs: a study of model averaging in dichotomous response risk estimation. Risk Anal *27*(3):659–670.

WHO [2002]. Silver and silver compounds: environmental aspects. Concise International Chemical Assessment Document 44. Geneva: World Health Organization, ISBN 92 4 153044 8, https://www.who.int/ipcs/publications/cicad/en/cicad44.pdf?ua=1.

WHO/IPCS (World Health Organization, International Programme on Chemical Safety) [2005]. Chemical-specific adjustment factors for interspecies differences and human variability: Guidance document for use of data in dose/concentration assessment. IPCS Harmonization Project Document No. 2. Geneva: World Health Organization, International Programme on Chemical Safety.

WHO/IPCS (World Health Organization, International Programme on Chemical Safety) [2010]. Guidance on principles of characterizing and applying PBPK models in risk assessment. Harmonization Project Document No 9. Geneva: WHO Library Cataloguing-in-Publication Data, International Programme on Chemical Safety.

Wijnhoven S, Peijnenburg W, Herberts C, Hagens WI, Oomen A, Heugens EHW, Roszek B, Bisschops J, Gosens I, Van De Meent D, Dekkers S, De Jong WH, Van Zijverden, Sips AJAM, Geertsma RE [2009]. Nano-silver: a review of available data and knowledge gaps in human and environmental risk assessment. Nanotoxicology *3*(2):109–138.

Wilding LA, Bassis CM, Walacavage K, Hashway S, Leroueil PR, Morishita M, Maynard AD, Philbert MA, Bergin IL [2016]. Repeated dose (928-day) administration of silver nanoparticles of varied size and coating does not significantly alter the indigenous murine gut microbiome. Nanotoxicology *10*(5):513–520.

Williams K, Milner J, Boudreau MD, Gokulan K, Cerniglia CE, Khare S [2016]. Effects of subchronic exposure of silver nanoparticles on intestinal microbiota and gut-associated immune response in the ileum of Sprague-Dawley rats. Nanotoxicology *9*(3):279–289.

Williams N [1999]. Longitudinal medical surveillance showing lack of progression of argyrosis in a silver refiner. Occup Med *49*(6):397–399.

Williams N, Gardner I [1995]. Absence of symptoms in silver refiners with raised blood silver levels. Occup Med *45*(4):205–208.

Wölbling RH, Milbradt R, Schopenhauer-Germann E, Euler G, Konig KH [1988]. Argyria in employees in the silver processing industry: dermatological investigations and quantitative measurements using atomic absorption spectrometry. Arbeitsmed Sozialmed Praventivmed *23*:293–297.

Xue Y, Zhang S, Huang Y, Zhang T, Liu X, Hu Y, Zhang Z, Tang M [2012]. Acute toxic effects and gender-related biokinetics of silver nanoparticles following an intravenous injection in mice. J Appl Toxicol *32*:890–899.

Youssef HF, Hegazy WH, Abo-Almaged HH, El-Bassyouni GT [2015]. Novel synthesis method of micronized ti-zeolite na-a and cytotoxic activity of its silver exchanged form. Bioinorg Chem Appl *2015*:428121, https://doi.org/10.1155/2015/428121.

Yu W-J, Son J-M, Lee J, Kim S-H, Lee I-C, Baek H-S, Shin I-S, Moon C, Kim S-H, Kim J-C [2014]. Effects of silver nanoparticles on pregnant dams and embryo-fetal development in rats. Nanotoxicology *8*(S1):85–91.

Yun J-W, Kim S-H, You J-R, Kim WH, Jang J-J, Min S-K, Kim HC, Chung DH, Jeong J, Kang B-C, Che J-H [2015]. Comparative toxicity of silicon dioxide, silver, and iron nanoparticles after repeated oral administration to rats. J Appl Toxicol *35*:681–693.

Zook JM, Long SE, Cleveland D, Geronimo CL, MacCuspie RI [2011]. Measuring silver nanoparticle dissolution in complex biological and environmental matrices using UV-visible absorbance. Anal Bioanal Chem *401*:1993–2002.

This page intentionally left blank.

# APPENDIX A

## Physiologically Based Pharmacokinetic (PBPK) Modeling

## A.1 Background and Objectives

Risk assessments with rodent bioassay data involve estimating human exposure concentrations that are equivalent to the animal effect level (e.g., $BMDL_{10}$; NOAEL). A physiologically based pharmacokinetic (PBPK) model can provide insight into the relationship between an external exposure (e.g., airborne mass concentration) and the internal tissue dose. NIOSH used estimates from a peer-reviewed, published PBPK model for silver nanoparticles in rats and humans by Bachler et al. [2013] to evaluate the airborne exposures that were estimated to result in silver tissue doses associated with adverse effects in humans (argyria) or in animals (lung or liver effects).

The objectives of these PBPK modeling analyses are to (1) examine the relationship between the exposure concentrations and the lung and liver tissue doses in rats after subchronic inhalation exposure; (2) estimate the rat effect levels based on lung and liver tissue doses, including the NOAELs, LOAELs, and benchmark dose (BMD) estimates; and (3) estimate the human-equivalent working lifetime exposure concentrations (up to 45 years) associated with the rat adverse effect levels, based on the tissue concentrations of either active/soluble silver (i.e., silver able to release ions and/or form complexes such as silver sulfide) or total silver (i.e., both active/soluble and complexed silver). The PBPK model of Bachler et al. [2013], with model extensions described in Bachler et al. [2015b] and Juling et al. [2016], was used by NIOSH to estimate the occupational exposures (as 8-hour time-weighted average [TWA] concentrations) of AgNPs for up to a 45-year working lifetime associated with the estimated tissue doses equivalent to those in rats with no or minimal adverse effects in the lungs or liver.

### A.1.1 Particle Mechanisms

Factors that can influence the retained tissue dose over time include the clearance and retention processes for inhaled particles and the physical-chemical properties of the particles (e.g., size, shape, solubility), including changes to the particles (e.g., dissolution or chemical transformation such as to silver-sulfur nanocrystals) after deposition or uptake in the body [Bachler et al. 2013]. Silver is processed in the body through various mechanisms, including sulfidation (binding with sulfur) or opsonization (binding with protein), which results in stabilization of the silver, although it is not known if these processes occur within or outside cells (e.g., macrophages). In human skin and eyes, precipitated granules (micrometer scale) can occur regardless of the form of silver taken/administered, including metallic, ionic, or colloidal silver/nanosilver (see Scroggs et al. 1992; Wang et al. 2009; Wadhera and Fung 2005; and Chang et al. 2006, respectively). In a 28-day oral administration study of silver nanoparticles or silver acetate in rats, Loeschner et al. [2011] measured sulfur and selenium in the precipitated granules of silver in cells (e.g., macrophages). In an in vitro study, silver reacted with sulfur, forming "bridges" between the nanoparticles—resulting in a decreased dissolution rate and decreased toxicity [Levard et al. 2011, 2012].

Silver nanoparticles have been shown to undergo dissolution in the lungs and translocation to blood, liver, skin, and other organs. Human exposures to silver resulting in argyria (bluish coloration of skin) have been reported [Hill and Pillsbury 1939; ATSDR 1990; Drake and Hazelwood 2005; Wijnhoven et al. 2009; Johnston et al. 2010; Lansdown 2012]. To better estimate the airborne exposures and tissue doses associated with argyria in humans, PBPK modeling is needed to estimate the relationship between external (airborne) exposure and internal tissue dose of Ag nanoparticles after inhalation.

### A.1.2 Model Evaluation Criteria

In the development and application of the PBPK models for nanoparticulate and ionic silver, Bachler et al. [2013] state that they followed as much as possible the International Programme on Chemical Safety (IPCS) guidelines [WHO/IPCS 2010]. The scientific evidence basis for the model structure, domain of applicability, and uncertainties are clearly stated. The model equations for the physiological

processes of absorption, distribution, metabolism, and excretion (ADME) and associated parameter values are provided in the main journal article or the supplementary material. The aim of Bachler et al. [2013] was to develop PBPK models for both particulate and ionic silver that can be used to estimate the internal tissue dose associated with exposure over a wider range of scenarios. Bachler et al. [2013] note that for a broad application domain of a PBPK model, "it is essential that mechanistic information is reflected in the model structures and that the number of parameters is consistent with the number of underlying data points," and they cite WHO/IPCS [2010]. The structure of the PBPK models of Bachler et al. [2013] for silver nanoparticles and ions was based on the available knowledge about disposition of ionic silver and silver nanoparticles in rats and humans (Figures 2A and 2B, in Bachler et al. [2013]).

Criteria for evaluating and selecting PBPK models for use in risk assessment have also been described by U.S. EPA [2006] in the following four questions: (1) Is the PBPK model available for the test species and humans? (2) Are the parameters for simulating relevant routes available? (3) Does the model simulate dose metrics of relevance to risk assessment? (4) Has the model been evaluated and peer-reviewed? If the answer is "yes" to all questions, then the outcome is to "use in risk assessment." For "no" answers, experimental data collection, model development, and/or evaluation and peer review are recommended prior to use. From the information referenced in this section, it would be reasonable to determine that the model of Bachler et al. [2013] meets all four criteria (i.e., "yes" to each question). The reasons are fourfold: (1) the PBPK model is available for both rats and humans; (2) the model parameters for simulating relevant routes are available, including inhalation; (3) the model simulates dose metrics relevant to risk assessment (silver nanoparticles of different diameters and ionic forms); and (4) the original model [Bachler et al. 2013] has been evaluated as a peer-reviewed, scientific journal article, as have subsequent versions of the model for different applications, materials, or routes of exposure [Bachler et al. 2015a,b; Juling et al. 2016].

The Organization for Economic Cooperation and Development [OECD 2006, 2007] has developed criteria for evaluation of (quantitative) structure-activity relationship [(Q)SAR] models for regulatory purposes, which include the following features of the (Q)SAR model: (1) a defined endpoint; (2) an unambiguous algorithm; (3) a defined domain of applicability; (4) appropriate measures of goodness-of-fit, robustness, and predictivity; and (5) a mechanistic interpretation, if possible. The need for flexibility in the application of these principles was noted in the OECD report [2006, 2007] because the decision to use a (Q)SAR model may depend on the specific application and on the needs and constraints of a regulatory or decision-making framework [OECD 2006, 2007]. (Q)SAR models are based on the premise that "similar chemical structures are expected to exhibit similar chemical behaviour" [OECD 2007], whereas PBPK models are "an important class of dosimetry models that are useful for predicting internal dose at target organs for risk assessment applications" [U.S. EPA 2006]. To the extent that these two model types may have overlapping characteristics and applications, the (Q)SAR model criteria could also be useful in the evaluation of PBPK models.

These OECD [2006, 2007] (Q)SAR criteria could be described as having been met, at least in part, in the PBPK model of Bachler et al. [2013], either in the original publication or in subsequent publications [Bachler et al. 2015a,b; Juling et al. 2016], for the following reasons.

1. The model of Bachler et al. [2013] was used to predict the endpoint of tissue doses of silver particle and ionic forms, and these forms were further evaluated in Juling et al. [2016].
2. The algorithms or model equations were clearly described in the journal articles and supplemental materials.
3. The domain of applicability was described, which includes silver particle diameters of 15 to 150

nm, pure silver and silver alloy particles, and some coated silver particles [polyvinylpyrrolidone (PVP)49 and carboxymethyl cellulose (CMC)31], and it excludes particles with coatings designed to alter opsonization (e.g., polysorbate 8084 or polyethylene glycol, PEG).

4. Model predictions were shown to agree with measured data in four studies of rats and three studies of humans [Bachler et al. 2013] and with additional experimental data on rats [Juling et al. 2016], with standard deviations and $R^2$ estimates reported in some comparisons for statistical evaluation of the model predictions and measured values.
5. Mechanistic interpretations were evaluated in the original publication [Bachler et al. 2013] and investigated further in a subsequent publication [Juling et al. 2016]. Juling et al. [2016] reported that silver ions form secondary particles in vivo, a finding which illustrates the difficulty in distinguishing between the effects of silver nanoparticles and ions in vivo.

The model of Bachler et al. [2013] provides a useful tool to investigate the relationship between airborne exposure concentrations and tissue doses, including doses associated with the development of argyria in humans or liver or lung effects in rats. In addition, the model enables exploration of the role of particle size and solubility on these tissue dose estimates. However, some uncertainties remain in applying the model of Bachler et al. [2013] to estimating occupational exposures by extrapolating exposure duration and across species. For example, limited data are available to evaluate the occupational exposure estimates associated with silver tissue doses that are related to lung or liver effects in rats following subchronic (12- to 13-week) inhalation exposure to AgNPs (15- to 19-nm diameter) [Song et al. 2009; Sung et al. 2013].

In the current analyses, the model of Bachler et al. [2013] is shown to overpredict silver tissue doses from these two rat subchronic inhalation studies, which are used in this risk assessment (Section A.4.2). This finding may have resulted from the original model calibration being based on shorter-term studies, during which clearance was not as important in prediction of tissue dose. An additional uncertainty is that the data on humans to validate the model predictions were limited and included findings from only one occupational exposure study; thus, there is uncertainty in estimating tissue doses in humans over a working lifetime (e.g., up to 45 years).

Further evaluation of the silver model structure would be useful, in light of subsequent revisions and extensions of the model to other applications [Bachler et al. 2015a, b; Juling et al. 2016]. Chronic exposure data, if available, would be preferred for further evaluations of model predictions against the data. Additional evaluations could reduce uncertainty regarding the structure and application of the model of Bachler et al. [2013]. Investigation of the model performance beyond the original domain of applicability could also be informative regarding relevant factors in quantitative risk assessment for workers (e.g., chronic duration of exposure; human interindividual factors that affect particle kinetics; and role of variations in AgNP form and chemistry).

### A.1.3 PBPK Model Structure and Development

The PBPK model of Bachler et al. [2013] was developed on the basis of rat data and was extrapolated to humans. It consists of two sub-models, one for ionic silver and one for silver nanoparticles. Both sub-models were validated with independent data from the literature. Figure 1 of Bachler et al. [2013] shows the structures and interdependencies between these sub-models. Routes of exposure include inhalation, oral, and dermal. The model of Bachler et al. [2013] was designed to be a membrane-limited model (vs. flow limited), as also used by Li et al. [2012]. Two specific modeling assumptions of the model are that (1) AgNPs are discretely distributed in 1-nm steps (Figure S1 of Bachler et al. [2013]) and (2) distribution of nanoparticles in the bloodstream is size-independent. Other

modeling assumptions are described in the supplementary materials of that journal article.

In the model of Bachler et al. [2013], both silver ions and nanoparticles can translocate from the lungs to the blood (Figures 2A and 2B in Bachler et al. [2013]). In the blood, both ionic and nanoparticle silver are predicted to translocate to other organs, including the liver, kidney, and spleen (Figures 7A and 7B in Bachler et al. [2013]). Soluble silver is considered to be the most active form, from which silver ions are released at a rate that depends on various factors such as the particle form and size and the tissue compartment. Some evidence indicates that silver ions readily react with sulfhydryl groups to form silver-sulfur complexes. Glutathione (GSH) is the most common mercaptan (source of sulfhydryl groups) in many cells and therefore plays a major role in the biodistribution of ionic silver [Bell and Kramer 1999; Hansen et al. 2009]. Because liver has by far the highest levels of GSH of any organs, most ionic silver is taken up by the liver. Bachler et al. [2013] defined organ silver uptake as being proportional to the relative organ GSH concentration, thus allowing for a reduction in the number of model parameters.

In the general population, the estimated lifetime storage of silver in the human body is less than 0.5 g, although in extreme cases the storage is 100 g or more [ICRP 1960; East et al. 1980; Wadhera and Fung 2005]. On the basis of this information, Bachler et al. [2013] modeled the storage compartments for each organ (except blood) as sinks from which no silver is released and which have infinite capacity. The total storage of ionic silver in the rat's body was set at 0.5%, based on experimental results after intravenous injection of an ionic silver solution [Furchner et al. 1968].

In the PBPK model of Bachler et al. [2013], two possible scenarios were considered for the metabolism of AgNPs (as shown in Figure 3 of that publication): (1) AgNPs dissolve and release soluble silver species, which are described in the ionic silver PBPK model, and (2) AgNPs are directly transformed to silver sulfide particles. Scenario 2 was found to result in the best model fit to the data. Bachler et al. [2013] attribute their model finding (of no substantial dissolution of AgNPs to silver ions) to the stabilization of the nanoparticles by proteins adsorbed to the particle surface and/or to the transformation of silver to silver-sulfur nanocrystals (either of which would reduce the dissolution rate). Scenario 2 was considered to be supported by the evidence that silver readily reacts with mercaptans, that silver sulfide is detected in tissue samples after exposure to ionic silver, and that the silver tissue burdens predicted by that model scenario agree well with the tissue burden data from Kim et al. [2008] after oral exposure to AgNPs in rats [Bachler et al. 2013, including supplementary material]. Thus, a direct storage mechanism of silver to silver sulfide particles (i.e., bypassing ion formation) was used in the main model calculations [Bachler et al. 2013].

The rat silver nanoparticle and ionic models in Bachler et al. [2013] were calibrated with data from Lankveld et al. [2010] and Klaassen [1979], respectively, with some of the individual rate parameters from other studies, as noted in Bachler et al. [2013]. Lankveld et al. [2010] and Klaassen [1979] administered silver intravenously to rats and measured the silver excretion or tissue doses for up to 16 or 7 days post-exposure, respectively. Silver particles of 20, 80, or 110 nm in diameter were used by Lankveld et al. [2010], and an ionic silver solution was administered by Klaassen [1979]. Bachler et al. [2013] reported that in the calibration and validation of their model, they utilized experimental data of only easily soluble silver species (silver nitrate and silver acetate) or ionic silver solutions. (Note: the form and solubility of the silver in the study of Lankveld et al. [2010] was not verified, as it was not found to be reported in their publication.)

Data from four additional studies of rats were compared to the rat model predictions of Bachler et al. [2013] (Figures 4 and 5 in that article), including two inhalation studies of AgNPs in rats [Takenaka et al. 2001; Ji et al. 2007b]. Bachler et al. [2013] then extrapolated the rat model to humans by adjusting for species-specific differences in the respective physiological factors and body or

organ weights [ICRP 2002]. Human model parameter values were based on those for the reference worker (adult male) [ICRP 2002]; possible kinetic differences by sex or age were not considered. This human PBPK model showed good correlation with human biomonitoring data from three sources [ICRP 1960; Bader 1966; DiVincenzo et al. 1985] (Figure 6A-C in Bachler et al. [2013]). Particularly relevant for an occupational exposure context is the good agreement of the model predictions with measured values of silver in blood and feces from a biomonitoring study of workers [DiVincenzo et al. 1985; Bachler 2013, Figure 6C].

Further revisions to the PBPK model of Bachler et al. [2013] for AgNPs have been described following studies of rodents in applications to other nanomaterials (gold, titanium dioxide) and routes of exposure (intratracheal, oral) [Bachler et al. 2015a,b]. In addition, Juling et al. 2016] used the PBPK model of Bachler et al. [2013] (which they called a PBTK, or physiologically based toxicokinetic, model) to study the distribution of silver in rats 24 hours after intravenous administration of silver particles and ions. The model version of Juling et al. [2016] added a compartment for the thymus; the intestine compartment was divided into small and large intestine compartments; and a "remainder" compartment, which had also been added earlier [Bachler et al. 2015b], was added to contain all organs and tissues that are not covered by other compartments of the model. The PBPK modeling estimates for rats and humans were based on a more recent version of the model of Bachler et al. [2013], which for rats has been published in Bachler et al. [2015b] and Juling et al. [2016].

Before estimation of the human-equivalent concentrations to the rat subchronic effect levels, analyses were performed to compare the airborne exposure and tissue concentrations of silver in the two rat subchronic inhalation studies [Sung et al. 2009; Song et al. 2013]. Analyses were also performed to compare the PBPK rat model predictions of Bachler et al. [2013] to the measured tissue concentrations of silver in both rat studies.

## A.2 Evaluation of Rat Subchronic Data and PBPK Model Predictions

Silver tissue doses were measured in rats following subchronic (13- or 12-week) inhalation of AgNPs (~19 or 15 nm in diameter, respectively) [Sung et al. 2009; Song et al. 2013]. These rat tissue burden data were used in the current analysis to estimate the human-equivalent tissue doses and working lifetime exposures associated with the adverse effects observed in the rat subchronic inhalation studies. These adverse effects included pulmonary inflammation and bile duct hyperplasia (Section 5.1). Thus, the lung and liver tissue doses in rats were used to estimate the human-equivalent lung and liver doses of silver, assuming occupational airborne exposure to silver nanoparticles (for up to a 45-year working lifetime).

First, the relationships between the airborne cumulative exposure concentration of AgNPs (19 or 15 nm in diameter) and the measured silver burden in lung or liver tissues in rats (male and female) following subchronic inhalation (13 or 12 weeks) [Sung et al. 2009; Song et al. 2013] were examined (Sections A.2.1 and A.2.2). The cumulative exposure metric was used to adjust for the exposure duration difference in these two studies (13 vs. 12 weeks in Sung et al. [2009] and Song et al. [2013], respectively). In both lung and liver, the variability in the silver tissue burdens increased with exposure concentration. Non-constant (heterogeneous) variance was observed in the tissue burdens in rats at a given exposure concentration, which may be due to interindividual rat differences in the clearance and retention of silver nanoparticles (toxicokinetics). Despite the increased variability in the silver tissue doses at the highest dose, the two lower doses—which are associated with no or minimal adverse effects—are most relevant to human health risk assessment.

### A.2.1 Lungs

The rat lung tissue burdens of silver varied by study [Sung et al. 2009; Song et al. 2013] and by sex

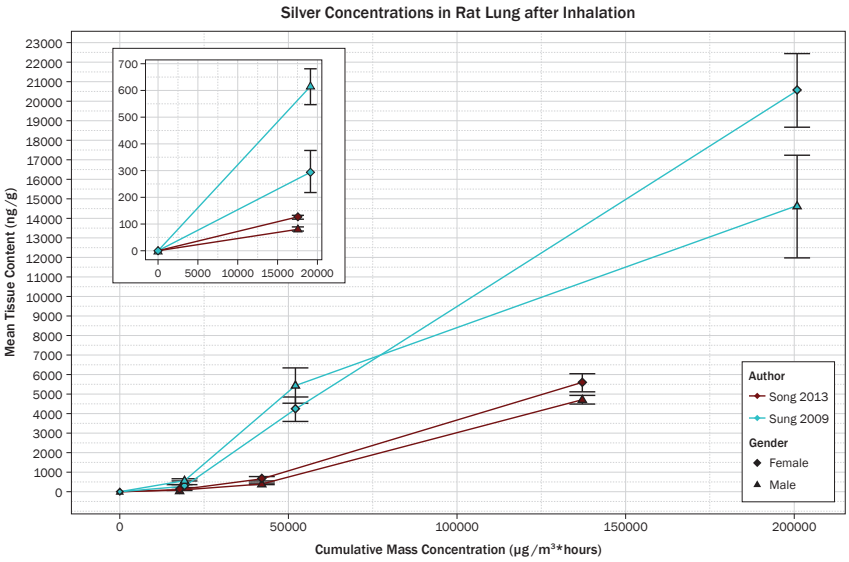


**Figure A-1. Lung silver burden (µg Ag/g wet tissue) by cumulative exposure (µg/m³ × hours) in male and female rats, measured at the end of the 13-week [Sung et al. 2009] or 12-week [Song et al. 2013] exposure.** Tissue concentrations are means ± 1 standard error. Lines fit to data, not modeled. Insert shows low exposure concentration (49 µg/m³) and control (unexposed) data only.

(Figure A-1). The measured burdens are higher in Sung et al. [2009] at all doses for both male and female rats, and a disproportionally higher Ag lung tissue dose is seen in rats at the highest exposure concentration (515 µg/m³) [Sung et al. 2009]. The higher burdens observed at all airborne exposure concentrations in Sung et al. [2009] could be due to higher deposition efficiencies of inhaled AgNPs in the lungs of rats in that study, although this is considered unlikely because rats in both studies were exposed to similar-sized particles (~19 vs. ~15 nm median diameter in Sung et al. [2009] and Song et al. [2013], respectively). Particles of similar diameter would be expected to have similar deposition efficiencies. Other, unexplained differences in the animals and/or experimental conditions may have resulted in these between-study differences. The relatively low number of animals also needs to be taken into account when comparing tissue burdens across groups (i.e., n = 3–5 rats per lung or liver tissue group of male or female rats in Sung et al. [2009]; n = 9 male rats and n = 4 female rats per lung or liver tissue group in Song et al. [2013]).

The steeper increase in the lung tissue burdens at the higher exposure concentration in Sung et al. [2009] (Figure A-1) is consistent with the possibility that impairment of lung clearance resulted in a disproportionate increase in the lung retention of silver particles at the highest exposure concentration (515 µg/m³). In general, the within-study lung tissue burdens (among males or females) were less variable than the between-study (Sung et al. [2009] or Song et al. [2013]) Ag lung tissue burdens, at the same (or similar interpolated) airborne exposure concentrations.

## A.2.2 Liver

The rat silver tissue burdens in the liver are generally more consistent across study and sex (Figure A-2) than those in the lungs (Figure A-1). At the two lower concentrations, the rat liver tissue burdens are relatively similar between the two studies [Sung et al. 2009; Song et al. 2013] and between males and females within each study. As was also observed in the lungs, the liver silver burdens seem to increase disproportionately at the highest

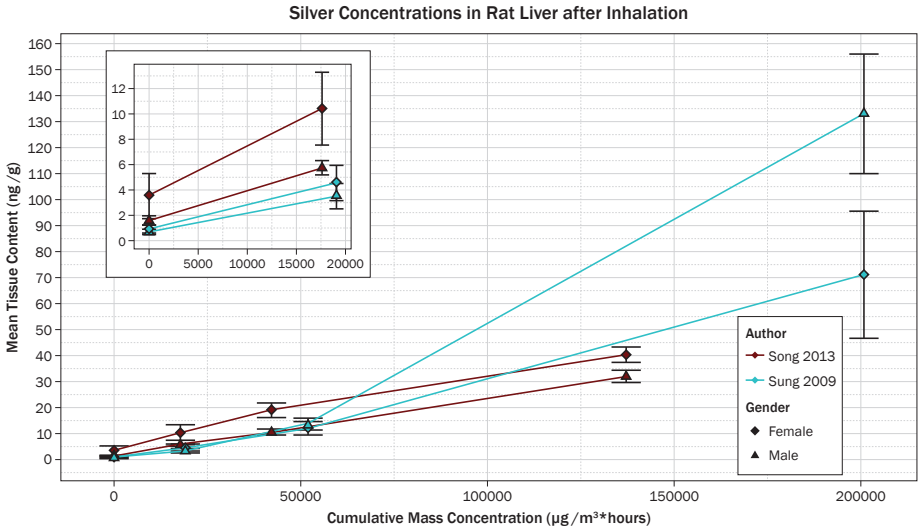


**Figure A-2. Liver silver burden (µg Ag/g wet tissue) by cumulative exposure (µg/m³ × hours) in male and female rats, measured at the end of the 13-week [Sung et al. 2009] or 12-week [Song et al. 2013] exposure.** Tissue concentrations are means ± 1 standard error. Lines fit to data, not modeled. Insert shows low exposure concentration (49 µg/m³) and control (unexposed) data only.

concentration (515 µg/m³ [Song et al. 2013]), suggesting increased tissue retention of silver at that concentration, especially in female rats. Male and female rat liver tissue doses of silver were similar in the Sung et al. [2009] study at the lower exposure concentrations and varied by a factor of approximately three between the studies [Sung et al. 2009; Song et al. 2013] at the lowest exposure concentration (49 µg/m³) (Figure A-2).

## A.3 Effect Level Estimates in Rats and Humans

The rat subchronic inhalation studies [Sung et al. 2008, 2009; Song et al. 2013] yielded NOAELs or LOAELs for minimal adverse lung or liver effects. The lung response of chronic pulmonary inflammation (minimal) and the liver response of bile duct hyperplasia (minimal) were selected as potentially adverse responses of relevance to humans. The silver tissue doses associated with either no significant increase (NOAEL) or a low (10%) increase ($BDML_{10}$) in these responses were selected as the target doses for risk assessment based on PBPK modeling [Bachler et al. 2013]. This model was used to estimate the working lifetime exposure concentrations that would result in the equivalent lung or liver tissue concentrations. In addition, for endpoints with sufficient data (at least one intermediate dose group with a response between that of the controls and the highest response), $BMDL_{10}$ values were estimated with dose-response modeling (as discussed in Appendix B).

Table A-1 shows estimated doses of silver in lung and liver tissues in rats after subchronic inhalation (for 12 or 13 weeks), at the NOAEL and $BMDL_{10}$ estimates. Dose-response data were not sufficient for modeling the chronic alveolar inflammation response in male or female rats in Sung et al. [2009] or in female rats in Song et al. [2013]. For those cases, only the NOAELs are provided in Table A-1. Dose-response data for chronic alveolar inflammation in male rats in Song et al. [2013] were minimally acceptable for $BMDL_{10}$ estimation (Appendix B). The highlighted doses are selected as representative target tissue doses of silver associated with either no or low estimated risk of adverse effects in the lungs or liver. These doses were selected as being

**Table A-1. Estimated target tissue doses of silver nanoparticles, based on rat subchronic inhalation studies.**

| Study/ Target organ | Adverse endpoint | Sex | Exposure concentration, μg/m³ | Tissue dose, measured or estimated, ng/g* | Type of effect level |
|---|---|---|---|---|---|
| | | **Song et al. [2013]** | | | |
| Lung | Chronic alveolar inflammation, minimal | M | 49 | 33† | $BMDL_{10}$ |
| | | | | 81 | NOAEL |
| | | F | 117 | **672** | NOAEL |
| | | **Sung et al. [2009]** | | | |
| Lung | Chronic alveolar inflammation, minimal | M | 133 | 5,450 | **NOAEL** |
| | | F | | **4,241** | |
| Liver | Bile duct hyperplasia, minimal | M | 133 | **11.6** | **$BMDL_{10}$** |
| | | | | 14 | NOAEL |
| | | F | | **6.3** | **$BMDL_{10}$** |
| | | | | 12 | NOAEL |

*Tissue doses of silver, as NOAEL or $BMDL_{10}$.

†Estimate was excluded from evaluation because of limited data and modeling options (see Appendix B).

$BMDL_{10}$: Benchmark dose (95% lower confidence limit) associated with a 10% response ($BMDL_{10}$), derived from benchmark dose modeling (U.S. EPA BMDS version 2.5) of the measured tissue dose and response data, including the following: liver bile dust hyperplasia, Sung et al. [2009] Table 9 (M) and Table 10 (F); lung inflammation, Song et al. [2013] Table XII (M). (See Appendix B for the BMD modeling results.)

NOAEL: No observed adverse effect level. The NOAEL is the highest dose group above the control (unexposed) group that did not have a statistically significantly greater proportion of rats with an adverse lung or liver response. NOAELs are as reported in Sung et al. [2009] Table 7 (M) and Table 8 (F); and Song et al. [2013] Table II (M) and Table III (F).

Notes: The human-equivalent tissue dose is assumed to be equal to the rat target tissue dose, expressed as ng Ag/g tissue. PBPK modeling was used to estimate the occupational airborne exposure to Ag (as 8-hour time-weighted average concentration, 40 hr/wk, up to 45 years) that would result in the same target tissue burden in humans (Section A.4). Estimated human equivalents to those in bold type are shown in Table A-9.

the lowest estimates for a given study, response endpoint, or sex and were used as target doses in the PBPK modeling.

As shown in Table A-1, the NOAEL lung tissue doses of silver vary substantially between the two studies [Song et al. 2013; Sung et al. 2009] (up to an order of magnitude or more), although the exposure concentrations and durations were similar. This suggests that rats in the study by Sung et al. [2009] retained considerably more silver in their lungs during the 13-week exposure than did the rats in the study by Song et al. [2013] (to a greater extent than the 1 additional week would suggest) but did not develop adverse lung effects at those doses. The generation method and particle size of the silver were similar between the two studies, which were performed in the same laboratory. The reason for the large difference in measured concentrations of silver in lung tissue in the two studies [Sung et al. 2009; Song et al. 2013] is not known, and it contributes to uncertainty in the lung tissue dose level for use in risk assessment. Sex differences in the mean lung tissue silver dose are also observed, although these sex differences are smaller than the between-study differences in silver lung tissue dose. It is also possible that there may have been an unknown difference in solubility of the AgNP used in the two

studies [Sung et al. 2009, diameter ~19 nm; Song et al. 2013, diameter ~15 nm], which could have resulted in different rates of clearance of AgNP from the lungs, or that the analytical method used for quantifying silver in tissues gave varying results.

Unlike the results for the lungs, the liver tissue doses of silver at the NOAEL were quite similar in male and female rats in Sung et al. [2009] (Table A-1) and in rats at the lower doses in Song et al. [2013] (who did not report any findings on bile duct hyperplasia) (see Figure A-2).

## A.4 PBPK Model Estimates

### A.4.1 Overview of PBPK Modeling Runs

A recently developed PBPK model for silver uptake and disposition in the body [Bacher et al. 2013] was used to estimate the internal tissue doses of silver in workers after up to 45 years of inhalation exposure to AgNPs [Bachler 2015, report to NIOSH]. Model simulations were performed to estimate the following:

- Occupational exposure concentration (8-hour TWA) of AgNP over a 45-year working lifetime (8 hr/d, 5 d/wk) associated with the retention of Ag in the skin at the target dose of 3.2 μg Ag/g skin, which is reported to be the lowest dose associated with argyria in humans [Bachler et al. 2013]; estimates are provided for AgNPs of different diameters and for ionic silver. The purpose of these estimates is to evaluate whether working lifetime exposures to AgNPs at the current NIOSH REL for silver (10 μg/m$^3$, 8-hour TWA concentration) would be likely to result in argyria.
- Tissue dose levels of silver in humans, assuming inhalation exposure to AgNPs (either 15 or 100 nm in diameter) or ionic silver over a 45-year working lifetime at 10 μg/m$^3$ (8-hour TWA) concentration. The purpose of these estimates is to evaluate whether working lifetime exposures to AgNPs would result in lung and liver tissue concentrations of silver above the rat adverse effect levels.
- Occupational exposure concentration (8-hour TWA) of AgNPs over a 45-year working lifetime that would result in the human-equivalent lung or liver tissue dose to that in the rat associated with adverse (early-stage) effects; estimates for either 15- or 100-nm-diameter AgNPs. No tissue dose data are available on humans exposed to AgNPs; thus, the rat subchronic inhalation data of AgNPs (median diameter, ~15–20 nm) are extrapolated to humans to estimate the target tissue doses associated with early-stage adverse lung or liver effects in rats.

All human model simulations are for an adult male, assuming light exercise (typically 1.2 m$^3$/d for 8 hours) and nasal breathing pattern, using the parameter values reported in Bachler et al. [2013]. Prior to these human model simulations, rat model simulations were performed to compare estimates from the rat model calibrated from other rat data on AgNP kinetics by inhalation and other routes of exposure [Bachler et al. 2013]. The parameters used in the rat model and the human model are reported in Tables A-2 and A-3, respectively.

Additional model runs (results not shown) included evaluations of rat models with increased lung clearance rate; human model estimates for mixed particle sizes of 1–100 nm, assuming uniform particle size distribution (these estimates are shown for argyria estimates only); and human model estimates for other rat-based target tissue doses, including the rat NOAEL estimates of 100 or 117 μg/m$^3$ and human-equivalent tissue dose estimates of 47 or 23 μg/m$^3$ (adult male, light exercise, nose breathing) estimated by Song et al. [2013] [Bachler 2015, report to NIOSH].

### A.4.2 Comparison of Model-Predicted and Measured Lung and Liver Tissue Burdens in Rats

The PBPK model of Bachler et al. [2013] was calibrated and validated on the basis of data on silver nanoparticles in rat studies, including inhalation exposure studies by Ji et al. [2007b] (same laboratory as the Sung et al. [2008, 2009] and Song et

**Table A-2. Physiological parameters for rat used in physiologically based pharmacokinetic (PBPK) model for silver nanoparticles [Bachler et al. 2013].**

| Rat | Organ weight as % of total body weight | SD | Blood flow amount as % of total blood volume | SD | GSH concentration µmol/g | SD |
|---|---|---|---|---|---|---|
| Skin* | 19.0 | 2.620 | 5.80 | 0.09 | 0.37 | 0.08 |
| Liver | 3.66 | 0.650 | 18.30 | 2.50 | 9.37 | 0.86 |
| Kidneys | 0.730 | 0.110 | 14.10 | 1.90 | 2.45 | 0.14 |
| Muscles* | 40.4 | 7.170 | 27.80 | 13.34 | 0.73 | 0.20 |
| Spleen† | 0.200 | 0.050 | 0.85 | 0.26‡ | 2.12 | 0.09 |
| Heart | 0.330 | 0.040 | 5.10 | 0.10 | 2.12 | 0.52 |
| Brain | 0.570 | 0.140 | 2.00 | 0.30 | 1.64 | 0.11 |
| Lung | 0.500 | 0.090 | 2.10 | 0.40 | 2.04 | 0.01 |
| Testes* | 1.03 | 0.060 | 0.79 | 0.16 | 3.41 | 0.20 |
| Small intestines* | 1.40 | 0.390 | 10.14 | 2.43 | 1.78 | 0.24 |
| Large intestine* | 0.840 | 0.040 | 1.64 | 0.44 | 2.10 | 0.22 |
| Thymus§ | 0.102 | 0.057 | 0.42 | 0.21 | 1.90 | 0.15 |
| Remainder | 31.2 | 7.67 | 26.26 | 13.94 | 1.22 | 0.09 |
| Cardiac output, L/min | 0.095 | 0.013 | | **Average:** | 1.22 | 0.09 |
| Blood, L | 0.022 | 0.002 | | | | |
| Body weight, kg | 0.300 | | | | | |

*Stott et al. [2006], for blood flow.
†Davies and Morris [1993], for blood flow.
‡Based on SDs from other organs because specific values were not available.
§Hatai et al. [1914]; Jansky and Hart [1968]; or Alhamdan and Grimble [2003], for organ weight, blood flow, or GSH concentration, respectively.
Notes: These parameters include those from more recent versions of the Bachler et al. [2013] model [Bachler et al. 2015b; Juling et al. 2016], which added a remainder compartment, containing all organs and tissue that are not covered by other compartments of the model. If not otherwise indicated, parameter values are from Brown et al. [1997]. SD: standard deviation.

al. [2013] studies) and by Takenaka et al. [2001]. These study reports described tissue burden/kinetics data only, not biological response. Reports of other rat studies [Sung et al. 2008, 2009; Song et al. 2013] presented both tissue burden and response data, which are used in this risk assessment. As discussed in this section, the lung and liver tissue burdens reported in those four rat studies [Takenaka et al. 2001; Ji et al. 2007b; Sung et al. 2009; Song et al. 2013] are compared to each other, and the model-predicted tissue burdens are compared to the data in Sung et al. [2009] and Song et al. [2013], which had not been used in the calibration or validation of the model by Bachler et al. [2013].

Ji et al. [2007b] performed a 28-day inhalation exposure study in rats (male and female, 6 weeks of age, specific-pathogen-free [SPF] Sprague-Dawley) exposed to 0, 0.5, 3.5, or 61 µg/m$^3$ AgNPs (6 hr/day,

**Table A-3. Physiological parameters for humans, used in physiologically based pharmacokinetic (PBPK) model for silver nanoparticles [Bachler et al. 2013].**

| Human | Organ weight as % of total body weight | SD | Blood flow amount as % of total blood volume | SD | GSH concentration µmol/g | SD |
|---|---|---|---|---|---|---|
| Skin | 4.36 | 0 | 5.92 | 1.13 | 0.46 | 0.20 |
| Liver | 2.47 | 0 | 21.3 | 4.84 | 6.40 | 0.40 |
| Kidneys | 0.420 | 0 | 18.1 | 2.32 | 4.00 | 0.30 |
| Muscles | 39.7 | 0 | 14.2 | 5.10 | 1.80 | 0.08 |
| Spleen | 0.210 | 0 | 3.43 | 1.24 | 2.12* | 0.09* |
| Heart | 0.450 | 0 | 4.91 | 1.32 | 1.20 | 0.20 |
| Brain | 1.99 | 0 | 11.8 | 1.77 | 1.40 | 0.30 |
| Lung | 0.680 | 0 | 3.38 | 2.49 | 2.04* | 0.01* |
| Testes | 0.048 | 0 | 0.10 | 0.00 | 3.41* | 0.20* |
| Small intestines | 1.40 | 0 | 9.10 | 2.20 | 1.78* | 0.24* |
| Large intestines | 0.490 | 0 | 3.80 | 0.40 | 2.10* | 0.22* |
| Thymus† | 0.034 | 0 | 0.42* | 0.21* | 1.90* | 0.15* |
| Remainder | 47.7 | 0 | 18.3 | 8.59 | 1.87 | 0.06 |
| Cardiac output, L/min | 6.5 | 1.300 | | **Average:** | 1.87 | 0.06 |
| Blood, L | 5.6 | 0.810 | | | | |
| Body weight, kg | 73 | | | | | |

* Values from the rat.

†Hatai et al. [1914]; Jansky and Hart [1968]; or Alhamdan and Grimble [2003], for organ weight, blood flow, or glutathione (GSH) concentration, respectively.

Note: These parameter values include those from a more recent version of the Bachler et al. [2013] model [Bachler et al. 2015b], which added a remainder compartment, containing all organs and tissue that are not covered by other compartments of the model. Reference value sources: weight, ICRP [2002]; blood flow, Williams and Legget [1989]; GSH, see Bachler et al. [2013].

5 d/wk, for 4 weeks). The AgNP diameter was ~12–15 nm (GSD ~1.5) in the three exposure concentrations. The AgNPs were generated by evaporation/condensation with use of a small ceramic heater [Ji et al. 2007a]; this is the same particle generation method used in the subchronic inhalation studies [Sung et al. 2008, 2009; Song et al. 2013]. Takenaka et al. [2001] conducted a 1-day inhalation exposure study in rats (female Fischer 344 rats; body weight, 150–200 g) that were exposed for 6 hours at 133 µg/m$^3$ to silver nanoparticles; rats were killed on days 0, 1, 4, and 7. The silver lung burden immediately after exposure was 1.7 µg Ag, which decreased rapidly to 4% of the initial lung burden by day 7. The AgNP median diameter was 17.1 ± 1.2 nm (GSD = 1.38). The AgNPs were generated by a spark discharging through an argon atmosphere [Takenaka et al. 2001].

In the two studies, the AgNP diameters were similar, although the particle generation methods were

different. These different generation methods could have resulted in different surface properties of the AgNPs, which could potentially have affected their toxicokinetic properties.

**Lungs:** Figure A-3 shows the end-of-exposure silver lung tissue burdens in these four rat studies by cumulative exposure (μg/m$^3$ × hours) (normalized) to account for the differences in exposure concentration and duration. These plots do not account for differences in the clearance of silver from the lungs during the exposure time, ranging from 1 day (6-hour exposure) in Takenaka et al. [2001] to 28 days in Ji et al. [2007], 12 weeks in Song et al. [2013], and 13 weeks in Sung et al. [2009]. The results show much higher lung silver burdens in Takenaka et al. [2001] and Ji et al. [2007b] at a given cumulative exposure concentration. These higher lung burdens could have been due to higher deposition fractions (although median particle sizes were similar) or clearing of a lower proportion of the deposited dose. Given the short duration of exposure (6 hours) in Takenaka et al. [2001], there would have been less time for alveolar macrophage–mediated clearance, although the silver lung burden cleared rapidly in the 1–7 days post-exposure [Takenaka et al. 2001, Table 1].

**Liver:** Figure A-4 shows the end-of-exposure liver tissue silver burdens in these four rat studies, also plotted by cumulative exposure (μg/m$^3$ × hours) (normalized) to account for the differences in exposure concentration and duration. Again, these plots do not account for differences in the amount of silver cleared from the liver during the exposure time (as mentioned above for the lungs). These results show similar liver silver burdens in the 4-, 12-, and 13-week exposure studies [Ji et al. 2007b; Song et al. 2013; Sung et al. 2009, respectively], suggesting similar build-up rates of silver in liver over

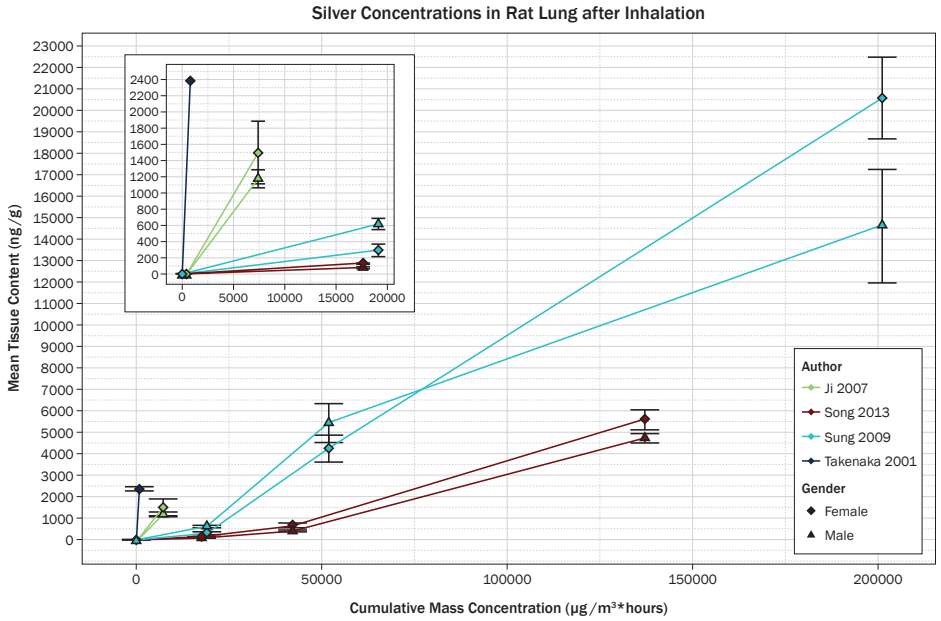


**Figure A-3. Comparison of lung silver burden (μg Ag/g wet tissue) by cumulative exposure (μg/m$^3$ × hours) in male and female rats, measured at the end of inhalation exposure (day 0, "immediately" after 6 hours in Takenaka et al. [2001]; 4 weeks in Ji et al. [2007b]; 13 weeks in Sung et al. [2009]; or 12 weeks in Song et al. [2013]).** Tissue concentrations are means ± 1 standard error. Lines fit to data, not modeled. Insert shows data at lowest exposure concentration only (i.e., 133, 0.5, 49, 49 μg/m$^3$, respectively, as cited above) and control (unexposed) data only.

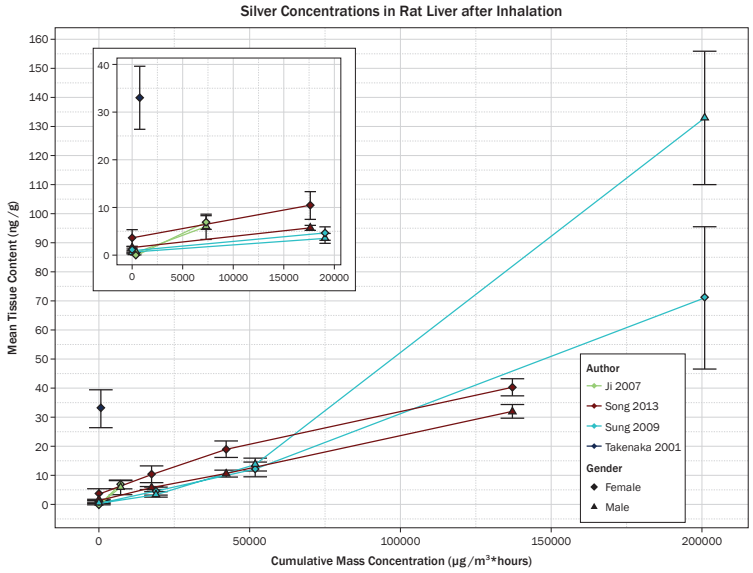


**Figure A-4. Comparison of liver silver burden (μg Ag/g wet tissue) by cumulative exposure (μg/m³ × hours) in male and female rats, measured at the end of inhalation exposure (day 0, "immediately" after 6 hours in Takenaka et al. [2001]; 4 weeks in Ji et al. [2007b]; 13 weeks in Sung et al. [2009]; or 12 weeks in Song et al. [2013]).** Tissue concentrations are means ± 1 standard error. Lines fit to data, not modeled. Insert shows data at lowest exposure concentration only (i.e., 133, 0.5, 49, 49 μg/m³, respectively, as cited above) and control (unexposed) data only; Takenaka et al. [2001] did not include a control group.

time. The highest liver silver burden is observed in the Takenaka et al. [2001] study, relative to similar cumulative exposure concentrations in the other studies, which may reflect the rapid initial translocation to the liver in this acute exposure. These findings illustrate the importance of accounting for the clearance pathways in the estimation of tissue doses over time. Cumulative exposure may be a good surrogate for the total deposited lung dose, but a PBPK model is needed to account for particle dissolution and clearance from the lungs and translocation to other organs.

The PBPK model–predicted tissue burdens of silver, based on the Bachler et al. [2013] rat model, were higher than the measured rat burdens of silver in lung and liver tissues at the end of the subchronic (12- or 13-week) inhalation exposure [Sung et al. 2009; Song et al. 2013] (Figures A-5 and A-6). For example, at the middle exposure concentration (133 μg/m³ in Sung et al. [2009] or 117 μg/m³ in Song et al. [2013]), the model-predicted rat lung burdens were higher by a factor of approximately 3 compared to the measured lung burdens in Sung et al. [2009] and by a factor of approximately 4–7 compared to the lung burdens in Song et al. [2013], among male and female rats. The model-predicted rat liver burden of silver was approximately 1.5- to 3-fold higher than the measured rat liver burdens in male and female rats in both studies [Sung et al. 2009; Song et al. 2013]. The number of rats per tissue-burden group were 3–5 males and 5 females in Sung et al. [2009] and 9 males and 4 females in Song et al. [2013]. The sample sizes for the Monte Carlo simulations in the PBPK model estimates were assumed to be equal to those of the same observed groups. (Note: Bachler et al. [2013] used 1,000 model iterations in the Monte Carlo simulations. Background levels of silver were not considered, although these would typically be low compared to the levels of silver from the inhalation exposure.)

The over-prediction of the lung and liver tissue burdens compared to the measured tissue burdens in the rat subchronic inhalation studies may be due to several factors. First, between-study variability and

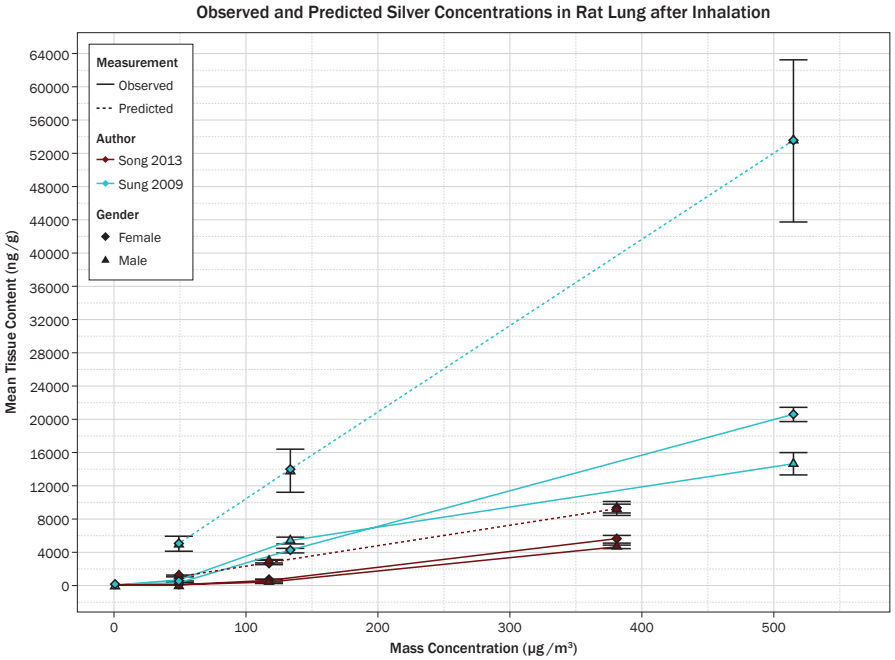


**Figure A-5: Observed and physiologically based pharmacokinetic (PBPK) model–predicted lung burdens in male and female rats at the end of the 13-week [Sung et al. 2009] or 12-week [Song et al. 2013] inhalation exposure.** (Note: the model predictions are the same for both sexes.)

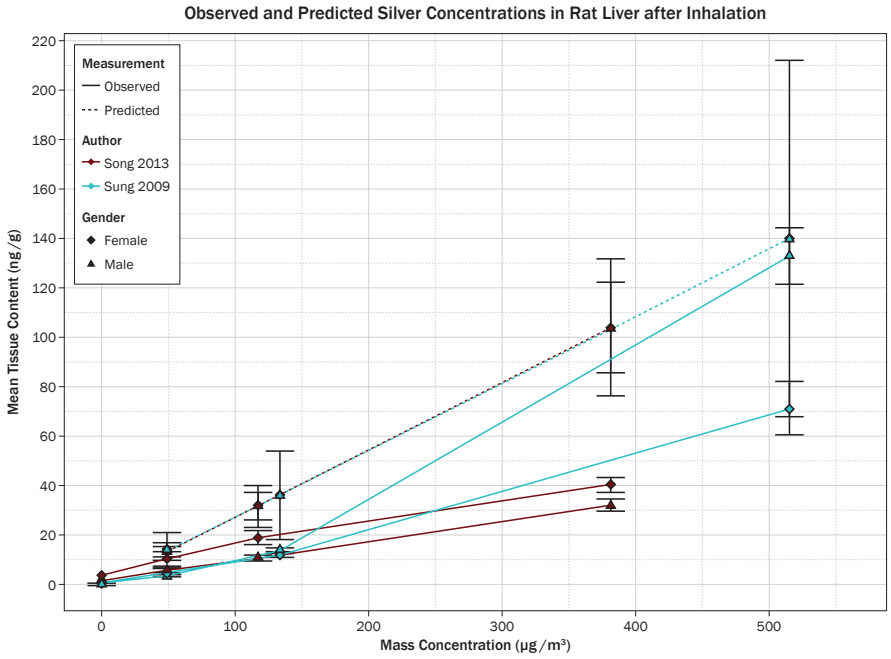


**Figure A-6: Observed and physiologically based pharmacokinetic (PBPK) model–predicted liver burdens in male and female rats at the end of the 13-week [Sung et al. 2009] or 12-week [Song et al. 2013] inhalation exposure.** (Note: the model predictions are the same for both sexes.)

the small numbers of animals could contribute to the apparent differences. Second, the PBPK model was calibrated and validated against rat data from shorter durations of exposure (1- or 28-day inhalation) at exposure concentrations of 133 μg/m$^3$ (1 d) or 0, 0.5, 3.5, or 61 μg/m$^3$ (28 days) in Takenaka et al. [2001] and Ji et al. [2007b]. By comparison, rats were exposed to generally higher concentrations (0, 49, 117, or 133 μg/m$^3$ and 381 or 515 μg/m$^3$) over longer durations (12 or 13 weeks) in Song et al. [2013] and Sung et al. [2009]. The higher tissue burdens in the shorter-term inhalation studies [Takenaka et al. 2001; Ji et al. 2007b] used in the PBPK modeling, extrapolated to longer-term exposures, may have contributed to over-estimation of the tissue burdens in the subchronic inhalation studies, in which there was apparently a higher clearance rate of silver from the rat lungs and liver [Sung et al. 2009; Song et al. 2013].

Another possibility is that the AgNPs differed (e.g., in solubility) across the studies; however, the particle sizes were similar (~12–19 nm in median diameter). The Ji et al. [2007b] study used the same AgNP generation method [Ji et al. 2007a] as used in the subchronic studies [Sung et al. 2009; Song et al. 2013]. As discussed above, a different AgNP generation method was used by Takenaka et al. [2010], and the different generation methods could have resulted in differences in the surface properties and toxicokinetics of the AgNPs in those studies.

An area of uncertainty is how this apparent model over-prediction of rat silver tissue doses would influence the estimates of human-equivalent exposure concentrations. Other model uncertainties suggest the silver tissue burdens could be underestimated, for example, by extrapolating the rat subchronic data to human working-lifetime exposures based on a long-term clearance model (ICRP 1994), as used in Bachler et al. [2013]. Human studies have shown that the ICRP [1994] model under-predicts the long-term retention of poorly soluble particles in the lungs of humans [Kuempel and Tran 2002; Gregoratto et al. 2010], although these models do not include particle dissolution pathways.

### A.4.3 Human-Equivalent Working Lifetime Exposure Concentrations

Estimations of working lifetime exposure concentrations of silver depend on the occupational exposure concentration and duration. The occupational route of exposure for these simulations is assumed to be inhalation. The deposited dose in the respiratory tract depends on the size of the airborne particles. The retained dose in the lungs and in other organs depends on the absorption rate of Ag from the lungs to the systemic circulation [Bachler et al. 2013].

### A.4.4 Worker Body Burden Estimates of Silver From Diet and Occupational Exposures

Apart from some workers' potential occupational exposure to silver, humans take in a certain amount of silver in the daily diet. The routes of exposure differ but are assumed to be primarily inhalation in the workplace and dietary (oral) intake. Studies of intravenous silver administration have also been reported [e.g., Park et al. 2011a]. Regardless of the route of exposure, silver nanoparticles can be absorbed into the adjacent tissue, enter the systemic circulation, and be taken into all organs in the body, including liver, kidney, spleen, bone marrow, and brain [Bachler et al. 2013; Song et al. 2013; Brune 1980].

A few studies have measured or estimated the tissue dose or body burdens of silver from the diet [Snyder et al. 1975; Kehoe et al. 1940] or occupational exposures [DiVincenzo et al. 1985; Wölbling et al. 1988]. Table A-4 shows findings from DiVincenzo et al. [1985] on Ag body burden in humans from the diet and from occupational exposure, as well as retention estimates based on Ag biomonitoring results in workers at a U.S. facility that produced silver for photographic processes and products. The study included workers with airborne exposure to silver (n = 30) and control workers (randomly selected) at the same facility without airborne exposures to silver (n = 35) (sample sizes from Table 2 of DiVincenzo et al. [1985]). Most of the workers with silver

**Table A-4. Estimated annual body burden of silver in humans, based on biomonitoring measurements and estimates [DiVincenzo et al. 1985] or physiologically-based pharmacokinetic (PBPK) model predictions [Bachler et al. 2013].**

| Study | Ag form | Annual body burden (µg Ag/kg body wt) | Retention, % |
|---|---|---|---|
| DiVincenzo et al. [1985]* | | | |
| Workers (workplace + diet) | NR | 14 | 1 |
| Controls (diet) | NR | 2 | 1 |
| Bachler et al. [2013]—Controls (diet) | Nanoparticle | 3 | 0.77 |
| | Ionic | 1 | 0.25 |

*As reported in Table 5 of DiVincenzo et al. [1985].
NR: not reported.

exposure had worked for 5 or more years in a production area with the highest potential exposure to airborne silver. Job descriptions included burner operators, maintenance workers, smelter operators, and mechanics. In both groups the mean duration of employment was approximately 20 years and the mean age was approximately 45 years.

The annual body burden of silver from the diet in unexposed workers (controls) estimated by DiVincenzo et al. [1985] (assuming 1% intestinal absorption) was 2 µg Ag/kg body weight (BW), or storage/retention of 1% silver (form of silver not reported) (Table A-4). Based on the PBPK model of Bachler et al. [2013] (assuming 4% intestinal absorption), the estimated annual body burden of silver nanoparticles is 1 µg Ag/kg BW, and that of ionic silver is 3 µg Ag/kg BW (corresponding to either 0.77% or 0.25% storage/retention after 45 years). These similar estimates reported in DiVincenzo et al. [1985] and calculated from the model of Bachler et al. [2013] provide information relevant to validation of the PBPK model predictions.

Table A-4 (as well as Table 5 of DiVincenzo et al. [1985]) provides information from which to estimate the average airborne concentration of the workers in that study. The estimated exposed worker daily Ag uptake (as reported in Table 5 of DiVincenzo et al. [1985]) is 0.054 µg Ag/kg BW (assuming 1% of the "silver intake" was retained in the body), or 3.78 µg Ag/d for a 70-kg adult male. Although not specifically stated in Divencenzo et al. [1985], it is implied that the "silver intake" is the inhaled dose and that the 1% silver retained in the body includes the fraction of the inhaled dose that is deposited in the respiratory tract and then absorbed and retained in the body.

Thus, the daily airborne exposure concentration can be estimated as follows, assuming a reference worker air intake of 9.6 $m^3$ in an 8-hour day:

3.78 µg/d uptake in Ag worker = X µg/$m^3$ * 9.6 $m^3$/d * 0.01 intake fraction

*or*

X µg/$m^3$ = 3.78 µg/d / [9.6 $m^3$/d * 0.01]

where X = 39.4 µg/$m^3$.

This estimate is consistent with the airborne exposure concentrations of 1–100 µg/$m^3$ measured over a 2-month period, as reported by DiVincenzo et al. [1985]. DiVincenzo et al. [1985] reported an estimated occupational airborne average exposure concentration of approximately 30 µg/$m^3$. (Note that DiVincenzo et al. [1985] used 3.38 µg/d, vs. 3.78 µg/d from the Table 5 value of 0.054 µg/kg × 70 kg.) An airborne concentration of 33.8 µg/$m^3$ is calculated from 3.38 µg/d / (10 $m^3$/d * 0.01), which supports the interpretation that DiVincenzo et al. [1985] considered the 1% "intake fraction" to include the

deposited respiratory tract dose and the retention/storage dose. "Insoluble silver" was considered to be the primary form of silver to which workers were exposed in that study [DiVincenzo et al. 1985, p. 208]. The worker annual body burden of silver was approximately 6-fold higher (12 μg Ag/kg BW) than that from diet (2 μg Ag/kg BW) (total of 14 μg Ag/kg BW in exposed workers), although the route of exposure and internal organs exposed differ.

No adverse health effects were reported in the study of DiVincenzo et al. [1985] (among workers with ~20-year exposure, age ~45 years). However, the purpose of that study was to estimate Ag body burdens on the basis of measurements in feces, urine, blood, and hair, and the report did not present any biomedical findings. Thus, there is uncertainty about whether any adverse health effects occurred in those workers, associated with their occupational exposure to silver.

Silver tissue burden estimates in humans, based on measurements or model predictions, are provided in Tables A-5 and A-6. Measured tissue burdens of silver in smelter workers and in workers without occupational exposure to silver (controls), as reported in Brune [1980], are reported in Table A-5. Estimates of silver tissue burdens from dietary intake are provided in Table A-6 and are based on PBPK model [Bachler et al. 2013] estimates of silver tissue burden that assume exposure up to 45 years and an average dietary intake of 80 μg/d (based on an upper estimate of 60–80 μg/d from Snyder et al. [1975] and Kehoe et al. [1940], as reported in DiVincenzo et al. [1985]).

## A.4.5 Estimated Working Lifetime Exposure Concentrations Associated with Argyria

Argyria (bluish pigmentation of the skin) has been observed in humans with Ag burdens of 3.2 μg/g skin tissue; this skin tissue dose was measured in an individual who developed argyria at the lowest administered dose of 1.84 g (intravenous) of silver arsphenamine [Triebig and Valentin 1982; Wadhera et al. 2005; Gaul and Staud 1935, as reported in Bachler et al. 2013].

Table A-7 shows the working lifetime exposure concentrations (8 hr/d, 5 d/wk, 52 wk/yr, for up to 45 years) estimated to result in an Ag skin concentration that has been associated with argyria at the lowest dose in humans (3.2 μg/g, as reported in Bachler et al. [2013]). These estimated working-lifetime exposure concentrations associated with argyria depend on the particle diameter (1–100, 15, 100 nm) and physical-chemical form (ionic, nanoparticle). The estimated average airborne exposure concentrations to reach the minimum skin tissue dose associated with argyria over a 45-year working lifetime range from 47 μg/m$^3$ for exposure to ionic silver to 78 μg/m$^3$ for exposure to 15-nm-diameter Ag nanoparticles or 253 μg/m$^3$ for exposure to 100-nm-diameter Ag nanoparticles. These estimated concentrations

**Table A-5. Silver tissue doses in smelter workers who had exposures to silver and in workers without silver exposures [Brune 1980].***

| Organ | Ag-exposed workers: Organ dose (μg Ag/g tissue) | Unexposed workers: Organ dose (μg Ag/g tissue) |
|---|---|---|
| Lung | 0.28 | 0.06 |
| Liver | 0.33 | 0.032 |
| Kidney | 0.18 | 0.045 |
| Skin | NR | NR |

*Values are upper end of reported range; lower values for all data entries were <0.005 μg Ag/g wet tissue weight [Brune 1980].
NR: not reported.

**Table A-6. Estimated silver tissue burdens after dietary intake of 80 µg/day in adult male (BW: 70 kg) for up to 45 years, by silver particle size and physical form —based on Bachler et al. [2013] human model.**

| Duration, years | Lung, µg Ag/g tissue | | Liver, µg Ag/g tissue | | Kidney, µg Ag/g tissue | | Skin, µg Ag/g tissue | |
|---|---|---|---|---|---|---|---|---|
| | Sol/Activ | Total | Sol/Activ | Total | Sol/Activ | Total | Sol/Activ | Total |
| **Nanoparticles (average diameter 15 nm)** | | | | | | | | |
| 15 | 0.000 | 0.000 | 0.001 | 0.008* | 0.002 | 0.020 | 0.000 | 0.008 |
| 30 | 0.000 | 0.001 | 0.001 | 0.015* | 0.002 | 0.038 | 0.000 | 0.016 |
| 45 | 0.000 | 0.001 | 0.001 | 0.023* | 0.002 | 0.056[a] | 0.000 | 0.024 |
| **Ionic silver** | | | | | | | | |
| 15 | 0.002 | 0.014 | 0.010[d] | 0.048*† | 0.003 | 0.027 | 0.000 | 0.036 |
| 30 | 0.002 | 0.026 | 0.010[d] | 0.086*† | 0.003 | 0.050[a] | 0.000 | 0.071 |
| 45 | 0.002 | 0.038 | 0.010[d] | 0.124*† | 0.003 | 0.074[a] | 0.000 | 0.107 |

Note. Intestinal absorption of silver is estimated to be 4% for silver nanoparticles, assuming that nanosilver is formed after the oral intake of soluble silver salts [Bachler et al. 2013]; this may be an upper estimate, given that the rat intestinal absorption is closer to 1%. Ionic silver absorption is also estimated to be 4%. For either silver nanoparticles or ions, model predictions include the following: intake, 1,314 mg; uptake, 52.6 mg (at 4% absorption). Predicted retained dose was 3.27 mg for ionic silver and 10.2 mg for silver nanoparticles over 45 years.

*Higher than the rat liver tissue levels (0.006 or 0.012 µg/g) associated with lower 95% confidence interval estimate of the benchmark dose ($BMDL_{10}$) associated with 10% excess of bile duct hyperplasia, minimal severity (Table A-1). Also exceeds the human reference level of silver in liver (~0.017 µg/g), based on a study in deceased persons in the United States [ICRP 1960] (Bachler et al. [2013], Figure 6).

†Higher than the Ag tissue burdens in unexposed workers (liver: 0.032 µg Ag/g tissue; kidney: 0.045 µg Ag/g tissue) [Brune 1980] (Table A-5).

**Table A-7. Estimated working lifetime (45-year) exposure concentrations of silver nanoparticles associated with argyria (retained skin dose of 3.2 µg Ag/g skin, minimum dose) [Bachler et al. 2013, citing Triebig et al. 1982].**

| Physical-chemical form | Particle diameter, nm | Airborne concentration (8-hour TWA), µg/m³ |
|---|---|---|
| Ionic | NA | 46.8 |
| Nanoparticle | 15 | 77.6 |
| Nanoparticle | 100 | 253 |
| Nanoparticle | 1–100 | 204 |

Assumptions: adult male (8 hr/d, 5 d/wk), 1.2 m³/hr breathing rate, nose breather.
NA: not applicable; TWA: time-weighted average.

are based on the skin tissue dose in a sensitive human, i.e., at the lowest administered dose reported to be associated with argyria.

All of these estimates of working lifetime exposure concentrations associated with argyria exceed the current NIOSH REL and OSHA PEL of 10 μg/m$^3$ (for any particle size, soluble or insoluble), by factors of approximately 5 to 25. These PBPK model-based estimates suggest that the current NIOSH REL and OSHA PEL of 10 μg/m$^3$ (8-hour TWA concentration, up to 45-year working lifetime) would be protective against the development of argyria in workers exposed to airborne AgNPs or ions. These estimates are consistent with the estimates of silver body burdens not expected to result in argyria that were used as the basis for the OSHA PEL and NIOSH REL (see Section 1.4).

## A.4.6 Estimated Silver Tissue Burdens in Workers with Inhalation Exposure to 10 μg/m$^3$ of AgNP

The estimated tissue doses of silver in workers with airborne exposures at the current NIOSH REL for silver (i.e., 10 μg/m$^3$, as an 8-hour TWA concentration; total airborne particle size sampling; soluble or insoluble particles) are shown in Table A-8. The soluble/active Ag tissue dose appears to reach an approximate steady-state tissue concentration in the lung, liver, and other tissues (due to first-order rate of transformation of active/soluble silver to insoluble silver in the PBPK model). The total silver tissue doses appear to continue increasing up to the 45-year working lifetime (because of the slow pulmonary clearance of insoluble particles). These Ag tissue doses (ng/g) in workers (up to a 45-year working lifetime) are compared to the rat Ag target tissue dose estimates (Ag ng/g) (NOAEL or BMDL10) associated with no or low adverse (early stage) lung or liver effects in the rat subchronic inhalation studies. No UFs were applied to the rat effect level estimates in these comparisons.

### *A.4.6.1 Lungs*

The PBPK model–based estimates of the human lung tissue dose after 45 years of exposure to silver at the NIOSH REL of 10 μg/m$^3$ (8-hour TWA, total silver) depended on particle size and form (i.e., 222, 690, or 1,640 ng/g for 100-nm, 15-nm, or ionic silver, respectively) (Table A-8). The female rat Ag lung-tissue doses at the NOAEL (no pulmonary inflammation) were 672 ng/g [Song et al. 2013] and 4,242 ng/g [Sung et al. 2009], which are lower than the male rat Ag lung-tissue dose of 5,450 ng/g at the NOAEL (Table A-1). Thus, the estimated soluble/active Ag tissue dose from a working lifetime exposure to 15-nm AgNP (690 ng/g) or ionic silver (1,640 ng/g) at 10 μg/m$^3$ (8-hour TWA) was estimated to exceed the rat NOAEL for pulmonary inflammation from one of the subchronic inhalation studies (672 ng/g) [Song et al. 2013] but did not exceed the rat NOAEL lung Ag tissue dose (4,241 ng/g) from the other rat study [Sung et al. 2009] (Table A-1).

Many of the lung tissue estimates of Ag (Table A-8) exceeded the maximum values reported in smelter workers (0.28 μg Ag/g lung tissue) (Table A-5) by more than two orders of magnitude. The airborne silver exposures of smelter workers are unknown [Brune 1980]. From information reported in DiVincenzo et al. [1985], the estimated exposure in a group of silver workers was 39.4 μg/m$^3$ for 20 years (Section A.4.4). Medical results were not reported by DiVincenzo et al. [1985].

### *A.4.6.2 Liver*

The PBPK model–based estimates of the human liver tissue dose after 45 years of exposure to silver at the NIOSH REL of 10 μg/m$^3$ (8-hour TWA, total silver) also depended on particle size and form (i.e., 3, 10, or 40 ng/g for 100-nm, 15-nm, or ionic silver, respectively) (Table A-8). The rat liver-tissue doses of silver at the NOAEL (no bile duct hyperplasia) were 12 ng/g in females and 14 ng/g in males, as reported by Sung et al. [2009] (Table A-1). The rat $BMDL_{10}$ estimates for bile duct hyperplasia were similar (6.3 and 12 ng/g) (Table A-1). Thus, the estimated soluble/active Ag tissue dose from a working lifetime exposure to 100-nm AgNP (3 ng/g) did not exceed the NOAEL or $BMDL_{10}$ tissue dose estimates (6–14 ng/g), whereas those for the 15-nm AgNP (10 ng/g) or ionic silver (40 ng/g) were similar to or higher than those rat effect level estimates.

**Table A-8. Estimated silver tissue burdens for up to a 45-year working lifetime inhalation exposure to 10 µg/m³ (current NIOSH REL for silver particles, soluble and insoluble), by particle size and physical form of Ag (assuming adult male, air intake 1.2 m³/hr, 8 hr/d, 5 d/wk)—based on human model of Bachler et al. [2013].**

| Duration, years | Lung, µg Ag/g tissue | | Liver, µg Ag/g tissue | | Kidney, µg Ag/g tissue | | Skin,* µg Ag/g tissue | |
|---|---|---|---|---|---|---|---|---|
| | Sol/Activ | Total | Sol/Activ | Total | Sol/Activ | Total | Sol/Activ | Total |
| **Particle average diameter: 15 nm** | | | | | | | | |
| 15 | 0.67†‡ | 25†‡§ | 0.01ᶜ | 0.090‖¶ | 0.024 | 0.22† | 0.0008 | 0.088 |
| 30 | 0.68†‡ | 31†‡§ | 0.01ᶜ | 0.17‖ | 0.025 | 0.42† | 0.0008 | 0.18 |
| 45 | 0.69†‡ | 36†‡§ | 0.01ᶜ | 0.25‖¶ | 0.026 | 0.62† | 0.0008 | 0.26 |
| **Particle average diameter: 100 nm** | | | | | | | | |
| 15 | 0.21‡ | 7.8†‡§ | 0.003 | 0.028‖¶ | 0.007 | 0.068 | 0.002 | 0.027 |
| 30 | 0.21‡ | 9.8†‡§ | 0.003 | 0.052‖¶ | 0.008 | 0.13 | 0.002 | 0.054 |
| 45 | 0.22‡ | 11†‡§ | 0.003 | 0.077‖¶ | 0.008 | 0.19† | 0.002 | 0.810 |
| **Ionic silver** | | | | | | | | |
| 15 | 1.59†‡ | 58.8†‡§ | 0.04‖¶ | 0.19‖¶ | 0.016 | 0.11 | 0.00 | 0.14 |
| 30 | 1.61†‡ | 74.4†‡§ | 0.04‖¶ | 0.35†‖¶ | 0.016 | 0.22† | 0.00 | 0.29 |
| 45 | 1.64†‡ | 84.8†‡§ | 0.04‖¶ | 0.50†‖¶ | 0.016 | 0.32† | 0.00 | 0.44 |

*The estimated skin tissue doses are all less than 3.2 µg/g, which is the minimum estimated Ag dose in skin associated with argyria, as reported in Bachler et al. [2013].

†Exceeds tissue levels of Ag reported in smelter workers (Table A-5) by Brune [1980], for whom airborne exposure concentrations of Ag were not reported.

‡Exceeds the lung tissue level of 0.081 µg Ag/g (male rats) associated with the estimated NOAEL for lung effects, following subchronic inhalation of Ag nanoparticles [Song et al. 2013] (Table A-1).

§Exceeds the lung tissue level of Ag of 4.2 µg Ag/g lung tissue (female rats) associated with the NOAEL (no observed adverse effect level), following subchronic inhalation of Ag nanoparticles [Sung et al. 20009] (Table A-1).

‖Similar to or exceeds the liver tissue levels (0.006 µg/g females; 0.012 µg/g males) associated with lower 95% confidence interval estimate of the benchmark dose ($BMDL_{10}$) associated with 10% of bile duct hyperplasia, minimal severity, in rats [Sung et al. 2009] (Table A-1) .

¶Exceeds the liver tissue level of silver in the general population (0.017 µg/g) [ICRP 1960] and/or that reported in unexposed workers (0.032 µg/g) [Brune 1980].

Note: An in vitro Ag dose of 1 µg/g was associated with adverse effects, as discussed in Bachler et al. [2013].

These results suggest that the estimated risk for developing bile duct hyperplasia (minimal or higher severity) depends on whether the relevant dose metric is the total silver or the soluble/active silver, as well as on the particle size and type. The total tissue dose of silver in workers would include both the background exposure (e.g., from diet) and the workplace exposure (e.g., from inhalation). Average human background level of silver in liver tissue (e.g., from dietary sources) has been reported

at 0.017 μg/g [ICRP 1960]. This measured background level of silver in liver tissue is similar to the PBPK model–predicted liver tissue dose of silver from the diet after a 45-year working lifetime (0.023 μg/g total silver) (Table A-6). In unexposed workers, the upper range of the silver concentration in liver tissue was 0.032 μg/g; in smelter workers, it was 0.33 μg/g [Brune 1980] (Table A-5), although the workplace exposure was not reported.

These estimated human liver tissue concentrations of silver are higher than the rat liver tissue silver concentrations at the estimated NOAEL and $BMDL_{10}$ (0.006–0.014 μg/g). Thus, it is difficult to interpret the significance of the rat study findings to humans, given that the rat effect levels are similar to the background level in humans (and presumably not associated with adverse effects in the general population). Possible explanations may include the following: (1) the silver nanoparticles in the rat study may be more toxic than the silver to which humans were exposed historically; (2) the rat may be more sensitive to silver at tissue doses equivalent to the human background level; (3) the silver liver tissue doses may be underestimated (e.g., if silver were lost in the analysis); and/or (4) the minimal severity liver effects near the rat effect levels may be subclinical in humans and therefore not observed. No information is available to assess these possible explanations, and thus, these quantitative estimates from the rat data are uncertain.

### A.4.7 Estimated 45-year Working Lifetime Airborne Exposure Concentrations Equivalent to Rat Effect Levels

Estimated human-equivalent 45-year working lifetime exposures of AgNP (8-hour TWA) equivalent to the rat effect levels ($BMDL_{10}$ or NOAEL) are shown in Table A-9, by particle size and type. Assuming total AgNP (both soluble and insoluble) is the relevant tissue dose metric, the 45-year working lifetime exposure concentration estimates that result in human lung or liver tissue doses equivalent to the rat target tissue doses (NOAEL or $BMDL_{10}$ estimates in Table A-1) are all lower than 10 μg/m$^3$. The airborne concentration estimates for the 15-nm Ag are lower than those for the 100-nm Ag (Table A-9).

Assuming that soluble/active AgNP is the relevant tissue dose metric, some of these working lifetime 8-hour TWA concentration estimates are less than the existing NIOSH REL of 10 μg/m$^3$ (i.e., those at the $BMDL_{10}$, which are the most sensitive target tissue dose estimates). Other estimates for the soluble/active Ag tissue burden are greater than 10 μg/m$^3$ (Table A-9). The most sensitive (lowest) dose metric is total silver; the 45-year working lifetime estimated 8-hour TWA exposure concentration at the $BMDL_{10}$ or NOAEL was 0.19–1.5 μg/m$^3$, which suggests a REL.

## A.5 Evaluation of PBPK Modeling Results

### A.5.1 Utility of PBPK Modeling Estimates

PBPK modeling permits evaluation of the predicted lung and liver doses in workers versus those measured in rat subchronic inhalation studies of silver nanoparticles (15- to 19-nm diameter) and associated with no or a low level of early-stage adverse effects in the lungs or liver. This PBPK model also permits evaluation of the skin tissue burden associated with argyria in humans and estimates of silver in workers based on occupational (inhalation) or dietary (oral) exposure.

The PBPK model of Bachler et al. [2013] was calibrated from AgNP kinetics data in rats and extrapolated to humans on the basis of interspecies adjustment of physiological and morphological parameters that influence the deposition and disposition of silver particles following inhalation. The human model of Bachler et al. [2013] was shown to provide good prediction of the limited biomonitoring data on workers exposed to silver (Section A.1).

Bachler et al. [2013] report certain limitations in their PBPK model that could bias an evaluation of the particle dissolution. For instance, model calibration

**Table A-9. Working lifetime (45-year) exposure concentration of silver (Ag) nanoparticles (soluble/active or total; 15- or 100-nm diameter) associated with Ag target tissue doses (NOAEL or $BMDL_{10}$) in the rat subchronic inhalation studies [Sung et al. 2009; Song et al. 2013] (adult male; reference worker air intake, 1.2 $m^3$/hr).***

| Rat Study, Sex | Type of effect level | Silver tissue dose, ng/g | Particle diameter in nm | Airborne exposure concentration (8-hour TWA) (µg/$m^3$) | |
|---|---|---|---|---|---|
| | | | | Assuming tissue dose metric of soluble/active Ag | Assuming tissue dose metric of total Ag |
| **Lung—Chronic alveolar inflammation, minimal†** | | | | | |
| Song [2013], Female | NOAEL (117 µg/$m^3$) | 672 | 15 | 9.7 | 0.19 |
| | | | 100 | 31 | 0.60 |
| Sung [2009], Female | NOAEL (133 µg/$m^3$) | 4,241 | 15 | 61 | 1.2 |
| | | | 100 | 195 | 3.8 |
| **Liver—Bile duct hyperplasia, minimal** | | | | | |
| Sung [2009], Female | $BMDL_{10}$ | 6.30 | 15 | 6.2 | 0.26 |
| | | | 100 | 20 | 0.83 |
| Sung [2009], Male | $BMDL_{10}$ | 11.6 | 15 | 11.4 | 0.47 |
| | | | 100 | 37 | 1.5 |

BMDL: Benchmark dose, 95% lower confidence limit estimate, associated with 10% added response; NOAEL: No observed adverse effect level; TWA: time-weighted average.

*Based on Ag absorption rate from lungs to systemic circulation in humans, as determined from an in vivo animal study [Takenaka et al. 2001], which is 7-fold higher than the Ag absorption rate from Ji et al. [2007b] that was used in simulations of studies by Sung et al. [2009] and Song et al. [2013]. Further information on the absorption rates are provided in the supplementary material of Bachler et al. [2013].

†Dose-response data from male rats in Song et al. [2013] were minimally acceptable for BMD estimation (Tables B-2 and B-8) but are not included here because of higher uncertainty. Subsequent analyses (not included in PBPK modeling) utilized pooled data from male and female rats in Sung et al. [2009] and Song et al. [2013] (Table B-11).

with the experimental data could have incorporated some dissolution that was not accounted for in the model (i.e., that may have occurred during the 5 days of intravenous administration of silver or during the 16 days post-exposure until Lankveld et al. [2013] investigated the silver tissue burdens and kinetics). In addition, because the ionic PBPK model of Bachler et al. [2013] was also calibrated with data after the intravenous injection (in this case of an ionic silver solution, with rats examined 7 days post-exposure [Klaassen 1979]), the model accounts only for silver ions that are able to freely distribute within the body. That means those that dissolve and transform to silver sulfide within cells would be outside of the application domain of the model, according to Bachler et al. [2013].

The pulmonary or intestinal absorption fraction of Ag ions or nanoparticles is an area of uncertainty in the human PBPK model [Bachler et al. 2013]. Although no human data are known to be available for these parameters, the sensitivity of the model estimates to the assumed parameter values

could be investigated. Another area of uncertainty is whether the smaller AgNPs (e.g., <15 nm) may translocate more efficiently from the lungs to the blood. If this occurs, as was shown recently for gold nanoparticles [Kreyling et al. 2014], then the silver burdens in the lungs and other organs may depend to a greater extent on the particle size. A key data gap in the evaluation of this PBPK model is the lack of chronic inhalation exposure data on AgNPs in rats on which to further test it.

## A.5.2 Comparison of Human Data to Rat-Based Estimates

A useful evaluation of the rat-based OEL estimates for silver nanoparticles is to compare those estimates to the occupational exposure and health effects data on workers exposed to silver in various processes (Section 2). Reports of studies in humans typically did not give the airborne particle sizes (Section 2). However, exposure to AgNPs would be anticipated in some types of production (e.g., in DiVincenzo et al. [1985]). Miller et al. [2010] did measure and report airborne exposures to AgNPs in workers' breathing zones, including airborne concentrations that exceed the NIOSH REL.

No researchers have reported adverse health effects other than argyria in workers with long-term inhalation exposures to silver (e.g., ~20 years at ~39 μg/m$^3$ [DiVincenzo et al. 1985], which is greater than the NIOSH REL of 10 μg/m$^3$ for up to 45 years); however, few studies have performed medical evaluations of workers exposed to silver dust and fumes (e.g., Pifer et al. [1989] and Rosenman et al. [1979, 1987], discussed in Sections 2 and 3). Researchers who have reported argyria in workers have not reported adverse lung or liver effects associated with exposure to silver (although their studies were relatively small, e.g., involving a few dozen workers). Adverse lung or liver effects are predicted from the rat studies to develop at similar or lower Ag tissue doses than those associated with argyria (Table A-7; Table A-10), and therefore adverse lung or liver effects would be expected to be observed in workers with sufficient exposures to cause argyria. This absence of reported lung or liver effects in workers (including those with argyria) suggests that the lung and liver effects in rats could be early-stage, pre-clinical effects that are not associated with adverse function. On the other hand, the absence of reported adverse health effects in workers could be due to insufficient study, especially of workers exposed to silver nanoparticles.

An evaluation of the available evidence from the human and rat studies, and from PBPK modeling, is discussed in detail below. Comparisons are made between the tissue dose levels of silver reported in the rat studies and as estimated in humans exposed for up to a 45-year working lifetime, including at the current NIOSH REL for silver of 10 μg/m$^3$. These findings are discussed for the measured and/or estimated silver tissue doses and responses in the skin, lungs, and liver of rats and humans.

## A.5.3 Argyria Risk

Comparison of the PBPK-model [Bachler et al. 2013] estimates of skin tissue burdens to those associated with argyria in humans suggests that workers exposed for up to a 45-year working lifetime at the current NIOSH REL for silver would not likely develop argyria (Table A-7). That is, the estimated working lifetime airborne exposure concentrations (8-hour TWA) resulting in the lowest skin tissue dose reported to be associated with argyria in humans (3.2 μg/g [Triebig et al. 1982]) were higher than the REL of 10 μg/m$^3$ for all particle sizes and types evaluated. These exposure estimates were 47, 78, and 253 μg/m$^3$, respectively, for ionic silver, AgNPs of 15-nm diameter, and AgNPs of 100-nm diameter.

These PBPK model–based estimates suggest an approximately 5- to 25-fold margin of exposure (MOE) between the current REL and the lowest reported human skin tissue dose of silver associated with argyria. An MOE is the ratio between an effect level and an exposure [Kim et al. 2016]. As discussed previously, no other adverse effects associated with silver exposure have been reported to occur in humans with argyria.

**Table A-10. Human-equivalent concentrations for silver nanomaterials from physiologically based pharmacokinetic (PBPK) modeling.[*]**

| Rat effect endpoint and sex [Study reference] | Rat PoD as silver tissue dose, ng/g[†] | Particle size: diameter, nm | Human-equivalent concentration, μg/m³[‡] |
|---|---|---|---|
| **Total Silver Dose Metric** | | | |
| Liver bile duct hyperplasia, $BMCL_{10}$, female [Sung et al. 2009] | 6.3 | 15 | 0.26 |
| | | 100 | 0.83 |
| Pulmonary inflammation, NOAEL, female [Song et al. 2013] | 672 | 15 | 0.19 |
| | | 100 | 0.60 |
| **Soluble/Active Silver Dose Metric** | | | |
| Liver bile duct hyperplasia, $BMCL_{10}$, female [Sung et al. 2009] | 6.3 | 15 | 6.2 |
| | | 100 | 20 |
| Pulmonary inflammation, NOAEL, female [Song et al. 2013] | 672 | 15 | 9.7 |
| | | 100 | 31 |

[*]This table is a subset of results shown in Table A-9, i.e., the results for the lowest silver tissue doses by endpoint and particle size.
[†]From Table A-1. Rat PoD value for liver bile duct hyperplasia was selected as the lowest PoD among the estimates for that endpoint. For pulmonary inflammation, the lowest PoD estimate ($BMDL_{10}$) in male rats from Song et al. [2013] was not selected because of the limited data and modeling options to estimate that PoD. The female PoD (NOAEL) from Song et al. [2013] was selected as the next higher estimate, which was ~6–8× lower than the NOAELs for the same response at similar exposure concentrations (117 or 133 μg/m³) in male or female rats in Sung et al. [2009]. Alternatively, the male rat NOAEL of 81 ng/g from Song et al. [2013] (which was ~70× lower than the NOAEL for male rats in Sung et al. [2009]) could be used as the pulmonary inflammation $PoD_{animal}$.
[‡]Estimated from the PBPK model of Bachler et al. [2013] for a 45-year working lifetime.

## A.5.4 Lung Inflammation Risk

The rat effect levels (NOAEL or $BMDL_{10}$) based on the lung tissue dose of silver (Table A-1) can be compared to the predicted human tissue doses of silver, given workplace exposure at the NIOSH REL of 10 μg/m³ (Table A-8). These predictions depend on particle size and solubility. According to the model of Bachler et al. [2013], the human total silver doses in lung tissue after a 45-year working lifetime at the REL are estimated to be 11, 36, or 85 μg/g for 100-nm-diameter AgNPs, 15-nm-diameter AgNPs, or ionic Ag, respectively. The estimated human soluble/active silver doses in lung tissue are lower, at 0.22, 0.69, or 1.6 μg/g for the same particle sizes and forms. These human silver lung tissue dose estimates exceed the rat $BMDL_{10}$ estimate of 0.033 μg/g and the rat NOAEL of 0.081 μg/g in male rats in Song et al. [2013] (Table A-1). The estimated human soluble/active silver doses in lung tissue do not exceed the NOAELs of 0.672 or 4.2 μg/g silver in lung tissue in female rats in Song et al. [2013] or Sung et al. [2009], respectively.

Available data on the human background lung tissue concentration of silver in unexposed workers were up to 0.06 μg Ag/g lung tissue (Table A-5) [Brune 1980]. In smelter workers, the lung tissue concentration was up to 0.28 μg/g. No data were available on airborne exposures to silver, nor on any adverse lung effects associated with that tissue concentration of silver.

The findings from the PBPK modeling indicate that the risk estimates of developing adverse lung effects after a working lifetime exposure to silver

nanomaterials depend on the assumed dose metric (total or soluble/active) and the rat effect level estimate. The rat lung tissue silver dose estimates ($BMDL_{10}$ or NOAEL) for pulmonary inflammation vary widely, depending on the study and sex (Table A-1). These large differences in the quantitative estimates of the rat lung tissue dose of silver associated with adverse pulmonary effects contribute to the uncertainty in the estimated human equivalent lung tissue dose after a working lifetime exposure at the current silver REL.

The wide difference in the effect level estimates for pulmonary inflammation in the same rat sex across the two studies raises uncertainty about the doses associated with that response (e.g., female rat NOAEL of 0.67 or 4.2 ng/g, associated with 117 or 133 mg/m$^3$ exposure concentration, in Song et al. [2013] and Sung et al. [2009]) (Table A-1). Thus, for similar airborne exposure concentrations, the associated silver lung tissue doses were nearly an order of magnitude different. This difference in tissue dose could be due to differences in the particles between the two studies (although these were generated by the same method and had similar characteristics) or to difficulties in obtaining consistent analytical results for quantifying the tissue burdens. The challenge of adequately recovering the silver administered to rodent lungs was reported in the NIEHS NanoGo consortium (http://ehp.niehs.nih.gov/1306866/) at SOT 2015 (http://www.toxicology.org/AI/MEET/am2015/ss.asp). High variability in the recovery amounts were also reported in the NIEHS studies, and it was difficult to achieve mass balance in many cases. The Sung et al. [2009] and Song et al. [2013] studies did not report mass balance (nor did the study design permit that estimate, because the initial deposited dose was not reported).

## A.5.5 Bile Dust Hyperplasia Risk

The rat liver effect levels (NOAEL or $BMDL_{10}$) (Table A-1) can be compared also to the predicted dose of silver in human liver tissue at the NIOSH REL of 10 μg/m$^3$ (Table A-8). These predictions depend on particle size and solubility, as seen also for the lung tissue dose estimates. From the model of Bachler et al. [2013], the human total silver dose in liver tissue after a 45-year working lifetime at the REL is estimated to be 0.077, 0.25, or 0.50 μg/g for 100-nm-diameter AgNPs, 15-nm-diameter AgNPs, or ionic Ag, respectively. The estimated soluble/active silver tissue doses are lower, at 0.003, 0.01, or 0.04 μg/g for the same particle size and form. The total silver doses exceed the rat effect levels ($BMDL_{10}$ estimates of 0.006 μg/g in females and 0.012 μg/g in males). The rat NOAELs for bile duct hyperplasia, 0.012 μg/g in females and 0.014 μg/g in males, are similar to the $BMDL_{10}$ estimates (Table A-1). The human estimated liver tissue doses of soluble/active silver are similar to the rat effect levels, with some estimates in humans above or below those in rats. These results suggest that the estimated risk for developing bile duct hyperplasia (minimal or higher severity) depends on whether the relevant dose metric is the total silver or the soluble/active silver, as well as the particle size and type.

Available data on human background tissue concentration of silver in the liver (from dietary sources) indicate background levels of approximately 0.017 μg/g [ICRP 1960] or 0.032 μg/g [Brune 1980]. These human liver tissue concentrations of silver are similar to or higher than the rat liver tissue silver concentrations at the NOAEL and $BMDL_{10}$ (0.0063–0.014 μg/g) (Table A-1). This finding suggests that on a mass basis, humans are exposed to background levels of silver that exceed the no or low effect level in rats for liver bile duct hyperplasia. It also suggests uncertainty in the quantification of the silver tissue doses. The estimated equivalent 45-year working lifetime exposures to the rat $BMDL_{10}$ estimate range from 0.26 to 1.5 μg/m$^3$ based on a total silver dose metric and range from 6 to 37 μg/m$^3$ based on soluble/active silver (8-hour TWA airborne concentrations) (Table A-9). The range reflects differences in estimates by particle size and by sex.

These findings indicate that the risk estimates at the NIOSH REL depend on the assumed dose metric (total or soluble/active) for silver. However, some

evidence suggests that the rat may be more sensitive or the effect level may be underestimated. First, the human predicted liver doses after dietary exposure to silver (0.023 μg/g total silver after 45 years) (Table A-9) exceed the rat effect levels. Second, the background concentrations of silver in liver tissue (from dietary sources) reported in the general U.S. population (~0.017 μg/g) also exceed the rat effect levels of 0.006 or 0.012 μg Ag/g tissue. Thus, the quantitative estimates from the rat data are uncertain, possibly because of (1) erroneous measurement of silver in rat tissue, (2) higher sensitivity of the rat to silver tissue levels, and/or (3) the subclinical nature of the effects.

### A.5.6 Silver Nanoparticle Form

The form of the silver in the human or rat tissues is not known. It may be reasonable to assume that the proportion of active/soluble silver in the rat subchronic inhalation studies would be greater than that in humans over a lifetime. This assumption is based on the hypothesis that opsonization (protein binding) of silver occurs essentially immediately in mammals, forming a "protein corona" that stabilizes the particles [Bachler et al. 2013; Landsiedel et al. 2011]. Thus, over time, the proportion of total silver that is in the soluble/active form would be smaller. If the soluble/active form of silver is more relevant to the toxicity, then it may be more relevant to use an equivalent active/soluble silver dose in the rat and human tissues, based on the PBPK model estimates. On the other hand, if the insoluble nanoparticle dose is related to the toxicity, then the total silver tissue dose should be used to estimate the airborne concentration. The role of the physical-chemical form of the silver on its toxicity remains an area of uncertainty, although the general findings from the literature suggest that the smaller particle size and greater solubility are more toxic (Section 5.6). In an updated version of the PBPK model of Bachler et al. [2013] in rats compared to new experimental data, silver ions were observed to form secondary particles [Juling et al. 2016]. This observation illustrates the difficulties in distinguishing the effects of the silver nanoparticles or ions.

This page intentionally left blank.

# APPENDIX B

## Statistical Analyses Supplement

## B.1 Benchmark Dose Modeling of Rat Subchronic Inhalation Studies

A standard benchmark dose (BMD) modeling method [U.S. EPA 2012b] was used to model the dose-response relationships in the rat subchronic inhalation studies of silver nanoparticles [Sung et al. 2009; Song et al. 2013]. The in vivo toxicological studies on silver nanoparticles in experimental animals are summarized in Appendix E, Table E-5. More detailed accounts of the studies are also provided in the text of Appendix E. The studies considered to be the most applicable to the development of an OEL were subchronic inhalation studies of Sprague-Dawley rats reported by Sung et al. [2009] (90 days, or about 13 weeks) and Song et al. [2013] (12 weeks). These studies were evaluated for dose-response data that were sufficient for BMD modeling. Criteria include a monotonic dose-response relationship, dichotomous responses, and at least one dose group with response proportion between 0 and 1.

A BMD is a maximum likelihood estimate of the dose associated with a low response (e.g., 10%); a BMDL is the 95% lower confidence limit estimate of the BMD [Crump 1984]. BMDL estimates are often treated as NOAELs for use as PoDs to estimate exposure limits in humans [U.S. EPA 2012b].

The U.S. Environmental Protection Agency (EPA) benchmark dose software (BDMS) version 2.5 [U.S. EPA 2014] was used to model the data in Sung et al. [2009] and Song et al. [2013]. A pooled analysis of pulmonary inflammation data from both Sung et al. [2009] and Song et al. [2013] was performed with U.S. EPA BMDS version 2.6 [U.S. EPA 2015].

Both point-of-impact (lung) and systemic (liver) target organ endpoints were evaluated. These response endpoints include (1) pulmonary inflammation (i.e., chronic alveolar inflammation); (2) bile duct hyperplasia; and (3) liver abnormality. The dose (as airborne exposure concentration) and response data used in these BMD models are shown in Table B-1 [Sung et al. 2009] and Table B-2 [Song et al. 2013]. Tables B-3 and B-4 show dose (as mean tissue concentration) for the same responses and studies as Tables B-1 and B-2, respectively. When chronic alveolar inflammation was evaluated separately by sex, only the male rat data were adequate for dose-response modeling. However, the pooled data from both studies and sexes were sufficient for modeling (Table B-11).

All of the available BMDS dichotomous response models were evaluated, which included gamma, logistic, log-logistic, probit, log-probit, multistage (polynomial degree 2 and/or 3), Weibull, and quantal linear. Model averaging (MADR) per Wheeler

**Table B-1. Response proportions in Sprague-Dawley rats following subchronic inhalation exposure to silver nanoparticles [Sung et al. 2009].**

| | Bile duct hyperplasia | | | |
|---|---|---|---|---|
| | Concentration, µg/m³ | | | |
| **Group** | **0** | **49** | **133** | **515** |
| Males | 0/10 | 0/10 | 1/10 | 4/9 |
| Females | 3/10 | 2/10 | 4/10 | 9/10 |
| | **Liver abnormality** | | | |
| | Concentration, µg/m³ | | | |
| **Group** | **0** | **49** | **133** | **515** |
| Males | 0/10 | 0/10 | 1/10 | 4/9 |
| Females | 3/10 | 5/10 | 5/10 | 9/10 |

**Table B-2. Response proportions in Sprague-Dawley rats following subchronic inhalation exposure to silver nanoparticles [Song et al. 2013].**

| Chronic alveolar inflammation (minimal) | | | | |
|---|---|---|---|---|
| | Concentration, μg/m³ | | | |
| **Group** | **0** | **49** | **117** | **381** |
| Males* | 0/5 | 0/5 | 3/5 | 5/5 |

*Female response proportions at same concentrations (0/4, 0/4, 0/4, 4/4) are inadequate for BMD modeling.

**Table B-3. Response proportions in Sprague-Dawley rats following subchronic inhalation exposure to silver nanoparticles [Sung et al. 2009].**

| Bile duct hyperplasia* | | | | |
|---|---|---|---|---|
| | Mean liver tissue concentration, ng/g | | | |
| **Group** | **0.90** | **4.55** | **12.07** | **71.08** |
| Females | 3/10 | 2/10 | 4/10 | 9/10 |
| | Mean liver tissue concentration, ng/g | | | |
| | **0.70** | **3.52** | **13.75** | **132.97** |
| Males | 0/10 | 0/10 | 1/10 | 4/9 |

*Severity level in female rats: minimum (3/10, 2/10, 4/10, 8/10) and moderate (0/10, 0/10, 0/10, 1/10), respectively, in increasing dose groups; severity level in male rats: minimum in all dose groups.

**Table B-4. Response proportions in Sprague-Dawley rats following subchronic inhalation exposure to silver nanoparticles [Song et al. 2013].**

| Chronic alveolar inflammation (minimal) | | | | |
|---|---|---|---|---|
| | Mean lung tissue concentration, ng/g | | | |
| **Group** | **0.82** | **80.65** | **417.40** | **4715.28** |
| Males* | 0/5 | 0/5 | 3/5 | 5/5 |

*Female response proportions at same concentrations (0/4, 0/4, 0/4, 4/4) are inadequate for BMD modeling.

and Bailer [2007], using the logistic, log-probit, multistage degree 2, and Weibull models, was also performed for comparison to the BMDS modeling results. All BMDS models were used to estimate a benchmark response (BMR) of 10% the excess (added) risk of early-stage adverse lung or liver effects in rats following subchronic inhalation of AgNP. The best-fitting model(s) were selected on the basis of optimal goodness-of-fit criteria, i.e., the models with the lowest Akaike Information Criteria (AIC) among the models with goodness-of-fit *p* values within the applicable range (>0.1). Care should be taken when selecting the model with the smallest AIC, as the EPA BMDS does not include parameters that are estimated to be at a boundary value (e.g., the background parameter) in the penalization of the log likelihood, which can misrepresent the best-fitting model for the given data.

For some models, such as the multistage, EPA BMDS did not report the standard errors for the parameter estimates, which can be used as an additional check for a statistically significant trend

(i.e., the slope parameter). In those cases, the fitted model was compared to the null model by means of the likelihood ratio test for nested models.

The resulting benchmark concentration ($BMC_{10}$) and lower 95% confidence interval ($BMCL_{10}$) estimates associated with 10% response, along with the goodness-of-fit parameters for the best-fitting model(s), are shown in Tables B-5, B-7, and B-12 [Sung et al. 2009] and Tables B-6 and B-8 [Song et al. 2013]. These best-fitting models are shown in Figures B-1 through B-8.

The MADR-derived estimates of $BMCL_{10}$ and $BMDL_{10}$ for all endpoints and dose metrics are provided in Tables B-9 and B-10. The $BMCL_{10}$ estimates based on BMDS and MADR were reasonably similar, but some differences (in part due to different criteria used for the model fit estimates) are observed. For example, for the Sung et al. [2009] endpoints, BMDS estimates of $BMDL_{10}$ are smaller; and for the Song et al. [2013], the MADR estimates of $BMDL_{10}$ are smaller.

All available alveolar lung inflammation data (on male and female rats from Song et al. [2013] and Sung et al. [2009]) were combined (pooled) and modeled. The fact that a best-fitting model was able to be found for the combined data suggests that the data may be sufficiently homogenous to combine, that is, the exposure concentration adequately explains the variability in the alveolar lung inflammation response without explicitly accounting for lab and sex effects. The resulting benchmark concentration ($BMC_{10}$) and lower 95% confidence interval ($BMCL_{10}$) estimates associated with the added 10% risk of response, along with the goodness-of-fit estimates for the best-fitting model, are shown in Table B-11. The best-fitting model is shown in Figure B-9.

The liver bile duct hyperplasia and liver abnormality data [Sung et al. 2009] were analyzed separately by sex. For each histopathological endpoint, the observed responses were statistically significantly different for females and males, suggesting that the observed responses should be modeled while considering both concentration and sex; the interaction effect was not statistically significant ($p > 0.05$) for both endpoints. The resulting benchmark concentrations ($BMC_{10}$) and lower 95% confidence interval ($BMCL_{10}$) estimates associated with the added 10% risk of response, along with the goodness-of-fit estimates for the best-fitting models, are shown in Table B-12. The best-fitting models are shown in Figures B-7 and B-8.

These $BMCL_{10}$ and $BMDL_{10}$ estimates are similar to or lower than the NOAELs (or LOAEL) reported in the animal studies (Table A-1). A $BMCL_{10}$ or $BMDL_{10}$ estimate may be considered equivalent to a NOAEL estimate [U.S. EPA 2012b], and equivalent uncertainty factors can be applied as described in Appendix A. The resulting OELs would be similar to or lower than those estimated with use of the NOAELs (or LOAEL). As discussed in Appendix A, the sources of uncertainty in the estimation of the $BMCL_{10}$ or $BMDL_{10}$ estimates include the small number of rats per group (n = 5) for the pulmonary inflammation endpoint and the large variability in the silver lung tissue doses between the two subchronic studies [Sung et al. 2008; Song et al. 2013].

**Table B-5. Best-fitting benchmark concentration (BMC) models of subchronic inhalation responses to silver nanoparticles in Sprague-Dawley rats [Sung et al. 2009].**

| Model | AIC | *P* value | BMC, µg/m³ | $BMCL_{10}$, µg/m³ |
|---|---|---|---|---|
| **Male: Bile duct hyperplasia** | | | | |
| Log-probit | 21.1114 | 0.9806 | 155.8 | 92.5 |
| **Female: Bile duct hyperplasia** | | | | |
| Logistic | 46.8796 | 0.7073 | 78.2 | 50.5 |

AIC = Akaike Information Criterion; $BMCL_{10}$: Benchmark concentration, 95% lower confidence limit estimate, associated with 10% added risk.

**Table B-6. Best-fitting benchmark concentration (BMC) models of subchronic inhalation responses to silver nanoparticles in Sprague-Dawley rats [Song et al. 2013].**

| Model | AIC | *P* value | BMC, μg/m³ | $BMCL_{10}$, μg/m³ |
|---|---|---|---|---|
| **Male: Alveolar inflammation (minimal)** | | | | |
| Multistage (degree = 2)* | 10.1497 | 0.843 | 44.8 | 13.6 |

AIC = Akaike Information Criterion; $BMCL_{10}$: Benchmark concentration, 95% lower confidence limit estimate, associated with 10% added risk.
*Multistage model only fit to these data, following the methodology described in Appendix A of NIOSH [2013].

**Table B-7. Best-fitting benchmark dose (BMD) models of subchronic inhalation responses to silver nanoparticles in Sprague-Dawley rats [Sung et al. 2009].**

| Model | AIC | *P* value | BMD, ng/g | $BMDL_{10}$, ng/g |
|---|---|---|---|---|
| **Male: Bile duct hyperplasia** | | | | |
| Gamma, MS2, MS3, QL, and Weibull* | 21.4821 | 0.9281 | 22.7 | 11.6 |
| **Female: Bile duct hyperplasia** | | | | |
| Logistic | 46.7501 | 0.7624 | 10.3 | 6.3 |

AIC = Akaike Information Criterion; $BMDL_{10}$: Benchmark dose, 95% lower confidence limit estimate, associated with 10% added risk.
*Identical model fits (AIC and *p* values) and BMD and $BMDL_{10}$ estimates for these five BMDS models: gamma, multistage polynomial degree 2 or degree 3 (MS2 or MS3), quantal linear (QL), and Weibull.

**Table B-8. Best-fitting benchmark dose (BMD) models of subchronic inhalation responses to silver nanoparticles in Sprague-Dawley rats [Song et al. 2013].**

| Model | AIC | *P* value | BMD, ng/g | $BMDL_{10}$, ng/g |
|---|---|---|---|---|
| **Male: Alveolar inflammation (minimal)** | | | | |
| Multistage (degree = 2)* | 9.0622 | 0.9818 | 145.8 | 33.0 |

AIC = Akaike Information Criterion; $BMDL_{10}$: Benchmark dose, 95% lower confidence limit estimate, associated with 10% added risk.
*Multistage model fit to only these data, following the methodology described in Appendix A of NIOSH [2013].

**Table B-9. Model-average benchmark concentration estimates from subchronic inhalation studies in Sprague-Dawley rats for all endpoints modeled.**

| Rat study | Endpoint | $BMCL_{10}$ estimate in rats (μg/m³)—BCa | $BMCL_{10}$ estimate in rats (μg/m³)—Percentile |
|---|---|---|---|
| Sung et al. [2009] | Bile duct hyperplasia in males | 30.20 | 112.49 |
| | Bile duct hyperplasia in females | 32.87 | 24.52 |
| Song et al. [2013] | Chronic alveolar inflammation in males | 48.17 | 36.86 |

$BMCL_{10}$: Benchmark concentration, 95% lower confidence limit estimate, associated with 10% added risk; BCa: Bias-corrected and accelerated (bootstrapping method); Percentile: 2.5th percentile of the bootstrap distribution.

**Table B-10. Model-average benchmark dose estimates from subchronic inhalation studies in Sprague-Dawley rats for all endpoints modeled.**

| Rat study | Endpoint | $BMDL_{10}$ estimate in rats (ng/g)—BCa | $BMDL_{10}$ estimate in rats (ng/g)—Percentile |
|---|---|---|---|
| Sung et al. [2009] | Bile duct hyperplasia in males | 2.61 | 14.55 |
| | Bile duct hyperplasia in females | 2.09 | 2.03 |
| Song et al. [2013] | Chronic alveolar inflammation in males | 57.18 | 43.50 |

$BMDL_{10}$: Benchmark dose, 95% lower confidence limit estimate, associated with 10% added risk; BCa: Bias-corrected and accelerated (bootstrapping method); Percentile: 2.5th percentile of the bootstrap distribution.

**Table B-11. Pooled data and best-fitting benchmark concentration (BMC) models for the subchronic inhalation responses to silver nanoparticles in male and female Sprague-Dawley rats [Sung et al. 2009; Song et al. 2013].**

| Chronic alveolar inflammation (minimal) | | | | | | |
|---|---|---|---|---|---|---|
| | Concentration, $\mu g/m^3$ | | | | | |
| Group | 0 | 49 | 117 | 133 | 381 | 515 |
| Pooled | 5/29 | 5/29 | 3/9 | 2/20 | 9/9 | 16/19 |

| Model | AIC | *P* value | BMC, $\mu g/m^3$ | $BMCL_{10}$, $\mu g/m^3$ |
|---|---|---|---|---|
| Multistage (degree = 3) | 108.324 | 0.125 | 124.9 | 62.8 |

AIC = Akaike Information Criterion; $BMCL_{10}$: Benchmark concentration, 95% lower confidence limit estimate, associated with 10% added risk.

**Table B-12. Best-fitting benchmark concentration (BMC) models of subchronic inhalation responses to silver nanoparticles in Sprague-Dawley rats [Sung et al. 2009].**

| Model | AIC | *P* value | BMC, $\mu g/m^3$ | $BMCL_{10}$, $\mu g/m^3$ |
|---|---|---|---|---|
| Male: Liver Abnormality | | | | |
| Quantal linear | 21.9566 | 0.888 | 111.1 | 57.3 |
| Female: Liver Abnormality | | | | |
| Logistic | 50.892 | 0.7993 | 76.6 | 44.5 |

AIC = Akaike Information Criterion; $BMCL_{10}$: Benchmark concentration, 95% lower confidence limit estimate, associated with 10% added risk.

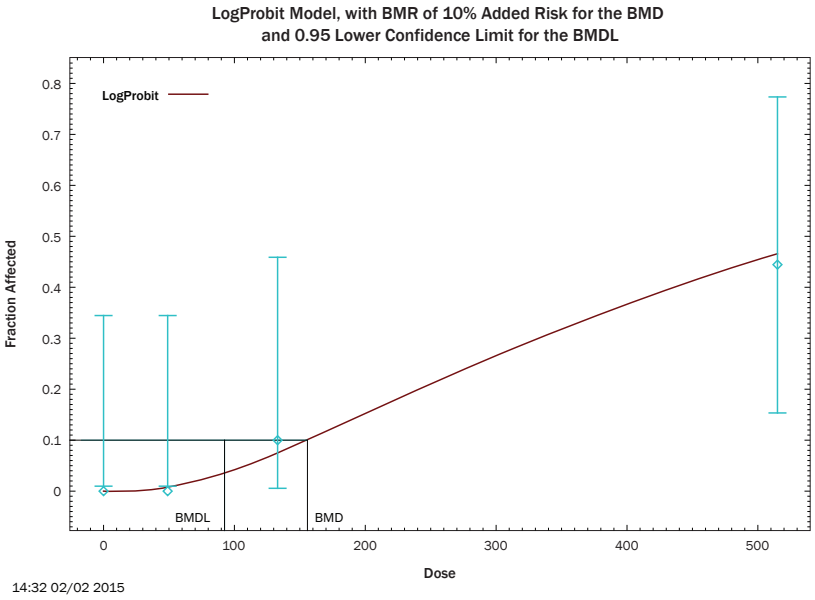


Figure B-1. Exposure-response model (log-probit) fit to the airborne exposure concentration of silver nanoparticles (µg/m³) and **liver bile duct hyperplasia proportion in male rats** [Sung et al. 2009]. (Data and model results in Tables B-1 and B-5.) Benchmark response (BMR) is defined as a 10% added risk of liver bile duct hyperplasia; BMC: Benchmark concentration estimate; $BMCL_{10}$: Benchmark concentration, 95% lower confidence limit estimate. BMC and $BMCL_{10}$ are associated with BMR, as shown with green lines to mark these point estimates on the dose-response curve.

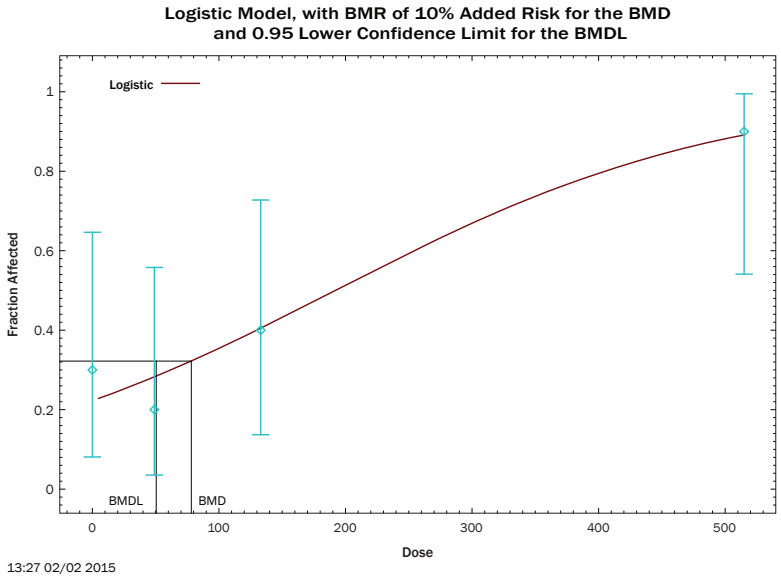


Figure B-2. Exposure-response model (logistic) fit to the airborne exposure concentration of silver nanoparticles (µg/m³) and **liver bile duct hyperplasia proportion in female rats** [Sung et al. 2009]. (Data and model results in Tables B-1 and B-5.) Benchmark response (BMR) is defined as a 10% added risk of liver bile duct hyperplasia; BMC: Benchmark concentration estimate; $BMCL_{10}$: Benchmark concentration, 95% lower confidence limit estimate. BMC and $BMCL_{10}$ are associated with BMR, as shown with green lines to mark these point estimates on the dose-response curve.

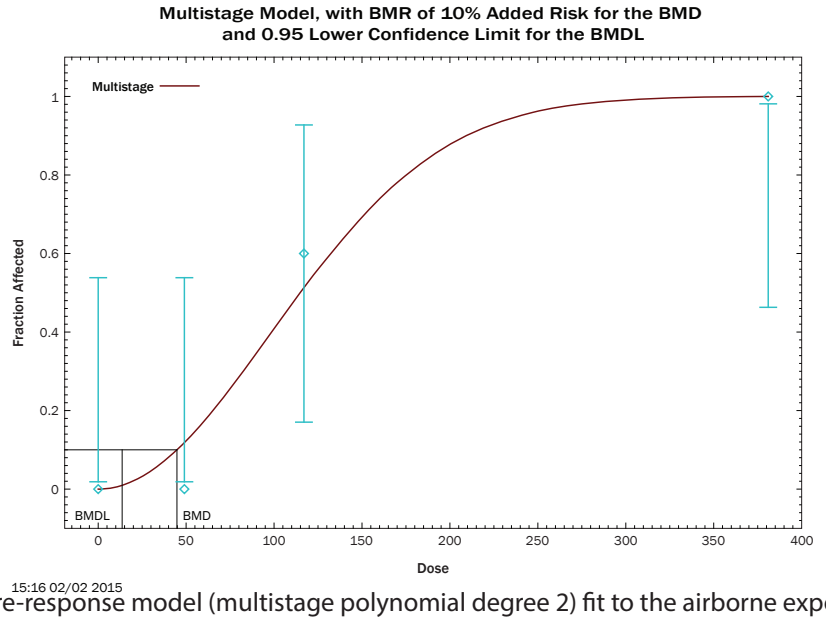


Figure B-3. Exposure-response model (multistage polynomial degree 2) fit to the airborne exposure concentration of silver nanoparticles (μg/m$^3$) and **chronic alveolar inflammation proportion in male rats** [Song et al. 2013]. (Data and model results in Tables B-2 and B-6.) Benchmark response (BMR) is defined as a 10% added risk of chronic alveolar inflammation; BMC: Benchmark concentration estimate; $BMCL_{10}$: Benchmark concentration, 95% lower confidence limit estimate. BMC and $BMCL_{10}$ are associated with BMR, as shown with green lines to mark these point estimates on the dose-response curve.

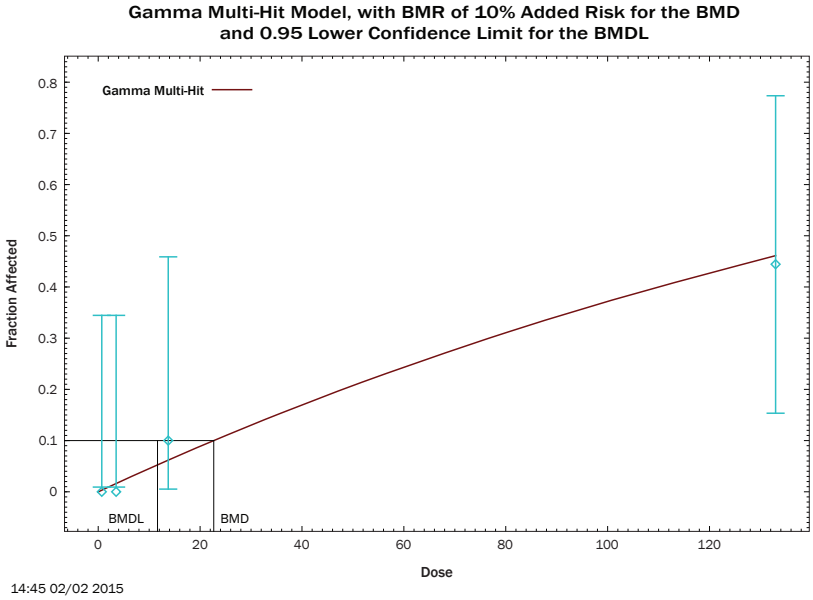


Figure B-4. Dose-response model (gamma) fit to the silver mass dose in liver tissue (ng/g) and **liver bile duct hyperplasia proportion in male rats** following subchronic inhalation exposure to silver nanoparticles [Sung et al. 2009]. (Data and model results in Tables B-3 and B-7; see Table B-7 for other models with equivalent fit as gamma model to these data.) Benchmark response (BMR) is defined as a 10% added risk of liver bile duct hyperplasia; BMD: Benchmark dose estimate; $BMDL_{10}$: Benchmark dose, 95% lower confidence limit estimate. BMD and $BMDL_{10}$ are associated with BMR, as shown with green lines to mark these point estimates on the dose-response curve.

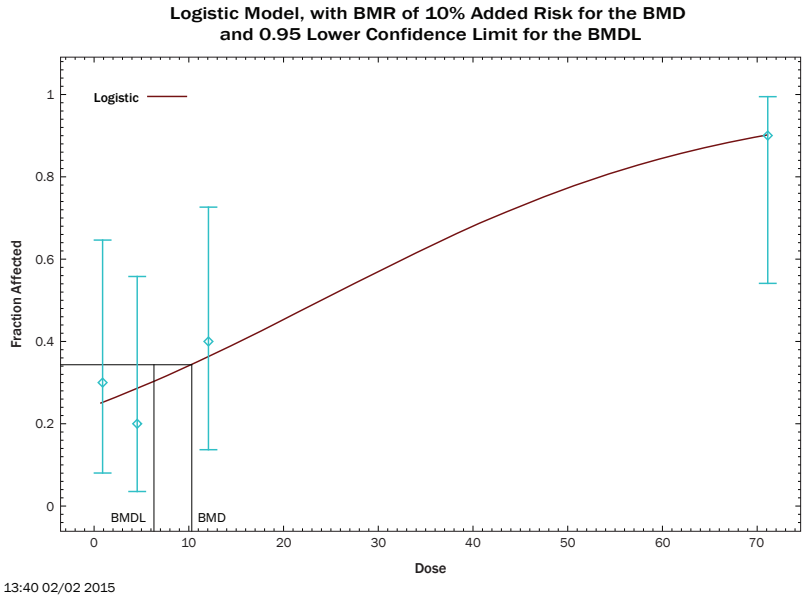


Figure B-5. Dose-response model (logistic) fit to the silver mass dose in liver tissue (ng/g) and **liver bile duct hyperplasia proportion in female rats** following subchronic inhalation exposure to silver nanoparticles [Sung et al. 2009]. (Data and model results in Tables B-3 and B-7.) Benchmark response (BMR) is defined as a 10% added risk of liver bile duct hyperplasia; BMD: Benchmark dose estimate; $BMDL_{10}$: Benchmark dose, 95% lower confidence limit estimate. BMD and $BMDL_{10}$ are associated with BMR, as shown with green lines to mark these point estimates on the dose-response curve.

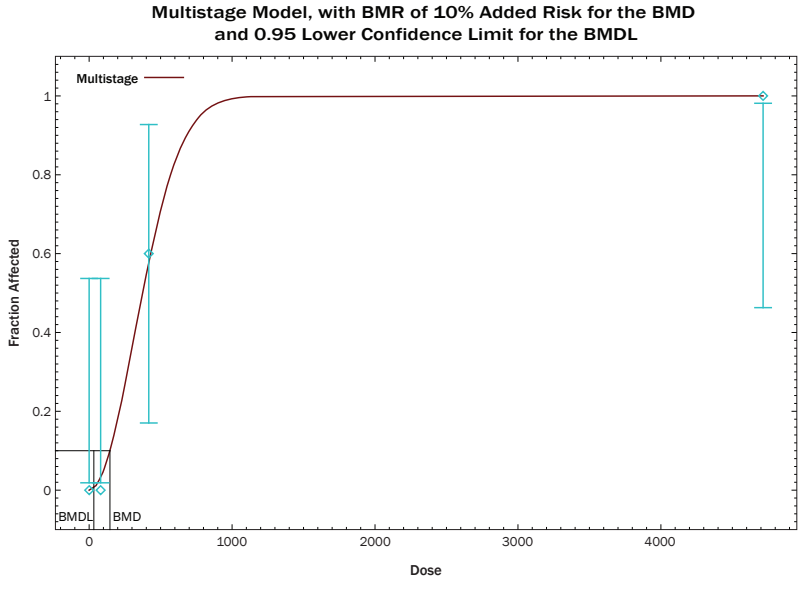


Figure B-6. Dose-response model (multistage polynomial degree 2) fit to the silver mass dose in lung tissue (ng/g) and chronic alveolar inflammation proportion in male rats following subchronic inhalation exposure to silver nanoparticles [Song et al. 2013]. (Data and model results in Tables B-4 and B-8.) Benchmark response (BMR) is defined as a 10% added risk of chronic alveolar inflammation; BMD: Benchmark dose estimate; $BMDL_{10}$: Benchmark dose, 95% lower confidence limit estimate. BMD and $BMDL_{10}$ are associated with BMR, as shown with green lines to mark these point estimates on the dose-response curve.

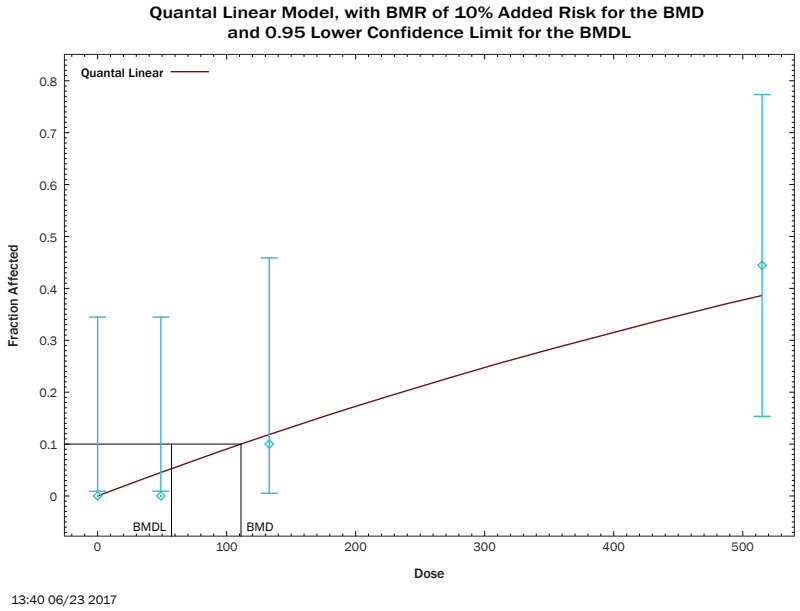


Figure B-7. Exposure-response model (quantal linear) fit to the airborne exposure concentration of silver nanoparticles (µg/m$^3$) and **liver abnormality proportion in male rats** [Sung et al. 2009]. (Data and model results in Tables B-1 and B-12.) Benchmark response (BMR) is defined as a 10% added risk of liver abnormality; BMC: Benchmark concentration estimate; $BMCL_{10}$: Benchmark concentration, 95% lower confidence limit estimate. BMC and $BMCL_{10}$ are associated with BMR, as shown with green lines to mark these point estimates on the dose-response curve.

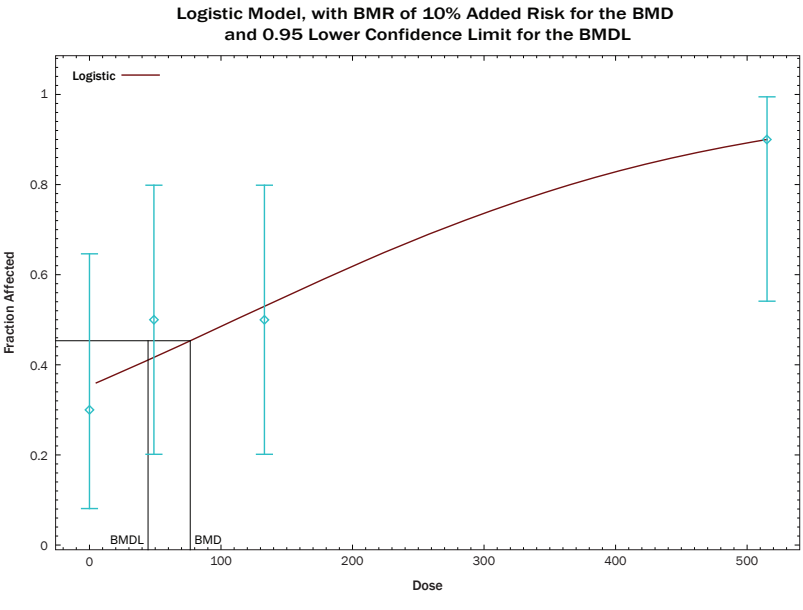


Figure B-8. Exposure-response model (logistic) fit to the airborne exposure concentration of silver nanoparticles (µg/m$^3$) and **liver abnormality proportion in female rats** [Sung et al. 2009]. (Data and model results in Tables B-1 and B-12.) Benchmark response (BMR) is defined as a 10% added risk of liver abnormality; BMC: Benchmark concentration estimate; $BMCL_{10}$: Benchmark concentration, 95% lower confidence limit estimate. BMC and $BMCL_{10}$ are associated with BMR, as shown with green lines to mark these point estimates on the dose-response curve.

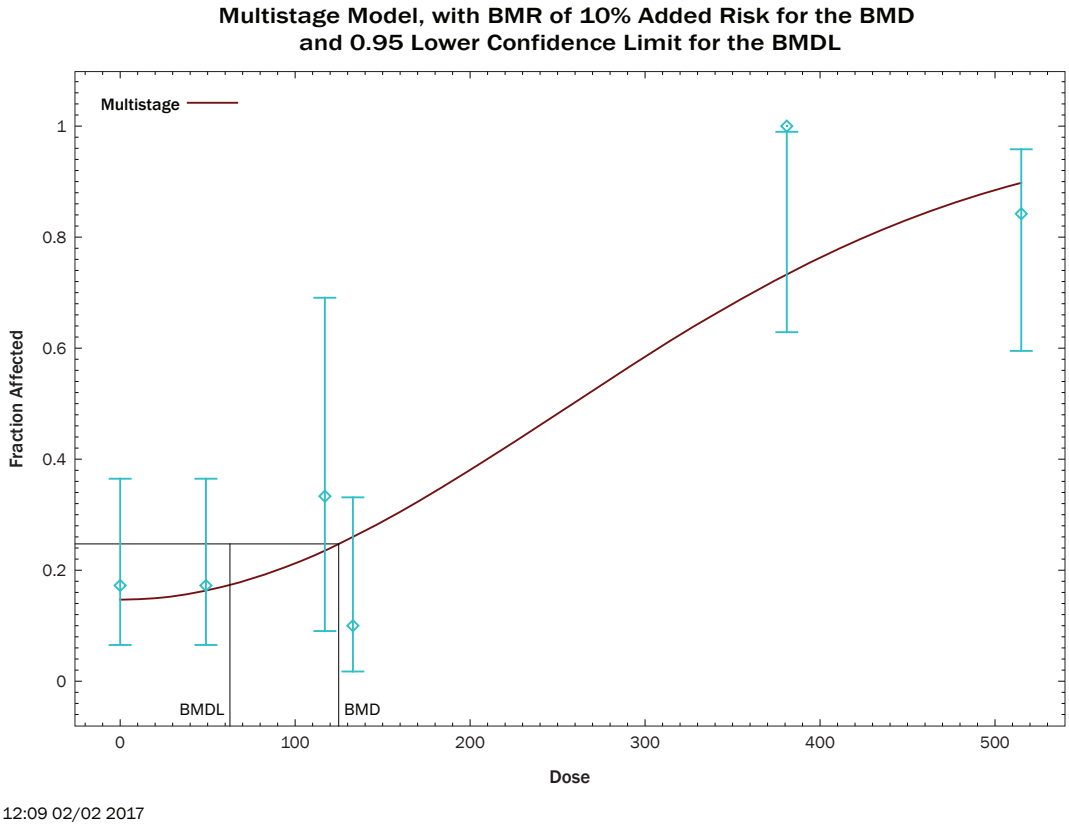


Figure B-9. Exposure-response model (multistage polynomial degree 3) fit to the **pooled data** on airborne exposure concentration of silver nanoparticles (μg/m$^3$) and **chronic alveolar inflammation proportion in male and female rats** [Sung et al. 2009; Song et al. 2013]. (Data and model results in Table B-11.) Benchmark response (BMR) is defined as a 10% added risk of chronic alveolar inflammation; BMC: Benchmark concentration estimate; $BMCL_{10}$: Benchmark concentration, 95% lower confidence limit estimate. BMC and $BMCL_{10}$ are associated with BMR, as shown with green lines to mark these point estimates on the dose-response curve.

## B.2 No Observed Adverse Effect Level (NOAEL) Estimation of Rat Liver Bile Duct Hyperplasia

### B.2.1 Background

A statistical examination of the rat dose and response data was performed to estimate the no observed adverse effect levels (NOAELs) in male and female rats with respect to liver bile duct hyperplasia in the subchronic inhalation study by Sung et al. [2009]. This analysis was performed to verify the NOAEL, which is defined as the highest dose group that was not statistically significantly different from the controls.

An omnibus test first identified whether an association exists between subchronic inhalation exposure to silver nanoparticles and liver bile duct hyperplasia. This test was followed by multiple comparisons to identify the levels of exposure that result in a response statistically significantly different from background.

### B.2.2 Data

The following data are taken from Sung et al. [2009], Tables 9 and 10. All hyperplasia responses (minimum and moderate) are combined for the female rats.

**Table B-13. Male rat liver bile duct hyperplasia (only minimum reported).**

| Dose | Response |
|---|---|
| Control (0 μg/m$^3$) | 0/10 |
| Low (49 μg/m$^3$) | 0/10 |
| Middle (133 μg/m$^3$) | 1/10 |
| High (515 μg/m$^3$) | 4/9 |

**Table B-14. Female rat liver bile duct hyperplasia (minimum and moderate hyperplasia combined).**

| Dose | Response |
|---|---|
| Control (0 μg/m$^3$) | 3/10 |
| Low (49 μg/m$^3$) | 2/10 |
| Middle (133 μg/m$^3$) | 4/10 |
| High (515 μg/m$^3$) | 9/10 |

## B.2.3 Analysis

### *B.2.3.1 Male rats*

Because these rodent data do not have large samples, and response proportions are near 0, the traditional tests relying on asymptotic normal or chi-square distributions are not applicable. Instead, an exact inferential method, Fisher's exact test, can be used. A level of significance of 5% was used for decision-making. Statistical analysis was completed with SAS 9.4.

The following hypothesis was tested:

$H_0$: Male Rat Hyperplasia is not associated with Dose

$H_A$: Male Rat Hyperplasia is associated with Dose

The *p* value is 0.0081, thus suggesting an association between liver bile duct hyperplasia and subchronic inhalation exposure to silver nanoparticles in male rats. However, this test does not indicate which dose group(s) have statistically significantly different proportions of male rats with hyperplasia. To obtain this information (which is required to determine the NOAEL), pairwise exact tests were used to compare each exposure group (low, middle, and high) to the control group (Table B-15). Results are not shown for the low (49 μg/m$^3$) vs. control comparison, as both have responses of 0/10.

**Table B-15. Comparisons of hyperplasia proportions, male rats.**

| Comparison | *P* value (two-sided) |
|---|---|
| 133 μg/m$^3$ vs. Control | 1.0000 |
| 515 μg/m$^3$ vs. Control | 0.0325 |

Thus, the high-dose group is statistically significantly different from the control group, whereas the low and middle groups are not. Therefore, 133 μg/m$^3$ is the NOAEL. Adjustments for multiple comparisons (e.g., Bonferroni) were not made.

### *B.2.3.2 Female rats*

The process above was also used for female rats.

$H_0$: Female Rat Hyperplasia is not associated with Dose

$H_A$: Female Rat Hyperplasia is associated with Dose

The *p* value is 0.0104; thus, these data do support an association between liver bile duct hyperplasia and subchronic inhalation exposure to silver nanoparticles in female rats.

Pairwise exact tests are used to compare each exposure group (low, middle, and high) to the control group (Table B-16).

**Table B-16. Comparisons of hyperplasia proportions, female rats.**

| Comparison | *P* value (two-sided) |
|---|---|
| 49 μg/m$^3$ vs. Control | 1.0000 |
| 133 μg/m$^3$ vs. Control | 1.0000 |
| 515 μg/m$^3$ vs. Control | 0.0198 |

Thus, the high dose group is statistically significantly different from the control group, whereas the low and middle groups are not. Therefore, 133 μg/m$^3$ is the NOAEL. Adjustments for multiple comparisons (e.g., Bonferroni) were not made.

### B.2.4 Conclusion

In an exact statistical test, subchronic inhalation exposure to silver nanoparticles is associated with liver duct hyperplasia in both male and female rats. In exact pairwise comparisons, the NOAEL is 133 μg/m$^3$ for both male and female rats.

## B.3 Pooled Data Analysis of Rat Subchronic Pulmonary Inflammation

### B.3.1 Background

In investigations of the potency of silver nanomaterials, data from two studies [Sung et al. 2009; Song et al. 2013] on pulmonary inflammation in rodents were analyzed separately by dose-response modeling. An exploratory plot illustrated variability in response due to lab effect.

This analysis investigates whether the information from these two studies can be combined in five phases:

1. Pool all data (both labs, both sexes)
2. Pool all male data (both labs, only males)
3. Pool all female data (both labs, only females)
4. Pool all Sung et al. [2009] data (one lab, both sexes)
5. Pool all Song et al. [2013] data (one lab, both sexes)

The traditional method to investigate pooled data would be to model the following multiple non-linear relationship:

$$Pulmonary\ Inflammation = Function\ (Dose, Lab, Sex) + \varepsilon$$

EPA BMDS 2.6 cannot handle a relationship with more than one covariate (i.e., dose). Other statistical software (e.g., SAS) allows the user to fit non-linear regression models with multiple covariates, but the estimation of a benchmark dose and its lower confidence limit is not automatically provided as in BMDS. As a result, the model above will be investigated in the five phases, where each phase is making an assumption of whether or not a covariate is statistically significant. For example, the model in phase 1, where all data are pooled, is assuming that Lab and Sex do not contribute statistically significantly to the variance in the response. Each of the five models can be evaluated separately in EPA BMDS.

Models will be fit to estimate the dose (concentration in μg/m$^3$) associated with an added 10% risk. The best-fitting model is that which has a goodness-of-fit *p* value greater than 0.1 and has the smallest AIC.

As previously investigated, EPA BMDS does not include model parameters that are estimated to be a boundary value (e.g., zero) in the AIC calculation, which is -2 times the log likelihood plus 2 times the number of parameters in the model. The result is that of the best-fitting models, the "best" may have a smaller AIC value than it should by constant factor of 2. If the best model does have non-estimable parameters, then the adjusted AIC will be computed. If this model still has the smallest AIC, then the process ends. If another model now has a smaller

AIC, then it will be checked for non-estimable parameters and the AIC will be adjusted. This process will be repeated until the best model is chosen.

## B.3.2 Analyses

### *B.3.2.1 Phase 1: Pool all data (both labs, both sexes)*

Binary data can be difficult to visualize, but there seems to be an association: below 200 μg/m$^3$, most rodents *didn't* exhibit pulmonary inflammation, whereas after 381 μg/m$^3$, most rodents *did* exhibit pulmonary inflammation (Figure B-10).

All models were fit with the default options, where BMR = added 10%: Quantal Linear, MS2, MS3, Gamma, Logistic, Log Logistic, Log Probit, Probit, and Weibull. The best-fitting model was the MS3, as it was the only one with adequate goodness-of-fit (Table B-17). A visual inspection of the fit is also satisfactory (Figure B-11). Note: the linear and cubic terms were estimated to be 0 (a boundary value) in the MS3 model (model parameter estimates not shown), but the MS2 model did not have the same quadratic and intercept parameter estimates and had a non-zero linear term. As previously identified, EPA BMDS does not include "boundary parameters" when computing AIC, which is -2*LL + 2*#parameters. "Correcting" the MS3 AIC adds 4 because there are 2 boundary parameters, but because MS3 is the only adequately fitting model, no conclusions change.

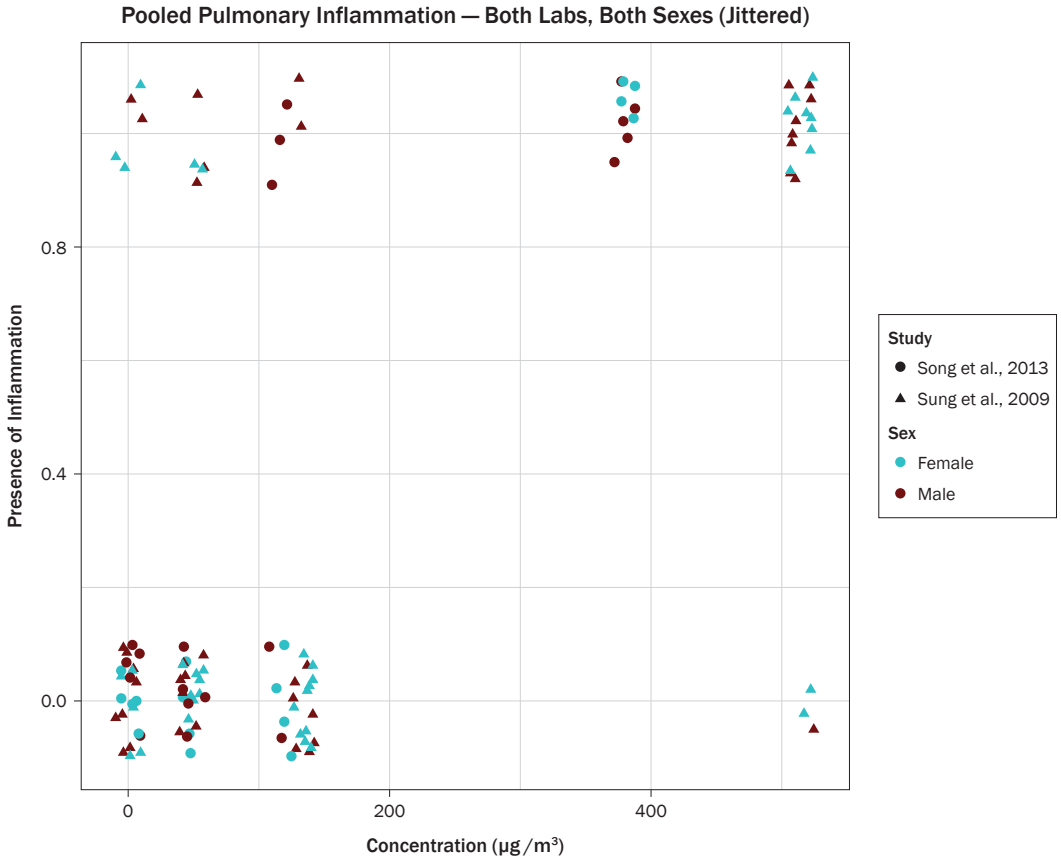


Figure B-10. Pooled data on chronic alveolar inflammation in male and female rats exposed to silver nanoparticles from the subchronic inhalation studies of Sung et al. [2009] and Song et al. [2013].

**Table B-17. Summary of models fit to the pooled data on chronic alveolar inflammation in male and female rats exposed to silver nanoparticles from the subchronic inhalation studies of Sung et al. 2009 and Song et al. 2013; benchmark response of added 10% risk.**

| Model name | Goodness-of-fit *p* value | AIC | BMC, µg/m³ | BMCL, µg/m³ | AIC adjustment | New AIC |
|---|---|---|---|---|---|---|
| Multistage Degree 3 | 0.125 | 108.324 | 124.879 | 62.7501 | +4 | 112.324 |
| Log Logistic | 0.0948 | 108.494 | 160.708 | 91.9108 | | |
| Log Probit | 0.0934 | 108.681 | 162.287 | 95.433 | | |
| Logistic | 0.0929 | 109.166 | 91.0083 | 71.6765 | | |
| Gamma | 0.0777 | 109.36 | 159.391 | 80.4167 | | |
| Probit | 0.0821 | 109.658 | 86.5785 | 70.1134 | | |
| Multistage Degree 2 | 0.066 | 109.814 | 172.124 | 68.9935 | | |
| Weibull | 0.0644 | 110.221 | 140.787 | 67.9829 | | |
| Quantal-Linear | 0.0123 | 115.165 | 43.8085 | 30.1885 | | |

AIC = Akaike Information Criterion; BMC = Benchmark concentration estimate; BMCL: Benchmark concentration, 95% lower confidence limit estimate, associated with 10% added risk.

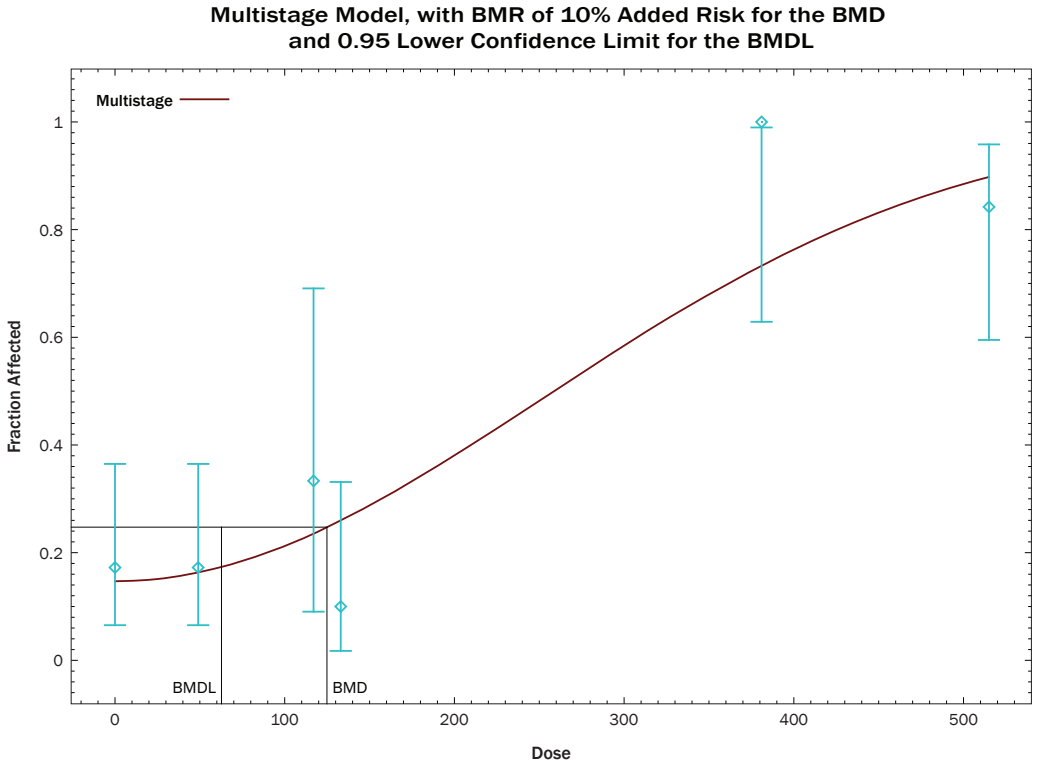


Figure B-11. EPA BMDS plot of the Multistage Degree (MS) 3 model fit to the pooled data on chronic alveolar inflammation in male and female rats exposed to silver nanoparticles from the subchronic inhalation studies of Sung et al. [2009] and Song et al. [2013]; Benchmark response of added 10% risk.

### *B.3.2.2 Phase 2: Pool all male data (both labs, only males)*

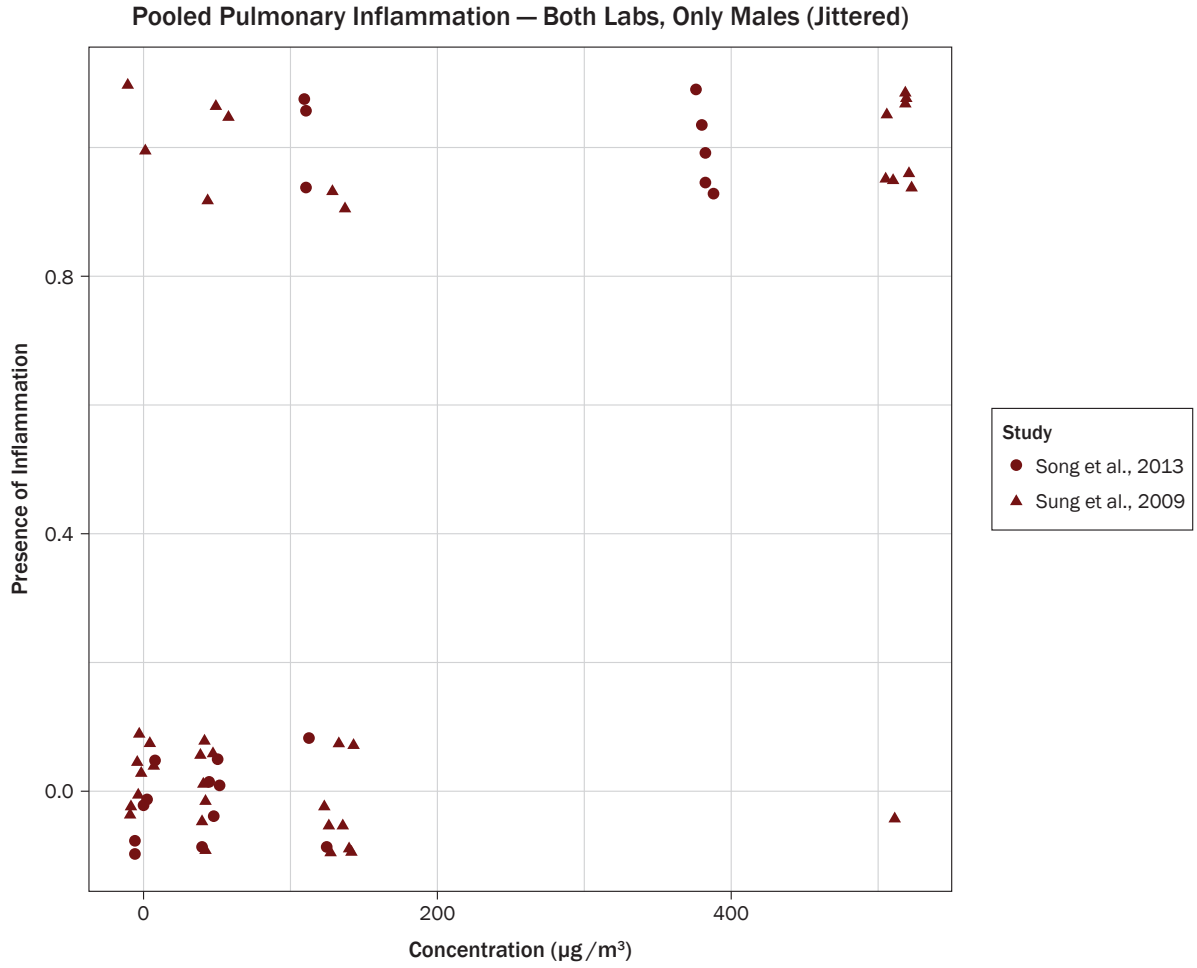


Figure B-12. Pooled data on chronic alveolar inflammation in only male rats exposed to silver nanoparticles from the subchronic inhalation studies of Sung et al. 2009 and Song et al. 2013.

For Phase 2, the male pulmonary inflammation data from both labs was combined, and an association is visible (Figure B-12). The best-fitting model was the Logistic, as all models had adequate goodness-of-fit and the Logistic model had the smallest AIC (Table B-18). All parameters were estimable. A visual inspection of the fit is also satisfactory (Figure B-13).

**Table B-18. Summary of models fit to the pooled data on chronic alveolar inflammation in only male rats exposed to silver nanoparticles from the subchronic inhalation studies of Sung et al. 2009 and Song et al. 2013; benchmark response of added 10% risk.**

| Model name | Goodness-of-fit *p* value | AIC | BMC, µg/m³ | BMCL, µg/m³ | AIC adjustment | New AIC |
|---|---|---|---|---|---|---|
| Logistic | 0.3594 | 58.7911 | 72.8551 | 51.5364 | 0 | |
| Probit | 0.3464 | 59.0091 | 71.7603 | 53.3993 | | |
| Quantal-Linear | 0.2822 | 60.1351 | 31.5999 | 19.588 | | |
| Log Logistic | 0.2412 | 60.6002 | 93.1509 | 30.0721 | | |
| Gamma | 0.2432 | 60.7511 | 76.9207 | 22.3897 | | |
| Log Probit | 0.2324 | 60.7747 | 93.2812 | 30.508 | | |
| Weibull | 0.2424 | 60.798 | 69.3448 | 22.2645 | | |
| Multistage Degree 2 | 0.2343 | 60.8748 | 64.0911 | 21.5788 | | |
| Multistage Degree 3 | 0.2343 | 60.8748 | 64.0907 | 22.0662 | | |

AIC = Akaike Information Criterion; BMC = Benchmark concentration estimate; BMCL: Benchmark concentration, 95% lower confidence limit estimate, associated with 10% added risk.

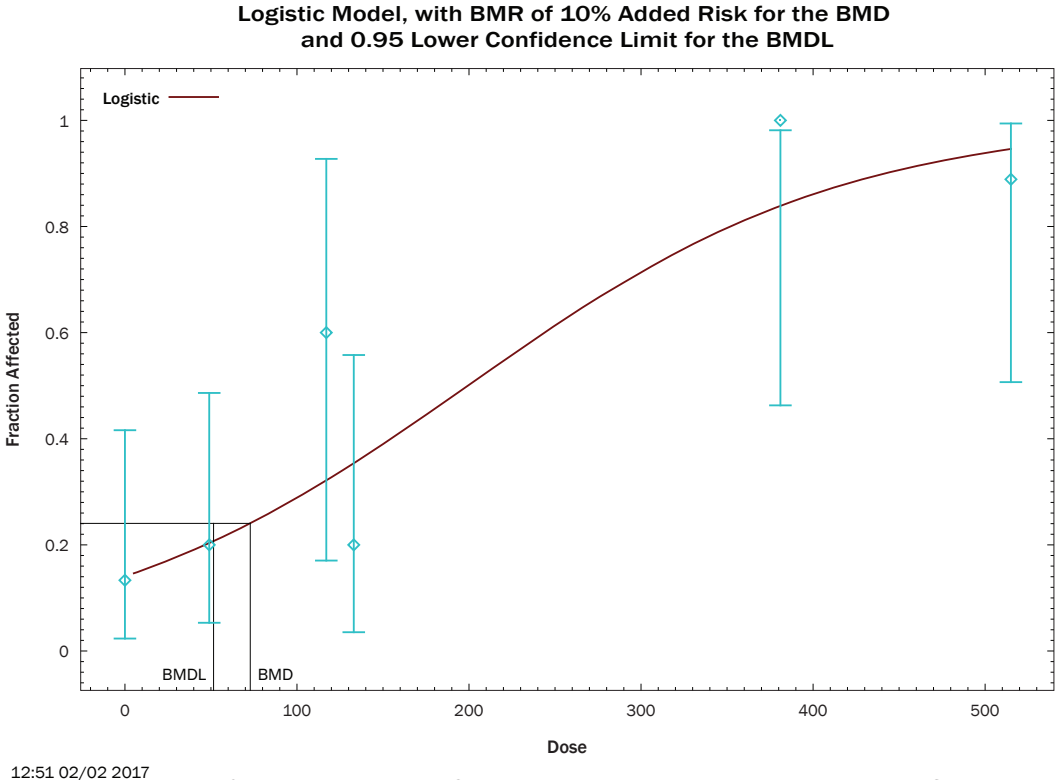


Figure B-13. EPA BMDS plot of the Logistic model fit to the pooled data on chronic alveolar inflammation in only male rats exposed to silver nanoparticles from the subchronic inhalation studies of Sung et al. 2009 and Song et al. 2013; Benchmark response of added 10% risk.

### *B.3.2.3 Phase 3: Pool all female data (both labs, only females)*

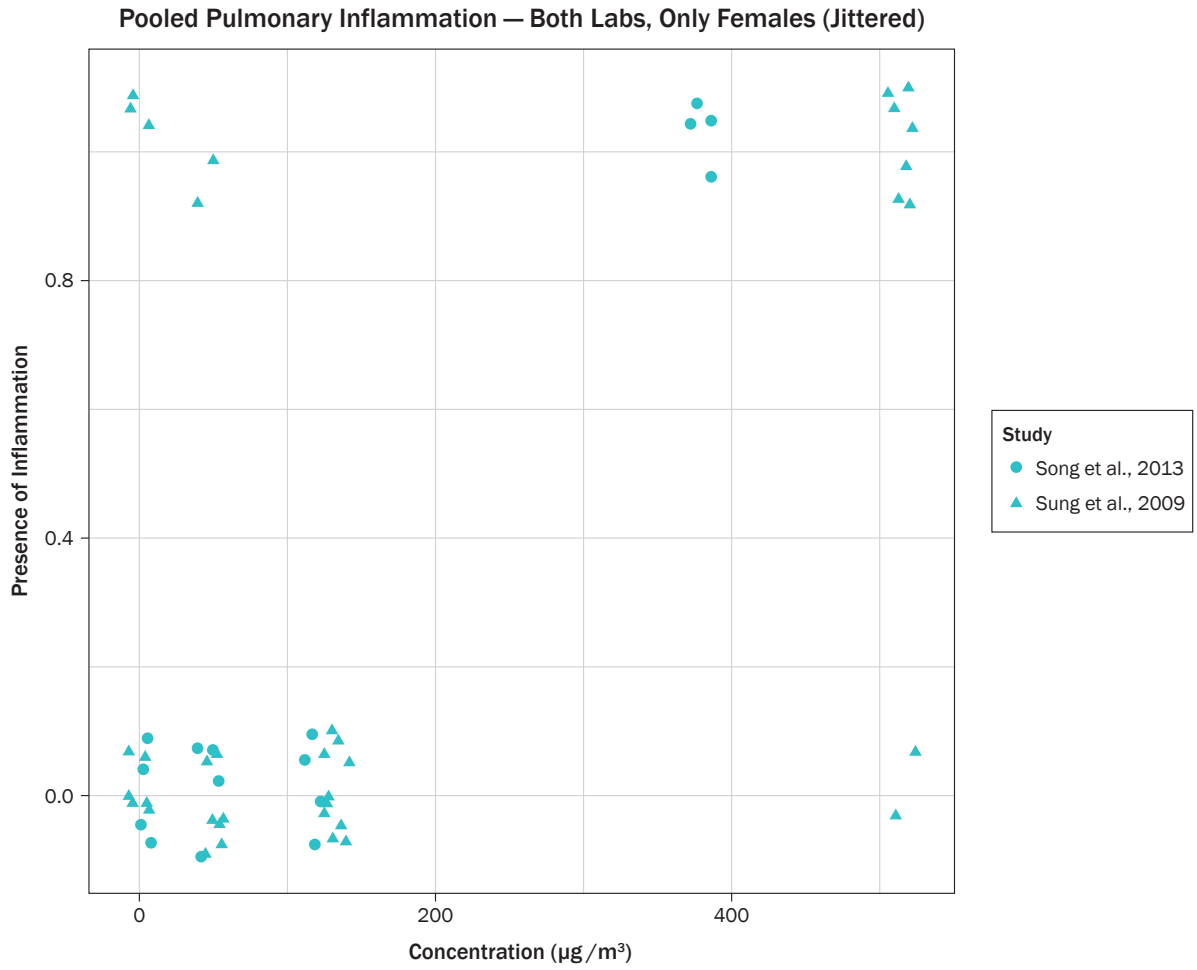


Figure B-14. Pooled data on chronic alveolar inflammation in only female rats exposed to silver nanoparticles from the subchronic inhalation studies of Sung et al. 2009 and Song et al. 2013.

The female pulmonary inflammation data from both labs was combined for Phase 3, and again an association is visible (Figure B-14). The MS2 model failed computationally, hence the goodness-of-fit *p* value of 0 and missing BMDL. The best-fitting model was the MS3, which also visibly fits the data. However, two parameters were estimated to be the boundary value and aren't included in the AIC calculation, so the new AIC selection process begins (Table B-19). The next best-fitting model is the Log Probit, which has no non-estimable parameters (Figure B-15).

**Table B-19. Summary of models fit to the pooled data on chronic alveolar inflammation in only female rats exposed to silver nanoparticles from the subchronic inhalation studies of Sung et al. 2009 and Song et al. 2013; benchmark response of added 10% risk.**

| Model name | Goodness-of-fit *p* value | AIC | BMC, µg/m³ | BMCL, µg/m³ | AIC adjustment | New AIC |
|---|---|---|---|---|---|---|
| Multistage Degree 2 | 0 | 41.7064 | 408.874 | | — | — |
| Multistage Degree 3 | 0.1508 | 50.0352 | 204.127 | 97.4488 | +4 | 54.0352 |
| Log Probit | 0.1233 | 50.5459 | 200.377 | 121.54 | | |
| Log Logistic | 0.1125 | 50.734 | 203.348 | 116.53 | | |
| Gamma | 0.1051 | 51.0656 | 207.192 | 114.868 | | |
| Weibull | 0.0819 | 52.0323 | 200.726 | 98.5956 | | |
| Logistic | 0.0741 | 52.1996 | 112.311 | 80.2723 | | |
| Probit | 0.0674 | 52.6595 | 103.843 | 76.7273 | | |
| Quantal-Linear | 0.0207 | 56.9876 | 59.7879 | 34.8319 | | |

AIC = Akaike Information Criterion; BMC = Benchmark concentration estimate; BMCL: Benchmark concentration, 95% lower confidence limit estimate, associated with 10% added risk.

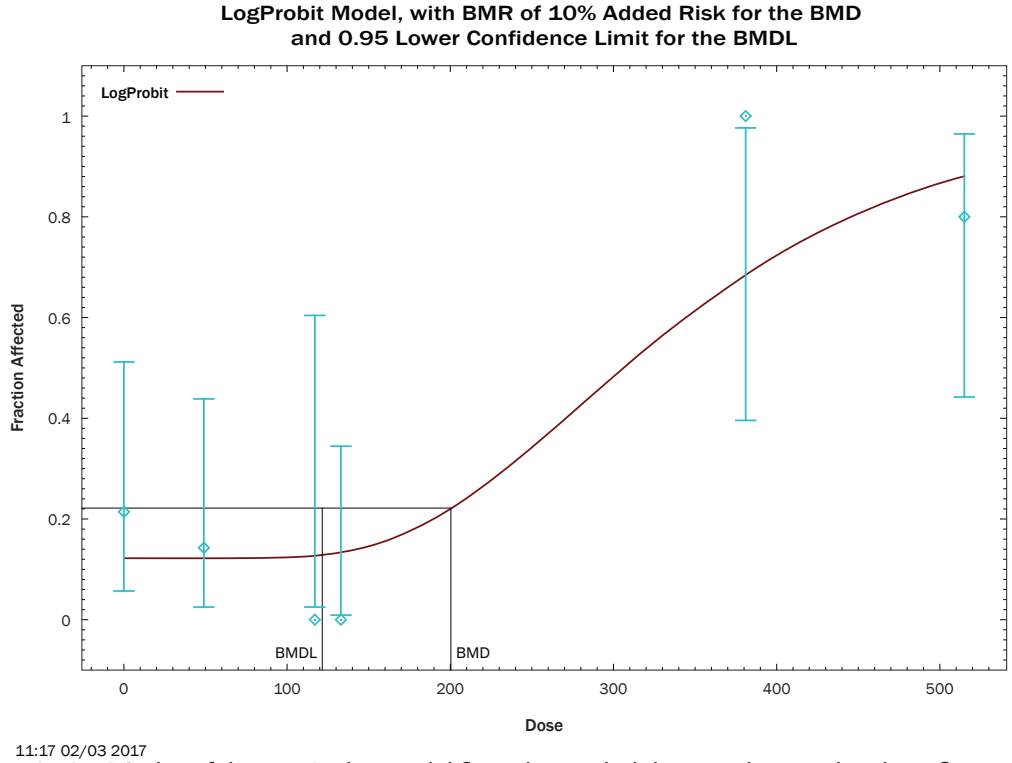


Figure B-15. EPA BMDS plot of the Log Probit model fit to the pooled data on chronic alveolar inflammation in only female rats exposed to silver nanoparticles from the subchronic inhalation studies of Sung et al. [2009] and Song et al. [2013]; benchmark response of added 10% risk.

### *B.3.2.4 Phase 4: pool all Sung [2009] data (one lab, both sexes)*

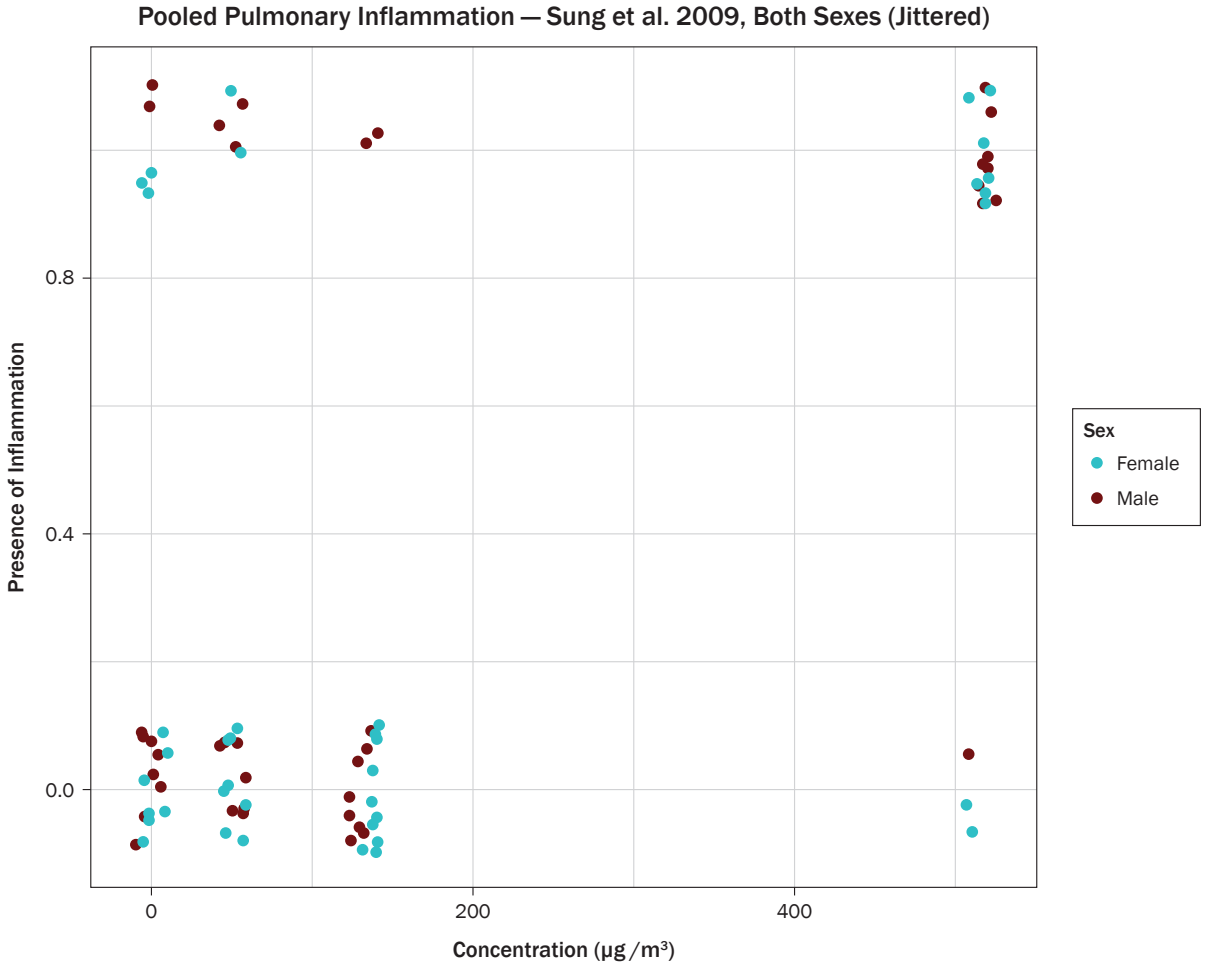


Figure B-16. Pooled data on chronic alveolar inflammation in male and female rats exposed to silver nanoparticles from the subchronic inhalation study of Sung et al. 2009

In Phase 4, the male and female pulmonary inflammation data were combined from the Sung et al. [2009] study (Figure B-16). The initial best-fitting model for these data is the Gamma, but one parameter was non-estimable. After AIC adjustment, the next best model was the MS2, but the visual fit is not monotonically increasing. The next best model is the MS3, which has two non-estimable parameters, so the AIC increases by 4. The Log Logistic now has the lowest AIC, just under that of the adjusted Gamma, with no adjustments needed for the AIC (Table B-20). The visual fit of the Log Logistic model is also acceptable (Figure B-17).

**Table B-20. Summary of models fit to the pooled data on chronic alveolar inflammation in male and female rats exposed to silver nanoparticles from the subchronic inhalation study of Sung et al. [2009]; benchmark response of added 10% risk.**

| Model name | Goodness-of-fit *p* value | AIC | BMC, µg/m³ | BMCL, µg/m³ | AIC adjustment | New AIC |
|---|---|---|---|---|---|---|
| Gamma | 0.3915 | 80.6229 | 318.101 | 136.966 | +2 | 82.6229 |
| Multistage Degree 2 | 0.4281 | 81.1782 | 318.297 | 179.964 | — | — |
| Multistage Degree 3 | 0.3089 | 81.1835 | 225.822 | 111.115 | +4 | 85.1835 |
| Log Logistic | 0.1709 | 82.6225 | 404.723 | 136.931 | | |
| Log Probit | 0.1709 | 82.6225 | 334.777 | 137.979 | | |
| Weibull | 0.1709 | 82.6225 | 425.373 | 135.438 | | |
| Logistic | 0.0672 | 84.5596 | 104.932 | 78.6943 | | |
| Probit | 0.0625 | 84.7756 | 99.4601 | 76.3518 | | |
| Quantal-Linear | 0.0129 | 88.6681 | 63.1267 | 37.9974 | | |

AIC = Akaike Information Criterion; BMC = Benchmark concentration estimate; BMCL: Benchmark concentration, 95% lower confidence limit estimate, associated with 10% added risk.

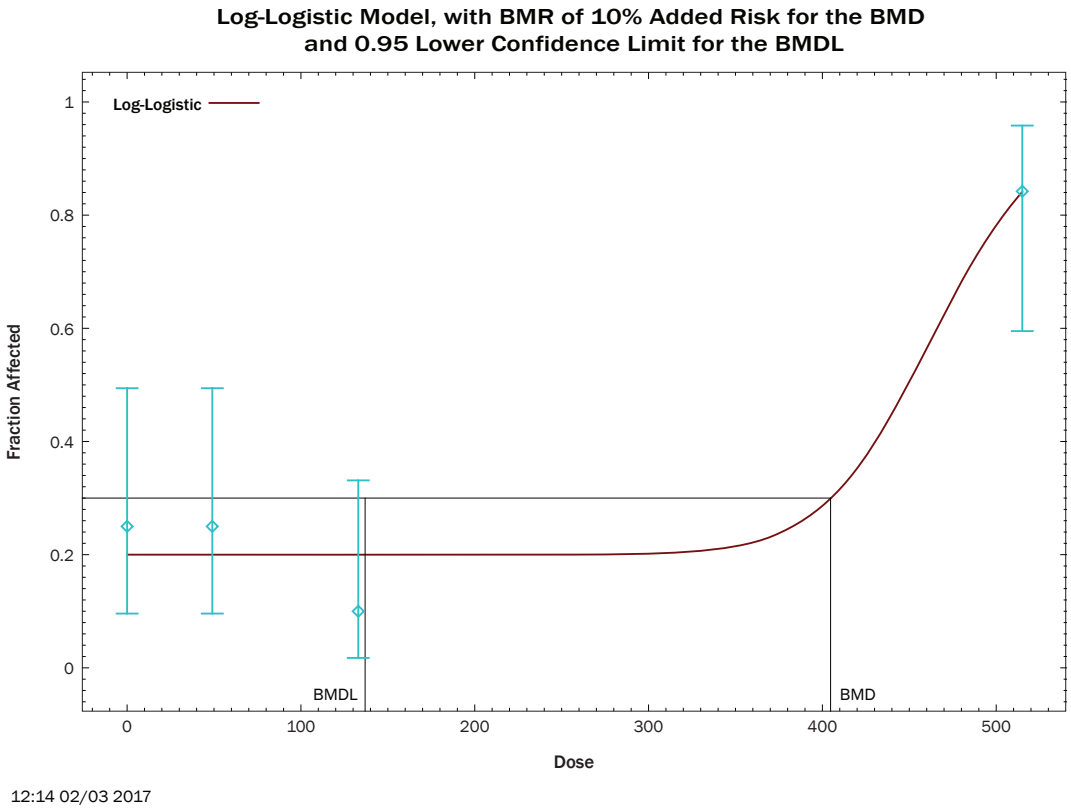


Figure B-17. EPA BMDS plot of the Log Logistic model fit to the pooled data on chronic alveolar inflammation in male and female rats exposed to silver nanoparticles from the subchronic inhalation study of Sung et al. [2009]; benchmark response of added 10% risk

### *B.3.2.5 Phase 5: pool all Song [2013] data (one lab, both sexes)*

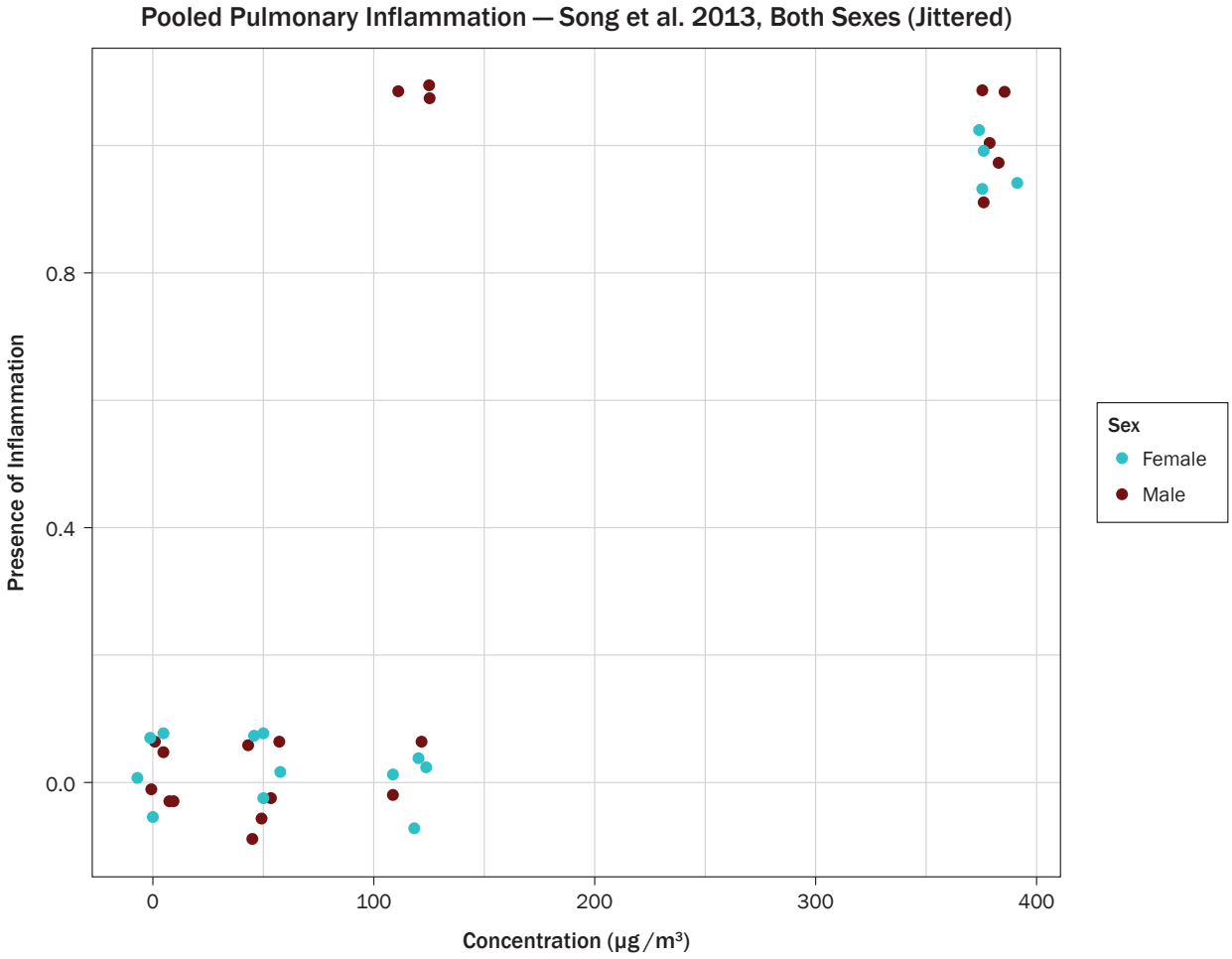


Figure B-18. Pooled data on chronic alveolar inflammation in male and female rats exposed to silver nanoparticles from the subchronic inhalation study of Song et al. 2013

For the final phase of this analysis, the male and female pulmonary inflammation data from Song et al. [2013] were combined (Figure B-18). This is a "noisy" relationship, and as a result the parameter estimations across the models are affected. For the initial best-fitting model, the Log Logistic, the background estimate was not as estimable as another parameter. Thus, the AIC was adjusted, and AICs had to be adjusted for the Gamma and MS3 models as well. The Logistic, Log Probit, and Probit models all had identical goodness-of-fit *p* values and AICs. The smallest BMD estimate came from the Log Probit model, but this had a non-estimate parameter. The next smallest BMD estimate was from the Probit (Table B-21). There was a large amount of variability around the background parameter estimate (95% CI: -3142.19 to 3123.16), but all parameters were estimable. Thus, the best-fitting model was chosen to be the Probit (Figure B-19).

**Table B-21. Summary of models fit to the pooled data on chronic alveolar inflammation in male and female rats exposed to silver nanoparticles from the subchronic inhalation study of Song et al. [2013]; benchmark response of added 10% risk.**

| Model name | Goodness-of-fit *p* value | AIC | BMC, µg/m³ | BMCL, µg/m³ | AIC adjustment | New AIC |
|---|---|---|---|---|---|---|
| Log Logistic | 1 | 13.4573 | 107.621 | 56.0969 | +4 | 17.4573 |
| Gamma | 1 | 13.4609 | 94.2444 | 49.2345 | +4 | 17.4609 |
| Multistage Degree 3 | 0.9654 | 13.9705 | 76.8451 | 31.9106 | +6 | 19.9705 |
| Logistic | 1 | 15.4573 | 111.425 | 58.8764 | N/A, but note that SE is large on the background estimate | |
| Log Probit | 1 | 15.4573 | 101.567 | 54.7316 | +2 | 17.4573 |
| Probit | 1 | 15.4573 | 106.041 | 54.4632 | N/A, but note that SE is large on the background estimate | |
| Weibull | 0.9999 | 15.4576 | 103.883 | 45.4488 | | |
| Quantal-Linear | 0.2178 | 21.1911 | 22.1765 | 13.4603 | | |
| Multistage Degree 2 | 0 | 1.95E+54 | Computation failed; BMD is larger than three times maximum input doses | | | |

AIC = Akaike Information Criterion; BMC = Benchmark concentration estimate; BMCL: Benchmark concentration, 95% lower confidence limit estimate, associated with 10% added risk; SE = Standard error.

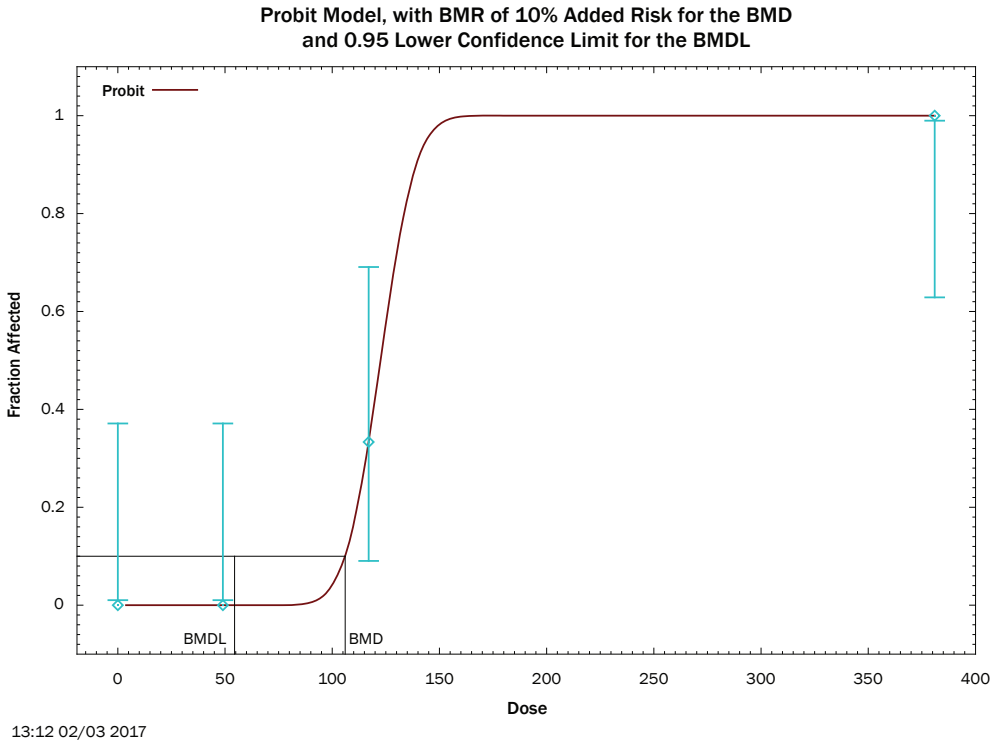


Figure B-19. EPA BMDS plot of the Probit model fit to the pooled data on chronic alveolar inflammation in male and female rats exposed to silver nanoparticles from the subchronic inhalation study of Song et al. [2013]; benchmark response of added 10% risk

## B.3.3 Conclusions

In conclusion, a model could be fit to and a BMD/BMDL estimate found for each pooled data scenario (Table B-22). The success of Phase 1, where all data were combined, suggests that accounting for Lab and Sex may not be necessary; that is, the Lab and Sex effects may not be statistically significant for explaining the variability in the response, and dose is sufficient. To estimate the effects of Lab and Sex and verify the conclusion that data for both labs and sexes may be pooled, a multiple logistic regression model was explored with SAS 9.4 (Table B-23).

For Phases 3 to 5, adjustments were made to AIC estimates because of the fact that EPA BMDS does not penalize the likelihood for parameters estimated to be a boundary value. BMD estimates did not tend to change by very much in these cases between the "best" model by the as-shown AICs and the "best" model by the adjusted AICs.

**Table B-22. Summary of best-fitting models of the data on chronic alveolar inflammation in male or female rats exposed to silver nanoparticles from the subchronic inhalation studies of Sung et al. [2009] or Song et al. [2013] across the five pooling phases; benchmark response of added 10% risk.**

| Phase | Best model | Goodness-of-fit *P* value | AIC | BMC, μg/m³ | BMCL, μg/m³ |
|---|---|---|---|---|---|
| 1. Pool all data (both labs, both sexes) | Multistage Degree 3 | 0.125 | 108.324 | 124.879 | 62.7501 |
| 2. Pool all male data (both labs, only males) | Logistic | 0.3594 | 58.7911 | 72.8551 | 51.5364 |
| 3. Pool all female data (both labs, only females) | Log Probit | 0.1233 | 50.5459 | 200.377 | 121.54 |
| 4. Pool all Sung et al. [2009] data (Sung lab, both sexes) | Log Logistic | 0.1709 | 82.6225 | 404.723 | 136.931 |
| 5. Pool all Song et al. [2013] data (Song lab, both sexes) | Probit | 1 | 15.4573 | 106.041 | 54.4632 |

AIC = Akaike Information Criterion; BMC = Benchmark concentration estimate; BMCL: Benchmark concentration, 95% lower confidence limit estimate, associated with 10% added risk

**Table B-23. Logistic model fit statistics for the modifying effects of concentration, sex, and study on chronic alveolar inflammation induced by subchronic exposure to silver nanoparticles from the studies by Sung et al. [2009] and Song et al. [2013].**

| Analysis of Maximum Likelihood Estimates | | | | | | | |
|---|---|---|---|---|---|---|---|
| Parameter | | DF | Estimate | Standard Error | Wald Chi-Square | *P* value | Exp(Est) |
| Intercept | | 1 | 2.0365 | 0.3594 | 32.1064 | <.0001 | 7.664 |
| Concentration | | 1 | -0.00816 | 0.00152 | 28.7423 | <.0001 | 0.992 |
| Sex | Female | 1 | 0.3477 | 0.2563 | 1.8405 | 0.1749 | 1.416 |
| Study | Song et al., 2013 | 1 | -0.0360 | 0.2607 | 0.0191 | 0.8902 | 0.965 |

DF: degrees of freedom; Exp(Est): Euler's constant raised to the power of the value in the Estimate column.

The exploratory logistic regression model confirms the conclusions of the phased approach above, as Sex and Lab are not statistically significant at the 5% level of significance. The variability in the proportion of rats determined to have chronic alveolar inflammation is sufficiently explained by dose alone.

## B.4 Exploration of Pooling Rat Subchronic Liver Effects Data

### B.4.1 Background

A previous analysis explored the potential of grouping the alveolar inflammation data from Sung et al. [2009] and Song et al. [2013]. It was found that a simple concentration-response model adequately fit the model without including covariates for Lab (Sung, Song) or Sex (Female, Male).

This section explores whether the female and male data can be combined from the Sung et al. [2009] report within two alternative endpoints: Liver Bile Duct Hyperplasia and Liver Abnormality.

Hyperplasia was already analyzed separately by Sex. Abnormality is also of interest, so points of departure (BMD and BMDL) will be estimated for those data.

### B.4.2 Analysis

#### *B.4.2.1 Liver Duct Hyperplasia*

The following pooled data (Table B-24) were considered for modeling.

The interaction term was found to be not statistically significant ($p = 0.7919$). In the resulting simpler logistic model, Sex was found to be statistically significant. Thus, the liver hyperplasia data for male and female rats should not be pooled, as the female rats were approximately 3.5 times more likely than males to develop liver bile duct hyperplasia (Table B-25). Visually, the dose-response curves are distinct, further supporting the statistically significant difference in liver hyperplasia development rates between male and female rats (Figure B-20).

To explore the significance of Sex, an exploratory Logistic model was fit to the pooled data in SAS 9.4.

$$\pi_i = \frac{\exp\{\beta_0 + \beta_1 * Concentration_i + \beta_2 * Sex_i + \beta_3 * Concentration * Sex_i\}}{1 + \exp\{\beta_0 + \beta_1 * Concentration_i + \beta_2 * Sex_i + \beta_3 * Concentration * Sex_i\}}$$

$$i = 1, \ldots, 79$$

Sex = 1 if female, 0 if male

$\pi_i$ is the expected probability of liver duct hyperplasia for rodent i

**Table B-24. Rat subchronic inhalation study data for silver nanoparticles—response proportion for liver bile duct hyperplasia (minimum or moderate).**

| | Response proportion | | | |
|---|---|---|---|---|
| | Exposure concentration, µg/m³ | | | |
| **Rat study and sex** | **0** | **49** | **133** | **515** |
| Sung et al. [2009]—Male | 0/10 | 0/10 | 1/10 | 4/9 |
| Sung et al. [2009]—Female | 3/10 | 2/10 | 4/10 | 9/10 |
| *Pooled** | *3/20* | *2/20* | *5/20* | *13/19* |

*Histopathology results from Tables 9 and 10 of Sung et al. [2009]; data at end of 13-week exposure.

**Table B-25. Logistic model fit statistics for the modifying effects of concentration and sex on liver bile duct hyperplasia in male and female rats induced by subchronic exposure to silver nanoparticles from the study by Sung et al. [2009].**

| Analysis of maximum likelihood estimates | | | | | | | |
|---|---|---|---|---|---|---|---|
| **Parameter** | | **DF** | **Estimate** | **Standard error** | **Wald Chi-Square** | ***P* value** | **Exp(Est)** |
| **Intercept** | | 1 | -2.5560 | 0.5686 | 20.2054 | <.0001 | 0.078 |
| **Concentration** | | 1 | 0.00692 | 0.00182 | 14.4495 | 0.0001 | 1.007 |
| **Sex** | Female | 1 | 1.2519 | 0.4096 | 9.3431 | 0.0022 | 3.497 |

DF: degrees of freedom; Exp(Est): Euler's constant raised to the power of the value in the estimate column.

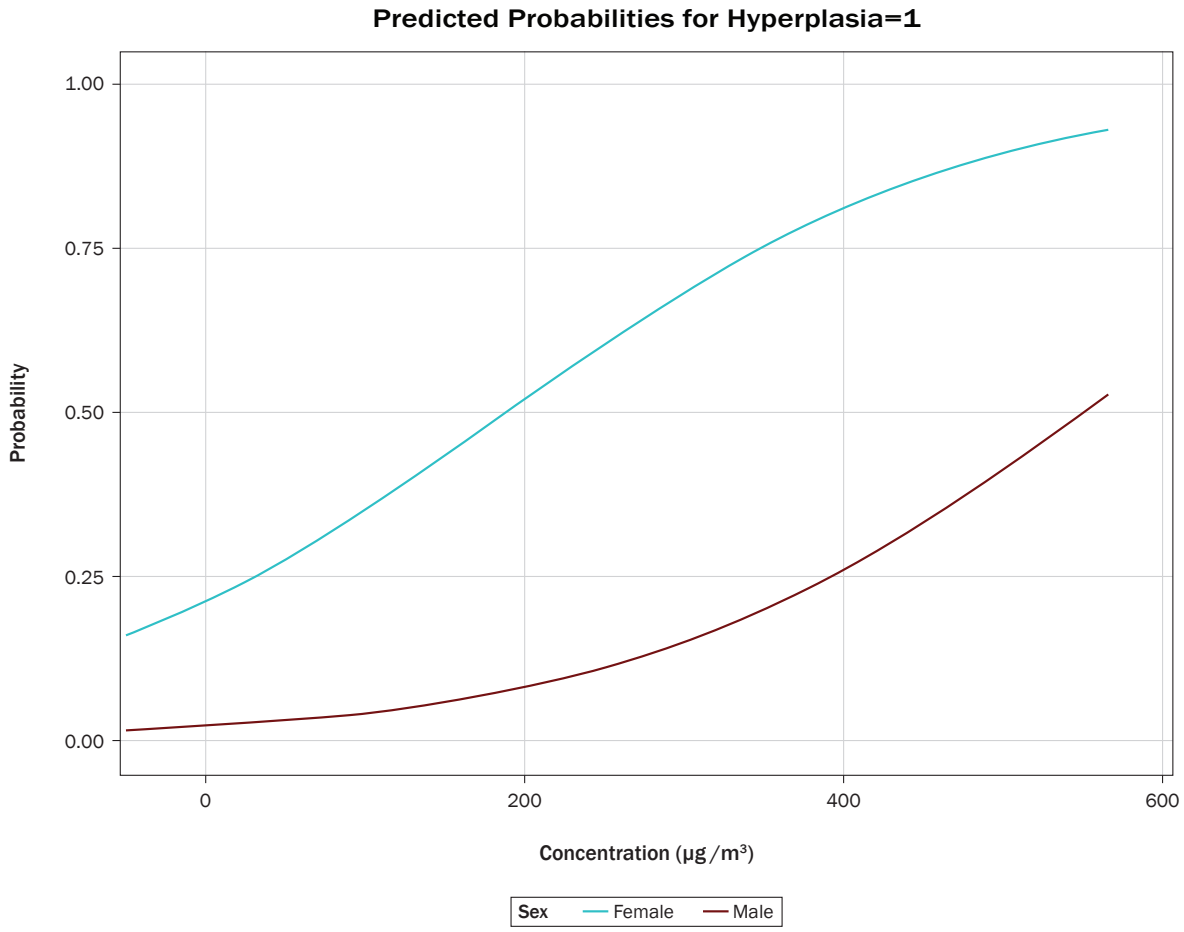


Figure B-20. Logistic model fits to data on male and female liver hyperplasia induced by subchronic exposure to silver nanoparticles from Sung et al. [2009].

### *B.4.2.2 Liver Abnormality*

In addition to bile duct hyperplasia, Sung et al. [2009] also considered necrosis, vacuolation, mineralization, granuloma, fibrosis, and pigment when histopathologically analyzing the rodent livers. All of these endpoints were combined into a category called Abnormality. The resulting data are below (Table B-26).

In male rats, Abnormality consists of bile duct hyperplasia, necrosis, vacuolation, and mineralization. In the female rats, Abnormality consists of bile duct hyperplasia, necrosis, vacuolation, granuloma, fibrosis, and pigment. The combination of histopathological responses observed in each rat is not clear because of the nature of the reported summary data; for example, some rats may have had only bile duct hyperplasia and others may have had some or all responses.

To explore the significance of Sex, an exploratory Logistic model was fit to the pooled data in SAS 9.4.

$$\pi_i = \frac{\exp\{\beta_0 + \beta_1 * Concentration_i + \beta_2 * Sex_i + \beta_3 * Concentration * Sex_i\}}{1 + \exp\{\beta_0 + \beta_1 * Concentration_i + \beta_2 * Sex_i + \beta_3 * Concentration * Sex_i\}}$$

$i = 1, \ldots, 79$

Sex = 1 if female, 0 if male

is the expected probability of liver abnormality for rodent i

**Table B-26. Rat subchronic inhalation study data used in NIOSH risk assessment—response proportion for liver abnormalities.**

| | Response proportion | | | |
|---|---|---|---|---|
| | Exposure concentration, µg/m³ | | | |
| Rat study and sex | 0 | 49 | 133 | 515 |
| Sung et al. [2009]—Male | 0/10 | 0/10 | 1/10 | 4/9 |
| Sung et al. [2009]—Female | 3/10 | 5/10 | 5/10 | 9/10 |
| Pooled* | 3/20 | 5/20 | 6/20 | 13/19 |

*Histopathology results from Tables 9 and 10 of Sung et al. [2009]; data at end of 13-week exposure.

The interaction term was found to be not statistically significant ($p = 0.5821$). In the resulting simpler logistic model, Sex was found to be statistically significant. Thus, the liver abnormality data for male and female rats should not be pooled, as the female rats were approximately 4.3 times more likely than males to develop a liver abnormality (Table B-27). Visually, the dose-response curves are distinct, further supporting the statistically significant difference in liver abnormality development rates between male and female rats (Figure B-21).

**Table B-27. Logistic model fit statistics for the modifying effects of sex on rat liver abnormalities induced by subchronic exposure to silver nanoparticles from Sung et al. [2009].**

| Analysis of maximum likelihood estimates | | | | | | | |
|---|---|---|---|---|---|---|---|
| **Parameter** | | **DF** | **Estimate** | **Standard error** | **Wald Chi-Square** | ***P* value** | **Exp(Est)** |
| **Intercept** | | 1 | -2.1516 | 0.5393 | 15.9179 | <.0001 | 0.116 |
| **Concentration** | | 1 | 0.00636 | 0.00185 | 11.8632 | 0.0006 | 1.006 |
| **Sex** | Female | 1 | 1.4493 | 0.4064 | 12.7205 | 0.0004 | 4.260 |

DF: degrees of freedom; Exp(Est): Euler's constant raised to the power of the value in the estimate column.

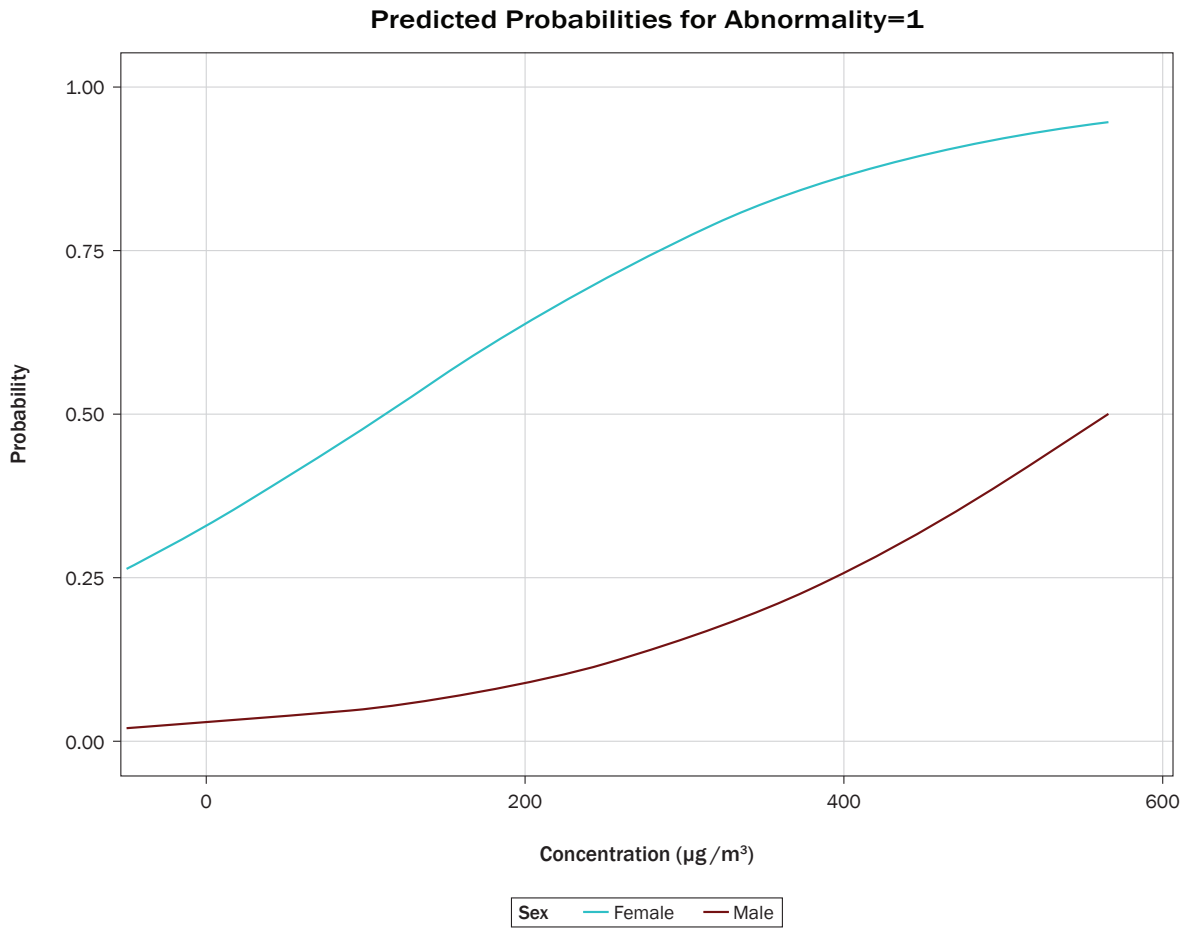


Figure B-21. Logistic model fits to data on male and female rat liver abnormalities induced by subchronic exposure to silver nanoparticles in Sung et al. [2009].

### *B.4.2.3 Point of Departure Estimation for Liver Abnormality*

The liver bile duct hyperplasia data were previously analyzed, and benchmark doses (the doses associated with 10% added risk of hyperplasia) were estimated for each sex separately.

The liver abnormality data for each sex were modeled separately with use of EPA BMDS 2.6. All available models were considered (Gamma, Quantal Linear, Logistic, Log-Logistic, Log-Probit, MS2, MS3, Probit, Weibull). Default modeling options were used. The benchmark response was set at added 10% risk. The best model chosen is that having the smallest AIC, where the goodness-of-fit *p* value is greater than 0.1.

#### B.4.2.3.1 Male Liver Abnormality

All models had adequate goodness-of-fit (Table B-28), and the best-fitting model was the Quantal Linear (Figure B-22).

**Table B-28. Summary of EPA BMDS model fits to data on male rat liver abnormalities induced by subchronic exposure to silver nanoparticles in Sung et al. [2009].**

| Model | *P* value | AIC | BMC, µg/m³ | BMCL, µg/m³ |
|---|---|---|---|---|
| Quantal-Linear | 0.888 | 21.9566 | 111.126 | 57.2667 |
| Log Probit | 0.9257 | 23.1059 | 152.078 | 48.1568 |
| Log Logistic | 0.8873 | 23.2415 | 159.484 | 43.6585 |
| Gamma | 0.8797 | 23.2533 | 163.03 | 62.2946 |
| Weibull | 0.8704 | 23.2952 | 165.104 | 61.9547 |
| Multistage Degree 3 | 0.8395 | 23.3923 | 173.845 | 61.1904 |
| Multistage Degree 2 | 0.8395 | 23.3923 | 173.845 | 49.1907 |
| Probit | 0.6167 | 24.057 | 244.293 | 158.211 |
| Logistic | 0.5749 | 24.2378 | 268.699 | 173.98 |

AIC: Akaike Information Criterion; BMC: Benchmark concentration estimate; BMCL: Benchmark concentration, 95% lower confidence limit estimate, associated with 10% added risk.

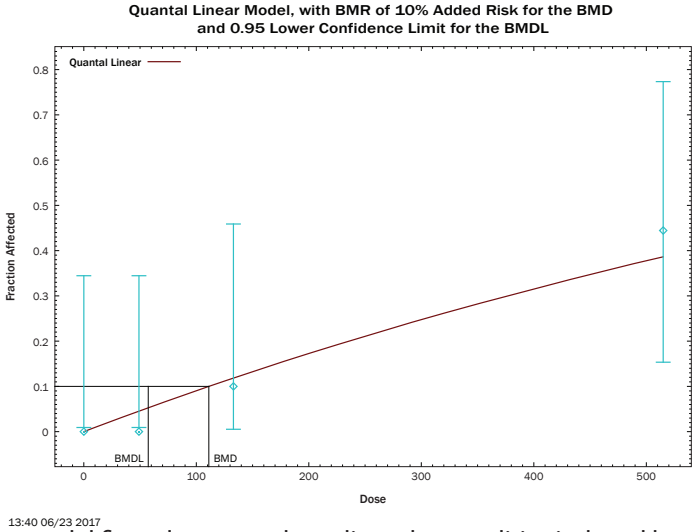


Figure B-22. Quantal linear model fit to data on male rat liver abnormalities induced by subchronic exposure to silver nanoparticles in Sung et al. [2009].

#### B.4.2.3.2 Female Liver Abnormality

All models had adequate goodness-of-fit, and the best-fitting model was the Logistic (Figure B-23). The Probit and Logistic models had equal AIC estimates, but the Logistic model had the smaller BMD estimate (Table B-29).

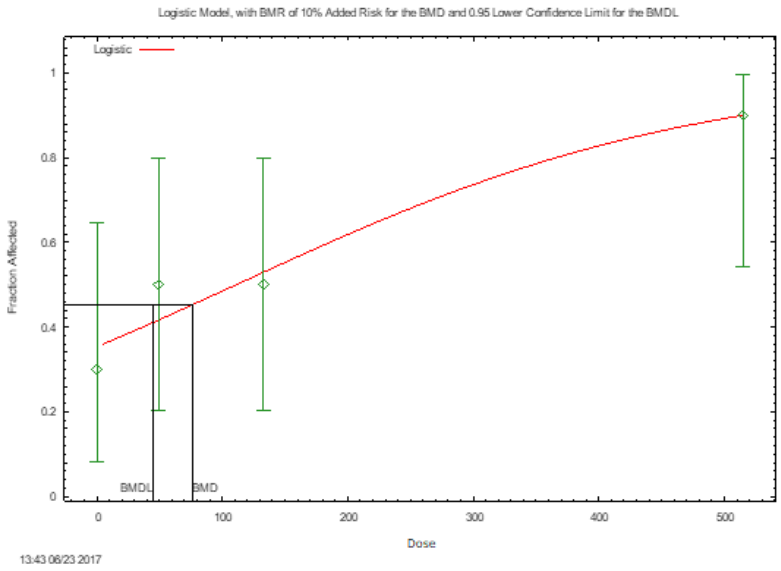


Figure B-23. Logistic model fit to data on female rat liver abnormalities induced by subchronic exposure to silver nanoparticles in Sung et al. [2009].

**Table B-29. Summary of EPA BMDS model fits to data on female rat liver abnormalities induced by subchronic exposure to silver nanoparticles in Sung et al. [2009].**

| Model | *P* value | AIC | BMC, µg/m³ | BMCL, µg/m³ |
|---|---|---|---|---|
| Logistic | 0.7993 | 50.892 | 76.629 | 44.541 |
| Probit | 0.7996 | 50.8919 | 80.359 | 50.3944 |
| Quantal-Linear | 0.7916 | 50.9086 | 45.9117 | 20.3863 |
| Multistage Degree 3 | 0.5298 | 52.8376 | 61.5382 | 20.5724 |
| Multistage Degree 2 | 0.5169 | 52.8622 | 59.9452 | 13.6063 |
| Weibull | 0.4966 | 52.9035 | 52.4935 | 20.3995 |
| Gamma | 0.4942 | 52.9086 | 46.0966 | 20.3863 |
| Log Logistic | 0.4144 | 53.1072 | 79.0148 | 0.136955 |
| Log Probit | 0.3922 | 53.171 | 67.6935 | 0.143749 |

AIC: Akaike Information Criterion; BMC: Benchmark concentration estimate; BMCL: Benchmark concentration, 95% lower confidence limit estimate, associated with 10% added risk.

### B.4.3 Conclusion

There were statistically significant differences in the observed proportions of rats with liver bile duct hyperplasia and liver abnormality between males and females in the Sung et al. [2009] study; females were roughly four times more likely to have a response. Therefore, the data for the two sexes should not be pooled.

Benchmark concentrations were estimated separately for male and female liver abnormality. In Table B-30 and Table B-31, the data and results are summarized.

**Table B-30. Response proportions in Sprague-Dawley rats following subchronic inhalation exposure to silver nanoparticles [Sung et al. 2009].**

| | Liver Abnormality | | | |
|---|---|---|---|---|
| | Concentration, µg/m³ | | | |
| Group | 0 | 49 | 133 | 515 |
| Males | 0/10 | 0/10 | 1/10 | 4/9 |
| Females | 3/10 | 5/10 | 5/10 | 9/10 |

**Table B-31. Best-fitting benchmark concentration (BMC) models of subchronic inhalation responses to silver nanoparticles in Sprague-Dawley rats [Sung et al. 2009].**

| Model | AIC | *P value* | BMC, µg/m³ | $BMCL_{10}$, µg/m³ |
|---|---|---|---|---|
| Male: Liver abnormality | | | | |
| Quantal Linear | 21.9566 | 0.888 | 111.1 | 57.3 |
| Female: Liver abnormality | | | | |
| Logistic | 50.892 | 0.7993 | 76.6 | 44.5 |

AIC: Akaike Information Criterion; BMC: Benchmark concentration estimate; BMCL: Benchmark concentration, 95% lower confidence limit estimate, associated with 10% added risk.

## B.5 Evaluation of Biomarker Findings in Silver Jewelry Workers

### B.5.1 Summary of findings

The findings of increased DNA damage and oxidative stress among jewelry workers who were exposed to silver nanomaterials [Aktepe et al. 2015] were statistically evaluated in this analysis to determine if these findings could be verified on the basis of the information provided in the report. The authors gave summary statistics that are sufficient for replication.

The authors measured differences in DNA damage and plasma parameters between a group of silver jewelry workers (n = 35) and a control group (n = 41) from a similar area in Mardin, Turkey. The authors state that the silver workers were exposed to silver particles via inhalation for at least 4 hours a day. The two groups were shown to be similar in socioeconomic status, mean age, mean BMI, and proportion of smokers. Comparisons (group characteristics and biological effects) were evaluated by Student's *t*-test at a significance level of 0.001. The authors conclude that DNA damage and oxidative stress measurements were statistically significantly higher in the group of silver workers; therefore,

"exposure to silver particles among silver jewelry workers caused oxidative stress and accumulation of severe DNA damage."

Review of the statistical methods and results highlighted several concerns. First, the conclusion of causality is tenuous, given the experimental design. Second, the descriptions of the working environment and exposures are lacking. No information was given about silver levels in the blood. Third, the results of several of the statistical tests could not be replicated with the provided summary statistics. Fourth, the statistical test used (Student's *t*-test) is not appropriate in some cases, given the types of measurements (e.g., severity scores). Despite these concerns, it does appear that being a silver worker in Mardin, Turkey, is associated with differences in the measured biological effects.

## B.5.2 Statistical evaluation of findings

This study reports a causal relationship between silver particle exposure and oxidative stress and severe DNA damage. This was not a completely randomized experiment, so establishing causality is not an automatic conclusion; other factors (i.e., lurking variables) could contribute to the effects seen but were not directly measured.

The authors state only that the silver jewelry workers were "working at least 4 h in a day." There is no further information about length of employment or job tasks (e.g., smelting would likely have a higher exposure than working with silver wires). There is no description of exposure controls or the working environment. There is no description about the form of the silver exposure other than "particle or nanoparticle," e.g., dust or fume.

The "control" group (in quotes because it is more of a comparison group; the subjects were volunteers, as stated by the author) and the exposed group were compared on Socioeconomic Status (SES), Age, BMI, and Proportion of Smokers. To establish if silver exposure is associated with the biological effects of interest, the two groups must be highly similar, with the only difference being the exposure to silver particles. No data are provided about SES, but the authors claim the SES of the two groups was similar. Summary statistics (mean, standard deviation, sample size) are provided for the measurements of Age and BMI. Comparisons were made by the authors, using Student's two-sample *t*-test (in SPSS 11.5), which assumes the following:

- The two groups are independent.
- Measurements within each group are independently and identically approximately normally distributed.

Student's *t*-test has been shown to be robust to some deviation from these assumptions, and the assumptions are probably met for these data.

The authors state there is not a statistically significant difference in average age between the two groups ($p < 0.231$), nor in average BMI ($p < 0.234$).

These results were replicated in SAS 9.3 with Proc TTEST (Table B-32). It was assumed that population variances were equal; this assumption was verified via the F-test at the 5% level of significance, and *p* values were greater than 5% (not shown).

**Table B-32. Replication results for age and BMI comparisons.**

| Variable | Author's *P* value | Replicated *P* value |
|---|---|---|
| Age, years | <0.231 | 0.2123 |
| BMI, kg/m$^2$ | <0.234 | 0.0226 |

The difference in average BMI was found to be more significant than stated by the authors; because the authors chose a 0.1% level of significance (presumably) *a priori*, their conclusions that the groups are similar with respect to Age and BMI remain the same in light of the replication differences.

There may have been a mistake by the authors when comparing the proportion of smokers between the two groups (41 control subjects, 35 silver workers). The authors report the proportion as $\frac{\#\text{Yes}}{\#\text{No}}$ rather

than $\frac{\#Yes}{n}$ and find a $p$ value of <0.427. If one conducts the two-sided hypothesis test for two incorrect proportions,

$$\text{Proportion of Smokers in Patients} = \frac{15}{20}$$
$$\text{Number of Patients} = 20$$
$$\text{Proportion of Smokers in Controls} = \frac{16}{25}$$
$$\text{Number of Controls} = 25$$

then the resulting $p$ value is 0.429, which is similar to that which was reported by the authors.

The comparison of the correct proportions was made with a chi-square test from Proc Freq. The resulting $p$ value was 0.7347, indicating that there is not a statistically significant difference in proportion of smokers between the two groups. Again, the author's conclusion that there isn't a difference remains the same in light of the replication difference (and possible computational error).

Thus, it does appear that the comparison group is similar to the silver worker group in the dimensions of SES, Age, BMI, and Smoking Proportion.

This same process follows for the comparison of mean responses for six biological effects: TAS (total antioxidant status), TOS (total oxidant status), OSI (oxidative stress index, the sum of TAS and TOS), Ceruloplasmin, Total thiol, and Mononuclear leukocyte DNA damage. All of these appear to be continuous measurements and could reasonably be approximately normally distributed, except for the last measurement, DNA Damage, meaning a two-sample $t$-test is sufficient for testing for differences in the average responses between the two groups.

DNA Damage is a total score of 100 slides, where each slide is rated 0, 1, 2, 3, or 4 (undamaged to maximally damaged). Thus, for each subject, the total score could range from 0 to 400. This is a combination of ordinal measures, which may not be suitable for Student's $t$-test; a non-parametric test would typically be used. Without the individual scores, a proper replication cannot be done. Interpreting the results of this $t$-test as indicating there is a difference in average DNA damage score may be incorrect, given the improper use of the statistical test.

The six comparisons were replicated with use of Proc TTest in order to check the reported $p$ value ranges (Table B-33).

**Table B-33. Replication results for biological response comparisons.**

| Variable | Author's $p$ value | Replicated $p$ value |
|---|---|---|
| TAS | <0.05 | 0.0041 |
| TOS | <0.001 | 0.0005 |
| OSI | <0.001 | <0.0001 |
| Ceruloplasmin | <0.01 | 0.0017 |
| Total Thiol | <0.001 | <0.0001 |
| DNA Damage | <0.001 | <0.0001 |

The replications tend to agree with the $p$ value ranges of the authors. It is unclear why the authors chose to report ranges rather than the actual $p$ value, but it seems to indicate that the $p$ value was larger than 0.001 (the author's chosen level of significance) for TAS or Ceruloplasmin.

## B.6 Conclusions

Despite replication differences and having only summary statistics, it does appear that the silver workers are being affected by their silver exposure. The comparison group and silver worker group do appear to have similar characteristics, with the exception being silver exposure. Their average levels of TOS, OSI, and Total Thiol are statistically significantly different from the comparison group. Comparisons of TAS and Ceruloplasmin were not significant at the author's chosen level of significance. The statistical evaluation of DNA Damage completed by the authors is flawed because the nature of the measurements is not commensurate with the assumptions of a $t$-test. Therefore, a conclusion is unclear at this point.

For all of these comparisons, it would be helpful to see a discussion of the practical effects. For example, is a decrease of 0.11 millimoles/L in the average TAS biologically significant? As another example, for the DNA Damage metric, the control group had an average score (standard deviation of scores) of 7.48 (5.46) and the silver workers had an average score of 15.37 (6.07). The minimum score per worker is 0 and the maximum score is 400. Is a total score of 15 out of 400 indicative of severe DNA damage?

Across these biological effect comparisons, it does appear that the silver jewelry workers have statistically significantly different measurements compared to a similar non-exposed group, which suggests a potential need for occupational safety measures for silver jewelry workers.

## B.7 References

See References (Section 9) in main document.

This page intentionally left blank.

# APPENDIX C

## Literature Search Strategy

The research question for these literature searches is "What evidence is available to evaluate the potential health risks associated with occupational exposure to silver nanomaterials?" Three main searches were conducted: (1) during 2012–2014, with findings reported in the external review draft NIOSH Current Intelligence Bulletin (CIB): Health Effects of Occupational Exposure to Silver Nanomaterials, December 18, 2015; (2) during 2016–2017, with findings reported in the revised external review draft of the CIB, August 24, 2018; and (3) during 2019, in a specific search to determine if any additional studies that might pertain to the risk assessment had been published since the previous searches.

During each of the literature searches, the articles were retrieved if found to be relevant following examination of titles and abstracts by the authors. The articles selected from the literature searches for full review included any in vivo studies on silver nanoscale or microscale particles. In the updated literature searches (2016), in vitro studies that provided information on the role of physicochemical properties on the toxicity of microscale or nanoscale silver were selected. All selected publications were individually reviewed and considered for inclusion in the CIB on the basis of relevance to occupational exposure or to toxicological effects in humans, animals, or cell systems. All relevant studies found are included in this review. Any issues identified with regard to study design or quality are discussed in the document.

The total number of publications on silver nanomaterials evaluated in this review includes seven studies of exposure in workers, 111 studies in animals, and 75 studies in cells. Of these, the primary studies that NIOSH selected for the quantitative risk assessment and derivation of the recommended exposure limit for silver nanomaterials are the two published subchronic inhalation studies of rats exposed to silver nanoparticles (Section 6). All other publications on studies in animals or cells were used in evaluations of the biodistribution and clearance of silver, the toxicological effects associated with exposure, the possible biological modes of action, and the physicochemical properties of silver nanomaterials that may affect the toxicity observed in the experimental studies. Details for each literature search are described below.

First, the initial literature search, record retrieval, and evaluation of studies were conducted by the Oak Ridge Institute for Science and Education (ORISE). A report was submitted to NIOSH in June 2012 that provided an evaluation of the experimental animal (in vivo) and cellular (in vitro) studies with silver nanoparticles. Studies cited in the report were identified from literature searches using PubMed, Toxline, Embase, and BIOSIS. Search terms included silver nanoparticles as well as other relevant key words (e.g., toxicology, physical and chemical properties, dosimetry). NIOSH conducted updated and expanded literature searches in January 2013 and June 2014 to identify studies with occupational exposure to silver and/or silver nanomaterials. Search terms were selected to ensure that all in vivo and in vitro studies with silver and/or silver nanomaterials were identified, as well as studies describing workplace exposure. Literature searches were conducted in the online databases CINAHL, PubMed, Compendex, Embase, HSDB, NIOSHTIC-2, Risk Abstracts, Toxicology Abstracts, Toxline, and Web of Science. The findings from these literature searches were reported in the December 18, 2015, external review draft of the CIB. The draft document at this stage included a total of 267 citations, including 42 cell studies, 51 animal studies, and 5 studies involving occupational exposure to silver nanomaterials (with known handling or production of silver nanomaterials or with silver nanomaterials being identified from exposure monitoring).

Second, following the public review of the draft CIB through April 2016, NIOSH responded to comments to update the literature search by conducting additional literature searches, covering the dates of January 1, 2011, to June 30, 2016. These searches were conducted with the online databases PubMed, Embase, and Toxline. Several discrete subject areas were identified, and a set of search

terms was identified for each study area. These were assembled into the following search strings:

human — ((Occupational OR occupation OR occupations OR workplace OR worksite OR worker OR workers OR employee OR employees) AND (silver OR nanosilver OR nano-silver)),

animal — ((Murine OR mouse OR mice OR rat OR rats OR rodent OR rodents OR hamster OR hamsters OR rabbit OR rabbits) AND (Inhalation OR inhaled OR inhale OR "intratracheal instillation" OR "pharyngeal aspiration") AND (silver OR nanosilver OR nano-silver)),

oral — ((Murine OR mouse OR mice OR rat OR rats OR rodent OR rodents OR hamster OR hamsters OR rabbit OR rabbits) AND (oral) AND (silver OR nanosilver OR nano-silver)),

dermal — ((Porcine OR pig OR pigs) AND (dermal OR skin) AND (silver OR nanosilver OR nano-silver)),

in vitro — ((In vitro) AND (lung OR liver OR pulmonary OR hepatic) AND (silver OR nanosilver OR nano-silver)),

cell-free — (("Cell-free") AND (silver OR nanosilver OR nano-silver)),

zebrafish — ((Zebrafish AND (silver OR nanosilver OR nano-silver)).

NIOSH conducted another literature search in October 2016 to update the search results through the end of the third quarter (September 2016). Searches were conducted in PubMed, Embase, Scopus, and Toxline. In addition to the previously described subject areas, two new subject areas were added, and their corresponding search strings were as follows:

kinetics — ((Silver OR nanosilver OR nano-silver) AND (PBPK OR "physiologically-based pharmacokinetic model" OR biodistribution OR bio-distribution OR clearance OR fate OR kinetics) AND (worker OR workers OR occupation OR occupations OR occupational OR workplace OR workplaces OR worksite OR worksites OR murine OR mouse OR mice OR rat OR rats OR rodent OR rodents OR hamster OR hamsters OR rabbit OR rabbits));

reproductive — ((Silver OR nanosilver OR nano-silver) AND (reproductive OR reproduction OR developmental)).

The results of the 2016 literature searches are reported in Table C-1, by database and subject area.

**Table C-1. Results of 2016 literature searches, by database and subject area.**

| String | PubMed | Embase | Toxline | Scopus |
|---|---|---|---|---|
| animal | 66 | 107 | 50 | NA |
| cell-free | 52 | 91 | 300 | NA |
| dermal | 41 | 317 | 13 | NA |
| human | 418 | 384 | 264 | NA |
| in-vitro | 172 | 372 | 171 | NA |
| oral | 149 | 197 | 86 | NA |
| zebrafish | 85 | 121 | 61 | NA |
| kinetics | 152 | 379 | 77 | 142 |
| reproductive | 1,020 | 677 | 352 | 1,472 |

NA: not applicable (search not performed in those topic areas).

The combination of the 2016 literature searches yielded 7,788 results, of which 4,448 remained after removing duplicate records in EndNote. Records were further curated to those which were topical (relating to silver toxicology, exposure, and epidemiology), with English-language full text available from accessible databases. An additional 121 references were selected for inclusion in the document, resulting in a total of 388 citations, including 33 new cell studies, 59 new animal studies, and 2 new studies involving occupational exposure to silver nanomaterials (with known handling or production of silver nanomaterials or with silver nanomaterials being identified from exposure monitoring).

In January 2017, NIOSH conducted a focused search in PubMed to evaluate further the biological significance of the rat biliary hyperplasia response to silver nanoparticles. The search terms included bile duct hyperplasia, etiology; hyperplasia, liver, etiology, human; and cholangiocarcinoma, biliary hyperplasia, and pathogenesis in various combinations. This specific review was designed to inform the evaluation of whether biliary hyperplasia seen in subchronic studies was or was not potentially related to general hepatobiliary damage. Titles and, where relevant, abstracts were reviewed and the publications relevant to the potential translational relevance of rat biliary hyperplasia were selected for inclusion. As a result, three additional references were included from this search. The findings from the 2016–2017 literature searches were reported in the August 24, 2018, revised external review draft of the CIB.

Third, in April 2019, NIOSH conducted a final literature review to determine if any additional subchronic or chronic studies of rodents or studies of humans had been published that might pertain to the risk assessment. The search was conducted from July 2016 forward, to ensure that any studies retroactively added to the database were not omitted. The following search string was used in PubMed:

- ((silver[Title/Abstract] OR nano-silver [Title/Abstract] OR nanosilver [Title/Abstract]) AND (human[Title/Abstract] OR worker[Title/Abstract] OR chronic[Title/Abstract] OR subchronic[Title/Abstract] OR sub-chronic[Title/Abstract])) AND ("2016/07/01"[PDAT] : "3000s"[PDAT])

This 2019 search returned 1,449 results. All articles without available full text in English were excluded, as were those with titles and abstracts not indicating an original subchronic or chronic rodent toxicology study, or human occupational study, with exposure to silver nanomaterials. Five studies were evaluated further, of which one was already cited. The two animal studies that reported on subchronic oral exposure to silver nanoparticles were selected for addition to the document. No additional studies pertaining to the quantitative risk assessment of inhalation exposure to silver nanomaterials were found in the 2019 search.

A focused search was conducted in December 2019 and January 2020 for examples (including from official organizations such as U.S. EPA, OSHA, and FDA) regarding the consequences of persistent lung inflammation and its role in hazard classification when present in animal studies. Searches were conducted in PubMed, Google Scholar, and government websites; search terms included lung inflammation, hazard identification, risk assessment, interspecies extrapolation, pneumoconiosis, byssinosis, cotton dust, endotoxin, pathogenesis, adverse respiratory health effect, and respiratory tract toxicity. No date exclusions were used. In addition, two major medical reference texts were consulted and cited. Seven references were added on this topic.

The number of studies selected from the three main literature searches is reported in Table C-2. These literature search findings were reported in the two external review draft documents and the final document.

**Table C-2. Number of studies of silver nanomaterials cited in the CIB based on experiments in cells or animals or with reported occupational exposure.**

| Study type | No. of studies cited in CIB | | |
|---|---|---|---|
| | 2015 Draft | 2018 Draft | 2020 Final |
| Cell | 42 | 75* | 75* |
| Animal | 51 | 110 | 112 |
| Occupational exposure | 5 | 7 | 7 |

*Indicates that more than one article by the same author regarding the same subject material and cell-type were considered as part of a single study.

This page intentionally left blank.

# APPENDIX D

## In Vitro/Mechanistic Studies

A considerable number of research reports address the impacts of AgNPs on isolated cellular systems. These studies provide inferential evidence of the capacity of AgNPs to bring about cellular changes of potential toxicological consequence, and in many cases they contribute to our understanding of what biochemical and physiologic mechanisms might be triggered when AgNPs interact with cellular systems. In an extensive database of in vitro studies, the predominant topic areas for cellular and subcellular changes brought about by AgNPs are (1) development of oxidative stress and the induction of apoptosis and (2) DNA damage/genotoxicity. In the following paragraphs, results of in vitro and mechanistic studies of AgNPs are discussed within these general topic areas. Other relevant studies highlight possible impacts of AgNP exposure on gene expression and regulation, neurologic changes, effects on skin cells, and cytotoxicity.

## D.1 Oxidative Stress/Induction of Apoptosis

A wide range of cellular isolates and cultures have been used to examine cellular uptake of AgNPs and the oxidative stress and apoptotic effects of AgNPs in vitro. These studies provide some evidence of the toxic potential of the particles and provide insight into the physiologic and biochemical mechanisms that may be responsible. Among the many cellular systems that have formed a platform for these investigations are liver/hepatoma cells [Piao et al. 2011; Liu et al. 2010a; Arora et al. 2009; Kim et al. 2009c; Hussain et al. 2005a; Avalos Funez et al. 2013; Gaiser et al. 2013; Garcia-Reyero et al. 2014; Kermanizadeh et al. 2012, 2013; Paino et al. 2015; Sahu et al. 2014a, 2014b, 2014c, 2016a, 2016b; Shannahan et al. 2015; Sun et al. 2013]; rat alveolar and mouse peritoneal macrophages [Park et al. 2010b; Carlson et al. 2008; Hussain et al. 2005b]; fibroblasts [Wei et al. 2010; Arora et al. 2009, 2009; Hsin et al. 2008; Avalos et al. 2015]; HeLa cells [Miura et al. 2009]; human acute monocytic leukemia cell lines (THP-1 monocytes) [Foldbjerg et al. 2009; Braakhuis et al. 2016]; tumoral leukemia cells (HL-60) [Avalos Funez et al. 2013]; rat vascular smooth muscle cells [Hsin et al. 2008]; bovine retinal endothelial cells [Kalishwaralal et al. 2009]; mouse blastocysts [Li et al. 2010]; mouse MC3T3-E1 cells, rat adrenal PC12 cells, human HeLa cervical cancer cells and hamster ovary CHO cells [Kim et al. 2012]; A549 human lung cells [Lee et al. 2011a; Liu et al. 2010a; Foldbjerg et al. 2011; Stoehr et al. 2011; Beer et al. 2012; Chairuangkitti et al. 2013; Han et al. 2014]; A431 human skin carcinoma cells [Arora et al. 2008]; SGC-7901 human stomach cancer cells [Liu et al. 2010]; MCF-7 human breast adenocarcinoma cells [Liu et al. 2010a]; murine alveolar cell line and human macrophage and epithelial lung cell lines [Soto et al. 2007; Braakhuis et al. 2016; Jeanette et al. 2016]; human colon carcinoma (CaCo2) cells [Sahu et al. 2014a, 2014b, 2014c, 2016a, 2016b]; prostate cancer (VcAP), pancreas cancer (BxPC-3), and lung cancer (H1299) [He et al. 2016]; hamster kidney (BHK21) and human colon adenocarcinoma (HT29) cell lines [Gopinath et al. 2010]; human mesenchymal stem cells (hMSCs) [Greulich et al. 2009, 2011; Hackenberg et al. 2011]; rat aortic endothelial cells [Shannahan et al. 2015]; human umbilical vein endothelial cells [Braakhuis et al. 2016; Guo et al. 2016]; peripheral blood and mononuclear cells [Paino et al. 2015; Sarkar et al. 2015]; and human adipose-derived stem cells (hASCs) [Samberg et al. 2012].

Examples of the general approach to in vitro experimentation with AgNPs may be found in studies conducted at Wright-Patterson Air Force Base in which rat alveolar macrophages were incubated with different sizes of AgNPs [Hussain et al. 2005b; Carlson et al. 2008]. The cells, at 80% confluence, were incubated for 24 hours with various concentrations of hydrocarbon-coated AgNPs in a physiologic medium. The particles were 15, 30, 55, or 100 nm in diameter. Parameters under investigation included cellular morphology and uptake of AgNPs, mitochondrial function, membrane integrity, generation of reactive oxygen species (ROS), glutathione content, mitochondrial membrane potential, and the inflammatory response.

Study results indicated that AgNPs with the smallest diameter were more effective than larger nanoparticles at bringing about physiologic and toxicological

changes. For example, at silver concentrations up to 75 μg/mL, 15-nm AgNPs appeared to be more effective at releasing lactate dehydrogenase (LDH) from the cells, as a measure of lowered cell viability. Similarly, when the fluorescence intensity of dichlorofluorescein (DCF) in the presence of AgNPs was assessed for the various incubation products, 15-nm silver nanoparticles appeared to induce a greater intensity of fluorescence, a response indicative of enhanced generation of ROS. Concomitant with the enhanced generation of ROS was a statistically significant depletion of cellular reduced glutathione (GSH) levels, lowered mitochondrial function as indicated in the 3-(4,5-dimethylthiazol-2-yl)-2,5-diphenyltetrazolium bromide (MTT) viability assay, and the loss of mitochondrial membrane potential.

Carlson et al. [2008] also demonstrated a treatment-related increase in tumor necrosis factor (TNF)-α, macrophage inflammatory protein-2, and interleukin (IL)-1β but not IL-6 in the supernatant of macrophage/AgNP incubations. The authors suggested that the depletion of GSH levels may have created an imbalance between antioxidants and ROS, thereby resulting in oxidative stress and cellular damage. However, the degree to which this effect was related to the release of cytokines/chemokines remained unclear, because these responses did not appear to be influenced by particle size.

Arai et al. [2015] investigated differences between ionic silver and AgNP in murine macrophages (J774.1). Exposures to 20-, 60-, or 100-nm AgNP or an equal concentration of $AgNO_3$ were conducted in medium with 1% albumin for 24 hours. It was observed that unfunctionalized AgNP grew 2.1 to 3.4 times larger in the presence of 1% albumin, whereas citrate-capped AgNPs retained their nominal size in solution. The cytotoxicity EC50 values were 34.8, 27.9, 51.8, and 4.51 μg Ag/mL, indicating that the 100-nm AgNPs were less toxic than the 20- or 60-nm AgNPs but that ions were more toxic than all the AgNPs. Inhibition of glutathione synthesis had no effect on $AgNO_3$ cytotoxicity, which may indicate that dissolved ions are cytotoxic by a different, non-ROS-dependent pathway. Additionally, HPLC-ICP-MS was used to determine preferential silver binding. Ionic silver was eluted with the metallothioneins, whereas silver was detected in the AgNP sample with high-molecular-weight proteins. The authors identified AgNPs in the lysozyme by microscopy and indicated an expectation that they would be present in other organelles but not free-floating in the cytoplasm. Finally, a parallel in vivo experiment demonstrated the dispersal of inhaled AgNPs throughout ICR mice to secondary organs.

Sarkar et al. [2015] studied how differing AgNP size and surface modification might yield different effects on human monocyte–derived macrophage function. Four AgNP types were studied: each combination of 20- or 110-nm particles with citrate or PVP stabilization. Exposures were 5, 10, 20, or 50 μg/mL, for 3, 6, or 24 hours. Reduced viability was noted only for 24-hour exposures, as measured by LDH leakage. Testing after 4-hour exposure showed an increase in mRNA coding for IL-1β only at 25 μg/mL, whereas a dose-dependent increase in IL-8 mRNA and a decrease in IL-10 were also noted, indicating an inflammatory response. Infection with *Mycobacterium tuberculosis* indicated AgNP exposure also suppressed the typical *M. tuberculosis*–induced expression of several NF-κB, which may inhibit immune responses. No statistically significant differences were noted in size or surface function, and comparison to both the stabilizers alone and carbon black NPs indicated that AgNPs were causing the toxicity.

Given the importance of the liver as an important target organ of toxicity associated with AgNPs, a number of research groups have used cultures of hepatocytes to investigate the possible toxic effects of AgNPs in vitro. For example, the Wright-Patterson Air Force Base group, using BRL 3A rat liver cells, studied a range of endpoints [Hussain et al. 2005a] similar to those previously evaluated with use of rat alveolar macrophages [Hussain et al. 2005b; Carlson et al. 2008]. The two species of AgNPs employed were defined by diameters of either 15 or 100 nm, although little additional information was provided about the method of formation or their potential for aggregation. Using dose concentrations of 5 to 50 μg/mL and incubation times of up to 24 hours, the authors measured cytotoxicity by leakage of LDH

and deficits in mitochondrial function in the presence of MTT. Other parameters under investigation included changes in cellular morphology, formation of ROS, depletion of GSH levels, and changes to mitochondrial membrane potential. Both sets of AgNPs appeared to effectively induce a concentration-dependent depletion of mitochondrial function and the release of LDH to the culture medium. Under the microscope, the cells displayed a range of distortions in comparison with untreated cells, and by analogy to the same group's results with rat alveolar macrophages, they showed a concentration-dependent increase in ROS and depletion of GSH. Hussain et al. [2005a] concluded that the cytotoxicity of AgNPs was likely to be mediated through oxidative stress.

Many of these same manifestations of oxidative stress and cell viability were evident when cultured HepG2 human hepatoma cells were incubated with commercially obtained 10-nm AgNPs dispersed in an aqueous medium [Kim et al. 2009c]. The researchers ensured that any deficits in these parameters could be unequivocally assigned to the effect of the AgNPs by using an ion exchange resin to remove any free silver ions that might have been associated with the nanoparticle preparations. Then, in parallel incubations, they compared the capacity of equivalent amounts of silver in AgNPs and solutions of silver nitrate to reduce cell viability and/or induce oxidative stress and DNA damage. Cytotoxicity was measured with MTT and AB reduction assays and by LDH leakage, and data were expressed as median inhibitory concentration ($IC_{50}$) values.

For each parameter under investigation, increasing concentrations of silver brought about a reduction in cell viability in a dose-dependent manner. However, for both dye-reduction assays, free silver ions reduced cell viability to a greater extent than did the silver nanoparticles. By contrast, release of LDH activity was brought about more completely and at a lower silver concentration by incubation with AgNPs than with free silver ions (with $IC_{50}$ of 0.53 ± 0.19 versus 0.78 ± 0.10 μg/mL). This difference was not statistically significant. Pre-incubation of the cells with N-acetylcysteine (NAC) abolished these manifestations of reduced cell viability by a presumed reduction in the oxidative stress that had become apparent whether the cells were incubated with either AgNPs or a silver solution. Moreover, further evidence of the importance of oxidative stress in relation to AgNP toxicity was obtained by including the antioxidant N-acetylcysteine in the incubation medium 2 hours prior to the addition of the AgNP or silver nitrate preparations. Deficits in mitochondrial function and cellular membrane integrity and the occurrence of oxidative stress were largely abolished by this pretreatment.

Kim et al. [2009c] used intracellular fluorescence as an indicator of the formation of ROS in the presence of either AgNP or silver anion preparations. In each case, ROS formation was abolished by pretreatment with NAC. In an effort to understand the mechanism(s) whereby AgNPs caused intracellular oxidative stress, the authors used RT PCR to study the expression of oxidative stress–related genes such as glutathione peroxidase 1 (GPx1), catalase, and superoxide dismutase 1. In contrast to the effect of aqueous silver nitrate, AgNPs did not induce messenger ribonucleic acid (mRNA) expression of GPx1. However, the mRNA levels of catalase and superoxide dismutase 1 were increased in response to 24-hour incubation with AgNPs. Detection of phosphorylation on the H2AX gene, indicative of DNA double-strand breaks, was also thought to be associated with oxidative stress, because this effect was abolished as well after pre-incubation with N-acetylcysteine. Kim et al. [2009c] concluded that silver in free solution or in nanoparticles induced cytotoxicity as a result of oxidative stress. However, because the expression of oxidative stress–related mRNA species appeared to be regulated differently by AgNPs than by silver cations, the precise mechanism of AgNP activity may be different from that of soluble silver.

HepG2 cells were also used as a platform for the study of AgNP toxicity by Liu et al. [2010]. The researchers used PVP-coated nanoparticles with defined sizes of 5, 20, and 50 nm. All AgNP preparations were formed chemically by the reduction of silver nitrate by sodium hypophosphite in the presence of sodium hexametaphosphate and PVP, adjusted to a concentration of 1 g/L in deionized

water, and dispersed by ultrasonication. In evaluating HepG2 responses to AgNPs, Liu et al. [2010a] observed changes to cell morphology, viability, membrane integrity, and induction of oxidative stress by experimental procedures that were closely similar to those previously described. Ultrastructural analysis using TEM revealed the presence of AgNPs inside the cells, with the smaller particles apparently more effective at penetrating the membrane and inducing the toxic effects.

Liu et al. [2010a] attempted to distinguish between apoptotic and necrotic cell death as a result of AgNP treatment with the double-staining technique, using annexin V-fluorescein isothiocyanate (FITC) for apoptosis and propidium iodide (PI) for necrosis. When HepG2 cells were incubated at 0.5 μg/mL for 24 hours, the relative amounts of apoptotic cells were 4.64%, 8.28%, 6.53%, and 4.58% for silver nitrate and AgNPs (5 nm, 20 nm, and 50 nm), respectively, all compared to an incidence in controls of 2.39%. The authors concluded that despite the increased fraction of apoptotic cells in the silver-exposed groups, there was no difference between the treated and control groups for necrosis. Therefore, the AgNP-induced cell death was caused mainly by apoptosis.

HepG2 cells, along with Caco2 human colon carcinoma cells, were the subject of several studies by Sahu et al. [2014a, 2014b, 2014c, 2016a, 2016b]. The initial studies used 20-nm AgNPs as well as $AgNO_3$ as a comparative source of Ag ions [Sahu et al. 2014a, 2014b, 2014c], whereas the later studies included analogous exposures of the same cells to 50-nm AgNP under similar conditions [Sahu et al. 2016a, 2016b]. Cells were exposed at concentrations of up to 20.0 μg/mL. Generally, it was also found that HepG2 cells were affected at lower doses than Caco2 cells. Stronger genotoxic responses and pro-apoptotic markers were observed in AgNPs than Ag ions from 0.1 to 1.0 μg/mL, but this trend reversed in the range of 10–20 μg/mL. Specifically, responses such as micronuclei formation were noted only in cases of AgNP exposure but not in cases of Ag ion exposure. Interestingly, the authors observed evidence of mitochondrial damage but did not directly detect a difference in oxidative stress.

Ávalos Fúnez et al. [2013] studied HepG2 cells and HL-60 tumoral human leukemia cells. After exposing cells to citrate-stabilized AgNP with a range of 30–123 nm for up to 72 hours, both had statistically significantly reduced viability (measured by MTT assay) and LDH release at concentrations as low as 0.84 μg/mL. However, this could be mitigated by the addition of the antioxidant N-acetyl-L-cystine to the medium, indicating toxicity through AgNP-induced oxidative stress.

Paino et al. [2015] studied the effects of polyvinyl-alcohol (PVA)-coated AgNP exposure on HepG2 cells and normal human peripheral blood mononuclear cells (PBMCs). Cells were exposed for 24 hours to PVA-AgNP (4.0–11.7 nm in diameter) at concentrations of 1.0 and 50.0 μM, resulting in decreased viability. Specifically, an increase in early apoptotic cells was noted for both concentrations and cell lines, as well as DNA damage (by comet assay). Likewise, an increase in necrotic cell population was present except for the 1.0 μM exposure in HepG2 cells. Isolated neutrophils also showed statistically significantly increased oxidative stress following PCA-AgNP exposure (by DCFDA assay).

Kermanizadeh et al. [2012, 2013] also observed indicators of oxidative stress in two studies on the human hepatoblastoma cell line C3A after exposure to AgNPs. In these studies, AgNPs (specifically 17-nm-diameter NM-300) were found to result in upregulation of IL-8 and increased oxidative stress (assayed by glutathione and reduced GSH levels) after 24 hours of exposure. However, pretreatment with the antioxidant 6-hydroxy-2,5,6,7,8-tetramethylchroman-2-carboxylic acid mitigated these effects. Additionally, after 8 weeks of exposure, there was statistically significant DNA damage (indicated by comet assay). The response to AgNPs occurred at higher concentrations relative to zinc oxide NPs, titanium oxide NPs, and multi-walled carbon nanotubes [Kermanizadeh et al. 2012]. A later study [Kermanizadeh et al. 2013] indicated that the $LC_{50}$ of NM300 AgNPs was approximately 24 hours at 2 μg/mL, but it could not detect a statistically significant change in IL-6, TNF-α, or C-reactive protein levels or any effect on albumin or urea concentrations.

Gaiser et al. [2013] conducted a study both in vitro and in vivo on AgNP toxicity to the liver. The in vitro portion of the study used the C3A cell line and NM300 AgNPs. Following a 24-hour exposure to 0-625 μg/cm$^2$ AgNPs, the medium was removed for LDH analysis and cells were stained with Alamar Blue. Quantitation of LDH yielded an $LC_{50}$ of 2.5 μg/cm$^2$. NP uptake by C3A cells into membrane-bound vesicles was observed with confocal microscopy. Reduced GSH was also examined following exposure to 1, 2, and 4 μg/cm$^2$ AgNPs at 2, 6, and 24-hour time points, with no statistically significant changes. Levels of IL-1β, IL-8, IL-10, TNF-α, MCP-1, and IL-1RI mRNA were examined by RT-PCR following 0.1, 0.5, and 1 μg/cm$^2$ AgNP exposures at 4- and 24-hour time points. IL-8 increased relative to control, except for the 24-hour time point of the 0.5-μg/cm$^2$ AgNP exposure; TNF-α increased after exposure to 0.1 μg/cm$^2$ AgNPs but decreased for 1 μg/cm$^2$ after 4 hours; and IL-1RI changed only at 0.1 μg/cm$^2$ at the 24-hour time point. FACS analysis of the medium of C3A cells after exposure to 1, 2, and 4 μg/cm$^2$ AgNPs indicated ICAM-1 and IL-8 release at 4 hours following 40 μg/cm$^2$ exposure and at 24 hours following 5 μg/cm$^2$ exposure.

Sun et al. [2013] investigated the effects of PVP-coated AgNPs of 10- or 30- to 50-nm diameter on primary rat hepatic stellate cells (HSCs). FITC-Annexin V and PI staining was used to identify apoptotic cells, and a dose-dependent increase in apoptotic rates was observed starting at 20 μg/mL, with 10-nm particles causing a higher apoptotic fraction than 30- to 50-nm particles. Cytokine analysis by ELISA indicated no statistically significant differences in HGF, Il-6, TGF-β1, or TNF-α levels, but both MMP-2 and -9 were reduced after a 48-hour exposure to 0.2 μg/mL AgNPs (of either size).

Shannahan et al. [2015] studied the effect of protein corona on AgNP toxicity in rat liver epithelial (RLE) and rat aortic endothelial (RAEC) cells. Citrate-stabilized 20-nm AgNPs were incubated with human serum albumin (HAS), bovine serum albumin (BSA), or high-density lipoprotein (HDL) at 10°C for 8 hours. Their hydrodynamic sizes were 69.99, 30.60, and 62.10 nm, respectively. HAS and BSA were found to reduce the dissolution rate, whereas HDL increased it. Several changes in protein structure were observed. In both RLE and RAEC, a protein corona reduced uptake, though no strong correlation with hydrodynamic size could be established. Hyperspectral analysis indicated that 2 hours after exposing RLE or RAEC to AgNPs, those AgNPs underwent a blue shift, indicating a loss of the protein corona. However, cytotoxicity of AgNPs was reduced by the protein corona after a 3- or 6-hour exposure of 50 μg/mL, and adding a scavenger receptor B inhibitor (SR-BI) further reduced cytotoxicity. In RLE, AgNP-HDL was found to increase IL-6 expression, and SR-BI could prevent this. This was also true for all AgNPs in RAEC.

Connolly et al. [2015] investigated the cytotoxicity of NM-300K AgNPs in several rainbow trout cell types: RTH-149 and RTL-W1 liver cells, RTG-2 gonadal cells, and primary hepatocytes. AgNP concentrations from 0.73 to 93.5 μg/mL were tested, as well as Ag ion concentrations of 0.0345 to 345 μg/mL ($AgNO_3$). Both relative cell sensitivities and absolute $IC_{50}$ values varied, depending on whether Alamar Blue, CFDA-AM, or neutral red uptake assays were used. In general, each assay–cell type pair showed $IC_{50}$ values for AgNPs over tenfold greater than $AgNO_3$, with AgNP $IC_{50}$ values ranging from 10.9 to 32.2 μg/mL in RTL-W1, 19.4 to 24.9 μg/mL in RTH-149, 37.2 to 43.1 μg/mL in RTG-1, and 30.6 to 45.2 μg/mL in primary hepatocytes.

Piao et al. [2011] incubated human Chang liver cells with AgNPs prepared by the THF approach to demonstrate oxidative stress and to probe the biochemical and physiologic mechanisms that might be associated with this phenomenon. The authors reported that the nanoparticles had undergone a degree of aggregation in the incubation medium, with a size distribution of 28 to 35 nm in diameter, an increase from the original 5 to 10 nm. Cellular morphology, viability, mitochondrial efficiency, intracellular formation of ROS, and GSH levels were measured by means of "standard techniques," with and without N-acetylcysteine. A comparison of equivalent amounts of silver on nanoparticles or in solution in the MTT assay gave $IC_{50}$ values that

differed by a factor of two. This suggested that silver in nanoparticle form was more damaging to the cells than silver in free solution ($IC_{50}$ of 4 μg/mL for AgNPs, versus 8 μg/mL for silver nitrate).

In mechanistic analysis, the spectrum of intracellular proteins was surveyed by Western blot analysis, and a comet assay was performed to determine the degree of oxidative DNA damage. Flow cytometry was used to determine the percentage of apoptotic sub-G1 hypodiploid cells, and the amount of cellular DNA fragmentation was assessed by cytoplasmic histone-associated DNA fragmentation. The expected picture of oxidative-stress-related cytotoxicity and partial blockade with N-acetylcysteine was obtained. The comet assay showed that incubating human Chang liver cells with silver nanoparticles increased the tail length and the percentage of DNA in the tails, as compared to control cells. Other markers of oxidative stress, such as the levels of lipid peroxidation and the degree of protein carbonyl formation, were increased in AgNP-treated cells compared to control cells.

The authors of the study compiled an array of mechanistic data that pointed to AgNP-induced induction of apoptosis via a mitochondrial and caspase-dependent pathway. For example, after treatment with AgNPs, the AgNP-associated decrease in Bcl-2 expression and concomitant increase in Bax expression resulted in the following increases in Bax/Bcl-2 ratio with time: 1.0, 7.0, 9.5, 12.8, and 24.5 at 0, 6, 12, 24, and 48 hours, respectively. A change in ratio at this level led to the release of cytochrome from the mitochondrion and the occurrence of active forms of caspases 9 and 3. The authors interpreted their data as indicating that AgNP-induced apoptosis might be mediated through a caspase-dependent pathway with mitochondrial involvement.

The importance of c-Jun $NH_2$-terminal kinase (JNK) in mediating the apoptotic effects in human Chang liver cells was demonstrated by its time-dependent phosphorylation in the presence of AgNPs. In parallel with the retention of cell viability, the effect was attenuated by pretreatment with the JNK-specific inhibitor SP600125 or by transfection with small, interfering RNA against JNK [Piao et al. 2011].

Many of the same responses that indicated induction of oxidative stress and apoptosis in macrophages and liver cells have also been observed in fibroblasts when incubated with AgNPs. For example, Arora et al. [2008] used a commercial preparation of AgNPs (7–20 nm in diameter) in an aqueous suspension to challenge HT-1080 human fibrosarcoma cells and A431 human skin carcinoma cells. With use of a variant of the MTT assay for mitochondrial function with the compound sodium 3′-[1-(phenylaminocarbonyl)-3, 4-tetrazolium]-bis (4-methoxy-6-nitro) benzene sulfonic acid hydrate, a dose-dependent effect on cell viability was obtained in the concentration range of 6.25 to 50 μg/mL. Subsequent incubation of the cultures at one half the median inhibitory concentration ($IC_{50}$) of approximately 11 μg/mL gave an array of responses indicative of oxidative stress, including a reduction in GSH content and SOD activity and an increase in lipid peroxidation. An increase in treatment-related DNA fragmentation and a biphasic response in caspase-3 activation (in which the enzyme was induced up to a AgNP concentration of 6.25 μg/mL but suppressed at higher concentrations) indicated that cell death occurred by apoptosis at AgNP concentrations up to 6.25 μg/mL but by necrosis at higher concentrations.

However, AgNP-induced oxidative stress and apoptosis were less evident when the same researchers carried out equivalent studies in primary mouse fibroblasts and liver cells [Arora et al. 2009]. Respective $IC_{50}$ values were 61 and 449 μg/mL, and little change was seen in intracellular GSH and lipid peroxidation at one half the $IC_{50}$. The AgNPs in these studies were synthesized by an unspecified proprietary process. They were reported to be stable in culture media, with >90% of the particles with diameters between 7 and 20 nm. Possible agglomeration of the particles in the culture media was not mentioned. The results suggest that the primary cell preparations contained sufficient antioxidant capacity to protect the cells from possible oxidative damage.

Similar to the results reported by Piao et al. [2011] from studies with human Chang liver cells, the study by Hsin et al. [2008] used NIH3T3 fibroblasts

to investigate the link between the mitochondria-related generation of ROS, the incidence of apoptosis, and the activation of JNK. Incubating mouse L929 fibroblasts with nanoparticles also resulted in an increased incidence of apoptosis and a greater percentage of cells arrested in the G2M phase of the cell cycle [Wei et al. 2010]. Larger-scale silver entities (silver microparticles with a range of shapes and diameters between 2 and 20 μm) did not bring about these changes and were not internalized by the cells to the same extent as AgNPs. Transmission electron micrographs appeared to provide direct evidence that AgNPs but not microparticles entered the cells via an endocytic pathway. The authors concluded that AgNPs were more cytotoxic than silver microparticles to L929 cells. Differences were characterized by the ability of nanoparticles to enter the cells, causing morphologic abnormalities and apoptosis, and the cell cycle being arrested in the G2M phase.

Avalos et al. [2015] investigated the effects of AgNPs (4.7 and 42 nm) and gold NPs (30, 50, 90 nm) on human pulmonary fibroblasts (HPF). Cytotoxicity was assayed 24, 48, and 72 hours after exposure to NP by both MTT and LDH assays. MTT assays detected viability loss at 0.84 μg/mL at 24- and 72-hr time points for 4.7-nm AgNP and at 1.68 μg/mL for the 48-hour time point; LDH assays detected differences at all time points at 3.36 μg/mL or less. For the 42-nm particles, LDH assay detected differences at all time points at 13.45 μg/mL or less, whereas MTT assay detected differences by 100 μg/mL. Addition of NAC reduced the cytotoxic effect, suggesting an oxidative stress mechanism. ROS assay by DCF fluorescence demonstrated a 1.32-fold increase after exposure to 7.66 μg/mL 4.7-nm AgNPs and a 1.55-fold increase after exposure to 1150 μg/mL 42-nm AgNPs. AgNP exposure also depleted total glutathione content, though no statistically significant change in superoxide dismutase (SOD) activity was detected by ELISA.

Foldbjerg et al. [2009] used a human acute monocytic leukemia cell line (THP-1 cells) as a platform for studying the relative capacity of AgNPs and ionic silver to induce ROS, apoptosis, and necrosis. As obtained from the supplier, the particles were 30 to 50 nm in diameter and coated with 0.2% PVP. When the AgNPs were prepared in a stock solution, a major peak size of 118 nm was obtained. This preparation, as well as an equimolar solution of silver cations, was used to incubate THP-1 at a dose range of 0 to 7.5 μg/mL (calculated as silver mass), with an incubation time of up to 24 hours.

The fluorescent marker, DCF, was used to measure the intracellular generation of ROS, and the annexin V/PI double-staining technique was used to discriminate between cells undergoing apoptosis or necrosis. The presence of apoptosis was confirmed with the terminal deoxynucleotidyl transferase dUTP nick-end labeling (TUNEL) assay. As indicated by the results of the annexin V/PI assay, both AgNPs and silver cations brought about a statistically significant reduction in the percentage of viable cells after 24 hours' exposure. The median effective concentrations ($EC_{50}$) were 2.4 and 0.6 μg/mL, respectively, indicating that silver cations were approximately four times more toxic than AgNPs. Silver nanoparticles and silver cations likewise increased the production of ROS, as indicated by the differential formation of DCF. A 35% increase in cells positive for DNA breakage was observed in comparison with controls when THP-1 cells were incubated with AgNPs for 6 hours at a concentration of 5 μg/mL.

In general, the findings of this study point to a strong correlation between the increase in intracellular ROS, DNA damage, and high levels of apoptosis and necrosis for both AgNPs and ionic silver. In a follow-up study, Beer et al. [2012] evaluated the degree to which the silver ion fraction of AgNP suspensions contribute to the toxicity of AgNPs, using the A549 human lung carcinoma epithelial-like cell line. PVP-coated (0.2%) spherical AgNPs, with dimensions ranging in size from 30 to 50 nm, were exposed to suspensions/supernatants containing either 39% (0.2 μg/mL) or 69% (1.6 μg/mL) silver ions for 24 hours. At 1.6 μg/mL total silver, A549 cells exposed to an AgNP suspension containing a 39% silver ion fraction showed a cell viability of 92%, whereas cells exposed to an AgNP suspension containing a 69% silver ion fraction had a cell viability of 54%, as measured by the

MTT assay. At initial silver ion fractions of 5.5% and above, AgNP-free supernatant had the same toxicity as AgNP suspensions. Flow-cytometric analyses of cell cycle and apoptosis confirmed that there was no statistically significant difference between the treatments with AgNP suspension and AgNP supernatant, as measured by MTT assays. A clear association was observed between the amount of silver ions present in the solution and the toxicity of the AgNP suspensions. As found in the study of Foldbjerg et al. [2011], ionic and/or nanoparticulate silver induces ROS in A549 cells.

Braakhuis et al. [2016] used a co-culture model of human bronchial epithelial (16HBE), umbilical vein endothelial (HUVEC), and acute monocytic leukemia (THP-1) cells to assess the toxicity of AgNPs. First, 16HBE cells were seeded and allowed to grow to confluence before addition of differentiated THP-1 cells. Then, on the basal side of a transwell insert membrane with 0.4-μm pores, HUVEC cells were seeded. Solutions of AgNPs 10, 20, 50, and 100 nm in diameter in 2 nM citrate were used as stock for preparing exposure medium. Cell activity of 16HBE cells, as assayed by WST-1 cell-proliferating agent absorbance, decreased after 24 hours of exposure to 30 μg/mL AgNPs, regardless of size. Electron spin resonance assay of ROS in buffer showed that 10- and 20-nm AgNPs were associated with additional $H_2O_2$-induced hydroxyl radical formation, but 50- and 100-nm AgNPs were not. Intracellular ROS, as measured by DCFDA assay, doubled on exposure to AgNPs but did not show a statistically significant dose-response relationship. AgNP exposure did create a dose-dependent decrease of MCP-1 and increase in IL-8 release, as measured by ELISA. The authors noted that dose-response correlations could be stronger for either AgNP mass or surface area, depending on the endpoint selected.

Liu et al. [2010a] examined the impact of different sizes of AgNPs on oxidative stress and incidence of apoptosis in HepG2 cells, also using cultures of SGC-7901 human stomach cancer cells, MCF-7 human breast adenocarcinoma cells, and A549 human lung adenocarcinoma cells to ensure the universality of the toxic effect. This study was followed up by Lee et al. [2011a] to investigate the cytotoxic potential of AgNPs and the pathways by which they impact A549 cells. In addition to findings that AgNPs induce the reduction in cell viability, increase LDH release, alter cell cycle distribution, and change the expression of Bax and Bcl-2, reflective of increased apoptosis, AgNPs were also found to alter mRNA levels of protein kinase C (PKC) isotypes.

Chairuangkitti et al. [2013] examined both ROS-dependent and ROS-independent pathways of AgNP toxicity in A549 cells. The AgNPs were approximately 40–90 nm in diameter. Cytotoxicity was assayed by MTT assay at 24- and 48-hour post-exposure time points following exposure to 0, 25, 50, 100, or 200 μg/mL AgNPs; a 35% and 50% loss of viability after 24 and 48 hours, respectively, was noted at 200 μg/mL. Cytotoxicity was assayed by DCFDA at 3 hours post-exposure to 0, 25, 50, 100, or 200 μg/mL AgNPs; at 200 μg/mL a twofold increase in ROS levels was noted. Mitochondrial membrane potential was assayed by TMRE assay at 24-, 48-, and 72-hr post-exposure time points following exposure to 0, 100, or 200 μg/mL AgNP, and the portion of TRME-positive cells decreased in a dose-dependent manner with AgNP exposure.

Pretreatment with 10 mM NAC could partially protect against the effects of AgNP exposure to viability and ROS levels, though the protective effect was greatest at time points of 24 hours or less. Cell cycle analysis by FACS with PI staining occurred at 24-, 48-, and 72-hour post-exposure time points following exposure to 0, 100, or 200 μg/mL AgNPs; both sub-G1 (including apoptotic) and S phase cell populations increased, while G1 populations decreased. Pretreatment with NAC reduced the sub-G1 population but did not affect the G1 or S populations, indicating cell cycle arrest not associated with ROS production. Western blot analysis of proliferating cell nuclear antigen (PCNA) at 72 hours post-exposure to 0, 100, or 200 μg/mL AgNPs indicated that PCNA is downregulated by AgNP exposure but is also not protected by NAC pretreatment. The combined results indicate both ROS- and non-ROS-mediated toxic pathways for AgNP exposure.

Han et al. [2014] investigated the oxidative stress response of A549 cells to two forms of 15-nm-diameter AgNP: one synthesized by addition of $AgNO_3$ to an *Escherichia coli* supernatant (bio-AgNP) and another by citrate-mediated synthesis (chem-AgNP). Comparing TEM and DLS showed that chem-AgNPs agglomerate more than bio-AgNPs. Viability was measured by MTT assay after 24 hours of AgNP exposure; the $IC_{50}$ was indicated as about 25 μg/mL for bio-AgNP and about 70 μg/mL for chem-AgNP. This disparity was also present in membrane integrity measurements: LDH assays after 24 hours of AgNP exposure showed greater leakage for chem-AgNP than for bio-AgNP, especially over concentrations of 20 μg/mL. ROS measured by DCFDA assay was shown to be concentration-dependent and to increase over post-AgNP exposure incubation times (6, 12, 24 hours). Mitochondrial transmembrane potential by JC-1 assay indicated AgNPs, particularly bio-AgNPs, resulted in depolarization of the mitochondrial membrane (this is often linked to apoptotic pathways). Cellular uptake by TEM analysis also noted AgNP uptake into autophagosomes and autolysosomes that differed in structure from those of unexposed cells, leading the authors to speculate that AgNP exposure triggered autophagosome formation.

Soto et al. [2007] also used the results from a series of assays with A549 cells to compare the cytotoxicity potential of a wide range of nanoparticle materials, including AgNPs, titanium dioxide ($TiO_2$), multiwall carbon nanotubes, chrysotile asbestos, $Al_2O_3$, $Fe_2O_3$, and $ZrO_2$, using both a murine lung macrophage cell line (RAW 264.7) and a human lung macrophage cell line (THB-1). Relative cell viabilities were measured at a constant nanoparticulate material concentration of 5 μg/mL for the different cell lines. All of the nanoparticulate materials, except for $TiO_2$, showed a cytotoxic response, and AgNPs were particularly cytotoxic to the murine lung macrophage cell line. The nanoparticulate materials were observed to have a greater toxic effect in A549 cells, with the $TiO_2$ samples demonstrating a slight cytotoxic response. The A549 cells were found to be more sensitive than the murine and human macrophages. No correlation was found when particle surface area was used as an index for comparing cytotoxicity. Particle morphology or aggregate morphology was also not correlated with the cytotoxicity response for either the murine or the human cell line exposure, because a variety of morphologies within the nano-size range exhibited equivalent or similar cytotoxicity.

The degree of cell viability after 24-hour incubation with AgNPs was assessed in HeLa cells with use of Alamar Blue reagent as a probe for cell viability [Miura and Shinohara 2009]. An $IC_{50}$ of 92 μg/mL silver was obtained. The AgNPs were provided by the supplier with a specified diameter of 5 to 10 nm and were stabilized with a proprietary protectant. TEM analysis confirmed the particle size but showed the presence of some aggregates as well. To analyze for apoptosis, the authors incubated cells for 3 hours with various concentrations of AgNPs, double-stained with Annexin V (FITC-conjugated) and PI, and then analyzed by flow cytometry. As charted by the authors, AgNPs appeared to induce apoptosis in a dose-dependent manner up to 120 μg/mL.

In an effort to assess the expression level of genes potentially associated with apoptosis, Miura and Shinohara [2009] extracted total RNA from HeLa cells that had been incubated with silver nanoparticles for 4 hours and used RT-PCR to determine the expression of stress-related genes such as those for heme oxygenase-1, metallothionein-2A, and heat shock protein 70. Silver nanoparticles were effective in increasing the expression of heme oxygenase-1 and metallothionein-2A several-fold but not heat shock protein-70. This discrepancy was different from the pattern of gene expression obtained when cells were exposed to cadmium sulfate, in which all three stress-related genes were strongly expressed in response to treatment.

Guo et al. [2016] investigated the effects of 10-, 75-, and 110-nm AgNPs or $AgNO_3$ in vitro and in vivo. HUVEC cultures were used to further probe the results of the mouse injection study. Histopathology showed that treating HUVEC cultures with 1 μg/mL AgNPs was sufficient to erode the dense VE-cadherin at the cell junction and reduce cytoskeleton

actin fiber length. It was noted that $AgNO_3$ had greater toxicity, followed by 110-nm AgNPs and, finally, by 10- and 75-nm AgNPs. However, Hoerscht/PI staining indicated that $AgNO_3$ promoted necrosis, whereas AgNPs promoted early apoptosis. The authors speculate that the reason is that AgNPs are uptaken, whereas $AgNO_3$ instead damages membranes directly. Additionally, a DCFDA assay showed that AgNPs increased ROS, whereas $AgNO_3$ did not, indicating that silver ions have a different mechanism of action.

Jeanett et al. [2016] compared the effects of exposure to spark-generated 20-nm carbon black NPs (CNPs) or AgNPs to human bronchial epithelial (HBE) cells. In addition to the BEAS-2B cell line, two additional HBE cultures were developed from organ donors: one normal, and one with cystic fibrosis (CF). Cell death was assessed by LDH assay after 4 and 24 hours of exposure. In normal HBE and BEAS-2B cells, necrosis at 24 hours was low for both CNPs and AgNPs; however, necrosis was increased in CF HBE relative to normal HBE by 12% to18% for AgNPs and 6% to 9% for CNPs. Similarly, CF HBE caspase-3 activity was twofold to fourfold greater than normal HBE caspase-3 activity in exposures. The authors concluded there are increased levels of IL-6 and IL-8 in all models after exposure to CNPs or AgNPs and an increase in MCP-1 in BEAS-2B.

Gopinath et al. [2010] examined the effects of AgNPs on gene expression in an endeavor to assess the fundamental mechanisms that contribute to AgNP-induced cell death through mediated apoptosis. Hamster kidney (BHK21) and human colon adenocarcinoma (HT29) cells were treated with <20-nm-diameter AgNPs for 30 minutes to 6 hours. In order to assess the mode of cell death induced by AgNPs, treated cells were stained with FITC Annein V and PI for flow cytometric analysis. An increase in the early apoptotic population was observed in treated BHK21 cells (9%) and HT29 cells (11%), compared to control cells. Expression profiles of apoptotic genes such as bak, bax, bad, C-myc, and caspase-3 were analyzed, and an upregulation of p53 gene in the AgNP-treated cells was observed. On the basis of these gene expression profiles, the investigators proposed that AgNP treatment of both BHK21 and HT29 cells leads to programmed cell death (that is, apoptosis) as a result of a cascade reaction that activates caspase-3, which penetrates the nuclear membrane to induce DNA fragmentation. This extracellular cytotoxic stress on the cell membrane upregulates p53, which in turn acts on other apoptotic molecules and causes the mitochondria to induce apoptosis.

Schaeublin et al. [2011] evaluated the response to silver nanowires (4 or 20 μm in length; ~90 nm in diameter) in an in vitro co-culture assay with human alveolar lung cells 24 hours after exposure to 200 ng/mL. Neither AgNW length was toxic to the cells (on the basis of normal cell morphologic appearance) or decreased the cell viability (on the basis of MTS assay of mitochondrial function). However, both AgNW lengths were associated with an increase in some inflammatory cytokines (IL-6, IL-8, and interferon gamma). These results showed that the AgNWs were not cytotoxic at the dose evaluated but did cause irritant and inflammatory responses.

## D.2 DNA Damage/Genotoxicity

Ahamed et al. [2008] used mouse embryonic stem (MES) cells and mouse embryonic fibroblasts (MEF) to study the link between AgNP-induced apoptosis and DNA damage. Two types of AgNPs were used: uncoated plasma gas-synthesized particles and polysaccharide-coated particles, both approximately 25 nm in diameter. As visualized with a Cell Tracker Green fluorescent probe and observed under confocal microscopy, both types of AgNPs were taken up by the cell, although uncoated particles showed a greater tendency to aggregate and were excluded from certain organelles such as the nucleus and mitochondria. Coated particles were distributed throughout the cell.

As determined by Western blot analysis, expression of annexin V protein was enhanced by both species of nanoparticles, confirming the role of AgNPs in the induction of apoptosis in these cell lines. This was accompanied by upregulation of the

p53 tumor suppressor gene, increased induction of the Rad51 double-strand-break repair protein, and enhanced phosphorylation of the histone H2AX at the serine-139 residue. Because the latter effect is also thought to occur in response to a DNA double break, the authors interpreted their data as an indication that both types of AgNPs had induced increased p53 expression and double-strand DNA breakage, with concomitant apoptosis in MES and MEF cells. Uncoated (and less agglomerated) particles appeared to be more effective in bringing about these responses.

Foldbjerg et al. [2011] detected perturbations in the genetic architecture of the human lung A549 cancer cell line in response to AgNPs and silver in solution. In the former case, the 30- to 50-nm particles were coated with 0.2% PVP. As before, the cytotoxicity of AgNPs and silver in solution was assessed by a decrease in mitochondrial activity with the MTT assay. Silver ions induced dose-dependent reductions in mitochondrial function to a greater extent than equivalent concentrations of silver in nanoparticle form. In both cases, these effects were reduced by pretreating the cells with NAC. However, AgNPs induced greater amounts of ROS, suggesting that these entities could not be solely due to the potential release of silver ions from the nanoparticles. AgNP-induced cytotoxicity and ROS formation were accompanied by the formation of bulky DNA adducts, as demonstrated by $^{32}P$ post-labeling. Although the chemical identity of adducts was not determined, the authors speculated that these endogenously formed "I-compounds" were similar to those found to accumulate in an age-dependent manner in the absence of exogenous carcinogens. The strongly correlated responses were both inhibited by pretreatment with the antioxidant N-acetylcysteine, suggesting the AgNPs had triggered ROS-induced genotoxicity.

The effect of particle shape and size of Ag particles on causing toxic and immunotoxic effects was investigated by Stoehr et al. [2011]. Silver nanowires (length, 1.5–25 μm; diameter, 100–160 nm), AgNPs (30 nm), and silver microparticles (<45 μm) were tested with alveolar epithelial cells (A549) for cell viability and cytotoxicity. AgNWs and AgNPs were synthesized by wet chemistry, whereas silver microparticles were synthesized by the reduction of silver salt with sodium citrate. AgNWs, AgNPs, and silver microparticles were all coated with PVP to make them biocompatible and to keep them dispersed in water. TEM analysis of sample preparations confirmed that AgNWs and AgNPs were mostly monodispersed with little agglomeration, while some sedimentation and minor agglomeration of the silver microparticles were observed. Eight different AgNW concentrations (range, 5.05–16.47 mg/mL) as well as single concentrations of AgNPs (0.33 mg/mL) and silver microparticles (13.5 mg/mL) were prepared that overlapped in mass concentration and surface area.

Ion release by the tested silver materials was determined by means of inductively coupled plasma mass spectrometry (ICP-MS), and the effects of the released ions on cell viability and LDH generation were measured. To compare the effects on an activated and a resting immune system, the epithelial cells were stimulated with rhTNF-α or left untreated. Changes in intracellular free calcium levels were determined with calcium imaging. No effects were observed with AgNPs and silver microparticles on A549 cells, whereas AgNWs induced a strong cytotoxicity, loss in cell viability, and early calcium influx; however, the length of the AgNWs had minimal effect on the observed level of toxicity. The investigators hypothesized that the increase in toxicity and the absence of specific immunotoxic responses to AgNWs may be a result of its needle-like structure, making it easier to penetrate the cell membrane. Also, because of the lengths of the AgNWs, entry into the cell may have been incomplete, causing cell membrane damage that resulted in impaired repair and eventually cell death.

Greulich et al. [2009] evaluated the biologic activity of AgNPs on human tissue cells by exposing hMSCs to PVP-coated AgNPs (~100 nm in diameter) and determining their effect on cell viability, cytokine release, and chemotaxis. AgNPs were prepared by the polyol process, and hMSCs were exposed to AgNP concentrations of 0.5, 1, 2.5, 3, 3.5, 4, 5, and 50 μg/mL or to silver ions (silver acetate) for up to 7 days.

At AgNP concentrations of 3.5 to 50 μg/mL, no viable cells were detected. When silver acetate was used, the cytotoxic effect of silver was observed at a silver concentration of 2.5 μg/mL, whereas no cytotoxic reactions of hMSC were observed with AgNPs at concentrations of ≤3 μg/mL and with silver acetate at concentrations of ≤1 μg/mL. There was also a statistically significant decrease in the release of IL-6, IL-8, and VEGF (typical set of cytokines from hMSCs) in the presence of AgNPs as well as with silver acetate in the concentration range of 5 to 50 μg/mL. Silver acetate concentrations below 2.5 μg/mL (for ions) and below 5 μg/mL (for AgNPs) did not lead to a decrease in cytokine formation. The findings indicate that AgNPs exert cytotoxic effects on hMSCs at high concentrations but also induce cell activation (as analyzed by the release of IL-8) at high but nontoxic concentrations of nanosilver.

The same investigators [Kittler et al. 2010] also studied the effect of aging on the toxicity of PVP- and citrate-coated AgNPs (diameter of metallic core, 50 ± 20 nm), using hMSCs at water-solution concentrations of 50, 25, 20, 15, 5, 2.5, and 1 mg/L. AgNPs were stored at these concentrations for 3 days, 1 month, and 6 months and evaluated for cell viability and morphology. Aged AgNPs (at 50 mg/L) stored for 1 and 6 months caused complete cell death, whereas at 3 days the reduction in viability was 70%. AgNPs that were stored in solution for 6 months had a lethal concentration that was about 20 times smaller than that of freshly prepared AgNPs, indicating the release of silver ions during storage. However, the released silver ions were probably bound by proteins and therefore rendered less toxic. Cell viability at 6 months increased as the concentration decreased. The dissolution rates for the PVP- and citrate-coated AgNPs were studied at different temperatures. Dissolution was only partial for each functionalized AgNP, and the degree of dissolution did not depend on the absolute concentration of silver nanoparticles but seemed to be an intrinsic (although temperature-dependent) property of the nanoparticles. The rate of dissolution and the final degree of dissolution were higher for the PVP-coated AgNPs than for the citrate-functionalized AgNPs.

In a follow-up study by the same investigators [Greulich et al. 2011], the uptake of AgNPs into hMSC was examined to determine if more than one endocytotic pathway was involved. PVP-coated AgNPs with a metallic core of 50 ± 20 nm in diameter were used. The uptake of AgNPs into hMSC was determined by exposing hMSC for 24 hours at concentrations of 2.5, 2.0, 1.5, 1.0, or 0.5 μg/mL silver ions (silver acetate) or 50, 30, 25, 20, or 15 μg/mL AgNPs and quantitatively analyzing the intracellular side scatter signal by flow cytometry. AgNP uptake by hMSCs was observed to occur by clathrin-dependent endocytosis and by micropinocytosis, and the ingested nanoparticles subsequently occurred as agglomerates in the perinuclear region but not in the cell nucleus, endoplasmic reticulum, or Golgi complex. The inhibition of the clathrin-mediated pathway did not result in complete suppression of endocytosis, indicating that more than one endocytotic pathway might be involved.

The widespread use of AgNP-treated dressings to heal wounds and prevent infection led Hackenberg et al. [2011] to investigate the dosimetry for the agent's ability to induce toxicity in hMSCs. As supplied, the nanoparticles had a mean diameter of 46 nm, although aggregation to a mean diameter of 404 nm was observed when the particles were dispersed in physiologic medium or situated within the cells. Statistically significant cytotoxicity was observed at a concentration of 10 μg/mL, and a degree of DNA damage was indicated in the comet assay and by an increase in chromosomal aberrations. Chromosomal aberrations consisting of chromatid deletions and exchanges were induced at concentrations of 0.1 μg/mL and above. Hackenberg et al. [2011] compared this concentration with published data on the growth inhibition of *Staphylococcus aureus*, for which AgNP concentrations of 3.5 μg/mL had been reported [Kim et al. 2007]. This led Hackenberg et al. [2011] to conclude that the cytotoxic and genotoxic potential of AgNPs in hMSCs occurred at higher doses than did their antimicrobial effects.

Similarly, Samberg et al. [2012] assessed the toxicity and cellular uptake of both undifferentiated and differentiated human adipose-derived stem cells

(hASCs) exposed to AgNPs and evaluated their effect on hASC differentiation. The stem cells were exposed to 10- or 20-nm AgNPs (confirmed by TEM analysis) at concentrations of 0.1, 1.0, 10.0, 50.0, and 100.0 μg/mL either before or after differentiation. Baseline-viable hASCs were first differentiated down the osteogenic and adipogenic pathways or maintained in their proliferative state for 14 days and then exposed for 24 hours at concentrations of 0.1 through 100.0 μg/mL. To evaluate potential cellular uptake of AgNPs into hASCs, undifferentiated hASCs were grown to 100% confluency in complete growth medium for 5 days, whereas the effects of AgNPs on hASC differentiation were determined also with use of undifferentiated hASCs grown to 100% confluency in complete growth medium for 5 days.

Exposure to either 10- or 20-nm AgNPs resulted in no statistically significant cytotoxicity to hASCs and minimal dose-dependent toxicity to adipogenic and osteogenic cells at 10 μg/mL. Adipogenic and osteogenic cells showed cellular uptake of both 10- and 20-nm AgNPs without morphologic changes to the cells, in comparison with controls. Exposure to 10- or 20-nm AgNPs did not influence the differentiation of the cells at any concentration and resulted in only a minimal decrease in viability at antimicrobial concentrations. Exposure to AgNPs also resulted in no statistically significant cytotoxicity to undifferentiated hASCs, either prior to differentiation or following 14 days of differentiation.

The association of AgNP incubation of IMR-90 human lung fibroblast cells and U251 human glioblastoma cells with genetic perturbations, as well as mitochondrial damage and ROS formation, was demonstrated by AshaRani et al. [2009]. The AgNPs employed in the study were administered at concentrations of 25, 50, or 100 μg/mL and were to have been synthesized by the reduction of silver nitrate solution with sodium borohydride, followed by the addition of a filtered starch solution with constant stirring. The starch-coated particles were 6 to 20 nm in diameter and were stated to have good stability in water. Consistent with the work of others, the study demonstrated uptake of the particles into the cell cytoplasm and nucleus, causing an alteration in cell morphology and reduced viability, deficits in mitochondrial performance, and ROS production. Whereas annexin-V staining showed that only a small percentage of cells underwent apoptosis, cell cycle arrest in the G2M phase and data from the comet and cytokinesis-blocked micronucleus assays gave an indication of treatment-associated DNA damage. For example, the comet assay of AgNP-treated cells showed a concentration-dependent increase in tail momentum, and chromosomal breaks were detected in the cytokinesis-blocked micronucleus assay. This effect was especially noticeable in the U251 cell line.

Nallathamby and Xu [2010] used a novel approach to chart the changes in cellular growth and subcellular morphology when mouse fibroblast (L929) tumor cells were incubated with AgNPs. The particles were synthesized by chemical reduction of silver chlorate with sodium borohydride and sodium citrate. The product was stable in aqueous solution and inside single living cells with a median diameter of 12 nm. When the cells were incubated in flasks with AgNPs at 0, 11, or 22 μg/mL, the uptake of particles and inhibition of growth occurred as a function of concentration and duration of exposure.

However, by culturing the cells on coverslips in Petri dishes, the impact of AgNPs on individual cells could be visualized by microscopy. The result was a dose- and exposure-related formation of cells with single giant nuclei or cells with two, three, or sometimes four nuclei per cell. After incubation for 72 hours, almost all of the L929 fibroblast cells displayed one of these altered nuclear states. The authors interpreted their data as indicating that AgNPs induce malsegregation of the chromosomes rather than having a direct effect on replication.

Mei et al. [2012] evaluated the mutagenic potential of uncoated AgNPs (average size, ~5 nm; range, 4–12 nm), using a mouse lymphoma assay system. Modes of action (MoA) were assessed by means of standard alkaline and enzyme-modified comet assays and gene expression analysis. The mouse lymphoma cells (L5178Y/TK$^{+/-}$) were treated with AgNPs at a concentration of 5 μg/mL for 4 hours, at which time

the AgNPs were observed to be in the cytoplasm of the lymphoma cells. AgNPs induced dose-dependent cytotoxicity and mutagenicity, with a marked increase in the mutation frequency at 4 and 5 μg/mL (<50% cell survival at ≥5 μg/mL), where nanosilver had a clastogenic MoA. In the standard comet assay there was no statistically significant induction of DNA damage, although the percentage of DNA in the tail increased slightly with increasing dose. However, in the oxidative DNA damage comet assays, addition of lesion-specific endonucleases resulted in statistically significant induction of DNA breaks in a dose-dependent manner.

Gene expression analysis with use of an oxidative stress and antioxidant defense polymerase chain reaction (PCR) array showed that the expressions of 17 of the 59 genes on the arrays were altered in the cells treated with AgNPs. These genes are involved in the production of ROS, oxidative stress response, antioxidants, oxygen transporters, and DNA repair. The investigators concluded the results indicated that the mutagenicity of AgNPs used in this study resulted from a clastogenic MoA.

Several of the studies cited above have revealed toxic effects on cells that often occurred in a dose-dependent manner; however, only a few studies have evaluated AgNPs and the role of particle size on cellular toxicity [Park et al. 2011c; Kim et al. 2012; Gliga et al. 2014]. The effects of AgNPs of different sizes (20, 80, 113 nm) have been compared in in vitro assays for cytotoxicity, inflammation, genotoxicity, and developmental toxicity [Park et al. 2011c]. Cytotoxicity was investigated in L929 murine fibroblasts and RAW 264.7 murine macrophages, and effects of AgNPs were compared to those of silver in ionic form. The role of AgNP size on the generation of ROS and on parameters of inflammation was also evaluated, as well as the dependence of particle size on developmental toxicity and genotoxicity in mouse embryonic cells and embryonic fibroblasts, respectively.

Metabolic activity of RAW 264.7 cells, embryonic stem cells, and L929 cells was evaluated with use of WST-1 cell proliferation reagent when the cells were exposed to AgNPs for 24 hours or for 10 days (embryonic stem cells). In both L929 fibroblasts and RAW 264.7 macrophages, metabolic activity was decreased (concentration dependently) by AgNPs as well as by ionic silver. For ionic silver, the decrease in metabolic activity was similar between the two cell types. In contrast, for AgNPs, the metabolic activity was more affected in 929 fibroblasts than in RAW 264.7 macrophages. In both cell types the 20-nm AgNPs were the most potent in decreasing metabolic activity.

In assessments of cell membrane integrity (LDH), 20-nm AgNPs were more potent in reducing the cell membrane integrity of L929 fibroblasts than was ionic silver, whereas ionic silver was more potent in RAW 264.7 macrophages. In addition, the cellular generation of ROS was observed to increase for 20-nm AgNPs but only marginally for the larger AgNPs when exposed to RAW 264.7 macrophages. The generation of ROS in macrophages occurred only at concentrations above those decreasing the metabolic activity of macrophages, suggesting a secondary effect rather than causing the onset of cytotoxicity. The 20-nm AgNPs were also found to be the most potent for causing embryonic stem cell differentiation. However, 20-nm AgNPs did not induce an increase in gene mutation frequencies (genotoxicity evaluation) at concentrations up to 3 μg/mL.

Kim et al. [2012] examined the size-dependent cellular toxicity of AgNPs, using three different sizes (~10, 50, and 100 nm in diameter). A series of cell lines, including osteoblastic MC3T3-E1 cells, rat adrenal PC12 cells, human cervical cancer HeLa cells, and hamster CHO cells, were exposed to AgNPs at doses of 10, 20, 40, 80, or 160 μg/mL to investigate the regulation of cell proliferation, ROS production, LDH release, apoptosis induction, and stress-related gene expression. Cell assays were conducted at 24, 48, and 72 hours after treatment with AgNPs. Results from assays suggested that AgNPs exerted statistically significant cytotoxic effects against all cell types, as indicated by decreased mitochondrial function, and that these effects occurred in a dose- and size-dependent manner. Both the MC3T3-E1 and PC12 cell lines were shown to be the most sensitive to toxic effects. In particular, the cytotoxic

response to AgNPs was cell-dependent, with apoptosis occurring in MC3T3-E1 and necrosis in PC12 cell lines. Moreover, 10-nm-diameter AgNPs had a greater apoptotic effect against the MC3T3-E1 cells than did AgNPs 50 and 100 nm in diameter.

Nymark et al. [2013] investigated the genotoxicity of PVP-coated AgNPs in BEAS-2B cells. The AgNPs had an average diameter of 42.5 nm; they were coated in PVP, characterized, and suspended in cell medium. Cytotoxicity was assessed by trypan blue dye exclusion, after exposure to 1.9 to 182.4 µg/mL AgNPs for 4, 24, or 48 hours. Approximately 50% viability was observed at 182.4 µg/mL after 4 hours or at doses exceeding 45.6 µg/mL at 48 hours, but with 34.2% cytotoxicity at the highest 24-hour dose.

Genotoxicity was assayed by alkaline comet assay after exposure to 7.6 to 182.4 µg/mL AgNPs for 4 or 24 hours, by micronuclear analysis with fluorescent microscopy after exposure to 10 to 240 µg/mL AgNP for 48 hours, and by chromosomal aberration assay with microscopy after exposure to 10–240 µg/mL AgNPs for 24 hours or 2.5 to 40 µg/mL for 48 hours. At 60.8 µg/mL and higher doses, 4- and 24-hour treatments caused at least a twofold comet tail increase, though micronuclei induction or chromosomal aberrations were not noted.

Gliga et al. [2014] also investigated the size- and coating-dependent toxicity of AgNPs following exposure of human lung cells (BEAS-2B). BEAS-2B cells were exposed to citrate-coated AgNPs of different sizes (10-, 40-, and 75-nm diameters) as well as to 10-nm PVP-coated and 50-nm uncoated AgNPs, at doses of 5, 10, 20, and 50 µg/mL. Study parameters included evaluation of particle agglomeration, cell viability, ROS induction, genotoxicity, γ$H_2$AX foci formation (a marker for DNA damage and repair), and intracellular localization. To assess cytotoxicity, BEAS-2B cells were exposed to AgNPs for 4 and 24 hours in an AB assay. After 4 hours, no statistically significant signs of toxicity of any of the AgNPs were observed, up to the highest dose tested. Statistically significant cell toxicity was evident only for the 10-nm citrate-coated AgNPs ($p \leq 0.05$) and 10-nm PVP-coated AgNPs ($p \leq 0.01$) after 24 hours for the doses of 20 and 50 µg/mL. No significant alterations of the mitochondrial activity of the BEAS-2B cells were observed at doses of 5 and 10 µg/mL or for the other AgNPs.

When the LDH assay was used for cytotoxicity determination, no statistically significant toxicity was observed after 4 hours for any of the AgNPs. However, statistically significant toxicity was observed after 24 hours for the 10-nm citrate-coated AgNPs ($p \leq 0.05$) and the 10-nm PVP-coated AgNPs ($p \leq 0.0001$) at the dose of 50 µg/mL. None of the larger AgNPs altered cell viability. In contrast, all AgNPs tested caused an increase in overall DNA damage after 24 hours when assessed by the comet assay, suggesting an independent mechanism for cytotoxicity and DNA damage. No γH2AX formation was detected, and no increased production of intracellular ROS was observed.

Despite different agglomeration patterns, there was no difference in the uptake or intracellular localization of the citrate- and PVP-coated AgNPs, and there was no coating-dependent difference in cytotoxicity. Furthermore, the 10-nm particles released more $Ag^+$ than did all other AgNPs (approximately 24% by mass, versus 4–7% by mass) following 24 hours in cell medium. The released fraction in cell medium did not induce any cytotoxicity, indicating that intracellular release of Ag could have been responsible for the toxicity.

The genotoxicity of AgNPs (range, 4–12 nm in diameter) was evaluated by Li et al. [2012], using a *Salmonella* reverse mutation assay (Ames) and an in vitro micronucleus test in TK6 human lymphoblastoid cells. The Ames assay was conducted according to OECD test guidelines, with use of *Salmonella typhimurium* tester strains TA98 and TA1537 for detection of frame-shift mutation and the use of tester strains TA100, TA1535, and TA102 for the measurement of base-pair substitution. For TA98 and TA100, frank toxicity (reduction of background revertant frequency and/or thinning of the background) was detected at 4.8 µg/plate and higher doses; toxicity was observed for TA1535 and TA1537 at 9.6 µg/plate and higher doses. At the highest dose of 76.8

μg/plate, all the bacteria from the five tester strains were killed. In general, AgNPs were found to be negative in the Ames test; this result may have been due to the agglomeration of the nanoparticles, making them too large to transport through the pores in the bacterial cell wall, or possibly due to the insensitivity of most tester strains to oxidative DNA damage.

Li et al. [2012] evaluated the cytotoxicity of AgNPs with use of lymphoblast TK6 cells treated at concentrations of 10 to 30 μg/mL. Cytotoxicity was measured with relative population doubling, which reflects a combination of cell growth, death, and cytostasis. A dose-response increase in micronuclei was observed at a dose of 25 μg/mL and was reported by the investigators as a weak positive, consistent with findings from other studies that tested various types of nanomaterials with mammalian cells.

To determine the mutagenic potential of colloidal AgNPs (average diameter, 10 nm), four histidine-requiring strains of *S. typhimurium* (TA98, TA100, TA1535, and TA1537) and one tryptophan-requiring strain of *Escherichia coli* (WP2uvrA) were used in the presence and absence of metabolic activation with S9 mix [Kim et al. 2013b]. In the absence of metabolic activation (that is, without S9 mix), cytotoxicity was found at ~62.5 μg/plate (TA98, TA1535, TA1537, and WP2uvrA) and at ~31.25 μg/plate (TA100). Cytotoxicity was also exhibited at concentrations of ~125 μg/plate (TA98, TA100, and TA1537) and ~250 μg/plate (TA1535 and WP2uvrA) in the presence of metabolic activation. Precipitation and aggregation of the AgNPs were also observed at a dose level greater than 1.25 μg/plate with and without metabolic activation. No statistically significant number of revertant colonies was observed for any of the bacterial strains, with or without metabolic activation, in comparison with the negative control. No dose-dependent increase of revertant colonies was observed for any of the bacterial strains.

Kim et al. [2013] also conducted a chromosome aberration test to identify chromosomal abnormalities. A preliminary cytotoxicity test was carried out at a relative cell count (RCC) concentration of ~50%. At this RCC, AgNPs were found to induce cytotoxicity. For groups treated for 6 and 24 hours without the S9 mix, a cytotoxic effect was induced at about 15.625 μg/mL, whereas for the group treated for 6 hours with the S9 mix, cytotoxicity was induced above 31.25 μg/mL. On the basis of these results, chromosome slide samples were prepared at 3.906, 7.813, and 15.625 μg/mL, with 50% of the RCC concentration as the highest concentration. AgNPs did not produce any statistically significant increase in the number of CHO-k1 cells with chromosome aberrations when compared to the negative controls with or without metabolic activation. AgNPs also did not cause a statistically significant increase in the number of cells with polyploidy or endoreduplication when compared with controls in the presence and absence of the S9 mix.

Induction of genotoxicity in CHO-K1 cells by AgNPs was also studied by Kim et al. [2013a]. A majority of the AgNPs were 40–59 nm, based on SEM, TEM, and DLS, though aggregates up to 315 nm were observed. Comet assays demonstrated an AgNP dose-dependent increase in DNA damage, with a 450% tail increase at 10 μg/mL exposure; that exposure was also sufficient to induce micronucleus formation.

However, bacterial mutagenicity was not detected in *Salmonella typhimurium* strains TA98, TA100, TA1535, and TA 1537 by Ames test, regardless of the presence of S9 mix, nor was AgNP exposure associated with changes in binucleated cells, cytokinesis-block proliferation index, or relative increase in cell counts in CHO-K1 cells.

## D.3 Changes in Gene Expression/Regulation

A number of research groups have employed DNA microarray analysis in an attempt to understand the cellular responses to AgNPs at the molecular level. For example, using 7- to 10-nm-diameter nanoparticles stabilized with PVP, Kawata et al. [2009] observed changes in cellular morphology, cell viability, and micronucleus formation when HepG2 human hepatoma cells were incubated with AgNPs

at noncytotoxic doses. However, micronucleus formation was greatly reduced in cells incubated with either a polystyrene nanoparticle preparation or a silver carbonate solution, but it was only partially reduced in response to AgNPs where the cells had been pre-incubated with the antioxidant NAC. Accompanying these well-characterized responses was an induction of genes associated with cell cycle progression. Thus, AgNPs altered the expression levels of 529 genes at least twofold, with 236 genes being induced and 293 repressed.

Patterns of induction featured genes classified as "M phase" (31 genes), microtubule-based processes (19 genes), DNA repair (16 genes), DNA replication (24 genes), and intracellular transport (32 genes). Many of the genes were involved in chromosome segregation, cell division, and cell proliferation. Striking levels of induction were also observed for some stress-inducible genes, including three coding for metallothioneins and three for different heat-shock proteins. Overlapping patterns of gene expression in this cell line were observed in silver carbonate–altered gene profiles. For example, in comparisons of AgNPs and silver carbonate, 66 upregulated genes and 72 downregulated genes were altered commonly in the same direction with both chemical treatments. Kawata et al. [2009] speculated that the upregulation of a number of genes associated with DNA repair and the increase in micronucleus in AgNP-exposed HepG2 cells might point to the DNA-damaging effects of silver in both nanoparticle and ionic form.

The A549 human lung adenocarcinoma cell line was used by Deng et al. [2010] as a platform for studying increased gap junction intercellular communication (GJIC) activity and increased expression of connexin43 (Cx43) mRNA in the presence of AgNPs. The particles were a proprietary formulation, 30 nm in diameter and coated with 0.2% PVP, although TEM and dynamic light scattering indicated that a degree of aggregation had occurred when the particles were dispersed in an aqueous medium. GJIC was assessed by means of a scrape loading/dye transfer technique, and Cx43 was detected by immunofluorescence. Furthermore, western blot assays were performed to determine the level of expression of Cx43 protein, and RT-PCR analysis showed that silver AgNPs upregulated the expression of Cx43 mRNA in a dose-dependent manner (1.2–1.8 times at concentrations ranging from 0.5 to 4.0 μg/mL after a 24-hour incubation). Deng et al. [2010] speculated that GJIC and Cx43 might mediate some of the biologic effects of AgNPs.

Ma et al. [2011] applied genomic analysis to responses to AgNPs (~20 nm in diameter) in human dermal fibroblasts. The particles employed had been prepared by reduction of a silver nitrate solution with sodium borohydride and were used at 200 micromolar (μM). However, TEM analysis showed a considerable degree of aggregation of the nearly spherical particles. For the microarray analysis, total RNA was isolated, amplified, labeled, and hybridized and cRNA probes were synthesized. A proprietary computer program (BeadStudio) used to survey changes in gene expression showed that 1,593 genes were impacted by AgNPs after 1, 4, or 8 hours of incubation. Only 237 genes were affected after 1 hour, as compared to 1,149 after 4 hours and 684 after 8 hours. Biologic pathway analysis of the affected genes identified five functional clusters associated primarily with disturbance of energy metabolism, disruption of cytoskeleton and cell membrane, gene expression, and DNA damage/cell cycle arrest.

Foldbjerg et al. [2012] studied the effect of AgNPs (average particle diameter, 15.9 nm) on gene expression, using human lung epithelial cell line A549 exposed to 12.1 μg/mL AgNPs for 24 and 48 hours. Results were compared to control (unexposed) and silver ion ($Ag^+$)–treated cells (1.3 μg/mL) with Affymetrix microarray analysis. AgNPs exposed for 24 hours altered the regulation of more than 1,000 genes (twofold regulation), compared to only 133 genes that responded to $Ag^+$ exposure. Nearly 80% of all genes induced by $Ag^+$ were also upregulated in AgNP-treated cells. Bioinformatic analysis of the upregulated genes in response to the 24-hour exposure with $Ag^+$ and AgNPs revealed similar functional gene groups that were enriched. Exposure of epithelial cells to AgNPs and $Ag^+$ resulted in intracellular production of ROS but did not induce apoptosis or necrosis at the concentrations used in the study.

Exposure to AgNPs influenced the cell cycle and led to an arrest in the G2/M phase, whereas exposure to $Ag^+$ caused a faster but less-persisting cellular response than did exposure to AgNPs. The investigators concluded that although the transcriptional response to exposure with $Ag^+$ is highly related to the responses caused by exposure to AgNPs, the particulate form and size of AgNPs "affect cells in a more complex way."

Huo et al. [2015] investigated the effects of NM-300K 20-nm AgNP exposure in 16HBE, HUVEC, and HEPG2 cells. Cellular viability showed both time- and dose-dependent toxicity. Additionally, 16HBE cells were more sensitive than HEPG2 cells, and HUVEC was the least sensitive of the three. Notably, 2 μg/cm$^2$ AgNP exposure statistically significantly upregulated both xbp-1s and chop mRNA levels in 16HBE cells, as well as chop mRNA levels in HEPG2. Other genes related to the endoplasmic reticulum (ER) stress signaling pathway were also upregulated in 16HBE by AgNP exposure. Western blot analysis showed upregulation of binding immunoglobulin protein and caspase-12 relative to caspase-3 in AgNPs exposed to 16HBE cells, which indicates a pro-apoptotic response through the ER-targeted pathway (rather than mitochondrial-targeted pathway). Huo et al. [2015] also found that lung, liver, and kidney tissues showed statistically significant increases in ER stress following intratracheal instillation of AgNPs in vivo.

Srivastava et al. [2012] investigated selenoprotein synthesis in A549 and HaCat keratinocyte cells. MTT and LDH assays were used to examine the effects of up to 10 μM AgNP exposure on viability; little change was observed. However, AgNP exposure did result in a dose-dependent reduction of $^{75}$Se radioisotope incorporation into known selenoproteins. No changes were observed in incorporation of $^{35}$S-methionine/cysteine, indicating the change was specific to selenoproteins and not proteins overall. These changes also occurred with exposure to Ag ions (as $Ag_2SO_4$). The authors indicated that the most likely mechanism was that leeched Ag ion interfered with Se binding; additional experiments eliminated other possible mechanisms. Activity assays showed that both AgNP and Ag ions also decreased thioredoxin reductase (TrxR1) activity but not protein levels. This indicates the possibility that AgNPs may interfere with selenoprotein synthesis.

## D.4 Modeling the Perturbation of the Blood–Brain Barrier

Tang et al. [2010] used co-cultures of rat brain microvessel vascular endothelial cells and astrocytes that were established on a polycarbonate membrane in a diffusion chamber to model the potential for AgNPs to cross the blood–brain barrier. The researchers used commercial preparations of AgNPs (diameter, 50–100 nm) and contrasted their passage with larger-scale silver microparticles (diameter, 2–20 μm) incubated in the same system. The use of ICP-MS showed that AgNPs readily crossed the barrier, whereas silver microparticles did not. TEM analysis demonstrated the capacity of AgNPs to be taken up by the mixed culture. Some of the endothelial cells showed signs of morphologic disruption, with large vacuole formation and signs of necrosis of cellular organelles.

Primary brain microvessel endothelial cells isolated from Sprague-Dawley rats were employed by Trickler et al. [2010] to determine the capacity of AgNPs to potentiate the release of proinflammatory mediators, with possible impacts on blood–brain barrier permeability. Obtained from a commercial supplier, the PVP-coated AgNPs used in these experiments conformed to their size requirements of 25, 40, and 80 nm in diameter and were mostly spherical, as indicated by TEM and dynamic light-scattering analysis. Cellular accumulation of silver was greater from the smaller nanoparticles, and cell viability was likewise more severely affected in those cultures exposed to the 25-nm-diameter particles. The cultures also showed a time-dependent preferential release of prostaglandin $E_2$ and the cytokines TNF-α, IL-1β, and IL-2, in relation to smaller AgNPs. According to the authors, these changes may be linked to ROS generation and an increase in microvascular permeability.

## D.5 Impact of Silver Nanoparticles on Keratinocytes

Two research reports have examined the effects of AgNPs on keratinocytes, focusing in particular on the different results that were obtained when the toxicity of particles of different sizes and coatings was compared [Amato et al. 2006; Samberg et al. 2010]. For example, Amato et al. [2006] reported in an abstract that hydrocarbon-coated AgNPs of 15, 25, or 55 nm in diameter induced greater degrees of toxicity than did uncoated forms of silver that were 80 or 130 nm in diameter. The use of a CytoViva 150 Ultra Resolution Imaging system showed AgNP aggregates on the surface of the cells, along with some evidence of particle uptake into the HEL-30 mouse keratinocytes. Measuring caspase activity and using confocal fluorescent microscopy provided evidence of the onset of apoptosis at sublethal doses.

These results differed from those of Samberg et al. [2010], who incubated human epidermal keratinocytes for 24 hours with eight different species of AgNPs. As supplied by nanoComposix, Inc. (San Diego, CA), these preparations included three unwashed colloids of 20-, 50-, and 80-nm-diameter AgNPs, three washed colloids of the same nominal size, and two carbon-coated powders that were 25 and 35 nm in diameter. In contrast to the findings of Amato et al. [2006], the loss of cell viability that was observed with unwashed AgNPs at silver concentrations of 0.34 or 1.7 µg/mL was not seen when the cells were incubated with washed or carbon-coated particles, even though all silver nanoparticles were taken up into cytoplasmic vacuoles to roughly the same extent. The inflammatory potential of AgNPs was demonstrated by increases of IL-1β, IL-6, IL-8, and TNF-α in the media of cells exposed at 0.34 µg/mL. The authors suggested that the toxicity of AgNPs to human epidermal keratinocytes might be influenced by residual contaminants in the AgNP preparations and not necessarily by the particles themselves.

## D.6 Effect of Silver Nanoparticles on Platelet Activation

Jun et al. [2011] carried out a series of experiments to investigate the effect of AgNPs on platelet aggregation. The commercial AgNPs averaged slightly less than 100 nm in diameter and were maintained in solution in nonaggregated form by ultrasonication and vortexing. A colloidal dispersion of AgNPs (5,000–8,000 nm in diameter) was used in comparison. The measured parameters that were indicative of platelet activation included platelet aggregation per single-cell counts, TEM analysis, low cytometric analysis of phosphatidylserine exposure (a measure of apoptosis), platelet pro-coagulant activity, serotonin secretion, detection of p-selectin expression, and determination of intracellular calcium levels. There was a dose-dependent increase in platelet aggregation with increased concentration of nanoparticle-borne but not microparticle-borne silver. Aggregation was further enhanced by the presence of thrombin.

Other determinants of coagulation dose-dependently associated with the presence of AgNPs included the degree of phosphatidylserine exposure, pro-coagulant activity, expression of p-selectin, and secretion of serotonin. The presence of the calcium chelator ethylene glycol-bis (β-amino-ethyl ether) N,N,N′,N′-tetra acetic acid in the incubation medium partially blocked the platelet aggregation activity of AgNPs, implicating a role for calcium ions in the induction of platelet aggregation. Overall, the results pointed to the capacity of AgNPs to enhance platelet aggregation and pro-coagulant activity, with a possible intermediary role for intracellular calcium and sub-threshold levels of thrombin.

## D.7 Antitumor and Antimicrobial Activity of Silver Nanoparticles

The in vivo experiments of Sriram et al. [2010], in which intraperitoneally injected AgNPs appeared to

enhance survival time and reduce the volume of ascites tumors in female Swiss albino mice, were supplemented by experiments in which Dalton's lymphoma cell lines were incubated for 24 hours with AgNPs in vitro. As described in Section 5.3.3, the researchers used 50-nm-diameter AgNPs that had been produced in *B. licheniformis* cultures incubated in the presence of silver nitrate. When the MTT assay was used as a measure of cell viability, a silver concentration of 500 nm was calculated for the $IC_{50}$. Measurement of caspase 3 in cell lysates showed a marked increase in activity compared to that in controls, and fragmentation of DNA indicated the presence of double-strand breaks. The authors speculated that their data indicated a potential antitumor property of AgNPs and the relevance of apoptosis to this process.

In light of the extensive use of AgNP-bearing dressings to deter infection in wounds, Lok et al. [2006] used proteomic analysis to examine their mode of antibacterial action by incubating cultures of *E. coli* (wild-type K12 strain MG1655) with samples of spherical, 9.3-nm-diameter bovine serum albumin–stabilized nanoparticles that had been produced by the borohydride reduction method. Two-dimensional electrophoresis was used to separate the spectrum of cellular proteins pre- and post-incubation; the resulting peptides were identified by MALDI-TOF MS and, in some cases, immunoblots. The initial concentrations of AgNPs and silver nitrate that inhibited bacterial proliferation were 0.4 nm and 6 μm, respectively, suggesting that silver presented in the nanoparticle form was more efficient at deterring bacterial growth.

With regard to changes in gene expression, induction of some cell envelope and heat-shock proteins appeared to be differentially enhanced, including outer membrane proteins A, C, and F (or their precursors), periplastic oligopeptide binding protein A, D-methionine binding protein (including body binding proteins A and B), and a 30S ribosomal subunit S6. However, the researchers reported that some of these stimulated proteins appeared to be in their precursor forms, which were said to generally contain a positively charged N-terminal signal sequence of about 2 kDa. In addressing the possible mode of action associated with the antimicrobial effect of AgNPs, the researchers found that short-term incubation of *E. coli* with AgNPs provided evidence of membrane destabilization, reduction in membrane potential, and depletion of intracellular potassium and ATP. These consequences were thought to be manifestations of the proteomic changes observed at the molecular level.

Swanner et al. [2015] investigated the cytotoxic and radiosensitizing effects of AgNP exposure on several triple-negative breast cancer (TNBC) and non-triple-negative breast cell lines. TNBC cell lines included MDA-MB-231, BT-549, and SUM-159 cells. Non-TNBC cell lines included ER/PR positive, luminal A-like breast cancer cells (MCF-7); noncancerous, transformed breast cells (MCF-10A); immortalized human mammary epithelial cells (HMECs) (184B5); and post-stasis HMECs. TNBC cells showed greater cytotoxic sensitivity to AgNP exposure than non-TNBC cells, as measured by MTT assay, by approximately 10 μg/mL. Similarly, cytotoxicity assessed by clonogenic assay showed that 10 μg/mL was 100% inhibitive of TNBC cells but not non-TNBC cells. However, all non-TNBC cells do uptake AgNP. Cystein thiols are more oxidized in TNBC cells than non-TNBC cells. Additionally, after exposure to AgNP and 4 Gy X-rays, DNA damage as quantified by γH2AX showed statistically significantly increased damage in TNBC cells relative to non-TNBC cells.

**Table D-1. Summary of in vitro studies of silver nanomaterials**

| Cell Type | Particle Characteristics | Exposure Details: Concentrations/ Dose | Exposure Details: Duration | Major Outomes | NOAEL/ LOAEL | Comments | Reference |
|---|---|---|---|---|---|---|---|
| **Human Cells** | | | | | | | |
| HepG2 human hepatoma | AgNPs and $Ag^+$ ions: 5–10 nm particles dispersed in an aqueous medium; agglomerates 100–300 nm | 0.2–1 µg/mL | 24- or 28-hour incubation | Release of LDH activity; mRNA levels of catalase and superoxide dismutase 1 increased; detection of phosphorylation on the H2AX gene; ROS formation | NA | AgNPs exhibited cytotoxicity with a potency comparable to that of $Ag^+$ ions | Kim et al. [2009c] |
| HepG2 human hepatoma cells; SGC-7901 human stomach cancer cells; MCF-7 human breast adenocarcinoma cells; and A549 human lung adenocarcinoma cells | PVP coated; 5, 20, and 50 nm in diameter | Cell viability test: 0.01–100 µg/mL | 6-, 12-, or 24-hr incubation | Apoptosis and necrosis test: 0.1, 0.5, 2.5 µg/mL; membrane damage and oxidative stress: 0.01–10 µg/mL | NA | Induced cell death caused by apoptosis; no difference between control group and exposed group for necrosis; smaller particles more effective at penetrating the membrane and inducing toxic effects | Liu et al. [2010a] |
| Human Chang liver cells | Particles started at 5–10 nm but aggregated to 28–38 nm after incubation in the medium | 4 µg/mL | 0- to 24-hr incubation | Increased levels of lipid peroxidation and protein carbonyl formation; decrease in Bcl-2 expression: increase in Bax. ROS formation | NA | Apoptosis via a mitochondrial and caspase-dependent pathway; the importance of JNK in mediating the apoptotic effects was demonstrated by its time-dependent phosphorylation in the presence of AgNPs | Piao et al. [2011] |

(Continued)

**Table D-1. Summary of in vitro studies of silver nanomaterials (Continued)**

| Cell Type | Particle Characteristics | Exposure Details: Concentrations/ Dose | Exposure Details: Duration | Major Outomes | NOAEL/ LOAEL | Comments | Reference |
|---|---|---|---|---|---|---|---|
| HT-1080 human fibrosarcoma cells; A431 human skin carcinoma cells | 7–20-nm diameter in an aqueous suspension | 6.25–50 µg/mL | | Reduction in GSH content and SOD activity; increase in lipid peroxidation; increase in treatment-related DNA fragmentation | NA | Oxidative stress; cell death by apoptosis and necrosis | Arora et al. [2008] |
| Human acute monocytic leukemia cell line (THP-1 cells) | 30–50 nm in diameter and coated with 0.2% PVP | 0–7.5 µg/mL (calculated as silver mass) | Up to 24-hr incubation | Increase in intracellular ROS, DNA damage | | Apoptosis; necrosis; statistically significant reduction of viable cells after 24-hr exposure | Foldbjerb et al. [2009] |
| A549 human lung carcinoma epithelial-like cell line | 30–50 nm, spherical, coated with 0.2% PVP | Suspensions/supernatants containing 39% (0.2 µg/mL silver ions) or 69% (1.6 µg/mL silver ions) | 24-hr incubation | Induced ROS | NA /1.6 µg/mL total silver, suspension containing 39% silver | AgNP-free supernatant had the same toxicity as AgNP suspensions | Beer et al. [2012] |
| HeLa cells | 5–10 nm in diameter, stabilized with a proprietary protectant | $IC_{50}$ of 92 µg/mL silver | 3- to 4-hr incubation | Increase in expression of heme oxygenase-1 and mettothionein-2A | | Apoptosis | Miura and Shinohara [2009] |
| A549 cells | ~500 nm (agglomerated) | Morphology: 10, 50, 200 µg/mL Cytotoxicity: 5, 10, 50, 200 µg/mL Apoptosis: 50 and 100 µg/mL | Morphology: 24-hr incubation Cytotoxicity: 12, 24, 48, 72 hr of incubation Apoptotic cell death: 24-hr incubation | Increased LGH release; altered cell cycle distribution; changes to expression of Bax and Bcl-2; altered mRNA levels of protein kinase C isotypes | | Reduction in cell viability; increased apoptosis; cytotoxicity at 48 hr | Lee et al. [2011a] |

(Continued)

**Table D-1. Summary of in vitro studies of silver nanomaterials (Continued)**

| Cell Type | Particle Characteristics | Exposure Details: Concentrations/ Dose | Exposure Details: Duration | Major Outomes | NOAEL/ LOAEL | Comments | Reference |
|---|---|---|---|---|---|---|---|
| Human colon adenocarcinoma (HT29) cells | <20 nm in diameter | 11 µg/mL | 30-min to 6-hr incubation | Cascade reaction, which activates caspase-3, which penetrates nuclear membrane to induce DNA fragmentation | | Programmed cell death (apoptosis) | Gopinath et al. [2010] |
| Human lung macrophage cell line (THB-1); human epithelial (A549) cells | Primary particle: 3-100 nm in diameter | 5 µg/mL | 52-hr incubation | Cytotoxic effect | | Epithelial cells more sensitive to effects | Soto et al. [2007] |
| Human lung A549 cancer cell line | 30–50 nm in diameter and coated with 0.2% PVP | AgNPs: 0–20 µg/mL $Ag^{+}$: 0–10 µg/mL | 24-hr incubation | Induced dose-dependent reductions in mitochondrial function to a greater extent than equivalent concentrations of silver in nano-form | | Induced cytotoxicity and ROS formation was accompanied by formation of bulky DNA adducts; responses inhibited by pretreatment with N-acetyl-cysteine | Foldbjerb et al. [2011] |
| Human mesenchymal stem cells (hMSCs) | Mean diameter of 46 nm; aggregation mean diameter of 404 nm when dispersed in medium | 0.1, 1.0, and 10 µg/mL | 1-, 3-, and 24-hr incubation | Chromosomal aberrations | NA / 0.1 µg/mL | Cytotoxic and genotoxic potential of Ag-NPs occurred at higher doses than did their antimicrobial effects | Hackenberg et al. [2011] |

(Continued)

**Table D-1. Summary of in vitro studies of silver nanomaterials (Continued)**

| Cell Type | Particle Characteristics | Exposure Details: Concentrations/ Dose | Exposure Details: Duration | Major Outomes | NOAEL/ LOAEL | Comments | Reference |
|---|---|---|---|---|---|---|---|
| Human mesenchymal stem cells (hMSCs) | PVP-coated, ~100 nm in diameter | Concentrations of 0.5, 1, 2.5, 3, 3.5, 4, 5 µg/mL or to silver ions (silver acetate) | Up to 7 days | Both types showed a decrease in release of IL-6, IL-8, and VEGF | Silver: 1 µg/mL; 2.5 µg/mL AgNP: 3 µg/mL; 3.5 µg/mL | AgNPs exert cytotoxic effects in hMSCs at high concentrations but also induce cell activation at high but nontoxic concentrations of nanosilver | Greulich et al. [2009] |
| Human mesenchymal stem cells (hMSCs) | PVP-coated, 50 nm ± 20 nm in diameter | Concentrations of 0.5, 1.0, 1.5, 2.0, or 2.5 µg/mL silver acetate (ions) or 15, 20, 25, 30, or 50 µg/mL AgNPs | 24-hr incubation | 80-nm AgNP agglomerates found in perinuclear region of hMSCs (clathrin-mediated endocytosis uptake) | | Possibly more than one endocytotic pathway for cell uptake | Greulich et al. [2011] |
| Human adipose-derived stem cells (hASCs), undifferentiated and differentiated | 10 or 20 nm in diameter | 0.1, 1.0, 10.0, 50.0, 100.0 µg/mL, either before or after differentiation | Cells were differentiated down the osteogenic or adipogenic pathways or maintained in their proliferative state for 14 days and then exposed for 24 hr to evaluate potential cellular uptake of AgNPs the hASCs grew in a medium for 5 days | No morphologic changes occurred in adipogenic and osteogenic cell uptake of both 10 & 20 nm; no statistically significant cytotoxicity to hASCs when exposed to 10- or 20-nm | NA/ 10 µg/mL | No statistically significant cytotoxicity to undifferentiated hASCs either prior to differentiation or following 14 days of differentiation | Samberg et al. [2012] |

(Continued)

**Table D-1. Summary of in vitro studies of silver nanomaterials (Continued)**

| | | Exposure Details | | | | | |
|---|---|---|---|---|---|---|---|
| Cell Type | Particle Characteristics | Concentrations/ Dose | Duration | Major Outomes | NOAEL/ LOAEL | Comments | Reference |
| IMR-90 human lung fibroblasts; U251 human glioblastoma cells | 6–20 nm in diameter; starch-coated | 25, 50, or 100 µg/mL | 2- to 72-hour incubation | Alteration in cell morphology; reduced viability; deficits in mitochondrial performance and ROS production | | Small percentage of cells underwent apoptosis; indication of treatment-associated DNA damage | AshaRani et al. [2009] |
| Human lung cells (BEAS-2B) | Citrate-coated: 10, 40, 75 nm in diameter PVP-coated: 10 nm in diameter Uncoated: 50 nm in diameter | 5, 10, 20, 50 µg/mL | 4- and 24-hr incubation | No cells showed signs of cell toxicity after 4 hr; after 24 hr, cell toxicity was present in 10-nm citrate-coated and 10-nm PVP-coated from doses of 20 and 50 µg/mL; all cells showed overall DNA damage after 24 hr | | Independent mechanism for cytotoxicity and DNA damage | Gliga et al. [2014] |
| TK6 human lymphoblastoid cells | 4–12 nm in diameter | 10–30 µg/mL | | Frank toxicity of TA98 and TA100; toxicity of TA1535 and TA1537; dose-response increase in micronuclei was observed at a dose of 25 µg/mL | Frank toxicity: 4.8 µg/plate; toxicity: 9.6 µg/plate | Results were weak-positive, consistent with results in similar studies | Li et al. [2012] |
| HepG2 human hepatoma cells | 7–10 nm in diameter; stabilized by PVP | 0, 0.1, 0.2, 0.5, 1.0, 1.5, 2.0, 2.5, 3.0 mg/L | 24-hr incubation | Changes in cellular morphology; cell viability; micronucleus formation; statistically significant cytotoxicity at >1.0 mg/L | | DNA-damaging effects; altered expression levels of 529 genes at least twofold | Kawata et al. [2009] |
| A549 human lung adenocarcinoma cell line | 30 nm in diameter; coated with 0.2% PVP | 0.5–4.0 µg/mL | 24-hr incubation | Upregulated the expression of Cx43 | | GJIC and Cx43 might mediate some of the biologic effects of AgNPs | Deng et al. [2010] |

(Continued)

**Table D-1. Summary of in vitro studies of silver nanomaterials (Continued)**

| Cell Type | Particle Characteristics | Exposure Details: Concentrations/ Dose | Exposure Details: Duration | Major Outomes | NOAEL/ LOAEL | Comments | Reference |
|---|---|---|---|---|---|---|---|
| Human dermal fibroblasts | ~20 nm in diameter | Reduction of silver nitrate solution with sodium borohydride at 200 micromolar | 1-, 4-, or 8-hour incubation | 1,593 genes were impacted after 1-, 4-, and 8-hour incubations | | Disturbance of energy metabolism; disruption of cytoskeleton, cell membrane, and gene expression; DNA damage/cell cycle arrest | Ma et al. [2011] |
| A549 human epithelial cell line | AgNPs: 30 nm in diameter; silver microparticles: <45 µm in diameter; AgNWs: 1.5–25 µm in length, 100–160 nm in diameter (all particles coated with PVP) | AgNPs: 0.33 mg/mL; silver nanoparticles: 13.5 mg/mL; AgNWs: 5.05–16.47 mg/mL | 24- and 48-hour incubation | Strong cytotoxicity, loss in cell viability, and early calcium influx with AgNWs; AgNPs and silver microparticles had minimal effect on A549 cells | | Cell damage and resulting cell death hypothesized by investigator as being caused by the needle-like structure of the AgNWs | Stoehr et al. [2011] |
| Human epithelial cell line | 15.9 nm average particle size | 12.1 µg/mL | 24- and 48-hour incubation | Altered the regulation of more than 1000 genes (two-fold regulation); intracellular production of ROS | | Did not induce apoptosis or necrosis | Foldbjerb et al. [2012] |
| Human epidermal keratinocytes | Three unwashed colloids of 20, 50, and 80 nm in diameter; 3 washed colloids of 20, 50, and 80 nm in diameter; 2 carbon-coated powders 25 and 35 nm in diameter | 0.000544–1.7 µg/mL | 24-hr incubation | Loss of cell viability observed in unwashed AgNPs; increases in TNF-α, IL-1β, IL-6, and IL-8; decrease in cell viability for unwashed AgNPs <1.7 µg/mL | NA / 0.34 µg/mL (unwashed AgNPs) | Toxicity of AgNPs might be influenced by residual contaminants in the AgNP preparations and not necessarily by the particles themselves | Samberg et al. [2010] |

(Continued)

**Table D-1. Summary of in vitro studies of silver nanomaterials (Continued)**

| Cell Type | Particle Characteristics | Exposure Details: Concentrations/ Dose | Exposure Details: Duration | Major Outomes | NOAEL/ LOAEL | Comments | Reference |
|---|---|---|---|---|---|---|---|
| Human platelets (washed) | 100 nm in diameter; solution in nonaggregated form by ultrasonication and vortexing; colloidal dispersion (microparticles 5,000–8,000 nm in diameter) used for comparison | 50, 100, and 250 µg/mL | 5 min | Dose-dependent increase in platelet aggregation with increased concentration of nanoparticles but not microparticle-borne silver | | Enhance platelet aggregation and procoagulant activity, with possible intermediary role for intracellular calcium and subthreshold levels of thrombin | Jun et al. [2011] |
| **Animal Cells** | | | | | | | |
| Rat alveolar macrophages | 15, 30, 55, 100 nm in diameter | 0, 5, 10, 25, 50, and 75 µg/mL | Cells at 80% confluence were incubated 24 hr | Same as Hussain et al. [2005b]; treatment-related increase in TNF-α, macrophage inflammatory protein-2, IL-1β, in the supernatant of macrophage/ AgNP incubations | NA | Oxidative stress; cellular damage. | Carlson et al. [2008] |
| Rat alveolar macrophages | 15, 30, 55, 100 nm in diameter | 5–50 µg/mL | Cells at 80% confluence incubated 24 hr | Smaller-diameter AgNPs more effective than larger NPs at physiologic and toxicological changes | NA | Oxidative stress; cellular damage | Hussain et al. [2005b] |
| BRL 3A rat liver cells | 15 or 100 nm in diameter | 5–50 µg/mL | Incubation times up to 24 hr | Both cell sizes induced a concentration-dependent depletion of mitochondrial function; release of LDH to culture medium | NA | Cytotoxicity through oxidative stress | Hussain et al. [2005a] |

(Continued)

**Table D-1. Summary of in vitro studies of silver nanomaterials (Continued)**

| Cell Type | Particle Characteristics | Exposure Details: Concentrations/ Dose | Exposure Details: Duration | Major Outomes | NOAEL/ LOAEL | Comments | Reference |
|---|---|---|---|---|---|---|---|
| NIH3T3 fibroblasts | Ag 1–100 nm in diameter; non-nano Ag <250 µm in diameter | 50 and 100 µg/mL | 24 hr for AgNPs; up to 72 hr for non-nano Ag | Link between mitochondrial-related generations of ROS and incidence of apoptosis and activation of JNK; non-nano Ag not cytotoxic and no effect on apoptosis | | Results similar to those for Piao et al. [2011] | Hsin et al. [2008] |
| Primary mouse fibroblasts and liver cells | >90% of particles 7–20 nm in diameter | $IC_{50}$ values were 61–449 µg/mL | 24-hr incubation | Primary cell preparations contained sufficient antioxidant capacity to protect cells from possible oxidative damage | | Study similar to Arora et al. [2008], but oxidative stress and apoptosis were less evident | Arora et al. [2009] |
| L929 fibroblasts | AgNPs: 50–100 nm; Ag microparticles: 2–20 µm | 10, 25, 50, 100 µg/mL | 24-hr incubation | Greater percentage of cells arrested in G2M phase of cell cycle | | Increased incidence of apoptosis; AgNPs caused greater level of apoptosis than did Ag microparticles at same dose | Wei et al. 2010 |
| Murine lung macrophage (RAW 264.7) | | 5 µg/mL | | | | Cytotoxic response | Soto et al. [2007] |
| Mouse embryonic stem cells, mouse embryonic fibroblasts | Uncoated plasma gas-synthesized AgNPs & polysaccharide-coated AgNPs, both approx. 25 nm in diameter | 50 µg/mL | 4-, 24-, 48-, and 72-hr incubation | Increased induction of the Rad51 double-strand break repair protein; enhanced phosphorylation of the histone H2AX at the serine-139 residue | | Increased p53 expression and double DNA breakage, with concomitant apoptosis in both cells within 4 hr after exposure | Ahamed et al. [2008] |

(Continued)

**Table D-1. Summary of in vitro studies of silver nanomaterials (Continued)**

| Cell Type | Particle Characteristics | Exposure Details: Concentrations/ Dose | Exposure Details: Duration | Major Outomes | NOAEL/ LOAEL | Comments | Reference |
|---|---|---|---|---|---|---|---|
| Mouse fibroblast (L929) tumor cells | Median diameter of 12 nm; synthesized by chemical reduction of silver chlorate with sodium borohydride and sodium citrate | 0, 11, 22 µg/mL | 72-hr incubation | Formation of cells with single giant nuclei or cells with two, three, or sometimes four nuclei per cell | | Induced malsegregation of the chromosomes rather than having direct effect on replication | Nallathamby and Xu [2010] |
| Mouse lymphoma assay system | 4–12 nm in diameter; average size ~5 nm; uncoated | 5 µg/mL | 4-hr incubation | Observed in the cytoplasm of the lymphoma; DNA breaks; expressions of 17 of the 59 genes on the arrays were altered in the cells | | Induced dose-dependent cytotoxicity and mutagenicity | Mei et al. [2012] |
| Rat brain microvessel vascular endothelial cells; astrocytes to model a blood-brain barrier | AgNPs: 50–100 nm in diameter; Ag microparticles: 2–20 µm in diameter | 100 µg/mL | 4-hr incubation | AgNPs readily crossed the barrier, whereas silver microparticles did not | | Morphologic disruption, with large vacuole formation and signs of necrosis of cellular organelles | Tang et al. [2010] |
| Sprague-Dawley rat primary brain microvessel endothelial cells (rBMECs) | 25, 40, and 80 nm in diameter; spherical; PVP-coated | Cytotoxicity: 1.95–15.63 µg/cm$^2$; prostaglandin $E_2$ and cytokine release in rBMECs: 10.4 µg/cm$^2$; cell morphology: 5.2 µg/cm$^2$ | 24-hr incubation | ROS generation; increase in microvascular permeability; release of prostaglandin $E_2$ and cytokines TNF-α, IL-1β, and IL-2 | | Cell viability more severely affected in cultures exposed to the 25- and 50-nm diameters; cerebral microvascular damage | Trickler et al. [2010] |
| HEL-30 mouse keratinocytes | 15-, 25-, or 55-nm diameter (coated with hydrocarbon); 80- or 130-nm diameter (not coated) | 25, 40, 50, 65, and 100 µg/mL | 24-hr incubation | Onset of apoptosis at 25 µg/mL | NA | The 15-, 25-, and 55-nm particles induced greater degrees of toxicity than the larger (uncoated) particles | Amato et al. [2006] |

(Continued)

**Table D-1. Summary of in vitro studies of silver nanomaterials (Continued)**

| Cell Type | Particle Characteristics | Exposure Details: Concentrations/ Dose | Exposure Details: Duration | Major Outomes | NOAEL/ LOAEL | Comments | Reference |
|---|---|---|---|---|---|---|---|
| L929 mouse fibroblasts, RAW 264.7 and D3 embryonic stem cells | 20-, 80-, 110-nm-diameter AgNPs, mostly spherical | 0.1–100 µg/mL | 24 hr for RAW 264.7 and L929; 10 days for D3 cells | For L929 and RAW 264.7: metabolic activity highest with 20-nm AgNPs; RAW 264.7: increased ROS generation with 20-nm AgNPs; L929: compromised cell membrane integrity with all sizes | NA | Toxicity of AgNPs and silver ions dependent on particle size and cell type | Park et al. [2011c] |
| Cell lines: Osteoblastic MC3T3-E1, PC12, rat adrenal medulla, human cervical cancer, HeLa, CHO | 10-, 50-, 100-nm-diameter AgNPs | 10, 20, 40, 80, or 160 µg/mL: after 24-hr incubation, concentrations were 1, 2, 4, 8, and 16 µg | Additional incubation for 24, 48, or 72 hr | Size- and dose-dependent cellular toxicity for all cell lines; ROS generation and cytotoxicity increased as size and concentration of AgNPs increased | NA | Toxicity of AgNPs dependent on particle size and cell type; effect may be related to cellular uptake processes from cell membrane to nuclear pores | Kim et al. [2012] |
| Dalton's lymphoma cell lines | 50 nm in diameter; produced in *Bacillus licheniformis* cultures incubated in the presence of silver nitrate | Silver concentration of 500 nM was calculated for the $IC_{50}$ | 24-hr incubation | Measurement of caspase 3 in cell lysates showed marked increase in activity in comparison with controls; fragmentation of DNA indicated presence of double-strand breaks | NA | Data indicated a potential antitumor property of AgNPs and the relevance of apoptosis to this process | Sriram et al. [2010] |
| J774.1 (murine macrophage) | AgNPs, spherical, citrate-capped, 20-, 60-, 100-nm; $AgNO_3$ (as Ag ion source) | 0, 5, 10, 50, 100 µg/mL | 24-hr incubation (cytotoxicity), 3-hr (speciation, lysosome imaging) | 20- and 60-nm more toxic than 100-nm; AgNO3 more toxic than AgNPs; AgNPs bound to high-MW proteins, whereas Ag ions bound to metallothioneins | NA | Ag ions only adversely affected viability at greater than 2.5 µg/mL. | Arai et al. [2015] |

(Continued)

**Table D-1. Summary of in vitro studies of silver nanomaterials (Continued)**

| | | Exposure Details | | | | | |
|---|---|---|---|---|---|---|---|
| Cell Type | Particle Characteristics | Concentrations/ Dose | Duration | Major Outomes | NOAEL/ LOAEL | Comments | Reference |
| HL-60 (tumoral human leukemia), HepG2 (hepatoma cells) | AgNPs, citrate-stabilized, 30–123-nm | 0.84, 1.68, 3.37, 6.72, 13.45 µg/mL | 24-, 48-, 72-hr incubation | N-acetyl-L-cysteine rescues AgNP-exposed cells, indicating AgNP toxicity has an oxidative stress–related mechanism | NA | | Avalos et al. [2013] |
| HPF (human pulmonary fibroblasts) | AgNPs, spherical, 4.7-, 42-nm | 0.84, 1.68, 3.37, 6.72, 13.45, 100, 500, 2000 µg/mL | 24-, 48-, 72-hr incubation | 4.7-nm AgNPs were more toxic than 42-nm; AgNP exposure depletes GSH, indicating oxidative stress | NA | | Avalos Funez et al. [2015] |
| 16HBE (human bronchial epithelial), HUVEC (human umbilical vein endothelial), THP-1 (human acute monocytic leukemia) differentiated to macrophages | AgNPs, spherical, 10-, 20-, 50-, 100-nm, in 2-mM Sodium Citrate | 0.03–30 µg/cm$^2$ | 24-hr incubation | AgNP exposure did not affect transepithelial cell resistance; dose response tended toward mass (rather than surface area) for co-culture models; lower MCP-1 and IL-8 production in co-culture models | NA | AgNPs did not release ions in culture medium or artificial lysosomal fluid (ph 4.6); 10- and 20-nm (but not 50- or 100-nm) AgNPs induced acellular ROS generation | Braakhuis et al. [2016] |
| A549 (human lung epithelial) | AgNPs, spherical, 40–90-nm | 25, 50, 100, 200 µg/mL | 24-, 48-, 72-hr incubation | AgNPs cause ROS formation, cytotoxic effects, apoptosis, S-phase cell-cycle arrest, and proliferating cell nuclear antigen; N-acetyl-L-cysteine rescues AgNP-exposed cells from cytotoxicity and apoptosis | NA | | Chairuangkitti et al. [2013] |
| SH-SY5Y (human blastoma), D384 (human astrocytoma), A549 (human lung epithelial) | AgNPs, 20–100-nm, $AgNO_3$ (as Ag ion source) | 1–100 µg/mL | 4–48 hours (short-term), 10-day (long-term) | Cerebral cell lines were more sensitive than lung cell lines to AgNP toxicity; Ag ions had stronger effects than AgNPs | NA | AgNP doses less than 18 µg/mL were not cytotoxic | Coccini et al. [2014] |

(Continued)

**Table D-1. Summary of in vitro studies of silver nanomaterials (Continued)**

| Cell Type | Particle Characteristics | Exposure Details: Concentrations/ Dose | Exposure Details: Duration | Major Outomes | NOAEL/ LOAEL | Comments | Reference |
|---|---|---|---|---|---|---|---|
| RTH-149 (rainbow trout liver), RTL-W1 (rainbow trout liver), RTG-2 (rainbow trout gonadal) | NM-300K AgNPs, 4- and 25-nm, $AgNO_3$ (as Ag ion source) | 0.73–93.5 µg/mL (AgNP); 0.0345–345 µg/mL (Ag ion) | 24-hr | AgNP is similarly toxic to Ag ion, but media conditions affect toxicity; this is expected to be a function of protein effects on agglomeration | NA | $IC_{50}$ values ranged from 0.4 to 3.8 µg/mL for RTH-149 and RTL-W1, or 10.9 to 32.2 µg/mL for RTG-1; authors postulated that AgNP acts on lysosome walls | Connolly et al. [2015] |
| C3A (human hepatoblastoma) | NM-300 AgNPs | 0–625 µg/cm$^2$ (LDH), 1 µg/cm$^2$ (microscopy), 1, 2, 4 µg/cm$^2$ (GSH), 0-40 µg/cm$^2$ (cytokine release) | 24-hr (LDH and microscopy), 2-, 6- 24-hr (GSH) | AgNPs are toxic to C3A cells (LD50 ~ 20 µg/cm$^2$); AgNPs identified in cytoplasm and nucleus; low dose does not affect C3A activity but upregulates IL-8 and TNF-α expression | NA | Study also included in-vivo component (not discussed here) | Gaiser et al. [2013] |
| HepG2 (hepatoma cells) | PVP-AgNPs, 30-nm, $AgNO_3$ (as Ag ion source) | 2–20 µg/L (PVP-AgNP), 5-211 µg/L (Ag ion) | 24-hr | PVP-AgNP affected transcription-factor pathways that $AgNO_3$ did not | NA | Study also included in-vivo component (not discussed here) | Garcia-Reyero et al. [2014] |
| HUVEC (human umbilical vein endothelial) | AgNPs, 10-, 75-, 110-nm in 2 mM sodium citrate; $AgNO_3$ (as Ag ion source) | 1–40 µg/mL | 24-hr | Cytotoxicity occurred at lower dose for Ag ion than AgNPs; Ag ions promoted necrosis; AgNPs promoted apoptosis, cell detachment, and ROS production and shortened cytoskeleton actin fibers | NA | Study also included in-vivo component (not discussed here) | Guo et al. [2016] |

(Continued)

**Table D-1. Summary of in vitro studies of silver nanomaterials (Continued)**

| Cell Type | Particle Characteristics | Exposure Details: Concentrations/ Dose | Exposure Details: Duration | Major Outomes | NOAEL/ LOAEL | Comments | Reference |
|---|---|---|---|---|---|---|---|
| C1C10 (mouse Balb/C NAL-1A type II pneumocyte), MLE12 (FVN/N mouse SV40 transformed lung epithelial), LA-4 (A/He mouse adenoma lung epithelial) | AgNPs, spherical, 20- and 100-nm, citrate- or PVP-stabilized | 6.25, 12.5, 25, and 50 µg/mL | 24-hr | Smaller AgNPs were more cytotoxic and faster to dissolve in lysosome; coating difference had no discernable effect | NA | Cell lines varied in response | Hamilton et al. [2015] |
| A549 (human lung epithelial) | AgNPs, 15-nm, two versions: one synthesized from an E. coli supernatant by addition of AgNO3 (bio-AgNP); the other by citrate-mediated synthesis (chem-AgNP) | 0–50 µg/mL (bio-AgNP) and 0–100 µg/mL (chem-AgNP) | 24-hr | Both AgNPs cause cytotoxicity, increase intracellular ROS, and localize in autophagosomes and autolysosomes; AgNPs promote apoptosis | NA | Bio-AgNP had a stronger effect than chem-AgNP in each case; no endotoxin assay reported | Han et al. [2014] |
| VcAP (prostate cancer), BxPC-3 (pancreas cancer), H1299 (lung cancer) | AgNPs, spherical, 8–22-nm | 2, 5, 8, 10, 20, and 30 µg/mL (viability); 2, 5, 10, 15, and 20 µg/mL (NF-κB); 10 µg/mL (Western blot) | 72-hr (viability), 24-hr (NF-κB), unknown (apoptosis, Western blot) | AgNP exposure reduced NF-κB activity, decreased BCL-2 expression, and increased caspase-3 and survivin expression | NA | Cell lines had differing sensitivity to AgNPs (H1299 > BxPC-3 > VCaP); LC50 of H1299 between 5- and 8-µg/mL | He et al. [2016] |

(Continued)

**Table D-1. Summary of in vitro studies of silver nanomaterials (Continued)**

| Cell Type | Particle Characteristics | Exposure Details: Concentrations/ Dose | Exposure Details: Duration | Major Outomes | NOAEL/ LOAEL | Comments | Reference |
|---|---|---|---|---|---|---|---|
| A549 (human lung epithelial), MDM (monocyte-derived macrophage), MDDC (monocyte-derived dendritic cells) | AgNPs, 33.4-nm, citrate-coated; $AgNO_3$ (as Ag ion source) | 30–278 ng/$cm^2$ | 4-h, 24-h | No statistically significant toxicity at most AgNP and $AgNO_3$ concentrations | NA | | Herzog et al. [2013] |
| A549 (human lung epithelial), MDM (monocyte-derived macrophage), MDDC (monocyte-derived dendritic cells) | AgNPs, PVP-coated | 10, 20 and 30 µg Ag/ mL | 4-, 24-hr | Cultures submerged expressed lower response than those at the air-liquid interface | NA | All cell lines were co-cultured | Herzog et al. [2014] |
| 16HBE (human bronchial epithelial), HUVEC (human umbilical vein endothelial), HEPG2 (human hepatoblastoma) | NM-300K AgNPs, 20-nm; $AgNO_3$ (as Ag ion source) | 1.5, 3, 6, 12, 24 µg/ $cm^2$ | 6-, 12-, 24-hr | AgNP exposure causes unfolded protein response in 16HBE cells, but not in HUVEC or HEPG2 cells; Ag ions were more cytotoxic than AgNPs to all cell lines | NA | Study also included in-vivo component (not discussed here) | Huo et al. [2015] |
| BEAS-2B (human bronchial epithelial), organ-donor derived HBE (human bronchial epithelial) | Spark-generated AgNPs and CNPs, 20-nm | $4\times10^7$, $4\times10^8$, $4\times10^9$, AgNP/$cm^2$; $3.5\times10^8$, $3.5\times10^9$, $2\times10^{10}$, CNP/$cm^2$ | 4-, 24-hr | AgNP exposure increased IL-6 and IL-8 secretion but reduced MCP-1 secretion; cystic fibrotic cells were more sensitive | NA | | Jeanett et al. [2016] |

(Continued)

**Table D-1. Summary of in vitro studies of silver nanomaterials (Continued)**

| | | Exposure Details | | | | | |
|---|---|---|---|---|---|---|---|
| Cell Type | Particle Characteristics | Concentrations/ Dose | Duration | Major Outomes | NOAEL/ LOAEL | Comments | Reference |
| C3A (human hepatoblastoma) | NM-300 AgNPs, 17-nm, ZnO, TiO2, MWCNT | 1.25, 2.5, 5, 10, 20, 40, 80 μg/cm$^2$ | 24-hr (anti-oxidants, GSH, DCFH-DA) , 6-hr (comet assay), 8 week (long term comet assay) | AgNPs had greater cytotoxicity than TiO2-NPs, ZnO NPs, or MWCNT; AgNP toxicity was prevented by pre-treatment with anti-oxidants; AgNPs were less genotoxic than other selected exposures at LC 20, and no statistically significant difference was found between the short- and long-term studies; IL-8 was upregulated for all NP exposures | NA | AgNP LC50 was between 1.25 and 2.5 μg/cm$^2$ | Kermanizadeh et al. [2012, 2013] |
| CHO-K1 (Chinese hamster ovary) | AgNPs, 40–59-nm | 0.01, 0.1, 1, 10 μg/mL | 24-hr | AgNP exposure induced genotoxicity in CHO-K1 cells | NA | Increase in DNA tail moment noted at 0.01-μg/mL Ag, micronucleus formation at 0.1-μg/mL Ag | Kim et al. [2013a] |
| Primary tenocytes from Sprague-Dawley rats | AgNPs, synthesized 5–10-nm | 1, 10, 20 μM | 42-days | AgNP exposure improved tendon healing and tensile modulus recovery | NA | No AgNP toxicity shown at under 20 μM | Kwan et al. [2014] |

(Continued)

**Table D-1. Summary of in vitro studies of silver nanomaterials (Continued)**

| Cell Type | Particle Characteristics | Exposure Details: Concentrations/ Dose | Exposure Details: Duration | Major Outomes | NOAEL/ LOAEL | Comments | Reference |
|---|---|---|---|---|---|---|---|
| BEAS-2B (human bronchial epithelial), | PVP-coated Ag-NPs, 42.5-nm | 0.5, 1, 2, 4, 6, 8, 12, 24 and 48 μg/cm$^2$ (corresponding to 1.9, 3.8, 7.6, 15.2, 22.8, 30.4, 45.6, 91.2, and 182.4 μg/mL) (cytotoxicity); 2, 4, 8, 16, 24, 36 and 48 μg/cm$^2$ (corresponding to 7.6, 15.2, 30.4, 60.8, 91.2, 136.8, 182.4 μg/mL) (comet, micronucleus, chromosomal aberration assays) | 4-, 24-, 48-hour (cytotoxicity); 4-, 24-hour (comet assay); 48-hour (micronucleus assay); 24-hour (chromosomal aberration assay) | At 60.8-μg/mL, DNA damage (tail moment) increased; micronuclei formation and chromosomal aberrations did not increase | NA | Cytotoxicity assays needed to extrapolate from pre-apoptotic populations | Nymark et al. [2013] |
| HepG2 (hepatoma cells), PBMC (peripheral blood and mononuclear cells) | PVA-coated Ag-NPs, 4.0–11.7-nm | 1.0 and 50.0 μM | 24-hour | 1 and 50 μM AgNP increased DNA damage, apoptosis, and necrosis (except for 1 μM in HepG2) | NA | | Paino et al. [2015] |
| HEPG2 (human hepatoblastoma), Caco2 (human colon carcinoma) | AgNPs, 50-nm; $AgC_2H_3O_2$ | 1.0, 2.5, 5.0, 10.0, 15.0 μg/mL | 4-, 24-, 48-hour | AgNPs cause micronuclei formation and potentially apoptosis; HepG2 cells are more sensitive than Caco2; AgNPs also decreased mitochondria membrane potential; no AgNP-induced ROS detected; AgNPs are more toxic from 0.1 to 1.0 μg/mL; Ag ions more toxic at 10–20 μg/mL | NA | Studies linked because of their similarity in materials, models, and endpoints, though specific methods varied | Sahu et al. [2014a, 2014b, 2014c] |

(Continued)

**Table D-1. Summary of in vitro studies of silver nanomaterials (Continued)**

| | | Exposure Details | | | | | |
|---|---|---|---|---|---|---|---|
| Cell Type | Particle Characteristics | Concentrations/ Dose | Duration | Major Outomes | NOAEL/ LOAEL | Comments | Reference |
| HEPG2 (human hepatoblastoma), Caco2 (human colon carcinoma) | AgNPs, 50-nm; $AgC_2H_3O_2$ | 1, 3, 5, 10, 20 µg/mL | 24-hr | Ag ions caused cytotoxicity at lower concentrations than AgNPs; 50-nm AgNPs induce micronuclei and are genotoxic to HEPG2 cells but not Caco2 cells; Ag ion exposure does not cause micronuclei | NA | Comparisons were made to the results of Sahu et al. [2014a, 2014b, 2014c] | Sahu et al. [2016a, 2016b] |
| Primary PBMC (peripheral blood and mononuclear cells) differentiated to MDM (macrophages) | AgNPs, spherical, 20- and 110-nm, citrate- or PVP-stabilized | 5, 10, 20 and 50 µg/mL | 3-, 6-, 24-hr | AgNPs can reduce MDM viability, increase IL-8 expression, and suppress immune responses to *Mycobacterium tuberculosis* (including IL-1B, IL-10, and TNF-α expression) and other NF-κB-related genes | NA | Toxic effects were noted regardless of whether citrate or PVP was used as a stabilizer | Sarkar et al. [2015] |
| BMM (bone marrow-derived macrophages from 8-week old wild-type C57/Bl6 mouse) | AgNWs, 3-, 5-, 10-, 14-, 28-µm length, 115 –122-nm diameter | 2.5 µg/cm$^2$ | Up to 30-hr | AgNW over 5-µm impair mobility in wound closure | NA | Study also included in-vivo component (not discussed here) | Schinwald et al. [2012] |
| RLE (rat liver epithelial) RAEC (rat aortic endothelial) | AgNWs, citrate coated | 25 µg/mL (uptake); 6.25, 12.5, 25, 50 µg/mL (cytotoxicity); 50 µg/mL (activation) | 2-hr (uptake); 3-, 6-hr (cytotoxicity); 1-hr (activation) | Protein corona reduces AgNP uptake by cells; corona lost after uptake; SR-BI mediates AgNP uptake; AgNPs induce IL-6 expression | NA | | Shannahan et al. [2015] |

(Continued)

**Table D-1. Summary of in vitro studies of silver nanomaterials (Continued)**

| Cell Type | Particle Characteristics | Exposure Details: Concentrations/ Dose | Exposure Details: Duration | Major Outomes | NOAEL/ LOAEL | Comments | Reference |
|---|---|---|---|---|---|---|---|
| 16HBE (human bronchial epithelial), THP-1 (human acute monocytic leukemia) | AgNPs, pristine (90-nm) and aged paint (652-nm) | 1, 3, 9, 27, 81 and 243 µg/mL | 24-hr | Aged paint NPs less toxic than pristine NPs | NA | A co-culture was used in this study; NPs studied were not from the same paints prior to aging | Smulders et al. [2015b] |
| A549 (human lung epithelial), HaCat (keratinocyte) | AgNPs, synthesized; $Ag_2SO_4$ (as Ag ion source) | 1.0, 2.5, 5.0, 10 µM AgNP; 100, 250, 500, 750 nM $Ag_2SO_4$ | 24-, 48hr | AgNPs and/or Ag ions inhibit selenoprotein synthesis | NA | Ag ions affected selenoprotein synthesis at lower concentrations | Srivastava et al. [2012] |
| HSC (rat hepatic stellate cells) | PVP-coated AgNPs, 10- and 30–50-nm | 20, 100, and 250 µg/mL (cytotoxicity); 20 and 100 µg/mL (cell IQ), 20 µg/mL (cytokine detection) | 96-hr (cytotoxicity), 24-hr (apoptosis), 4-hr (LDH assay); 72-hr (cell IQ); 2-days (cytokine detection) | PVP-AgNP have low acute (sub 4-hr) toxicity, but exposure causes apoptosis in a dose- and inversely size-dependent manner; AgNP exposure inhibits MMP-2 and -9 production | NA | | Sun et al. [2013] |
| 184B5, MCF-7, MCF-10A, TNBC (triple-negative breast cancer) [MDA-MB-231 (human mammary epithelial cells), BT-549, SUM-159] | PVP-coated AgNPs, 20–30-nm | 0–100 µg/mL | 24-hr | TNBCs were more sensitive to AgNPs than other models; Ag ions did not have same effects as AgNPs | NA | Study also included in-vivo component (not discussed here) | Swanner et al. [2015] |
| isolated mitochondria from Wistar rat livers | AgNPs, 40- or 80-nm | 2, 5 µg AgNP/mg protein | Unknown | AgNPs increase mitochondrial permeability, decrease function | NA | | Teodoro et al. [2011] |

(Continued)

**Table D-1. Summary of in vitro studies of silver nanomaterials (Continued)**

| Cell Type | Particle Characteristics | Exposure Details: Concentrations/ Dose | Exposure Details: Duration | Major Outomes | NOAEL/ LOAEL | Comments | Reference |
|---|---|---|---|---|---|---|---|
| HEPG2 (human hepatoblastoma), HCT116 (human colon carcinoma), A549 (human lung epithelial), MCF-7 (human caucasian breast adenocarcin-oma) | Ag-incorporating zeolites | 0.78, 1.56, 3.125, 6.25, 12.5, 25, 50, 100 µg/mL | 48-hour | Cell responses vary between cell lines; all lines had LD50s under 15-µg/mL AgNPs | NA | Ag incorporation into zeolites was part of experimental procedure | Youssef et al. [2015] |
| **Bacteria/Viruses** | | | | | | | |
| Four histidine-requiring strains of *Salmonella typhimurium* (TA98, TA100, TA1535, TA1537); one tryptophan-requiring strain of *Escherichia coli* (WP2uvrA) | 10 nm average particle size; colloidal; absence of metabolic activation; presence of metabolic activation | 0, 7.8, 15.6, 31.2, 62.5, 125, 250, 500 and 1000 µg/mL | 6- and 24-hr incubation | No statistically significant number of revertant colonies observed in any strain, regardless of metabolic activation; no statistically significant increase in cells with polyploidy or endoreduplication, regardless of metabolic activation | NA | Absence of metabolic activation: cytotoxic effect at 15.6 µg/mL; Presence of metabolic activation: cytotoxicity induced above 31.2 µg/mL | Kim et al. [2013] |
| *E. coli* (wild-type K12 strain MG1655) with bovine serum albumin | Spherical AgNPs: 9.3 nm in diameter | AgNPs: 0.4 and 0.8 nm; $AgNO_3$: 6 and 12 nm | 5–30 min | Short-term incubation of *E. coli* with AgNPs provided evidence of membrane destabilization; reduction in membrane potential; depletion of intracellular potassium and ATP | NA | Silver presented in the nanoparticle form was more efficient at deterring bacterial growth | Lok et al. [2006] |

## D.8 Dermal Absorption (in Vitro)

A series of experiments by Larese et al. [2009] examined the capacity of AgNPs to penetrate human skin in vitro. The researchers used Franz diffusion cells to monitor the penetration of silver through either intact or abraded previously frozen, full-thickness skin preparations. The preparation was a 0.14-weight percent suspension of PVP-coated AgNPs in ethanol, with a mean diameter of 25 ± 7.1 nm (range, 9.8–48.8 nm). The use of a PVP coat ensured structural stability of the particles and deterred aggregation. The particles were applied to the skin in a 1:10 dilution of synthetic sweat (pH, 4.5). After 24 hours, median silver concentrations of 0.46 and 2.32 nanograms per square centimeter ($ng/cm^2$) were obtained in the receptor fluid for intact and damaged skin, respectively. Penetration of silver proceeded in a linear fashion between 4 and 24 hours through abraded skin but leveled off after approximately 8 hours in intact skin. The absorption rates of silver through abraded skin were about fivefold higher than for intact skin. Using TEM, the authors observed silver deposition in the stratum cornea and upper layers of the epidermis.

This page intentionally left blank.

# APPENDIX E

## Toxicological and Toxicokinetic Effects of Silver Nanoparticles in Experimental Animal Studies

# E.1 Inhalation Exposure

## E.1.1 Toxicokinetics

The absorption and distribution of AgNPs via the inhalation route were studied in 16 female F344 rats that received a single 6-hour exposure to AgNPs at a concentration of 133 μg/m$^3$ and subsequently were killed (four animals per timepoint) at 0, 1, 4, or 7 days post-exposure [Takenaka et al. 2001]. The AgNPs, as generated by a spark discharging through an argon atmosphere, were compact and spherical, with a median diameter of 17 ± 1.2 nm (GSD = 1.38) and minimal aggregation. Immediately after exposure, silver was detected at elevated concentrations in the lungs, nasal cavity, liver, and blood, but the concentrations declined over time.

The researchers detected a total of 1.7 μg of silver in the lungs immediately after exposure had ended, by using inductively coupled plasma mass spectroscopy (ICP-MS cannot differentiate elemental from ionic silver). However, this amount dropped quickly, and only about 4% of the initial pulmonary burden was present after 7 days. Evidence that absorption of the nanoparticles had occurred came from the detection of 8.9 nanograms per gram wet weight (ng/g) silver in the blood on the first day. This was lower in subsequent analyses, as silver was distributed to secondary target tissues such as the liver, kidney, heart, and tracheobronchial lymph nodes. Absorption data for inhaled AgNPs were compared with those obtained when 150 microliters (μL) of an aqueous solution of silver nitrate was intratracheally instilled in 12 animals. Similarly, in another phase of the experiment, a 150-μL aqueous suspension of AgNPs was intratracheally instilled in seven animals. Increased aggregation of the AgNPs had occurred in the latter preparation, and in contrast to the findings with monodispersed AgNPs, up to 32% of the silver from the aggregated preparation was retained in the alveolar macrophages after 4 or 7 days. The water-soluble silver was rapidly cleared from the lungs in a manner similar to that of the monodispersed AgNPs, suggesting that both entities can be readily absorbed via the lungs and undergo systemic distribution. Additional studies addressing toxicokinetics following inhalation are addressed in Section E.1.2, in conjunction with toxicological findings in those studies.

## E.1.2 Toxicological Effects

Inhalation studies reported by Ji et al. [2007a,b], Sung et al. [2008, 2009, 2011], and Song et al. [2013] exposed Sprague-Dawley rats to AgNPs that were generated by using a small ceramic heater and an air supply to disperse defined amounts of AgNPs from a bulk silver source material into the inhalation chambers [Ji et al. 2007a]. Ji et al. [2007a] describe a nanoparticle generation method involving heating of a source material, but do not specify the nature of that material beyond saying it was "bulk silver." They also state that for a "long-term stability test, a wound silver wire with 0.8 mm diameter was placed on the heater surface." The particles were found to be composed of elemental silver, monodispersed and spherical, with diameters predominantly in the 15- to 20-nm range.

In the acute study, five rats per sex per group received a single 4-hour exposure to 0 particles (fresh air controls); 0.94 × 106 particles/cm$^3$ (76 μg/m$^3$ silver; low concentration); 1.64 × 106 particles/cm$^3$ (135 μg/m$^3$ silver; mid concentration); or 3.08 × 106 particles/cm$^3$ (750 μg/m$^3$ silver; high concentration) [Sung et al. 2011]. Mortality, clinical signs, body weight changes, food consumption, and lung function were monitored over a 2-week period after exposure. At necropsy, weights of the major organs were compared to those of controls.

Lung function parameters examined included tidal volume, minute volume, respiration rate, inspiration and expiration times, and peak inspiration and expiration flows. All animals survived exposure and the 2-week observation period, and there were no clinical signs of toxicity. Food consumption and body weights were closely similar to those of controls among the groups. Likewise, lung function tests showed no statistically significant differences between the groups and controls. Sung et al. [2011] pointed to the difficulty of generating higher concentrations of monodispersed nanoparticles in

their system. Nonetheless, the authors determined that the high concentration of 750 μg/m$^3$ was 7.5 times higher than the ACGIH TLV (100 μg/m$^3$) for silver dust and probably more than 600 times the particle surface area for silver dust, assuming a 4-μm diameter for the latter and a nanoparticle surface area of $8.69 \times 10^9$ nm$^2$/cm$^3$. However, no acute toxicological effects of AgNPs at this exposure concentration were evident in these studies.

In a 28-day inhalation study, the same researchers exposed ten 8-week-old specific-pathogen-free (SPF) Sprague-Dawley rats per sex per group, 6 hours/day, 5 days/week, for 4 weeks to 0 particles (fresh air controls); $1.73 \times 10^4$ AgNPs/cm$^3$ (0.48 μg/m$^3$ silver; low concentration); $1.27 \times 105$/cm$^3$ (3.48 μg/m$^3$ silver; mid concentration); or $1.32 \times 10^6$/cm$^3$ (61 μg/m$^3$ silver; high concentration), following OECD Test Guideline 412 [Ji et al. 2007b]. Respective geometric mean particle diameters (and geometric standard deviations) were 11.93 nm (0.22), 12.40 nm (0.15), and 14.77 nm (0.11); the higher diameter at the high concentration was explained as being due to agglomeration of particles. Parameters monitored included clinical signs, body weight changes, and, at term, hematology and clinical chemistry values, organ weights, tissue silver, and histopathologic effects.

The body weight changes among the groups did not differ statistically significantly from those of controls, and there were no statistically significant organ weight changes in either males or females after 28 days of exposure to AgNPs. Although isolated fluctuations in food consumption, hematology, or clinical chemistry parameters were not considered related to treatment, Ji et al. [2007b] observed instances of cytoplasmic vacuolization in the liver of exposed animals. This response was likely due to lipid accumulation and, as a common response to hepatic injury [Eustis et al. 1990], was probably treatment related.

For males there was one such case among controls, and there were four cases in the low-concentration group and one each in the mid- and high concentration groups. For females, the effects were more dose-related; there were two cases each in the control and low-concentration groups, six in the mid-concentration group, and seven in the high concentration group. Other histopathologic effects on the liver included two cases of hepatic focal necrosis at high concentration in males and a single case at high concentration among females. No histopathologic effects of AgNPs were seen in the kidney, spleen, lungs, adrenals, heart, reproductive organs, brain, or nasal cavity. There was also a concentration-dependent increase in the concentration of silver deposited in the lungs. Likewise, silver was readily detected in the liver and brain of animals exposed at the high concentration but only marginally so in the blood, suggesting rapid clearance from the bloodstream to the tissues after inhalation.

Hyuan et al. [2008] also examined the potential effects of inhaled AgNPs on the respiratory mucosa of Sprague-Dawley rats. Ten animals per sex per group were exposed 6 hours/day, 5 days/week, for 28 days to 0 particles (fresh air controls); $1.73 \times 10^4$ particles/cm$^3$ (0.5 μg/m$^3$; low concentration); $1.27 \times 10^5$ particles/cm$^3$ (3.5 μg/m$^3$; mid concentration); or $1.32 \times 10^6$ particles/cm$^3$ (61 μg/m$^3$; high concentration). Histochemical staining of the respiratory mucosa showed the number and size of neutral mucin-producing goblet cells to be increased, whereas those producing acid mucins were unchanged. No histopathologic changes were observed in the lungs or nasal cavity. Foamy alveolar macrophages were observed in rats exposed to 3.5 and 61 μg Ag/m$^3$. The toxicological significance of these changes was uncertain.

Sung et al. [2008, 2009] reported the toxicological effects of inhaled AgNPs from a single experiment (following OECD Test Guideline 413) in which ten Sprague-Dawley rats per sex per group were exposed 6 hours/day, 5 days/week, for 90 days. The study was designed to identify possible adverse effects not detected in the 28-day study by Ji et al. [2007b] and Hyun et al. [2008]. AgNPs were generated and concentrations and size distributions were measured as described by Ji et al. [2007 a,b]. As reported by Sung et al. [2008], rats were exposed to 0 particles (fresh air controls); $0.7 \times 10^6$ particles/cm$^3$ (48.94 μg Ag/m$^3$); $1.4 \times 10^6$ particles/cm$^3$ (133.19 μg Ag/m$^3$); or $2.9 \times 10^6$ particles/cm$^3$ (514.78 μg Ag/m$^3$).

**Table E-1. Incidence and severity of histopathologic changes in the lungs of Sprague-Dawley rats following inhalation exposure to silver nanoparticles in Sung et al [2008].**

| Exposure Parameters | Males | | | | Females | | | |
|---|---|---|---|---|---|---|---|---|
| | Control | Low | Mid | High | Control | Low | Mid | High |
| Number (particles/$cm^3$) × $10^5$ | 0 | 6.64 | 14.3 | 28.5 | 0 | 6.64 | 14.3 | 28.5 |
| Surface area ($nm^2/cm^3$) × $10^9$ | 0 | 1.08 | 2.37 | 6.61 | 0 | 1.08 | 2.37 | 6.61 |
| Mass (μg/$m^3$) | 0 | 48.94 | 133.19 | 514.78 | 0 | 48.94 | 133.19 | 514.78 |
| **Tissue deficits** | | | | | | | | |
| Accumulation (macrophage, alveolar) | 3/10 | 5/10 | 5/10 | 8/10 | 7/10 | 4/10 | 4/10 | 6/10 |
| Inflammation (chronic, alveolar) | 2/10 | 3/10 | 2/10 | 7/10 | 3/10 | 2/10 | 0/10 | 8/10 |
| Infiltration (mixed-cell perivascular) | 3/10 | 4/10 | 6/10 | 8/10 | 0/10 | 0/10 | 1/10 | 7/10 |

Lung function was tested weekly on four animals per dose group, 40 minutes after the end of exposure. Respective geometric mean diameters (and geometric standard deviations) were 18.30 nm (1.10), 18.71 nm (1.78), and 18.93 nm (1.59). As a mark of pulmonary inflammation, the appearance of albumin, lactate dehydrogenase, and total protein was monitored in bronchoalveolar lavage (BAL) fluid obtained at term. Cell counts of macrophages, polymorphonuclear cells, and lymphocytes in BAL fluid were obtained histologically. Excised pieces of lung were examined by histopathology.

Pulmonary function was evaluated weekly in four rats per sex per group by means of ventilated bias-flow whole-body plethysmography to determine tidal volume, minute volume, respiratory frequency, inspiration and expiration times, and peak inspiration and expiration flow [Sung et al. 2008]. Among the lung function test results, tidal volume, minute volume, and peak inspiration flow showed dose-related deficits in response to AgNP inhalation. In addition, stained slides of lung sections indicated treatment-related increases in the incidence of mixed cell infiltrate perivascular and chronic alveolar inflammation, including alveolitis, granulomatous lesions, and alveolar wall thickening and macrophage accumulation (Table E-1).

In discussing their data, Sung et al. [2008] compared the lung function deficits with those reported for subjects exposed to welding fumes, drawing the conclusion that the cumulative lung dose of AgNPs at the high dose (514.78 μg Ag/$m^3$) was 10–15 times less than the welding fume exposure in terms of mass dose for a similar level of response. Therefore, it was hypothesized that surface area or particle number may be a more meaningful determinant of exposure than mass when correlated with lung function deficits and associated histopathologic changes.

In the second report, data were presented on hematology and clinical chemistry parameters, and excised pieces of the major organs and tissues were examined for histopathology changes and silver deposition [Sung et al. 2009]. There were few, if any, effects of AgNP administration during the in-life phase of the experiment, although one high-concentration male died during an ophthalmologic examination. No treatment-related effects on body weight change, food consumption or, at term, organ weights, hematology, or clinical chemistry parameters were observed in the remaining rats. Tissue content of silver was dose-dependently increased in lung, liver, kidney, olfactory bulb, brain, and whole blood, and some histopathologic lesions were noted in the liver that appeared to be related to dose. For example, as shown in Table E-2, bile-duct hyperplasia was noted

**Table E-2. Incidence and severity of histopathologic changes in the livers of Sprague-Dawley rats following inhalation exposure to silver nanoparticles in Sung et al [2009].**

| Exposure Parameters | Males | | | | Females | | | |
|---|---|---|---|---|---|---|---|---|
| | Control | Low | Mid | High | Control | Low | Mid | High |
| Number (particles/$cm^3$) × $10^5$ | 0 | 6.64 | 14.3 | 28.5 | 0 | 6.64 | 14.3 | 28.5 |
| Surface area ($nm^2/cm^3$) × $10^9$ | 0 | 1.08 | 2.37 | 6.61 | 0 | 1.08 | 2.37 | 6.61 |
| Mass (μg/$m^3$) | 0 | 48.94 | 133.19 | 514.78 | 0 | 48.94 | 133.19 | 514.78 |
| **Tissue deficits** | | | | | | | | |
| Bile duct hyperplasia | 0/10 | 0/10 | 1/10 | 4/9 | 3/10 | 2/10 | 4/10 | 9/10 |
| Hepatocellular necrosis (single cell) | 0/10 | 0/10 | 0/10 | 0/9 | 0/10 | 0/10 | 0/10 | 3/10 |

with increased incidence in higher-concentration groups. Furthermore, single-cell hepatocellular necrosis was seen in three of 10 female rats exposed to the high concentration. The authors of the study suggested that their data were indicative of a no observed adverse effect level (NOAEL) in the region of 100 μg/$m^3$ that was consistent with the ACGIH TLV of 100 μg/$m^3$ for silver dust.

The finding of bile duct hyperplasia, in parallel with the lung function deficits plotted by Sung et al. [2008], indicated statistically significant decrements. However, hepatic effects can also be characteristic of aging rats as well as a common response to the administration of some chemicals [Eustis et al. 1990], although the findings of dose-dependent increases in lesions is most likely a result of AgNP exposure.

Lee et al. [2010] screened for differentially expressed genes in the brains of C57Bl/6 mice exposed to AgNPs via inhalation. The nanoparticles were produced by the same procedure described in the first paragraph of this section and had characteristics similar to those used by other researchers [Sung et al. 2011, 2009, 2008; Hyun et al. 2008; Ji et al. 2007a,b]. Two groups of seven male mice were exposed to silver nanoparticles (1.91 × $10^7$ particles/$cm^3$; geometric mean diameter, 22.18 ± 1.72 nm) 6 hours/day, 5 days/week, for 2 weeks. One of the exposure groups was observed for a 2 week recovery period before being killed for necropsy. Two other groups of seven mice served as untreated and sham-exposed controls.

When total ribonucleic acid (RNA) from the cerebrum and cerebellum was analyzed by gene microarray, the expression of 468 and 952 genes, respectively, showed some degree of response to AgNP exposure, including several associated with motor neuron disorders, neurodegenerative disease, and immune cell function.

The use of real-time quantitative reverse-transcription polymerase chain reaction (RT-PCR) to analyze the expression of selected genes in whole blood identified five genes that were downregulated in response to AgNP exposure. Expression of three of the five remained suppressed throughout the 2-week recovery period, but expression of the other two returned to control levels during the recovery phase. Lee et al. [2010] considered these genes to have potential as biomarkers for recent exposure to AgNPs.

Kim et al. [2011a] reported on the evaluation of genotoxic potential of AgNPs that were generated as described by Ji et al. [2007a] and Sung et al. [2008]. Male and female Sprague-Dawley rats were exposed by inhalation for 90 days according to OECD Test Guideline 413. Rats were exposed to AgNPs (18 nm in diameter) at concentrations of 0.7 × $10^6$ particles/$cm^3$ (low dose), 1.4 × $10^6$ particles/$cm^3$ (middle dose), and 2.9 × $10^6$ particles/$cm^3$ (high dose) for 6 hours per day and then killed 24 hours after the last administration. The femurs were removed and bone marrow was collected and evaluated for micronucleus induction according to OECD Test Guide-

line 474. The in vivo micronucleus test was used for detection of cytogenetic damage.

Although a dose-related increase was found in the number of micronucleated polychromatic erythrocytes (MNPCEs) in the male rats, no statistically significant treatment-related increase in MNPCEs was found in the male and female rats in comparison with the negative controls. These findings were consistent with those reported by Kim et al. [2008], in which no genotoxicity (per in vivo micronucleus test) was found in rats following the oral administration of AgNPs for 28 days.

Song et al. [2013] reported the lung effects in male and female Sprague-Dawley rats (17 males and 12 females per exposure group) following 12-week inhalation exposure to AgNPs (14–15 nm in diameter). Exposure concentrations were 49 μg/m$^3$ (0.66 × 10$^6$ particles/cm$^3$; low dose), 117 μg/m$^3$ (1.41 × 10$^6$ particles/cm$^3$; middle dose), or 381 μg/m$^3$ (3.24 × 10$^6$ particles/cm$^3$; high dose) for 6 hours per day. Lung function was measured every week during the exposure period and after cessation of exposure.

Animals were killed after the 12-week exposure period and at 4 and 12 weeks after the exposure cessation. Lungs were analyzed for silver concentration with use of NIOSH Analytical Method 7300. Song et al. [2013] noted that histopathologic examination of rat lung tissue showed "a significant increase in the incidence of mixed cell infiltrate, perivascular and chronic alveolar inflammation, including alveolaritis, granulomatous lesions, and alveolar wall thickening and alveolar macrophage accumulation in both the male and female rats." These effects were observed in the middle- and high-dose groups of male rats and in the high-dose group of female rats, at the end of the 12-week exposure. Gradual clearance of AgNPs and decreased inflammation of the lungs were observed in female rats but not in the high-dose males during the 12-week recovery period.

The findings suggest a possible NOAEL of 49 μg/m$^3$ (low dose) and a lowest observed adverse effect level (LOAEL) of 117 μg/m$^3$ (middle dose), although the authors suggested that the effects at the middle dose could be considered a NOAEL on the basis of similar effects (minimal accumulation of macrophages and inflammation in the alveoli) to those observed in the control group of the study by Sung et al. [2009]. Some of the lung effects noted by Song et al. [2013] were reported to persist at the end of the 12-week exposure period, and male rats were observed to be more susceptible than the females to the lung effects of AgNP exposure. Lung function decreases (including in tidal volume, minute volume, and peak expiratory flow) and lung inflammation were observed in male rats and persisted in the high-dose group at 12 weeks post-exposure. In female rats, no decrease in lung function was observed, and the lung inflammation showed gradual recovery after cessation of exposure [Song et al. 2013].

A dose-dependent, statistically significant increase in silver concentration was observed in all tissues from the male and female rat groups exposed to AgNPs for 12 weeks, except for the female brain. Silver accumulation was still observed in some tissues at 4 weeks after the end of exposure (including in the liver, kidneys, spleen, and blood, and in the ovaries in female rats). Silver concentrations remained statistically significantly increased (in comparison with the unexposed control rats) in the liver and spleen at 12 weeks post-exposure. The silver concentrations in the kidneys also showed a sex difference, with the female kidneys containing five times more accumulated silver than the male kidneys. No histopathologic effects of silver in organs other than the lungs were reported [Song et al. 2013]. Exposure parameters and lung histopathology are summarized in Table E-3.

In a follow-up study, Dong et al. [2013] investigated the sex-dependent effect of AgNPs on the kidney gene level, based on toxicogenomic studies of kidneys from rats exposed to AgNPs via inhalation for 12 weeks. The exposure conditions were the same as those employed by Song et al. [2013], and the study included both male and female SPF Sprague-Dawley rats, divided into four groups. The male groups (n = 17) consisted of 5 rats for 12-week exposure, 4 for 4-week recovery, 4 for 12-week recovery, and 4

**Table E-3. Incidence and severity of silver nanoparticle–related histopathologic changes in the lungs of Sprague-Dawley rats.**

| Exposure Parameters | Males | | | | Females | | | |
|---|---|---|---|---|---|---|---|---|
| | Control | Low | Mid | High | Control | Low | Mid | High |
| Number (particles/cm$^3$) × 10$^{-5}$ | 0 | 6.6 | 14.1 | 32.4 | 0 | 6.6 | 14.1 | 32.4 |
| Surface area (nm$^2$/cm$^3$) × 10$^{-9}$ | 0 | 0.76 | 1.70 | 4.85 | 0 | 0.76 | 1.70 | 4.85 |
| Mass (µg/m$^3$) | 0 | 48.76 | 117.14 | 381.43 | 0 | 48.76 | 117.14 | 381.43 |
| **Tissue deficits—12-week exposure** | | | | | | | | |
| Accumulation (macrophage, alveolar) | 0/5 | 1/5 | 3/5 | 5/5 | 0/4 | 0/4 | 0/4 | 4/4 |
| Inflammation (chronic, alveolar) | 0/5 | 0/5 | 3/5 | 5/5 | 0/4 | 0/4 | 0/4 | 4/4 |
| Infiltration (mixed-cell perivascular) | 1/5 | 1/5 | 3/5 | 5/5 | 0/4 | 0/4 | 0/4 | 4/4 |
| **Tissue deficits—4-week recovery** | | | | | | | | |
| Accumulation (macrophage, alveolar) | 0/4 | 0/4 | 1/4 | 2/4 | 0/4 | 0/4 | 1/4 | 2/4 |
| Inflammation (chronic, alveolar) | 0/4 | 0/4 | 0/4 | 0/4 | 0/4 | 0/4 | 0/4 | 0/4 |
| Infiltration (mixed-cell perivascular) | 2/4 | 0/4 | 0/4 | 0/4 | 0/4 | 1/4 | 0/4 | 0/4 |
| **Tissue deficits—12-week recovery** | | | | | | | | |
| Accumulation (macrophage, alveolar) | 1/5 | 0/4 | 2/4 | 3/4 | 0/4 | 0/4 | 1/4 | 0/4 |
| Inflammation (chronic, alveolar) | 0/5 | 0/4 | 0/4 | 1/4 | 0/4 | 0/4 | 0/4 | 0/4 |
| Infiltration (mixed-cell perivascular) | 0/5 | 0/4 | 1/4 | 0/4 | 0/4 | 0/4 | 1/4 | 0/4 |

Source: Song et al. [2013].

for micronucleus testing after 12-week exposure. The female groups (n = 13) consisted of 5 rats for 12-week exposure, 4 for 4-week recovery, and 4 for 12-week recovery. The air-control exposure group included four male and female rats. Exposure target doses were as follows: for the low-dose group, $0.6 \times 10^6$ particles/cm$^3$ ($1.0 \times 10^9$ nm$^2$/cm$^2$, 48.76 µg/m$^3$); for the medium-dose group, $1.4 \times 10^6$ particles/cm$^3$ ($2.5 \times 10^9$ nm$^2$/cm$^2$, 117.14 µg/m$^3$); and for the high-dose group, $3.0 \times 10^6$ particles/cm$^3$ ($5.0 \times 10^9$ nm$^2$/cm$^2$, 381.43 µg/m$^3$). AgNPs were spherical, with diameters <47 nm (range, 4–47 nm; GSD, 1.71).

After a 12-week exposure, silver concentrations in the kidneys confirmed a sex difference: in the low- and medium-dose groups, the silver concentration was twofold higher in the kidneys of female versus male rats [Dong et al. 2013]; and in the high-dose group, a fourfold higher silver concentration in the kidneys of females was consistent with results previously reported [Kim et al. 2008; Sung et al. 2009;

Song et al. 2013]. These sex differences have been suggested to be related to metabolism and hormonal regulation, because the kidneys are a target organ for several hormones such as thyroid hormones and testosterone [Kim et al. 2009a].

Gene expression changes were evaluated in the study by means of a deoxyribonucleic acid (DNA) microarray of the kidneys for the low- and high-dose groups of male and female rats. The genes that were upregulated or downregulated by more than 1.3-fold ($p < 0.05$) were regarded as statistically significant. As a result, 104 genes were found to have been upregulated or downregulated by more than 1.3-fold in male rats. Among the 104 genes changed by exposure, 24 genes were involved in the KEGG pathway and related to 49 biologic pathways. In the female kidneys, 72 genes were found to have been upregulated or downregulated by more than 1.3-fold. Among the 72 genes changed by exposure to either the low or high dose, 21 genes were involved in the KEGG pathway and related to 33 biologic pathways. The sex gene profiling in the study showed a predominant expression of metabolic enzyme–related genes in the male rat kidneys, versus a predominant expression of extracellular signaling–related genes in the female rat kidneys. However, no statistically significant gene alterations were observed in the redox system, inflammation, cell cycle, and apoptosis-related genes in either sex.

The capacity of AgNPs to bring about toxicological changes in the lung as a result of subacute inhalation was investigated in C57Bl/6 mice by Stebounova et al. [2011]. Twenty-six male C57Bl/6 mice underwent whole-body exposure to 3300 μg/m$^3$ AgNPs 4 hours/day, 5 days/week, for 2 weeks. Along with 13 sham-exposed controls, equal numbers of mice were necropsied within 1 hour or 3 weeks after exposure to determine BAL fluid composition (5 per group), lung histopathology (3 per group), and silver deposition to the major organs (5 per group). The AgNPs were a commercial product with a stated particle size of 10 nm. The PVP-coated particles were ultrasonicated in water, nebulized to an aerosol, and then dried at 110°C prior to introduction into the exposure chamber.

The AgNPs showed a bimodal particle size distribution, with peak maxima at 5 nm (85%–90% of the particle count) and 22 nm (<15%). However, in use, the aerosolized nanoparticles showed a degree of aggregation (with a geometric mean diameter of 79 nm). Stebounova et al. [2011] reported a median of 31 μg silver per gram (g) dry weight in the lungs of mice necropsied immediately after exposure. Those necropsied after a 3-week recovery period had a median silver content of 10 μg/g; two of the five mice had none detected. Silver was also detected in the BAL fluid of exposed animals, with mean concentrations of 13.9 μg/L in animals necropsied at cessation of exposure and 1.7 μg/L in those necropsied 3 weeks post-exposure. However, the silver content in the heart, liver, and brain was below the detection limit.

In examining the cell content and presence of biomarkers in BAL fluid from silver-exposed mice, the authors reported that the numbers of macrophages and neutrophils were approximately double those in the BAL specimens of controls, although no biologic significance was assigned to this change. Furthermore, there were no treatment-related changes in total protein levels or lactate dehydrogenase (LDH) activity, and most cytokines assayed were below their limits of detection. Lung histopathology yielded unremarkable findings, allowing Stebounova et al. [2011] to conclude that overall, C57Bl/6 mice showed minimal pulmonary inflammation or cytotoxicity when exposed to AgNPs under the prevailing exposure conditions.

An acute inhalation exposure study examining lung effects was conducted by Seiffert et al. [2016]. In this study, the investigators generated an AgNP aerosol by a spark generation method, yielding AgNP with a count mean diameter of 13 to 16 nm and geometric standard deviation of ~1.6. In this study, two different strains of rats, Sprague-Dawley (SD; outbred) and Brown Norway (BN; inbred), were exposed via nose-only inhalation to a dose of $3.68–4.55 \times 10^7$ particles/cm$^3$ (0.6–0.8 mg/m$^3$) for 3 hours (low dose) or 3 hours/day for 4 days (high dose). Lung and alveolar silver burden were estimated to be 8 and 6 μg for the low dose and 26–28

and 18–19 μg for the high dose, respectively, for the two strains. Animals were euthanized 1 and 7 days following exposure, and AgNP lung distribution, lung mechanics (airway resistance and tissue elastance) and BAL fluid parameters were evaluated (n = 8–12 per group per time point).

Silver burden in the lung and in macrophages was higher for BN rats at day 1 compared to SD rats, although silver levels decreased with time in both strains. In SD rats, silver staining showed particles localized in macrophages in the alveolar region and lung interstitium. In BN rats, silver-positive macrophages were located in alveolar septum, airway mucosa, and lamina propria of blood vessels, as well as in termina bronchioles. No changes in airway mechanics were observed for SD rats, whereas increased airway resistance and tissue elastance were observed in BN rats 1 day post-exposure, which resolved by 7 days post-exposure. Inflammatory cells in the lung were increased at day 1, characterized by neutrophils in SD rats and by neutrophils and eosinophils in BN rats, at the high dose, with resolution over time. Malonaldehyde levels in BAL fluid, an index of oxidative stress, were elevated at day 1, along with phospholipid levels in both strains. Surfactant protein-D was lower overall in BN rats compared to SD rats and was increased at the low dose at day 1 in BN compared to air controls. It was reduced at the high dose in SD rats at day 7.

The authors suggest that changes in phospholipid and protein may influence uptake and aggregation of particles in vivo. BAL fluid cytokines related to immune and inflammatory responses (KC, IL-1β, MCP-1, MIP-2, IL-17a) were increased at day 1 in both strains in the high-dose rats and to a greater degree in the BN rats. IL-6 was also increased in BN rats at day 1. At the low dose, there were greater elevations of cytokine in the BN rats. Cytokine responses resolved with time in both strains. Overall, AgNP exposure caused increased toxicity that showed some degree of resolution over time, and strain-related differences were attributed to the underlying inflammatory state of the lungs in BN rats.

An acute nose-only inhalation study was also conducted by Kwon et al. [2012], using a system similar to that in the studies by Jie et al. [2007a; b]. Male C57BL/6 mice were exposed to ~2.9 mg/m$^3$ AgNPs ($1.93 \times 10^7$ particles/cm$^3$) with diameter of 20–30 nm for 6 hours. Silver biodistribution, lung pathology, and BAL fluid parameters were analyzed at 0 and 24 hours following exposure (n = 5 per group per timepoint). Lung burden decreased substantially between 0 and 24 hours post-exposure. Silver levels were increased in brain, heart, spleen, and testes at 0 hours. No silver was detected in the kidney, and silver in the liver was not above control levels. There was a trend for an increase in silver in liver and testis at 24 hours. Silver measured in the heart and spleen decreased over time. Changes in mitogen-activated protein kinase (MAPK) signaling were detected at the molecular level in lung tissue. Despite changes at the molecular level in tissue, no differences in neutrophil influx or LDH in BAL specimens were observed; only a statistically insignificant increase in total protein in BAL fluid was observed at 0 hours, and no histopathological changes were observed in the lungs.

Roberts et al. [2013] reported on the results of an inhalation study with rats exposed to silver nanoparticles to assess pulmonary and cardiovascular responses from acute exposure. Two sources of AgNPs were used in the study: the first was a commercial antimicrobial product that contained 20 mg/L total silver (75% colloidal silver and 25% silver ions), and the other was a synthesized AgNP sample from the National Institute of Standards and Technology (NIST), reported to be 1,000 mg/L stock silver in deionized water (100% colloidal silver). Male Sprague-Dawley rats were exposed by inhalation for 5 hours to a low concentration (100 μg/m$^3$) of the commercial antimicrobial product (20 mg/L total silver; ~33 nm count median aerodynamic diameter [CMAD]) or to 1000 μg/m$^3$ in a suspension from the NIST sample (200 mg/L total silver; ~39 nm CMAD). Estimated lung burdens determined from deposition models were 0 (control aerosol), 1.4 μg Ag/rat (low dose), and 14 μg Ag/rat (high dose). The low dose was selected to be equivalent to the TLV set by the ACGIH for particulate silver (100 μg/m$^3$). Two sets of exposures with paired controls were conducted for each dose.

For each exposure set and each dose, 12 rats were exposed to air (n = 6 for day 1 and n = 6 for day 7) and 12 rats were exposed to AgNPs (n = 6 for day 1 and n = 6 for day 7). Rats from one set of exposures were killed on days 1 and 7 for evaluation of pulmonary response (inflammation, cell toxicity, alveolar air/blood barrier damage, macrophage activity, blood cell differentials) and for microvascular studies (responsiveness of tail artery to vasoconstrictor or vasodilatory agents, heart rate and blood pressure in response to isoproterenol or norepinephrine, respectively).

Rats from the second set of exposures were killed on days 1 and 7 following measures for hemodynamic response. No statistically significant changes in pulmonary or cardiovascular parameters were observed for either the commercial or NIST samples at days 1 and 7 post-exposure, although slight cardiovascular changes were observed in the 1.4-μg exposure group, possibly because of the higher fraction of ionic silver in the commercial product than in the NIST sample.

A series of acute inhalation studies were conducted that compared effects of particle size on lung and tissue distribution [Anderson et al. 2015a; Braakhuis et al. 2014], pulmonary toxicity [Braakhuis et al. 2014; Silva et al. 2016], and translocation and effects in the olfactory bulb [Patchin et al. 2016]. Braakhuis et al. [2014] compared tissue distribution and lung effects in male Fischer rats (F344/DuCrl) following nose-only exposure to 15- or 410-nm particles at concentrations of 179 and 169 μg/m$^3$, respectively, for 6 hours per day for 4 consecutive days. Surface area and particle number were about 1 and 2 orders of magnitude greater for the 15-nm particles on a mass basis.

Lung burden of silver measured by ICP-MS was determined at 1 day post-exposure to be about 5.5 and 8.5 μg for 15- and 410-nm particles, respectively, with a degree of clearance for both particle sizes by day 7 post-exposure. Silver content was also measured in lung-associated lymph nodes, liver, kidney, spleen, testes, and brain. For all but the liver, silver levels were below the limit of detection. In the liver, silver was detected following exposure to the smaller particle only, with clearance over time. Pulmonary toxicity—measured as neutrophil influx, BAL fluid cytokines, and glutathione level—and lung injury markers were statistically significantly increased at 1 day post-exposure to the smaller particle when compared to the larger particle. Effects resolved by 7 days post-exposure. Effects were attributed in part to differences in internal dose and dissolution rate of the particles.

Exposure conditions for the Anderson et al. [2015a], Silva et al. [2016], and Patchin et al. [2016] studies were identical. Male Sprague-Dawley rats underwent a 6-hour nose-only inhalation of 20- or 110-nm citrate-stabilized AgNPs aerosolized at a concentration of 7.2 mg/m$^3$ or 5.3–5.4 mg/m$^3$, respectively, or citrate buffer aerosol as a control. In these studies, agglomerate size following aerosolization was measured to be 81% and 82% less than 1.6 μm, and the count mean diameter determined by SMPS was 77.4 and 78.2 for 20- and 110-nm particles, respectively. Anderson et al. [2015a] examined lung deposition and clearance at 0, 1, 7, 21, and 56 days post-exposure (n = 6 per group per time point). Investigators used ICP-MS to evaluate tissue silver burden, as well as hyperspectral analysis and autometallography of tissue and BAL fluid macrophages to assess tissue distribution and clearance of silver.

Thoracic deposition at day 0 was 321 and 357 ng for the 20- and 110-nm particles, respectively, and did not differ in distribution among lung lobes for the different particle sizes. One third of the initial load remained for both groups at day 56. Tissue clearance and distribution were comparable, with particles localized to the terminal bronchiole/alveolar duct junction. Macrophage uptake and burden over time were greater with 20-nm AgNPs in comparison to 110-nm AgNPs. The authors attributed this difference in part to the particle number per mass being greater in the 20-nm exposure versus the 110-nm exposure.

In a parallel study, Silva et al. [2016] examined pulmonary toxicity, following the same exposure paradigm as Anderson et al. [2015]. Histopathology and BAL were performed at 1, 7, 21, and 56 days post-exposure

(n = 6 per group per time point). BAL fluid LDH was equivalently elevated at 7 days post-exposure in both groups. BAL fluid protein was statistically significantly elevated in both the 20- and 110-nm AgNP groups at 1 and 7 days post-exposure; however, this occurred to a greater degree among the rats exposed to 20-nm particles. Neutrophil influx was statistically significantly elevated at 7 and 21 days post-exposure in the 20-nm-exposed group only.

Histopathological changes included increased inflammatory cells and cellular exudate in airspaces, a degree of eosinophil influx, Type II cell hypertrophy, and sloughing of airway epithelium in the most severe instances. Responses for both groups peaked at day 7 and resolved by day 21 for the rats exposed to larger particles, and by day 56 for rats exposed to 20-nm particles. In agreement with Anderson et al. [2015a], macrophages from rats exposed to 20-nm particles had a greater particle load than those exposed to 110-nm particles. In this study, the 20-nm particles produced a greater and more persistent response than the 110-nm particles, with responses resolving toward the end of the time course.

In a related study, using the same exposure paradigm, Patchin et al. [2016] examined size-dependent silver particle transport to the brain following inhalation of 20- or 110-nm AgNPs. In this study, the investigators examined deposition and clearance from the nasal cavity and the olfactory bulb (OB), using ICP-MS and autometallography of tissue, and assessed microglial activation as an index of toxicity in the OB at 0, 1, 7, 21, and 56 days post-exposure (n = 8 per group per time point). Silver deposition in the nasal cavity at day 0 was comparable for 20- and 110-nm particles; however, there was a statistically significantly greater amount of silver in the OB following exposure to 20-nm particles. At days 1 to 56, silver content in the OB after exposure to 20-nm particles remained relatively constant, whereas exposure to 110 nm resulted in a slight increase over time and a greater amount of silver in the OB at day 56 when compared to exposure to 20-nm particles. Nasal cavity silver decreased dramatically by day 1 for both particle sizes. Microglia activation was identified by Iba1- and/or TNF- $\alpha$ -positive staining of tissue. Activation increased at day 0 following exposure to both particle sizes, whereas activation was statistically significantly increased following only the 20-nm particle exposure at 1 and 7 days. The results taken together show that size affects the temporal translocation to the OB.

In addition to evaluations of the direct effects of AgNPs on toxicity following inhalation, studies have been conducted that assess the effects of AgNP inhalation on the course of the allergic response, using the ovalbumin (OVA) model of asthma in mice [Chuang et al. 2013; Jang et al. 2012; Su et al. 2013]. The OVA model of asthma consists of an initial sensitization phase to OVA, followed by a pulmonary challenge with OVA in order to establish the elicitation phase of allergic response. Allergic (OVA sensitization and elicitation without AgNP exposure) and non-allergic controls (no OVA sensitization with or without AgNP exposure) were employed in all studies.

In a pair of related studies by Chuang et al. [2013] and Su et al. [2013], the investigators delivered 33-nm AgNPs to female BALB/c mice at a dose of 3.3 $mg/m^3$ for 7 consecutive days between the OVA sensitization and challenge phase of the model to assess the effect of AgNP exposure on the elicitation phase of allergic response (n = 5–6 per group). Chuang et al. [2013] found that AgNP alone in the absence of OVA sensitization did not enhance BAL fluid IgE levels but did cause a statistically nonsignificant increase in neutrophils and eosinophils in the lungs, and it increased airway reactivity versus non-allergic control animals. In the allergy model, AgNP exposure caused a statistically significant increase in lung eosinophils, BAL fluid IgE and IL-13 levels, and airway reactivity following the elicitation phase, compared to allergic and non-allergic controls, suggesting that the particle exposure exacerbated the allergic response.

Su et al. [2013] used a proteomic evaluation of BAL fluid and plasma in the same animal model and found differentially altered protein levels in both allergic and nonallergic mice exposed to AgNPs, with 18 proteins associated with systemic lupus

erythematosus in both groups of mice. Jang et al. [2012] exposed female BALB/c mice to 6-nm AgNPs by nebulization at 20 ppm (40 mg/kg) once per day for 5 days immediately before OVA challenge in the elicitation phase of the allergy model. In addition, they investigated the role of the vascular endothelial growth factor (VEGF) pathway, using a VEGF receptor tyrosine kinase inhibitor in the model. They found AgNPs to attenuate the allergic response, reducing mucus secretion, eosinophil influx, airway reactivity, and activity in the VEGF signaling pathway relative to allergic controls. It is unclear why the two groups have conflicting results, although it may be attributed in part to study design differences in particle size, dose, and timing of particle delivery.

## E.2 Oral Exposure

### E.2.1 Toxicokinetics

The absorption and distribution of AgNPs via the oral route were studied by Loeschner et al. [2011] in groups of seven or nine female Wistar rats. The AgNPs were made by reducing silver nitrate with hydrazine in the presence of polyvinylpyrrolidone (PVP). The resulting nanoparticles were sedimented by centrifugation and dialyzed against deionized water. Size analysis showed the existence of two populations. The first, comprising about 90% of the material, was spherical, with a mean diameter of 14 ± 2 nm. Although the second population was larger (with a mean diameter of 50 ± 9 nm), these particles were also shown to be distinct nanoparticles rather than agglomerates. Female Wistar rats (n = 9) received 12.6 milligrams per kilogram body weight per day (mg/kg-day) of silver for 28 days via twice-daily gavage with the AgNP suspension, while seven rats underwent similar gavage with 9 mg/kg-day silver from an 11.5-mg/mL aqueous solution of silver acetate. Nine animals underwent gavage with an 11.5-mg/mL aqueous solution of PVP as vehicle controls.

During the third week of the study, rats were kept for 24 hours in metabolic cages to obtain samples of urine and feces. At term, samples of blood, brain, stomach, liver, kidney, lung, and muscle were taken for silver analysis (by ICP-MS), histopathology, scanning electron microscopy (SEM), and TEM characterization, as well as auto-metallography (AMG) and EDS.

A substantial proportion of the oral load of silver appeared in the feces of animals exposed to AgNPs (63 ± 23%) and the silver acetate solution (49 ± 21%), indicating some absorption of silver in the stomach, small intestine, liver, kidney, muscle, and lungs. However, Loeschner et al. [2011] were unable to assess the contribution of hepatobiliary recirculation to these values. A greater proportion of the oral load of silver acetate was absorbed than of AgNPs, although the use of AMG to locate silver within target tissues did not reveal statistically significant differences in the disposition of the element between the two administered forms. For example, silver was located in the lamina propria at the tips of the villae in the ileum but not in the epithelial cytoplasm. The use of EDS confirmed that granules in the lysosomes of macrophages consisted of silver, and additional signals identified as selenium and sulfur were also detected. In the liver there was intense staining of the Kupffer cells and around the central veins and portal tracts. In both cases, staining the kidney for silver located it in the glomeruli and proximal tubules.

The authors concluded that although silver concentrations in target organs were generally lower after administration of AgNPs than with water-soluble forms of the element, there were few if any differences in the distribution pattern of silver from either source. Given the similarities in disposition within the tissues, Loeschner et al. [2011] were unable to determine whether AgNPs were absorbed as an entity or whether they had dissolved in the gastrointestinal tract, followed by re-deposition in the tissues.

An experiment by Park et al. [2011a] determined the bioavailability and toxicokinetics of citrate-coated AgNPs in male Sprague-Dawley rats. As obtained from a commercial vendor, the particles were 7.9 ± 0.95 nm in diameter and coated with citrate; they

were employed by the researchers from a 20% (w/v) aqueous solution. Other physical and chemical data included a mean particle volume of $1.9 \times 10^3$ nm$^3$, a mean surface area of $7.53 \times 10^2$ nm$^2$/particle, and a mean particle mass of $2 \times 10^{-17}$ g. Animals received AgNPs at concentrations of 1 or 10 milligrams per kilogram body weight (mg/kg) orally or intravenously. After treatment, blood samples were taken at 10 minutes and then at 1, 2, 4, 8, 24, 48, and 96 hours. Feces and urine samples were collected for 24 hours after treatment, and excised pieces of liver, lung, and kidney were obtained at 24 and 96 hours post-dosing for silver analysis by ICP-MS.

With regard to absorption, a comparison of the ratio of the plasma areas under the curves for oral versus intravenous administration gave measures of the bioavailability for oral exposure to this species of nanoparticles. Values of 1.2% to 4.2% of the oral load were obtained, depending on the size of the applied dose. For distribution, no AgNPs were detected in lung or kidney after oral administration. However, there was a slight elevation of silver content in the liver of animals orally exposed to 10 mg/kg. In fact, most of the orally applied AgNPs were recovered in the feces, suggesting that only a small proportion of the load had been absorbed. However, it is unclear how much of the fecal recovery of silver had been recycled through the hepatobiliary circulation after absorption. The fact that some silver was released to the feces after intravenous injection suggests that AgNPs could be voided after passage through the bile duct. Park et al. [2011a] speculated that gastrointestinal absorption of AgNPs might be low because of the citrated coat. It was thought that the presence of this hydrophilic center might render gastrointestinal absorption more difficult. However, the portion of the load that was absorbed was predominantly sequestered in the liver.

Although the citrate-coated AgNPs employed by Park et al. [2011a] appeared not to be readily absorbed via the oral route and showed no signs of tissue deposition other than in the liver, an earlier experiment by Kim et al. [2009a] detected silver deposition in the kidney, urinary bladder, and adrenal gland of F344 rats after oral administration of a proprietary preparation of 60-nm AgNPs dispersed in 0.5% carboxymethyl cellulose (CMC). The authors provided little physical and chemical information about the nanoparticles employed but stated that the preparation was at least 99.98% pure. As determined by specific staining of thin sections of excised tissue pieces, it appeared that silver deposition in these tissues was much more prevalent in female than male F344 rats. There was no obvious explanation for this disparity.

Hendrickson et al. [2016] measured tissue distribution of silver by atomic absorption spectroscopy, as well as hematological and biochemical parameters in blood, following acute or subacute exposure of male Sprague-Dawley rats to uncoated AgNPs. The AgNPs were spherical, with an average diameter of 12.3 nm, and were stabilized in a 1% starch solution with 0.1% Tween-80 prior to gavage. For the acute study, a dose of 2000 mg/kg was administered one time and measures were taken at 1 and 7 days post-exposure. In the repeated-dose study, AgNPs were administered at a dose of 250 mg/kg once a day for 30 days. Distribution and blood parameters were measured on days 7, 14, and 30 of the exposure. In both dosing studies, the majority of the AgNPs were excreted (estimated at >99%), similar to the findings of Loeschner et al. [2011] and Park et al. [2011a]. Outside the gastrointestinal tract (stomach and small intestine), silver was detected in liver, kidney, and spleen following both exposures. In the acute exposure, silver was measured in the liver ≥ kidney > spleen at day 7. On day 7 of the repeated exposure, silver was detectable only in the spleen. On days 14 and 30 of exposure, silver was present in kidney > spleen ≥ liver. Silver was not detected in blood, lung, brain, adrenal glands, testes, heart, thymus, skin, muscle, or adipose tissue following either exposure. Irrespective of the dosing regimen, no changes in blood parameters were measured, in contrast to some findings of toxicology studies discussed in section E7.2.1.

Of relevance to absorption as well as the toxicological impacts of silver nanoparticles, Park et al. [2010b] orally administered repeated doses of 1 mg/kg AgNPs to ICR mice daily for 14 days. The

AgNPs were initially suspended in tetrahydrofuran (THF) with sonication. Subsequently, the solvent was allowed to evaporate and was replaced with the same volume of de-ionized water. A critical feature of the experiment was the use of batches of AgNPs that had been screened by size. Thus, groups of five mice were orally administered AgNPs of 22, 42, or 71 nm or silver particles that averaged 323 nm in diameter. The distribution of silver, the clinical chemistry fluctuations, the histopathologic findings, and the detection and measurement of cytokines were then described in relation to particle size.

A critical finding was that silver from the smaller nanoparticles (up to and including 71 nm) was detected in brain, lung, liver, kidney, and brain, whereas the larger AgNPs (323 nm) were not detected in these tissues. Another response that was observed after administration of AgNPs, but not the larger silver microparticles, was increased serum concentrations of transforming growth factor-beta (TGF-β). Some differences in the subpopulations of whole-blood lymphocytes were also reported with varying particle size, but the data were less robust. However, the findings were consistent with the concept that small AgNPs are more active in exerting toxicological responses because of their expedient transport to susceptible sites.

A subacute oral AgNP exposure study with Sprague-Dawley rats was reported by Lee et al. [2013a], who focused on the clearance kinetics of tissue-accumulated silver. Rats were assigned to three groups, with 20 rats per group: control (no exposure), low dose (100 mg/kg body weight), and high dose (500 mg/kg body weight). The groups were exposed to two different sizes of citrate-coated AgNPs (average diameter, 10 and 25 nm) over 28 days. Rats were observed during recovery for 4 months to identify clearance of the tissue-accumulated silver. Regardless of the AgNP size, the silver content in most tissues gradually decreased during the 4-month recovery period. The exceptions were the silver concentrations in the brain and testes, which did not clear after the 4-month period, indicating an obstruction of the transporting of accumulated silver out of these tissues. Although the clearance half-times differed according to dose and sex, the tissues with no biologic barrier, such as the liver, kidneys, and spleen, showed a similar clearance trend. The silver concentration clearance was in this order:

> blood > liver = kidneys > spleen > ovaries > testes = brain

The different AgNP sizes used in the study had minimal effect on absorption, distribution, metabolism, and excretion, although the size difference was relatively narrow. The authors suggested that these findings support the hypothesis that silver toxicity originates mainly from silver ions, and in this study it was generated from the surface of the AgNPs. The findings also indicate that coated AgNPs and size differences may have minimal effect on absorption, distribution, metabolism, and excretion.

Effects of size, coating, and solubility were also investigated by Bergin et al. [2016]. The study was conducted in two parts: one examined biodistribution and the other evaluated organ weight and histopathological changes as indices of toxicity. For the toxicological evaluation, male C57BL6/6NCrl mice (6 per group) were exposed to 20- or 110-nm colloidal AgNP coated with PVP or citrate at doses of 0.1, 1.0, or 10 mg/kg/day for 3 days in the presence or absence of an antibiotic. Additional exposure groups included controls for citrate and PVP buffers and a soluble form of silver, silver acetate. Body weight was monitored on days 1–3 and 1 week following the last exposure. On the last day of exposure and 1 week following the last exposure, the following organs were collected for toxicity assessment: brain, heart, lung, liver, spleen, thymus, gonads, GI tract (esophagus to rectum), left kidney and adrenal gland, right kidney and adrenal gland, salivary glands, mammary glands, quadriceps muscle, bone marrow from sternum, bladder, skin, and mesenteric lymph nodes. No changes in body weight were observed and no statistically significant changes in histopathology were found.

In the second part of the study, mice were exposed to 10 mg/kg of AgNPs, buffer controls, or soluble Ag at time 0. Urine and feces were collected at 0, 3, 6, 9,

12, 18, 24, and 48 hours after exposure. Organ silver levels were measured by inductively coupled optical emission spectroscopy at 48 hours post-exposure. The majority of administered silver (70.5% to 98.6%) was recovered in the feces, regardless of size, coating, or solubility. Silver was detected in liver, kidney, spleen, gastrointestinal tract, and urine, and to a slightly greater degree for the soluble form of silver, although levels in these tissues totaled less than 0.5% the administered dose at the highest levels measured. The findings corroborate those of Lee et al. [2013a], indicating that size and coating had minimal effects on absorption, distribution, metabolism, and excretion following acute exposure.

## E.2.2 Toxicological Effects

Experimental studies of humans are limited. Smock et al. [2014] examined effects of oral administration of 15 ml of 32 ppm silver nanocolloid (average particle size ranging from 25 to 40 nm) for 14 days on platelet aggregation (PA) as a risk factor for thrombosis in 18 healthy volunteers 18 to 60 years of age. The estimated daily dose equivalent was 480 µg/day. Sterile water was used as a placebo control. Blood was collected for testing prior to the first exposure following 8 hours of fasting, to obtain a baseline measure of PA, and following 8 hours of fasting after the last exposure. Unstimulated PA and PA in the presence of collagen or adenosine diphosphate were evaluated. Additionally, total concentration of silver in serum was assessed by ICP-MS.

The peak serum silver concentration was reported to be 6.8 ± 4.5 µg/L. Spontaneous PA in the absence of an agonist was not found. The collagen agonist at a dose of 0.5 µg/mL caused a statistically significant decrease in PA, and a trend for a decrease was also noted at 1.0 µg/mL collagen. The authors note that these findings are in contrast to previous in vitro studies that showed increased PA [Jun et al. 2011; Kim et al. 2009d]; however, concentrations of silver were lower by an order of magnitude or greater in the human study. The authors also note that the clinical significance of the findings are not clear but warrant further investigation.

In a survey of the acute toxicity of AgNPs, Maneewattanapinyo et al. [2011] attempted to determine a median lethal dose ($LD_{50}$) for AgNPs in ICR mice. The AgNPs were produced by reducing a silver nitrate solution with sodium borohydride in the presence of soluble starch as a stabilizer. The particles were stated to be of high purity (99.96% silver), spherical, and with a narrow size range of 10–20 nm. Additionally, the content of free silver ions was very low (<0.04%). There were no deaths among mice observed for 14 days after a dose of 5,000 mg/kg, and there were no clinical signs of toxicity, reduced weight gain, hematologic or clinical chemistry changes, or gross and histopathologic findings. In this study, the oral $LD_{50}$ in ICR mice was thus designated as >5,000 mg/kg.

Dasgupta et al. [2019] also performed an acute toxicity test with 60-nm AgNPs generated by thermal co-reduction processes. Female Wistar rats were treated with 0, 500, 1000, or 2000 mg/kg AgNP for 14 days. No mortality, change in body weight, or change in water and food consumption was found. There was an increase in ALP in serum found at the highest dose. The $LD_{50}$ for this study was assessed at >2000 mg/kg.

In a 28-day study by Kim et al. [2008] of the toxicological impacts of oral exposure to AgNPs, 4-week-old male and female SPF Sprague-Dawley rats (10 per dose group) underwent gavage with AgNPs (average diameter, 60 nm; range, 53–71 nm) in an aqueous solution of 0.5% carboxymethyl cellulose (CMC) as the vehicle. The authors provided little physical and chemical information about the nanoparticles employed but stated that the preparation was at least 99.98% pure. The experiment followed OECD Test Guideline 407, using doses of silver at 0, 30, 300, or 1,000 mg/kg that were given for 28 days. At the conclusion of the dosing phase, animals were unfed for 24 hours and then anesthetized to facilitate the withdrawal of blood for measuring hematologic and clinical chemistry parameters. Major organs and tissues were excised, weighed, and processed for silver determination and histopathologic examination. The rat bone marrow micronucleus test was carried out according to OECD Test Guideline 474 to assess genotoxicity.

**Table E-4. Serum cholesterol concentration and alkaline phosphatase activity in Sprague-Dawley rats that underwent gavage with AgNPs for 28 days.**

| | Serum Cholesterol Concentration (mg/dL) | | Alkaline Phosphatase Activity (IU/L) | |
|---|---|---|---|---|
| Dose Group (mg/kg) | Males | Females | Males | Females |
| 0 | 69.0 ± 8.2 | 89.6 ± 9.1 | 427.2 ± 70.6 | 367.6 ± 125.7 |
| 30 | 73.1 ± 16 | 85.6 ± 12.2 | 475.4 ± 98.5 | 335.4 ± 79.0 |
| 300 | 82.1 ± 21.7 | 102.9 ± 17.7† | 613.7 ± 128.6† | 403.3 ± 75.9 |
| 1,000 | 87.5 ± 13.1* | 117.5 ± 14.1† | 837.7 ± 221.5† | 499.0 ± 107.3† |

*$p < 0.05$; †$p < 0.01$ versus controls, as calculated by the authors.
IU/L: International units per liter.
Source: Kim et al. [2008].

Clinical signs were unremarkable during the in-life phase of the experiment, and no compound-related changes in body weight gain or food consumption were observed. At term, there were no dose-dependent changes in organ weights, hematologic parameters, or bone marrow cytotoxicity. However, there were treatment-related increases in serum cholesterol concentration and alkaline phosphatase (AP) activity that, at the highest dose, were statistically significantly different from levels in controls (Table E-4).

As tabulated by the authors, dose-related increases in silver content were noted in the blood and tissues such as testis, kidney, liver, brain, lung, and stomach, with a twofold higher accumulation in the kidneys of female rats versus males. Though difficult to explain mechanistically, this difference was consistent with that observed in F344 rats by Kim et al. [2009a]. Histopathologic examination of the liver showed an increased incidence of bile duct hyperplasia in AgNP-receiving rats. Other hepatic responses included infiltration of inflammatory cells in the hepatic lobe, portal tract, and dilated central veins. These changes are consistent with the clinical chemistry data, pointing collectively to a possible silver-related perturbation of the metabolism and structural architecture of the liver.

In a second oral study, scientists from the same research group carried out an exposure regimen identical to that used by Kim et al. [2008] but with the primary focus on silver deposition and changes to the structure of the ileum, colon, and rectum [Jeong et al. 2010]. The AgNPs were about 60 nm in diameter on average and were dispersed in an aqueous solution of 0.5% CMC at doses of 0 (vehicle control), 30, 300, or 1,000 mg/kg-day for 28 consecutive days. The ileum, colon, and rectum were assessed for general histologic structure and amounts of mucins in the mucosa. Specific histochemical staining procedures were used to detect and distinguish between mucins, and the intensity of staining was subjectively scored to assess the amounts of mucins.

In addition to the use of hematoxylin/eosin stain on mounted sections of these tissues, periodic acid–Schiff stain was used to detect neutral mucins, Alcian blue was used for acidic mucins, and high-iron diamine plus Alamar Blue (AB) was used to distinguish sulfated from nonsulfated mucins. There was a dose dependent accumulation of AgNPs in the lamina propria of the small and large intestine, with higher numbers of goblet cells that had released their mucus, as compared to the number in controls. Given the detection of fluctuating amounts of differentially stained mucins among the groups, the researchers suggested that AgNPs might induce the discharge of mucus granules with abnormal compositions.

Sharare et al. [2013] also investigated effects of subacute silver exposure on the murine intestinal mucosa at lower doses than those used in the Kim et al. [2008] study. AgNPs, 3 to 220 nm, synthesized from silver nitrate in deionized water, were administered to male Swiss albino mice at doses of 0, 5, 10, 15, or

20 mg/kg-day for 21 days. Body weights were monitored once a week and animals were euthanized on the last day of treatment. Histopathology and TEM analysis were performed on the small intestine.

A degree of weight loss was noted over the time course in mice treated with AgNPs (greatest at 10 mg/kg). In addition, histological findings included loss of microvilli, increased inflammatory cells in the villus, and increased mitotic figures in the intestinal glands (proliferation response to replace damaged epithelial cells). TEM confirmed damage to the microvilli. The authors hypothesized that the weight loss may be due to decreased intestinal absorption of nutrients because of AgNP-induced damage.

Further related to responses in the ileum, a subchronic study was conducted on male and female Sprague-Dawley rats to examine effects of silver nanoparticles on gut-associated immune responses and on intestinal microbiota populations across phyla and genre, as well as within one family of gram-negative bacteria [Williams et al. 2015]. Rats (10/sex/group) were exposed to 9, 18, or 36 mg/kg AgNPs that ranged in size (10, 75, or 110 nm), stabilized in 2 mM citrate, divided into two doses a day for 13 weeks. An additional study examined effects of 100, 200, or 400 mg/kg silver acetate in the same dosing regimen. Bacteria populations and growth were assessed, and expression of Enterobacteriaceae family–specific genes in the ileum (*MUC2, MUC3, TLR2, TLR4, IL10, TGF-β, FOXP3, GPR43,* and *NOD2*) was measured following the final exposure.

Findings showed that AgNPs caused a size- and dose-dependent change in the populations of gut microbiota, with decreases in Firmicutes phyla and Lactobacillus genus and a shift toward gram-negative bacteria, whereby the smallest particles had the greatest effect. Sex differences were greatest in effects on gene expression in the ileum. In general, genes associated with family-specific bacterial immune response were decreased with decreasing particle size, particularly at the lower doses. TLR4 and MUC3 were downregulated to a greater degree in females, whereas TLR2 was downregulated to a greater degree in males. Less change in gene expression was observed at the higher dose (36 mg/kg), which followed a pattern similar to the 100-mg/kg soluble silver. The authors suggest that the higher dose was less effective possibly because of greater agglomeration of material and/or more efficient dissolution with decreasing particle size.

In addition to their experimental administration of differently sized AgNPs to ICR mice, as described in E.2, Park et al. [2010a] undertook a 28-day gavage study in which three mice per sex per group underwent gavage with 0 (vehicle control), 250, 500, or 1,000 μg/kg AgNPs (average particle diameter, 42 nm) dispersed in an aqueous medium, doses that were statistically significantly lower than those discussed above. Major organs and tissues were excised at term for silver analysis and histopathologic examination. Blood samples were measured for clinical chemistry parameters and the presence of cytokines.

Although there were no histopathologic changes in the livers or small intestines of the treated groups, some liver-related clinical chemistry parameters changed in relation to dose, including the activities of AP and aspartate aminotransferase (AST) in high-dose mice (both sexes). Additionally, the activity of alanine aminotransferase (ALT) was increased in high-dose females but not males. The only organ or tissue where histopathologic changes were observed was the kidney, where signs of slight cell infiltration were noted in the cortex of high-dose mice of either sex. Changes in the levels of cytokines and immunoglobulin (Ig)-E were also noted in high-dose mice, in comparison with the control group. These differences are listed in Table E-5. The authors noted that their doses were far lower than those that induced histopathologic responses in the liver of Sprague-Dawley rats after oral exposure [Kim et al. 2008]. Therefore, they concluded that doses of AgNPs at these low concentrations can induce inflammatory responses by repeated oral administration.

In a follow-up study to Park et al. [2010a], Kim et al. [2010a] treated 10 F344 rats per sex per group by gavage with AgNPs (average diameter, 56 nm; range, 25–125 nm) for 13 weeks at silver doses of 0, 30, 125, or 500 mg/kg-day. The monodisperse and nonaggregated AgNPs were dispersed in an aqueous

**Table E-5. Levels of cytokines in the serum of high-dose and control mice as a result of oral administration of AgNPs to ICR mice for 28 days.**

| Parameter | Controls ($n$ = 3) | High-dose group ($n$ = 3) |
|---|---|---|
| **Pro-inflammatory cytokines (pg/mL)** | | |
| Interleukin (IL)-1 | ND* | 8.8 ± 0.7† |
| Tumor necrosis factor (TNF)-α | 1.21 | 3.41 ± 0.06 |
| IL-6 | 1.44 | 13.75 ± 0.57† |
| **Thyroid helper (Th)1–type cytokines (pg/mL)** | | |
| IL-12 | 35.5 | 76.86 ± 5.2† |
| Interferon (IFN)-γ | ND | 0.52 ± 0.04 |
| **Th-2-type cytokines (pg/mL)** | | |
| IL-4 | ND | 2.7 ± 0.07‡ |
| IL-5 | ND | 1.34 ± 0.01 |
| IL-10 | ND | 29.02 ± 1.7† |
| | | |
| TGF-β (pg/mL) | ND | 6.73 ± 0.52† |
| Ig E (ng/mL) | 3.28 | 6.04 ± 0.74‡ |

* Nondetectable.
†$P < 0.01$.
‡$P < 0.05$.
Source: Park et al. [2010a].

solution of 0.5% CMC that also constituted the vehicle control. As before, clinical signs, body weights, and food consumption were monitored in the in-life phase of the experiment. At term, blood was withdrawn to measure hematologic and clinical chemistry parameters. Organ weights were recorded, and excised pieces of the major tissues and organs were processed for histopathologic examination and measurement of silver content.

Most major organs and tissues showed a dose-dependent increase in silver content. However, as observed in other studies of AgNPs in experimental animals [Kim et al. 2009a, 2008], there was an increased deposition of silver in female versus male kidneys at equivalent doses. The authors of the study did not mention whether any of the exposed animals showed clinical signs of toxicity, but there were no statistically significant changes in food consumption and water intake among the groups. Likewise, there were no dose-related changes in body weights of female rats, although high-dose males showed less body weight gain than controls after 4, 5, and 7 weeks of exposure. Body weight gain was also less in mid-dose males than in controls after 10 weeks. At term, there were few if any changes in organ weights associated with exposure to AgNPs. However, high-dose males showed an increase in the weight of the left testis and low- and mid-dose females showed decreases in weight of the right kidney. In a manner similar to the 28-day oral study in Sprague-Dawley rats [Kim et al. 2008], the most clear-cut treatment-related changes in clinical chemistry parameters were increases in AP activity in high-dose females (versus controls), which achieved statistical significance, as well as statistically significant increases in serum cholesterol concentration in high-dose rats of both sexes.

Perhaps the most noteworthy toxicological responses to AgNPs in this study were histopathologic changes to the liver that showed a dose-related trend.

Specifically, there were increased incidences in minimal to mild bile duct hyperplasia in both sexes of F344 rats. The proportions of males affected were 4/10 (controls), 7/10 (low dose), 9/10 (mid dose), and 6/10 (high dose); the respective proportions of affected females were 3/10, 7/10, 8/10, and 7/10. These responses are similar to those in Sprague-Dawley rats described by Kim et al. [2008] following their 28-day oral exposure study and by Sung et al. [2009] following their 90-day inhalation study. However, related changes in such clinical chemistry parameters as serum cholesterol concentration or AP activity were not observed in the latter study. In summarizing their data, Kim et al. [2010a] concluded that a LOAEL of 125 mg/kg, with a NOAEL of 30 mg/kg, would be appropriate from their data. However, because the incidences of bile duct hyperplasia in the low-dose groups were elevated in comparison with controls and were clearly part of a dose-related trend, the point of departure for these responses could be lower than 30 mg/kg.

Liver effects following oral exposure to AgNP were found in a subchronic study by Dasgupta et al. [2019]. Female Wistar rats, 6–8 weeks of age, were orally administered 60-nm AgNPs generated by thermal co-reduction processes once daily for 12 weeks at a dose of 0, 20, 40, 60, 80, or 100 mg/kg. Body weight and water/food consumption were monitored over the time course. At the end of the exposure period, whole blood was collected for hematology and biochemical analysis, and major organs were collected for histopathology and analysis of silver burden.

Lower body weight gain and lower food/water consumption were found in the 80- and 100-mg/kg groups. In the 60-, 80-, and 100-mg/kg groups, blood cholesterol, bilirubin, AST, and ALT were elevated. However, at 80 and 100 mg/kg, levels of LDH, glucose, ALP, γ-glutamyltranspeptidase (GGTP), and triglycerides were also elevated. Hematology was also altered in the 80 and 100 mg/kg groups, with increased MCV, WBC counts, and neutrophil counts and decreased platelets, eosinophils, basophils, MCHC values, and hematocrit. Histopathologic analysis was conducted and tissue burdens of silver were measured in the 100-mg/kg group in lung, liver, kidney, pancreas, and heart. Kidney pathology findings included tubular degeneration and dilation. Other findings included mild congestion in lung tissue; congestion with increased mononuclear cells in liver; and particles in liver tissue sections. ICP-MS analysis of the tissues showed silver accumulation in liver (~36 μg/g), kidney (~28 μg/g), lung (~11 μg/g), and pancreas (~1 μg/g). No silver was detected in heart. The authors concluded that the liver was a target organ for toxicity and accumulation, with effects in the kidney as well.

Investigators in other subchronic studies have also reported kidney and liver pathology. Taking together the data of Park et al. [2010a], who observed kidney damage following oral exposure, and Kim et al. [2010a], who noted increased silver in the kidneys of females, Tiwari et al. [2017] performed a subchronic study of kidney-specific toxicity following a 60-day oral exposure to PVP-stabilized AgNPs in female Wistar rats. Rats were exposed to 50 or 200 ppm AgNPs (10–40 nm, average of ~27 nm diameter, <1% ionic) daily for 60 days. Accumulation of silver (ionic and non-ionic) was measured in kidneys immediately following the last exposure, and excretion was monitored at 1, 7, 28, and 60 days of exposure.

There was a dose-dependent increase in silver accumulation in the kidneys, with approximately 70% to 75% of silver in the particulate form and, correspondingly, 30% to 25% in the ionic form. After the first day of exposure, 62.5% of the low dose and 72.6% of the high dose were excreted, and excretion increased over time. Markers of nephrotoxicity in urine were observed to increase over time, starting at 7 days of exposure, and included an increase in total protein in urine, as well as clusterin, kidney injury molecule-1 (KIM-1), TIMP-1, and VEGF. Additionally, osteopontin was elevated at later times in the low-dose exposure group only.

Following the 60-day exposure, serum levels of creatinine were elevated in both exposures. Kidney pathology was observed in the proximal and distal tubule as well as the glomerulus and Bowman's capsule. Structural changes included necrotic cells, damage to mitochondria, damage to villi in the brush border, and damage to organelles associated with the endocytic system. Proteins associated with immune response, inflammation, and tissue injury were elevated in both serum and kidney tissue (erythropoietin, VEGF,

RANTES, IL-7, IL-1β, and TNF-α). Additionally, serum levels of IL-6, Il-12p70, IFN-γ, GM-CSF, and MIP-2 were elevated, and IL-18 and Il-17A were also elevated in kidney tissue. mRNA expression of factors related to cell survival, proliferation, and autophagy were evaluated at the low dose in conjunction with immunohistochemistry. Markers of autophagy were not altered; however, markers for necrosis were increased and apoptotic markers were decreased. In addition, levels of ROS and 8-oxoG (oxidative DNA damage) were elevated in kidney tissue, whereas levels of anti-oxidants were found to decrease. The data implicate oxidative stress and inflammation in the promotion of kidney injury (necrosis) following subchronic exposure in female rats at a dose of 50 ppm.

Yun et al. [2015] also performed a 13-week exposure study in male and female Sprague-Dawley rats. This study was designed to compare toxicity of oral administration of three NPs that differed in composition (AgNPs, $SiO_2$ NPs, and $Fe_2O_3$ NPs). Parameters measured included body weight, organ weight, blood chemistry, urinalysis, and organ histopathology. In addition, silver distribution in blood, liver, kidney, spleen, lung, brain, urine, and feces was measured by ICP-MS. The dose was determined from a 14-day dose-response study (515, 1030, or 2060 mg/kg daily).

In the subacute dose-response study, no statistically significant effects were observed for the iron and silica NPs. AgNPs cause increased AP levels in males at the two higher doses and in females at all doses, suggesting greater effects in liver of females. The middle dose (~1000 mg/kg) was selected for subchronic study. No statistically significant changes were observed in body weight across the course of the study. Silver was detectable in all organs, blood, urine, and feces. The majority of silver was measured in the feces.

No differences in distribution due to sex were observed. In both male and female rats, AP was statistically significantly elevated following subchronic exposure, and lymphocyte infiltration into kidney and liver was noted for both sexes. Sex differences were observed in blood, with white blood cells elevated in females and platelets elevated in males. In addition, a statistically significant elevation in serum calcium levels occurred in females, along with increased observation of calcification in the kidney. The study suggests liver and kidney as target organs, with potential sex differences in response to oral exposure to AgNPs, similar to findings in other studies discussed above [Kim et al. 2009a; Park et al. 2010a; Kim et al. 2010a].

The potential mechanism of the effects of subchronic exposure to AgNPs, particularly in relation to the effects in the liver, was investigated by Elle et al. [2013], with an emphasis on the role of oxidative stress in injury. AgNPs were delivered to Sprague-Dawley rats by gavage as collargol (70%–80% 20-nm AgNPs and 20% protein gel) for 81 days at a dose of 500 mg/kg. One day following the last exposure, blood was collected for plasma analysis of lipids, liver enzymes, and antioxidant capacity. Liver and heart were harvested to evaluate biomarkers of oxidative stress, and inflammation was measured in liver.

Food intake and body weight were found to be statistically significantly lower in exposed rats. In plasma, total cholesterol was statistically significantly elevated, along with an increased ratio of LDL to HDL cholesterol; triglycerides were statistically significantly reduced; and ALT was statistically significantly increased, indicating effects on the liver. Malondialdehyde (MDA) levels (lipid peroxidation) were increased and antioxidant capacity was decreased, along with decreased superoxide dismutase levels and paraoxonase activity. Superoxide anion as a biomarker of oxidative stress was increased in heart and liver of exposed rats; however, MDA and superoxide dismutase activities were not. In addition, IL-6 and TNF-α were elevated in the liver of exposed rats. These findings, taken together, support the concept that oxidative stress is at least a contributing mechanism in AgNP toxicity.

An additional subacute exposure study also supports the involvement of oxidative stress in toxicity of AgNPs in vivo [Shrivastava et al. 2016]. In this study, male Swiss albino mice were exposed to a dispersion of 20-nm AgNPs or colloidal gold NPs at a dose of 1 or 2 μM by oral gavage for 14 days. Blood, brain, liver, kidney, and spleen were collected after the last exposure. A battery of assays were employed to

assess blood and tissue ROS and antioxidant capacity. Liver and kidney function were measured as AP and ALT, and urea and creatinine in serum, respectively. Systemic inflammatory potential was assessed as IL-6 and nitric oxide synthase in plasma, and DNA damage due to oxidative stress was measured as 8-hydroxy-2'-deoxyguanosine (8-OHdG) in urine. AgNP findings included statistically significant elevations in IL-6 and nitric oxide synthase in plasma. ALT, AP, and urea were also elevated in plasma. Metallothionein levels were increased in both liver and kidney but to a greater degree in kidney. In addition, ROS in blood and all tissues collected were increased. Antioxidant capacity was decreased in plasma, whereas the various enzymes measured were altered in tissues differentially, depending on the enzyme and the tissue, and 8-OHdG increased in the urine following AgNP exposure. As with the subchronic study by Elle et al. [2013], the study by Shrivastava et al. [2016] supports the role of oxidative stress in AgNP toxicity.

In contrast to the subchronic studies discussed above [Kim et al. 2010a; Yun et al. 2015; Elle et al. 2013] that suggest liver and kidney as primary targets of AgNP toxicity following oral exposure, in addition to effects in other organ systems, a subchronic study by Garcia et al. [2016] did not find adverse effects in kidney or liver. In this study, male Sprague-Dawley rats were exposed to 20–30-nm PVP-coated AgNPs by gavage at a dose of 0, 50, 100, or 200 mg/kg per day for 90 days. Silver accumulation in tissues (liver, kidney, spleen, thymus, brain, and ileum), subcellular distribution in those tissues, distribution of other metals in tissues, Ag excretion (urine and feces Ag levels), and plasma biochemical and hematological parameters were analyzed, and histopathology of tissues was performed.

The majority of excreted Ag was found in feces (~10,000–18,000 μg/g, depending on dose), although there were low but detectable amounts in urine (<0.1 μg/g). Ag was found in all tissues measured, with the greatest amount in the ileum. At the subcellular level, AgNPs could be found in liver and intestinal cells. No changes in blood cell differentials, blood chemistry (including BUN, creatinine, AST, ALT, AP), or histopathological parameters were found. The only statistically significant difference in tissues was observed in the analysis of redistribution of Cu, Fe, Mg, and Zn. Differential elevations and decreases in Cu and Zn were found, depending on organ and dose. The lack of effects in kidney and liver, and in pathology in the ileum, in contrast to observations in other studies (Kim et al. 2010a; Yun et al. 2015; Elle et al. 2013; Jeong et al. 2010; Williams et al. 2015], could be due to a number of factors such as dose (the highest dose was lower than in many of the studies, with the exception of Williams et al. [2015]). Another factor could be particle coating, which may affect absorption and/or dissolution rate. Many of the discussed studies did not specifically examine dissolution or effect of the ion or coating of the materials.

However, several studies involved toxicological comparisons of one or more of the following parameters within a study: size, solubility, and coating or capping agent. Park [2013] investigated toxicokinetic differences and toxicities of AgNPs and silver ions in rats after a single oral administration of 2 mg/kg (low dose) or 20 mg/kg (high dose). Male Sprague-Dawley rats (n = 5) were given a dose of either AgNPs (diameter, ~7.9 nm) or silver ions ($Ag^+$). The $AUC_{24hr}$ of $Ag^+$ was 3.81 ± 0.57 μg/d/mL when rats were treated with a dose of 20 mg/kg, whereas that of AgNPs was 1.58 ± 0.25 μg/d/mL. Blood levels, tissue distributions, and excretion of silver were measured up to 24 hours after oral administration.

Tissue distribution of silver in liver, kidneys, and lungs was higher when $Ag^+$ was administered than when AgNPs were administered. Silver concentrations in blood of rats treated with AgNPs were lower than those of rats treated with $Ag^+$ at the same dose. Blood silver concentrations in rats treated with 20 mg/kg AgNPs were also found to be lower than those of rats administered 2 mg/kg $Ag^+$. Decreased red blood cell counts, hematocrit levels, and hemoglobin levels were found in $Ag^+$-treated groups, whereas increased platelet counts and mean platelet volume were noted in the AgNP-treated rats. The concentrations of silver in both the lung and liver were lower in rats treated with AgNPs than in rats treated with $Ag^+$, and the highest concentration of silver was found in the liver of rats

treated with $Ag^+$ (20-mg/kg dose). Orally administered AgNPs were not absorbed in the gastrointestinal tract but excreted via feces; however, excretion of silver through feces was negligible for rats treated with the same dose of $Ag^+$, a finding indicating that bioavailability of $Ag^+$ may be greater than with AgNPs. Findings related to greater biodistribution of the soluble form of silver are in agreement with those of Bergin et al. [2016] previously discussed.

Qin et al. [2016] evaluated biodistribution and toxicity following a subacute exposure to AgNP (28–44 nm stabilized in PVP) or soluble silver ($AgNO_3$). Male and female Sprague-Dawley rats (10 per group per sex) were orally dosed with 0.5 or 1.0 mg/kg AgNP or $AgNO_3$ daily for 28 days. On day 28, blood was collected for hematology and biochemical analysis, and liver, kidney, spleen, stomach, small intestine, and gonads underwent histopathological analysis. Additionally, silver was measured in liver, spleen, kidney, testes, and plasma by atomic absorption spectroscopy. No statistically significant differences in body weight, food consumption, or organ/body weight ratio were found for either exposure. In male and female rats, AgNP exposure led to increased red blood cells and decreased platelet counts. In addition, white blood cells were increased in female rats at the high dose of AgNPs. In males, AgNP exposure led to an increase in AST in the plasma. The only change associated with soluble silver was an increase in red blood cells in females at the low dose.

No histopathologic changes were observed in spleen, stomach, small intestine, or gonads for either sex following AgNP or soluble silver exposure. Minor pathological changes were noted in kidneys and livers of both sexes following exposure to AgNP and soluble silver, which did not differ statistically significantly from each other. AgNP distribution was statistically significantly lower compared to soluble silver for both sexes. In males both AgNP and $AgNO_3$ were greatest in liver and kidney, followed by testes and spleen, then plasma. $AgNO_3$ distribution in females followed a similar pattern, with liver having the highest burden (ovaries were not measured), followed by the kidneys and spleen. In females, organ burden of silver following AgNP exposure did not follow a similar distribution pattern, with equal amounts of silver detected across liver, kidney, spleen, and plasma. The results indicate that the soluble form is more readily absorbed, as had been indicated by others [Bergin et al. 2016; Lee et al. 2013a; Park et al. 2013]. The authors suggest that the biochemical and hematological changes that were greater for AgNP versus $AgNO_3$ indicate that the particle itself contributes in part to the overall toxicity.

In a study to examine the toxicokinetics and tissue distribution of two types of AgNPs, $AgNO_3$ (soluble silver), and two negative controls, five groups of Sprague-Dawley rats (five per group) were exposed by gavage daily for 28 days to <20-nm uncoated or <15-nm PVP-coated AgNPs and to $AgNO_3$ [van der Zande et al. 2012]. All groups of rats were followed for 8 weeks. Dissection was performed on day 29 and at 1 week and 8 weeks post-exposure. Silver was present in all examined organs (liver, spleen, kidney, testis, lungs, brain, heart), and the highest levels in all silver-treatment groups were in the liver and spleen. Silver concentrations in the organs were highly correlated to the amount of $Ag^+$ in the silver nanoparticle suspension, indicating that mainly $Ag^+$ (and to a lesser extent, AgNPs) passed the intestines in the AgNP-exposed rats, a finding similar to Qin et al. [2016]. In all groups, silver was cleared from most organs at 8 weeks post-exposure, except for the brain and testis.

By means of single-particle ICP-MS, AgNPs were detected in the AgNP-exposed rats but also in $AgNO_3$-exposed rats, demonstrating the in vivo formation (or precipitation) of nanoparticles from $Ag^+$ that were probably composed of silver salts. Biochemical markers and antibody levels in blood, lymphocyte proliferation and cytokine release, and NK-cell activity did not reveal hepatotoxicity (unlike the findings of Qin et al. [2016]) or immunotoxicity from the silver exposure. The authors noted that the consequences of in vivo formation of AgNPs and the long retention of silver in the brain and testis warrant further assessment of the potential health risk.

Subacute toxicity of 14-nm AgNPs stabilized with PVP and ionic silver in the form of silver acetate was investigated in 4-week-old male (6 per dose)

and female (10 per dose) Wistar Hannover Galas rats for 28 days [Hadrup et al. 2012a]. Animals received by gavage a vehicle control and AgNP doses of 2.25 or 9 mg/kg bw/day or silver acetate doses of 9 mg silver/kg bw/day for 28 days. Clinical, hematologic, and biochemical parameters, organ weights, and macroscopic and microscopic pathologic changes were evaluated. No increase in AP or cholesterol was found for AgNPs at doses of up to 9 mg/kg/day. However, effects were observed for silver acetate (ionic form) at a dose of 14 mg/kg/day, including an increase in AP, decrease in plasma urea, and decrease in thymus weights.

Additionally, Hadrup et al. [2012a] found no observable effects in the microbiologic status of the rats' gastrointestinal tract caused by ingesting AgNPs. This finding is confirmed in a study by Wilding et al. [2016] that examined the role of size and surface coating on the murine microbiome following 28 days of exposure to 10 mg/kg/day of 20- or 110-nm AgNP stabilized in citrate of PVP. Silver acetate was employed as a control for effects of the ion (an antibiotic control group was also employed). At 1 day following the last exposure, male C57BL/6Crl mice were euthanized and cecal tips were processed for microbial sequencing and molecular analysis. No differences in diversity, populations, or structures of the microbiome were found, regardless of size or coating following the subacute exposure. However, as previously mentioned, longer subchronic exposure to AgNPs did result in effects on the microbiome, with the smallest particles (10 nm) utilized in the study having the greatest effect [Williams et al. 2015]. The findings together suggest that effects may be related primarily to duration of silver exposure and particle size; however, further studies are needed for definitive conclusions to be made.

In a study related to Hadrup et al. [2012a], Hadrup et al. [2012b] exposed male and female Wistar rats to 0, 2.25, 4.5, or 9.0 mg/kg AgNPs (14 nm, PVP-coated) or 9.0 mg/kg ionic silver (silver acetate) for 28 days. On day 18 of exposure, urine was collected for a 24-hour period for measures of metabolites. No effects on metabolites were found in male rats. However, in female rats, uric acid was statistically significantly increased following exposure to the middle and high dose of particles, but not following exposure to silver acetate. Allantoin was statistically significantly elevated following exposure to particles and to ionic silver. The findings suggest a greater sensitivity in females. In addition, the authors suggest that the increase in urine metabolism resulting in the increase in these metabolites is indicative of oxidative stress and cytotoxicity, resulting in DNA degradation, and that these are potential mechanisms for AgNP toxicity. The theory is supported by other studies discussed above that suggest oxidative stress is present following AgNP exposure [Elle et al. 2013; Shrivastava et al. 2016].

Hadrup et al. [2012c] also compared the neurotoxic effects, in vivo and in vitro, of PVP-stabilized AgNPs (average diameter, 14 nm) and silver acetate. Following 28 days of oral administration, AgNPs (4.5 and 9 mg/kg/day) and silver acetate (9 mg/kg/day) statistically significantly increased the concentration of dopamine in the brains of Wistar female rats, whereas the brain concentration of 5-hydroxytryptamine (5-HT) was increased only by AgNPs at a dose of 9 mg/kg/day. However, in the 14-day range-finding study, the brain dopamine concentration decreased in rats treated with AgNPs at doses of 2.25 and 4.5 mg/kg/day. Three solutions consisting of (1) AgNPs, (2) an ionic silver solution obtained by filtering a nanosilver suspension, and (3) silver acetate were found in neuronal-like PC12 cells in vitro. AgNPs were not observed to cause necrosis. However, cell viability was decreased, and apoptosis (involving both the mitochondrial and the death receptor pathways) was found for all three solutions, with silver acetate being most potent. The findings suggest that the ionic silver and 14-nm AgNP preparations have similar neurotoxic effects, possibly due to the release of ionic silver from the surface of AgNPs.

Wesierska et al. [2018] and Dabrowska-Bouta et al. [2016] also examined neurological effects. In the study by Wesierska et al. [2018], male Wistar rats (8–10 weeks old) were administered bovine serum albumin–coated AgNPs (20 nm primary size, 197 nm hydrodynamic diameter) 5 days a week for 4

weeks at a dose of 1 or 30 mg/kg, or saline control. Silver accumulation was measured in various regions of the brain: whole brain, frontal cortex, lateral cortex, hippocampus, or cerebellum. At the higher dose, silver was statistically significantly increased in whole brain, as well as in the frontal cortex and hippocampus. A statistically significant increase in the hippocampus at the low dose was also observed. The study found no changes in non-cognitive behavior (motor movement); however, long- and short-term memory, evaluated by the carousel maze test, were affected at both doses, indicating effects on the hippocampus.

Dabrowska-Bouta et al. [2016] examined effects related to behavior and effects on cerebral myelin following low-dose subacute exposure to AgNPs. Male Wistar rats were exposed to saline, 0.2 mg/kg AgNPs (10 nm, citrate stabilized), or 0.2 mg/kg silver citrate (ionic silver) for 14 days. Body weight and temperature were monitored on days 1, 8, and 14. On days 15 and 16 a battery of tests to evaluate behavioral effects were performed, including locomotor activity (distance traveled in 30 minutes), motor coordination (rotarod performance test), memory (novel object recognition test), anxiety performance (elevated plus-shaped maze apparatus), and nociceptive reaction (tail-immersion test). TEM was performed to assess myelin structure, and expression of myelin-specific proteins was quantified. AgNPs and ionic silver caused an increase in body temperature on day 8, which persisted in the ionic silver group on day 14, and an increase in body weight on day 14 following AgNP exposure was observed.

Similar to the results of Wesierska et al. [2018], no differences in any groups were noted for tests assessing motor activity or motor coordination; however, unlike Wesierska et al. [2018], this study showed no effect on memory. The exposure in the Wesierska et al. [2018] study was a higher dose and was administered 2 weeks longer than that administered by Dabrowska-Bouta et al. [2016]. Only exposure to ionic silver decreased sensitivity to noxious stimuli (nociceptive test) and increased behavioral anxiety. However, similar forms of damage to myelin were observed in brain of rats exposed to AgNPs or ionic silver. Both forms of silver decreased expression of three myelin-related proteins. AgNPs increased the mRNA expression of these three proteins, whereas ionic silver exposure increased only one of these proteins. The authors suggested that molecular and structural effects in myelin following low-dose exposure to AgNPs indicate that the brain may be a target organ for silver and that more studies are required to better understand neurotoxicity outcomes.

In addition to the subacute oral exposure studies discussed above that try to establish the role of particle size and solubility in toxicity, one subchronic study examined tissue distribution and toxicity following a 13-week exposure to ionic silver or citrate-coated AgNPs that vary in size [Boudreau et al. 2016]. In this study, which is related to that of Williams et al. [2015] discussed above, male and female Sprague-Dawley/CD-23 rats were orally exposed to 9, 13, or 36 mg/kg of 10-, 75-, or 110-nm AgNPs or 100, 200, or 400 mg/kg silver acetate daily for 13 weeks. Control groups included 2 mM citrate to control for the coating material, or water as a vehicle control.

Following the last exposure, histopathology and tissue distribution of silver were evaluated in testes, uterine horn, mesenteric lymph nodes, femur bone marrow, eyes, proximal ileum, jejunum, proximal colon, kidney, liver, spleen, and heart. Localization of silver deposits in tissues was analyzed in TEM images. Additionally, micronuclei formation in blood was measured and reproductive toxicity was evaluated by vaginal cytology, sperm count, sperm mobility, and sperm morphology studies. Direct comparison of soluble silver exposure to AgNP exposure in this study is difficult because the dose ranges were drastically different for the two materials; however, testing of both compounds provided information on distribution and toxicity in their own right.

The authors report that AgNP exposure did not result in any treatment-related pathology in tissues, nor did it cause any changes in blood chemistry or hematology values. Silver acetate exposure resulted in statistically significant mortality at the high dose used in the study, with most animals removed

before termination of the 13-week exposure. Those that survived the 400-mg/kg dose had an increased incidence and severity of lesions characterized by mucosal hyperplasia in small and large intestine and thymic atrophy/necrosis. Differences in hematological values were described as sporadic for animals exposed to the soluble silver (lower mean corpuscular volumes and higher red blood cell counts), and no differences in blood chemistry were noted. AgNP did not increase micronuclei formation, whereas the highest dose of soluble silver did result in increases at week 4 of the 13-week study. No differences in results of vaginal cytology or sperm analysis were detected.

In the silver distribution portion of the study, light microscopy revealed pigmentation in tissues following AgNP or silver acetate exposure that the authors deemed a product of silver translocation to these organs, and this was quantified. Pigmentation was greater in females than in males following AgNP exposure, particularly in lymph nodes, large intestine, stomach, kidney, and spleen, but size differences could not be discerned. In males, a size difference could be detected whereby the smallest particle showed the greatest prevalence. Pigmentation was greatly increased in rats exposed to soluble silver. TEM examination further showed that the distribution of silver was different between AgNP and soluble silver at the cellular level, with AgNP found primarily within the cell, whereas the soluble silver localized to the extracellular membranes of the cells. Silver burden in tissues was measured by ICP-MS. Blood, bone marrow, and heart had the lowest measured values for silver content in both AgNP- and soluble silver–exposed groups. Blood and bone marrow levels were higher in the 10-nm AgNP group compared to the other sizes of AgNPs, and levels in the soluble-silver group were higher than in the AgNP group, as would be anticipated because of dosing differences. In general, silver levels in the gastrointestinal tract were higher than in other tissues. Accumulation was greater in females in most portions of the gastrointestinal tract, with the exception of the ileum. The mesenteric lymph nodes had the highest concentration of silver.

The AgNP and soluble-silver groups exhibited similar profiles of deposition in the gut. In the major organs outside the gastrointestinal tract, particle size and sex differences were observed, with exposure to smaller particles leading to greater deposition than larger particles. In female rats, levels in kidney and spleen were statistically significantly higher than in male rats. Concentrations in organs were higher with the soluble silver exposure; however, the patterns of deposition were similar to those of the AgNPs. To summarize, the major findings suggest that the smaller particle size led to increased tissue distribution relative to larger particles. At the organ level, patterns of distribution were similar between soluble and particle silver, with prominent sex differences, whereas distribution within cells differed according to solubility.

In addition to studies of systemic toxicity in potential target organ systems such as liver, kidney, spleen, and brain, a number of studies have been performed that assess effects of oral exposure to AgNPs on reproduction and reproductive development in both males [Lafuente et al. 2016; Thakur et al. 2014; Miresmaeili et al. 2013; Mathiu et al. 2014; Sleiman et al. 2013] and females [Fennell et al. 2016; Philbrook et al. 2011; Yu et al. 2014]. Lafuente et al. [2016] conducted a subchronic exposure study in adult male Sprague-Dawley rats to assess effects on sperm count, motility, viability, and morphology, as well as epididymal and testicular pathology. Rats were orally administered 0, 50, 100, or 200 mg/kg of 20- to 30-nm AgNPs coated with PVP, for 90 days. Similar to the lower-dose study by Boudreau et al. [2016], no statistically significant changes in sperm number or motility were found. However, an increase in changes in sperm morphology was found, including alterations in the shape of the tail (100 mg/kg) or the head (50 mg/kg) and in some instances a detached head. Histopathological analysis of tissues showed no changes to testes or epididymis; however, a trend was noted for an increment of desquamation into the tubular lumen following the highest dose.

Another 90-day oral exposure study was conducted by Thakur et al. [2014] in adult male Wistar rats. Rats received 0 or 20 μg/kg/day of citrate-stabilized AgNPs (5–20 nm) for 90 days, a considerably lower

dose than that used in the study by Lafuente et al. [2016]. Histopathology and TEM analysis of the testis were performed following exposure. Histopathological analysis indicated abnormalities in the testis related to atrophy of the seminiferous tubules, abnormalities in germinal epithelium, loss of spermatogenic cells, and exfoliation of germ cells. TEM analysis revealed thickened and fibrous seminiferous tubules, depletion and necrosis of germ cells, and abnormal structure among Sertoli cells, spermatocytes, and spermatids. Reasons for differences in observations between Lafuente et al. [2016] and Thakur et al. [2014] could be attributable to the difference in AgNP coating or to the rat strain.

Three studies have been conducted on pre-pubertal male rats [Mathias et al. 2104; Sleiman et al. 2013; Miresmaeili et al. 2013]. Pre-pubertal male Wistar rats ($n$ = 30) were orally treated with 15 or 30 μg/kg/day AgNPs (~86 nm in diameter, citrate stabilized) from postnatal day 23 to postnatal day 58 (35 days, at a total dose of 131–263 μg Ag/rat) to evaluate the effects on sexual behavior and reproduction; they were killed on postnatal day 102 [Mathias et al. 2014]. The acrosome integrity, plasma membrane integrity, mitochondrial activity, and morphologic alterations of the sperm were analyzed. Sexual partner preference, sexual behavior, and serum concentrations of follicle stimulating hormone (FSH), luteinizing hormone (LH), testosterone, and estradiol were also recorded. No measurements of blood silver were made.

Exposure to AgNPs was found to reduce the acrosome and plasma membrane integrities, reduce mitochondrial activity ($p < 0.05$), and increase the abnormalities of the sperm (<0.01) in both the 15- and 30-μg/kg groups versus controls. AgNP exposure also delayed the onset of puberty, although no changes in body growth were observed in either treatment group. The animals did not show changes in sexual behavior or serum hormone concentrations. The serum concentrations of FSH, LH, testosterone, and estradiol were not statistically significantly different between the experimental groups. Because the hormone profiles of testosterone, estradiol, FSH, and LH were not altered by AgNP treatment, the investigators suggested that the defective sperm function and morphology observed in this study may have resulted from defective spermatogenesis due to direct effects of AgNPs on spermatic cells.

Similar findings of increased sperm morphologic abnormalities were observed by Gromadzka-Ostrowska et al. [2012], following a single intravenous dosing of AgNPs in rats, and by Lafuente et al. [2016] and Thakur et al. [2014] following oral exposure, the latter having examined a similar dose in a longer subchronic study in adult rats as discussed above. Another commonality with the study by Thakur et al. [2014] was the citrate-coating or stabilizing agent, although the particle in Mathias et al. [2014] was larger, and the strain of rat used in the study was the same.

In a second oral study, scientists from the same research group [Sleiman et al. 2013] carried out a similar exposure regimen with male Wistar rats ($n$ = 30) exposed to AgNPs (~86 nm, citrate stabilized) during the pre-pubertal period and killed on postnatal days 53 and 90. Animals were treated orally with either 15 μg/kg bw or 50 μg/kg bw, from postnatal day 23 until postnatal day 53. Growth was assessed by daily weighing. The progress of puberty in the rats was measured by preputial separation, while spermatogenesis was assayed by measuring the sperm count in testes and epididymis and examining the morphologic and morphometric characteristics of seminiferous epithelium by stereologic analysis. In addition, testosterone and estradiol levels were assayed by radioimmunoassay. The weight of animals during postnatal days 34 to 53 was lower in the 50-μg/kg treatment group than in the control group and the 15-μg/kg treatment group; however, at 90 days postnatally, the growth among groups was not markedly different.

A numerical reduction in total and daily sperm production was observed in the 50-μg/kg AgNP group on postnatal day 53. On postnatal day 90, both treatment groups had statistically significantly lower total and daily sperm production ($p < 0.05$) in comparison with the control group. Decreased sperm reserves in the epididymis and diminished sperm transit time were also observed on postnatal day 53. However, no alterations of testosterone and estradiol serum concentrations

were found on postnatal days 53 and 90. On postnatal days 53 and 90, discontinuity and disorganization of seminiferous epithelium, cellular debris in the lumen, and sloughing of the germinal cells from the epithelium into the tubular lumen were found. The presence of cellular debris and germinal epithelial cells in the tubular lumen and vesicles was suggested as being a possible impairment to the spermatogenesis process.

In a separate study on pre-pubertal male Wistar rats, Maresmaeili et al. [2013] administered 70-nm AgNPs (coating and stabilizing agent not characterized) to rats 45–50 days of age, twice a day for 48 days (equating to one spermatogenesis period), for a total dose per day of 0, 25, 50, 100, or 200 mg/kg. The epididymis was collected for spermatogenic cell counts and histology, and the acrosome reaction assay was performed; dead or viable sperm with and without acrosome reaction were measured. Statistically significant differences for viable sperm with and without acrosomal reaction were noted at the two lower doses of AgNPs. Thickening of connective tissue in seminiferous tubules was noted following AgNP exposure; however, tubule diameter did not increase. There was a statistically significant reduction in the number of spermatocytes, spermatids, and spermatozoa in all groups. At the high dose, spermatogonia were also reduced. This study further substantiates the potential for the testis, and particularly the process of spermatogenesis, to be a target following oral exposure to AgNPs.

Studies have also been conducted on pregnant dams and embryo/fetal development (Fennel et al. 2016; Philbrook et al. 2011; Yu et al. 2014]. Fennell et al. [2016] conducted a study that compared effects of AgNP size and solubility on tissue distribution, plasma biomarkers, and urine metabolites in pregnant Sprague-Dawley rats following oral gavage or intravenous administration. In this study, rats were dosed with 10 mg/kg of silver acetate stabilized in PVP or 20-nm or 110-nm PVP-coated AgNPs by oral gavage on gestation day 18. At 24 and 48 hours, tissues were collected for measurements of silver content by ICP-MS. Urine and feces were collected to measure excreted silver. Cardiovascular markers of injury were measured in plasma, and metabolites and 8-OH-dG (an oxidative stress marker) were measured in urine. The same set of measurements were made in a separate group of rats administered 1 mg/kg of the different sample by intravenous exposure.

Because of a limited number of animals per group per parameter evaluated (n = 1–3), clear trends within a route of exposure were difficult to assess; however, following oral exposure, the majority of silver in the silver acetate group and the 110-nm group was recovered in the feces (total silver recovered in the 20 nm group was 28%, indicating a potential issue in measurement of that group). In all groups at 48 hours, outside of the GI tract tissue, silver content was highest in placenta and was also measurable in the fetus. In the liver, the highest levels were observed in the silver acetate group, potentially indicating a difference in distribution due to solubility. Following intravenous exposure, silver measurements in tissues, urine, and excretion indicated a recovery rate of 23% to 57% of the dose.

Silver was detectable in most organs, including the placenta and the fetus, with the highest levels measured in the spleens for the particle-exposed groups and the lungs for the silver acetate–exposed groups at 48 hours, indicating again the differences in distribution related to solubility. No differences were observed in markers of toxicity in plasma or urine due to exposure or route of exposure; however, carbohydrate and amino acid metabolites were affected following silver exposure.

A size and particle comparison study was conducted by Philbrook et al. [2011] on female CD-1 mice. Mice were administered a single oral dose of 10, 100, or 1000 mg/kg of 20-nm AgNPs, 3 μm Ag microparticles, 50-nm $TiO_2$ NPs, or 1–2 μm $TiO_2$ microparticles on gestation day 9 or vehicle control (0.5% tragacanth gum in deionized water). Effects of exposure on the fetus were assessed 1 day before spontaneous delivery. Skeletons were examined for defects in vertebrae and sternebrae, as well as cleft palate and polydactyl, braincase abnormalities. TEM analysis of liver and kidney tissue was performed to evaluate translocation of silver to the fetus, and inflammation and cell death were assessed histologically in liver, kidney, and placenta. Additional studies were also performed on *Drosophila melanogaster* to assess effects on reproduction and egg and larval development.

NP exposure did not alter weight gain in pregnant dams, litter size, fetal resorption, fetal length, or fetal weight. AgNPs at 10 mg/kg and $TiO_2$ NPs at 100- and 1000-mg/kg exposure did reduce the number of viable fetuses. In addition, $TiO_2$ NPs at the two higher doses led to developmental abnormalities in fetuses (encephalopathy, open eye lids, and leg and tail defects). Neither NPs caused cell death or inflammation in liver, kidney, or placenta; however, AgNPs could be detected in kidney and liver. Similar to findings in the mammalian toxicity study, $TiO_2$ NPs had greater effects in the fruit fly than AgNPs, although both NPs had greater effects than the micron-sized counterpart.

Yu et al. [2014] conducted a subacute dose-response exposure in pregnant Sprague-Dawley rat dams. Rats were administered 100, 300, or 1000 mg/kg/day of 6.45-nm AgNPs in 0.5% CMC on gestational days 6 to 19. Cesarean sections were performed on gestational day 20. Blood chemistry was performed for dams, and livers were homogenized to evaluate oxidative stress. Ovaries and uteruses of dams were also removed, and corpus lutea and implantation sites were evaluated. Fetuses were evaluated for viability, malformations, and morphological abnormalities.

The only statistically significant finding related to fetal effects in pregnancy was an increase at the highest dose in loss of pre-implanted embryos, and only one fetus in the high-dose group had skeletal malformation. Other skeletal variations existed among groups, but differences were not statistically significant. No effects were observed regarding number of fetuses or litters. Weight gain and blood chemistry parameters of dams, including indices of kidney and liver function, were normal. Catalase and glutathione reductase were elevated in liver homogenates of dams in all dose groups, and glutathione content was elevated in the high-dose group, indicating the potential of AgNP to cause oxidative stress in pregnancy. The authors concluded the NOEL to be <100 mg/kg/day for dams because of hepatic oxidative stress and 1000 mg/kg/day for fetal and embryo development.

In terms of genotoxic potential, Kovvuru et al. [2015] examined the potential for genotoxicity and DNA damage due to AgNP exposure in male and female mice, as well as offspring of pregnant mice. They used a strain of knockout mice deficient in *Mhy (MutY homologue)*, a DNA glycosylate involved in base excision repair to correct for promutagenic activity, whereby adenosine mispairs with 8-oxoguanine or formation of 2-hydroxyladenine (2-OH-A) occurs. These mice would be more susceptible to genotoxic events involving DNA repair. The goal of the study was to determine whether genotoxicity following AgNP exposure is related to oxidative DNA damage.

In this study, male and female C57BL/6J $p^{un}/p^{un}$ background mice or $Mhy^{-/-}$ mice were exposed to 96.1-nm AgNP (determined by DLS) at a dose of 500 mg/kg/day for 5 days. Pregnant mice of each background were exposed to 500 mg/kg on gestational days 9.5 to 13.5. Wildtype and knockout mice were evaluated for micronuclei formation (chromosomal damage) and positive staining for γ-H2AX (double-strand breaks) in the blood and bone marrow and positive staining for 8-oxoguanine (oxidative DNA damage) in the blood. Liver tissue was evaluated by PCR array profiling of genes involved in DNA repair. Offspring of dams were evaluated for DNA deletions, evidenced as eye spot formation visualized in the retinal epithelium at 20 days of age. AgNP exposure in wildtype mice increased micronuclei formation in blood and bone marrow, and this response was further increased in knockout mice. Induction of γ-H2AX foci and 8-oxoG was also increased in both groups of AgNP-exposed mice.

Gene profiling showed that 36 or 84 DNA repair genes were modulated (24 downregulated, 12 upregulated) in AgNP-exposed mice, several of which were differentially upregulated or downregulated between the wildtype and knockout groups. In offspring of both wildtype and knockout mice, AgNP exposure led to increased eye spot formation on the retina epithelium, indicative of DNA deletion events in utero. Results taken together suggest that AgNP induces genotoxicity, which may be in part due to oxidative stress and damage to DNA. The role of oxidative stress in DNA damage is corroborated by oral exposure studies discussed previously [Shrivastava et al. 2016; Hadrup et al. 2012b].

## E.3 Exposure via Other Routes

### E.3.1 Dermal

Wahlberg [1965] reported on a series of percutaneous studies with guinea pigs in which various metal compounds were used to evaluate the rate of absorption. The rate of absorption for silver nitrate (2 ml applied to skin and observed 3 weeks post-exposure) was found to be small (<1% per 5-hour period) compared to the rate of absorption of the other metals. The rates of dermal absorption were compared to the toxicity of silver nitrate and the other metals following intraperitoneal administration at a dose of 2 ml. The relative toxicity (mortality) observed for the various metals following intraperitoneal administration was comparable to the rate of dermal absorption found with guinea pigs; the lowest mortality rate was among guinea pigs exposed to silver.

Recently published studies examined the dermal toxicity of AgNPs in female weanling pigs [Samberg et al. 2010] and guinea pigs [Maneewattanapinyo et al. 2011; Kim et al. 2013b; Korani et al. 2011]. In the study by Samberg et al. [2010], female pigs were topically exposed to washed and unwashed AgNPs (average diameters of 20 and 50 nm) that were suspended in deionized water solutions of 0.34, 3.4, or 34 μg/mL over a 14-day period. The site of application was then examined for irritation with use of the Draize scoring system, and excised pieces of skin were examined by light and electron microscopy.

Other than a general graying of the skin, there were no direct signs of topical irritation, although some indications of focal inflammation and edema were seen when the skin was viewed under light microscopy. For example, the authors noted the occurrence of epidermal hyperplasia with an extension of rete pegs into the dermis. However, the AgNPs themselves appeared to be limited to the superficial layers of the stratum cornea. These findings were consistent with those reported by Maneewattanapinyo et al. [2011] and Kim et al. [2013].

Maneewattanapinyo et al. [2011] evaluated the dermal toxicity and irritation potential of 10–20-nm AgNPs, following the OECD 434 Guideline (acute dermal toxicity—fixed dose procedure). Male guinea pigs were exposed to 50 or 100,000 ppm AgNPs, which remained in contact with the skin for 24 hours. Symptoms, along with weight and morbidity, were monitored at 1, 3, 7, and 14 days after exposure, and histopathological examination was done at day 14. No abnormal findings were reported. This study also examined eye irritation and found transient eye irritation at a dose of 5,000 mg/kg at 24 hours after exposure, resolving by 72 hours.

Kim et al. [2013] evaluated acute dermal toxicity in Sprague-Dawley rats (with the OECD 402 Guideline), irritation potential in New Zealand White rabbits (OECD 404 Guideline), and sensitization potential in SPF guinea pigs (OECD 406 Guideline), using 10-nm AgNPs. No toxicity, change in body weight, or mortality was reported for doses of 2,000 mg/kg following 24 hours of skin exposure, up to 2 weeks following exposure. During the study with rabbits, no statistically significant clinical signs or deaths were observed. In the initial ocular test at a dose of 100 mg per animal, no signs of irritation to the cornea, iris, or conjunctiva were observed 1, 24, 48, and 72 hours after removal of the test substance. When AgNPs were applied to the skin of SPF guinea pigs in accordance with OECD Test Guideline 406, a sensitization protocol that involves an induction phase with adjuvant as well as a challenge phase, none of the tested animals died or showed any statistically significant body weight change or abnormal clinical signs during the experimental period. Only 1 out of 20 animals had patchy erythema, yielding a 5% skin sensitization rate (classification of weak sensitizer).

However, these findings contrasted with those reported by Korani et al. [2011], in which an array of changes to the skin of Hartley guinea pigs were observed following dermal application of aqueous solutions of colloidal AgNPs (<100-nm diameters) at concentrations of 100 and 1,000 μg/mL in an acute study (6 animals/dose) using OECD Test Guideline 402 and three concentrations of 100, 1,000, and 10,000 μg/mL (6 animals/dose) in a subchronic study. In the acute study, 10% of the body surface

was exposed and examined 1, 24, 48, and 72 hours post-exposure for presence of edema, erythema, or any type of dermal change. Observations continued for 14 days. In the subchronic study, a shaved skin area of 5 cm × 5 cm was applied 5 days/week with 100, 1000, or 10,000 μg/mL AgNPs for 13 weeks; skin of the positive controls was rubbed with 100 μg/mL of $AgNO_3$. Korani et al. [2011] described an array of changes to the skin as a result of either dosing regimen, with increasing severity in such responses as epidermal thickness, inflammation, presence of round and clear cells, and reduced papillary in relation to dose and exposure duration. Similar skin inflammatory responses were recorded in all treatment groups in the subchronic study. Increased incidence of histopathologic responses in the liver and spleen were also reported for the subchronic study, with signs of necrosis at the highest dose.

The results indicate that dermal contact with AgNPs causes slight histopathologic abnormalities of the skin, liver, and spleen of animals that can occur at dermal concentrations >0.1 mg/kg (>100 μg). In a follow-up study by Korani et al. [2013], the subchronic dermal exposure (5 days per week for 13 weeks to 0, 100, 1,000, or 10,000 ppm of colloidal AgNPs, or silver nitrate at 100 μg/mL, as aqueous solutions applied to skin) was repeated with focus specifically on effects in kidneys, bone, and heart. Tissue distribution following dermal exposure was measured with an atomic absorption spectrophotometer, and degree of accumulation was reported as follows: kidney > muscle > bone > skin > liver > heart > spleen.

Pathological studies were performed on heart, kidney, and bone. Bone was evaluated for inflammation, osteoclast formation, narrowing of marrow space, and line separating of lamellar bone. Abnormalities were observed with all doses, and dose-dependent increases in severity occurred for all parameters except inflammation. Heart tissue was evaluated for inflammation, cardiocyte deformity, clear zone around nucleus, and congestion/hemorrhage, with dose-dependent increases found in all parameters. Toxicity in the kidney was evaluated as inflammation, proximal convoluted tubule (PCT) degeneration, adhesion of glomerular epithelial cells to Bowman's capsule (BC), capsular thickening, membranous thickening, and increased mesangial cells. Again, a dose-dependent increase was observed for most parameters, with the most severe effects including PCT degeneration, followed by effects in BC and capsular thickening. In all instances, the 100-μg/mL silver nitrate control scored similarly in severity to the 100-ppm dose. Both studies together indicate the potential for silver to translocate to other organ systems following subchronic exposure; however, it is unclear whether this effect is related to dissolution rate and consequently delivery of ion or particle to tissue.

Ling et al. [2012] reported on the potential dermal exposure risk to workers for nanoscale zinc oxide powder, multiwall carbon nanotubes, and nanoscale silver (Ag-colloid, Ag-liquid) so that appropriate risk management practices could be incorporated in the workplace to protect workers. The assessment of workers' risk of exposure to nanoscale silver focused on the potential for dermal absorption of silver during the handling of nanoscale silver-colloid (average diameter, 9.87 nm) and silver-liquid (average diameter, 13.04 nm). Based on criteria by OECD [2004], WHO [2010], and U.S. EPA [2004], two skin exposure techniques were used (transdermal Franz diffusion cell drive and tape stripping) to evaluate dermal absorption of nanoscale silver. Excised porcine skin was used as a model for human skin in the transdermal Franz diffusion cell test.

Nanoscale silver-colloid and silver-liquid samples flowed with specific rates through a portion of the skin for 18 hours. The sampled porcine skin and remaining fluids were analyzed for silver with use of flame atomic absorption spectrometry (FAAS); silver concentrations from the remaining skin and fluids were then added and compared with the original amounts. For the tape stripping technique, nanoscale silver-colloid and silver-liquid at concentrations of 20 μg/mL and 300 μg/mL, respectively, were applied evenly on human skin for 2 hours. After this, tapes with areas of 5 $cm_2$ were patched on the human skin and subjected to pressure, followed by immediate tape stripping. Stripping was repeated 5 times, with each taking up 6 to 8 layers of the stratum cornea, yielding removal of about 30

to 40 cell layers of the stratum cornea. The stripping tapes were analyzed with inductively coupled plasma mass spectrometry (ICP/MS) to quantify silver contents.

Results of the tape stripping analysis showed that the distribution of nanoscale silver colloid and silver liquid was predominantly on the first and second strippings of the stratum cornea. This occurred at both the 20-µg/mL and 300-µg/mL concentrations, indicating a low rate of skin penetration over a short period of exposure. In addition, the experiments showed that organic modifiers affected the infiltration of nanoscale silver. When a less-polar solvent such as isopropyl alcohol was used, the penetration rate was higher than for other polar solvents.

Although the dermal toxicity data from studies of animals and studies using porcine skin are limited, they suggest that AgNPs can penetrate the skin epidermis [Larese et al. 2009; Ling et al. 2012], can induce some systemic toxicity [Korani et al. 2011; 2013], and can cause topical irritation at the site of contact [Samberg et al. 2010; Korani et al. 2011], depending on dose and duration of exposure.

## E.3.2 Intratracheal Instillation, Oropharyngeal Aspiration, or Intranasal Instillation

### *E.3.2.1 Silver nanoparticles*

Alternatives to inhalation exposure, including intratracheal (IT) instillation, oropharyngeal aspiration, or intranasal (IN) instillation, have been employed to study the in vivo responses to AgNPs in the lungs of experimental animals. All the studies in Table E-5 examined various lung effects following exposure. A number of studies have focused on the pulmonary effects and/or lung distribution following exposure to a single form and size of AgNP alone or in comparison with other metal NPs [Arai et al. 2015; Haberl et al. 2013; Kaewamatawong et al. 2014; Katsnelson et al. 2013; Liu et al. 2013a; Park et al. 2011b; Roberts et al. 2012; Smulders et al. 2014, 2015a]. Other studies have focused on systemic effects in addition to lung responses following exposure to AgNPs [Davenport et al. 2015; Genter et al. 2012; Gosens et al. 2015; Holland et al. 2015; Huo et al. 2015; Liu et al. 2012; Minchenko et al. 2012; Wen et al. 2015]. Additionally, several studies have examined the effects of size and capping/coating agent on toxicity and biodistribution [Anderson et al. 2015b; Botelho et al. 2016; Silva et al. 2015; Seiffert et al. 2015].

Studies examined acute responses up to 1 day post-exposure to a single IT instillation of AgNPs [Arai et al. 2015; Haberl et al. 2013; Katsnelson et al. 2013]. Haberl et al. [2013] examined lung injury and inflammation in BAL fluid following a dose-response (0, 50, or 250 µg per rat) to AgNPs ~70 nm in diameter with PVP coating in female Wistar-Kyoto rats. In this study, a trend for a dose-dependent increase in inflammation was measured as BAL fluid neutrophil influx and increased BAL fluid cytokines (IL-1β, IL-6, IL-12p70, MIP-1 α , MIP-2, CINC-1, M-CSF); however, increases were statistically significant only when compared to control at the highest AgNP dose administered. The high dose also caused statistically significant lung injury (increased BAL fluid LDH and protein levels) 24 hours post-exposure.

Katsnelson et al. [2013] investigated pulmonary effects 24 hours after a single IT administration of 49-nm AgNPs generated by laser ablation of a metal target, in comparison to gold NPs or micron-sized silver particles (1.1 µm diameter) at a dose of 0.5 mg in 1 ml of vehicle in female rats. Inflammatory cell infiltration, phagocytosis, and cell distribution of particles were evaluated. AgNP exposure caused a greater degree of neutrophil influx into the lungs when compared to both the micron-size silver and gold NPs. A greater degree of phagocyte-uptake of AgNPs occurred in comparison with micro-size silver particles, measured as pit number and size on the surface of alveolar macrophages by atomic force microscopy. TEM showed a difference in distribution of AgNPs versus gold NPs, where AgNPs did not penetrate cell nuclei but did have affinity for the mitochondria. The study demonstrated that cytotoxicity and distribution varied according to size and chemical composition of particles.

Arai et al. [2015] examined lung effects and systemic distribution in male ICR mice at 4 and 24 hours post-exposure to 10 μg of 20-nm citrate-coated AgNP or $AgNO_3$ solution as a control for effects of the ionic/soluble form of silver. Silver was measured by ICP-MS in lung, liver, kidney, spleen, and urine. Lung levels of silver were lower in mice administered the ionic form of silver, suggesting a faster rate of lung clearance versus AgNPs. Both AgNPs and the ionic form of silver were detected in the liver, and the increase was statistically significantly greater for the ionic form as compared to AgNPs, suggesting a faster rate of biodistribution for the ionic form. No significantly increased silver levels were detected for either form in kidney, spleen, or urine at these early time points post-exposure. Both forms of silver caused an increase in lung neutrophils. The increase was statistically significant only for the ionic form at 24 hours. AgNPs increased BAL fluid IL-1β statistically significantly at 4 hours post-exposure. In a parallel in vitro study in J774.1 cells, AgNPs were shown to distribute to metallothioneins and were found sequestered in the lysosome, with gradual dissolution over time. This study indicated that the soluble form of silver caused greater inflammation at 24 hours post-exposure and was cleared faster from the lung (related to greater distribution to the liver), in comparison with AgNPs.

Park et al. [2011b] and Kaewamatawong et al. [2014] examined lung responses up to 1 month following a single IT instillation of AgNPs. Park et al. [2014] administered AgNPs at doses up to 500 μg/kg to ICR mice and evaluated the resulting inflammation by measuring the concentration of cytokines in BAL fluid and in the blood. The commercially supplied AgNPs were originally suspended in THF with sonication. After all the solvent had been allowed to evaporate, the particles were reconstituted in phosphate-buffered saline (PBS). A histopathologic analysis was also carried out on excised pieces of lung, and changes in gene expression were assessed by a microarray method.

The AgNPs were dispersed in an aqueous medium, and there was evidence of aggregation in that the average diameter of particles was 243.8 nm. A considerable number of dose-related changes were evident in the cytokine composition of BAL fluid and blood as a result of exposure to AgNPs. In BAL specimens, the most dramatic increases in cytokine levels were manifested in IL-1, IL-6, IL-10, and TGF-β. These agents appeared to reach a maximum concentration 28 days after exposure. In the blood, concentrations of IL-6, IL-12, IFN-γ, and IL-10 showed statistically significant increases on the day after instillation. Histopathologic analysis indicated inflammatory responses, such as infiltration of alveolar macrophages, in lung tissue on day 1 but not on days 14 and 28. The responses were characterized by the presence of cell debris, dead neutrophils, and foreign bodies. A substantial number of changes in gene expression resulted from IT instillation of AgNPs, with 261 genes being upregulated and 103 genes downregulated. Changes in the functionality of induced genes appeared to be related to tissue damage.

Kaewamatawong et al. [2014] measured parameters of lung injury, inflammation, and oxidative stress in male ICR mice at 1, 3, 7, 15, and 30 days post-exposure to colloidal AgNPs (0 or 100 ppm, 10–20-nm diameter). Cytotoxicity in the cells of BAL fluid was increased at days 1 and 3 post-exposure to AgNPs. Neutrophil influx was statistically significantly increased at 3 days post-exposure, and lymphocyte influx increased at 7 and 15 days post-exposure. Histopathological findings showed increased neutrophils and macrophages 1 and 3 days after instillation, mild-to-moderate multifocal alveolitis in areas with macrophages that contained AgNPs, and type II cell hypertrophy and hyperplasia.

Histopathology responses peaked by 7–15 days post-exposure, with the additional findings of cellular necrosis, lymphocytic infiltration, and mild to moderate loss of structural architecture. Areas of lung injury in tissue corresponded to increased immunohistochemical staining of superoxide dismutase, suggesting that AgNP exposure increased oxidative stress. Immunohistochemical staining of metallothionein in tissue also correlated to areas high in AgNPs, further suggesting affinity of AgNPs for these proteins.

Repeated-dose, subacute exposure studies using IT instillation [Liu et al. 2013a; Roberts et al. 2012] or oropharyngeal aspiration [Smulders et al. 2014, 2015a] have also been performed to assess lung toxicity and distribution of AgNPs. Intratracheal instillation of AgNPs in male Sprague-Dawley rats was observed to cause an increase in the cellular and protein content of BAL fluid, as well as increased injury, as determined by histopathological analysis. Liu et al. [2013a] exposed Wistar rats by IT instillation to 3.5 or 17.5 mg/kg of 52-nm AgNPs once every 2 days for 5 weeks (19-nm ZnO NPs and 23-nm TiO2 NPs were also evaluated).

Lung effects were observed 1 day following the last exposure. Inflammation (IL-1, IL-6, MIP-2, TNF-α levels) and oxidant damage (GSH, SOD, MDA, and NO levels) were measured in BAL fluid. Both doses of AgNPs caused increases in all parameters of oxidant damage as well as increases in IL-6 and MIP-2. The high dose of AgNPs also caused increased TNF-α levels in BAL fluid. The study implicates oxidative stress as a pathway for increased immune and inflammatory responses following exposure to AgNPs.

In a study by Roberts et al. [2012], male Sprague-Dawley rats were exposed to AgNPs (20 nm in diameter) with a 0.3%-by-weight coating of PVP. Dispersion of AgNPs in a physiologic medium caused some degree of aggregation, as indicated by the average particle size of 180 nm. AgNPs were administered weekly for 8 weeks at a dose regimen lower than that of Liu et al. [2013a], at 0, 9.35, or 112 μg per rat (~0, 0.03, or 0.3 mg/kg), with subsequent evaluation after 7, 28, or 84 days. The high dose of AgNPs was observed to induce acute pulmonary injury and inflammation that appeared to resolve to a degree over time. The low dose produced very little lung injury or inflammation.

Smulders et al. [2014] conducted a comparative toxicity study that examined the effects of a repeated aspiration exposure to AgNPs (25–28-nm diameter, 90-nm-diameter aggregated) relative to other metal-based ENMs and paints containing ENMs. Oropharyngeal aspiration in male BALB/c mice was conducted once a week for 5 weeks at 20 μg per exposure, for a cumulative dose of 100 μg per mouse. At 2 and 28 days after the last exposure, BAL fluid and blood cell and cytokine responses were measured, as well as silver levels in lung, kidney, liver, spleen, and heart. Regarding findings related to the AgNPs, BAL fluid neutrophil influx was increased at 2 days after the last exposure, along with BAL fluid IL-1β and KC, indicating increased inflammation following AgNP exposure. Inflammatory responses resolved by 28 days post-exposure. Silver levels in the lung were lower at day 28 versus 2 days post-exposure, showing a slight degree of clearance over time. Silver was increased in liver, kidney, and spleen at 2 days post-exposure, but not in the heart, and was shown to be cleared by 28 days post-exposure in those organs.

In a follow-up study [Smulders et al. 2015a], using a similar exposure regimen, the investigators examined distribution of AgNPs (heterogeneous mixture, 20-nm spherical and 80–90-nm rods, with average agglomeration of ~500 nm) in the lung along with co-localization with other metals and speciation of silver at 2 days following the last exposure. A high percentage of macrophages in both the airways and alveolar regions contained AgNPs. A large portion of the AgNPs were dissolved and were determined to be complexed to thiol-containing proteins, likely metallothioneins.

Several studies have examined pulmonary and extrapulmonary toxicity following IT or IN instillation of AgNP. Holland et al. [2015] examined the effects of a single IT instillation of 0 or 1 mg/mL of 20-nm citrate-capped AgNPs on pulmonary and cardiovascular responses in a model of cardiac ischemic reperfusion (I/R) injury in rats. Responses were evaluated at 1 and 7 days after exposure and were compared to a dose-response of silver acetate (AgAc) as a soluble/ionic form of silver. Histopathology of the lung revealed no effects 1 day post-exposure. By 7 days, only a thickening of the alveolar wall was noted in AgNP-exposed rats. AgNP exposure did not increase neutrophil influx or protein content in the lungs; however, increased neutrophils, lymphocytes, and total lung protein were measured in the AgAc group. Serum cytokine analysis showed increased

pro-inflammatory cytokines (IL-1β, IL-6, IL-18, and TNF-α) at 1 day and elevated IL-2, IL-13, and TNF-α at 7 days in AgNP-exposed mice. AgAc did not statistically significantly elevate serum cytokines. AgNPs also caused expansion of I/R injury and depression of coronary vessel reactivity. AgAc produced vascular effects at the high dose, but this occurred in the absence of increased cytokines in BAL fluid or serum. The differences led the authors to conclude that the soluble form of silver is not entirely responsible for effects of AgNPs on the cardiovascular system.

Pulmonary and systemic inflammation was assessed by Gosens et al. [2015] following a single IT instillation of AgNPs (3–4 nm, capped with polyoxylethylene glycerol trioleate and Tween-20) in C57BL/6NT mice at doses ranging from 1 to 128 μg per mouse. BAL fluid parameters of injury and inflammation, blood cell profiles, and liver glutathione levels were measured 1 day after exposure, along with liver silver content. No increases in pulmonary neutrophil influx, cytokines, LDH, albumin, or AP levels were measured following AgNP exposure. In addition, no alterations in blood cell profiles were found. However, despite the lack of lung and systemic inflammatory parameters, silver content in liver was increased and glutathione levels were decreased, suggesting the sensitivity of the liver to effects following AgNP respiratory exposure, as suggested by inhalation studies discussed previously.

Huo et al. [2015] also examined lung and systemic responses in mice following a single IT instillation of the same AgNPs utilized by Gosens et al. [2015], at doses of 0.1 or 0.5 mg/kg. Lung, trachea, arterial tissue, liver, and kidney were analyzed for markers of stress to endoplasmic reticulum (ER) and apoptosis at 8 and 24 hours post-exposure. Silver content in tissues was also evaluated. Increased silver was detected in the liver at 8 hours after both doses and in the kidney at 24 hours following the high dose of AgNPs. Rate of apoptosis was increased in the lung at the low and high doses and in the kidney at the high dose at 24 hours. mRNA levels of several ER markers were increased in the lung, liver, and kidney but not in the trachea or arterial tissue, at different times following exposure. The findings also suggest liver sensitivity to AgNP exposure, as well as kidney sensitivity.

A study by Minchenko et al. [2012] also detected changes in gene expression in different tissues following AgNP exposure (single IT instillation in rats). mRNA expression of genes related to circadian factors was analyzed at 1, 3, and 14 days post-exposure to 0.05 mg/kg AgNPs (28–30-nm diameter, 30% in solution). Alterations in several genes, including PER1, PER2, and CLOCK, were observed at different times and to different degrees in lung, liver, kidney, brain, heart, and testes.

Genter et al. [2012] assessed organ distribution and systemic effects following a single IN instillation of AgNPs (25-nm diameter) in mice. Whole blood, brain, kidney, liver, spleen, and nasal cavity specimens were collected at 1 and 7 days after exposure to 0, 100, or 500 mg/kg AgNPs. In addition to deposition in the nasal cavity, AgNPs were found to distribute to the lung, brain (olfactory bulb and lateral brain ventricles), spleen (localized in the red pulp to a greater degree than in the white pulp), and kidney. Pathology in the nasal cavity included mucosal erosion. Glutathione levels were found to be increased in the nasal cavity and blood, indicating a degree of oxidative stress in those tissues. No microglial cell activation or inflammation was noted in the brain. However, reduced cellularity in spleen was observed, localized to the red pulp, suggesting erythrocyte destruction in the spleen.

In a related study, Davenport et al. [2015] examined systemic and behavioral responses following a single IN instillation (doses ranging from 10 to 500 mg/kg) or repeated IN instillation (50 mg/kg per day for 7 days). Silver content in tissues, spleen cellularity and glutathione levels, Hmox1 expression, and protein in brain were evaluated 7 days after the single IN exposure. Neurobehavioral response was measured with the Morris water maze in association with the 7-day exposure. Silver was detected in liver, gut-associated lymphoid tissue, choroid plexus, and lateral ventricles. Effects in the spleen included increased glutathione levels, increased monocyte and macrophage populations at 25 and 50 mg/kg, and a reduction in NK cells at doses of 25–500 mg/kg. Oxidative stress responses measured as Hmox1 were noted in the hippocampus but not in the cortex. Despite changes in oxidative stress in regions

of the brain associated with learning and memory, no changes in learning behavior were observed, and only modest change in spatial reference memory was noted following AgNP exposure.

Two additional studies examined brain effects and distribution of silver to the brain following repeated IN instillation in rats [Liu et al. 2012; Wen et al. 2015]. Liu et al. [2012] administered 0, 3, or 30 mg/kg of 50–100-nm AgNPs (agglomerating to 33–380 nm) to male rats once every 2 days for 14 days. Histology was performed and ROS in hippocampus were measured, along with cognitive function as performance in the Morris water maze test and long-term potentiation tests. Dose-dependent impairment of cognitive function was found. Increased neuronal damage and ROS in the hippocampus were observed, in the area involved in learning and memory.

Wen et al. [2015] conducted a repeated IN exposure in neonatal male and female rats with 20-nm PVP-coated AgNPs or soluble $AgNO_3$ at doses of 0.1 or 1.0 mg/kg once a day for 4 or 12 weeks, to assess organ distribution and retention. Silver was measured by ICP-MS in heart, liver, spleen, lung, kidney, pancreas, ovaries or testes, fat, and brain. In this study, no sex differences were observed. Exposure to ionic silver did cause 18% mortality at the highest dose, whereas no weight loss or mortality was observed following AgNP exposure, suggesting that a greater degree of toxicity is associated with the ionic form of silver.

For both forms of silver at a dose of 0.1 mg/kg per day, the highest levels at 4 weeks were detected in the liver, with statistically significantly greater accumulation of ion versus particle in these organs. At 4 weeks, silver ion in the liver was measured at 424.8 ng/g of tissue, whereas AgNPs were measured at 35.5 ng/g of tissue. Silver ion was also detectable in the brain at 4 weeks. Dose-dependent increases were observed in liver and brain for both forms of silver at 4 weeks. After 12 weeks of exposure to the lower dose, the brain contained the highest levels of silver for both ionic silver (58 ng/g) and AgNPs (9 ng/g). Silver ion also accumulated in kidney after 12 weeks of exposure (23 ng/g). Ionic silver was below 20 ng/g in all other tissues, and AgNPs in all other organs were below 5 ng/g. These studies, taken together, suggest the brain may be a target for AgNPs, particularly following intranasal exposure, and that there is a greater degree of translocation of the ionic form of silver than of the particle form.

The effects of the properties of size and particle coating/capping agent on AgNP distribution and toxicity were also evaluated in several studies [Anderson et al. 2015b; Botelho et al. 2016; Seiffert et al. 2015; Silva et al. 2015]. All four studies examined 20- and 110-nm PVP- and citrate-coated AgNPs. In the study by Seiffert et al. [2015], strain-related differences were also investigated. BN or Sprague-Dawley (SD) rats were administered 0.1 mg/kg of the four different AgNPs by a single IT instillation. Controls for the coating materials were also examined, along with a soluble ion sample at a concentration of 1 μg per animal in the form of silver nitrate. Histological analysis was performed and lung function, BAL fluid cell and protein levels, and gene expression of proteins in lung tissue were measured at 1, 7, and 21 days post-exposure.

Ion exposure at the concentration of 1 mg per rat did not produce any adverse effects in the lung. The greatest effects on lung function parameters were observed in BN rats, a strain that has a degree of pre-existing inflammation in the lung. In BN rats, airway resistance was increased following exposure to all AgNPs, regardless of size and coating, at 1 day post-exposure. At 7 days, only the citrate-capped particle caused an increase in resistance in the BN group, which resolved by day 21. At day 21, an increase was observed in resistance following exposure to the 20-nm PVP-coated particle. Compliance in BN rats was decreased on day 1 after exposure to all particles, with the exception of 110-nm citrate-capped AgNPs; the decrease persisted for the 20-nm PVP-coated particle to day 7 and for the 20-nm citrate-coated particle to day 21. Airway resistance and hyperreactivity following acetylcholine challenge were increased following exposure to 20-nm PVP-coated particles at day 1.

At day 7, hyperresponsiveness was increased with both sizes of citrate-coated particles, and at day 21, both 20-nm particles increased hyperresponsiveness in BN rats. AgNP particle exposure did not

alter baseline measure of resistance or resistance following acetylcholine challenge in SD rats. A decrease in compliance was observed at 1 day post-exposure to 20-nm citrate-capped particles, and airway hyperresponsiveness was increased on day 21 after exposure to 20-nm PVP-coated particles. BAL fluid cell differentials showed increased neutrophils and eosinophils for BN rats 1 day following exposure, regardless of particle type and size, with a statistically significant increase for only citrate-coated particles at day 7.

Neutrophil and lymphocyte numbers were increased in BAL specimens of SD rats at 1 day post-exposure to the smaller particles for each coating, with a statistically significant increase persisting to day 7 for only the 20-nm citrate-coated material. BAL fluid protein levels, malondialdehyde (MDA), cytokines (KC, CCL11, IL-13, eosinophil cationic protein), and IgE were increased in BN rats at 1 day post-exposure to varying degrees with all particles. Increases in total protein and KC persisted following exposure to the 20-nm AGNPs at day 7, and MDA remained elevated following PVP-coated particle exposure at 7 days. In SD rats, MDA and eosinophil cationic protein were increased at day 1 following exposure to 20-nm particles, and KC was elevated following exposure to 20-nm PVP-coated particles.

The authors concluded that the greatest differences could be attributed primarily to size, with differential and less critical differences due to particle coating. The greater degree of response in BN rats suggests there may be concern for responses related to immune effects such as those attributed to asthma.

Botelho et al. [2016] conducted a study to further examine size on innate immune defense and lung function following a single IT instillation of 0.05 mg/kg of 20- or 110-nm citrate- or PVP-coated particles in C57BL/6 mice. BAL fluid cell counts, protein levels, phospholipid levels, and LDH were measured, and lung histology and tissue analysis of Cd11b (monocyte recruitment) were performed at 1 day post-exposure for all particles and at 7 and 21 days after exposure with PVP-coated particles. LDH, cell counts, and proteins levels were not statistically significantly increased in BAL fluid at 1 day following exposure to any of the particles. Surfactant protein D was decreased following PVP-coated particle exposure. The 110-nm PVP-coated particle had the greatest effect on lung mechanical function. Increased cell counts in BAL fluid and reduced lung function were observed for the PVP-coated particles at 7 days post-exposure, with resolution by 21 days post-exposure. In this study, the PVP-coated particles and specifically the larger PVP-coated particle produced the greatest disruption in lung function. The authors attributed effects in part to particle solubility. Citrate-coated materials were not investigated beyond 1 day post-exposure in this study.

Two related studies examined lung toxicity [Silva et al. 2015] and lung distribution [Anderson et al. 2015b] following a single IT instillation of 20- or 110-nm PVP- or citrate-coated AgNPs in rats. In the toxicity study, rats were exposed to 0, 0.1, 0.5, or 1.0 mg/kg of particles or buffers as controls. BAL fluid and tissue analysis was performed at 1, 7, and 21 days post-exposure. All AgNPs caused increased polymorphonuclear cells in BAL fluid at 1 and 7 days post-exposure at the 0.5 and 1.0 mg/kg dose, and this increase remained statistically significant following the larger PVP- and citrate-coated particle exposures at day 21. Lung injury measured at LDH was greatest on day 7 following all particle exposures at the 0.5 and 1.0 mg/kg dose. Lung tissue analysis showed the greatest difference at day 7 versus day 21 post-exposure for all particles examined. At day 1, AgNP exposure caused increased cellularity in the airspaces and centriacinar inflammation, which continued and increased to day 7, accompanied by cellular exudate and debris in airspaces. At day 21, inflammation continued, although not to the same degree as at day 7, and a foaminess and irregular multi-nucleated appearance of macrophages were noted in all exposure groups but to the greatest degree in the 110-nm citrate- and PVP-coated groups. Results taken together showed the most persistent toxicity following exposure to the larger particles, regardless of coating.

In a related study, Anderson et al. [2015b] examined the lung distribution of these particles following 0.5 or 1.0 mg/kg administered by a single IT instillation, at 1, 7, and 21 days post-exposure.

Findings indicated that citrate-coated AgNPs persisted to a greater degree in the lung up to day 21 (90% retention at day 21) than did the PVP-coated particles (30% retention at day 21). Silver-positive macrophages in the lung decreased at a greater rate in the PVP-coated particle groups than in the citrate-coated groups. In terms of size, at 1 day post-exposure more 100-nm particles were located in the proximal airways than 20-nm particles. Larger particles were also more rapidly cleared from the lungs, whereas the 20-nm citrate-coated particles persisted to the greatest degree.

Some commonalities exist in the studies that utilize IT instillation, IN instillation, or oropharyngeal aspiration. Silver is observed to translocate to other organ systems, primarily to liver, kidney, and brain as targets (with temporal differences in tissue burden observed), as well as to spleen, testes, and heart in select studies. In most instances where study recovery points were carried out up to 1 month post-exposure, pulmonary responses appeared to resolve to varying degrees over time. In studies that examined ionic forms in comparison to particles at equal mass doses, the ionic form was usually the more toxic form in the lung, and it was usually found to clear at a faster rate from the lung. There are discrepancies in responses related to size and coatings among studies that examined the same batteries of AgNPs, suggesting more research is needed in this area to understand the role of these properties and how the properties relate to ion release from particles, as well as potential subsequent toxicity over time in vivo.

### *E.3.2.2 Silver nanowires*

Kenyon et al. [2012] studied the lung toxicity of silver nanowires (AgNWs) of varying lengths in male Sprague-Dawley rats (by intratracheal instillation of long [20 μm] or short [4 μm] AgNWs, about 50 nm in diameter). Rats were administered AgNW doses of 10, 50, 125, or 500 μg, alpha-quartz (positive control) at 500 μg, or dispersion medium (vehicle control). Both wire samples caused a dose-dependent increase in lung injury (lactate dehydrogenase activity and albumin content in lavage fluid) and inflammation (increased lung neutrophils and phagocyte oxidant production). Neither the short nor the long wires at the 10-μg dose had any effect on lung toxicity. The longer wires caused slightly more lung injury immediately following exposure, whereas the shorter wires induced greater toxicity over the time course. The authors suggested this finding may be due to greater wire number and surface area in the short-wire sample when samples were compared on an equivalent mass basis.

Schinwald et al. [2012] studied the role of length of silver nanowires (AgNWs) on the acute lung responses in mice (C57BL/6, female, 9 weeks old). Mice (five per group) were exposed by pharyngeal aspiration to AgNWs of different lengths (3, 5, 10, or 14 μm) or to short or long fibers of amosite (SFA or LFA). The doses were selected to equalize the number of fibers per mouse, which resulted in mass doses of 10.7, 10.7, 17.9, 35.7, 50, and 50 μg/mouse for SFA, AgNW3, AgNW5, AgNW10, AgNW14, and LFA, respectively. The 50-μg dose was selected from an initial dose-response series as one that resulted in a persistent inflammatory response with AgNW14 and LFA.

The acute inflammation response was evaluated 24 hours after aspiration exposure. A length-dependent trend in the pulmonary inflammatory response was observed for the AgNWs, yet only the mice exposed to the longest (14-μm) AgNWs showed a statistically significant increase in the granulocytes in BAL fluid. A nonlinear relationship was observed between exposure to AgNWs by length and inflammation response, which suggested a length threshold based on a "discernible step-increase in granulocyte recruitment at a length between 10 and 14 μm" [Schinwald et al. 2012; Schinwald and Donaldson 2012]. Frustrated phagocytosis (defined as incomplete uptake of fibers by cells) was observed in mice exposed to AgNW14 or LFA. Histopathology performed 24 hours after aspiration showed minor granulomas and lymphocyte infiltrates in mice exposed to AgNW5 or AgNW10. More extensive granuloma and lymphocyte infiltrates were observed in mice exposed to AgNW14 and LFA, which was consistent with the BAL findings of inflammation. Although the AgNW14 produced more granulomatous areas compared to shorter fibers, that response was still relatively minor

compared to the "extensive interstitial thickening and remodeling of the alveolar spaces after LFA treatment" [Schinwald et al. 2012]. The authors noted that their results need to be confirmed in long-term inhalation studies using a range of different nanofibers at plausible exposure concentrations, before these thresholds can be used for risk assessment.

Silva et al. [2014] examined the effects of long and short AgNWs in rats after a single IT instillation of 0, 0.1, 0.5, or 1.0 mg/kg AgNW per rat. Short wires were characterized to be 2 μm in length and ~33 nm wide with an aspect ratio of 62.1, whereas long wires were 20 μm in length and ~65 nm wide, with an aspect ratio of 321.4. BAL fluid cell differentials and protein levels were assessed, along with pathological analysis of tissue, at 1, 7, and 21 days following exposure. At 1 day post-exposure, short and long AgNWs statistically significantly increased neutrophils and eosinophils in the lung at the highest dose. Short AgNWs also increased neutrophils and eosinophils at the dose of 0.5 mg/kg. Both long and short AgNWs increased total protein in the lung at doses of 0.5 and 1.0 mg/kg. The increase persisted with the long wires at day 7 at the high dose. BAL fluid parameters of injury and inflammation showed resolution by day 21.

Microscopic examination of alveolar macrophages recovered by BAL indicated both long and short wires produced increased foreign body macrophages; however, only long wires produced a degree of frustrated phagocytosis following exposure. Histopathology showed increased inflammation in tissue at doses of 0.5 and 1.0 mg/kg. Responses to the short wires appeared to increase with time, whereas responses following long-wire exposure were worse at day 7 versus day 21.

Despite trends for temporal differences in the pattern of injury, there were no statistically significant differences between short and long wires in histopathological scores. Pathology was characterized by cellular exudate in the alveolar region and sloughing of cells in the terminal bronchioles, as well as tissue granulomas. By day 21, AgNWs were localized in granulomas and in terminal bronchiole/alveolar duct junctions with macrophage infiltrates.

Immunohistochemistry showed TNF-α- and TGF-β-positive cells at 1 and 7 days, respectively, following exposure to both long and short wires. The difference in BAL fluid parameters at 1 and 7 days post-exposure to short versus long wires was attributed to a greater number of wires per mass instilled with the short-wire sample compared to the long-wire sample. The investigators suggest that further study by inhalation is necessary to determine if responses are related to delivery of a bolus dose from IT instillation.

## E.3.3 Subcutaneous, Intravenous, or Intraperitoneal Injection

### *E.3.3.1 Kinetics following subcutaneous injection*

Tang et al. [2008] investigated the potential of AgNPs (50–100 nm in diameter) and silver microparticles (2–20 μm in diameter) to cross the blood–brain barrier. Wistar rats (90 females) were given a subcutaneous injection of either AgNPs or silver microparticles, and five rats from each group were killed at weeks 2, 4, 8, 12, 18, and 24 to obtain brain tissue to measure silver concentrations. Silver concentrations were higher for the AgNP group than for the silver microparticle and control groups and reached statistical significance at 4 weeks ($p < 0.05$). In the AgNP group, silver concentrations reached a peak of 0.41 μg ± 0.16 μg at week 12 and did not change statistically significantly by week 24. No statistically significant difference in silver concentrations between the silver microparticle group and control group was detected ($p > 0.05$).

It could not be determined whether the silver concentrations in the brain were a result of AgNPs or $Ag^+$. However, in ultrastructural analysis, AgNPs were detected in vascular endothelial cells from the abnormal blood–brain barrier, which could have resulted from transcytosis of the endothelial cells of the brain–blood capillary. No abnormal substance was detected in the brains of rats from the control group and the silver microparticle group. However, many pyknotic, necrotic neurons were detected in the brain of the AgNP exposure group between 2 and 24 weeks.

Tang et al. [2009] also studied the distribution of AgNPs over a 24-month period after the subcutaneous injection of elemental AgNPs or silver microparticles in female Wistar rats at a single dose of 62.8 mg/kg. The preparation of nanoparticles (5 mg/mL in physiologic medium) was reported to be 50–100 nm in diameter, mostly spherical, and with a low degree of aggregation. The tissue and subcellular distribution of silver associated with this preparation was compared with that of a preparation of silver microparticles. These were said to be of various shapes and sizes, ranging from 2 to 20 μm.

Although most of the silver from both nanoparticles and microparticles accumulated at the site of administration, ICP-MS showed that about 0.15% of the nanoparticle load reached the bloodstream and was distributed to remote sites, including kidney, liver, spleen, brain, and lung. By contrast, silver microparticles did not pass to the general circulation to any great extent (no more than 0.02% of the injected load), and their distribution to the tissues was therefore markedly less than that of AgNPs. However, fecal excretion of silver from silver microparticles was greater than that from nanoparticles during early follow-up (2 weeks after injection). This pattern was reversed on later sampling dates (up to 24 weeks). For AgNPs, histopathologic examination of these target organs by TEM and EDS revealed localization of internalized silver. This showed silver-containing electron-dense droplets (as opposed to dissolute silver ions) in the renal tubular epithelial cells, at the margin of the renal capsule, and in hepatocytes, hepatic sinusoidal and perisinusoidal spaces, lymphocytes in the splenic cord, cerebral neurons, vascular endothelial cells of the blood-brain barrier, and alveolar epithelial cells.

#### *E.3.3.2 Kinetics following intravenous injection*

Corroborative evidence of the distribution of internalized AgNPs to the liver has come from studies in which the deposition of intravenously injected $^{125}$iodine-labeled AgNPs was monitored by single-photon emission computerized tomography (SPECT) imaging in Balb/c mice and Fischer CDF rats [Chrastina and Schnitzer 2010]. The PVP-coated AgNPs were spherical and largely monodispersed, with an average diameter of 12 nm. In addition to the SPECT imaging, the major organs were excised from the animals at term and counted for radioactivity.

SPECT imaging gave a strong signal in the abdominal area that was thought to be associated with the liver and spleen. Less-intense signals were associated with the lung and bone. The level of activity in the blood after 24 hours was comparatively low, suggesting translocation from the blood via the mononuclear phagocyte system. Ashraf et al. [2015] also studied tissue distribution, using SPECT. A rabbit was administered dextran-coated AgNPs (15.7 nm median size) or uncoated AgNPs (53 nm median size) that had been labeled with technicium at a dose of ~200 μg/mL in a 1-mCi/mL solution. Following intravenous administration, the animal was monitored up to 30 minutes.

Similar to the findings of Chrastina and Schnitzer [2010], the greatest accumulation of silver was observed in the liver/spleen region and the rate of uptake was faster for the uncoated AgNPs. Silver was observed in the heart and lungs in the first 2 minutes and cleared rapidly. Silver was also observed in the stomach region but not in the thyroid (a location where free technicium may be found). Silver was monitored in kidney and bladder for clearance studies, which indicated that uncoated AgNPs were cleared faster.

With respect to accumulation in liver following intravenous administration, Su et al. [2014a] utilized a push-pull probe-based system in male Sprague-Dawley rats to study translocation of silver to extracellular space in the liver. In this study, the probe was placed surgically into the center of the left lateral lobe of the liver; 30 μg/kg of AgNPs (measuring 35 nm for primary particle size and ranging from 69 to 92 nm in agglomeration size) in vehicle (10% fetal bovine serum in DMEM) was administered intravenously. Accumulation in extracellular space was monitored every 10 minutes for 130 minutes. At the 180$^{th}$ minute, a second administration was given,

and animals were monitored similarly up to the 350th minute. Blood was collected at various time points, and five sections of liver were taken at the end of the study for measurement of silver content.

Silver content in the blood increased rapidly up to 10 minutes post-administration and then declined rapidly over the subsequent 15–40 minutes. After the first administration, silver in the extracellular space of the liver increased to maximum by 10 minutes. Following the second administration, nearly twice as much entered the extracellular space. The authors suggest that the first administration may have blocked the reticuloendothelial system to a degree, a mechanism for cellular uptake of silver, leading to a greater rate of accumulation of silver in the extracellular space following the second administration.

The studies by Chrastina and Schnitzer [2010], Afshar et al. [2015], and Su et al. [2014a] followed the acute kinetics of silver distribution, from minutes up to 1 day following exposure. In a study to assess the distribution and excretion of silver, Klaassen [1979] intravenously administered silver nitrate, a soluble form of silver, in the femoral vein of rats (0.01, 0.03, 0.1, or 0.3 mg/kg Ag/kg), rabbits (0.1 mg/kg Ag/kg), and dogs (0.1 mg/kg Ag/kg), up to 4 days post-exposure. Within 4 days post-administration of silver to rats dosed at 0.1 mg/kg Ag/kg, 70% of the silver was excreted in the feces and <1% in the urine. The disappearance of silver from the plasma and its excretion in the bile were measured for 2 hours after the intravenous administration of 0.01, 0.03, 0.1, and 0.3 mg/kg of silver to rats. The concentration of silver in the bile was 16–20 times higher than that in the plasma. For the two lower doses, the overall plasma-to-bile gradient was due almost equally to the plasma-to-bile gradient and the liver-to-bile gradient, whereas for the doses at the two higher concentrations of silver, the liver-to-bile gradient became more important. Marked species variation in the biliary excretion of silver was observed. Rabbits and dogs excreted silver at rates about 1/10 and 1/100, respectively, of that observed in the rat. Although it is difficult to determine the excretion rate of silver in the bile of humans, the results indicate that biliary excretion is an important route for the elimination of silver.

Lee et al. [2013c] also found the serum kinetics, tissue distribution, and excretion of citrate-coated AgNPs in rabbits to be similar to those of the soluble form examined by Klaassen [1979] following intravenous injection. Citrate-coated AgNPs (~7.9-nm diameter) were intravenously injected into the ear vein of four SPF New Zealand White male rabbits at doses of 0.5 mg/kg and 5 mg/kg, based on a dose selection following the OECD Test Guideline 417. Blood was sampled from the vein of the collateral ear before and after treatment, at 5, 10, and 30 minutes; at 1, 2, 6, and 12 hours; at the end of days 1 through 7; and at days 14, 21, and 28. Blood samples were also collected from the non-treated control group, at 1, 7, and 28 days.

The concentration of AgNPs in the serum was at its highest 5 minutes following treatment, and 90% of the AgNPs were eliminated from the serum at 28 days. Tissue distribution of AgNPs was determined in the liver, lung, kidney, brain, spleen, testis, and thymus, revealing that the liver, spleen, and kidney were the main target organs. This finding was consistent with findings in other studies [Lankveld et al. 2010; Loeschner et al. 2011; Park et al. 2011]. Although the accumulated level of silver in the 5-mg/kg dose group was higher than that in the 0.5-mg/kg dose group, tissue accumulations of AgNPs observed in the high-dose group were not always 10-fold higher than in the low-dose group.

The excretion of AgNPs through urine, in comparison with feces, was very low during the entire experimental period; more than 90% of AgNPs were still present in the body in the high-dose group at day 7, and 85% still remained in the low-dose group over the same period. Pigmentation in the liver was the main finding of histopathology at 7 and 28 days, whereas no pigmentation was observed in the non-treated control rabbits. Inflammatory cell infiltration was statistically significantly increased in the liver, lung, and kidneys of the AgNP-treated rabbits. However, there were no statistically significant histologic findings in the brain and thymus.

The distribution and biokinetics of AgNPs were also evaluated by Xue et al. [2012], following intravenous administration of AgNPs in the tail vein

of ICR mice. Mice (three exposure groups and a control group, with six male and female mice per group) were exposed to doses of AgNPs at 7.5, 30, or 120 mg/kg. Average primary particle size of purchased AgNPs, as determined by TEM, was 21.8 nm (10–30 nm), but agglomeration of particles (up to 117-nm diameter) was observed to occur at the time of intravenous administration. Toxic effects were assessed via general behavior, serum biochemical parameters, and histopathologic observation of the mice. Biokinetics and tissue distribution of AgNPs were evaluated at a dose of 120 mg/kg. Silver analysis with ICP-MS was used to quantify silver concentrations in blood and tissue samples at predetermined time intervals.

After 2 weeks, AgNPs exerted no obvious acute toxicity in the mice; however, inflammatory reactions in lung and liver cells were induced in mice treated at the 120-mg/kg dose level. The distribution of silver was observed in all major organs, with the highest levels found in the spleen and liver, followed by the lungs and kidneys. Silver was retained in the spleen for the entire experiment, whereas the 120-μg/g silver concentration found in the liver slowly decreased over 14 days. In the lungs, silver concentrations decreased from days 1 through 7 but increased slightly from days 7 through 14. The elimination half-lives and clearance rates of AgNPs were, respectively, 15.6 hours and 1.0 ml/hr for male mice and 29.9 hours and 0.8 ml/hr for female mice. A sex-related difference in the biokinetic profiles of blood, as well as the distribution of silver to the lungs and kidneys, was observed, with statistically significantly higher levels of silver found in the female mice than in male mice at 14 days post-injection. This sex difference in organ-specific silver concentration is consistent with findings reported by Kim et al. [2008] and Sung et al. [2008] in rats exposed to AgNPs. Mild histopathologic changes were also found in the lungs and liver of mice in the 120-mg/kg exposure group [Xue et al. 2012]. These findings are similar to those previously reported by Kim et al. [2008], in which liver damage was found in Sprague-Dawley rats exposed by oral administration to 300 mg AgNPs.

Dziendzikowska et al. [2012] evaluated the time-dependent biodistribution and excretion of AgNPs of two different sizes by administering intravenously 20- and 200-nm AgNPs to male Wistar rats at a dose of 5 mg/kg bw (2 exposure and 1 control group of 23 rats each). The study was designed to (1) analyze the effect of AgNP size on rat tissue distribution at different time points, (2) determine the accumulation of AgNPs in target organs, (3) analyze the intracellular distribution of AgNPs, and (4) examine the excretion of AgNPs by urine and feces. Biologic material was collected at 24 hours and at 7 and 28 days after injection and analyzed by ICP-MS and TEM.

AgNPs were found to translocate from the blood to the main organs (lungs, liver, spleen, kidneys, and brain), and the highest concentration of silver was in rats treated with 20-nm AgNPs, in comparison with 200-nm AgNPs. The highest concentration of silver was found in the liver after 24 hours, indicating that the liver may be the first line of defense as a consequence of intravenous administration and/or because of the activation of metallothioneins, involved in detoxication of heavy metals such as silver [Wijnhoven et al. 2009]. In addition, the high silver deposition in the liver (8 μg/g wet weight) may have been associated with effective filtration and the presence of specific subpopulations of mononuclear phagocytic cells that can be involved in the sequestration of nanoscale particles.

The concentration of silver in the liver decreased over time and reached the lowest concentration at 28 days post-administration. These findings possibly indicate a purification of the liver and redistribution of AgNPs to other organs or its excretion from the body in bile [Kim et al. 2010a; Park et al. 2011a]. Silver concentrations found in the lungs (that is, accumulated in alveolar macrophages) were similar to those observed in the spleen after 7 days, and the concentration of silver in the kidneys and brain increased with time and peaked at 28 days. Despite the high concentration of silver in the kidneys, the rate of silver excretion in the urine was low, which might be explained by the lack of renal glomerular filtration and tubular excretion of

the kidneys. In addition, the smaller size of AgNPs (20-nm particles) had the highest rate of accumulation in various organs.

These findings are consistent with those of Lankveld et al. [2010], who showed a higher level of small (20-nm) AgNPs in the liver and a lower level in the kidneys, brain, and heart, whereas large AgNPs (80 and 100 nm) were concentrated mainly in the spleen and (in smaller amounts) in the liver and lungs. Repeated administration of AgNPs resulted in accumulation of silver in the liver, lung, and spleen, indicating a possible mechanism responsible for the distribution of different-sized nanoscale particles. These findings were consistent with those suggested by Li and Huang [2008], who found that particles smaller than the pores of liver fenestrae (about 100 nm) are captured more efficiently by the liver, whereas larger particles are absorbed with greater affinity in the spleen.

In addition to size, other physical-chemical properties, including dissolution rate and surface coatings, have been implicated in toxicological effects of AgNPs. Recordati et al. [2016] investigated both size and coating of AgNPs in comparison to a soluble form of silver, silver acetate. Male CD-(ICR) mice (n = 3/group) were injected via the tail vein one time with a dose of 10 mg/kg of PVP- or citrate-coated AgNPs at sizes of 10, 40, or 100 nm, or 15.5 mg/kg silver acetate, equal to 10 mg/kg silver. Blood, liver, kidney, spleen, brain, and lung were collected for distribution analysis, as well as histopathological analysis.

Irrespective of particle coating, the 10-nm particles had the greatest total tissue accumulation, a finding in agreement with Dziendzikowska et al. [2012]. All particles had the highest accumulation in liver and spleen but were also measurable in lung and kidney, except for the 10-nm particle, which also had a high degree of accumulation in lung. Silver acetate accumulated to the highest degree in liver and to a lesser degree in kidney and spleen, where accumulation was comparable. In the kidney, silver acetate had the highest levels with respect to all treatments. The authors suggest a difference in target organs for soluble versus particle, with kidney being a greater target for soluble silver, and liver and spleen for particulate silver; however, soluble silver accumulated to the highest degree in the liver, and only one time point post-exposure was examined.

Target organ toxicity may be highly dependent on the kinetic differences in clearance rate of the two forms of silver. In addition to tissue distribution, the authors investigated cellular localization of silver tissues, using autometallography. In the spleen, silver was found in the cytoplasm of macrophages in white and red pulp, as well as endothelial cells. In the liver, silver was found primarily in Kupffer cells along sinusoids, and occasionally in endothelial cells associated with sinusoids and portal endothelial cells. A size difference was noted, with the larger particles localizing primarily to the Kupffer cells and the smaller particles in both Kupffer and endothelial cells. The smallest particle was associated with uptake in gall bladder epithelial and endothelial cells as well. Silver was also detected in localized areas in kidney and lung following particle exposure, but not in brain.

Toxicity was also evaluated in this study. A single 10-mg/ kg intravascular injection of 10-nm citrate- or PVP-coated AgNPs caused overt hepatotoxicity characterized by gall bladder hemorrhage, periportal hemorrhage, midzonal hepatic necrosis, portal vasculitis, and thrombosis. The same mass dose (10 mg/kg) of 40-nm nanoparticles caused similar gall bladder changes in one mouse, which also had hepatocellular necrosis, whereas in the remaining five mice in that exposure group, liver changes were restricted to the gall bladder and were milder. Mice injected with 100-nm particles had only mild and occasional gall bladder edema or hyperemia, whereas mice receiving an equivalent silver ion exposure by silver acetate injection had kidney and not hepatobiliary changes, despite having the highest degree of silver accumulation in the liver for soluble silver. This corroborates the authors' hypothesis that kidney is the primary target for soluble versus particulate silver at this time point post-exposure. In this study, size appeared to be a more critical factor than the coatings of the materials for both distribution and toxicity, and differences were solubility-dependent as well.

To better understand kinetics-related dissolution and distribution or redistribution of AgNPs, Su et al. [2014b] employed a knotted reactor-based differentiation scheme to monitor the ratio of ion to particle in tissues following intravenous administration of AgNP. In this study, male Sprague-Dawley rats were administered 125 μg/50 μl vehicle (10% fetal bovine serum in DMEM) of AgNPs (35 nm primary particle size; 69 nm particle size agglomerated in vehicle), ~ 500 μg/kg body weight AgNPs, or vehicle. Blood, liver, spleen, kidneys, lungs, and brains were collected at 1, 3, and 5 days post-exposure. Samples were processed for determination of the ion and particle fractions and silver was quantified by ICP-MS.

Total silver was highest in the liver and spleen at all times. The ion-to-particle ratio was 100% for kidney, lung, brain, and blood. The ratio was <20% for liver, and it gradually decreased in spleen over time. This indicated that the silver was primarily in particle form in the liver and was in soluble form in the other tissues, suggesting AgNP degradation and redistribution. Histopathology was also performed on the tissues. The only organ with positive pathological findings was the liver, whereby inflammation and necrosis were noted at days 3 and 5 post-exposure. The study demonstrates the kinetics of dissolution and the potential role of the particle in liver effects.

Pang et al. [2016] examined effects of various surface coatings of AgNPs on biodistribution and pharmacokinetics in male Balb/c mice. The particles used in this study had a similar primary particle size of ~30 nm and were coated with one of the following compounds: citrate (negative charge), polyethylene glycol (PEG; negative charge), PVP (negative charge), or branched polyethylenimine (BPEI; positive charge). Silver nitrate was also tested as reference material for ionic silver. In solution, the hydrodynamic diameters of PVP and citrate AgNP were ~36 nm, PEG was ~55 nm, and BPEI was ~63 nm. BPEI had the lowest particle concentration per ml (~3 times lower than all other particles) and the highest Ag concentration per ml (~2 times higher than all other particles). Particles and silver nitrate were administered intravenously with 5 animals per group. Tissue burden was measured as μg/g tissues as well as total silver per tissue by ICP-MS at 24 hours post-exposure in liver, spleen, lung, kidneys, intestines, and brain. Blood concentration was measured at 2, 10, 30, and 60 minutes post-exposure and at 6, 12, 24, and 72 hours post-exposure.

Ionic silver accumulated in liver to the greatest degree, followed by lower levels in all other organs. All particles had the greatest accumulation in liver and spleen, findings similar to those of Chen et al. [2016] (discussed below) and Xue et al. [2012]. PVP and citrate AgNPs followed similar distribution patterns, with liver > spleen > lung = intestines > kidney = brain, a finding similar to that of Recordati et al. [2016]. PEG AgNPs had the highest burden of all particles in the spleen, followed by BPEI AgNPs, whereas BPEI had the greatest deposition in lung compared to all other particles. PEG AgNPs were distributed as follows: liver ≥ spleen > intestines ≥ lungs ≥ kidney = brain. BPEI were distributed as follows: liver ≥ spleen ≥ lung > kidney = intestines = brain.

In terms of total body silver burden as a sum of the data per tissue measured, PEG AgNPs were greatest, followed by BPEI AgNP. Ionic silver was lowest across tissues. This could be due to a faster clearance rate of the soluble form of the material or a greater accumulation in other organs not measured. Blood kinetic studies showed that PEG AgNPs remained in the circulation the longest in the first 60 minutes and had a longer elimination half-life than all other particles. PEG AgNPs also had the lowest affinity for bovine serum albumin in an acellular test, indicating resistance to opsonization by protein in the blood. The authors suggest that a lower degree of protein-binding affinity may lead to slower uptake into tissues.

In the same study, authors examined toxicity of the particles and silver nitrate in a hepatoma cell line (Hepa1c1c7). A dose-response study was conducted to determine viability/cytotoxicity as EC50. BPEI had the lowest EC50 (10.38 μg/mL), followed closely by ionic silver, citrate AgNPs, and PVP AgNPs (12.39–14.28 μg/mL). PEG was the least toxic, with an EC50 of 63.14 μg/mL. This finding correlated with particle uptake in cells, whereby PEG AgNPs had the lowest

levels of uptake in 24 hours. These findings correspond well with the biodistribution and elimination half-life data from the in vivo studies.

Taken together, the data suggested that the BPEI AgNP may be slightly more cytotoxic due to surface charge or chemistry, whereas PEG AgNPs, the more neutral of the negatively charged particles, was less toxic, had lower binding affinity for protein, and persisted to the greatest degree in vivo. The authors note that the study does not account for effects of coating on dissolution rate of particles, which may also affect the toxicity, kinetics, and distribution.

Additional studies that examine toxicity in conjunction with pharmacokinetics are discussed along with toxicological studies in section E.3.3.3.

### *E.3.3.3 Toxicological effects following intravenous or intraperitoneal injection*

Kim et al. [2009b] administered AgNPs intravenously to Sprague-Dawley rats (two per sex per group) to correlate clinical chemistry, histopathologic, and toxicogenomic responses, with the aim of identifying biomarkers for AgNP exposure. Animals were exposed to an unstated number of injections of AgNP preparations over a 4-week period. Exposure groups included a nonexposed control group, group I (receiving 100 mg/kg silver in 50 to 90-nm particles), and group II (receiving 1 mg/kg silver in 1- to 10-nm particles). The AgNPs were dispersed in an aqueous medium containing amino acids. The only clinical chemistry changes observed were statistically significant increases in serum cholesterol concentrations in the two exposed groups and reductions in serum creatinine levels that also achieved statistical significance. Histopathologic examination of major tissues and organs showed silver particle deposition in the hepatic sinusoids and Kupffer cells. These effects were associated with moderate lymphocyte aggregation, destruction of hepatocytes, and lymphocytic infiltration of the hepatic perivenular area. Though not necessarily associated with histopathologic disorders, other sites of silver deposition were the lung alveolar septum, kidney glomerulus, and spleen white pulp. The most striking hematologic finding was a marked increase in the lymphocyte/granulocyte ratio in the AgNP exposure groups, compared to controls.

Kim et al. [2009b] also observed alterations in gene expression in rats exposed to AgNPs when total RNA was extracted from the livers of control and exposed groups and used as a basis for microarray analysis. Using a threshold of 1.2 to assign genes into upregulated or downregulated categories, the researchers sorted 191 and 187 genes into these respective categories when the findings for groups I and II were considered together. Twenty genes were found to be commonly expressed in groups I and II, four of which (SLC7A13 [solute carrier family 7, member 13], PVR [poliovirus receptor], TBXAS1 [thromboxane A synthetase 1], and CKAP4 [cytoskeleton-associated protein 4]) were proposed as size-independent genomic biomarkers. Ten other genes were proposed as sentinels for the AgNP-induced histopathologic and clinical chemistry changes.

The same researchers also injected two male Sprague-Dawley rats per group with 50-nm AgNPs at doses of 0 (control), 1, or 100 mg/kg at 2- to 3-day intervals over a 4-week period, prior to performing a proteomic analysis of liver, lung, and kidney tissues [Kim et al. 2010b]. Protein extracts from liver, lung, and kidney were separated by means of two-dimensional gel electrophoresis. Protein spots selected as differentially expressed were cut from the gels, digested, and then identified with matrix-assisted laser desorption/ionization time-of-flight mass spectrometry (MALDI-TOF MS) and peptide mass fingerprinting. Functional analysis of the differentially expressed proteins, as related to exposure to AgNPs, demonstrated outcomes such as apoptosis, generation of ROS, thrombus formation, and inflammation. Differentially expressed proteins in the kidney also appeared to be associated with indicators of metabolic disorders such as diabetes.

Katsnelson et al. [2013] conducted a subacute intraperitoneal exposure study in outbred female white rats, using 50-nm AgNPs, similar in size to those used by Kim et al. [2009; 2010b]. The study was conducted in comparison with similar-sized

gold NPs (AuNPs). Rats were injected three times per week up to 20 injections (~3 weeks). Following exposure, the following were completed: blood hematology and biochemistry, urine analysis, CNS functional and behavioral tests (withdrawal reflex test and head dips into hole-boards for behavioral testing), genotoxicity tests in multiple organ tissues, histopathology, and metal content determinations (liver, kidney, and spleen). In a separate study, effects of administration of a bioprotective complex (mixture of dietary supplements and vitamins high in anti-oxidants and free radical scavengers as well as metals that act antagonistically to silver) given orally with AgNP exposure were measured.

Both nanoparticles caused decreased red blood cells, succinate dehydrogenase activity in blood lymphocytes, and ceruloplasmin levels in serum, the latter to a greater degree in AgNP-exposed rats. AuNPs additionally caused an increase in blood monocytes, a decrease in hemoglobin, and a decrease in kidney mass. A similar trend was present for AgNPs, although it was not statistically significant. Both nanoparticles were detected in liver, kidney, and spleen. AuNPs deposited to a greater extent in liver compared to AgNPs, and AgNPs deposited to a greater extent in kidney compared to AuNPs. Both particles increased the number of binucleate hepatocytes in liver (AuNPs > AgNPs) and Kupffer cells (AuNPs = AgNPs). A trend for an increase in particle load in Kupffer cells was present following AgNP exposure. Both particles caused equivalent decreased levels of white to red pulp ratio in spleen and caused increased thickness to the glomerular basal membrane in kidneys.

Overall, genotoxicity measured by the rapid amplification of polymorphic DNA (RAPD) test was greater for AgNP-exposed animals than AuNP-exposed animals, with both inducing genotoxicity. Increases were greatest in liver and spleen, followed by bone, kidney, and blood cells. Administration of the bioprotective complex attenuated the toxicity to a degree, possibly because of increased anti-oxidant activity. The authors concluded that the primary difference in particles occurred in tissue distribution and genotoxicity, with AgNPs causing a slightly greater toxicity than AuNPs.

Increased oxidative and endoplasmic reticular stress have been implicated as mechanisms of toxicity following oral exposures to AgNPs (Elle et al. 2013; Hadrup et al. 2012a; Kovvuru et al. 2015; Shrivastava et al. 2016; Yu et al. 2014) and pulmonary exposure to AgNPs (Aria et al. 2015; Genter et al. 2012; Huo et al. 2015; Kaewamatawong et al. 2014; Liu et al. 2012; Liu et al. 2013a; Seiffert et al. 2016; Smulders et al. 2015a). Evidence of this mechanism of action is present in intravenous exposure studies also (Chen et al. 2015; Tiwari et al. 2011). Tiwari et al. [2011] reported an increase in ROS levels when Wistar rats were injected intravenously through the tail vein at doses of 4, 10, 20, and 40 mg/kg AgNPs (15–40 nm in diameter) at 5-day intervals over 32 days.

Histopathologic examination revealed statistically significant changes ($p < 0.01$) in hematologic parameters (WBCs, platelets, hemoglobin, and RBCs) in the 20- and 40-mg/kg groups. In the 40-mg/kg group, statistically significant increases were also found in the liver function enzymes alanine aminotransferase (ALT), aspartate aminotransferase (AST), AP, gamma glutamyl transpeptidase, and bilirubin. AgNP deposition was reported to be found primarily in the liver and kidney of rats exposed at doses of 20 and 40 mg/kg. ROS was found to increase in all groups in a dose-related manner. The investigators suggested that the deposited AgNPs are endocytosed and interact with mitochondria to produce ROS. These increased levels of ROS (AgNP in doses >20 mg/kg) enhance $H_2O_2$ levels, which can cause damage in the DNA strand, chromosome aberration, and conformational changes in proteins. AgNP doses <10 mg/kg were considered to be safe for biomedical application.

Chen et al. [2016] evaluated biodistribution, endoplasmic reticulum stress, and oxidative stress following intravenous exposure to AgNPs. AgNPs (NM-300K) had a primary particle size of 20 nm and a hydrodynamic diameter of ~38 nm in dispersant, consisting of 4% Tween-20 and 4% polyoxyethylene (NM-300K-DIS). Balb/c mice were administered 0, 0.2, 2.0, or 5.0 mg/kg by the tail vein 1 time and were euthanized 8 hours after exposure. Tissue burden was measured by ICP-MS and was determined, by

concentrations of deposits from highest to lowest, as spleen > liver > lung >> kidneys > heart > brain. IL-6 was found to be increased in serum only at the highest dose; however, there were no statistically significant differences in serum TNF-α.

Protein analysis by western blot for markers of endoplasmic reticulum stress and oxidative stress were measured in spleen and liver, and most were statistically significantly elevated in a dose-dependent manner in both tissues when compared to control. Gene expression of endoplasmic reticulum stress markers *xbp-1s* and *chop* was elevated in liver at the high dose but not in spleen or other organs. Gene expression of *sod-1* and *ho-1* was also elevated in liver, indicating a greater degree of stress in this tissue. Kidney gene expression of *ho-1* was also elevated at the high dose.

No histopathologic changes were observed in brain, heart, spleen, or kidneys. Lungs showed thickened alveolar walls and inflammation. Liver tissue showed necrosis in hepatic lobules, disorganized hepatic cords, and edema. The high dose of AgNPs caused increased levels of apoptosis (DNA damage assessed by TUNNEL assay) in lung, liver, spleen, and kidneys but not in heart or brain. In this study, toxicity appeared to be associated with target organs, mainly liver and spleen, followed by lung and kidney, and primarily occurred at the highest dose administered.

Lee et al. [2013b] intraperitoneally injected Sprague-Dawley rats (300–350 g/bw) with AgNPs (10–30 nm in diameter) at concentrations of 500 mg/kg to test the hypothesis that autophagy plays a role in mediating hepatotoxicity in animals. Autophagy is a homeostatic mechanism promoting cell survival by facilitating the removal of malformed or injured proteins or organelles [Lee et al. 2013c]. This study focused on the interrelationships between energy metabolism, autophagy, apoptosis, and hepatic dysfunction. All animals were killed on days 1, 4, 7, 10, or 30 post-exposure, and the concentration of silver in the liver was found to be 58–81 μg/g. Uptake of AgNPs was observed to be rapid but not proportional to the blood Ag concentration. Declination of ATP (-64% in day 1) and autophagy (determined by LC3-II protein expression and morphologic evaluation) increased and peaked on the first day. ATP content remained at a low level even though the autophagy had been activated. Apoptosis began to rise sigmoidally at days 1 and 4, peaked at day 7, and remained constant during days 7–30 post-exposure. Meanwhile, autophagy exhibited a gradual decrease from days 1 to 10, and the decrease at day 30 in comparison with the control group was statistically significant. The decline in autophagy, along with a high concentration of silver in the liver, was interpreted by the authors as causing insufficient self-protection, which contributed to the observed hepatotoxicity. An inflammatory response in the liver was observed by histopathologic evaluation on day 10 and was seen to progress to an advanced degree on day 30, when liver function was impaired.

Hepatotoxicity was also observed in a study by Wang et al. [2013]. To assess biodistribution and target organ toxicity, female Balb/c mice (5-10 per group) were exposed to 25-nm PVP-coated AgNPs at a dose of 0, 22, or 108 μg/kg, or silver nitrate at a dose of 108 μg/kg intravenously or intraperitoneally, every 2 days for weeks. Tissue distribution and histopathology were evaluated at 2 weeks after the last exposure. Following intraperitoneal exposure, silver, detected by ICP-MS, accumulated in a dose-dependent manner to the greatest degree in terms of ng/g tissue in liver and spleen, and to a greater degree for the high dose of particle versus ion, indicating ionic silver was cleared more rapidly. Silver could also be detected at much lower levels in kidney, heart, and spleen. Silver content in tissue was approximately 100-fold greater following intraperitoneal exposure versus intravenous exposure. At 2 weeks post-exposure, silver was detected in spleen > liver = kidney only for the high dose of AgNPs.

Because of particle persistence, histopathology was performed on liver, kidney, and spleen from the intraperitoneally exposed mice. Only liver showed pathological changes, including disorganized hepatic cords and enlarged central veins; this was more marked with the high-dose AgNP versus ionic silver exposure. No pathology was observed in kidney or spleen, and no hematological changes

were observed. The data again suggest that liver is a target organ following exposure.

As part of the same study, an additional experiment using similar exposure durations was performed to determine pharmacokinetics across time following exposure. For the pharmacokinetic study, female mice were exposed only intravenously, with the same regimen as described for the previous study, at a dose of 1.3 mg/kg per dose (n = 3 per group). Liver, spleen, kidney, heart, lung, and serum were collected at 15, 39, and 78 days following the last exposure. The highest tissue burden of silver on day 15 was in liver, kidney, and spleen; silver content was less in lung and heart. Burden decreased over time but was still measurable in liver, spleen, and kidney at day 78.

In the same study, Wang et al. [2013] also examined transport across the blood-testis barrier, as well as transport across placenta and effects on fetal liver. In the placental transport study, male and female mice were exposed by intraperitoneal injection to 0, 22, or 108 μg/kg or 108 μg/kg of silver nitrate, with the same exposure paradigm discussed above. After the 4 weeks of exposure, mice were mated. Placenta, fetal liver, and remaining fetus without liver were collected on gestational day 14.5 (n = 3–5/group) and silver content was evaluated. Silver was detected in placenta, fetus without liver, and fetal liver for all groups. Silver in the placenta was highest for the high dose of AgNPs, whereas in the fetus without liver and fetal liver, silver was highest with the low dose of AgNPs.

The authors suggest this may be due to higher agglomeration in the high dose, resulting in a decreased ability to cross placenta because of agglomerate size. Soluble silver content was comparable to the low-dose AgNPs in placenta and the high-dose AgNPs in fetus and fetal liver, and this may be attributable to faster clearance for the males and females during exposure and prior to mating. To assess transport across the blood-testes barrier, male mice were exposed to 1.3 mg/kg intravenously, according to the same regimen described above. Silver burden was measured in liver, spleen, kidney, heart, lung, muscle, testis, and serum 4 months after the last exposure. Silver content was greatest and comparable in terms of ng/g tissue in liver, spleen, and testis. Silver was also detected in kidney, heart, lung, and muscle but not serum. These studies, taken together, indicate kidney and spleen as target organs, but particularly liver, and indicate that AgNP exposure can lead to silver crossing biological barriers such as placenta and blood-testis barriers.

A number of other studies have examined effects on the reproductive system of males [Gromadzka-Ostrowska et al. 2012] and effects during pregnancy in females [Austin et al. 2012; Fennell et al. 2106; Mahabady 2012]. A study by Fennell et al. [2016] was discussed in a previous section. In this study, the investigators intravenously injected 1 mg/kg of 20-nm or 110-nm PVP-coated AgNPs, silver acetate, or vehicle control on gestation day 18 into pregnant Sprague-Dawley rats. At 1 and 2 days post-exposure, silver content was measured in tissues (blood, brain, heart, liver, kidneys, spleen, lung, gastrointestinal tract, skin, bone, carcass, fetus, and placenta). Urine and feces were collected to measure excreted silver. Cardiovascular markers of injury were measured in plasma, and metabolites and 8-OH-dG (oxidative stress marker) were measured in urine.

The percentages of administered silver recovered were 56.7%, 22.6%, and 32.9% for silver acetate, 20-nm particles, and 110-nm particles, respectively. At 24 and 48 hours, the highest tissue concentration of silver was measured in the spleens for both sizes of particles. At 24 hours for the soluble silver, the highest tissue level was also in the spleen, and at 48 hours the highest level was detected in the lungs. In general, silver was detected in most tissues measured, including kidney and liver. Silver was detected in the placenta and fetus irrespective of the form or size of silver and was measured to a greater degree in the placenta than the fetus. There were no differences in plasma biomarkers or urinary 8-OH-dG. Urinary metabolic analysis indicated possible changes in carbohydrate and amino acid metabolism.

Austin et al. [2012] intravenously injected pregnant CD-1 mice with AgNPs (average diameter, 50 nm; range, 30–60 nm) on gestation days (GDs) 7, 8, and 9 at dose levels of 0 (citrate buffer), 35,

or 66 μg Ag/mouse (group sizes of 6–12) to evaluate the distribution of AgNPs in pregnant mice and their developing embryos. Additional groups of mice were treated with silver nitrate (dissolved in 0.25 M mannitol) at dose levels of 9 and 90 μg Ag/mouse. Group sizes were nine and three mice for the 9- and 90-μg dose levels, respectively. Mice were euthanized on GD 10, and tissue samples were collected and analyzed for silver content. A statistically significant increase ($p < 0.05$) in AgNP content, as compared to that in silver nitrate–treated animals, was observed in nearly all tissues. AgNP accumulation was higher in liver, spleen, lung, tail (injection site), visceral yolk sac, and endometrium; the highest levels of silver were found in the liver, spleen, and visceral yolk sac. Concentrations of silver in embryos were about 25-fold less than those seen in the placenta or visceral yolk sac, suggesting that AgNPs become sequestered in visceral yolk sac vesicles and do not reach the fetal circulation in statistically significant amounts; no adverse morphologic effects on the developing embryos were observed. Austin et al. [2012] proposed that pinocytosis might be responsible for AgNP uptake by the visceral yolk sac.

The teratogenicity potential of AgNPs in pregnant 3- to 4-month-old Wistar rats was investigated by Mahabady [2012]. Pregnant rats ($n = 30$) were randomly divided into five groups (24 pregnant rats in treatment group and six pregnant rats in saline control group). Two subgroups of six rats in one treatment group were given either 0.4 or 0.8 mg/kg nanosilver intraperitoneally on GD 8. The same doses of nanosilver were also administered to a second treatment group (two groups of six rats) on GD 9. All animals were killed on GD 20; the uterus was exteriorized and the number and location of fetuses and resorptions were noted. The mean of weight, volume, and width of fetuses' placenta decreased statistically significantly ($p < 0.05$) in both treatment groups in comparison with the saline control group; no observed skeletal abnormalities were observed in the fetuses. No information was provided on the size of the AgNPs or whether the AgNPs were coated.

Gromadzka-Ostrowska et al. [2012] described the results of a study in which male Wistar rats (four groups, 24/group) were intravenously injected (tail vein) with AgNPs to assess the effects on spermatogenesis and seminiferous tubule morphology. The described experimental study featured changes to the applied concentration and dimensions of the AgNPs. Thus, animals received either 5 or 10 mg/kg AgNPs that were roughly 20 nm in diameter, 5 mg/kg of AgNPs that measured 200 nm, or 0.9% NaCl for the control group. Rats were killed at 24 hours, 7 days, or 4 weeks after treatment. Additionally, sperm counts were taken and germ cells assessed for DNA damage by means of the comet assay.

Silver nanoparticles at different doses and particle sizes appeared to be associated with increased comet tail moments after different durations. The frequency of abnormal spermatozoa in epididymal semen from experimental groups was not statistically significantly different, as compared with the NaCl group at the given time points. However, in all treated groups, the number of abnormal spermatozoa found 1 or 4 weeks after treatment was higher ($p < 0.05$). The comet assay showed that DNA damage (% DNA in tail) in the germ cells was statistically significantly increased at 24 hours in the 5- and 10-mg/kg (20-nm Ag) groups ($p \leq 0.05$) but declined with time post-exposure. No difference in the DNA damage level was found between the control group and the 5-mg/kg group (200-nm Ag) at all post-exposure time points. The results were interpreted "as suggestive" that AgNP genotoxicity was more pronounced in mature sperm cells in the epididymis than in spermatozoa in seminiferous epithelium. Histologic examination of the testes showed change in the testes seminiferous tubule morphometry in the rats treated with 200-nm AgNPs.

In addition to examination of reproductive effects, studies have also focused on neurological effects [Liu et al. 2013b; Sharma et al. 2010]. A series of experiments by Sharma et al. [2010] in Sprague-Dawley rats examined the capacity of aqueous dispersions of manufactured AgNPs (50–60 nm in diameter) to disrupt the blood-brain barrier. Silver nanoparticles were administered intravenously (30

mg/kg), intraperitoneally (50 mg/kg), or as a cortical superfusion (20 μg/10 μL) in a 0.7% sodium chloride solution containing 0.05% Tween 80. The authors measured the permeability of the blood-brain barrier to a sterile solution of Evans blue albumin or a $^{131}$iodine tracer given intravenously and assessed the potential for edema formation in the brain by measuring tissue water content.

AgNPs altered the blood-brain barrier to Evans blue albumin and radioiodine when administered intravenously or as a cortical superfusion but not by intraperitoneal administration. The leakage of Evans blue albumin was evident on the ventral surface of the brain and in the proximal frontal cortex. Cortical superfusion with nanoparticles gave moderate opening of the blood-brain barrier to protein tracers, with leakage of Evans blue albumin as well. A statistically significant increase in brain water content was seen after administration of AgNPs intravenously or by cortical superfusion. As before, intraperitoneal administration was ineffective.

In discussing their results, Sharma et al. [2010] stated that the increase in brain water content in areas where leakage of Evans blue albumin was observed was consistent with the capacity of systemically applied AgNPs to bring about edema formation and subsequent brain damage. A possible result of these changes could be AgNP-induced brain dysfunction, thereby raising the possibility of an association between acute exposure to AgNPs and neurodegenerative changes.

Although the intraperitoneal injection of AgNPs was ineffective in bringing about changes to the blood-brain barrier in Sprague-Dawley rats [Sharma et al. 2010], a study by Rahman et al. [2009] showed this route of application to be useful in bringing about changes in gene expression to regions of the brain in male C57BL/6N mice. They were intraperitoneally injected with 100, 500, or 1,000 mg/kg of 25-nm-diameter AgNPs and then killed after 24 hours. Total RNA was extracted from the caudate nucleus, frontal cortex, and hippocampus and analyzed by means of RT-PCR. Differential alterations in gene expression implicated AgNP-induced changes in apoptosis and free-radical-induced oxidative stress.

Liu et al. [2013b] reported that AgNPs do not affect spatial cognition or hippocampal neurogenesis in adult male ICR mice ($n$ = 15 per dose, $n$ = 10 for control). Mice were administered, via intraperitoneal injection, uncoated AgNPs with an average diameter of 36.3 nm at doses of 0 (control), 25, or 50 mg/kg, once a day in the morning for 7 consecutive days. Another group of mice received scopolamine (3 mg/kg) as a positive control for the behavioral studies. Spatial learning and memory ability were assessed with the Morris water maze test; after the behavioral test, mice were injected with bromodeoxyuridine and killed on days 1 and 28 post-exposure, and the brains were evaluated for proliferating cells. The test results showed that AgNP exposure did not alter either reference memory or working memory in the mice, in comparison with those in the non-exposed control group. Also, in the AgNP-treatment groups, no differences were revealed in hippocampal progenitor proliferation or in the survival and differentiation of newly generated cells.

**Table E-6. Summary of in vivo toxicological studies of silver nanoparticles (AgNPs) and nanowires (AgNWs)**

| Species | Particle Characteristics | Exposure Details: Concentration/ Dose | Exposure Details: Duration | Critical Effect(s) | NOAEL/ LOAEL | Comments | Reference |
|---|---|---|---|---|---|---|---|
| **Inhalation Exposure—Acute or Subacute** | | | | | | | |
| Sprague-Dawley rats; 5 of each sex per group | Mostly spherical, 15–20 nm in diameter | 0, 76, 135, or 750 μg/m$^3$ | Single 4-hr exposure | Clinical signs and lung function parameters | –/– | No adverse effects observed | Sung et al. [2011] |
| Sprague-Dawley rats; 10 of each sex per group | Mostly spherical, diameter range 2–65 nm (median, 16 nm) | 0, 0.48, 3.48, or 61 μg/m$^3$ | 6 hr/day, 5 days/ week for 4 weeks | Slight cytoplasmic vacuolization of the liver | 0.48/3.48 μg/ m$^3$ | Dose-response effect in females only | Ji et al. [2007b] |
| Sprague-Dawley rats; 10 of each sex per group | Mostly spherical, diameter range 2–65 nm (median, 16 nm) | 0, 0.48, 3.48, or 61 μg/m$^3$ | 6 hr/day, 5 days/ week for 4 weeks | Increase in number and size of the neutral mucin-producing goblet cells | 0.48/3.48 μg/ m$^3$ | | Hyun et al. [2008] |
| C57Bl/6 mice; 3×26 test animals, 13 controls | Spherical PVP-coated particles, >85% approx. 5 nm in diameter, but with 79-nm (GM) aggregates | 0, 3,300 μg/m$^3$ | 4 hr/day, 5 days/ week for 2 weeks | Minimal pulmonary inflammation | 3,300 μg/m$^3$ | Single concentration tested | Stebounova et al. [2011] |
| Sprague-Dawley male rats; 12 exposed and 12 controls | Two types of mostly spherical Ag [75% colloidal and 25% silver ions with 33-nm CMAD; and 100% colloidal with 39-nm CMAD] | 0, 100 μg/m$^3$ (1.4 μg Ag/rat lung) or 1000 μg/m$^3$ (14 μg Ag/rat lung) | Single 5-hr exposure; evaluated 1 and 7 days post-exposure | No acute toxicity in pulmonary or cardiovascular parameters | -/- | No adverse effects observed | Roberts et al. [2013] |

(Continued)

**Table E-6. Summary of in vivo toxicological studies of silver nanoparticles (AgNPs) and nanowires (AgNWs) (Continued)**

| Species | Particle Characteristics | Exposure Details: Concentration/ Dose | Exposure Details: Duration | Critical Effect(s) | NOAEL/ LOAEL | Comments | Reference |
|---|---|---|---|---|---|---|---|
| C57BL/6 male mice (2 groups of 7) | AgNPs geometric mean diameter, 22.18 ± 1.72 nm | AgNPs ($1.91 \times 10^7$ particles/$cm^3$) | 6 hr/day, 5 days/week for 2 weeks; one of the groups was observed for 2 weeks of recovery before necropsy | RNA analysis of cerebrum and cerebellum showed several genes associated with motor neuron disorders, neurodegenerative disease, etc.; genes from whole blood modulated in parallel to those in the brain | NA | Investigators believe that these genes could serve as biomarkers for AgNP exposure | Lee et al. [2010] |
| Fischer rats (F344/DuCrl); 12 males in each of 3 groups | 15-nm and 410-nm (200-nm primary particles) | (1) 15-nm group: mass, 179 μg/$m^3$; particle number, $3.8 \times 10^6$. (2) 410-nm group: mass, 167 μg/$m^3$; particle number, $2.0 \times 10^4$. (3) Air-only group (control, 0 μg/$m^3$) | Nose only, 6 hr per day, followed by 4 consecutive days to air only; 6 rats from each group killed 24 h after 4 days' exposure to air; remaining 6 rats killed 7 days after air exposure | No lung lesions observed; acute pulmonary inflammation response to 15-nm AgNPs post-exposure after 4 days of air exposure, but effects resolved after 7 days post-exposure | NA | AgNPs observed inside lung cells at 24 h post-exposure; average particle size reduced to <5 nm, attributed to dissolution; toxicity related to lung dose and particle number/ surface area | Braakhuis et al. [2014] |

(Continued)

**Table E-6. Summary of in vivo toxicological studies of silver nanoparticles (AgNPs) and nanowires (AgNWs) (Continued)**

| | | Exposure Details | | | | | |
|---|---|---|---|---|---|---|---|
| Species | Particle Characteristics | Concentration/ Dose | Duration | Critical Effect(s) | NOAEL/ LOAEL | Comments | Reference |
| Male C57BL/6 mice, 5 per group | 20-nm AgNP | $1.93 \times 10^7$ particles/cm$^3$ (~2.9 mg/m$^3$) | Nose only, 6 hours for 1 day, responses examined at 0 and 1 day after exposure | Distribution to brain, heart, liver, spleen, and testes with rapid clearance from lung. Activation of MAPK signal pathway, increased total protein in BAL fluid with recovery by 1 day, no lung pathology. | ND | | Kwon et al. [2012] |
| Sprague-Dawley rats and Brown Norway (BN) rats, 8-12 males per group | 13–16-nm AgNP, spark-generated | 3.68-4.55 $\times 10^7$ particles /cm$^3$ (~600-800 μg/m$^3$) | Nose only, 3 hours for 1 day (low dose) or 3 hours/day for 4 days (high dose), responses measured at 1 and 7 days post-exposure | Increased inflammatory cells and proteins with high dose, increased lung phospholipids, transient effects on lung mechanics | ND | Strain-related differences were attributed to the pre-existing inflammatory state in BN rats. | Seiffert et al. [2016] |
| Male Sprague-Dawley rats, 6 per group per time point | Citrate capped 20- or 110-nm AgNP | Aerosolized citrate buffer (control), 7.2 mg/m$^3$ for 20nm AgNPs and 5.4 mg/m$^3$ for 110-nm AgNPs; equivalent deposited dose in nasal epithelium of 4 and 1 μg/cm$^2$, respectively | Nose only, single 6-hour exposure, recovery time points of 0, 1, 7, 21 and 56 days | Increased deposition at terminal bronchiole/alveolar duct junction, 33 % persistence of particle in lung for both sizes, higher macrophage particle burden for smaller particle | ND | | Anderson et al. [2015a] |

(Continued)

**Table E-6. Summary of in vivo toxicological studies of silver nanoparticles (AgNPs) and nanowires (AgNWs) (Continued)**

| Species | Particle Characteristics | Exposure Details: Concentration/ Dose | Exposure Details: Duration | Critical Effect(s) | NOAEL/ LOAEL | Comments | Reference |
|---|---|---|---|---|---|---|---|
| Male Sprague-Dawley rats, 6 per group per time point | Citrate capped 20- or 110-nm AgNPs | Aerosolized citrate buffer (control), 7.2 mg/m$^3$ for 20-nm AgNPs and 5.3 mg/m$^3$ for 110-nm AgNPs; equivalent deposited dose in nasal epithelium of 4 and 1 μg/cm$^2$, respectively | Nose only, single 6-hour exposure, recovery time points of 1, 7, 21 and 56 days | Lung injury and inflammation peaked day 7; 20-nm AgNPs caused slightly greater inflammation and persisted longer, responses resolved over time | ND | | Silva et al. [2016] |
| Male Sprague-Dawley rats, 8 per group per time point | Citrate-capped 20- or 110-nm AgNPs | Aerosolized citrate buffer (control), 7.2 mg/m$^3$ for 20-nm AgNPs and 5.4 mg/m$^3$ for 110-nm AgNPs; equivalent deposited dose in nasal epithelium of 4 and 1 μg/cm$^2$, respectively | Nose only, single 6-hour exposure, recovery time points of 0, 1, 7, 21 and 56 days | Translocation to the olfactory bulb (OB); OB microglia activation was increased acutely up to 7 days post-exposure to 20-nm AgNPs and at day 0 only for 110-nm AgNPs | ND | Translocation greatest at day 0 for 20-nm AgNPs, whereas the greatest burden was at day 56 for the 110-nm AgNPs; particles differed in temporal rate of translocation | Patchin et al. [2016] |

(Continued)

**Table E-6. Summary of in vivo toxicological studies of silver nanoparticles (AgNPs) and nanowires (AgNWs) (Continued)**

| | | Exposure Details | | | | | |
|---|---|---|---|---|---|---|---|
| Species | Particle Characteristics | Concentration/ Dose | Duration | Critical Effect(s) | NOAEL/ LOAEL | Comments | Reference |
| BALB/c mice, 5-6 females per group | 33 nm average diameter, spherical | 0 or 3.3 mg/m$^3$ | 6 hours/day for 7 days from day 16- day 22 (after OVA sensitization and before OVA challenge) | Exacerbated allergic response (lung eosinophils, BAL fluid IgE and IL-13, airway reactivity); silver distributed to heart, spleen, liver, kidneys, and brain | ND | Histologic changes in capsule of liver and spleen, focal and mild inflammation in perirenal soft tissue AgNP exposed mice (allergic and non-allergic) and in allergic control mice. | Chuang et al. [2013] |
| BALB/c mice, 5-6 females per group | 33 nm average diameter, spherical | 0 or 3.3 mg/m$^3$ | 6 hours/day for 7 days from day 16- day 22 (after OVA sensitization and before OVA challenge) | Increased OVA-specific IgE; altered protein levels in BAL fluid and plasma in both allergic and non-allergic AgNP-treated mice; altered 18 proteins related to systemic lupus erythematosus in allergic and non-allergic mice | ND | | Su et al. [2013] |

(Continued)

**Table E-6. Summary of in vivo toxicological studies of silver nanoparticles (AgNPs) and nanowires (AgNWs) (Continued)**

| Species | Particle Characteristics | Exposure Details: Concentration/ Dose | Exposure Details: Duration | Critical Effect(s) | NOAEL/ LOAEL | Comments | Reference |
|---|---|---|---|---|---|---|---|
| BALB/c mice, 8 females per group | 6 nm, agglomerating to 24 nm, OVA control for allergy, control for VEGF activity (VEGF receptor tyrosine kinase inhibitor) | 20 ppm (40 mg/ kg) AgNPs or control for VEGF pathway activation (VEGF receptor tyrosine kinase inhibitor) | Nebulization 1× /day for 5 days before each OVA challenge (days 20-24), VEGF control 3 times intraperitoneally at 24 hour intervals for 5 days (days 0-24) | Attenuated allergic response, including mucus secretion, airway reactivity, and allergic cytokines and suppressed the P13/HIF-1 α /VEGF signaling pathway | NA | | Jang et al. [2012] |
| **Inhalation—Subchronic** | | | | | | | |
| Sprague-Dawley rats; 10 of each sex per group | Mostly spherical, diameter range 2–65 nm (median, 16 nm) | 0, 49, 133, or 515 μg/m$^3$ | 6 hr/day, 5 days/ week for 90 days (whole body exposure) | Lung function deficits, alveolar inflammation, macrophage accumulation | 133 (49) /515 μg/m$^3$ | Lung function and histologic deficits at high dose | Sung et al. [2008] |
| Sprague-Dawley rats; 10 of each sex per group | Mostly spherical, diameter range 2–65 nm (median, 16 nm) | 0, 49, 133, or 515 μg/m$^3$ | 6 hr/day, 5 days/ week for 90 days (whole body exposure) | Bile duct hyperplasia; hepatocellular necrosis | 133/515 μg/ m$^3$ | Same experiment as Sung et al. [2008] | Sung et al. [2009] |
| Sprague-Dawley rats; 17 males and 12 females per group | Spherical, non-agglomerated; diameter range 4–45 nm (median, 14–15 nm) | 0, 49, 117, or 381 μg/m$^3$ | 6 hr/day, 5 days/ week for 12 weeks (whole body exposure) | Lung function decrease, persistent lung inflammation in male rats; lung inflammation with gradual recovery in female rats | 117 (49) /381 (117) μg/m$^3$ | Silver nanoparticles generated as reported previously [Ji et al. 2007a] | Song et al. [2013] |

(Continued)

**Table E-6. Summary of in vivo toxicological studies of silver nanoparticles (AgNPs) and nanowires (AgNWs) (Continued)**

| Species | Particle Characteristics | Exposure Details: Concentration/ Dose | Exposure Details: Duration | Critical Effect(s) | NOAEL/ LOAEL | Comments | Reference |
|---|---|---|---|---|---|---|---|
| Sprague-Dawley male and female rats; 4 groups of 10 | AgNPs with 18-nm diameter | $0.7 \times 10^6$ particles/ $cm^3$ (low dose), $1.4 \times 10^6$ particles/ $cm^3$ (middle dose), $2.9 \times 10^6$ particles/ $cm^3$ (high dose) | 6 hr/day for 90 days; killed 24 hr after last treatment | Bone marrow tested for toxicity with micronucleus assay; no treatment-related genetic toxicity observed | NA | | Kim et al. [2011] |
| Sprague-Dawley male and female rats; 17 male and 12 female per group | Spherical AgNPs with diameters <47 nm (range, 4–47 nm) | $0.6 \times 10^6$ particles/ $cm^3$ (low dose), $1.4 \times 10^6$ particles/ $cm^3$ (middle dose), $3.0 \times 10^6$ particles/ $cm^3$ (high dose) | 6 hr/day, 5 days/ week for 12 weeks; rats given micronucleus gene test at end of 12 weeks or after 4- or 12-week recovery | Genes found to be up- and downregulated for the kidney by more than 1.3-fold ($P < 0.05$): 104 genes for males and 72 for females | NA | Female rats show a 2–4-fold higher Ag concentration in kidneys, possibly due to metabolism and hormonal regulation | Dong et al. [2013] |
| **Oral Exposure** | | | | | | | |
| Sprague-Dawley rats (male and female), 3 groups of 20 | Citrate-coated (avg. diameters 10 and 25 nm) | Control (0.9% citrate), 100 mg/kg bw, 500 mg/kg bw) | Subacute; exposed once/ day for 28 days; killed at 1, 2, and 4 months | AgNPs remained in brain and testes at 4 months | NA | Bio-persistence study; silver clearance concentration in blood > liver = kidneys > spleen > ovaries > testes = brain | Lee et al. [2013a] |

(Continued)

**Table E-6. Summary of in vivo toxicological studies of silver nanoparticles (AgNPs) and nanowires (AgNWs) (Continued)**

| Species | Particle Characteristics | Exposure Details: Concentration/ Dose | Exposure Details: Duration | Critical Effect(s) | NOAEL/ LOAEL | Comments | Reference |
|---|---|---|---|---|---|---|---|
| Male Sprague-Dawley rats (n = 9/group/time point) | 12.3-nm uncoated AgNPs in 1% starch with 0.1% Tween-80 | Acute exposure: 2000mg/ kg Subacute exposure: 250 mg/ kg | Acute: 1× administration with recovery points at 1, 7, and 14 days Subacute: 1x/ day for 30 days; assessment at 7th, 18th, and 30th day during exposure | No hematologic changes due to either exposure; >99% excreted for both acute and subacute exposure | ND | Acute biodistribution beyond the GI tract at day 7 was liver ≥ kidney > spleen; repeated exposure distribution beyond GI tract was highest in spleen at day 7, and kidney > spleen ≥ liver at days 14 and 30 | Hendrickson et al. [2016] |
| C57BL/6NCrl mice; 6 males per group/ time point | 20- or 110-nm AgNPs with gold core, PVP and citrate coated, or silver acetate (ion control),with or without antibiotic treatment | 0, 0.1, 1.0, or 10 mg/kg | 3 days with recovery at 1 and 7 days post-exposure | No changes in weight or organ histopathology; 70.5-98.6 % of dose recovered in feces; ionic silver was more bioavailable to a degree | NA | Size and coating did not affect distribution; ionic silver was higher than AgNPs in kidney, liver, and spleen | Bergin et al. [2016] |
| Human (18 healthy volunteers) | 25-40-nm colloidal AgNPs | 480 µg/day (32 ppm in 15 ml water) | 14 days | Decreased platelet aggregation in the presence of an agonist | NA | Peak silver concentration in blood was 6.8 ± 4.5 µg/L | Smock et al. [2014] |
| ICR mice (up-down procedure for oral lethality) | Spherical, starch-stabilized (colloidal) particles of 10–20-nm diameter | 5,000 mg/kg | Single dose | No lethality or signs of toxicity | ND | Oral $LD_{50}$ was >5,000 mg/kg | Maneewattana-pinyo et al. [2011] |

(Continued)

**Table E-6. Summary of in vivo toxicological studies of silver nanoparticles (AgNPs) and nanowires (AgNWs) (Continued)**

| Species | Particle Characteristics | Exposure Details: Concentration/ Dose | Exposure Details: Duration | Critical Effect(s) | NOAEL/ LOAEL | Comments | Reference |
|---|---|---|---|---|---|---|---|
| Wistar rats; females 6-8 weeks old; 5 per group | 60-nm AgNPs (thermal co-reduction) | 0, 500, 1000, 2000 mg.kg | 14 days | No lethality; normal weight gain and food/ water consumption | ND | Oral $LD_{50}$ was >2,000 mg/ kg; serum ALP increased at the high dose | Dasgupta et al. [2019] |
| Sprague-Dawley rats; 10 of each sex per group | 60-nm diameter in aqueous 0.5% carboxymethyl-cellulose (CMC), shape not specified* | 0, 30, 300, or 1,000 mg/kg-day by gavage | 28 days | Increases in serum cholesterol and alkaline phosphatase; liver histopathology | 30/300 mg/ kg-day | Silver deposited in major organs and tissues | Kim et al. [2008] |
| Sprague-Dawley rats, 4 males per group/time point | Citrate-coated 7.9-nm diameter in an aqueous medium, shape not specified | 1 or 10 mg/kg | Single exposure | Silver deposition in plasma, feces, urine, and the major tissues and organs | –/1 mg/kg | Citrate-coating of the particles may have deterred absorption | Park et al. [2011a] |
| ICR mice; 5 of each sex per group | 22-, 42-, 71-, and 323-nm-diameter particles in an aqueous medium, shape not specified | 1 mg/kg-day | 14 days | Silver deposition in a wide range of tissues; increased serum concentrations of TGF-β | NA | Smaller particles were more effective | Park et al. [2010b] |
| ICR mice; 3 of each sex per group | 42-nm diameter in an aqueous medium, shape not specified | 0, 250, 500, or 1,000 µg/kg-day by gavage | 28 days | Increases in serum AP, AST, ALT, and cytokines; kidney histopathology | 500/1,000 µg/ kg-day | | Park et al. [2010a] |
| F344 rats; 5 of each sex per group | 60-nm diameter in aqueous 0.5% CMC, shape not specified* | 0, 30, 125, or 500 mg/kg-day by gavage | 90 days | Kidney histopathology and silver deposition | ND | Heavier silver deposition was observed in females | Kim et al. [2009a] |

(Continued)

**Table E-6. Summary of in vivo toxicological studies of silver nanoparticles (AgNPs) and nanowires (AgNWs) (Continued)**

| Species | Particle Characteristics | Exposure Details: Concentration/ Dose | Exposure Details: Duration | Critical Effect(s) | NOAEL/ LOAEL | Comments | Reference |
|---|---|---|---|---|---|---|---|
| F344 rats; 10 of each sex per group | 60-nm diameter in aqueous 0.5% CMC, spherical and monodisperse | 0, 30, 125, or 500 mg/kg-day by gavage | 90 days | Increases in serum cholesterol and AP; liver histopathology | 30/125 mg/ kg-day | NOAEL and LOAEL are as specified by the study authors | Kim et al. [2010a] |
| Sprague-Dawley rats; 10 of each sex per group | 60-nm diameter in aqueous 0.5% CMC, shape not specified* | 0, 30, 300, or 1,000 mg/kg-day by gavage | 28 days | Intestinal silver deposition: Goblet cell activation | ND | Data are semi-quantitative | Jeong et al. [2010] |
| Male Swiss albino mice; 5 mice per group | 3–20-nm AgNPs (average diameter = 10.15 nm) | 0, 5, 10, 15, or 20 mg/kg | 21 days | Loss of microvilli, increased inflammatory cells in villus, increased mitotic figures in intestinal glands | ND | | Shahare et al. [2013] |
| Male and female Sprague-Dawley rats; 10/sex/group | 10-, 75-, or 110-nm citrate-stabilized AgNPs in 1% CMC, or silver acetate (ion control) | 0, 9, 18, or 36 mg/ kg AgNPs; 100, 200, or 400 mg/kg silver acetate | 13 weeks | AgNPs induce size-and dose-dependent changes in populations of gut microbiota; sex differences found for AgNP effects on expression of *Enterobacteriaceae-family* genes | ND | Higher doses of silver acetate were selected to ensure a response rather than matching amounts present in AgNP | Williams et al. [2015] |

(Continued)

**Table E-6. Summary of in vivo toxicological studies of silver nanoparticles (AgNPs) and nanowires (AgNWs) (Continued)**

| Species | Particle Characteristics | Exposure Details: Concentration/ Dose | Exposure Details: Duration | Critical Effect(s) | NOAEL/ LOAEL | Comments | Reference |
|---|---|---|---|---|---|---|---|
| Female Wistar rats, 6-8 weeks old; 5 per group | 60-nm AgNPs (thermal co-reduction) | 0, 20, 40, 60, 80, 100 mg/kg | Daily for 12 weeks | Increased liver enzymes in blood starting at 60 mg/kg. Greater effects in the 80 and 100 mg groups including reduced gain in body weight, increased cholesterol, triglycerides, and glucose, increased WBC and neutrophils, and decreased platelets and hematocrit | NOAEL = 30 mg/kg LOAEL = 60 mg/kg | Histopathology and silver accumulation in organs measured in only 100-mg/kg group; pathology observed in liver, lung and kidney; silver accumulation was liver > kidney > lung > pancreas | Dasgupta et al. [2019] |
| Female Wistar rats; 5/group/ parameter evaluated | 10–40-nm PVP-stabilized AgNPs; hydrodynamic diameter 87–230 nm | 0, 50, or 200 ppm | Daily for 60 days | Increased necrosis and damage to organelles in kidney; increased marker of inflammation systemically and in kidney; increased indices of oxidative stress in kidney | ND | ~60–70% of the dose was excreted on day 1 of exposure and increased over time; dose-dependent accumulation of AgNPs in kidney at day 60 (70–75% non-ionic, 25–30% ionic) | Tiwari et al. [2017] |

(Continued)

**Table E-6. Summary of in vivo toxicological studies of silver nanoparticles (AgNPs) and nanowires (AgNWs) (Continued)**

| Species | Particle Characteristics | Exposure Details: Concentration/ Dose | Exposure Details: Duration | Critical Effect(s) | NOAEL/ LOAEL | Comments | Reference |
|---|---|---|---|---|---|---|---|
| Male and female Sprague-Dawley rats; 5/sex/group Male and female Sprague-Dawley rats; 12/sex/group | 11-nm citrate-coated AgNPs; 12-nm $SiO_2$ NPs; 60-nm $Fe_2O_3$ NPs; 11-nm citrate-coated AgNPs; 12-nm $SiO_2$ NPs; 60-nm $Fe_2O_3$ NPs | ~0, 500, 1000, or 2000 mg/ kg~0, 250, 500, or 1000mg/kg | Subacute: 14 days Subchronic:13 weeks | AgNPs resulted in increased serum AP in males at the middle and high dose and in females at all doses; Ag detected in major organs; AP elevated in serum after high-dose AgNPs in males and females; histological changes in liver of both sexes; platelets elevated in males at high dose; increased white blood cells, serum calcium, and kidney calcification in females | | No toxicity associated with iron or silica NP; no toxicity associated with iron and silica NP and no translocation of silica or iron NP to other organ systems | Yun et al. [2015] |
| Male Sprague-Dawley rats; 16 per group | 70-80% 20-nm AgNPs and 20% protein gel (Collargol) | 820 mg/kg Collargol (500 mg/ kg AgNP) daily | 81 days | In plasma: increased cholesterol, increased ratio of LDL to HDL, decreased triglycerides; increased oxidative stress markers in heart and liver; increased inflammatory markers in liver | ND | | Elle et al. [2013] |

(Continued)

**Table E-6. Summary of in vivo toxicological studies of silver nanoparticles (AgNPs) and nanowires (AgNWs) (Continued)**

| Species | Particle Characteristics | Exposure Details: Concentration/ Dose | Exposure Details: Duration | Critical Effect(s) | NOAEL/ LOAEL | Comments | Reference |
|---|---|---|---|---|---|---|---|
| Male Swiss albino mice; 8 per group | 20-nm colloidal AgNPs or gold NPs | 1 or 2 μM/day | 14 days | Increased markers of systemic inflammation and kidney and liver injury; increased marker of oxidative stress in blood, urine, kidney, and liver; increased metallothionein greater in kidney than liver | ND | | Shrivastava et al. [2013] |
| Male Sprague-Dawley rats; 12 per group | 20–30-nm AgNPs, PVP-coated | 0, 50, 100, or 200 mg/kg/day | 90 days | AgNPs distributed to all major organs, also located in hepatic and ileum cells; no statistically significant pathology in any tissues collected including liver and kidney | ND | Thymus and brain copper and zinc levels were altered following AgNP exposure | Garcia et al. [2016] |
| Male Sprague-Dawley rats ($n$ = 5) | AgNPs (~7.9-nm diameter) | 2 mg/kg or 20 mg/kg | Up to 24 hr | Silver concentrations in blood, liver, and lungs higher with $Ag^+$ than with AgNPs at all doses | ND | Bioavailability of $Ag^+$ appears to be greater than with AgNPs | Park [2013] |

(Continued)

**Table E-6. Summary of in vivo toxicological studies of silver nanoparticles (AgNPs) and nanowires (AgNWs) (Continued)**

| Species | Particle Characteristics | Exposure Details: Concentration/ Dose | Exposure Details: Duration | Critical Effect(s) | NOAEL/ LOAEL | Comments | Reference |
|---|---|---|---|---|---|---|---|
| Male and Female Sprague-Dawley rats; 10 group/sex | 28–44-nm PVP-coated AgNPs or silver nitrate (ionic silver) | 0, 0.5 or 1.0 mg/kg | 28 days | AgNP distribution lower than soluble silver distribution; distribution noted in liver, kidney, spleen, and testes; minor pathological changes in kidney and liver of both sexes; sex differences noted in blood chemistry and distribution patterns | | Sex differences: increased AST in males and increased white blood cells in females, male tissue distribution of AgNPs was liver and kidney > testes and spleen whereas female distribution of AgNPs was equal across liver, kidney and spleen | Qin et al. [2016] |
| Sprague-Dawley rats; 5 groups of 5 | < 20-nm uncoated, <15-nm PVP and $AgNO_3$ particles | Ag = 90 mg/kg bw; $AgNO_3$ = 9 mg/kg bw, by gavage | 28 days | Silver deposition; silver cleared from organs except for brain and testis | ND | AgNPs similar to exposure to silver salts | Van der Zande et al. [2012] |

(Continued)

**Table E-6. Summary of in vivo toxicological studies of silver nanoparticles (AgNPs) and nanowires (AgNWs) (Continued)**

| | | Exposure Details | | | | | |
|---|---|---|---|---|---|---|---|
| Species | Particle Characteristics | Concentration/ Dose | Duration | Critical Effect(s) | NOAEL/ LOAEL | Comments | Reference |
| Hannover Galas male rats; 3 groups of 6 Hannover Galas rats: 4 groups of females,11 per group; 2 groups of males, 6 per group | 14-nm AgNPs (stabilized with PVP), or Ag acetate (ionic silver) | Control (PVP, 11.5 mg/mL), 4.5 mg Ag/kg bw/ day once or twice daily, for total dose of 4.5 or 9 mg/ kg bw Control (PVP, 11.5 mg/ mL) administered to 10 females and 6 males twice/day; AgNPs at 2.25 mg Ag/kg bw/day (8 females), 4.5 mg Ag/kg bw/day (8 females), or 9.0 mg Ag/kg bw/day (10 females and 6 males twice/day at 4.5); or 14 mg Ag acetate/kg bw/day in 11 mg/mL PVP (8 females twice/ day) | Killed on day14; killed on day 28 | No evidence of toxicological effects in AgNP exposed groups; decreased body weights; increases in plasma alkaline phosphatase absolute and thymus weights in Ag acetate–exposed groups | ND | Some toxicity at 9 mg/kg bw/ day ionic silver dose but not at an equimolar AgNP dose | Hadrup et al. [2012a] |
| Male C57BL/6Ncrl; 6 per group | Colloidal 20- or 110-nm over gold core, PVP- or citrate-coated, or silver acetate (AgAC ionic silver) | 10 mg/kg/day with and without antibiotics | 28 days | Study focused on murine gut microbiome: AgNPs, regardless of size and coating, did not alter the gut microbiome | ND | Cecal tips were processed to evaluate microbiome | Wilding et al. [2016] |

(Continued)

**Table E-6. Summary of in vivo toxicological studies of silver nanoparticles (AgNPs) and nanowires (AgNWs) (Continued)**

| Species | Particle Characteristics | Exposure Details: Concentration/ Dose | Exposure Details: Duration | Critical Effect(s) | NOAEL/ LOAEL | Comments | Reference |
|---|---|---|---|---|---|---|---|
| Male and female Wistar rats; 8-10 females per group, 6 males in the control and 9 mg/kg AGNP group | 14-nm PVP-coated AgNPs or AgAc (ionic silver) | 0, 2.25, 4.5, or 9 mg/kg day AgNPs, or 9.0 mg/kg/day ionic silver | 28 days—urine collected on day 18 for 24 hours | Metabolomics on urine showed increased allantoin and uric acid in female urine only indicating oxidative stress | ND | AgAC only increased allantoin in female urine | Hadrup et al. [2012b] |
| Female Wistar rats; 5 groups of 6 | 14-nm-diameter AgNPs or AgAc (ionic silver) | Control (PVP, 11.5 mg/mL), 2.25, 4.5, or 9 mg AgNP/ kg bw/day, or 14 mg ionic silver /kg bw/day | 28 days | Decrease in dopamine concentration (5-HT) in brain at 14 days but increase at 28 days for AgNPs; increase in noradrenaline brain concentration at 28 days for AgAc but not AgNPs | ND | Ionic silver and 14-nm AgNPs have similar neurotoxic effects | Hadrup et al. [2012c] |
| Male Wistar rats 8-10 weeks old; 8-10/group | 20-nm BSA-AgNPs (197 nm hydrodynamic diameter) | 0, 1, or 30 mg/kg | 1 time daily, 5 times per week for 4 weeks | No effect on body weight; short-term and long-term memory impairment measured by carousel maze test at both doses; normal non-cognitive effects | ND | Silver was increased in whole brain and in frontal cortex and hippocampus at high dose, and in the hippocampus at the low dose | Wesierska et al. [2018] |

(Continued)

**Table E-6. Summary of in vivo toxicological studies of silver nanoparticles (AgNPs) and nanowires (AgNWs) (Continued)**

| Species | Particle Characteristics | Exposure Details: Concentration/ Dose | Exposure Details: Duration | Critical Effect(s) | NOAEL/ LOAEL | Comments | Reference |
|---|---|---|---|---|---|---|---|
| Male Wistar rats; 12/group | 10-nm citrate-coated AgNPs or silver citrate (ionic silver) | 0.2 mg/kg/day | 14 days | No effect on memory, locomotor activity, or motor coordination; ionic silver decreased sensitivity to noxious stimuli and increase behavioral anxiety; both forms caused myelin sheath damage and altered myelin-related protein expression | ND | Also noted increased body temperature which persisted longer after ionic silver exposure | Dabrowska-Bouta et al. [2016] |
| Male and female Sprague-Dawley/ CD-23 rats; 10/ group/sex | 0 10, 75, or 110-nm citrate-coated AgNPs or AgAc (ionic silver) | AgNPs: 0, 9, 18, or 36 mg/kg/day AgAc: 0, 100, 200, or 400 mg/kg/day | 13 weeks | AgNPs appeared in cells whereas AgAc was localized to cell membranes; increased tissue deposition with decreased size and increased solubility; higher Ag levels in females in kidney, liver, and intestines; highest soluble dose led to statistically significant mortality | ND | AgNPs did not produce pathological results in major organs and no changes in blood chemistry or hematology | Boudreau et al. [2016] |

(Continued)

**Table E-6. Summary of in vivo toxicological studies of silver nanoparticles (AgNPs) and nanowires (AgNWs) (Continued)**

| Species | Particle Characteristics | Exposure Details: Concentration/ Dose | Exposure Details: Duration | Critical Effect(s) | NOAEL/ LOAEL | Comments | Reference |
|---|---|---|---|---|---|---|---|
| Male Sprague-Dawley rats; 6 per group | 20–30-nm PVP-coated AgNPs | 0, 50, 100, or 200 mg/kg/day | 90 days | AgNPs increased alteration in sperm morphology; trend for increased damage to tubular lumen | ND | No changes in sperm motility or number were noted; no statistically significant pathological changes in testes or epididymis | Lafuente et al. [2016] |
| Male Wistar rats; 8 per group | 5–20-nm AgNPs synthesized in citrate | 0 or 20 µg/kg/day | 90 days | Pathological abnormalities in testes and seminiferous tubules; abnormal structures in Sertoli cells, spermatids and spermatocytes; necrosis/depletion of germ cells | ND | | Thakur et al. [2014] |
| Pre-pubertal male Wistar rats ($n$ = 30) | AgNPs (~86-nm diameter) | 15 or 50 µg/kg bw | Exposed from post-natal day 23 to day 53 and killed on days 53 and 90 | Reduction in total and daily sperm production observed in 50-µg/kg group at day 53; at 90 days both exposure groups had lower sperm production ($P < 0.05$) | ND | Presence of cellular debris and germinal epithelial cells in tubular lumen and vesicles, suggestive of possible impairment to spermato-genesis process | Sleiman et al. [2013] |

(Continued)

**Table E-6. Summary of in vivo toxicological studies of silver nanoparticles (AgNPs) and nanowires (AgNWs) (Continued)**

| Species | Particle Characteristics | Exposure Details: Concentration/ Dose | Exposure Details: Duration | Critical Effect(s) | NOAEL/ LOAEL | Comments | Reference |
|---|---|---|---|---|---|---|---|
| Pre-pubertal male Wistar rats ($n$ = 30) | AgNPs (~86-nm diameter) | 15 or 30 µg/kg bw | Exposed from post-natal days 23 through 58 (35 days at a total dose of 131–263 µg Ag/ rat) and killed on postnatal day 102 | Reduction in acrosome and plasma membrane integrities, reduced mitochondrial activity, and abnormalities of sperm in both dose groups; no change in sexual behavior or serum hormone | ND | Possible direct effect of AgNPs on spermatic cells | Mathias et al. [2014] |
| Pre-pubertal male Wistar rats; 8 per group | 70-nm AgNPs | 0, 25, 50, 100, or 200 mg/kg/day | 48 days of exposure | Reduced spermatogonia at highest dose; reduction in spermatocytes, spermatozoa, and spermatids in all groups but the lowest dose; minor changes in connective tissue in seminiferous tubules | ND | No differences in Sertoli cell number or seminiferous tubule diameter noted | Miresmaeili et al. [2013] |
| Female Sprague-Dawley rats; | 6.45-nm AgNPs in 0.5% CMC | 0, 100, 300, or 1000 mg/kg/day | 14 days, on gestation days 6-19 | Dams: increased indices of oxidative stress in liver homogenates Fetuses: increased loss of pre-implanted embryos at highest dose | NOEL reported as < 100 mg/ kg/day for dams and 1000 mg/ kg/day for embryo-fetal development | No abnormal blood chemistry in dams; no pathology of liver or kidney | Yu et al. [2014] |

(Continued)

**Table E-6. Summary of in vivo toxicological studies of silver nanoparticles (AgNPs) and nanowires (AgNWs) (Continued)**

| Species | Particle Characteristics | Exposure Details: Concentration/ Dose | Exposure Details: Duration | Critical Effect(s) | NOAEL/ LOAEL | Comments | Reference |
|---|---|---|---|---|---|---|---|
| Female CD-1 mice; 3 pregnant dams per group with 10–18 litters per group | 20-nm or 3 μm Ag particles, 50-nm or 1–2-μm $TiO_2$ particles | 0, 10, 100, or 1000 mg/kg/day | 1 time on gestation day 9 | AgNPs at 10 mg/kg and $TiO_2$ NP at 1 and 1000 mg/kg reduced number of viable fetuses; AgNPs could be detected in kidney and liver; only $TiO_2$ NPs at high doses led to fetal developmental abnormalities; smaller particle had greater effect than larger particles | ND | No effects were observed in weight of dams or fetus, fetal resorption, or litter size; $TiO_2$ NP had greater effect than AgNP; no adverse pathology of kidney or liver | Philbrook et al. [2011] |
| Female Sprague-Dawley rats; 1-3 per group per time point | 20-nm or 110-nm PVP-coated AgNPs, or silver acetate | 10 mg/mL | 1 time on gestation day 18; parameters assessed 1 and 2 days post-exposure | Silver was detectable in placenta and fetus at both times and to a greater degree in fetus; markers of cardiovascular effects and oxidative stress were not altered | ND | Silver was detectable in all major organs; to a greater degree in spleen, lung, liver, kidney, placenta, and cecum/ large intestine; urine analysis showed changes in carbohydrate and amino acid metabolism | Fennell et al. [2016] |

(Continued)

**Table E-6. Summary of in vivo toxicological studies of silver nanoparticles (AgNPs) and nanowires (AgNWs) (Continued)**

| Species | Particle Characteristics | Exposure Details: Concentration/ Dose | Exposure Details: Duration | Critical Effect(s) | NOAEL/ LOAEL | Comments | Reference |
|---|---|---|---|---|---|---|---|
| Male and female C57BL/6J $p^{un}/p^{un}$ background mice or $Mhy^{-/-}$ mice; 4-6 mice per group | 96.1-nm AgNPs (determined by DLS) with PVP coating | 0 or 500 mg/kg/ day | 5 days, on gestation days 9.5–13.5 | Dams: increased micronuclei formation in blood and bone marrow in AgNP-exposed mice, which was greater in knockout; induction of oxidative stress markers in both groups of mice; Fetuses: increased eye-spot formation indicative of DNA deletion events | ND | Differences in upregulation and downregulation of gene expression of DNA repair genes between wildtype and knockout mice | Kovvuru et al. [2015] |
| **Dermal Exposure** | | | | | | | |
| Pigs; strain, sex, and number not stated | Spherical, 20- and 50-nm washed and unwashed particles | Up to 34 µg/mL applied to the shaved dorsal surface | 14 days | No observed erythema or edema; slight epidermal hyperplasia was seen microscopically | ND | | Samberg et al. [2010] |
| Male guinea pigs, 9 per group | Spherical, starch-stabilized (colloidal) particles of 10–20-nm diameter | 0, 50, or 100,000 ppm applied to shaved surface | 24-hour application, observation at 1, 3, 7, and 14 days; skin pathology at 14 days | No abnormalities reported in skin | ND | Ocular irritation and corrosion tests showed transient eye irritation with 5000 ppm at 24 hours—resolved by 72 hours | Maneewattanapinyo et al. [2011] |
| Sprague-Dawley rats, 10 per group (5 male, 5 female) | 10 nm, colloidal, stabilized in citric acid (1%) | 0 or 2000 mg/kg applied to shaved surface | 24-hour application, observed twice a day for 15 days | No irritation or toxicity observed | ND | | Kim et al. [2013] |

(Continued)

**Table E-6. Summary of in vivo toxicological studies of silver nanoparticles (AgNPs) and nanowires (AgNWs) (Continued)**

| Species | Particle Characteristics | Exposure Details: Concentration/ Dose | Exposure Details: Duration | Critical Effect(s) | NOAEL/ LOAEL | Comments | Reference |
|---|---|---|---|---|---|---|---|
| Male New Zealand White rabbits | 10 nm, colloidal, stabilized in citric acid (1%) | 0.5 ml test substance according to OECD guideline 404 | Various duration from 3 min to 4 hours application, observed 1, 24, 48, and 72 hours post-exposure | No irritation or corrosion observed | ND | Ocular irritation/ corrosion test resulted in conjunctival redness, edema, and discharge at 1 hour with resolution over time; no effects on cornea | Kim et al. [2013] |
| Male SPF guinea pigs, 20 animals | 10 nm, colloidal, stabilized in citric acid (1%) | 102.4 mg in 0.5 ml | Applied for 48 hours on day 6 following induction period with a 24 hour challenge on day 21 | 1/20 animals showed discrete and patchy erythema 24 and 48 hours following challenge indicating 5% skin sensitization rate (weak sensitizer) | ND | | Kim et al. [2013] |
| Male Hartley guinea pigs; 6 per group F | <100-nm particles of various shapes and degrees of aggregation | 0,100, or 1000 µg/ mL | Single acute exposure with a 14-day observation period | No lethality: some histopathologic changes to skin | –/100 µg/mL | | Korani et al. [2011] |
| Male Hartley guinea pigs; 6 per group | <100-nm particles of various shapes and degrees of aggregation | 0, 100, 1000, or 10,000 µg/mL | Subchronic; once daily, 5 days/week for 13 weeks | Skin perturbation; liver and spleen histopathology | –/100 µg/mL | | Korani et al. [2011] |

(Continued)

**Table E-6. Summary of in vivo toxicological studies of silver nanoparticles (AgNPs) and nanowires (AgNWs) (Continued)**

| | | Exposure Details | | | | | |
|---|---|---|---|---|---|---|---|
| Species | Particle Characteristics | Concentration/ Dose | Duration | Critical Effect(s) | NOAEL/ LOAEL | Comments | Reference |
| Male Hartley guinea pigs; 12 per treatment group | <100-nm particles of various shapes and degrees of aggregation | 0, 100, 1000, 10,000 ppm AgNPs or 100 μg/ mL silver nitrate | Subchronic, 13 weeks | Dose-dependent increase of silver in kidney > muscle > bone > skin > liver >heart > spleen; middle and high dose induced kidney pathology; all doses resulted in degrees of bone pathology; high dose caused pathological effects in heart | ND | Kidney, heart, and bone were the focus for histopathology analysis; liver and spleen were previously analyzed | Korani et al. [2013] |
| **Intratracheal Instillation and Pharyngeal Aspiration** | | | | | | | |
| Male ICR mice, 3-4 per group | 20-nm citrate-coated AgNPs and $AgNO_3$ (soluble control) (60- and 100-nm citrate-coated AgNPs and PVP-coated particles were used additionally for in vitro studies) | 10 μg of 20 nm citrate-stabilized AgNPs or $AgNO_3$ per mouse | Single IT instillation, assessment at 4 and 24 hr | Increased IL-1β at 4 hr in AgNPs versus soluble, greater neutrophil influx due to soluble form at 24 hours; increased lung burden for AgNPs versus soluble Ag, indicating faster clearance for soluble Ag and greater translocation to liver for soluble Ag; no detectable Ag in kidney, spleen, or urine | | In vitro, Ag distributed to metallothioneins and macrophages sequester AgNPs in the lysosome, with gradual dissolution over time | Arai et al. [2015] |

(Continued)

**Table E-6. Summary of in vivo toxicological studies of silver nanoparticles (AgNPs) and nanowires (AgNWs) (Continued)**

| Species | Particle Characteristics | Exposure Details: Concentration/ Dose | Exposure Details: Duration | Critical Effect(s) | NOAEL/ LOAEL | Comments | Reference |
|---|---|---|---|---|---|---|---|
| Female Wistar-Kyoto rats, 5 per group | 70-nm PVP-coated AgNPs | 0, 50, or 250 µg per rat (~ 0, 0.2, or 1 mg/kg) | Single IT instillation with recovery time point of 24 hours | Increased BAL fluid inflammatory cells, inflammatory cytokines, and lung injury at high dose | ND | | Haberl et al. [2013] |
| Male imprinting control region mice; 7-9 per group for BAL fluid parameters and 2-3 per group for histopathology | 99.96 % colloidal, 10–20 nm, spherical | 0 or 100 ppm/50 µl distilled water | Single IT instillation, recovery time points at 1, 3, 7, 15, and 30 days post-exposure | Cytotoxicity and neutrophil number in BAL fluid increased acutely after exposure, lymphocyte influx occurred at 7 and 15 days post-exposure, lung injury was characterized by inflammatory nodules, necrotizing alveolitis, and type II cell hyperplasia | ND | Increased indices of oxidative stress correlated to particle laden areas and cells at acute time points post-exposure; lung injury and inflammation resolved with time | Kaewamata-wong et al. [2014] |
| Female rats (in-house breeding colony), 8-14 in control and exposed groups | 49-nm AgNPs, 50-nm AuNPs, 1.1 µm Ag particles | 0 (water) or 0.5 mg/mL | Single IT instillation, evaluation at 24 hours | Increased neutrophil influx into lungs (AgNP> AuNP >micron Ag), Increased phagocytosis in macrophages and mitochondria affinity in macrophages and neutrophils with Ag versus Au; no nuclear penetration with AgNPs | | | Katsnelson et al. [2013] |

(Continued)

**Table E-6. Summary of in vivo toxicological studies of silver nanoparticles (AgNPs) and nanowires (AgNWs) (Continued)**

| | | Exposure Details | | | | | |
|---|---|---|---|---|---|---|---|
| Species | Particle Characteristics | Concentration/ Dose | Duration | Critical Effect(s) | NOAEL/ LOAEL | Comments | Reference |
| Wistar rats (sex not specified), 6 rats per group | 52-nm spherical AgNPs, 19-nm hexagonal ZnO NPs, 23-nm spherical $TiO_2$ NPs | 0, 3.5 and 17.5 mg/kg | IT instillation once every 2 days for 5 weeks with analysis 1 day post-exposure | Elevated indicators of oxidative stress, lung injury and inflammation in BAL fluid; cytotoxicity was ZnO> Ag=$TiO_2$ | ND | Comparative analysis suggests particle composition and stability as factors for toxicity | Liu et al. [2013a] |
| Sprague-Dawley rats; number and sex not stated | 20-nm PVP-coated particles that aggregated in a physiologic medium | 0, 9.35, or 112 μg/ rat | IT instillation once weekly for 8 weeks, with various recovery periods up to 84 days | Albumin, LDH, neutrophils, and lymphocytes increased in BAL fluid in comparison with controls | 9.35/112μg | Pulmonary injury and inflammation resolved with time | Roberts et al. [2012] |
| Male ICR mice ($n$ = 48); 12 per group | AgNPs at 243.8-nm average diameter | 0, 125, 250, and 500 μg/kg | Single IT instillation; histopathologic analysis at different time points from treatment (1, 7, 14, and 28 days) | Dose-related change in cytokine composition of BAL fluid and blood, with maximum concentration found at 28 days; changes in gene expression; marked inflammatory response from day 1 to 28 | NA | Changes in functionality of induced genes appears to be related to tissue damage | Park et al. [2011b] |

(Continued)

**Table E-6. Summary of in vivo toxicological studies of silver nanoparticles (AgNPs) and nanowires (AgNWs) (Continued)**

| Species | Particle Characteristics | Exposure Details: Concentration/ Dose | Exposure Details: Duration | Critical Effect(s) | NOAEL/ LOAEL | Comments | Reference |
|---|---|---|---|---|---|---|---|
| Male BALB/c OlaHsd mice, 4 per group | 25–28-nm AgNPs (90-nm aggregated), 15-nm $TiO_2$ NPs (396 nm aggregated), 19-nm $SiO_2$ NPs (192-nm aggregated), paints containing individual metal NPs | 0 or 20 µg per mouse per dose | Oropharyngeal aspiration once a week for 5 weeks with recovery at 2 and 28 days after last exposure | Increased silver in liver, spleen and kidney, but not heart, 2 days after last exposure, with clearance from all organs but lung at 28 days; increased lung inflammation with recovery over time | ND | Ag NP distribution differed from $TiO_2$ which was only present in the lung and $SiO_2$ which was found in lung and liver only. AgNPs were more toxic than $TiO_2$ and $SiO_2$ | Smulders et al. [2014] |
| Male BALB/c OlaHsd mice, number per group not specified | Heterogenous, 20-nm spherical and 80–90-nm rod-shaped AgNPs, aggregating to ~500 nm average. | 0 or 20 µg per mouse per dose | Oropharyngeal aspiration once a week for 5 weeks with recovery at 2 days after last exposure | High degree of macrophage phagocytosis in airways and alveolar region, high degree of dissolution and conjugation to thiol-containing molecules | ND | Presence of Fe and Cu in Ag-rich areas indicate metallothionein conjugation | Smulders et al. [2015a] |
| Male C57BL/6 mice, 2-4 per group | 25 nm, noted to agglomerate in delivery vehicle | 0, 100 or 500 mg/kg | Single IN instillation with recovery times of 1 and 7 days | AgNPs measured in brain (OB and lateral brain ventricles), spleen (red pulp more than white pulp), kidney, lung, and nasal cavity | ND | Elevated glutathione levels in nasal cavity and blood; nasal mucosal erosion and reduced cellularity in spleen; no alterations in cell infiltrates or microglial activation in the brain | Genter et al. [2012] |

(Continued)

**Table E-6. Summary of in vivo toxicological studies of silver nanoparticles (AgNPs) and nanowires (AgNWs) (Continued)**

| Species | Particle Characteristics | Exposure Details: Concentration/ Dose | Exposure Details: Duration | Critical Effect(s) | NOAEL/ LOAEL | Comments | Reference |
|---|---|---|---|---|---|---|---|
| Male C57BL/6 mice, 13-17 per group for repeated exposures, group number not stated for single exposures | 25 nm, noted to agglomerate in delivery vehicle | Single dose of 10-500 mg/kg, repeated dose of 50 mg/kg | Single or repeated (1 time per day for 7 days) intranasal instillation, 1 week recovery following repeated exposure | Silver deposition in liver, gut associated lymphoid tissue, and brain; oxidative stress responses elevated in hippocampus but not cortex; no change in learning or memory related behaviors (Morris Maze Test) | ND | | Davenport et al. [2015] |
| Female C57BL/6NT mice, 3 per group for AgNP | 8–47-nm AgNPs (NM-300) capped with polyoxyethylene glycerol trioleate and Tween-20, 70–100-nm ZnO NPs, 58–90-nm functionalized ZnO NPs; aggregates ~200 nm | 0, 1, 4, 8, 16, 32, 64, and 128 μg/ mouse | Single IT instillation, responses evaluated 1 day post-exposure | AgNPs decreased liver glutathione levels; no adverse pulmonary effects due to AgNPs | ND | ZnO NP were more inflammatory in the lung than AgNP | Gosens et al. [2015] |
| Male Sprague-Dawley rats, 4-5 per group | 20-nm citrate-capped (AgNPs), 26.2-nm hydrodynamic diameter; silver acetate (AgAc) | naïve, 2 mM citrate buffer vehicle, 1 mg/mL AgNP, or 0.01, 0.1, or 1 mg/mL AgAc | Single IT with recovery 1 and 7 days for AgNPs and 1 day for AgAc | Both AgAc and AgNPs caused a cardiac ischemic reperfusion injury but only AgNPs resulted in changes in serum cytokines levels | ND | | Holland et al. [2015] |

(Continued)

**Table E-6. Summary of in vivo toxicological studies of silver nanoparticles (AgNPs) and nanowires (AgNWs) (Continued)**

| Species | Particle Characteristics | Exposure Details: Concentration/ Dose | Exposure Details: Duration | Critical Effect(s) | NOAEL/ LOAEL | Comments | Reference |
|---|---|---|---|---|---|---|---|
| Male Wistar rats, 3 groups of 8 for behavioral measures (half the group for histopathology and half for markers of oxidative stress in the brain and hippocampus. | 50–100-nm AgNPs, primary size, 33–380 nm aggregated in deionized water (vehicle) | 0, 3, or 30 mg/kg | IN administration (nose drops) once every 2 days for 14 days | Dose-dependent impairment in cognitive function, increased neuronal damage in hippocampus, and increased ROS in hippocampus was observed | | Morris water maze tests were the basis for cognitive function; long-term potentiation tests also showed impairment of synaptic connectivity in the AgNP groups | Liu et al. [2012] |
| Male ICR mice, 6 per group | 20-nm AgNPs (NM-300K) in polyoxyethylene glycerol trioleate and Tween-20 (NM-300K DIS), NM-300K DIS control | 0, 0.1, and 0.5 mg/kg | Single IT instillation, assessment at 8 and 24 hours | Increased endoplasmic reticulum stress marker primarily in lung, liver and kidney, dose-dependent increased apoptosis in lung, apoptosis in kidney (high dose), increased Ag deposition in liver at 8 hours and kidney at 24 hours | NA | In vitro studies showed ER stress response in human bronchial epithelial cells but not in umbilical vein endothelial cells or hepatocytes | Huo et al. [2015] |

(Continued)

**Table E-6. Summary of in vivo toxicological studies of silver nanoparticles (AgNPs) and nanowires (AgNWs) (Continued)**

| Species | Particle Characteristics | Exposure Details: Concentration/ Dose | Exposure Details: Duration | Critical Effect(s) | NOAEL/ LOAEL | Comments | Reference |
|---|---|---|---|---|---|---|---|
| Male Wistar rats, 3 per group | 28–30-nm, 30% AgNPs in NaCl matrix | 0 or 0.05 mg/kg | Single IT instillation with recovery times of 1, 3, and 14 days | Alterations in mRNA expression of circadian regulatory genes (including PER1, PER2, CLOCK) were observed in lung, liver, brain, heart, kidney, and testes at varying degrees and times across the study | | | Minchenko et al. [2012] |
| Neonatal male and female rats, animal number varied by group from 5 - 30 | 20-nm PVP-coated AgNPs or $AgNO_3$ (ion control) | 0, 0.1 or 1 mg/kg AgNPs or silver ion | IN instillation 1x/day for 4 weeks or 12 weeks; organ samples taken immediately following 4 week exposure, and various times throughout the 12 week study up to 4 weeks | Silver detected in all major organs and to a greater degree for ionic Ag compared to AgNPs; for both forms of silver, the highest level of Ag was in liver at 4 weeks, followed by brain, and highest in brain at 12 weeks; dose-dependent differences were greater in AgNP groups than in ionic silver groups | ND | No sex-specific tissue accumulation observed; increased mortality noted in the 1-mg/kg/d silver ion group | Wen et al. [2015] |

(Continued)

**Table E-6. Summary of in vivo toxicological studies of silver nanoparticles (AgNPs) and nanowires (AgNWs) (Continued)**

| Species | Particle Characteristics | Exposure Details: Concentration/ Dose | Exposure Details: Duration | Critical Effect(s) | NOAEL/ LOAEL | Comments | Reference |
|---|---|---|---|---|---|---|---|
| Male C57BL/6, 4 per group | 20- and 110-nm PVP-capped and 20- and 110-nm citrate-capped AgNPs | 0.05 µg/g (0.05 mg/kg) | Single IT instillation with recovery at 1, 7, or 21 days | PVP-stabilized particles reduced surfactant protein D in BAL fluid at 1 day and increased inflammation and reduced lung function (7 days); larger particles had a greater effect; responses resolved by 21 days | ND | Subtoxic particle dose (0.05 µg/g) was determined by evaluating lung leakiness (injury) 1 day following a dose-response study, where no leakiness was observed | Botelho et al. [2016] |
| Male Sprague-Dawley (SD) rats and Male Brown Norway (BN) rats, 5-6 per group | 20- and 110-nm PVP-capped and 20 and 110-nm citrate-capped AgNPs | 0.1 mg.kg AgNPs, or controls for coating material (1mM citrate, 33 or 62 µg/mL PVP for 20- and 110-nm PVP-coated AgNPs, respectively) | Single IT instillation, responses measured at 1, 7, and 21 days post-exposure | Increased bronchial hyper-responsiveness (smaller particles > larger particles), increased inflammation, increased irritant response in BN rats | ND | Most cellular responses returned to baseline by day 21 | Seiffert et al. [2015] |
| Male Sprague-Dawley rats, 72 rats per particle type with 6 rats per group | 20- and 110-nm citrate-stabilized AgNPs, 20- and 110-nm PVP-stabilized AgNPs | 0, 0.1, 0.5, and 1 mg/kg (buffer as control) | Single IT instillation, recovery evaluated at 1, 7, and 21 days | The larger particle produced more persistent effects in the lung based on mass; no differences in toxicity due to coating were noted | ND | Increased alveolar neutrophils and airway cytotoxicity, variable degrees of resolution with time, based on size and parameter examined | Silva et al. [2015] |

(Continued)

**Table E-6. Summary of in vivo toxicological studies of silver nanoparticles (AgNPs) and nanowires (AgNWs) (Continued)**

| Species | Particle Characteristics | Exposure Details: Concentration/ Dose | Exposure Details: Duration | Critical Effect(s) | NOAEL/ LOAEL | Comments | Reference |
|---|---|---|---|---|---|---|---|
| Male Sprague-Dawley rats, 6 per group | 20- and 110-nm citrate stabilized AgNPs, 20- and 110-nm PVP-stabilized AgNPs | 0, 0.5, and 1.0 mg/kg | Single IT instillation, recovery evaluated at 1, 7, and 21 days | Increased deposition in proximal airways for small vs large particles; faster airway clearance for larger particles, faster rate of lung clearance for 20-nm PVP AgNPs vs 20-nm citrate AgNPs | ND | | Anderson et al. [2015] |
| Male Sprague-Dawley rats | Ag nanowires approx. 50-nm diameter; lengths 4 or 20 μm | 10, 50, 125, or 500 μg; alpha-quartz positive control at 500 μg or dispersion medium vehicle control | Single IT instillation | Both samples showed dose-dependent lung injury and inflammation | NA | Shorter wires' greater toxicity over time was possibly due to more wires/surface area per equivalent mass dose | Kenyon et al. [2012] |
| Female C57BL/6 mice; 5 per exposure group | Ag nanowires with lengths of 3, 5, 10, or 14 μm | Doses set to equalize number of wires/mouse: 10.7, 17.9, 35.7, and 50 | Single pharyngeal aspiration; acute inflammation response evaluated 24 hr post-exposure | Nanowire length-dependent trend in pulmonary inflammation; statistically significant increase in granulocytes in BAL fluid only with 14-μm Ag wires | NA | Suggested Ag nanowire threshold between 10- μm and 14-μm lengths | Schinwald et al. [2012] |

(Continued)

**Table E-6. Summary of in vivo toxicological studies of silver nanoparticles (AgNPs) and nanowires (AgNWs) (Continued)**

| | | Exposure Details | | | | | |
|---|---|---|---|---|---|---|---|
| Species | Particle Characteristics | Concentration/ Dose | Duration | Critical Effect(s) | NOAEL/ LOAEL | Comments | Reference |
| Male Sprague-Dawley rats, 63 rats per wire length | ~2 µm × 33 nm and 20 µm × 64 nm (length × width) AgNWs | 0, 35, 175, or 350 µg/rat (0, 0.1, 0.5 and 1 mg/kg, respectively) | Single IT instillation with recovery evaluated at 1, 7, and 21 days | Both sizes increased lung inflammation and injury at high dose; increased giant cell formation, terminal bronchiolar cell damage, and AgNW encapsulation in granulomas at day 21 | ND | Only long wires induced a degree of frustrated phagocytosis by macrophages | Silva et al. [2014] |
| **Intravenous Administration** | | | | | | | |
| Male Sprague-Dawley rats 9 n = 4/group/time point) | 35-nm AgNPs, primary size; agglomerating to 69 nm in vehicle | 125 µg/50 µl vehicle (~0.5 mg/kg); vehicle (10% fetal bovine serum in DMEM) | Single exposure with recovery points at 1, 3, and 5 days post-exposure | Inflammation and necrosis in liver only at days 3 and 5; silver levels highest in liver and spleen at all times; most of silver in liver was particulate; ion/particle ration decreased in spleen over time; silver in all other organs was primarily ionic. | | No pathology noted in kidney, spleen, lung, or brain | Su et al. [2014b] |

(Continued)

**Table E-6. Summary of in vivo toxicological studies of silver nanoparticles (AgNPs) and nanowires (AgNWs) (Continued)**

| Species | Particle Characteristics | Exposure Details: Concentration/ Dose | Exposure Details: Duration | Critical Effect(s) | NOAEL/ LOAEL | Comments | Reference |
|---|---|---|---|---|---|---|---|
| Male Balb/c mice; n= 5 for biodistribution studies and n= 3-5 for pharmacokinetic studies | PVP, citrate, PEG, or BPEI coated AgNPs ~30 nm; $AgNO_3$ soluble control | 20 µg of silver per mouse in 200 µl volume | Single exposure; biodistribution assessed at 1 day; blood collected at 2, 10, 30, and 60 min, and at 6, 12, 24, and 72 hours | All particles distributed to the greatest degree to the liver and spleen; BPEI had the greatest biopersistence in tissues at 24 hours; PVP and citrate AgNPs were similar in pharmacokinetics; PEG-coated particle also had a high biopersistence and remained in the circulation the longest in the first hour after exposure | ND | Complemen-tary in vitro studies showed DNA fragmentation and cytotoxicity with positively charged surface coating in liver cells | Pang et al. [2016] |
| Male CD-1 (ICR) mice (n = 3/ group0 | PVP- or citrate-coated 10-, 40-, or 100-nm AgNPs; or silver acetate | 10 mg/kg of AgNO or 15.5 mg/ kg silver acetate (10 mg/kg silver equivalent) | Single exposure with 24-hour recovery point | Coating did not influence distribution or toxicity; smaller particles accumulates to a greater degree in tissues than larger and were more hepatotoxic and splenotoxic | | Soluble silver accumulated in liver but also in a kidney, to a greater degree than particulate silver, and caused kidney toxicity | Recordati et al. [2016] |
| Male Wistar rats; 4 groups of 24 | 20- or 200-nm, almost spherical, agglomerated in solution | 0, 5, or 10 mg/ kg for the 20-nm particles, 0 and 5 mg/kg for the 200-nm particles | Single exposure (tail vein) with various recovery periods up to 4 weeks | Reduced sperm count, increased comet tail moments in germ cells | –/5 mg/kg | | Gromadzka-Ostrowska et al. [2012] |

(Continued)

**Table E-6. Summary of in vivo toxicological studies of silver nanoparticles (AgNPs) and nanowires (AgNWs) (Continued)**

| Species | Particle Characteristics | Exposure Details: Concentration/ Dose | Exposure Details: Duration | Critical Effect(s) | NOAEL/ LOAEL | Comments | Reference |
|---|---|---|---|---|---|---|---|
| Sprague-Dawley rats; sex not stated; 5–8 per group | 50–60-nm particles in 0.7% NaCl containing 0.05% Tween 80, shape not specified | 30 mg/kg | Single exposure | Leakage of Evans blue dye into the brain, brain edema | –/30 mg/kg | | Sharma et al. [2010] |
| Sprague-Dawley rats; 2 of each sex per group | Spherical, 50–90 nm or 1–10 nm in diameter, but with aggregation in aqueous medium | 100 mg/kg for the larger species, 1 mg/kg for the smaller | One injection in tail vein 3 days/ week for 4 weeks | Silver deposition, changes to the lymphocyte/ granulocyte ratio, changes in gene expression | NA | Dosing regimen insufficiently described | Kim et al. [2009b] |
| Sprague-Dawley rats; 2 males per group | Spherical, 50-nm-diameter particles in an aqueous medium; some larger particles (up to 100 nm in length) were rod-shaped | 0, 1, or 100 mg/kg | One injection in tail vein every 2–3 days for 4 weeks | Proteomic analysis of liver, kidney, and lung | NA | Functional analysis of proteomic changes implicated ROS formation and apoptosis in relation to silver nanoparticles treatment | Kim et al. [2010b] |
| Wistar rats; 4 dose groups and a control group; male and female rats; *n* per group not stated | Spherical 15–40-nm-diameter particles dispersed in ethylene glycol | 4, 10, 20, or 40 mg/kg; phosphate buffer saline as control substance | One injection in tail vein at 5-day intervals over 32 days | Hematologic changes in WBC, platelet counts, hemoglobin, and RBC in 20- and 40-mg/kg groups; increase in liver function enzymes, ALT, AST, AP, GGTP in 40-mg/kg group | NOAEL at 10 mg/kg | ROS increased in all groups in a dose-related manner | Tiwari et al. [2011] |

(Continued)

**Table E-6. Summary of in vivo toxicological studies of silver nanoparticles (AgNPs) and nanowires (AgNWs) (Continued)**

| Species | Particle Characteristics | Exposure Details: Concentration/ Dose | Exposure Details: Duration | Critical Effect(s) | NOAEL/ LOAEL | Comments | Reference |
|---|---|---|---|---|---|---|---|
| Balb/c mice (sex not specified); n = 3-6/group | 20-nm AgNPs (NM-300K) in medium 4% Tween-20 + 4% polyoxyethylene (NM-300K-DIS) | 0,0.2,2.0, or 5.0 mg/kg | Single dose, parameters assessed at 8 hours post-exposure | Highest dose caused lung and liver pathology; markers of oxidative and endoplasmic reticulum stress in liver and spleen; apoptosis in lung, liver, spleen, and kidney | ND | Tissue distribution spleen > liver > lungs >> kidneys > heart > brain | Chen et al. [2016] |
| Female Sprague-Dawley rats; 1-3 per group per time point | 20-nm or 110-nm PVP-coated AgNPs, or silver acetate | 1 mg/mL | 1 time on gestation day 18; parameters assessed 1 and 2 days post-exposure | Silver was detectable in placenta and fetus at both times and to a greater degree in fetus; markers of cardiovascular effects and oxidative stress were not altered | ND | Silver was detectable in all major organs but to a greater degree in spleen, lung, liver, kidney, placenta, and cecum/ large intestine; urine analysis show changes in carbohydrate and amino acid metabolism | Fennell et al. [2016] |

(Continued)

**Table E-6. Summary of in vivo toxicological studies of silver nanoparticles (AgNPs) and nanowires (AgNWs) (Continued)**

| Species | Particle Characteristics | Exposure Details: Concentration/ Dose | Exposure Details: Duration | Critical Effect(s) | NOAEL/ LOAEL | Comments | Reference |
|---|---|---|---|---|---|---|---|
| Female Balb/c mice; n = 5-10/ group<br>Female Balb/c mice; n = 3/group<br>Male Balb/c mice; n = 3-5/group | 25-nm PVP-coated AgNPs or silver nitrate<br>25-nm PVP-coated AgNPs<br>25-nm PVP-coated AgNPs | 0, 22, or 108 µg/kg AgNPs or 108 µg/kg silver nitrate<br>1.3 mg/kg AgNPs<br>1.3 mg/kg AgNPs | Every 2 days for 4 weeks, with recovery at 2 weeks after last exposure;<br>Every 2 days for 4 weeks with recovery at 15, 39, and 72 days after last exposure; Every 2 days for 4 week with recovery at 4 months after last exposure | High dose of AgNPs detected in Spleen > liver = kidney; Silver highest in liver, kidney, and spleen at d 15, lower in heart and lung; clearance occurred over time for liver spleen and kidney, but was still measurable at day 78. Silver was highest in liver, spleen, and testis (ng/g tissue), followed by kidney, heart, lung, and muscle | ND | Comparative study: intraperitoneal deposition and persistence were greater than with intravenous exposure; silver not detectable in serum; silver not detectable in serum | Wang et al. [2013] |
| CD-1 pregnant mice; groups of 6 to 12 | Spherical 50-nm-diameter particles of $AgNO_3$ | Doses of 0 ($n$ = 11), 35 ($n$ = 12), 66 ($n$ = 6) µg AgNPs on the 7$^{th}$, 8$^{th}$, and 9$^{th}$ day of gestation; doses of 9 ($n$ = 9) and 90 ($n$ = 3) µg $AgNO_3$ on same days of gestation | One injection of each dose on the 7$^{th}$, 8$^{th}$, and 9$^{th}$ day of gestation; killed 24 hr after 3$^{rd}$ injection | AgNPs identified in most maternal organs, extra-embryonic tissues, and embryos | NA | | Austin et al. [2012] |

(Continued)

**Table E-6. Summary of in vivo toxicological studies of silver nanoparticles (AgNPs) and nanowires (AgNWs) (Continued)**

| | | Exposure Details | | | | | |
|---|---|---|---|---|---|---|---|
| Species | Particle Characteristics | Concentration/ Dose | Duration | Critical Effect(s) | NOAEL/ LOAEL | Comments | Reference |
| Male Wistar rats; 2 exposure groups and 1 control group; 23 per group | 20- and 200-nm-diameter AgNPs | Doses of 0 (control group) and 5 mg/kg (exposure groups) | One injection; killed at 24 hr, 7 days, and 28 days | AgNPs identified in liver, lungs, spleen, kidneys, and brain; highest concentration of Ag in liver at 24 hr | NA | Highest concentration of Ag found with 20-nm AgNPs | Dziedzikowska et al. [2012] |
| ICR mice; 3 exposure groups and 1 control group; 6 male and female mice per group | 21.8-nm average primary AgNPs (range, 10–30 nm) | Doses of 0 (control group) and 7.5, 30, or 120 mg/kg | One injection; killed 10 min to 24 hr post-injection for biokinetics; at 7 and 14 days post-injection for histopathology | No acute effects at 14 days; Ag found in all major organs, with highest concentration in liver and spleen | NA | Highest concentration of Ag found in lungs and kidneys of female mice | Xue et al. [2012] |
| Female Balb/c mice ($n$ = 4) and female Fisher CDF rats; $n$ not stated | PVP-coated AgNPs were spherical with 12-nm avg. diameter | Iodine-125-labeled AgNPs Mice: 4 µCi of the $^{125}$I-AgNPs Rats: 20 µCi of the $^{125}$I-AgNPs | One injection; Ag distribution evaluated at 30 min, 4 hr, and 24 hr with CT-SPECT imaging of organs | Prominent uptake of AgNPs in liver and spleen; level of AgNPs in blood relatively low at 24 hr | NA | | Chrastina and Schnitzed [2010] |
| Sprague-Dawley male rats; New Zealand white male rabbits; male dogs; n not stated | Particle characterization not given | Ag nitrate mixed with $^{110}$Ag given in femoral vein of rats (0.01, 0.03, 0.1, 0.3 mg/kg), rabbits (0.1 mg/kg), and dogs (0.1 mg/kg) | One injection; $^{110}$Ag measured in urine and feces at 24-hr periods for 4 days | 25%–45% of Ag excreted into bile during first 2 hr; 70% excreted within 4 days; highest concentration of Ag occurred in liver at 2 hr | NA | Ag concentration in bile 16–20 times higher than that found in plasma | Klaassen [1979] |

(Continued)

**Table E-6. Summary of in vivo toxicological studies of silver nanoparticles (AgNPs) and nanowires (AgNWs) (Continued)**

| Species | Particle Characteristics | Exposure Details: Concentration/ Dose | Exposure Details: Duration | Critical Effect(s) | NOAEL/ LOAEL | Comments | Reference |
|---|---|---|---|---|---|---|---|
| SPF New Zealand white male rabbits ($n$ = 4) | Citrate-coated AgNPs (~7.9-nm diameter) | Injected into ear vein at doses of 0.5 mg/kg and 5 mg/kg | One injection; blood taken for Ag analysis from other ear at post-treatment times of 5, 10, and 30 min; 1, 2, 6, and 12 hr; days 1 through 7; and days 14, 21, and 28 | Concentration of AgNPs in serum at highest concentration 5 min from treatment; 90% of AgNPs eliminated from serum at 28 days; tissue distribution of AgNPs highest in liver, spleen, and kidney | ND | Pigmentation found in liver at 7 and 28 days; inflammatory cell infiltration increased in livers, lungs, and kidneys | Lee et al. [2013c] |
| **Intraperitoneal Injection** | | | | | | | |
| Outbred white female rats (n = 8-14 per group) | 50-nm AgNPs, 50-nm AuNPs, vehicle control (deionized water); 50-nm AgNPs with bioprotective complex or bioprotective complex only as control | 10 mg/kg | 3 times/week for 20 injections (~3 weeks; bioprotective complex supplied orally | Pathological alteration in kidney, liver and spleen; genotoxicity AgNPs > AuNPs in liver, spleen, bone, kidney, and RBC; minor differences between particles in blood chemistry parameters with greater decrease in ceruloplasmin in AgNP exposure | ND | Particles deposited in liver, kidney, and spleen with greater AgNPs in kidney and greater AuNP in liver; similar trends for decreased RBC, monocytes, and hemoglobin (AuNPs > AgNPs) | Katsnelson et al. [2013] |

(Continued)

**Table E-6. Summary of in vivo toxicological studies of silver nanoparticles (AgNPs) and nanowires (AgNWs) (Continued)**

| Species | Particle Characteristics | Exposure Details: Concentration/ Dose | Exposure Details: Duration | Critical Effect(s) | NOAEL/ LOAEL | Comments | Reference |
|---|---|---|---|---|---|---|---|
| Female Balb/c mice; n = 5-10/ group Female and Male Balb/c; exposed, then mated and fetuses collected; n = 3-5 per group | 25-nm PVP-coated AgNPs or silver nitrate; 25-nm PVP-coated AgNPs or silver nitrate | 0, 22, or 108 µg/kg AgNPs or 108 µg/ kg silver nitrate; 0, 22, or 108 µg/kg AgNPs or 108 µg/ kg silver nitrate | Every 2 days for 4 weeks, with recovery at 2 weeks after last exposure; males and females were exposed every 2 days for 4 weeks, then mated; placenta, fetal liver, remaining fetus collected gestational day 14.5 | Silver burden in tissue was dose-dependent and greatest in liver and spleen; burden was greater for high-dose AgNPs versus high-dose ionic silver; all forms of silver detected in placenta, fetal liver, and remaining fetus; high dose of AgNPs greatest in placenta and low dose of AgNPs greatest in fetal liver and remaining fetus | | Tissue deposition was 100-fold greater following intraperitoneal exposure versus intravenous exposure; authors suggest particle agglomeration as a barrier to particles crossing placenta | Wang et al. [2013] |
| Male C57BL/6N mice | 25-nm particles, shape not specified | 0, 100, 500, or 1,000 mg/kg | Single exposure | Altered gene expression in extracted regions of the brain | ND | RT-PCR analysis used oxidative stress and antioxidant defense arrays | Rahman et al. [2009] |
| Female Wistar pregnant rats (*n* = 30); 4 treatment groups and 1 control group | Nanosilver, size and type not specified | 4 groups given either 0.4 and 0.8 mg/kg at 8$^{th}$ day gestation or 0.4 and 0.8 mg/kg at 9$^{th}$ day gestation | Single exposure; killed at 20$^{th}$ day gestation | No evidence of teratogenicity; mean weights and lengths decreased in comparison with controls | NA | | Mahabady [2012] |

(Continued)

**Table E-6. Summary of in vivo toxicological studies of silver nanoparticles (AgNPs) and nanowires (AgNWs) (Continued)**

| Species | Particle Characteristics | Exposure Details: Concentration/ Dose | Exposure Details: Duration | Critical Effect(s) | NOAEL/ LOAEL | Comments | Reference |
|---|---|---|---|---|---|---|---|
| Sprague-Dawley rats; sex not stated; 5 to 8 per group | 50–60-nm particles in 0.7% NaCl containing 0.05% Tween 80, shape not specified | 50 mg/kg | Single exposure | No evidence of blood-brain barrier permeability or brain edema | NA | | Sharma et al. [2010] |
| Sprague-Dawley rats; sex not stated; 6 to 8 per group | 10–30-nm particles dispersed in deionized water | 500 mg/kg$^{-1}$ | Single exposure | Decrease in autophagy; liver function impairment; hepatotoxicity | NA | | Lee et al. [2013b] |
| Male ICR mice; control group ($n$ = 10); 3 experimental groups ($n$ = 15) and 1 positive control group ($n$ = 10) | Generally spherical with average diameter of 36.3 nm | Control group ($n$ = 10) received 0.9% normal saline; 3 experimental groups ($n$ = 15) received 10, 25, or 50 mg/kg bw AgNPs; 1 positive control group ($n$ = 10) received scopolamine (3 mg/kg bw) | Daily for 7 days | No evidence of an effect on altering the reference memory or working memory | NA | Exposure to AgNPs did not affect neurocognitive outcome or hippocampal neurogenesis | Liu et al. [2013b] |
| **Subcutaneous Injection** | | | | | | | |
| Wistar rats; 90 females | AgNPs: 50–100-nm diameter; Ag microparticles: 2–20-µm diameter, control group | Single exposure: 62.8 mg/kg in a volume of 1 ml | Single exposures; 5 rats from each group killed at weeks 2, 4, 8, 12, 18, and 24 for analysis of Ag concentration in brain | Ag concentration higher for AgNPs than for Ag microparticles; Ag concentration peaked at 12 weeks and remained constant | NA | Could not determine whether Ag concentrations in brain were result of AgNPs or Ag+ | Tang et al. [2008] |

(Continued)

**Table E-6. Summary of in vivo toxicological studies of silver nanoparticles (AgNPs) and nanowires (AgNWs) (Continued)**

| | | Exposure Details | | | | | |
|---|---|---|---|---|---|---|---|
| Species | Particle Characteristics | Concentration/ Dose | Duration | Critical Effect(s) | NOAEL/ LOAEL | Comments | Reference |
| Wistar rats; 90 females | AgNPs: 50–100-nm diameter; Ag microparticles: 2–20-µm diameter, control group | Single exposure: 62.8 mg/kg in a volume of 1 ml | Single exposure; 5 animals from each group killed at weeks 2, 4, 8, 12, 18, and 24 for analysis of Ag concentration in brains, liver, spleen, lung, and kidney | Concentrations of AgNPs in organs statistically significantly higher than those of Ag microparticles | NA | Ag microparticles did not pass to the general circulation (~0.02% of the injected load) | Tang et al. [2009] |

CMAD = count median aerodynamic diameter; CMC = carboxymethyl cellulose; GGTP = gamma glutamyl transpeptidase; GM = geometric mean; 5-HT = 5-hydroxytryptamine; NA = not applicable; ND = not determined; PVP = polyvinylpyrrolidone.

*By analogy to the findings in Kim et al. [2010a], these particles are likely to have been spherical.

# APPENDIX F

## Rat Respiratory Parameters Pertaining to Interspecies Equivalent Dose Estimation

## F.1 Estimating Lung Tissue Concentration of Silver Relative to Steady-State Tissue Concentration in Rats

The objective of the analysis in this section is to investigate the question of whether silver had reached steady-state concentration in the rat tissues at the end of the subchronic inhalation exposure. Data to address this question are reported in Song et al. [2013]. This information is relevant to the extrapolation of subchronic to chronic responses in the rat, which is also relevant to estimating the dose associated with potential responses in humans over a working lifetime (e.g., dosimetric adjustment factor for subchronic to chronic exposure, DAF 3) (Section 6.2.4). To the extent that steady-state tissue concentration has not been achieved, the tissue dose with continued exposure at a given concentration would result in greater tissue doses and therefore a higher likelihood of adverse response.

The concentration of a substance in the body at any point in time depends on the rates of intake and elimination. Half-life is the time required for a property (such as concentration or activity) of a substance in the body to decrease by half. At steady-state, the intake of a substance is in approximate dynamic equilibrium with its elimination. The time required to reach a steady-state concentration is approximately four to five half-lives for a substance administered at a regular interval [ITO 2011]. Thus, for a 12-week (84-day) study, the half-life would need to be less than approximately 21 days in order to achieve steady-state concentrations in that subchronic study.

Lung tissue concentrations of silver after subchronic inhalation are shown in male and female rats in Figure 7 of Song et al. [2013]. The lung silver concentration declined by a factor of approximately three during the 12-week post-exposure duration. Other tissue concentrations of silver cleared faster than those in lungs (shown in male and female rats separately in Tables IV, V, VII, and IX in Song et al. [2013]). However, the systemic tissue concentrations of silver depend on uptake from the lungs (portal of entry), such that steady state would not likely be achieved in the systemic tissues if not achieved in the lungs.

The concentration of a substance in the tissue at any time relative to the steady state concentration can be estimated as follows:

**Equation F-1**

$$\frac{C(t)}{Css} = 1 - e^{-kt}$$

where C(t) is the concentration of a substance in tissue at time t, Css is the steady-state tissue concentration, and k is the clearance rate constant; k is equal to ln(2)/half-life.

For example, in male rats exposed at the highest airborne exposure concentration (381 μg/m$^3$) of silver for 12 weeks (84 days), the retention half-life ($t_{1/2}$) of silver in lung tissue was 42.3 days (as shown in Table X of Song et al. [2013]), and ln(2) is 0.693, as follows:

**Equation F-2**

$$\frac{C(t)}{Css} = 1 - e^{\left(\left(\frac{0.693}{42.3}\right)x84\right)} = 0.75$$

That is, after 12 weeks of exposure, approximately 75% of the Css lung concentration of silver had been achieved in those rats. Estimates for the other exposure groups in male rats and female rats are shown in Tables F-1 and F-2. These estimates suggest the steady-state concentration of silver in lung tissue had not been achieved. Thus, with chronic exposure at the same exposure concentrations, higher tissue burdens would be expected than those in the subchronic study. Higher tissue concentrations of silver would be expected to increase the risk of adverse effects associated with that exposure.

## F.2 Rat Ventilation Rates

Some of the rat parameter values used in the dosimetric adjustment factors (DAFs) (Section 6.2.4.2)

are estimated from the average body weights. These include the DAFs for ventilation rate (DAF 1), deposition fraction of inhaled particles (DAF 2), and in some cases, dose normalization (DAF 4). Average body weight in female rats in Sung et al. [2009] was calculated as 196 g over the 13-week study, from the average body weights of 162 g at 8 weeks of age (start of study, all female rats) and 230.6 g at 21 weeks of age (end of study, control female rats). Average body weight of male rats in Sung et al. [2009] was calculated here as 345 g over the 13-week study, from the average body weights of 253 g at 8 weeks of age (start of study, all male rats) and 437 g at 21 weeks of age (end of study, control male rats).

Minute ventilation (L/min) was estimated with use of the average body weight in male or female rats, as shown in the following allometric [U.S. EPA 1994]:

**Equation F-3**

$$\ln(V_E) = b_0 + b_1 \ln(BW)$$

where $V_E$ is the minute ventilation (L/min); BW is body weight (kg); and $b_0 + b_1$ are the species-specific parameters, which for rat are -0.578 ($b_0$) and 0.821 ($b_1$) [Table 4-6 of U.S. EPA 1994].

Thus, minute ventilation is calculated as

**Equation F-4**

$$V_E \text{ (L/min)} = \text{Exp}[b_0 + b_1 \times \ln(BW)]$$

which results in $V_E$ of 0.15 L/min for a 196-g female rat and 0.23 L/min for a 345-g male rat.

By comparison, for a 300-g rat, as used in the MPPD default Long-Evans rat model, $V_E$ is 0.21 L/min. Tidal volume is 2.1 mL, assuming 102 breaths/min, calculated as follows:

**Equation F-5**

$$\text{Tidal volume (mL)} = V_E \text{ (L/min)} / [\text{breaths (min}^{-1}) \times 0.001 \text{ (L/mL)}]$$

These values differ from those reported in Sung et al. [2008] and Song et al. [2013], which also differ from each other. Sung et al. [2008] report minute ventilation (called minute volume) of ~25 mL/min (i.e., ~0.025 L/min) and tidal volume of ~0.25 mL; these values are approximately 10× lower than those for a standard (300-g) rat. Song et al. [2013] report minute volume of ~800 mL/min (i.e., ~0.8 L/min) and tidal volume of ~8 mL; these values are approximately 4× higher than those for a 300-g rat. Given these differences in the measured values reported in the two studies, and the resulting uncertainty, these values were estimated in this analysis from the allometric equation by using body weight (Equations F-3 through F-5). The estimation of these respiratory parameters can influence the estimates of the DAF and the HEC.

Air intake per exposure day ($m^3$) was calculated as follows, based on a 6-hour exposure day in the rat studies:

**Equation F-6**

$$\text{Air intake } (m^3) = V_E \text{ (L/min)} \times (60 \text{ min/hr} \times 6 \text{ hr}) \times 0.001 \text{ m}^3\text{/L}$$

which results in 0.053 $m^3$ in female rats and 0.084 $m^3$ in male rats in Sung et al. [2009]; these values are used in DAF 1 (Section 6.2.4.2).

## F.3 Rat Measured and Dosimetry Model–Predicted Lung Burdens

DAF 2 is the ratio of the deposition fractions of particles in the target respiratory tract region in humans and rats. Thus, the measured and predicted rat lung burdens of silver are evaluated in this section to compare to those predicted from the multiple-path particle deposition (MPPD) model [ARA 2011]. The Long-Evans rat model had been the only rat model in MPPD until the recent addition of a Sprague-Dawley rat model in MPPD v. 3.04. The estimates from each of these models is compared to the measured lung doses of silver in male rats (Table F-3) and female rats (Table F-4) at the end of the 13-week exposure in the Sung et al. [2009] study.

Each of these models over-predicted the measured lung burdens of silver, but the estimates from the Sprague-Dawley rat model were the closest to the reported values. Each model predicted that approximately half of the total deposited silver was retained at 13 weeks of exposure, based on clearance kinetics of poorly soluble particles. The lower retained doses may be due to dissolution in addition to alveolar macrophage–mediated clearance of silver particles.

## F.4 Interspecies Dose Normalization Factors

Estimating the equivalent dose in humans to the critical effect dose in rats involves adjusting for differences in the body or organ weight or surface area across species. Typical values used in the dose normalization factor DAF 4 in the risk assessment of inhaled particles are shown in Table F-5. NIOSH used the total respiratory tract surface area or the pulmonary surface area, respectively, in extrapolating the rat airborne exposure concentration associated with either liver bile duct hyperplasia or pulmonary inflammation (Section 6.2.4.2). For adverse effects beyond the lungs, as in the liver, body weight is also commonly used to extrapolate the rodent effect levels to humans, especially for oral routes of exposure. The ratios of the human/rat values are broadly similar for total respiratory tract surface area, pulmonary surface area, or body weight (Table F-5). For reasons that are not entirely clear, the ratios from U.S. EPA [1994] are smaller than the ratios from the other sources (Table F-5).

**Table F-1. Lung clearance kinetics and tissue concentration estimates in male rats in Song et al. [2013].**

| Exposure group | Half-time ($t_{1/2}$, d)* | Clearance rate constant $k = ln(2)/t_{1/2}$ | Lung tissue concentration at end of exposure as proportion of estimated steady-state concentration | Number of half-lives by end of 12-week exposure ($84\ d / t_{1/2}$) |
|---|---|---|---|---|
| Low | 28.5 | 0.0243 | 0.8704 | 2.95 |
| Medium | 84.9 | 0.0082 | 0.4963 | 0.99 |
| High | 42.3 | 0.0164 | 0.7475 | 1.99 |

*From Table X in Song et al. [2013].

**Table F-2. Lung clearance kinetics and tissue concentration estimates in female rats in Song et al. [2013].**

| Exposure group | Half-time ($t_{1/2}$, d)* | Clearance rate constant $k = ln(2)/t_{1/2}$ | Lung tissue concentration at end of exposure as proportion of estimated steady-state concentration | Number of half-lives by end of 12-week exposure ($84\ d / t_{1/2}$) |
|---|---|---|---|---|
| Low | 38.7 | 0.0179 | 0.7779 | 2.17 |
| Medium | 112.9 | 0.0061 | 0.4029 | 0.74 |
| High | 40.4 | 0.0172 | 0.7634 | 2.08 |

*From Table XI in Song et al. [2013].

**Table F-3. Comparison of measured and predicted rat lung burden of silver after subchronic (13-week) inhalation of silver nanoparticles in male Sprague-Dawley rats [Sung et al. 2009] and as predicted by the Multiple-Path Particle Dosimetry (MPPD) model, v. 3.04 [ARA 2015].**

| Measured exposure and dose | | Predicted dose by MPPD model and rat average body weight (BW) | | | |
|---|---|---|---|---|---|
| | | Retained lung dose (µg), estimated by model[†] | | Deposited lung dose (µg), estimated by model and equations[‡§] | |
| Airborne exposure concentration (µg/m³) | Rat retained lung dose (µg) after 13-week exposure[*] | Long-Evans, semi-symmetric (default), BW 300 g | Sprague-Dawley rat, symmetric, BW 345 g | Long-Evans rat, semi-symmetric (default), BW 300 g (DFalv: 0.28) | Sprague-Dawley rat, symmetric, BW 345 g (DFalv: 0.0635) |
| 0 | 0.0011 | 0 | 0 | 0 | 0 |
| 49 | 0.88 | 30.1 | 7.5 | 75 | 17 |
| 133 | 7.96 | 93.2 | 22.5 | 205 | 46.3 |
| 515 | 21.82 | 445.2 | 104 | 790 | 179 |

[*]Calculated from data reported in Tables 1 and 7 of Sung et al. [2009], as follows:
Ag in whole organ (µg) = ng Ag/g tissue × g tissue × 0.001 µg Ag/ng tissue, with use of female control rat mean body weight at end of exposure (437.05 g).

[†]Symmetric or semi-symmetric refers to the airway branching pattern in the MPPD model.

[‡]Average deposited rat lung dose was calculated as follows:

Deposited lung dose (total) =

Exposure concentration (µg/m³) × Exposure duration (5 d/wk × 13 wk) × Alveolar deposition fraction (DFalv) × Air intake per exposure day (m³/6-hr d)

where exposure concentration and duration are as reported in Sung et al. [2009]; DFalv was estimated by the stated model; and air intake volume per exposure day was estimated from the average rat body weight during the 13-week study (Section F-2). For 345-g males, minute ventilation was 0.23 L/min, and air intake volume was 0.084 m³/6-hr d.

[§]Deposition fraction in the alveolar region (DFalv) was estimated with use of the default respiratory parameters in the stated MPPD model (including as adjusted by BW); note that minute ventilation is similar, but not identical, to that calculated on the basis of the allometric equation in Section F-2.

**Table F-4. Comparison of measured and predicted rat lung burden of silver after subchronic (13-week) inhalation of silver nanoparticles in female Sprague-Dawley rats [Sung et al. 2009] and as predicted by the Multiple-path Particle dosimetry (MPPD) model, v. 3.04 [ARA 2015].**

| Measured exposure and dose | | Predicted dose by MPPD model and rat average body weight (BW) | | | |
|---|---|---|---|---|---|
| | | Retained lung dose (μg), estimated by model[†] | | Deposited lung dose (μg), estimated by model and equations[‡§] | |
| Airborne exposure concentration (μg/m³) | Rat retained lung dose (μg) after 13-week exposure[*] | Long-Evans, semi-symmetric, BW 300 g | Sprague-Dawley rat, symmetric, BW 196 g | Long-Evans rat, semi-symmetric, BW 196 g (DFalv: 0.19) | Sprague-Dawley rat, symmetric, BW 196 g (DFalv: 0.0635) |
| 0 | 0.001 | 0 | 0 | 0 | 0 |
| 49 | 0.31 | 30.1 | 3.08 | 32 | 7.04 |
| 133 | 4.31 | 93.2 | 9.08 | 87 | 19.1 |
| 515 | 23.55 | 445.2 | 40.8 | 337 | 74.0 |

[*]Calculated from data reported in Tables 2 and 8 of Sung et al. [2009], as follows:
Ag in whole organ (μg) = ng Ag/g tissue × g organ tissue × 0.001 μg Ag / ng tissue, with use of female control rat mean body weight at end of exposure (230.60 g).

[†]Symmetric or semi-symmetric refers to the airway branching pattern in the MPPD model.

[‡]Deposited rat lung dose was calculated as follows:

Total deposited lung dose (μg) =
Exposure concentration (μg/m³) × Exposure duration (5 d/wk × 13 wk) × Alveolar deposition fraction (DFalv) × Air intake per exposure day (m³/6-hr d)

where exposure concentration and duration are as reported in Sung et al. [2009]; DFalv was estimated by the stated model; and air intake volume per exposure day was estimated on the basis of the average rat body weight during the 13-week study (Section F.2). For 196-g females, minute ventilation was 0.15 L/min, and air intake volume was 0.053 m³/6-hr d.

[§]Deposition fraction in the alveolar region (DFalv) was estimated with use of the default respiratory parameters in the stated MPPD model (including as adjusted by BW). Tidal volume of 1.47 mL for input to MPPD for female rat (196 g BW) was calculated as in Equation F-5 (using values of 0.15 L/min and 102 breaths/min).

**Table F-5. Dose normalization factors in humans and rats.**

| Reference | Normalization factor (unit) | Human | Rat | Ratio (human/rat)* |
|---|---|---|---|---|
| Stone et al. [1992] | Alveolar surface area ($m^2$) | 102 | 0.4 | 255 |
| Miller et al. [2011] | | 63.462 | 0.2422 | 262 |
| U.S. EPA [1994] | | 54 | 0.32 | 169 |
| Miller et al. [2011]† | Total respiratory tract surface area ($m^2$) | 63.8969 | 0.2464 | 259 |
| U.S. EPA [1994]‡ | | 54.34 | 0.34375 | 158 |
| ICRP [1994] (human); Sung et al. [2009] (rat) | Body weight (kg) | 70 | 0.345 (male) | 203 |
| | | 70 | 0.196 (female) | 357 |
| | | 70 | 0.270 (both) | 259 |

*Note that the normalization factor ratio is expressed as the inverse ratio (i.e., rat/human) in the dosimetric adjustment factor approach shown in Equations 6.1 and 6.2.

†Miller et al. [2011] (values are from Tables 4 and 5 of that reference, except head region in humans, as shown in equation (a) below, which is from U.S. EPA [1994]) for the following respiratory tract regions: head, tracheobronchial, and alveolar surface area ($cm^2$), respectively; rat: 18.5 + 24.2 + 2,422 = 2,464.5 $cm^2$ total; human (a): 200 + 4,149 +634,620 = 638,969 $cm^2$ total.

‡U.S. EPA [1994; values are from Table 4-4 of that reference] for the following respiratory tract regions: head, tracheobronchial, and alveolar surface area ($cm^2$), respectively; rat: 15 + 22.5 + 3,400 = 3,437.5 $cm^2$ total; human: 200 + 3,200 + 540,000 = 543,400.

This page intentionally left blank.

# APPENDIX G

## Other Quantitative Risk Assessments for Silver Nanoparticles

## G.1 Christensen et al. [2010]

Christensen et al. [2010] calculated INELs (indicative no effect levels) for silver nanoparticles, following the EU European Chemicals Agency [ECHA 2010] guidelines. The data used were from one subchronic (90-day) inhalation study in rats (as reported in two publications [Sung et al. 2008, 2009]).

The lowest exposure concentration (49 μg/m$^3$) [Sung et al. 2008, 2009] for decreased lung function in female rats [Sung et al. 2008] was used as a LOAEL by Christensen et al. [2010], although they noted that the severity of the effects at the LOAEL was unclear. A NOAEL of 133 μg/m$^3$ for lung and liver effects [Sung et al. 2009] was also used in the analysis by Christensen et al. [2010].

Following the ECHA [2008] guidelines, Christensen et al. [2010] adjusted the NOAEL or LOAEL for the difference in exposure duration in the rats (6 hours/day) and in humans (8 hours/day), as well as adjusting for resting (comparable to rat study) versus light work activity in workers (that is, 6.7 m$^3$ vs. 10 m$^3$).

Thus, the human-equivalent concentration (HEC) corresponding to a LOAEL of 49 μg/m$^3$ was calculated as follows:

**Equation G-1**

$$49\ \mu g/m^3 \times 6\ hr/8\ hr \times 6.7\ m^3/10\ m^3 = 25\ \mu g/m^3$$

(The same adjustments result in 67 μg/m$^3$ as the HEC to 133 μg/m$^3$ in rats.)

Uncertainty factors of 3 and 10 (for two different exposure scenarios) were used for adjusting the rat subchronic LOAEL to estimate a NOAEL. Additional factors included 2.5 for interspecies toxicodynamics and 1 for interspecies toxicokinetics (because the local effects were assumed to be independent of metabolic rate); a factor of 5 for interspecies extrapolation to workers; and a factor of 2 for subchronic to chronic uncertainty.

Thus, the HEC of 25 μg/m$^3$ was divided by either of these factors:

**Equation G-2**

$$3 \times 2.5 \times 5 \times 2 = 75$$

or

**Equation G-3**

$$10 \times 2.5 \times 5 \times 2 = 250$$

Thus, the derived OEL estimates (INELs) based on the rat LOAEL of 49 μg/m$^3$ were calculated by dividing the human-equivalent LOAEL of 25 μg/m$^3$ by an overall adjustment factor of 75 or 250:

**Equation G-4**

$$25\ \mu g/m^3 / 75 = 0.33\ \mu g/m^3 \quad \text{(OEL estimate 1)}$$

**Equation G-5**

$$25\ \mu g/m^3 / 250 = 0.1\ \mu g/m^3 \quad \text{(OEL estimate 2)}$$

Similar calculations were applied to the rat NOAEL of 133 μg/m$^3$ for lung inflammation (male and female rats) from Sung et al. [2009]. In this case, the worker-equivalent concentration and OEL estimate was 67 μg/m$^3$. The assessment factors included 10 for interspecies (animal to human, TK and TD) systemic liver effects; 5 for intraspecies variability; and 2 for subchronic to chronic extrapolation:

**Equation G-6**

$$10 \times 5 \times 2 = 100$$

**Equation G-7**

$$67\ \mu g/m^3 / 100 = 0.67\ \mu g/m^3 \quad \text{(OEL estimate 3)}$$

## G.2 Weldon et al. [2016]

A dosimetric adjustment approach was applied by Weldon et al. [2016] in estimating an OEL for silver nanoparticles on the basis of data in one of the subchronic inhalation studies [Sung et al. 2008, 2009]. Weldon et al. [2016] reference NIOSH [2013] for the version of the DAF method used in their HEC estimation. A separate evaluation of the individual factors used in the DAF method is provided in Section 6.2.4.2. The DAF values used by Weldon et al. [2016] are shown in Table G-1 and compared to the values used in the NIOSH analysis (Section 6.2).

Weldon et al. [2016] evaluated the various effects observed in the rat lungs or liver shown in Table 9 of Sung et al. [2009], including pulmonary inflammation and liver bile duct hyperplasia. The specific endpoints were quantified as the proportion of rats examined in each group observed to have a given response and degree of severity, based on histopathological examination results in Table 9 of Sung et al. [2009]. Weldon et al. [2016] applied BMDS modeling (EPA BMDS v. 2.6) to those dose-response data. A multistage polynomial degree 2 model was selected as the best-fitting model (although the fit statistics for the BMDS models were not reported in Weldon et al. [2016]). The rat liver tissue burden (μg Ag in the liver) in female rats associated with a 10% added risk of bile duct hyperplasia, 95% lower confidence limit estimate ($BMDL_{10}$), was selected as the critical effect level for use as the $PoD_{animal}$. Although not the lowest $BMDL_{10}$ ($BMDL_{10}$ for liver abnormalities was lower), bile duct hyperplasia was selected as "a specific, quantitative endpoint" to represent "the most sensitive level of biological effect."

The rat tissue doses used in the BMDS dose-response modeling in Weldon et al. [2016] (μg per organ) were presumably estimated from the silver tissue dose (ng Ag/g tissue) reported in Tables 1 and 2 of Sung et al. [2009]. In those tables, the organ weights are reported as a percentage of body weight in male and female rats. Although not stated in Weldon et al. [2016], the total silver dose (μg) in an organ could be estimated by multiplying the organ weight (g) (calculated from the percentage of body weight) by the silver tissue dose concentration (ng/g) and adjusting units. The estimates by NIOSH of the lung and liver organ doses of silver (Tables G-2 and G-3) were very similar, but not identical, to the silver organ doses reported in Figures 2 and 3 of Weldon et al. [2016]. These slight differences in the dose data would only have a slight influence on the $BMDL_{10}$ estimates derived from the best-fitting model.

The rat $BMDL_{10}$ based on silver liver tissue dose (μg) was converted to an equivalent airborne concentration (μg/m$^3$) by fitting the tissue dose and airborne concentrations in the rat study with a linear regression model (shown in Supplementary Figure 1 of Weldon et al. [2016]) to identify the airborne concentration associated with a liver tissue dose equivalent to the $BMDL_{10}$ estimate. The $R^2$ for the linear relationship between airborne exposure concentration (μg/m$^3$) of silver and the lung tissue dose of silver (μg) was 0.87 in males and 0.96 in females. Although the specific $BMDL_{10}$ estimate is not reported, the values shown in Figure 4 and Supplementary Figure 1 of Weldon et al. [2010] are roughly consistent with the ~0.015 μg (i.e., ~15 ng) estimate described above.

On the basis of the results of the linear regression (Supplemental Figure 1), Weldon et al. [2016] estimated a $PoD_{animal}$ of 25.5 μg/m$^3$, which is called a benchmark concentration (BMC) and is the 95% lower confidence limit estimate ($BMCL_{10}$) of the dose-response relationship for liver bile duct hyperplasia in female rats. Weldon et al. [2016] note that this estimated effect level (i.e., $PoD_{animal}$) is lower (more health protective) than the NOAEL of 133 μg/m$^3$ reported in Sung et al. [2009] for bile duct hyperplasia in male or female rats.

After estimating the $PoD_{animal}$, Weldon et al. [2016] derived the HEC_PoD by dividing the $PoD_{animal}$ by the total DAF (as shown in Equations 6-1 and 6-2 in Section 6.2.4.1).

Specifically, the Weldon et al. [2016] analysis included the following values:

**Equation G-8**

$$\text{HEC\_PoD } (5.66\ \mu g/m^3) = 25.5\ \mu g/m^3 \,/\, [(10\ m^3/d \,/\, 0.1015\ m^3/d) \times (0.348/0.29) \times (10/1) \times (2{,}422\ cm^2 \,/\, 634{,}620\ cm^2)]$$

where the numerator is the $PoD_{animal}$ (25.5 μg/m$^3$) and the denominator is the total DAF (4.51), consisting of individual factors for ventilation rates (H/A), deposition fraction (pulmonary region) (H/A), relative rates for pulmonary retention half-time (H/A), and interspecies dose normalization (pulmonary surface area) (A/H), in humans (H) or animals (A).

The air intake value of 10 $m^3$/d in humans is similar to the 9.6 $m^3$/d worker reference value [ICRP 1994], and the air intake of 0.1015 $m^3$/d in rats is based on the ventilation rate reported in Pauluhn [2010] of 0.29 $m^3$/kg body weight for male Wistar rats (0.350 kg) in a subchronic inhalation study of carbon nanotubes [NIOSH 2013, Section A.6.3.1]. The ratio 0.348/0.29 includes the pulmonary deposition fractions in humans and rats, respectively, estimated in MPPD v. 2.11 (the Long-Evans was the only rat model available in v. 2.11). Weldon et al. [2016] cite Snipes [1989] for the ratio of 10/1 for the human-to-rat relative values for the pulmonary retention half-times of poorly soluble particles, assuming first-order clearance kinetics. Weldon et al. [2016] cite Miller et al. [2011] for the pulmonary surface area values of 2,422 $cm^2$ and 634,620 $cm^2$, respectively, in rats and humans.

Following this method, Weldon et al. [2016] derived an OEL of 0.19 μg/$m^3$ by dividing the HEC_PoD estimate of 5.66 μg/$m^3$ [Equation G-8] by a total uncertainty factor of 30. The total uncertainty factor of 30 includes individual uncertainty factors of 3 for toxicodynamic differences in animals and humans, 2 for extrapolation of subchronic to chronic effects, and 5 for interindividual variability in workers (i.e., $2 \times 3 \times 5 = 30$), as described in Weldon et al. [2016].

NIOSH used similar DAF values for air intake and interspecies dose normalization, although individual values differed (Table G-1). NIOSH used a different rat pulmonary deposition fraction of 0.0635 for the Sprague-Dawley rat (from MPPD v. 3.04) because it is the rat strain used in the Sung et al. [2009] and Song et al. [2013] studies of Ag-NPs. The pulmonary deposition fraction of 0.29 in the Long-Evans rat was higher than that in the Sprague-Dawley rat, apparently because of greater deposition efficiency of nanoparticles in the nasal–pharyngeal (head) region in the Sprague-Dawley rat (according to MPPD v. 3.04, which includes models for both rat strains).

NIOSH did not include a DAF for the relative pulmonary retention half-times of AgNPs in humans and rats because of insufficient data on the role of particle dissolution (and the lower retained silver in rat lung tissue than estimated for poorly soluble particles; Section F-3); NIOSH addressed this uncertainty by applying uncertainty factors (Section 6.2.4.3). Finally, in estimating the HEC to the rat effect level for liver bile duct hyperplasia, NIOSH normalized the doses across species by using the total respiratory tract surface area, because particles that deposit anywhere in the respiratory tract can potentially reach the liver, e.g., through translocation or dissolution into the blood circulation or the swallowing of particles that deposit in the nasopharyngeal region or were cleared from the lower respiratory tract (Section 6.2.4.2). Table G-1 provides a summary of the DAF values used by Weldon et al. [2016] and compares these to the values used in the NIOSH risk assessment (Section 6.2).

## G.3 Ji and Yu [2012]

Ji and Yu [2012] estimated an HEC to their estimated rat PoD of 100 μg/$m^3$. A worker-equivalent PoD of 59 μg/$m^3$ was estimated by adjusting the 100-μg/$m^3$ rat PoD by interspecies differences in the deposition fraction of silver nanoparticles (18 nm in diameter; GSD, 1.5) in the alveolar region of the respiratory tract (0.4 $m^2$ for rats; 62.7 $m^2$ for humans) [Ji and Yu 2012]. Inhalation exposure with light exercise in workers over a total of 13 weeks (5 days/week) was assumed [Ji and Yu 2012]. The alveolar deposition fractions in rats and humans were estimated with the multiple-path particle dosimetry (MPPD) 2.0 model [ARA 2009]. This worker-equivalent concentration estimate is similar to those estimated according to ECHA [2008] guidelines by Christensen et al. [2010] (Section G.1) and higher than that estimated in Weldon et al. [2016] (Section G.2). No OELs were proposed by Ji and Yu [2012].

## G.4 Acute Inhalation Exposure to Silver

In an acute (5-hr) inhalation study of two types of silver (ionic and AgNP) in rats (male, Sprague-Dawley), no adverse pulmonary effects were observed

1 day or 7 days post-exposure [Roberts et al. 2013]. The ionic silver was a commercial antimicrobial spray, administered at an exposure concentration of 100 μg/m$^3$ (count median aerodynamic diameter [CMAD] of 33 nm). The AgNP sample was a NIST reference material of total silver nanoparticles with low ionic content, administered at 1,000 μg/m$^3$ (CMAD of 39 nm).

A transient significant increase in blood monocytes was observed 1 day after exposure to the high concentration (AgNP), but not in rats exposed to the low concentration (ionic Ag). Slight cardiovascular changes (significant reduction in vascular responsiveness to ACh-induced re-dilation) were observed at the low concentration (ionic Ag) at 1 day post-exposure but not at the high concentration (AgNP). Both of these responses had resolved by 7 days post-exposure. Given the minimal, transient responses, each of these concentrations could be considered NOAELs for the respective types of silver.

In order to evaluate the short-term effects of exposure to silver nanoparticles, data from an acute (5-hr) inhalation study in rats was used to identify the rat NOAELs for airborne exposure to two types of silver (ionic and nanoparticles) [Roberts et al. 2013]. Benchmark doses were not estimated because there was only one exposure group for each type of silver. The HECs to the rat acute NOAELs were calculated by normalizing of lung weights (i.e., 1.5 g assumed for 9-week male Sprague-Dawley rats, approximately 300 g body weight; human lung weight of 1,200 g [ICRP 2002]), and by using a human alveolar deposition fraction of 0.17 (33 nm) or 0.15 (39 nm), based on the MPPD human deposition (Yeh and Schum) model [ARA 2011].

Lung dose estimates are shown for rats and humans in Table G-6. The estimated human-equivalent single-day (8-hour) exposure concentration is 620 μg/m$^3$ or 7.7 mg/m$^3$, respectively, for the commercial spray (ionic Ag) or NIST reference material (AgNP) (Table G-6). These HECs (to the rat acute NOAEL for ionic or nanoparticle silver spray) are approximately 60 or 700 times higher than the NIOSH REL for total silver (10 μg/m$^3$). These factors provide information relevant to a margin of exposure (MOE) assessment [Kim E et al. 2016]. The MOE in this example is the ratio of the HEC (to the rat effect NOAEL) and the REL. These HEC NOAEL estimates of a single acute exposure are 62 to 770 times greater than the NIOSH REL for total silver of 10 μg/m$^3$, or 688 or 8,555 times greater than the NIOSH proposed REL of 0.9 μg/m$^3$. Thus, the MOE estimates would be these same factors. However, these estimates are based on only one acute study of two materials, and the possible effects of repeated exposures at these concentrations are not known.

**Table G-1. Dosimetric adjustment factors used in Weldon et al. [2016], and comparison with values used in NIOSH risk assessment of silver nanoparticles (Section 6.2).**

| Dosimetric Adjustment Factor (DAF) | Weldon et al. 2016 — Liver bile duct hyperplasia | NIOSH (current analysis) — Lung inflammation | NIOSH (current analysis) — Liver bile duct hyperplasia |
|---|---|---|---|
| 1. Ventilation rate* (VE) [Human, H/ Animal, A] | 10/0.1015 = 99 $(m^3/d)/(m^3/d)$ | 9.6/0.084 = 114 $(m^3/d)/(m^3/d)$ | 9.6/0.053 = 181 $(m^3/d)/(m^3/d)$ |
| 2. Deposition fraction, by respiratory tract region (DF) [H/A] | 0.3848/0.29 = 1.2† | 0.386/0.0635 = 6.1† | 0.6634/0.949 = 0.699‡ |
| 3. Retention rate of particles in tissue [H/A] | 10/1 = 10 | NA [1/1] | NA [1/1] |
| 4. Normalization of dose across species [A/H] | 2,422/634,620† = 0.0038 $(cm^2)/(cm^2)$ | 0.4/102 = 0.0039 $(m^2)/(m^2)$† | 0.24647/63.8979 = 0.0038 $(m^2)/(m^2)$† |
| Total DAF $= (VE_H/VE_A) \times (DF_H/DF_A) \times (RT_H/RT_A) \times (NF_A/NF_H)$ | 4.51 | 2.72 | 0.49[1] |

*Ventilation rate differences pertain to the assumed body weight of the rat; for the NIOSH estimates, the sex associated with the most sensitive response is used (liver bile duct hyperplasia in females and lung inflammation in males), although the data were ultimately pooled on the basis of consistent exposure-response (Appendix B).

†Pulmonary (alveolar) region: particle deposition fraction (MPPD v. 3.04); alveolar surface area [Stone et al. 1992].

‡Total respiratory tract region: particle deposition fraction (MPPD v. 3.04); respiratory tract surface area [U.S. EPA 1994].

**Table G-2. Male rats—mean tissue doses of silver in Sung et al. [2009].**

| Organ and silver tissue concentration or total mass | Exposure group | | | |
|---|---|---|---|---|
| | Control (0 μg/m³) | Low (49 μg/m³) | Medium (133 μg/m³) | High (515 μg/m³) |
| Liver (ng Ag/g tissue)* | 0.70 | 3.52 | 13.8 | 133 |
| Liver (μg) in organ †‡ | 0.0078 | 0.038 | 0.16 | 1.50 |
| Lung (ng Ag/g tissue)* | 0.77 | 613 | 5,450 | 14,645 |
| Lung (μg) in organ†‡ | 0.0011 | 0.88 | 7.96 | 21.82 |

*From Table 7 of Sung et al. [2009].

†Calculated as Ag in whole organ (μg ) = ng Ag/g tissue × g tissue × 0.001 μg Ag/ng tissue, with use of male control rat mean organ weights (Table G-4).

‡Should match doses used in Weldon et al. [2016].

**Table G-3. Female rats—mean tissue doses of silver in Sung et al. [2009].**

| Organ and silver tissue concentration or total mass | Exposure group | | | |
|---|---|---|---|---|
| | Control (0 μg/m³) | Low (49 μg/m³) | Medium (133 μg/m³) | High (515 μg/m³) |
| Liver (ng Ag/g tissue)* | 0.90 | 4.55 | 12.07 | 71.08 |
| Liver (μg) in organ†‡ | 0.0055 | 0.026 | 0.07 | 0.46 |
| Lung (ng Ag/g tissue)* | 1.01 | 296 | 4,241 | 20,586 |
| Lung (μg) in organ†‡ | 0.0010 | 0.31 | 4.31 | 23.55 |

*From Table 8 of Sung et al. [2009].
†Calculated as Ag in whole organ (μg ) = ng Ag/g tissue × g tissue × 0.001 μg Ag/ng tissue, with use of female control rat mean organ weights (Table G-5).
‡Should match doses used in Weldon et al. [2016].

**Table G-4. Male rats—mean body and organ weights in Sung et al. [2009].**

| Body or organ (weight or percent)* | Exposure group | | | |
|---|---|---|---|---|
| | Control (0 μg/m³) | Low (49 μg/m³) | Medium (133 μg/m³) | High (515 μg/m³) |
| Body weight (BW) (g) | 437.05 | 435.62 | 456.22 | 451.44 |
| Liver (% of BW) | 2.54 | 2.51 | 2.48 | 2.50 |
| **Liver (g)**† | 11.10 | 10.93 | 11.31 | 11.29 |
| Lung (left + right) (% of BW) | 0.32 | 0.33 | 0.32 | 0.33 |
| Lungs (g)† | 1.40 | 1.44 | 1.46 | 1.49 |

*From Table 1 of Sung et al. [2009].
†Calculated as percentage of BW.

**Table G-5. Female rats—mean body and organ weights in Sung et al. [2009].**

| Body or organ (weight or percent)* | Exposure group | | | |
|---|---|---|---|---|
| | Control (0 μg/m³) | Low (49 μg/m³) | Medium (133 μg/m³) | High (515 μg/m³) |
| Body weight (BW) (g) | 230.60 | 237.95 | 221.13 | 248.70 |
| Liver (% of BW) | 2.64 | 2.43 | 2.52 | 2.59 |
| **Liver (g)**† | 6.09 | 5.78 | 5.57 | 6.44 |
| Lung (left + right) (% of BW) | 0.45 | 0.44 | 0.46 | 0.46 |
| **Lung (g)**† | 1.04 | 1.05 | 1.02 | 1.14 |

*From Table 2 of Sung et al. [2009].
†Calculated as percentage of BW.

**Table G-6. Acute (5-hr) inhalation exposure in rats—No observed adverse effect level (NOAEL) [Roberts et al. 2013] and human-equivalent exposure concentration.***

| Type of Ag | Count median aerodynamic diameter (nm) | Rat Ag lung dose (µg) [NOAEL] | Human-equivalent Ag lung dose (µg) | Airborne concentration (mg/m³) in 1 d (8-hour TWA) resulting in human-equivalent lung dose |
|---|---|---|---|---|
| Commercial spray (ionic) | 33 | 1.4 | 1,000 | 0.62 |
| NIST reference (particulate) | 39 | 14 | 11,000 | 7.7 |

*Calculations based on the following: Rat (male rat Sprague-Dawley, 9 weeks old) estimated body weight: 300 g; estimated lung weight: 1.5 g; Human lung weight: 1,200 g [ICRP 2002]; Human alveolar deposition fraction (DFalv): 0.17 (33 nm) or 0.15 (39 nm), MPPD Yeh and Schum model [ARA 2011]. Reference worker air inhaled (AI): 9.6 $m^3$/8 hour day [ICRP 1994]. The 8-hour time-weighted average (TWA) airborne concentration was calculated as: X $mg/m^3$ = Lung dose (mg) / [DFalv × AI].

This page intentionally left blank.

Promoting productive workplaces through safety and health research

DHHS (NIOSH) Publication No. 2021-112
DOI: https://doi.org/10.26616/NIOSHPUB2021112